STUDY OF THE ASPHALT PAVEMENT DAMAGE THROUGH NONDESTRUCTIVE TESTING ON OVERWEIGHT TRUCK ROUTES

A Thesis

by

SONIA INES RAMOS APARICIO

Submitted to the Office of Graduate Studies of
Texas A&M University
in partial fulfillment of the requirements for the degree of

MASTER OF SCIENCE

May 2004

Major Subject: Civil Engineering

STUDY OF THE ASPHALT PAVEMENT DAMAGE THROUGH NONDESTRUCTIVE TESTING ON OVERWEIGHT TRUCK ROUTES

A Thesis

by

SONIA INES RAMOS APARICIO

Submitted to Texas A&M University
in partial fulfillment of the requirements
for the degree of

MASTER OF SCIENCE

Approved as to style and content by:

_____
Robert L. Lytton
(Chair of Committee)

_____
Dallas N. Little
(Member)

_____
F. Michael Speed
(Member)

_____
Paul Roschke
(Interim Department Head)

May 2004

Major Subject: Civil Engineering

ABSTRACT

Study of the Asphalt Pavement Damage through Nondestructive Testing on Overweight

Truck Routes. (May 2004)

Sonia Inés Ramos Aparicio, B.S., National

Engineering University, Lima, Peru

Chair of Advisor Committee: Dr. Robert L. Lytton

Many highway facilities experience deterioration due to high traffic volumes and a service life that has been extended beyond facility design life. The 75th and 76th Texas Legislatures passed bills allowing trucks of gross vehicle weights (GVW) up to 125,000 lbs to routinely use a route in south Texas. Since the Texas Department of Transportation (Tx DOT) is concerned about the impact of overweight truck traffic (OTT) on its highways, there is a need to establish how the impact of this OTT on Texas roads will be incorporated into a long-term strategy for identifying and developing solutions to this problem.

In this study the effects of overweight truck traffic was investigated on a permitted truck route in the city of Brownsville. This route proceeds from the Veterans International Bridge to the Port of Brownsville via US77, SH4 and SH48 (SH 4/48).

The objective of this study is to establish the impact of heavy loads on the pavement structure through nondestructive testing. The problem increased in severity due to the increased flow of trade from the Port of Brownsville to Mexico, thus the expecting deterioration on the routes is mainly along the southbound lanes K6 and K7.

To accomplish this objective two nondestuctive testings were conducted as GPR and FWD tests. The K6 and K7 lanes were divided on 56 and 50 FWD stations, respectively. In addition, AC core samples were taken to be tested with frequency sweep test. All collected-data helped to analyze the route profile, layers thickness, static and dynamic backcalculated AC moduli, dynamic (complex) modulus from laboratory

testing, creep compliance parameters from the laboratory testing and dynamic analysis, and corrected AC moduli by temperature using three differents equations. In addition, it analyzed the effect of the cumulative 18-kip Equivalent Single Axle (ESAL) in both K6 and K7 lanes.

The results from the first analysis provided evidence of damage in the K6 lane; however, more significant results were found in the traffic analysis. This study confirms that because of greater amount of truck traffic (OTT) travels on K6 has lesser AC moduli than the K7 lane.

DEDICATION

This thesis is dedicated to my family: Victoria and Floren my lovely parents, my aunt Juana, my brothers, my sister and Chris, who encourages me to pursuit my goal.

ACKNOWLEDGMENTS

I would like to express my sincere gratitude to Dr. Emmanuel Fernando, my Supervisor and Dr Robet Lytton , my advisor and chair of my committee, for their guidance and support during this research. Their creativity and engineering vision inspired me during the course of this thesis work. I also extend my appreciation to my other committee members, Dr. Dallas Little and Dr Michael Speed, for their comments on my research.

This research has been sponsored by the Texas Department of Transportation. I would like to express a special thanks to Joe Leidy, the Project Director, to Mr. Luis Carlos Peralez, from Pharr District, and Rene Castro, who made possible the FWD data collection and traffic control. In addittion, I would like to extend my gratitude to Richard Peters, from Transportation Planning and Programming (TP&P) Division, who provided the weight-in-motion (WIM) data for fiscal year 2003 and Rhonda Christensen and Betty Hohensee who provided the lane distribution data at the WIM site along SH 4/48.

I would like to express my gratitude to Gerry Harrison and Lee Gustavus, research technicians, for their valuable support in the laboratory testing of this study.

Finally, I would like to express my gratitude to Lupe Fattorini, my colleagues, and anyone who assisted and encouraged me during the process of this research.

TABLE OF CONTENTS

LIST OF FIGURES

LIST OF TABLES

CHAPTER I

INTRODUCTION

Many highway facilities experience deterioration due to high traffic volumes and a service life that has been extended beyond facility design life. As aging road network conditions deteriorate, there is a need to increase investments and rehabilitation treatments in order to restore and maintain the road conditions at acceptable levels. The 75th and 76th Texas Legislatures passed bills allowing trucks of gross vehicle weights (GVW) up to 125,000 lbs to routinely use a route in south Texas, along the Mexican border. Since the Texas Department of Transportation (Tx DOT) is concerned about the impact of overweight truck traffic (OTT) on its highways, there is a need to establish how the impact of this OTT on Texas roads will be incorporated into a long-term strategy for identifying and developing solutions to this problem. These solutions could effectively promote future economic growth within the state Texas by preserving its highway infrastructures.

In this thesis was investigated the effects of overweight truck traffic on a permitted truck route in the city of Brownsville. This route proceeds from the Veterans International Bridge to the Port of Brownsville via US77, SH4 and SH48. The portion of the route along US77 is on a new concrete pavement and includes an elevated structure over half of its length. Most of the permitted truck route runs along SH4 and SH48. This research focused on studying the behaviour of the asphalt pavement supporting routine overweight truck traffic on SH4/48. Ninety-five percent of the truck traffic originates from the Port of Brownsville where the route starts at the FM 511 bridge, and runs along SH 48 until its intersection with Boca Chica Blvd. From there, truckers proceed along SH4 up to the US77 intersection, where they turn left to go to Mexico. Figure 1 gives an overview of the permitted truck route.

_____

The thesis follows the style and format of the *Transportation Research Board.*

FIGURE 1 Permitted Truck Route in Brownsville SH 4/48.

The payloads carried by permitted trucks are mostly coiled metal sheets, oil, and powder mineral (fluorite), which are transported from the Port of Brownsville to Mexico and vice versa. Figure 2 illustrates the types of payloads transported along the permitted truck route. The route was established in response to the need expressed by truckers to haul cargo at their trucks' operating capacities to improve operational efficiency. This meant hauling in excess of legal load limits, thus requiring permits to be issued.

The permit fee is US $30 per one-way trip. Even though the Pharr District retains 85% of the permit fee, it is too small an amount to cover the route's maintenance because of the potential for accelerated pavement deterioration. Therefore, it is relevant to study the effects of these routine overweight loads that run on SH 4/48 in order to identify requirements for building pavements to sustain routine overweight truck traffic. This information could help in maximizing trucking productivity and in enhancing the economic competitiveness of the state.

OBJECTIVES

The primary objectives of this research are to:

- characterize the effects of routine overweight truck loads on the performance of SH 4/48; and
- establish the impact of heavy truck loads on pavement performance.

These objectives were accomplished by carrying out nondestructive pavement testing, laboratory materials testing, evaluation of material properties from field and laboratory test data, and modeling of pavement response The expected benefits from this study are recommendations regarding an analysis procedure to determine the feasibility of using existing routes for overweight truck traffic. This project offered the first opportunity to study the effects of OTT on Texas highways. The data collected from this research are expected to be useful in establishing and developing ways to achieve the best accommodation of increased truck use on Texas highways.

FIGURE 2   Types of Loads Carried by Permitted Trucks.

PROBLEM STATEMENT

The nature of this complex problem can be stated as follows:

- the initial design for this route was based on conventional truck traffic conforming to legal load limits. Routine use of SH4/48 by overweight trucks began in March 1998.

- the problem increased in severity due to the increased flow of trade from the Port of Brownsville to Mexico. The deterioration on the routes is mainly along the southbound lanes K6 and K7.

- the impact of overweight truck traffic is a concern because the service life of highways under these conditions is unknown.

SCOPE OF THE RESEARCH

This thesis is documented in nine chapters. Chapter 1 is the introductory Chapter that gives the impetus for this study. Chapter II describes the concepts involved in the nondestructive test methods used to evaluate the effects of routine overweight truck traffic on SH4/48. Chapter III details the field data and laboratory testing methodology. It also describes how the SH4/48 route was segmented into different sections on the K6 and K7 lanes for the purpose of field data collection. The Chapter also identifies the locations (FWD stations) where cores were taken for laboratory testing. These FWD stations are named "core stations" in this study. Chapter IV summarizes the results of the analyses of the field data collected during the project. The field data taken with the falling weight deflectometer (FWD) and ground penetrating radar (GPR) are analyzed in this Chapter in order to predict pavement layer thickness profiles and static layer moduli values. Chapter V reports on the analysis of FWD data to characterize the dynamic modulus and the creep compliance properties of the asphalt concrete layer using dynamic analysis. The dynamic moduli backcalculated by system identification are compared to the backcalculated moduli from the static analysis. The dynamic analysis of full-time FWD data was conducted using the Dynamic Backcalculation by System Identification (DBSID) program developed by the Texas Transportation Institute (TTI). Static backcalculations were performed using MODULUS.

Chapter VI presents the results of laboratory tests of the field cores taken from SH4/48. The test carried out to characterize the asphalt layer was the frequency sweep test. Chapter VII presents the temperature corrections of backcalculated moduli beginning with the pavement temperature predictions. It was examined the corrected moduli as well as the modulus-temperature relationships determined from the test data as part of assessing the pavement damage along the route. For this analysis, the FWD stations on the K6 and K7 lanes were grouped, taking into consideration their values and the stations' proximity to each other. The temperature corrections of backcalculated moduli were done using three methods: the Chen equation, the TxDOT equation, and the Wictzak-Fonseca equation.

Chapter VIII discusses the comparison between the results obtained from field data presented in Chapters IV and V, and the laboratory data presented in Chapter VI. In addition, this Chapter takes the results obtained from the Witczak-Fonseca equation in order to show the current damage to the different sections along the route. Chapter IX summarizes the conclusions and recommendations stemming from this study.

CHAPTER II

LITERATURE REVIEW

This chapter presents relevant information regarding the test methods used to characterize the effects of permitted overweight loads on SH4/48.

GPR APPLICATIONS

Applying GPR techniques for nondestructive testing on highways and bridge decks has become more common in recent years. GPR has been demostrated to be an accurate and practical tool for nondestructive evaluation and inspection of highway structures. Different types of radar may be used for different applications on highway pavements. Depending on the way they operate, radar falls into two categories: air-launched and ground-coupled.

Air-launched GPR operates with the antena mounted at a specific height perpendicular to the pavement surface. This type of GPR is ideal for highway speed data collection, since there is no contact between the pavement surface and the antenna *(1)*.

Ground-coupled GPR operates with its plannar antennas in close contact with the pavement. This contact allows a better horizontal resolution, in the direction of the survey motion. This antenna is particularly suited to investigating defects in concrete pavements and bridge decks. The drawback is its data acquisition speed, which is limited to less than 6 mph. Defects such as surface cracks, voids, etc., or those of with relative profundity, one meter below the surface, can sometimes be detected with low frequency ground-coupled radar.

Air-launched radar systems work at the central frequency of approximately 1 GHz, while most ground-coupled radar systems work at lower frequencies, typically from 20 to 500 MHz *(2)*. The lower the frequency, the greater the penetration depth, but those lower frequencies offer less in near-surface resolution. For instance, under similar soil conditions, 100 MHz antennas may provide subsurface information to depths of 50 ft.

However, they will not be able to identify the presence of thin surface layers. On the other hand, a high frequency ground-coupled systems may only penetrate to a depth of 3 ft, but it can identify thin layers close to the surface. The Texas Transportation Institute's air-launched GPR unit operates at highway speeds (60 mph), and transmits and receives 50 pulses per second. It can effectively penetrate to a depth of two feet.

For the practical implementation of a GPR system, a automated signal processing is needed so that the mass of waveforms collected in a GPR survey can be transformed into information meaningful to highway engineers. In the past, TTI researchers used a signal processing system named DACQ to analyze GPR data *(3)*. Its main feature is an automated peak tracking system, in which the user identifies significant peaks within the GPR trace. The software then automatically traces those peaks throughout the entire file *(3)*. For each peak, the amplitudes and arrival times was of reflections were determined from the GPR data and used to compute the layer diealectrics and thicknesses. Other advanced features of DACQ is a correction procedure for antenna bounce, and several signal clean-up routines, which are applied prior to processing. However, there were several drawbacks with DACQ such as slow data processing if long lengths of highway were to be processed. Additionally, it was difficult to identify section breaks and the peak tracking system was difficult to use on several projects with badly distressed pavements..

Because of these limitations, a new processing package was subsequently developed to match Tx DOT's needs more closely. These needs are the capability of rapidly evaluating long sections of highway, of defining section changes, estimating layer thickness, and locating subsurface problem areas. COLORMAP is the software package that succeeded DACQ *(4)*. It was developed to provide a simple program that non-GPR experts can easily understand and use to interpret GPR data for pavement evaluation. In order to evaluate massive amounts of data in a timely fashion, COLORMAP employs several innovative data processing techniques. It relies on a color graphics display of GPR data to identify breaks and surface problems, and the manual tracking of layer interfaces in the layer computation routine.

FALLING WEIGHT DEFLECTOMETER

A nondestructive test is one from which the necessary information can be obtained to define physical properties of a sample without destroying it. In pavement evaluation, this involves a large mechanical device to duplicate vehicle loads without breaking up the pavement. By measuring the pavement response induced by loads, the structural integrity or stress-strain properties of the pavement structure can be determined (*5*).

The FWD is an impulse device used in the nondestructive testing of pavements because it reasonably simulates the shape and temporal nature of a moving wheel loading *(5)*. In addition, during FWD tests, the pavement's stress and strain conditions are similar to the conditions under a heavy vehicle load *(6)*. The major advantages of FWD testing are that:

- The impulse dropweight force on the pavement simulates traffic loads at highway speed.

- It is nondestructive.
- Pavement layer materials remain undisturbed.
- AC creep compliance data can be computed from FWD full-time history data and dynamic analysis. Pavement cracking and rutting can then be predicted from the creep compliance properties.

FWD is used in pavement evaluations to estimate pavement layer moduli for predicting remaining life. Most backcalculation procedures currently implemented predict the layer moduli from the peak load and the peak deflections measured by geophones. In this analysis, it is assumed that the FWD load is applied statically to the pavement, which is represented as an elastic layered system with linear or non linear (stress-dependent) material properties. These properties are backcalculated by minimizing the sum of the absolute or square of the errors between the predicted and the measured peak deflections at the geophone locations.

FWD works by applying an impulse load to the pavement which generates body waves and surface waves *(7)*. These waves travel at finite velocities and are recorded at different times by the geophones. The time lag of the response of the geophones is determined by transforming the load and the deflection histories from the time domain to the frequency domain by using the fast Fourier transform (FFT) method. Then, the FFT of the deflection history is divided by the FFT of the load history in order to obtain the pavement system transfer function. The magnitude of the deflection per unit force and the phase angle are then determined, frequency by frequency.

The layered elastic backcalculation program MODULUS 6.0 *(8)* developed by TTI, was used to analyze the FWD deflection data, specifically, to backcalculate layer moduli at different locations along the permitted truck route.

DYNAMIC ANALYSIS OF FWD DATA FOR PAVEMENT EVALUATION

Lytton *(7)* explained that there are more information in the FWD data than load and displacement amplitudes, and showed how other properties may be backcalculated using the load and displacement histories from the FWD. These properties include the creep compliance coefficients that may be determined from the analysis of the FWD load and deflection time histories:

$$D(t) = D_o + D_1 t^m \qquad (2.1)$$

where,

$D(t)$ = creep compliance at loading time t,

D_o, D_1 and m = coeficients of the power law model given by Eq. (2.1).

The slope m of the log creep compliance vs log time curve is directly related to the material damping as characterized by the phase angle.

There are several computer programs used to analyze the full time history data. These programs predict the transfer function or the FWD dispacement history for each sensor. Among them are PUNCH *(9)*, UTFWIBM *(10)*, SCALPOT *(11)*, and FWD-DYN

(12). The first three methods predict the tranfer function and the fourth, FWD-DYN, predicts the displacement history for a given sensor and pavement.

The FWD-DYN predicts the displacement history for each sensor, given the material properties and thickness of each pavement layer. In this program, the FWD load is first decomposed into its frequency components using FFT. Then, the transfer function, which defines the response of the pavement system to a steady-state unit load, is evaluated. Finally, the transfer function is multiplied by the FFT of the load to determine the Fourier transform of the displacement time history. FWD-DYN performs an inverse FFT on this Fourier transform to determine the time history of the displacement for each FWD sensor. It is significant to point out that the procedure assumes a linear system in view of the use of superposition to predict pavement response to the impulse load *(13)*.

The computer program DBSID determines the material properties using FWD data and full time load and displacement histories. DBSID was the result of adding a system identification routine to the FWD-DYN program. In this computer program, the pavement structure is limited to three layers of pavement, the first layer (AC) being a viscoelastic material following the power law creep compliance relationship of Eq. (2.1). The other two unbound layers are modeled as damped elastic solids characterized by Young's modulus and the damping coefficient. The equations to backcalculate the creep compliance parameters of Eq. (2.1) represent the relationship between the complex compliance and the complex modulus, and are given by Lytton *(7)*.

$$D'(\omega) \;=\; D_o + D_1 \frac{\Gamma(1+m)}{\omega^m} \cos\left[\frac{\pi m}{2}\right] \tag{2.2}$$

$$D''(\omega) \;=\; D_1 \frac{\Gamma(1+m)}{\omega^m} \sin\left[\frac{\pi m}{2}\right] \tag{2.3}$$

$$E'(\omega) \;=\; \frac{D'(\omega)}{\left[D'(\omega)^2 + D''(\omega)^2\right]^{\frac{1}{2}}} \tag{2.4}$$

$$E'(\omega) = \frac{D''(\omega)}{\left[D'(\omega)^2 + D''(\omega)^2\right]^{\frac{1}{2}}} \qquad (2.5)$$

$$\zeta(\omega) = \frac{E'(\omega)}{2E'(\omega)} \qquad (2.6)$$

where,

$D'(\omega)$	=	real part of the complex compliance,
$D''(\omega)$	=	imaginary part of the complex compliance,
$E'(\omega)$	=	real part of the complex modulus,
$E''(\omega)$	=	imaginary part of the complex modulus,
$\zeta(\omega)$	=	damping ratio,
$\Gamma(1+m)$	=	gamma function with parameter $(1+m)$, and
ω	=	loading frequency, radians/sec.

TEMPERATURE CORRECTIONS OF BACKCALCULATED AC MODULUS

The use of surface deflection measurements to evaluate pavements has steadily increased in the majority of highway agencies since the American Association of State Highway Officials (AASHO) road test was conducted. Deflection testing is used to evaluate a variety of pavement characteristics, including axle or vehicle load capacity, structural life, and uniformity. Deflection results are dependent upon seasonal variations that are affected by the underlying aggregate base course and subgrade. It is more significant in asphalt pavements which are dependent on the temperature of the asphalt (*14*). In fact, those factors that influence deflections are loading, environment, and pavement conditions. The environmental conditions related to seasonal variations are the temperature and moisture distributions within and around the pavement structures. The importance of these major factors is that they change the strength of the pavement materials and their resistance to traffic-induced stresses.

For pavement applications, the asphalt concrete moduli backcalculated from FWD data must be corrected to reference or standard conditions of temperature and loading

frequency. Before the temperature correction may be made, it is first necessary to determine the pavement temperature one is correcting from. This temperature is referred to herein as the base temperature, and correspond to the pavement temperature when the FWD data were collected. For this purpose, pavement temperatures may be measured directly with a temperature probe, or predicted from measured air and surface temperatures. In this regard, Lukanen *(14)* developed a set of equations for predicting pavement temperatures. These equations, referred to in the literature as BELLS2 and BELLS3, were developed using pavement temperature data from 41 Seasonal Monitoring Program (SMP) sites in North America.

BELLS2 is the equation used for the FWD testing protocol employed in the Long-Term Pavement Performance (LTPP) program, while BELLS3 is used for routine testing. The latter was developed to account for the effects of shading on the infrared temperatures measured at the SMP sites. Both equations require use of the infrared (IR) surface temperature at the time of the FWD measurements, and the average of the previous day's minimum and maximum air temperatures in the area of the project surveyed. The BELLS2 and BELLS3 equations have the following form and are different only in the coefficients β_i:

$$T_d = \beta_o + \beta_1\, IR + [\, \log_{10}(d) - 1.25][\beta_2\, IR + \beta_3\, T_{(1\text{-day})} + \beta_4 \sin(hr_{18} -15.5)]$$

$$+\beta_3\, IR \sin (hr_{18} - 13.5) \tag{2.7}$$

where,

T_d =   pavement temperature at depth, d (mm), within the asphalt layer in °C,

IR   =   surface temperature measured with the infrared temperature gauge in °C,

$T_{(1\text{-day})}$ =   the average of the previous day's high and low air temperature in °C,

hr_{18}	=	time of day in the 24-hour system, but calculated using an 18-hour asphalt temperature rise and fall time according to Stubstad (*15*),
β_i	=	coefficients of Eq. (2.7), which are given in Table 1 for both the BELLS2 and BELLS3 equations.

In TxDOT Project 0-1863, (*16*) TTI researchers developed an alternative equation, named the Texas-LTPP equation, which is considered more applicable for use in Texas. This equation is given by :

$$T_d = \beta_o + \beta_1 (IR+2)^{1.5} + \log_{10}(d) \times \{\beta_2 (IR+2)^{1.5} + \beta_3 \sin^2(hr_{18} -15.5) + \beta_4 \sin^2(hr_{18} - 13.5) + \beta_5 [T_{(1\text{-day})} + 6]^{1.5}\} + \beta_6 \sin^2(hr_{18} -15.5) \sin^2(hr_{18} -13.5) \qquad (2.8)$$

The coefficients, β_i, of Eq. (2.8) were determined using multiple linear regression with measured IR and pavement temperature data from the asphalt concrete SMP sites in Texas, New Mexico, and Oklahoma, and from asphalt sections located at the Texas A&M Riverside Campus. Table 2 presents the coefficients of the Texas –LTPP equation. The interested reader is referred to Fernando, Liu and Ryu (*16*) for additional details on the development of this equation. Comparing the predictions of the BELLS2, calibrated BELLS2, and the Texas-LTPP equations, these researchers found that the most accurate predictions for Texas conditions are obtained using the Texas-LTPP equation.

Project 0-1863 led to the development of the TxDOT Modulus Temperature Correction Program (MTCP), which may be used to correct asphalt concrete moduli backcalculated from FWD data to reference or standard conditions of temperature and loading frequency (*17*). MTCP provides users with the option of using BELLS2, BELLS3, or the Texas-LTPP equation for predicting pavement temperature. The program uses the output from MODULUS as an input to the modulus temperature correction.

TABLE 1   Coefficients of the BELLS2 and BELLS3 Equations.

Coefficient	BELLS 2	BELLS 3
β_0	+ 2.78	+0.950
β_1	+ 0.912	+0.892
β_2	-0.428	-0.448
β_3	+0.553	+0.621
β_4	+2.63	+1.83
β_5	+0.027	+0.042

TABLE 2   Coefficients of the Alternative Model for Predicting Pavement Temperature.

Coefficient	Estimate	t-statistic for testing the null Hypothesis that $\beta_i = 0$	p-value
β_0	6.46	21.1	0.0000
β_1	0.199	60.79	0.0000
β_2	-0.083	-43.08	0.0000
β_3	-0.692	-3.46	0.0000
β_4	1.875	7.5	0.0000
β_5	0.059	50.11	0.0000
β_6	-6.784	-11.5	0.0000

CHAPTER III

FIELD DATA COLLECTION

The field data collection on SH4/48 involved the following tasks:

- An initial site investigation,
- Establishing FWD monitoring sections,
- Material sampling.

This chapter documents the tasks carried out to collect data for characterizing the effects of overweight truck traffic on SH4/48 in Brownsville.

INITIAL SITE OF INVESTIGATION

The main objective of the initial site investigation was to collect information that may be used to establish test segments for field monitoring. For this purpose, the following tasks were conducted:

- Ground penetrating radar measurements along SH4/48;
- Identification of homogeneous segments from GPR surveys according to the predicted layer thickness profiles;
- Selection of FWD stations on each homogeneous segment;
- Prediction of layer thicknesses of the asphalt and flexible base materials; and
- Core sampling to verify GPR predictions, assist in data interpretation, and provide cores for laboratory testing.

It began with inputting a name for of different lanes of the route in both directions. The route lanes that run from Mexico to the Port of Brownsville, northbound, were called K1 and K2, which were the outside and inside lanes, respectively. In the same way the route lanes which run from the Port of Brownsville to Mexico, southbound, were named K6, the outside lane and K7, the inside lane.

Two GPR surveys were conducted to estimate the pavement layer thickness profiles along SH4/48 as first tasks. The first survey, conducted in September 2000, was done using TxDOT's air-launched GPR system. From the data collected was predicted

the surface layer thickness variations along SH4/48. However, information on the layering beneath the surface material was difficult to get, as the reflections coming after the surface layer were either not visible or very faint. Consequently, it was conducted another survey in February 2001, using ground-coupled radar antennas manufactured by Geophysical Survey Systems Incorporated (GSSI). This second survey was conducted along the outside and inside southbound lanes of SH4/48 corresponding, respectively, to the K6 and K7 lanes of the permitted truck route. Since most of the permitted trucks (about 95 percent) travel from the Port of Brownsville to Mexico, the decision was made to monitor these lanes during the project.

Two ground-coupled radar antennas were used. One was a GSSI 200 MHz unit that was primarily used to check the depth of the water table along the route. The other was a 1.5 GHz antenna that it was used to collect data on the near-surface pavement layers. Figure 3 shows the ground-coupled antennas used by researchers. Data from the 1.5 GHz antenna, along with coring information taken at various locations, were used to establish the base layer thickness profiles along the K6 and K7 lanes. It was not possible to see the ground water table from the GPR data collected with the 200 MHz antenna. Researchers note that Pharr District personnel drilled a hole on the shoulder near the location of a weigh-in-motion (WIM) site along SH48. No water table was encountered to a depth of 13 ft from the pavement surface at this location.

ESTABLISHING FWD MONITORING STATIONS

Based on the GPR measurements, it was established FWD stations along the K6 and K7 lanes of the permitted truck route. The portion of the route monitored in this study begins at the FM511 and SH48 intersection and ends approximately 0.14 miles south of Cleveland Street along SH4. The K6 lane was segmented into 16 homogeneous sections (A to P), while the K7 lane was divided into 6 homogeneous sections (A to F). Tables 3 and 4 summarize the locations of the different sections established, respectively, on the K6 and K7 lanes. The locations of the section endpoints are referred to the south end of the bridge over FM511.

FIGURE 3   Ground-Coupled GSSI Antennas Used on the Second GPR Survey.

TABLE 3   Locations of the K6 Lane Sections.*

Section	From		To	
	(miles)	(feet)	(miles)	(feet)
K6-A	0	1254	0	1610
K6-B	0	1610	0	1809
K6-C	0	1809	0	1954
K6-D	0	1954	1	1484
K6-E	1	1484	1	2874
K6-F	1	2874	2	1894
K6-G	2	1894	2	2639
K6-H	2	2639	3	3269
K6-I	3	3269	3	3544
K6-J	3	3544	3	3879
K6-K	3	4794	4	49
K6-L	4	49	4	3269
K6-M	4	3269	4	3514
K6-N	4	3514	4	3914
K6-O	4	3914	5	1189
K6-P	5	1189	5	1404

* Referred from south end of bridge over FM511

TABLE 4   Locations of the K7 Lane Sections.*

Section	From		To	
	(miles)	(feet)	(miles)	(feet)
K7-A	0	505	3	3159
K7-B	3	4064	3	4504
K7-C	3	4504	3	5174
K7-D	3	5174	4	399
K7-E	4	399	4	3199
K7-F	4	3199	5	669

* Referred from south end of bridge over FM511

Once the homogeneous sections in each lane were defined, researchers established the locations of the FWD stations in each section. Altogether, there were 56 FWD stations established on the K6 lane, and 50 stations on the K7 lane. Tables 5 and 6 show the locations of the FWD stations on which data were collected at different times during the project. In this regard, personnel from the Pharr District provided FWD data for evaluating and monitoring pavement performance along the K6 and K7 lanes.

TABLE 5 Locations of the FWD Stations in the K6 Lane.

Section	FWD Station	Distance of Station from FM 511 Bridge (miles)
K6-A	6-1	0.267
K6-B	6-2	0.314
K6-D	6-3	0.379
K6-D	6-4	0.466
K6-D	6-5	0.560
K6-D	6-6	0.655
K6-D	6-7	0.750
K6-D	6-8	0.845
K6-D	6-9	1.009
K6-D	6-10	1.091
K6-D	6-11	1.166
K6-D	6-12	1.261
K6-E	6-13	1.356
K6-E	6-14	1.451
K6-F	6-15	1.545
K6-F	6-16	1.668
K6-F	6-17	1.739
K6-F	6-18	1.829
K6-F	6-19	1.924
K6-F	6-20	2.019
K6-F	6-21	2.113
K6-F	6-22	2.208
K6-F	6-23	2.303
K6-G	6-24	2.398
K6-G	6-25	2.435
K6-G	6-26	2.492
K6-H	6-27	2.530
K6-H	6-28	2.606
K6-H	6-29	2.701
K6-H	6-30	2.805
K6-H	6-31	2.890
K6-H	6-32	2.985
K6-H	6-33	3.079
K6-H	6-34	3.193
K6-H	6-35	3.288

TABLE 5 Continued

Section	FWD Station	Distance of Station from FM 511 Bridge (miles)
K6-H	6-36	3.382
K6-H	6-37	3.477
K6-H	6-38	3.572
K6-I	6-39	3.657
K6-J	6-40	3.685
K6-K	6-41	3.951
K6-K	6-42	3.988
K6-L	6-43	4.083
K6-L	6-44	4.178
K6-L	6-45	4.273
K6-L	6-46	4.339
K6-L	6-47	4.416
K6-L	6-48	4.547
K6-L	6-49	4.613
K6-M	6-50	4.642
K6-O	6-51	4.796
K6-O	6-52	4.838
K6-O	6-53	4.932
K6-O	6-54	5.033
K6-O	6-55	5.163
K6-P	6-56	5.238

TABLE 6   Locations of the FWD Stations in the K7 Lane.

Section	FWD Station	Distance of Station from FM 511 Bridge (miles)
K7-A	7-1	0.288
K7-A	7-2	0.382
K7-A	7-3	0.430
K7-A	7-4	0.523
K7-A	7-5	0.618
K7-A	7-6	0.713
K7-A	7-7	0.808
K7-A	7-8	0.902
K7-A	7-9	0.997
K7-A	7-10	1.092
K7-A	7-11	1.177
K7-A	7-12	1.272
K7-A	7-13	1.366
K7-A	7-14	1.461
K7-A	7-15	1.613
K7-A	7-16	1.707
K7-A	7-17	1.802
K7-A	7-18	1.897
K7-A	7-19	1.991
K7-A	7-20	2.086
K7-A	7-21	2.181
K7-A	7-22	2.389
K7-A	7-23	2.470
K7-A	7-24	2.559
K7-A	7-25	2.654
K7-A	7-26	2.749
K7-A	7-27	2.844
K7-A	7-28	2.938
K7-A	7-29	3.033
K7-A	7-30	3.128
K7-A	7-31	3.222
K7-A	7-32	3.317
K7-A	7-33	3.412
K7-A	7-34	3.506
K7-A	7-35	3.601
K7-A	7-36	3.686
K7-B	7-37	3.961
K7-C	7-38	4.088
K7-D	7-39	4.160
K7-E	7-40	4.255
K7-E	7-41	4.349
K7-E	7-42	4.444
K7-E	7-43	4.539
K7-E	7-44	4.595
K7-E	7-45	4.650
K7-E	7-46	4.747
K7-F	7-47	4.842
K7-F	7-48	4.927
K7-F	7-49	5.022
K7-F	7-50	5.145

According to the initial GPR survey in Appendix A was detected variations on the asphalt concrete (AC) thickness and the posibility of the stripping layers. The extreme cases of AC thickness variation are seen in the sections K6-H, K6-I, K6-K, K7-C and K7-E. Possible stripping layers are seen in the sections K6-L and at some points in sections K7-E. Consequent to these possible issues, each section of the lanes K6 and K7 were divided into homogeneous sub-segments. The FWD stations were chosen from these sub-segments.

In COLORMAP Figures 4 to 23 the location of all FWD stations for lanes both K6 and K7 are indicated. Each trace marker indicates the respective FWD station.

The average distance between two consecutive stations is approximately 152 m (500 feet). These stations were selected on the asphalt pavement, skipping the FM 511 (bridge), and the intersecion FM 802 and Central Ave and the intersection between Boca Chica Blvd. with SH 48.

To locate the FWD stations, the distance measured between them were referred to the center of the street intersections or culverts. The streets used as references were the FM 511-bridge, FM 802, Minnessota Ave, Central Ave, Fruitdale Rd, Price Rd, Intersection SH4/SH48, Security Dr., Southmost Rd and Cleveland St

In this study, FWD data were monitored from February of 2001 to April of 2003 through intervals between four and seven months. In 2001, FWD data were collected in February, May, July and August; in 2002 in March, July, October and December, and in 2003, data was collected only in April. FWD data was taken in K6 lane four times in 2001: in February, May, July and August; and three times in 2002: in March, July and December. FWD data were collected in K7 lane three times in 2001: in February, May and August; four times in 2002: in March, July, October and December; and once in April of 2003.

In addition, the FWD stations K6-9, K7-8 and K7-9 were removed and no longer used after March of 2002 due to construction work on the road. There were other FWD stations which were omitted once in the FWD data collection because of road

maintenance or construction work. They were K6-8 in March of 2002, K6-33 in July of 2002, K7-11, K7-12 and K7-22 in October of 2002 and K7-43 in April of 2003.
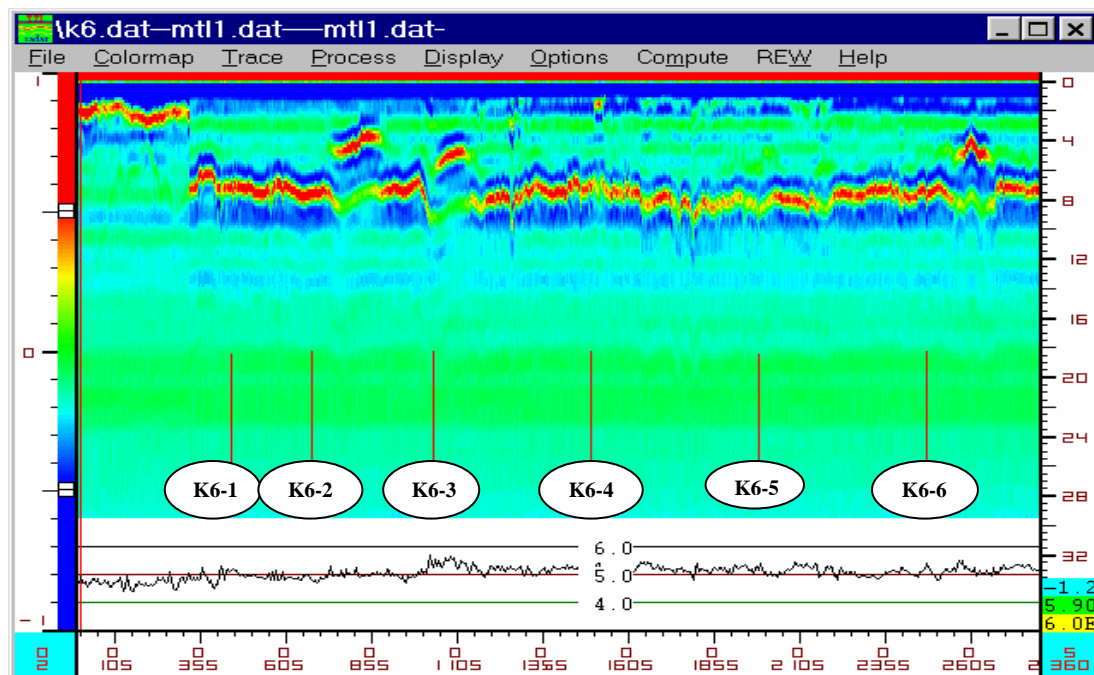
FIGURE 4   K6-1, K6-2, K6-3, K6-4, K6- 5, and K6-6 FWD Stations.
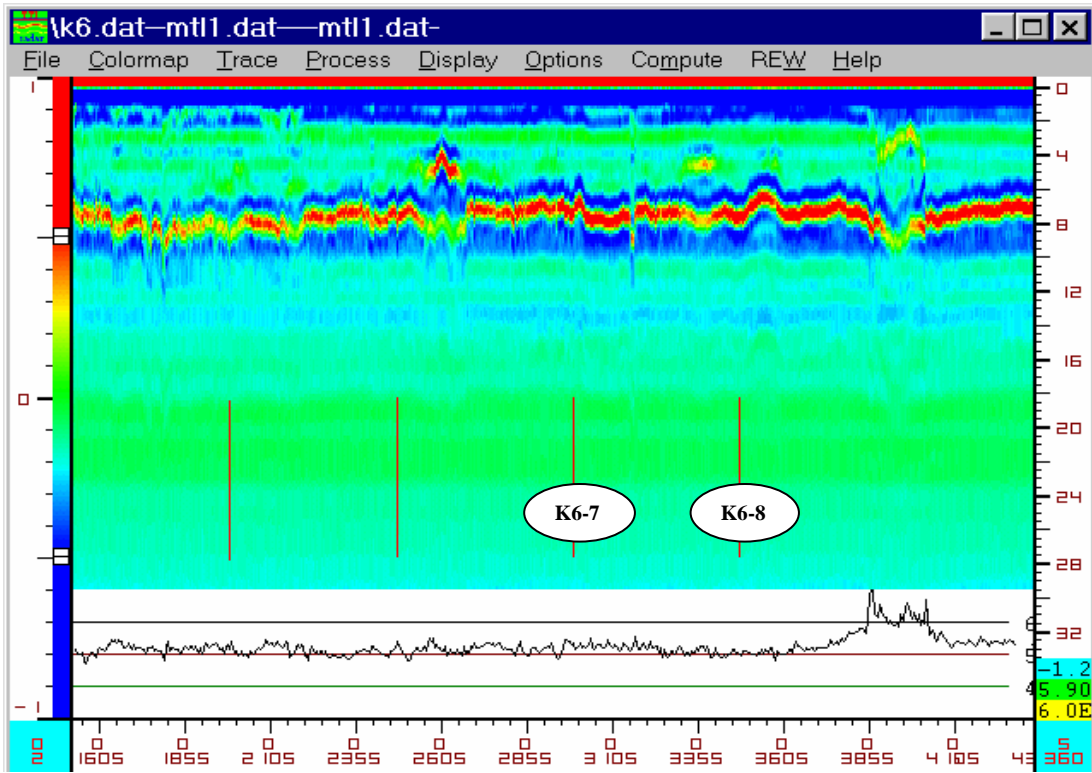
FIGURE 5   K6-7 and K6-8 FWD Stations.
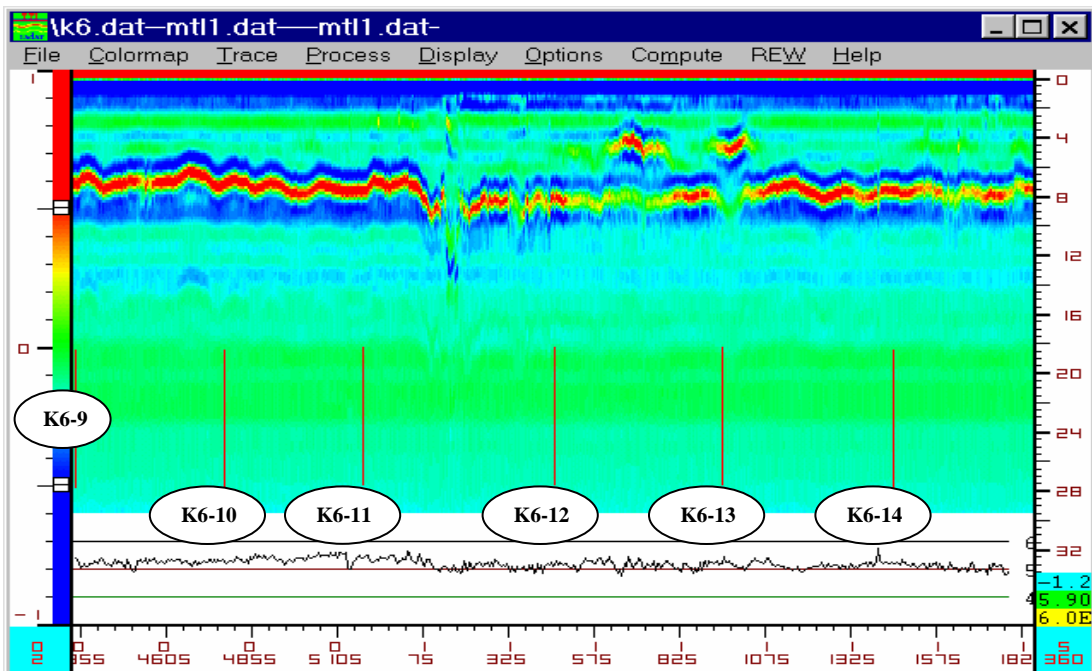
FIGURE 6   K6-9, K6-10, K6-11, K6-12, K6-13, and K6-14 FWD Stations.
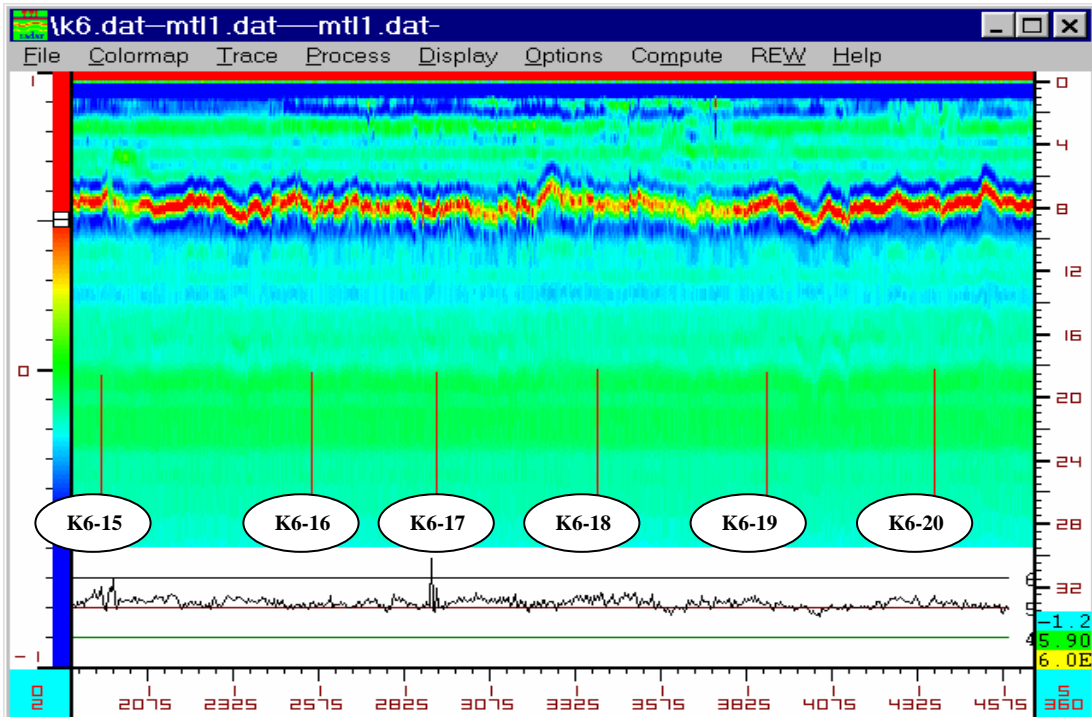
FIGURE 7   K6-15, K6-16, K6-17, K6-18, K6-19, and K6-20 FWD Stations.
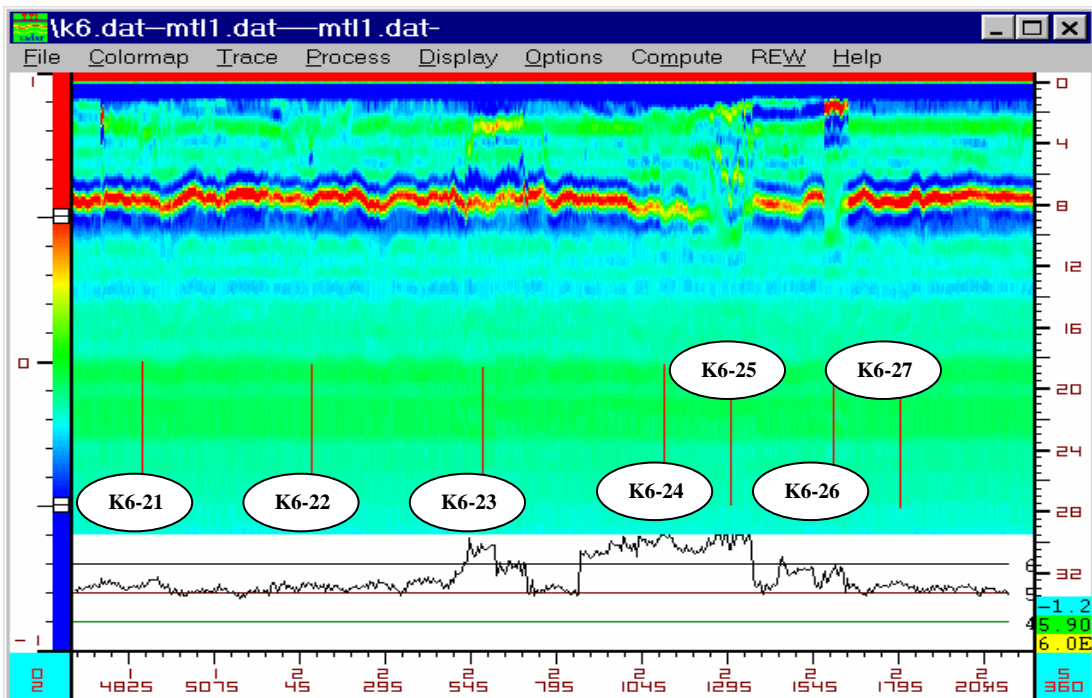
FIGURE 8   K6-21, K6-22, K6-23, K6-24, K6-25, K6-26, and K6-27 FWD Stations.
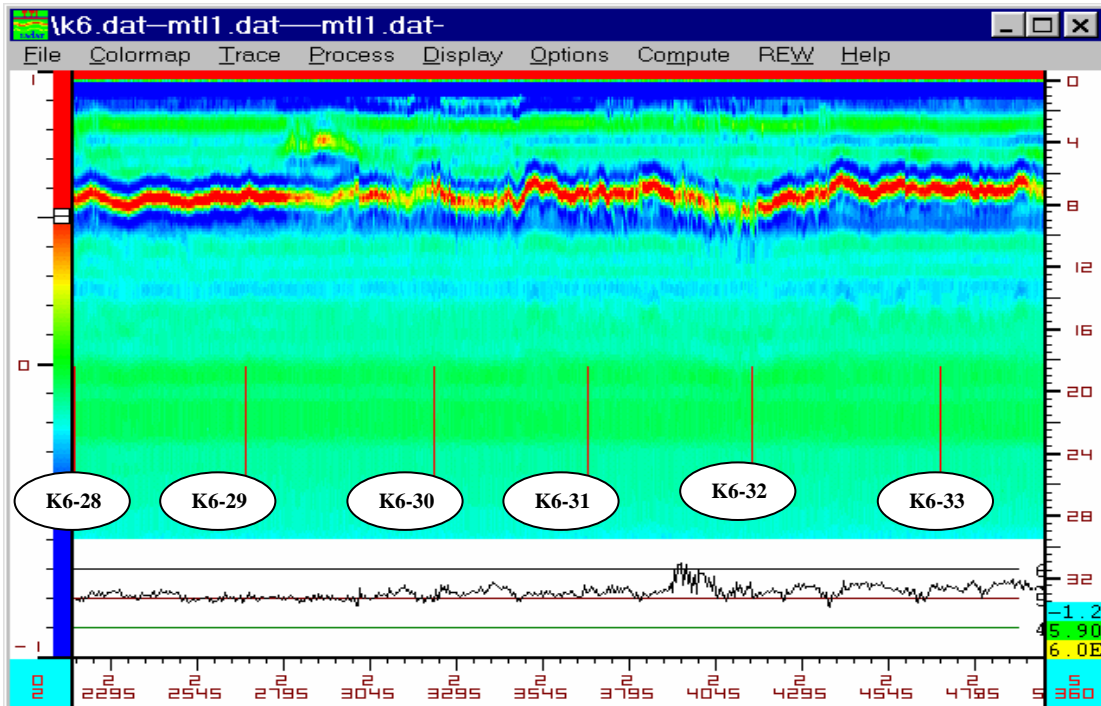
FIGURE 9   K6-28, K6-29, K6-30, K6-31, K6-32, and K6-33 FWD Stations.
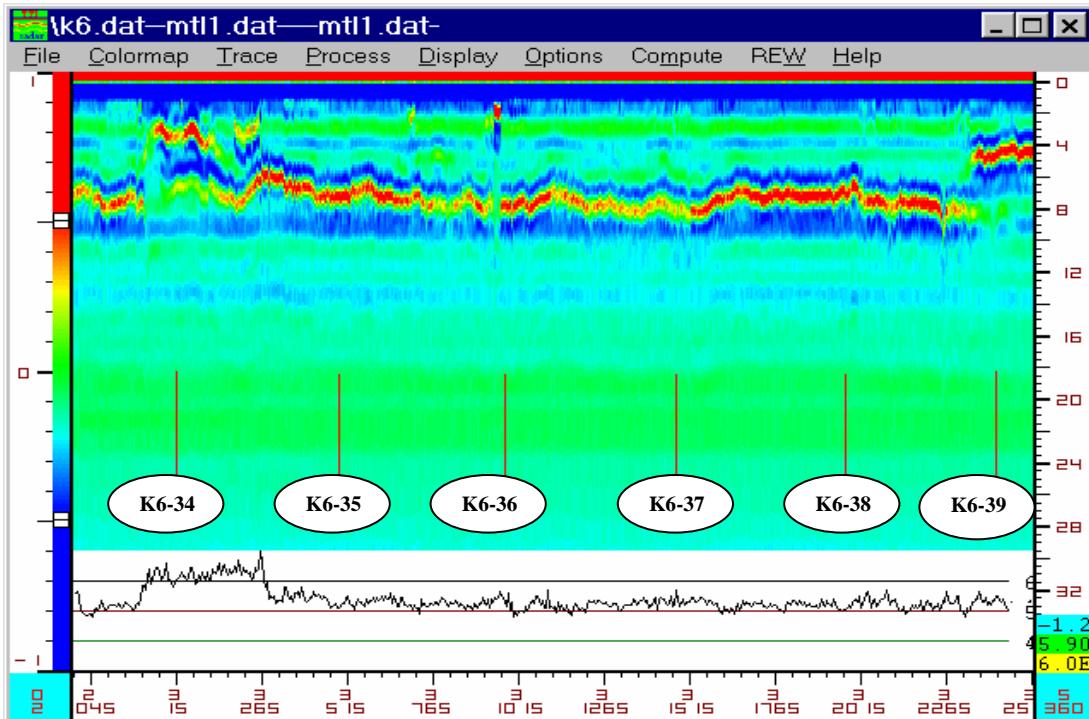
FIGURE 10   K6-34, K6-35, K6-36, K6-37, K6-38, and K6-39 FWD Stations.
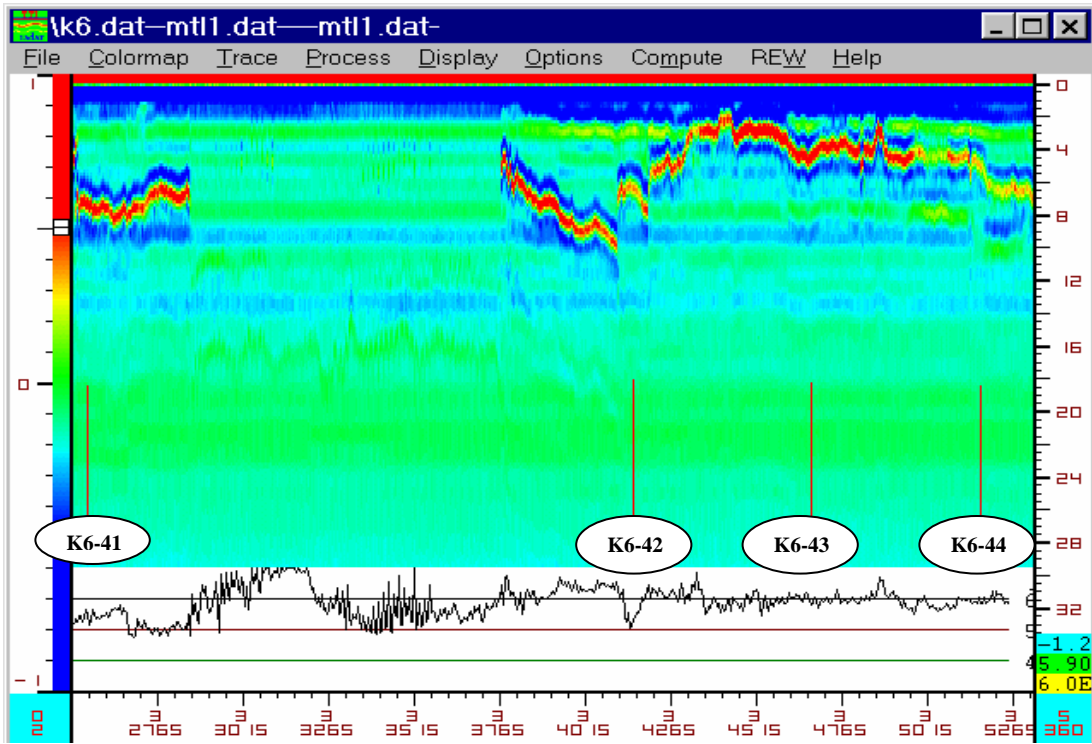
FIGURE 11   K6-41, K6-42, K6-43, and K6-44 FWD Stations.
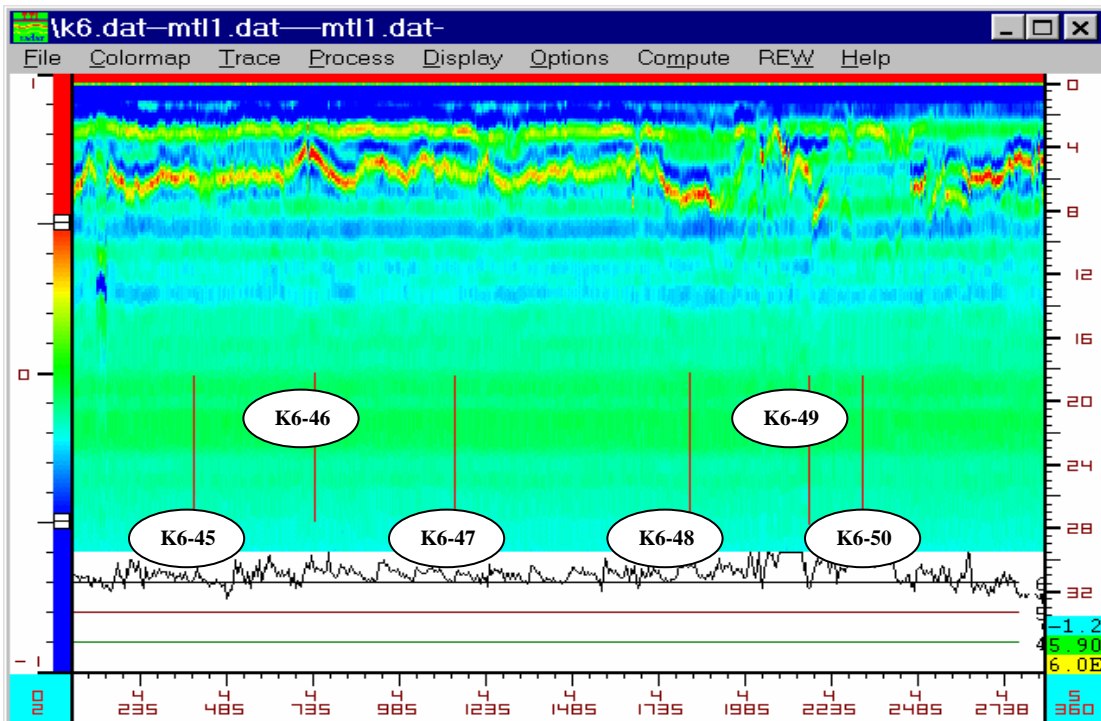
FIGURE 12   K6-45, K6-46, K6-47, K6-48, K6-49, and K6-50 FWD Stations.
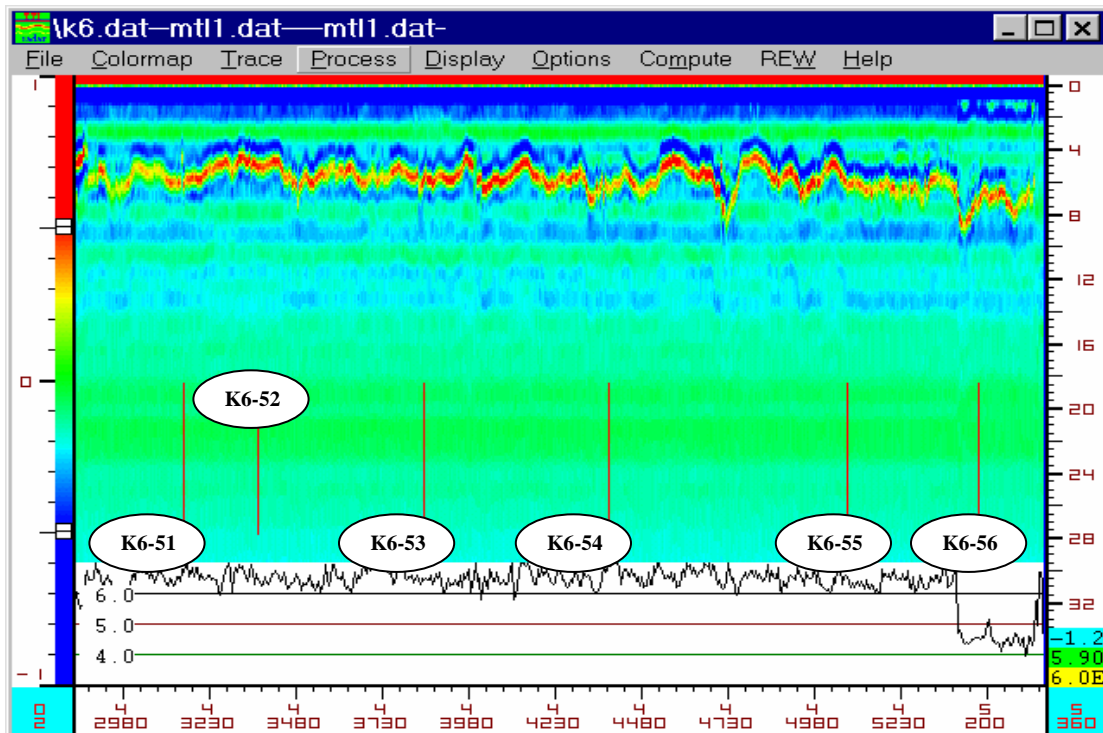
FIGURE 13   K6-51, K6-52, K6-53, K6-54, K6-55, and K6-56 FWD Stations.
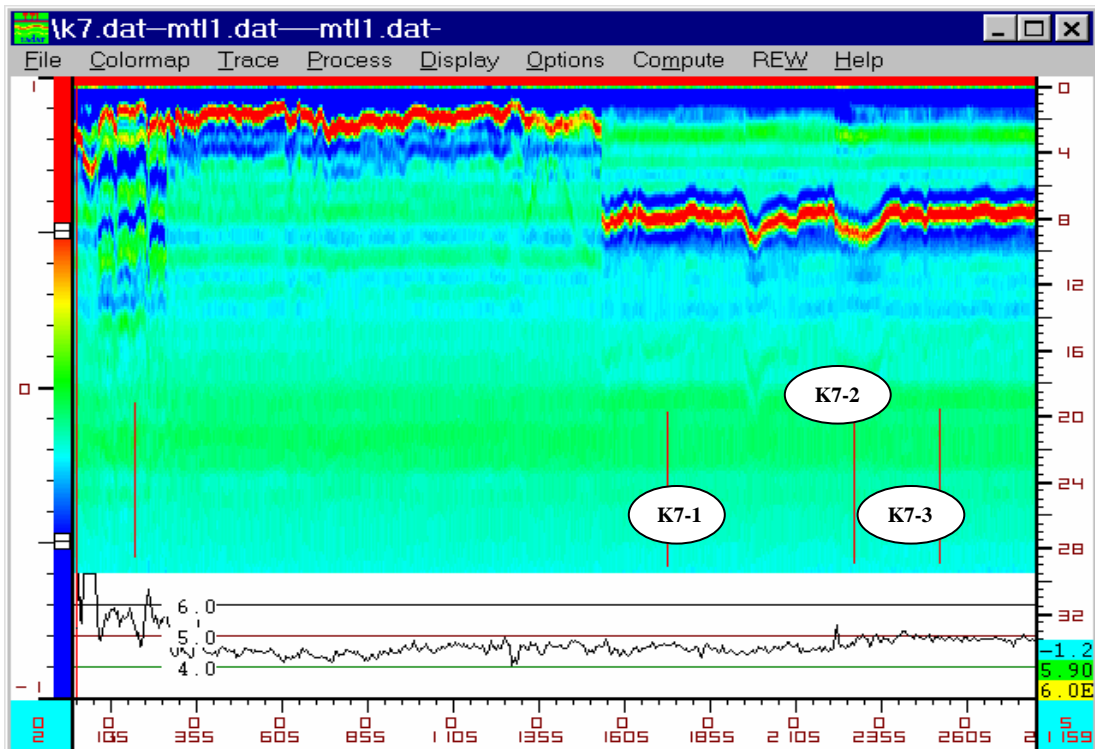
FIGURE 14   K7-1, K7-2, and K7-3 FWD Stations.
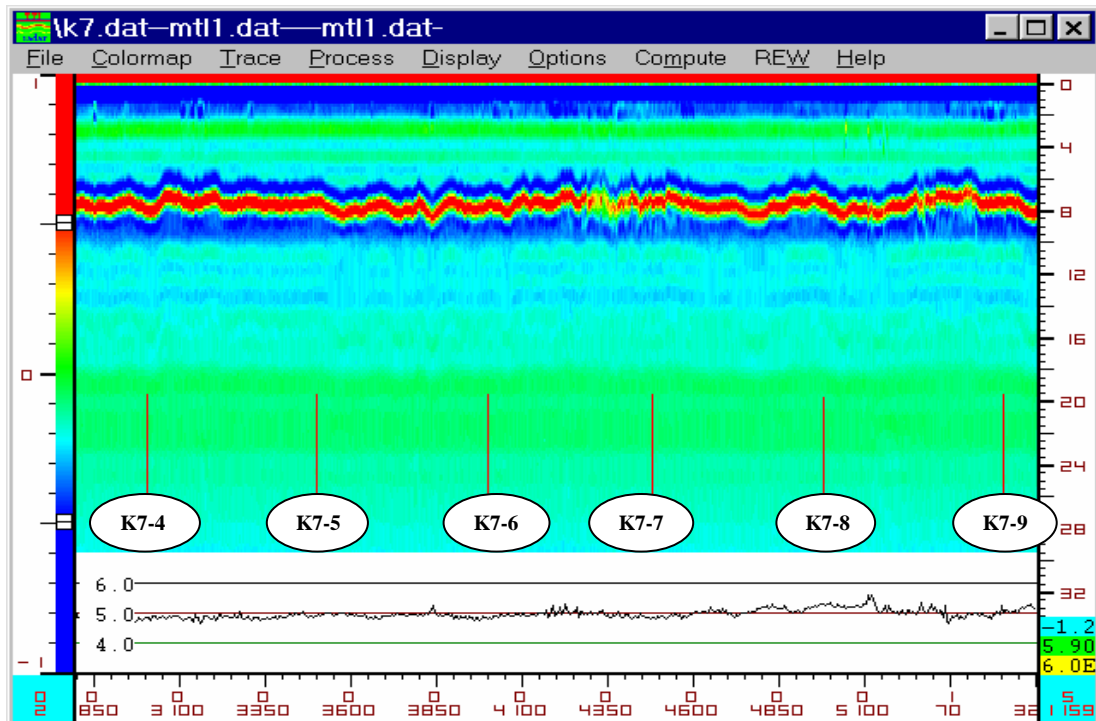
FIGURE 15   K7-4, K7-5, K7-6, K7-7, K7-8, and K7-9 FWD Stations.
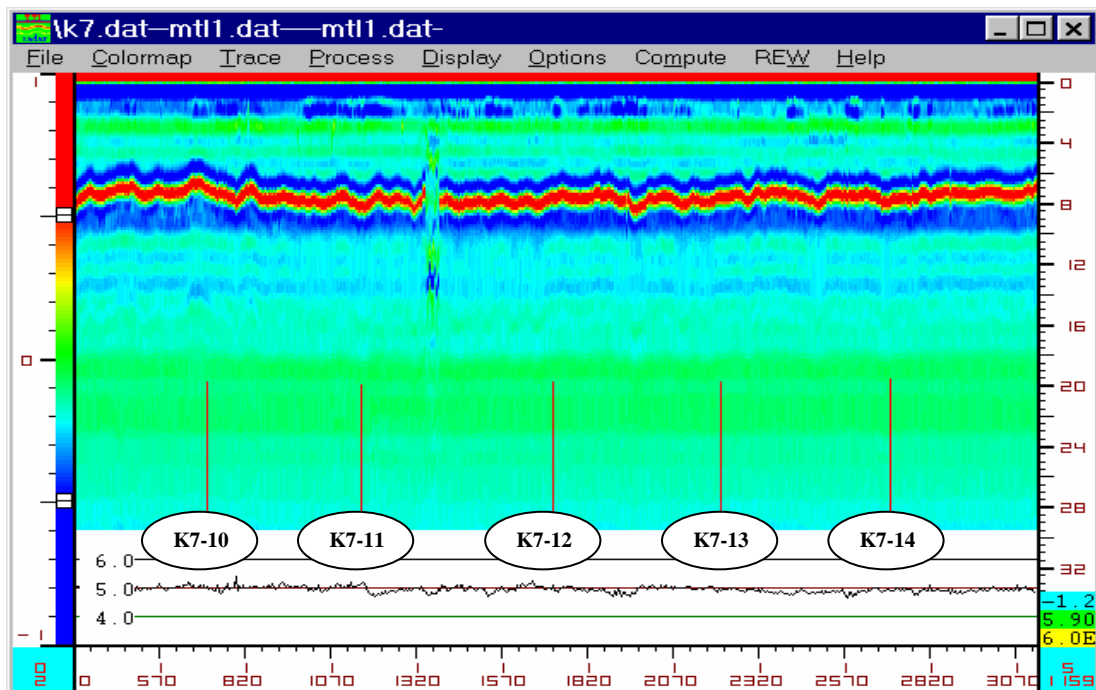
FIGURE 16   K7-10, K7-11, K7-12, K7-13, and K7-14 FWD Stations.
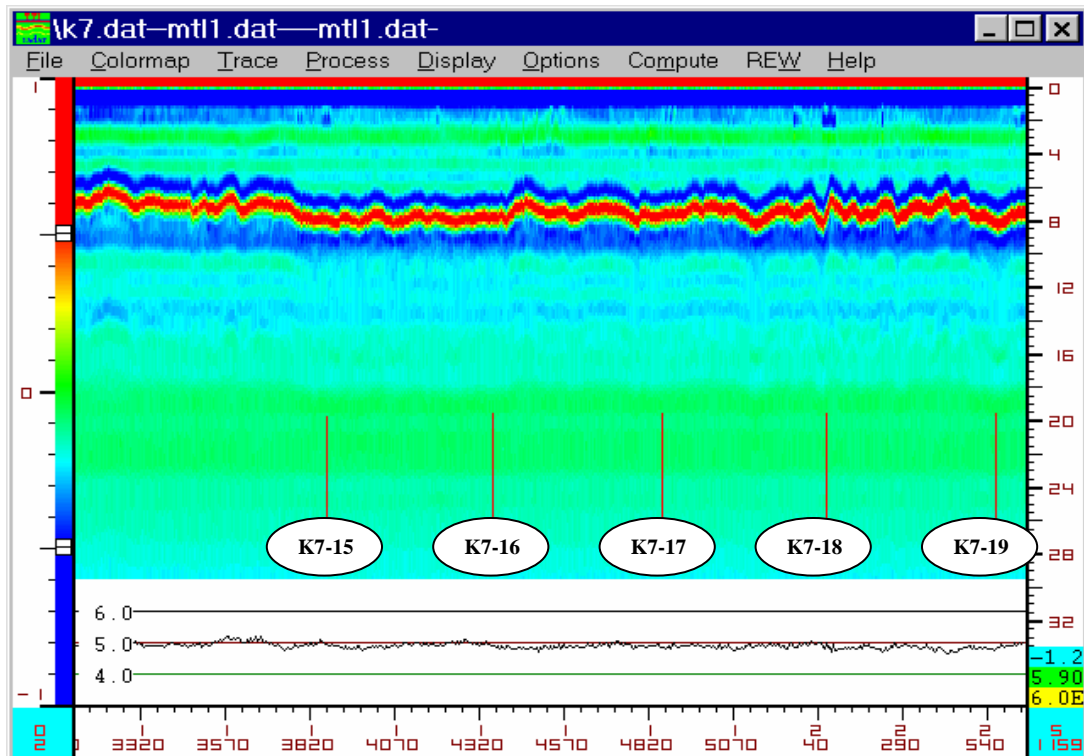
FIGURE 17   K7-15, K7-16, K7-17, K7-18, and K7-19 FWD Stations.
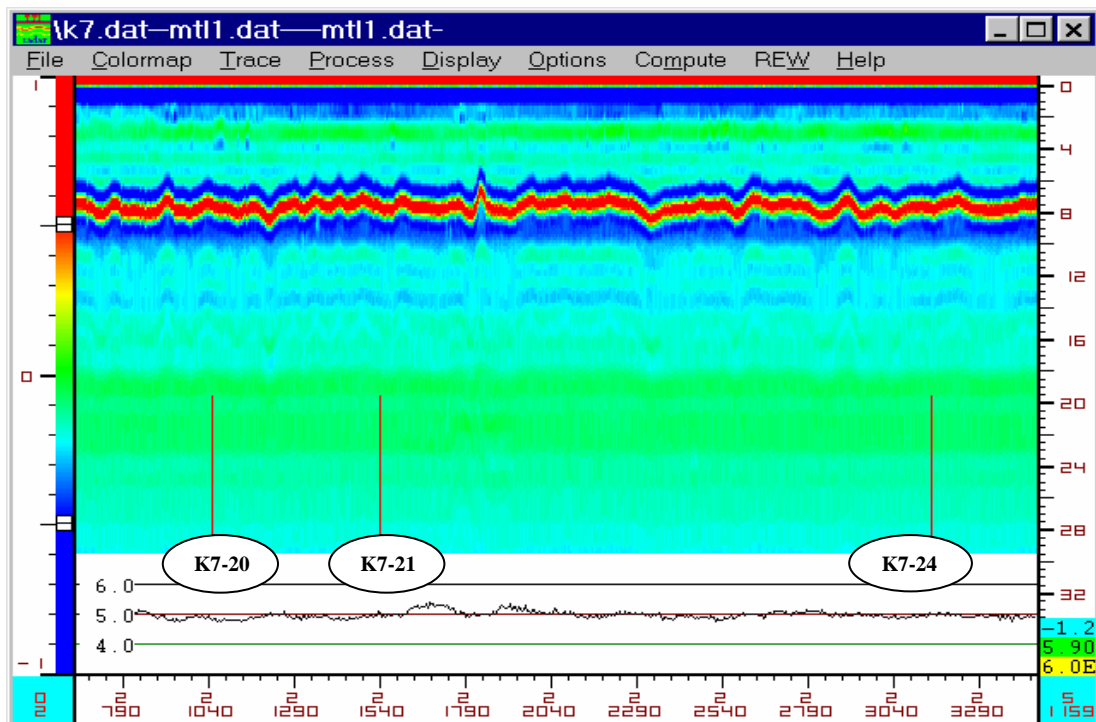
FIGURE 18   K7-20, K7-21, and K7-24 FWD Stations.
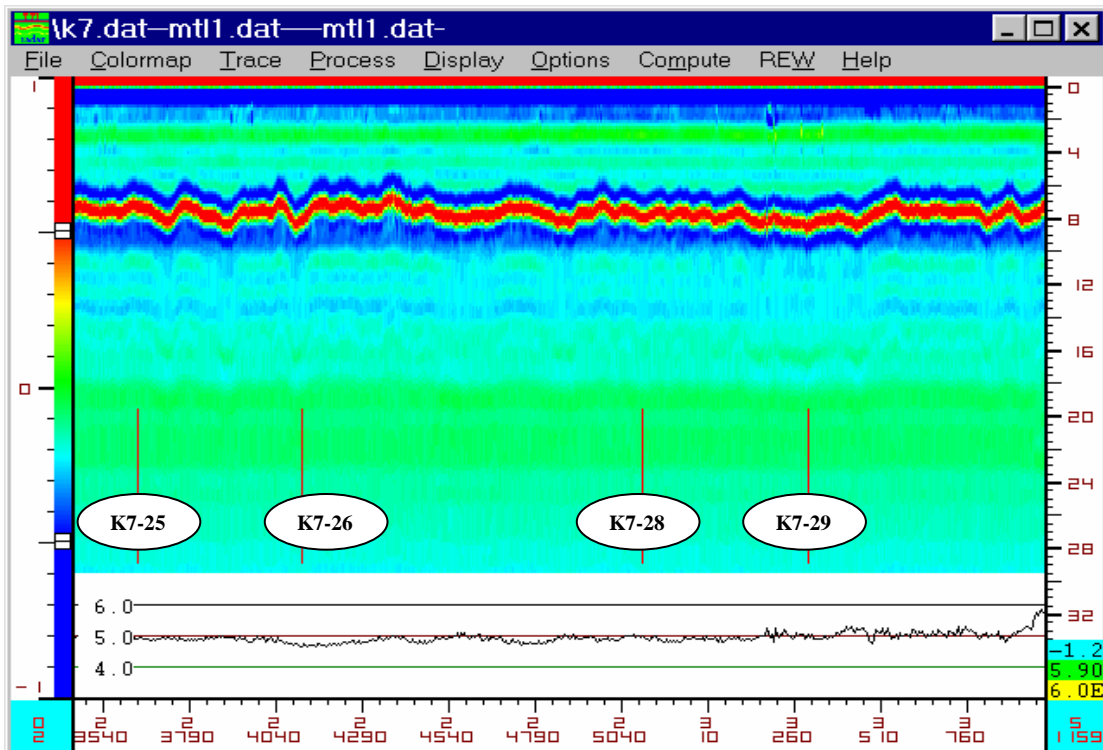
FIGURE 19   K7-25, K7-26, K7-28, and K7-29 FWD Stations.
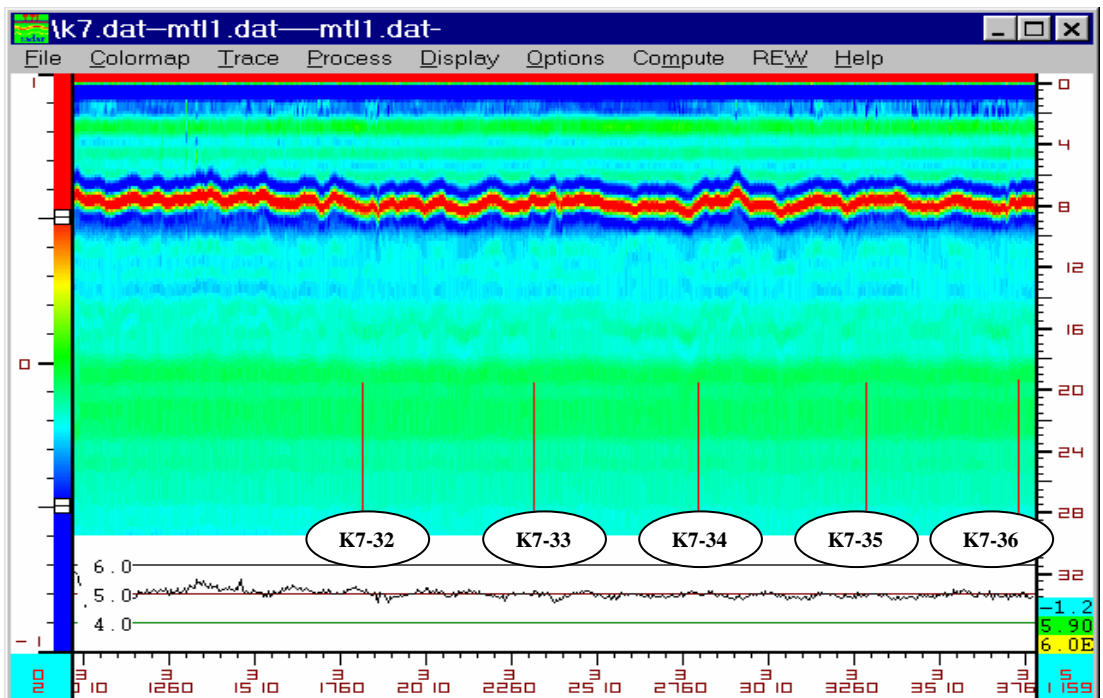
FIGURE 20   K7-32, K7-33, K7-34, K7-35, and K7-36 FWD Stations.
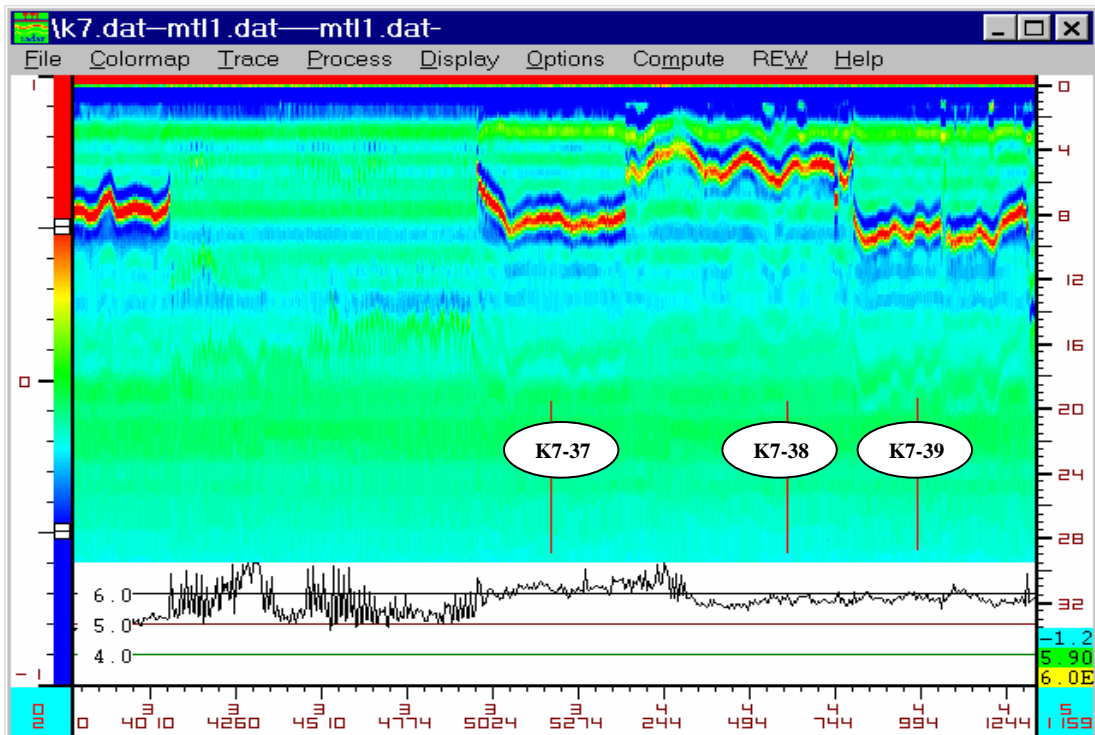
FIGURE 21   K7-37, K7-38, and K7-39 FWD Stations.
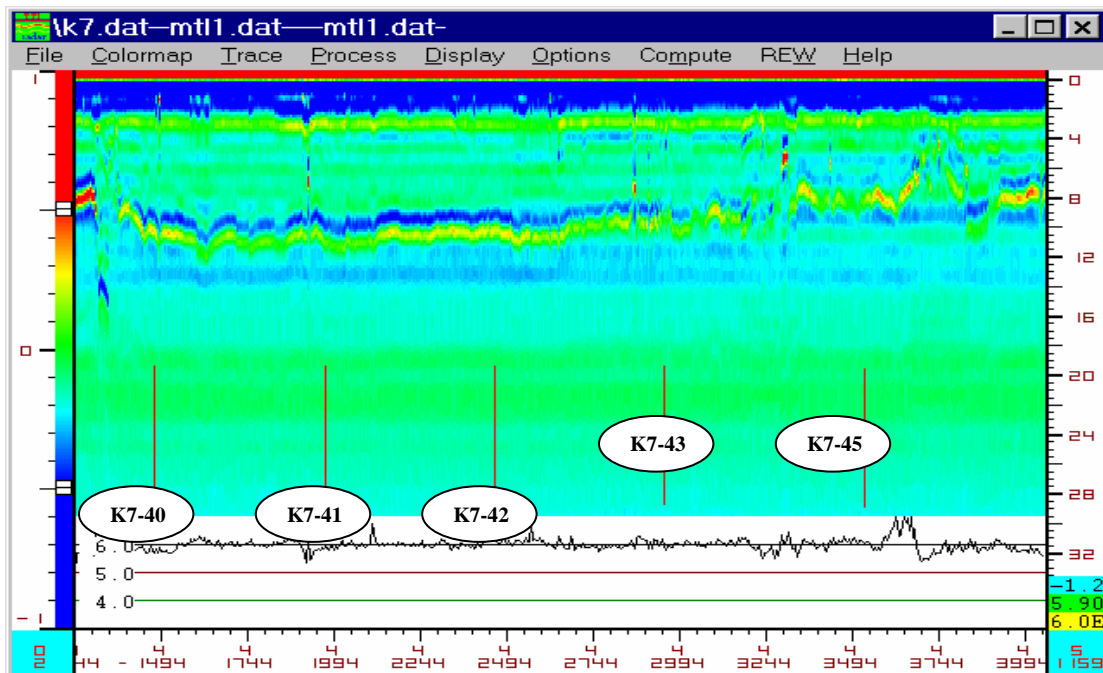
FIGURE 22   K7-40, K7-41, K7-43, and K7-45 FWD Stations.
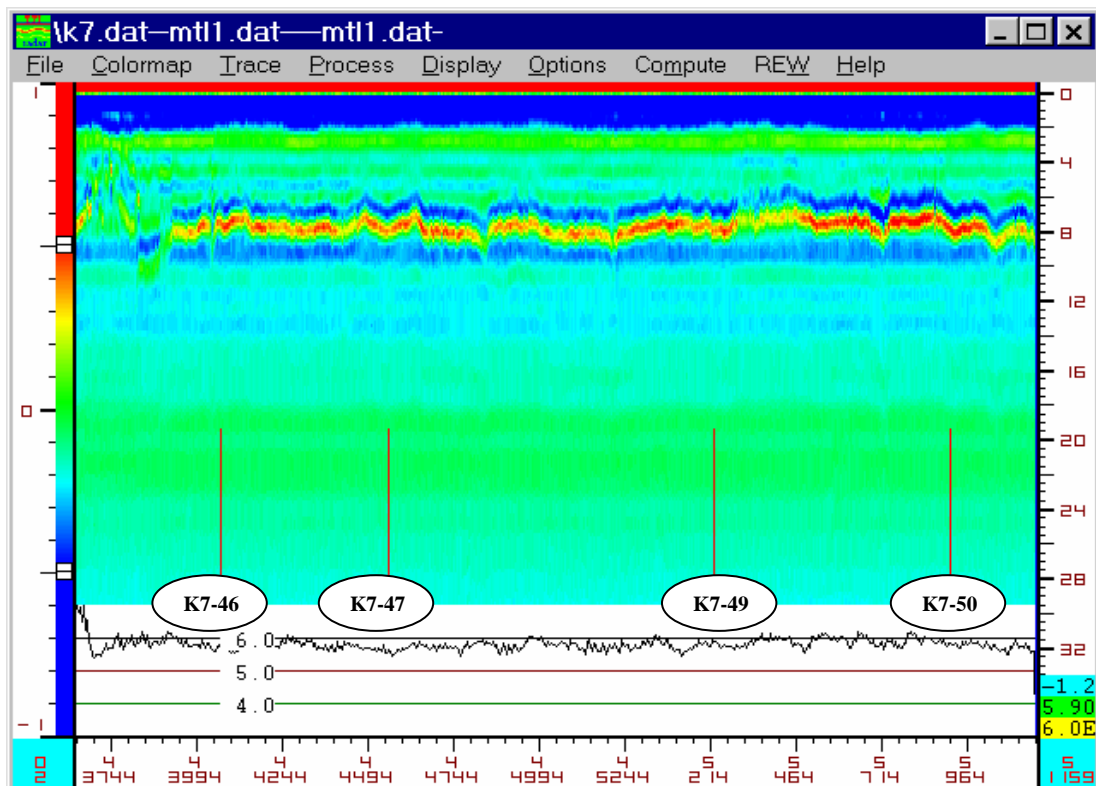
FIGURE 23   K7-46, K7-47, K7-49, and K7-50 FWD Stations.

MATERIAL SAMPLING

For GPR data interpretation and verification, a total of 20 cores were initially taken from SH4/48, 10 samples in each of the K6 and K7 lanes. Tables 7 and 8 show the locations were cores were taken. At these locations, the coring crew also measured the base thickness. The measured base thicknesses at the coring locations are also given in Tables 7 and 8.

During coring, a number of the six-inch diameter cores broke. These occurred in the downtown area along SH4, where difficulty was encountered in getting intact cores. Disintegration of the asphalt material during coring suggested possible stripping within the mix. In order to get additional cores for laboratory testing, Pharr District personnel took several more cores from the K6 lane along SH4, specifically at FWD stations K6-48,

K6-50, K6-51, and K6-53. This time, three-inch diameter cores were taken. Table 9 shows the thicknesses of the additional cores.

In addition, a set of five cores were taken at the WIM site along SH48. These are identified as C2 to C6 in Table 9. C2 and C3 were taken from the wheelpaths of the K6 lane, while C4 and C5 were taken from the K7 lane. C6 was taken from the center lane along SH48, which receives very little traffic at the vicinity of the WIM site.

TABLE 7   Thickness Measurements at Initial Coring Locations in the K6 Lane.

				Thickness			
N°	ID	Diameter		AC		Base	
		mm	in	mm	in	mm	in
1	K6-1	144	5.7	202	8.0	305	12
2	K6-4	142	5.6	182	7.2	279	11
3	K6-11	142	5.6	204	8.0	305	12
4	K6-23	142	5.6	192	7.6	330	13
5	K6-29	144	5.7	217	8.5	305	12
6	K6-35	145	5.7	197	7.8	305	12
7	K6-42	142	5.6	159	6.3	330	13
8	K6-45	142	5.6	216	8.5	203	8
9	K6-50	142	5.6	263	10.4	152	6
10	K6-53	144	5.7	191	7.5	330	13

TABLE 8   Thickness Measurements at Initial Coring Locations in the K7 Lane.

Nº	ID	Diameter		Thickness			
				AC		Base	
		mm	in	mm	in	mm	in
1	K6-1	144	5.7	202	8.0	305	12
2	K6-4	142	5.6	182	7.2	279	11
3	K6-11	142	5.6	204	8.0	305	12
4	K6-23	142	5.6	192	7.6	330	13
5	K6-29	144	5.7	217	8.5	305	12
6	K6-35	145	5.7	197	7.8	305	12
7	K6-42	142	5.6	159	6.3	330	13
8	K6-45	142	5.6	216	8.5	203	8
9	K6-50	142	5.6	263	10.4	152	6
10	K6-53	144	5.7	191	7.5	330	13

TABLE 9   Measurements of Additional AC Cores Taken in the K6 Lane.

Nº	ID	Field measurements			
		Diameter		Thickness	
		mm	in	mm	in
1	K6-48-16	92	3.6	208	8.2
2	K6-48-12	92	3.6	164	6.4
3	K6-50-16	92	3.6	127	5.0
4	K6-50-12	92	3.6	157	6.2
5	K6-51	92	3.6	133	5.3
6	K6-53-10	92	3.6	140	5.5
7	C2	102	4.0	164	6.5
8	C3	102	4.0	202	8.0
9	C4	102	4.0	202	8.0
10	C5	102	4.0	205	8.1
11	C6	102	4.0	188	7.4

CHAPTER IV

STATIC ANALYSIS

ANALYSIS OF THE LAYER THICKNESS

As was explained in Chapter III, TTI conducted a two GPR survey with a Ground-Coupled Antenna (200 MHz) and another GPR survey with an Air-launched Antenna (1.5GHz) on the SH 4/48 in Brownsville, Texas. This study was conducted for both lanes K6 and K7, covering 106 FWD stations.

The data processing, positioning and interpretations of these measurements were done by Roadscanner Oy which analyzed the data using Road Doctor™ software. The processing methods were the static background removal, signal amplification and horizontal and vertical filtering. Roadscanner Oy reported the layer thickness of the AC and the flexible base course after verifing with the thickness of the cores. Because the FWD stations are located at approximately 150 m (500 feet) spacing and Roadscanner Oy made the analysis of layer thickness every foot the average layer thickness was calculated for each 100 feet. Tables 10 and 11 show the predicted thicknesses reported by Roadscanners Oy, the average thickness and standard deviation calculated by +/- 50 feet of FWD stations.

The thicknesses of the AC and the flexible base (FB) for both lanes were plotted and can be seen in Figures 24, 25, 26 for the K6 lane, and 27, 28 and 29 for the K7 lane. These charts show four significant points, upon which it is necessary to remark: first, the thickness calculated by Roadscanner Oy; second, the average thickness; third, the core thickness taken in the initial 20 FWD stations; and finally, the layer thickness at each FWD station. It should be noted that there are more variations of AC thickness in the K6 lane than in the K7 lane, as seen in Figures 25 and 27. In addition, in both lanes, the AC thicknesses increase and the FB thicknesses decrease in the downtown area, as seen in Figures 24 and 29.

TABLE 10   AC and FB Predicted Thickness in the K6 Lane.

FWD	Predicted Thickness (cm)		Mean thickness (cm)		Std. Dev. (cm)	
Section	AC	FB	AC	FB	AC	FB
K6_1	22.20	28.80	21.88	29.05	1.35	0.80
K6_2	22.20	27.40	21.88	29.05	1.35	0.80
K6_3	24.30	30.90	21.88	29.05	1.35	0.80
K6_4	17.10	30.10	18.33	29.24	1.16	0.80
K6_5	22.20	30.10	20.39	29.05	1.49	0.80
K6_6	21.20	28.90	20.39	29.05	1.49	0.80
K6_7	19.10	28.30	20.39	29.05	1.49	0.80
K6_8	22.00	30.10	20.39	29.05	1.49	0.80
K6_9	17.60	29.80	18.95	29.17	1.08	0.80
K6_10	19.10	28.30	18.95	29.17	1.08	0.80
K6_11	20.70	29.10	18.95	29.17	1.08	0.80
K6_12	22.80	28.40	20.74	29.31	1.41	1.69
K6_13	22.80	29.80	20.74	29.31	1.41	1.69
K6_14	20.20	28.80	20.74	29.31	1.41	1.69
K6_15	19.70	28.70	20.74	29.31	1.41	1.69
K6_16	22.00	29.40	20.74	29.31	1.41	1.69
K6_17	22.80	29.10	20.74	29.31	1.41	1.69
K6_18	19.70	29.10	20.74	29.31	1.41	1.69
K6_19	20.40	28.60	20.74	29.31	1.41	1.69
K6_20	20.70	29.20	20.74	29.31	1.41	1.69
K6_21	20.70	29.00	20.74	29.31	1.41	1.69
K6_22	20.70	30.80	20.74	29.31	1.41	1.69
K6_23	19.10	32.60	20.74	29.31	1.41	1.69
K6_24	23.30	29.30	20.74	29.31	1.41	1.69
K6_25	22.80	28.40	20.74	29.31	1.41	1.69
K6_26	22.80	28.70	20.74	29.31	1.41	1.69
K6_27	20.70	29.90	20.74	29.31	1.41	1.69
K6_28	20.20	29.30	20.74	29.31	1.41	1.69
K6_29	19.70	31.10	20.74	29.31	1.41	1.69
K6_30	16.60	30.40	18.49	29.68	1.68	1.69
K6_31	18.10	29.40	18.49	29.68	1.68	1.69
K6_32	22.80	28.00	18.49	29.68	1.68	1.69
K6_33	17.30	30.90	18.49	29.68	1.68	1.69
K6_34	16.80	30.90	18.49	29.68	1.68	1.69
K6_35	19.70	30.00	18.49	29.68	1.68	1.69
K6_36	19.70	29.30	18.49	29.68	1.68	1.69
K6_37	20.70	30.80	20.78	29.33	1.56	1.69
K6_38	17.10	29.90	17.84	30.03	0.58	1.69
K6_39	22.80	29.60	20.53	29.34	1.34	1.69
K6_40	21.20	27.80	20.53	29.34	1.34	1.69
K6_41	17.30	33.90	17.76	30.10	1.18	1.69
K6_42	18.60	31.70	17.76	30.10	1.18	1.69
K6_43	16.60	29.60	15.09	31.17	1.99	1.69
K6_44	22.80	29.60	21.10	30.55	2.24	1.69
K6_45	18.60	28.00	17.04	28.89	1.11	1.69
K6_46	15.50	30.00	17.04	28.89	1.11	1.69
K6_47	16.60	28.40	17.04	28.89	1.11	1.69
K6_48	23.50	23.10	24.32	21.92	1.62	1.69
K6_49	28.00	17.50	24.32	21.92	1.62	1.92
K6_50	24.40	20.40	24.32	21.92	1.62	1.92

TABLE 10   Continued

FWD	Final Thickness (cm)		Mean thickness (cm)		Std. Dev. (cm)	
Section	AC	FB	AC	FB	AC	FB
K6_51	16.60	29.60	17.71	27.19	1.48	2.05
K6_52	19.70	25.60	17.71	27.19	1.48	2.05
K6_53	19.10	33.30	19.68	30.77	1.32	2.03
K6_54	23.50	21.60	22.88	23.02	1.65	1.23
K6_55	23.30	21.50	22.88	23.02	1.65	1.23
K6_56	20.70	23.80	22.88	23.02	1.65	1.23
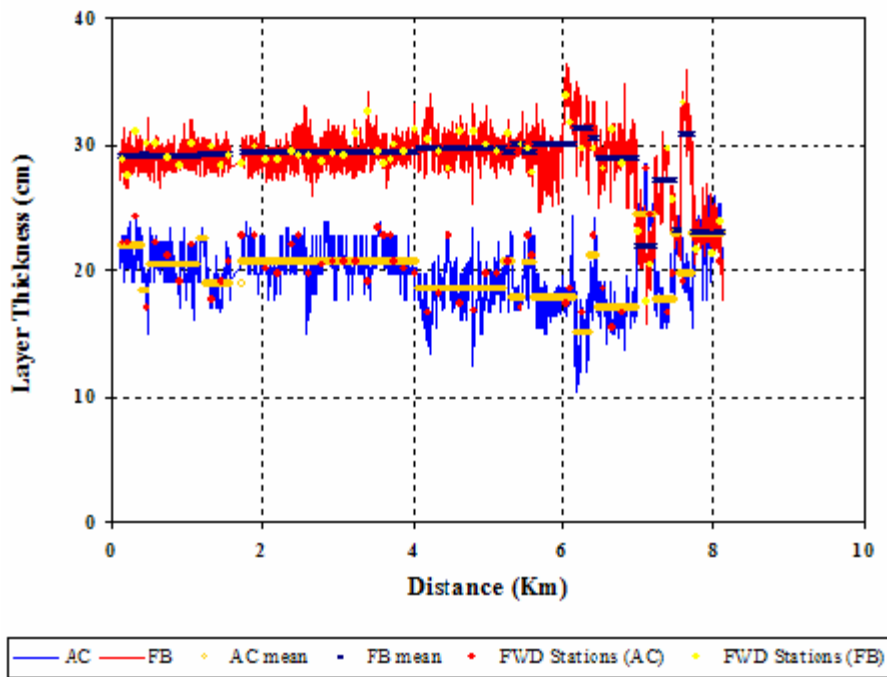
FIGURE 24   AC and FB Predicted Thickness in the K6 Lane.
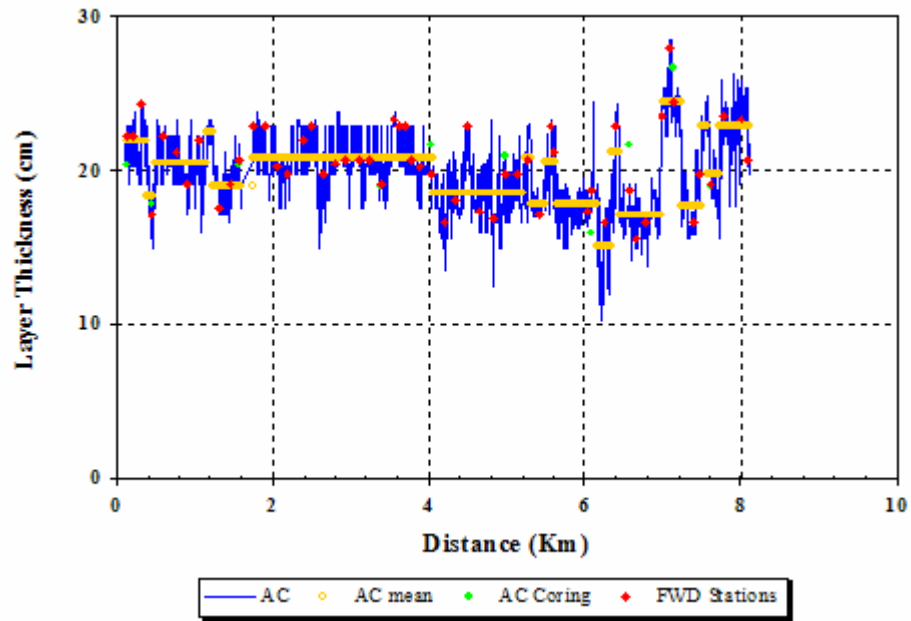
FIGURE 25   AC Predicted Thickness in the K6 Lane.
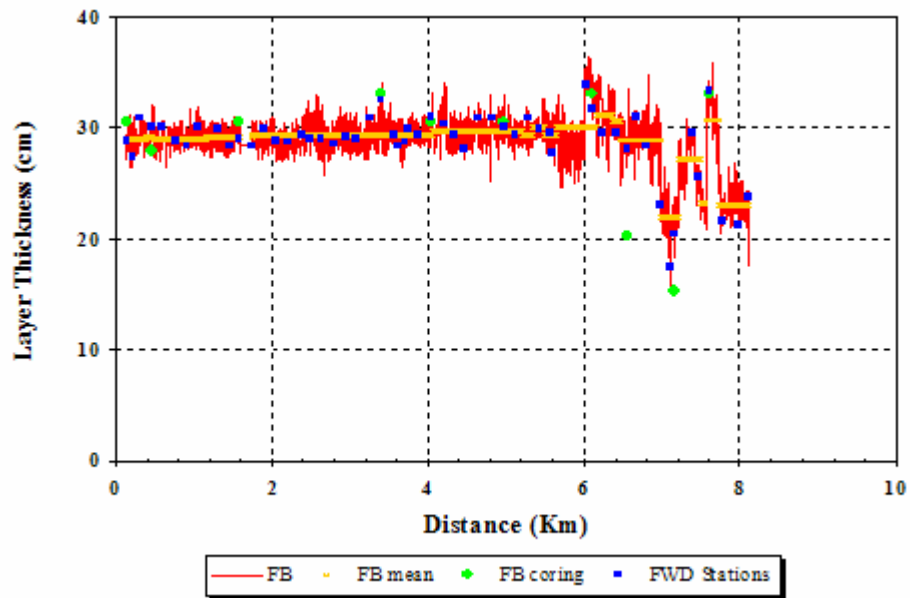
FIGURE 26   Flexible Base Predicted Thickness in the K6 Lane.
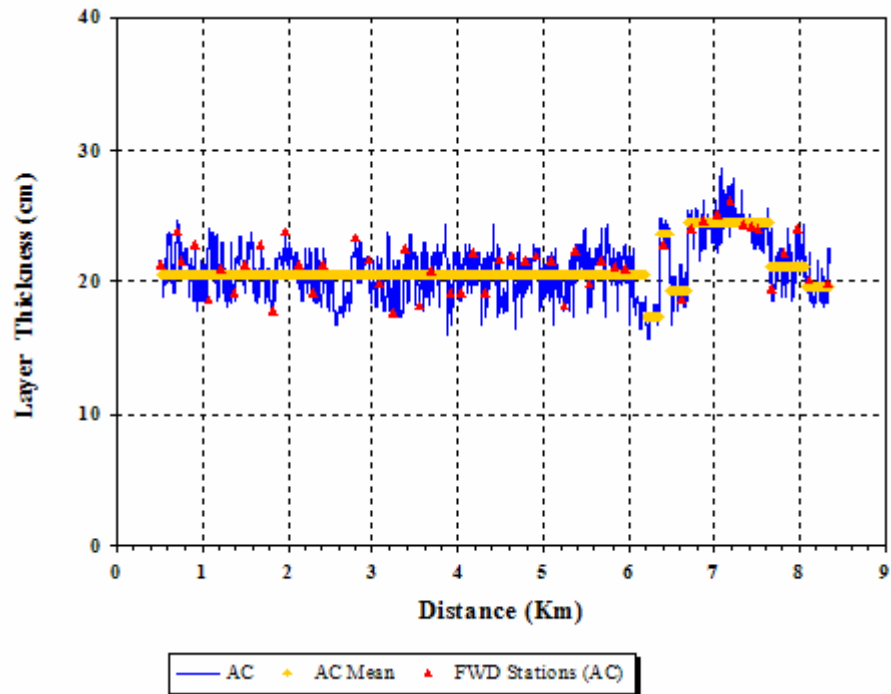
FIGURE 27   AC Predicted Thickness in the K7 Lane.
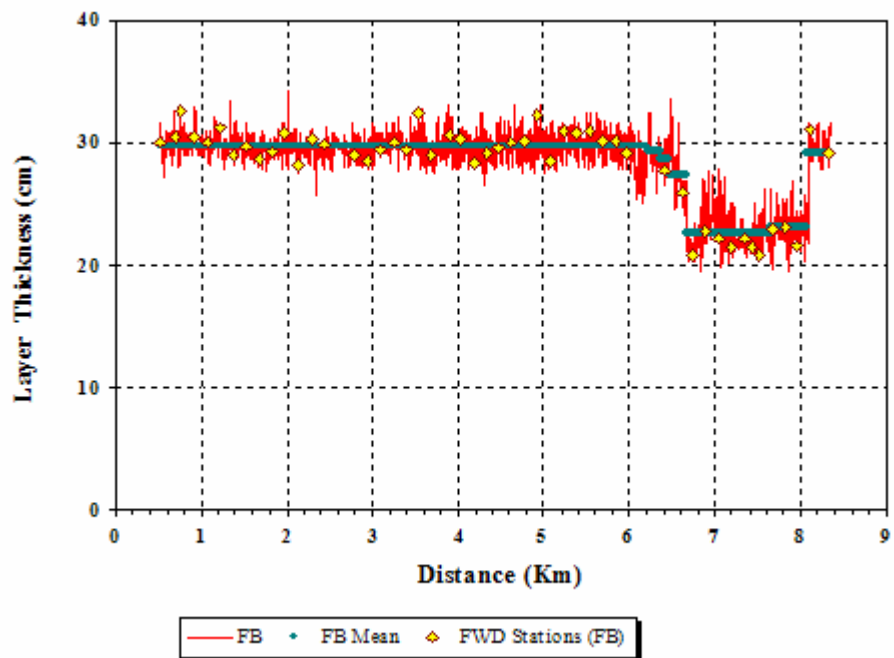
FIGURE 28   Flexible Base Predicted Thickness in the K7 Lane.
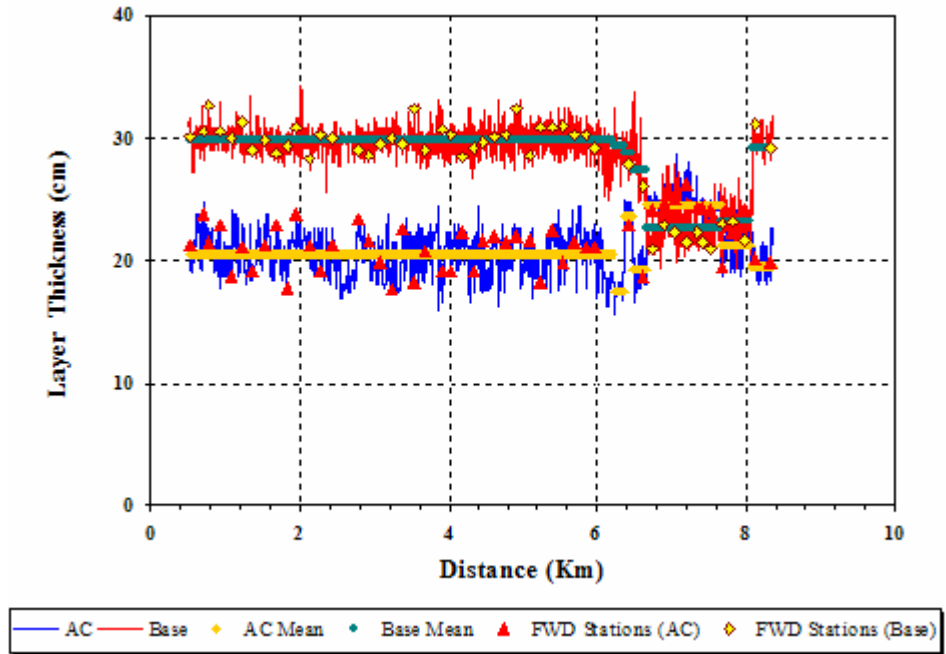
FIGURE 29   AC and FB Predicted Thickness in the K7 Lane.

TABLE 11   AC and FB Predicted Thickness in the K7 Lane.

FWD Section	Final Thickness (cm)		Mean thickness (cm)		Std. Dev.(cm)	
	AC	FB	AC	FB	AC	FB
K7_1	21.20	30.00	20.50	29.64	1.63	1.06
K7_2	23.80	30.50	20.50	29.64	1.63	1.06
K7_3	21.50	32.60	20.50	29.64	1.63	1.06
K7_4	22.80	30.50	20.50	29.64	1.63	1.06
K7_5	18.60	30.00	20.50	29.64	1.63	1.06
K7_6	21.00	31.30	20.50	29.64	1.63	1.06
K7_7	19.10	29.00	20.50	29.64	1.63	1.06
K7_8	21.20	29.80	20.50	29.64	1.63	1.06
K7_9	22.80	28.70	20.50	29.64	1.63	1.06
K7_10	17.80	29.30	20.50	29.64	1.63	1.06
K7_11	23.80	30.80	20.50	29.64	1.63	1.06
K7_12	21.20	28.20	20.50	29.64	1.63	1.06
K7_13	19.10	30.30	20.50	29.64	1.63	1.06
K7_14	21.20	29.90	20.50	29.64	1.63	1.06
K7_15	23.30	29.00	20.50	29.64	1.63	1.06
K7_16	21.70	28.50	20.50	29.64	1.63	1.06
K7_17	19.90	29.50	20.50	29.64	1.63	1.06
K7_18	17.60	30.00	20.50	29.64	1.63	1.06
K7_19	22.50	29.50	20.50	29.64	1.63	1.06
K7_20	18.20	32.40	20.50	29.64	1.63	1.06
K7_21	20.80	29.00	20.50	29.64	1.63	1.06
K7_22	19.10	30.70	20.50	29.64	1.63	1.06
K7_23	19.10	30.30	20.50	29.64	1.63	1.06
K7_24	22.20	28.40	20.50	29.64	1.63	1.06
K7_25	19.10	29.20	20.50	29.64	1.63	1.06
K7_26	21.70	29.60	20.50	29.64	1.63	1.06
K7_27	22.00	30.10	20.50	29.64	1.63	1.06
K7_28	21.50	30.20	20.50	29.64	1.63	1.06
K7_29	22.00	32.30	20.50	29.64	1.63	1.06
K7_30	21.60	28.60	20.50	29.64	1.63	1.06
K7_31	18.20	30.90	20.50	29.64	1.63	1.06
K7_32	22.40	30.80	20.50	29.64	1.63	1.06
K7_33	19.90	31.00	20.50	29.64	1.63	1.06
K7_34	21.50	30.20	20.50	29.64	1.63	1.06
K7_35	21.10	30.20	20.50	29.64	1.63	1.06
K7_36	21.00	29.20	20.50	29.64	1.63	1.06
K7_37	22.80	27.80	23.64	29.64	0.98	1.06
K7_38	18.60	26.00	19.24	29.64	1.07	1.06
K7_39	24.10	20.90	24.50	22.82	0.93	1.33
K7_40	24.60	22.80	24.50	22.82	0.93	1.33
K7_41	25.00	22.20	24.50	22.82	0.93	1.33
K7_42	26.10	21.50	24.50	22.82	0.93	1.33
K7_43	24.30	22.20	24.50	22.82	0.93	1.33
K7_44	24.20	21.50	24.50	22.82	0.93	1.33
K7_45	24.10	20.90	24.50	22.82	0.93	1.33
K7_46	19.40	23.00	21.14	22.82	1.31	1.33
K7_47	22.20	23.10	21.14	22.82	1.31	1.33
K7_48	24.10	21.60	21.14	22.82	1.31	1.33
K7_49	20.20	31.10	19.52	29.65	0.92	0.75
K7_50	19.90	29.20	19.52	29.65	0.92	0.75

ANALYSIS OF THE LAYER MODULI

As it was stayed previously, FWD data was collected seven different times during three years: 2001, 2002, and 2003. The MODULUS 6.0 software (*18*) was used for the determination of moduli values. Due to the apparent thickness variations along the K6 lane, the backcalculated modulus was done by station using the predicted thickness from Tables 10 and 11. Several trials have been made to adjust the backcalculated modulus beginning with the predicted thickness. Figure 30 gives the initial idea about the pavement structural layers used to determine the backcalculated moduli. They are asphalt concrete (AC), flexible base (FB), and subgrade (SG). Unfortunately, the first attempt had a high error rate between the measured and predicted deflections more than 10% in all the downtown stations in the K6 lane, from K6-42 up to K6-56. In addition, in some of the stations such as K6-11, K6-33, K7 -31 the backcalculated moduli did not have variations over time. It means that they did not show any time-temperature relationships. Therefore, it was evaluated different ways of modeling the pavement materials underlying the AC surface.

Legend   Layer Thickness

AC	20 cm (8 in)
FB	30 cm (12 in)
SG	Variable
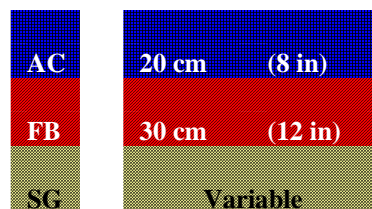
FIGURE 30   Initially Assumed Pavement Structure Layers.

The next attempts at reducing the error rate were made by combining the flexible base predicted thickness with lower layer thicknesses such as the salvaged flexible base (Salv.) and treated limestone (LT). This gave a new flexible base thickness (NFB). These lower layer thicknesses were checked out in the field, at the K6-4 FWD station as seen in Figure 31, and with the maintenance records of the Pharr District. The representation of

the pavement layering for modulus backcalculation resulting in lower errors is shown in the Figure 32.

Since the backcalculated modulus is determined by station using the predicted thickness from Tables 10 and 11, the thickness values that appear on the Figures 30, 31 and 32 are only approximated.
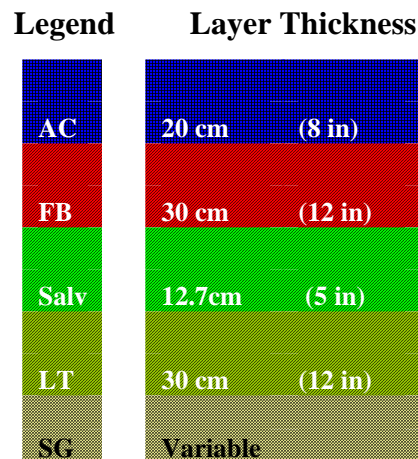
FIGURE 31   Pavement Structure Thickness in the K6-4 FWD Station.
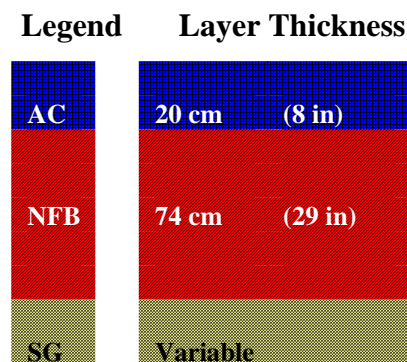
FIGURE 32   Pavement Structure Layers Used in Backcalculated Modulus.

The backcalculated modulus has been plotted vs. time by station. This means that the AC, NFB and SG moduli can be seem in same plot in the bar chart. Appendix B shows all these plots for both lanes K6 and K7. Tables 12 and 13 indicate the percentage of error in backcalculated modulus found in these analyses.

TABLE 12 Percentage of the Backcalculated Modulus Error by Stations for the K6 Lane.

Section	FWD Stations	2001				2002		
		Feb	May	Jul	Aug	Mar	Jul	Dec
K6-A	6-1	5	5	4	6	5	5	4
K6-B	6-2	3	3	2	2	2	3	1
K6-D	6-3	3	4	2	3	3	3	4
K6-D	6-4	1	2	4	1	2	3	2
K6-D	6-5	4	3	3	3	2	2	3
K6-D	6-6	2	2	5	4	2	4	2
K6-D	6-7	4	2	5	4	1	2	4
K6-D	6-8	1	4	2	3	*	2	2
K6-D	6-9	2	2	4	2	*	*	*
K6-D	6-10	1	2	2	1	3	2	2
K6-D	6-11	2	1	3	1	2	1	2
K6-D	6-12	1	2	2	2	1	3	4
K6-E	6-13	3	3	5	4	4	2	5
K6-E	6-14	3	1	3	2	3	2	4
K6-F	6-15	2	2	3	4	1	3	1
K6-F	6-16	2	2	4	4	5	4	2
K6-F	6-17	5	2	2	4	2	5	2
K6-F	6-18	5	5	3	4	3	5	4
K6-F	6-19	2	1	5	5	3	3	4
K6-F	6-20	4	2	5	3	4	3	2
K6-F	6-21	3	4	5	2	3	3	3
K6-F	6-22	3	2	3	2	6	4	1
K6-F	6-23	3	4	6	5	5	5	4
K6-G	6-24	1	4	5	5	5	5	2
K6-G	6-25	3	4	4	5	5	5	4
K6-G	6-26	5	2	5	6	1	4	2
K6-H	6-27	2	4	2	4	2	4	5
K6-H	6-28	3	5	5	5	2	4	5
K6-H	6-29	1	3	5	3	3	4	3
K6-H	6-30	5	5	5	3	2	5	3
K6-H	6-31	1	4	3	4	3	3	5
K6-H	6-32	2	2	4	5	5	4	5
K6-H	6-33	1	5	4	6	4	*	5
K6-H	6-34	2	2	3	1	3	3	2
K6-H	6-35	1	5	5	5	5	5	4
K6-H	6-36	4	3	4	1	2	3	4
K6-H	6-37	0	4	2	5	5	5	5
K6-H	6-38	1	3	4	6	2	5	5
K6-I	6-39	1	6	5	5	5	5	4
K6-J	6-40	4	5	5	5	5	6	5
K6-K	6-41	4	3	5	5	2	5	5
K6-K	6-42	9	7	12	12	5	2	2
K6-L	6-43	7	9	10	19	9	8	6

TABLE 12   Continued

Section	FWD Stations	2001				2002		
		Feb	May	Jul	Aug	Mar	Jul	Dec
K6-L	6-44	2	2	2	2	1	2	4
K6-L	6-45	1	3	3	4	3	3	2
K6-L	6-46	5	5	3	4	4	5	4
K6-L	6-47	3	3	3	4	3	5	2
K6-L	6-48	1	3	3	3	2	2	2
K6-L	6-49	4	4	4	5	2	5	2
K6-M	6-50	4	3	4	3	3	5	3
K6-O	6-51	3	3	3	4	3	5	3
K6-O	6-52	4	5	4	4	4	5	3
K6-O	6-53	1	2	1	3	1	2	5
K6-O	6-54	4	6	7	7	7	7	3
K6-O	6-55	1	3	4	5	3	4	4
K6-P	6-56	2	4	5	6	3	3	4

* No data.

TABLE 13   Percentage of the Backcalculated Modulus Error by Stations for the K7 Lane.

Section	FWD	2001			2002				2003
	Stations	Feb	May	Aug	Mar	Jul	Oct	Dec	Apr
K7-A	K7-1	1	2	4	1	2	2	1	*
K7-A	K7-2	1	2	5	2	1	2	1	2
K7-A	K7-3	1	1	2	2	1	1	1	4
K7-A	K7-4	1	1	1	1	1	1	5	1
K7-A	K7-5	3	2	3	3	3	2	2	3
K7-A	K7-6	2	1	*	2	2	2	3	3
K7-A	K7-7	1	1	1	1	1	4	2	1
K7-A	K7-8	1	2	2	*	*	*	*	*
K7-A	K7-9	1	2	3	*	*	*	*	*
K7-A	K7-10	1	1	5	2	3	1	4	2
K7-A	K7-11	2	2	4	2	2	*	5	2
K7-A	K7-12	2	5	1	2	4	3	2	1
K7-A	K7-13	1	3	1	2	2	1	2	1
K7-A	K7-14	2	1	2	2	2	1	1	5
K7-A	K7-15	4	5	4	4	5	5	3	1
K7-A	K7-16	1	4	1	3	4	3	3	4
K7-A	K7-17	1	3	1	1	2	3	2	1
K7-A	K7-18	2	2	3	1	4	4	3	1
K7-A	K7-19	2	5	4	4	3	4	1	4
K7-A	K7-20	1	*	3	1	1	1	2	2
K7-A	K7-21	1	5	0	5	1	1	5	4
K7-A	K7-22	0	1	1	1	1	*	4	1
K7-A	K7-23	1	1	2	2	2	2	3	3
K7-A	K7-24	4	1	1	3	1	2	3	1
K7-A	K7-25	2	1	2	3	2	3	4	2
K7-A	K7-26	1	2	2	0	2	5	2	1
K7-A	K7-27	1	2	2	1	4	3	1	1
K7-A	K7-28	4	1	2	1	1	2	2	1
K7-A	K7-29	3	3	4	2	*	3	3	3
K7-A	K7-30	4	5	4	4	5	2	2	3
K7-A	K7-31	4	3	3	3	4	3	4	3
K7-A	K7-32	4	2	4	3	2	2	4	2
K7-A	K7-33	1	3	4	2	2	1	3	3
K7-A	K7-34	1	2	3	2	1	1	1	1
K7-A	K7-35	1	2	3	4	1	2	2	4
K7-A	K7-36	1	5	4	5	1	2	1	6
K7-B	K7-37	4	5	2	5	5	4	4	4
K7-C	K7-38	8	10	6	8	9	11	7	13
K7-D	K7-39	1	3	1	3	2	4	4	2
K7-E	K7-40	1	2	3	0	2	4	2	1
K7-E	K7-41	2	1	3	2	2	2	3	1
K7-E	K7-42	4	2	4	1	2	5	5	3
K7-E	K7-43	2	2	2	3	3	4	1	*

TABLE 13   Continue

Section	FWD Stations	2001			2002				2003
		Feb	May	Aug	Mar	Jul	Oct	Dec	Apr
K7-E	K7-44	1	5	2	1	5	5	1	2
K7-E	K7-45	4	3	3	5	3	4	4	3
K7-E	K7-46	2	4	4	4	4	4	4	4
K7-F	K7-47	2	3	2	5	3	5	3	2
K7-F	K7-48	2	1	3	3	4	4	2	1
K7-F	K7-49	2	2	2	3	2	3	1	2
K7-F	K7-50	3	2	4	3	2	2	4	9

* No data.

CHAPTER V

DYNAMIC ANALYSIS

DYNAMIC MODULUS AND CREEP COMPLANCE PARAMETERS

For the dynamic analysis the computer program DBSID was used, (*18*). This program uses the FWD full time histories of load and displacement for the backcalculation of pavement material properties. This program permits the simulation of a pavement layer structure consisting of up to three layers. The consideration taken for this analysis was that the first layer (AC) is modeled as a viscoelastic material and the second layer (flexible base) and third layer (subgrade) as damped elastic material. Since the maximum iteration number of DBSID is 40 iterations, there is a variety of results that may be analyzed. These results were analyzed by two criteria: by plotting the measured and predicted displacement history data and by the root mean square error (RMSE) of deflections of each iteration.

Even though there is a significant amount data to process in dynamic analysis, in this study, only the core stations were analyzed. These FWD stations are K6-1 K6-4, K6-11, K6-23, K6-29, K6-35, K6-48, K7-3, K7-11, K7-20, K7-31, K7-37 and K7-40. The stations K6-50, K6-51 and K6-53 were omitted because they did not give clear results in the laboratory testing. In addition, K7-9 was not analyzed due to the fact that FWD data was stopped due to construction that resulted ina change of pavement at this station.

In Appendix C one may see the plots of the measured and predicted displacement histories by the FWD stations and the time corresponding to both the K6 and K7 lanes. These plots show that the predicted measurement fit the measured values quite adequately in most of the FWD stations. However, there were some FWD stations that did not provide a good results in dynamic analysis, such as K7-3 during any months, K6-1 and K6-4 in the month of February of 2001, and K6-35 in May and August of 2001, March, July and August of 2002.

In addition, Tables 14 to 26 present the creep compliance parameters, layer modulus, depth to a rigid layer (DB), and RMSE in the predicted deflections by station and time.

Lane K6

TABLE 14   Creep Compliance Parameters and Modulus from K6-1 FWD Station.

				MODULUS (MPa)			DB	RMSE
Month	Do	D1	m	AC	FB	SG	(m)	(μm)
May 01	3.3E-05	5.6E-02	0.344	684	66	66	66	22
Jul 01	1.7E-05	3.4E-02	0.417	1602	87	87	87	13
Aug 01	1.9E-06	6.2E-02	0.354	648	48	48	48	28
Mar 02	1.0E-03	4.5E-02	0.474	1322	56	56	56	31

TABLE 15   Creep Compliance Parameters and Modulus from K6-4 FWD Station.

				MODULUS (MPa)			DB	RMSE
Month	Do	D1	m	AC	FB	SG	(m)	(μm)
May 01	1.0E-05	1.5E-02	0.430	3718	88	90	6	9
Jul 01	1.7E-05	1.5E-02	0.435	3903	75	70	6	11
Mar 02	1.3E-05	1.5E-02	0.415	3530	86	86	6	10
Jul 02	1.3E-05	2.7E-02	0.497	2854	111	71	7	14

TABLE 16   Creep Compliance Parameters and Modulus from K6-11 FWD Station.

				MODULUS (MPa)			DB	RMSE
Month	Do	D1	m	AC	FB	SG	(m)	(μm)
Feb 01	3.3E-06	2.8E-03	0.322	1227	869	93	6	1
May 01	7.3E-06	1.7E-02	0.476	4052	818	80	6	2
Jul 01	1.4E-05	5.0E-02	0.539	1881	911	82	6	4
Aug 01	1.9E-05	9.9E-02	0.577	1138	816	75	5	3
Mar 02	8.3E-06	1.2E-02	0.443	5113	758	88	7	3
Jul 02	1.0E-05	3.0E-02	0.498	2653	1007	89	6	2

TABLE 17   Creep Compliance Parameters and Modulus from K6-23 FWD Station.

Month	Do	D1	m	MODULUS (MPa)			DB (m)	RMSE (μm)
				AC	FB	SG		
Feb_01	5.00E-06	1.37E-02	0.384	3358	551	73	6	2
May_01	1.67E-05	6.66E-02	0.500	1185	316	76	6	8
Jul_01	1.58E-05	5.35E-02	0.398	918	542	67	5	5
Aug_01	3.33E-05	1.77E-01	0.485	416	501	74	5	5
Mar_02	1.04E-05	1.93E-02	0.413	2723	503	68	5	3
Jul_02	1.48E-05	4.59E-02	0.427	1223	656	73	5	5

TABLE 18   Creep Compliance Parameters and Modulus from K6-29 FWD Station.

Month	Do	D1	m	MODULUS (MPa)			DB (m)	RMSE (μm)
				AC	FB	SG		
Feb_01	3.50E-06	3.54E-03	0.308	9028	438	99	7	2
May_01	1.04E-05	1.33E-02	0.390	3538	337	89	7	4
Jul_01	2.78E-07	1.38E-02	0.399	3582	564	82	6	3
Aug_01	2.27E-05	8.24E-02	0.572	1332	326	81	6	6
Mar_02	8.77E-06	8.60E-03	0.374	5070	519	85	7	3
Jul_02	1.25E-05	1.41E-02	0.441	4244	574	81	6	3

TABLE 19   Creep Compliance Parameters and Modulus from K6-35 FWD Station.

Month	Do	D1	m	MODULUS (MPa)			DB (m)	RMSE (μm)
				AC	FB	SG		
Feb_01	4.55E-06	4.55E-03	0.294	6564	111	109	5	11
Jul_01	3.13E-05	1.02E-01	0.580	1116	95	96	6	15

TABLE 20   Creep Compliance Parameters and Modulus from K6-48 FWD Station.

Month	Do	D1	m	MODULUS (MPa)			DB (m)	RMSE (μm)
				AC	FB	SG		
Feb_01	1.95E-05	3.21E-02	0.416	1663	73	83	6	5
Jul_01	5.51E-05	1.99E-01	0.549	496	66	69	5	12
Aug_01	8.74E-05	2.40E-01	0.483	304	75	59	4	14
Mar_02	3.54E-05	8.67E-02	0.486	853	72	75	5	8
Jul_02	3.98E-05	1.14E-01	0.514	739	70	76	5	9

Lane K7

TABLE 21   Creep Compliance Parameters and Modulus from K7-11 FWD Station.

| Month | Do | D1 | m | MODULUS (MPa) | | | DB | RMSE |
				AC	FB	SG	(m)	(μm)
May_01	7.01E-06	1.37E-02	0.387	3426	481	108	7	4
Aug_01	8.33E-06	1.20E-02	0.337	3077	478	102	6	4
Mar_02	5.00E-06	2.01E-03	0.202	9488	364	105	7	2
Jul_02	1.41E-05	3.27E-02	0.444	1871	477	90	6	3
April_03	5.81E-06	5.95E-03	0.315	5588	456	111	7	3

TABLE 22   Creep Compliance Parameters and Modulus from K7-15 FWD Station.

| Month | Do | D1 | m | MODULUS (MPa) | | | DB | RMSE |
				AC	FB	SG	(m)	(μm)
May_01	7.14E-06	1.88E-02	0.356	2156	390	118	8	5
Aug_01	7.14E-06	9.73E-03	0.289	3013	407	108	8	4
Mar_02	3.33E-06	4.30E-03	0.229	5107	439	115	8	4
Jul_02	1.19E-05	3.13E-02	0.430	1833	285	116	7	6
Oct_02	9.09E-06	2.96E-02	0.553	3431	230	92	7	11
April_03	4.89E-06	2.74E-03	0.214	7418	287	93	6	2

TABLE 23   Creep Compliance Parameters and Modulus from K7-20 FWD Station.

| Month | Do | D1 | m | MODULUS (MPa) | | | DB | RMSE |
				AC	FB	SG	(m)	(μm)
Feb_01	3.70E-06	2.98E-03	0.221	7076	471	82	7	2
Aug_01	8.33E-06	6.48E-03	0.332	5539	498	72	7	3
Mar_02	3.65E-06	3.85E-03	0.298	7967	508	72	7	3
Jul_02	1.11E-05	1.75E-02	0.424	3189	511	73	6	3
Oct_02	1.22E-05	3.22E-02	0.488	2336	540	72	7	3
April_03	4.07E-06	3.07E-03	0.241	7547	405	82	7	3

TABLE 24   Creep Compliance Parameters and Modulus from K7-31 FWD Station.

Month	Do	D1	m	MODULUS (MPa) AC	FB	SG	DB (m)	RMSE (μm)
May_01	7.14E-06	5.80E-03	0.415	9165	593.011	84	5	3
Aug_01	1.25E-05	2.44E-02	0.671	7067	839.375	17	2	15
Jul_02	1.11E-05	1.20E-02	0.501	6606	580.725	72	5	3
Oct_02	1.04E-05	3.79E-02	0.528	2382	781.693	78	4	6
April_03	6.10E-06	2.70E-03	0.341	13824	682.988	87	5	3

TABLE 25   Creep Compliance Parameters and Modulus from K7-37 FWD Station.

Month	Do	D1	M	MODULUS (MPa) AC	FB	SG	DB (m)	RMSE (μm)
Feb_01	2.63E-06	8.67E-03	0.356	4664	436	108	8	2
May_01	1.90E-07	3.28E-02	0.456	1981	337	105	8	4
Aug_01	1.25E-05	4.35E-02	0.467	1572	408	107	8	3
Mar_02	4.55E-06	1.19E-02	0.356	3399	382	112	8	3
Jul_02	1.79E-05	5.01E-02	0.447	1241	276	100	9	9
Oct_02	2.00E-05	5.90E-02	0.562	1788	190	99	8	12
April_03	7.14E-06	2.71E-02	0.496	2877	355	117	7	6

TABLE 26   Creep Compliance Parameters and Modulus from K7-40 FWD Station.

Month	Do	D1	m	MODULUS (MPa) AC	FB	SG	DB (m)	RMSE (μm)
Feb_01	6.35E-06	8.20E-03	0.347	4732	123	85	6	3
May_01	1.25E-05	2.77E-02	0.452	2290	122	74	6	4
Aug_01	1.79E-05	2.90E-02	0.461	2280	144	76	5	4
Mar_02	8.05E-06	9.34E-03	0.343	4075	133	77	6	3
Jul_02	2.32E-05	7.32E-02	0.519	1186	95	69	5	9
Oct_02	1.67E-05	6.39E-02	0.586	1840	98	68	6	11
April_03	1.02E-05	1.63E-02	0.401	3075	119	79	6	3

In Chapter VIII the backcalculated AC modulus obtained from dynamic analysis will be discussed and compared to those from static analysis. In addition, the correlation between the creep compliance parameters from the dynamic analysis and laboratory testing will be analyzed.

CHAPTER VI

LABORATORY TESTING

The main purpose of laboratory testing is to get helpful information about the changes in the AC layer of the pavement as it is affected by routine overweight truck traffic. Due to the fact that AC undergoes time-dependent changes, it is significant to consider this condition in material characterizations. According to the AASHTO 2002 Design Guide *(19)*, the long-term, time-dependent property changes come about because of one of these conditions: the chemical and physical hardening of the asphalt binder due to short or long–term aging of the AC binder, curing caused by evaporation of the moisture inside of asphalt emulsion system, and pozzuolanic reactions of cementitious materials.

In addition, the 2002 Design Guide *(19)* indicates that materials subjected to load-related fatigue distress may undergo a severe degradation of properties with time and load repetitions. Microcracks may develop, leading to a reduced modulus. The possible reduction of modulus due to this, would lead to an increase in a stress and larger possibility of permanent deformation.

DYNAMIC MODULUS OF THE ASPHALT CONCRETE MIXTURE /E*/

The standard tests in the NCHRP 1-37 DM1 Draft Standard Test Method for the Dynamic Modulus of Asphalt Concrete Mixtures ASU May –2002 *(20)*, and ASTM D3497-79, Standard Test Method for Dynamic Modulus of Asphalt Mixtures *(21)* cover procedures for preparing and testing to determine the dynamic modulus and phase angle over a range of temperature and loading frequencies. Both tests are carried out by applying a sinusoidal (haversine) axial compression stress to the asphalt concrete sample at a given temperature and loading frequency. The applied stress and recoverable axial strain response of the samples are measured to calculate the dynamic modulus and phase angle. The method produces results that differ with the frequencies and temperatures used

in the testing. While ASTM D3497-79 (*21*) uses temperatures such as 5, 25 and 40 $^{\circ}$C with frequencies of 1, 4 and 16 Hz, the NCHRP 1-37 (*20*) has a greater range of temperatures and frequencies used, such as -10, 4, 20, 37.8 and 54.4 $^{\circ}$C, and 25, 10, 5, 1, 0.5 and 0.1 Hz, respectively.

On the other hand, the number of replications indicated by ASTM D3497-79 is 6 samples of the pavement cores, while the NCHRP 1-37 is limited to 4 specimens if it is used with two LVDTs per specimen. Therefore, with the purpose of getting the best simulation of the field's AC properties the NCHRP 1-37 standard was selected to determine the dynamic (complex) modulus of the AC cores.

It is known that the temperatures in the city of Brownsville do not drop a grade below zero during the winter season. In addition, since the laboratory testing was begun during Summer of 2002 and the only pavement temperatures from the FWD data available by that time, as seen in Table 27, reflect that the pavement temperature at 25.4 mm (1 in) or predicted pavement temperature at middle depth had a range between 21.1°C and 54.4°C (70 $^{\circ}$F and 130 $^{\circ}$F). Consequently, the temperatures used in the test were six: 21.1, 29.4, 37.8, 43.3 and 54.4 $^{\circ}$C (70, 85, 100, 110 and 130 $^{\circ}$C).

TABLE 27 Field and Predicted Pavement Temperatures by March 2002.

Lane	Month	Field Pav. Temperature 25.4 mm (1")						Predicted Pav Temperature at middle depth					
		Min		Max		Mean		Min		Max		Mean	
		$^{\circ}$F	$^{\circ}$C	$^{\circ}$F	$^{\circ}$C	$^{\circ}$F	$^{\circ}$C	$^{\circ}$F	$^{\circ}$C	$^{\circ}$F	$^{\circ}$C	$^{\circ}$F	$^{\circ}$C
K6	Feb_01	76	24	91	33	85	30	79	26	88	31	83	28
	May_01	103	39	124	51	115	46	97	36	108	42	103	39
	Jul_01	112	44	127	53	119	48	109	43	116	47	112	45
	Aug_01	135	57	145	63	135	57	116	46	126	52	121	49
	Mar 02	108	42	119	48	113	45	99	37	105	41	102	39
K7	Feb_01	78	26	92	33	85	29	89	32	94	34	91	33
	May_01	115	46	128	53	122	50	99	37	108	42	103	39
	Aug_01	*	*	*	*	*	*	107	42	111	44	108	42
	Mar 02	89	32	104	40	96	36	94	35	112	44	103	40

* No data.

As was mentioned in Chapter II the number of AC cores taken initially were reduced by handling or breaking problems. The final number of tested cores were 12 cores for the lane K6, and 9 for the lane K7, and an additional 4 samples collected in the vicinity of the K6-4 FWD station. Tables 28, 29 and 30 specify core measurements from the laboratory testing. Even though in the NCHRP 1-37 standard specifies that the dynamic modulus testing ought to be tested on cores with nominal diameters of 101,6 mm (4 in), the second set of samples taken in the downtown area were cored with smaller diameters due to their lower stiffness. It is significant that the cores did not have a homogenous AC material with height (thickness). For that reason the position of the linear variable differential transformer (LVDT) clamps were set up 25mm (1") from the top and the bottom ends of the surface cores. The LVDT gauge length (GL) that was employed on the tested cores is detailed in Figure 33.

The set of frequencies and number of cycles used were those indicated in the selected standard. They are 25, 10, 5, 1, 0.1 and 0.5 Hz, and with 200, 200, 100, 20, 15, and 15 cycles, respectively. Before cores could be tested, they were placed in the environmental chamber to equilibrate them to the required temperature. The specimen C2 was used as a dummy specimen in the preparation of this test.

TABLE 28 Laboratory Measurements of the AC Cores of the K6 Lane.

Nº	ID	Diameter (mm)	Height (mm)	GL (mm)	Diameter (in)	Height (in)	GL (in)
1	K6-1	102	195	142	4	8	6
2	K6-4	102	165	117	4	6	5
3	K6-11	102	193	114	4	8	4
4	K6-23	102	170	116	4	7	5
5	K6-29	102	204	124	4	8	5
6	K6-35	102	194	105	4	8	4
7	K6-48-16	92	208	130	3.6	8	5
8	K6-48-12	92	164	102	3.6	6	4
9	K6-50-16	92	127	76	3.6	5	3
10	K6-50-12	92	157	102	3.6	6	4
11	K6-51	92	133	83	3.6	5	3
12	K6-53-10	92	140	102	3.6	6	4

TABLE 29   Laboratory Measurements of the AC Cores of the K7 Lane.

Nº	ID	Diameter (mm)	Height (mm)	GL (mm)	Diameter (in)	Height (in)	GL (in)
1	K7-3	102	208	157	4	8	6
2	K7-9	102	192	141	4	8	6
3	K7-11	102	209	151	4	8	6
4	K7-12	102	206	152	4	8	6
5	K7-15	102	208	141	4	8	6
6	K7-20	102	209	151	4	8	6
7	K7-31	102	206	141	4	8	6
8	k7-37	102	206	155	4	8	6
10	K7-40	102	207	152	4	8	6

TABLE 30   Laboratory Measurements of the AC Cores on K6-4 FWD Station.

Nº	ID	Diameter (mm)	Height (mm)	GL (mm)	Diameter (in)	Height (in)	GL (in)
1	C2	102	164	115	4.0	6.5	5
2	C3	102	195	151	4.0	7.7	6
3	C4	102	202	150	4.0	8.0	6
4	C5	102	205	152	4.0	8.1	6
5	C6	102	188	90	4.0	7.4	4
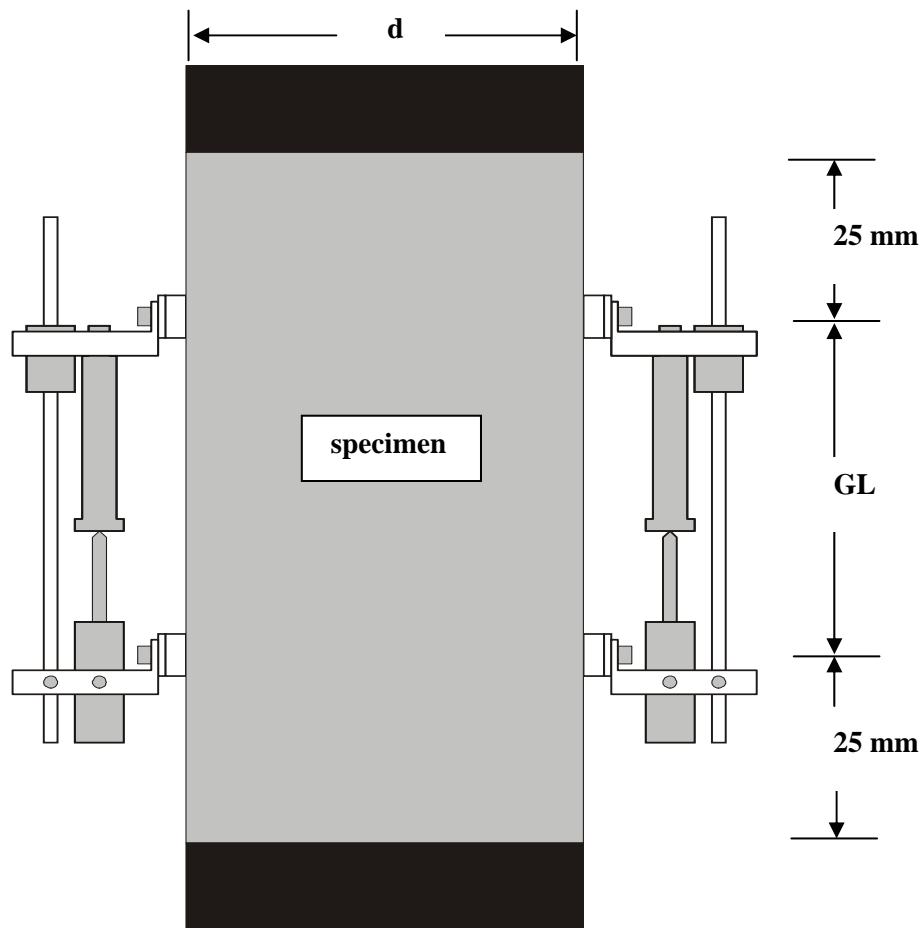
FIGURE 33   Location of the LVDTs at the AC Cores.

The laboratory data were processed by computer program to get complex modulus (E*) and creep compliance (D) with their corresponding real and imaginary parts. The dynamic complex modulus (/E*/) is got from the absolute value of the complex modulus.

The calculations of the angle phase (ϕ)

$$\phi = (t_i/ t_p) \times 360$$

were determined from max (min) points and not from the mid point values. Figure 34 shows the time lag (t_i) and loading cycle period (t_p) used.

All of these properties (E*, D and /E*/) were calculated with four approaches named Case 1, Case 2, Case 3, and Case 4.

- Case 1: The amplitude of the load and deformation were from regresion data and the angle phase was calculated from the regression at minimun points.

- Case 2: The amplitude of the load and deformation were from raw data and the angle phase was from the regression at minimum points.

- Case 3: The amplitude of the load and deformation were from regresion data and the angle phase was from the regression at maximum points.

- Case 4: The amplitude of the load and deformation were from raw data and the angle phase was from the regression at maximum points.

Appendix D shows all of the possible combinations (a max 12 combinations in each testing temperature) neccesary to get the curves of the dynamic modulus at different frequencies. Figures 35 to 49 present the best results in each tested core.
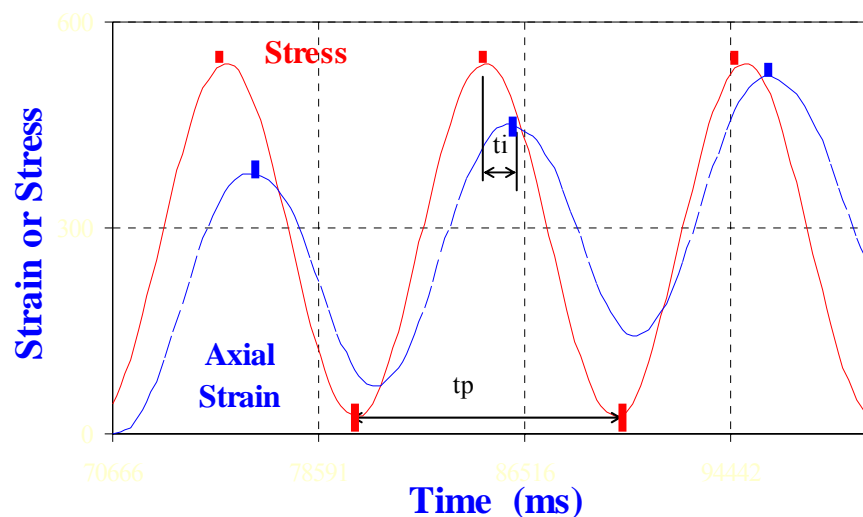
FIGURE 34   Stresses and Strains in Complex Modulus Test.

Lane K6
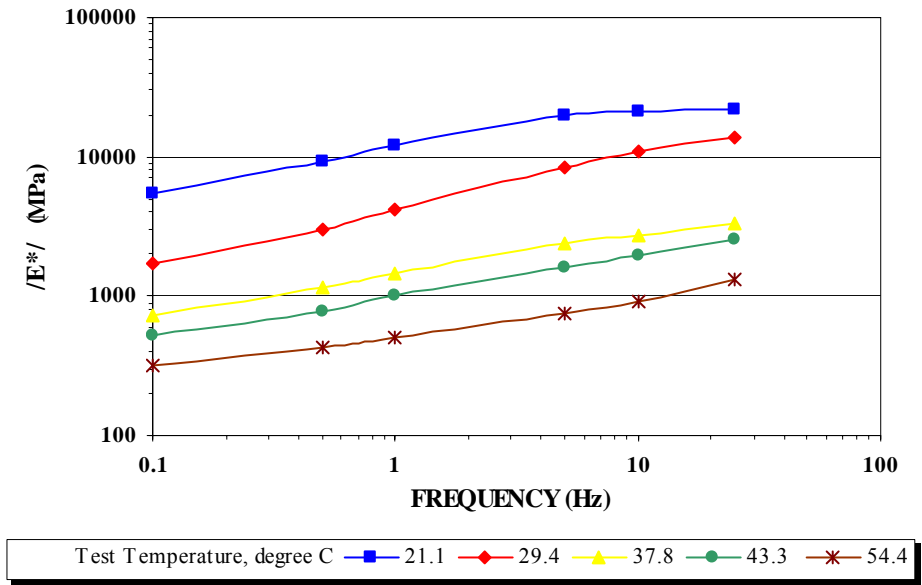
FIGURE 35   Dynamic (Complex) Modulus of the K6-1 FWD Station.
                      Case 1 and Case 3.
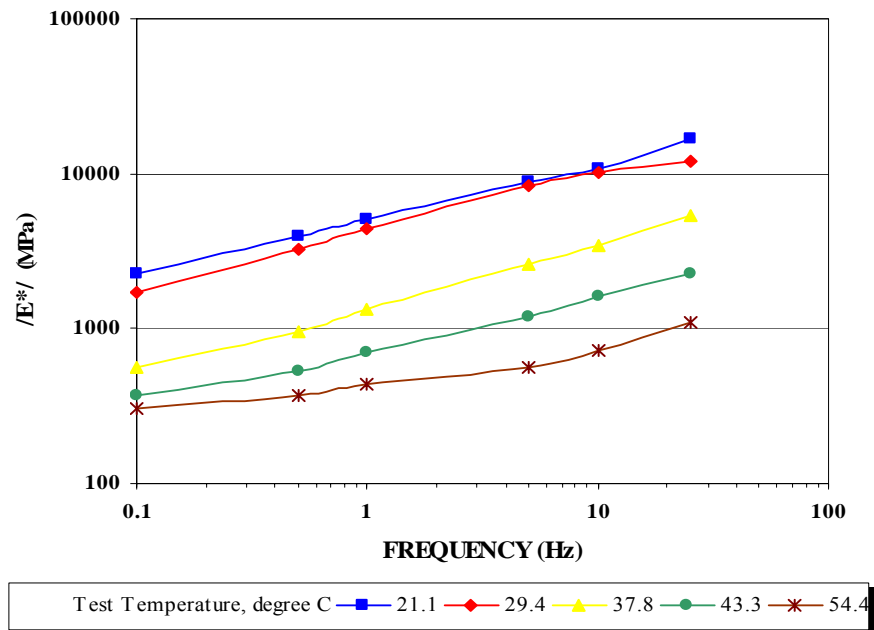
FIGURE 36   Dynamic (Complex) Modulus of the K6-4 FWD Station.
                      Case 1 and Case 3.
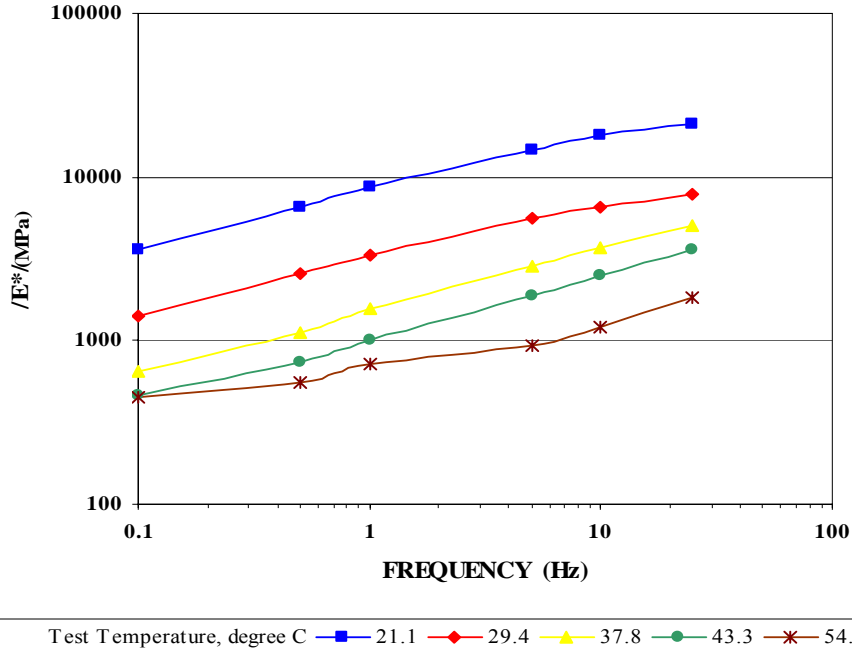
FIGURE 37   Dynamic (Complex) Modulus of the K6-11 FWD Station. Case 1 and Case 3.
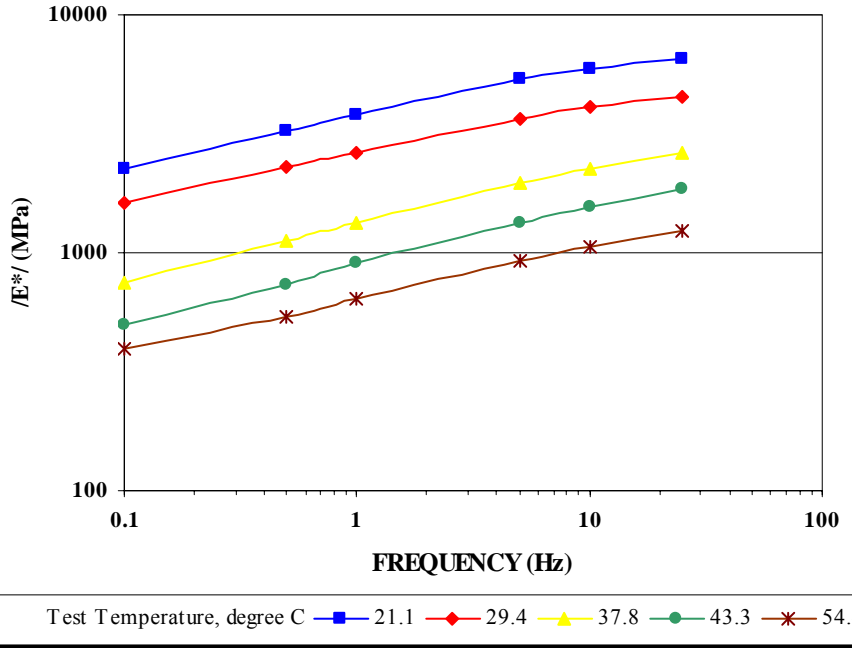
FIGURE 38   Dynamic (Complex) Modulus of the K6-23 FWD Station. Case 1 and Case 3.
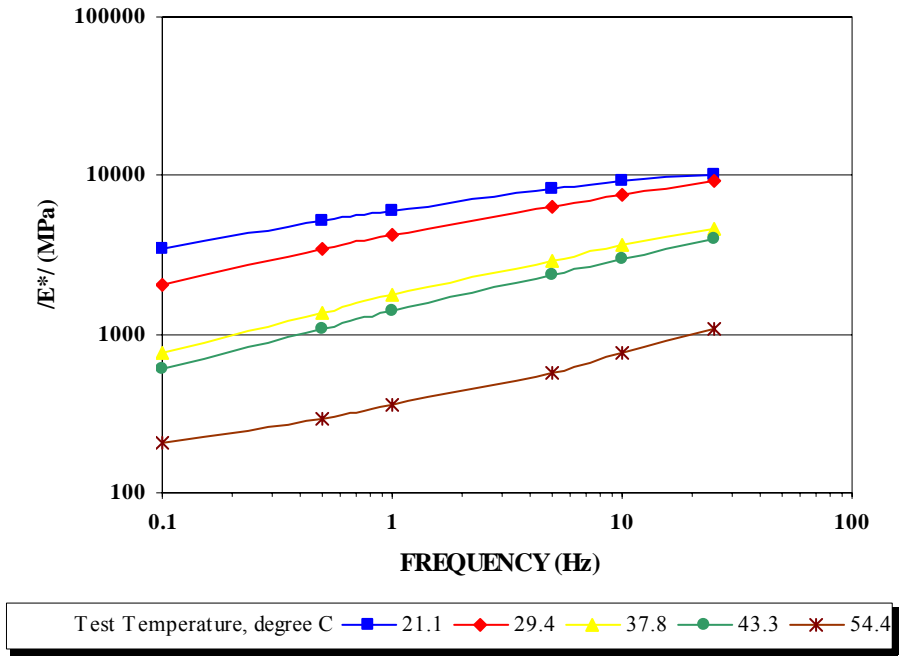
FIGURE 39 **Dynamic (Complex) Modulus of the K6-29 FWD Station. Case 2 and Case 4.**
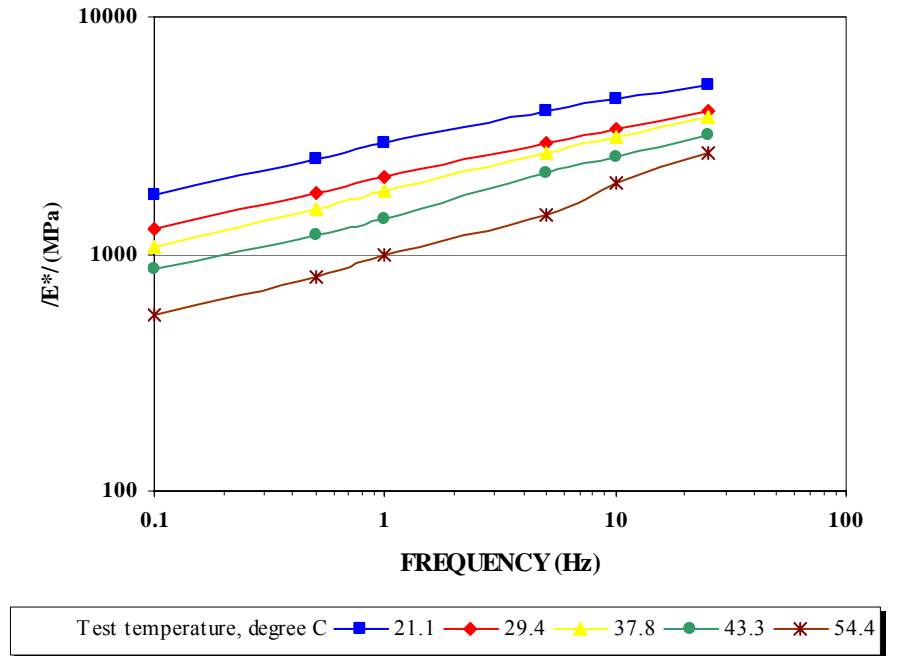
FIGURE 40 **Dynamic (Complex) Modulus of the K6-48 FWD Station. Case 1 and Case 3.**

Lane K7
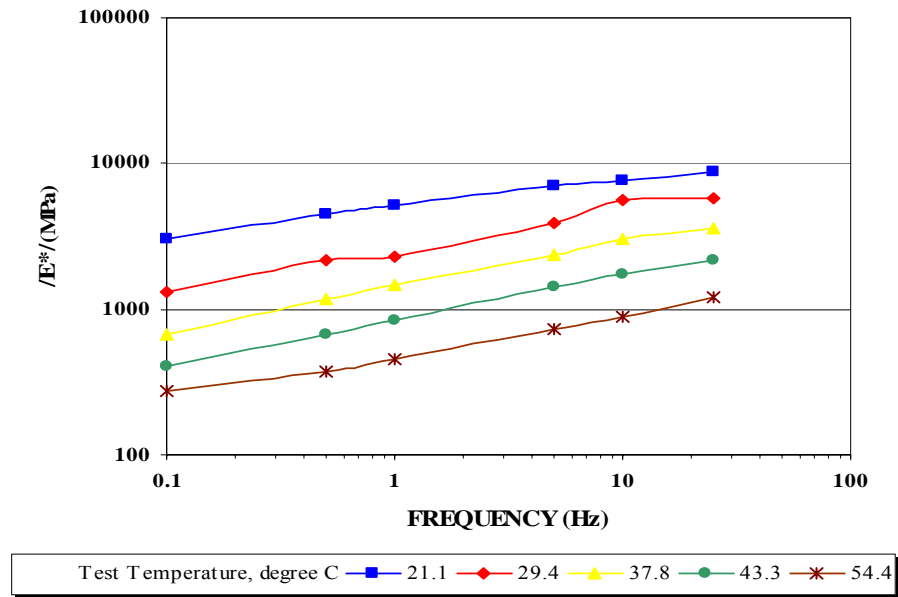
FIGURE 41 Dynamic (Complex) Modulus of the K7-3 FWD Station. Case 2 And Case 4.
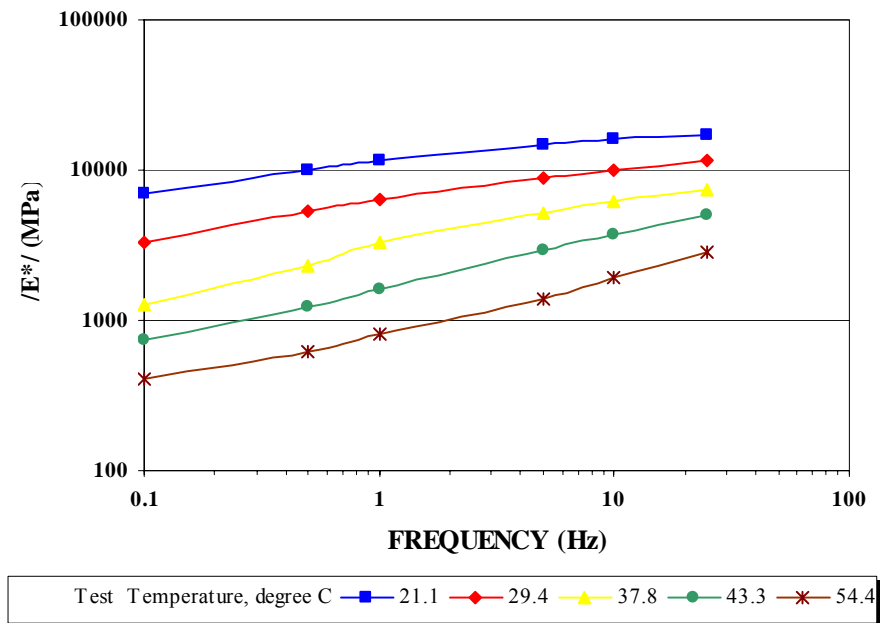
FIGURE 42 Dynamic (Complex) Modulus of the K7-9 FWD Station. Case 1 and Case 3.
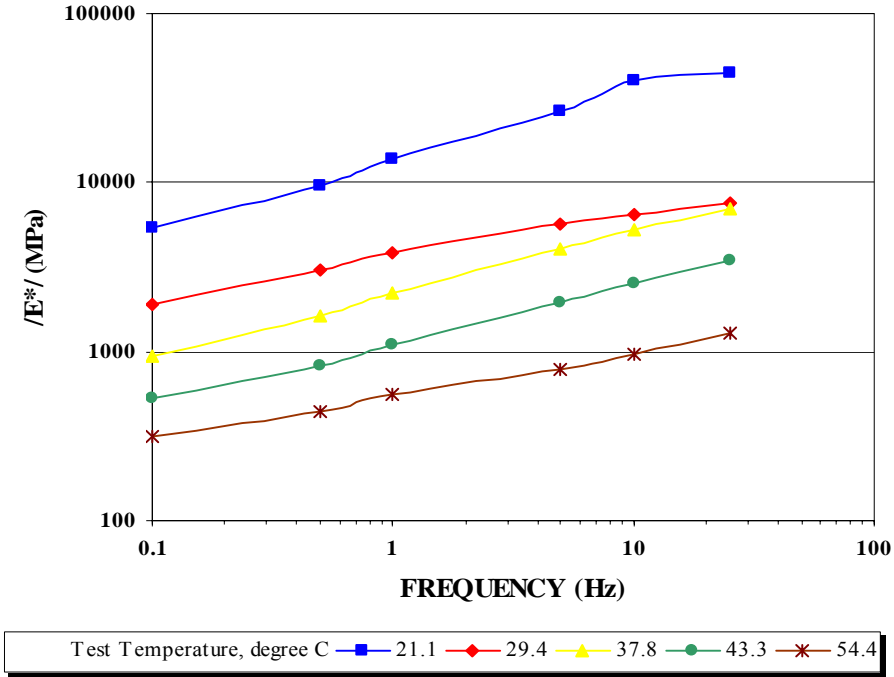
FIGURE 43 **Dynamic (Complex) Modulus of the K7-11 FWD Station. Case 1 and Case 3.**
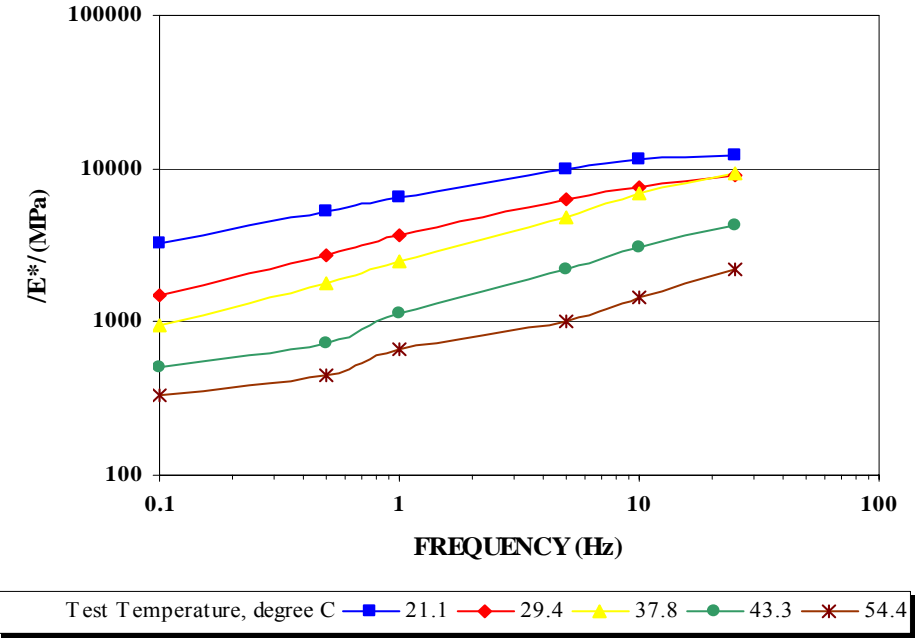
FIGURE 44 **Dynamic (Complex) Modulus of the K7-15 FWD Station. Case 1 and Case 3.**
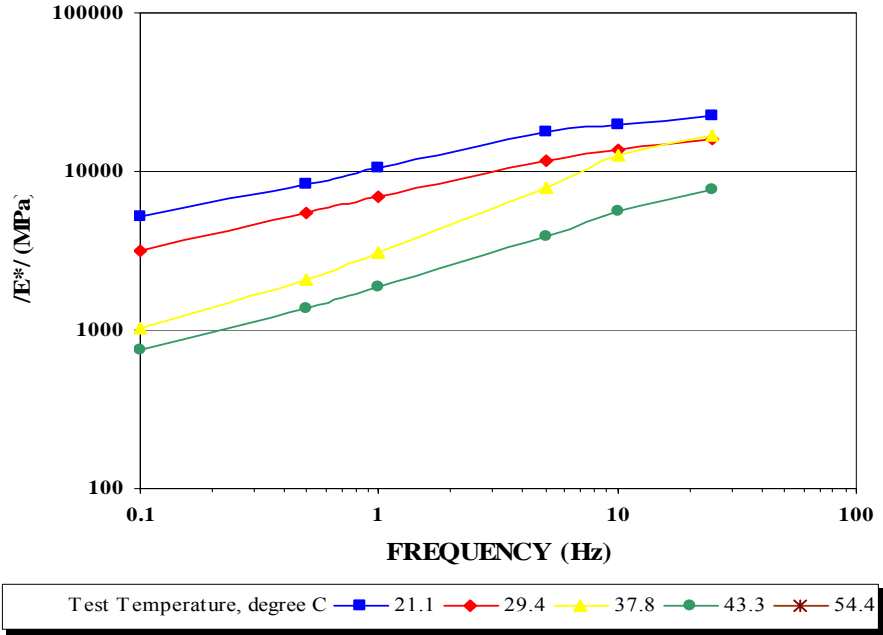
FIGURE 45   Dynamic (Complex) Modulus of the K7 20 FWD Station.
Case 2 and Case 4.
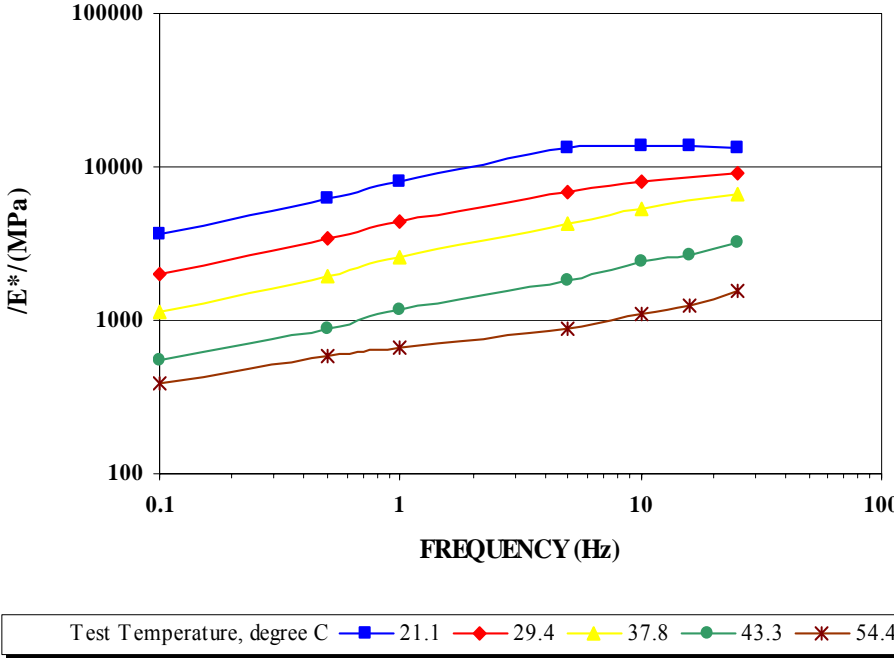
FIGURE 46   Dynamic (Complex) Modulus of the K7-31 FWD Station.
Case 1 and Case 3.
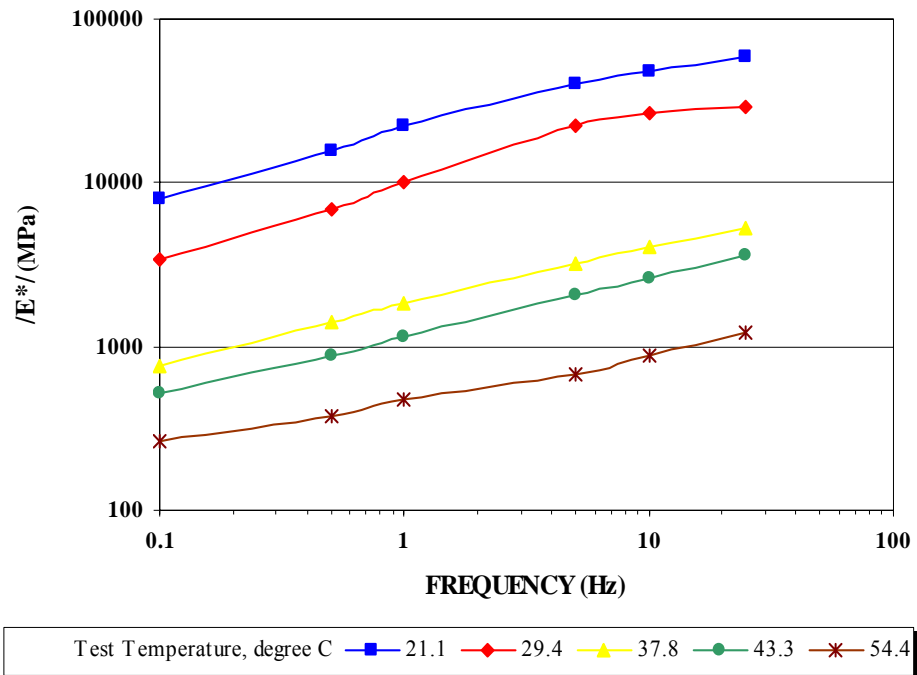
FIGURE 47   Dynamic (Complex) Modulus of the K7-37 FWD Station. Case 1 and Case 3.
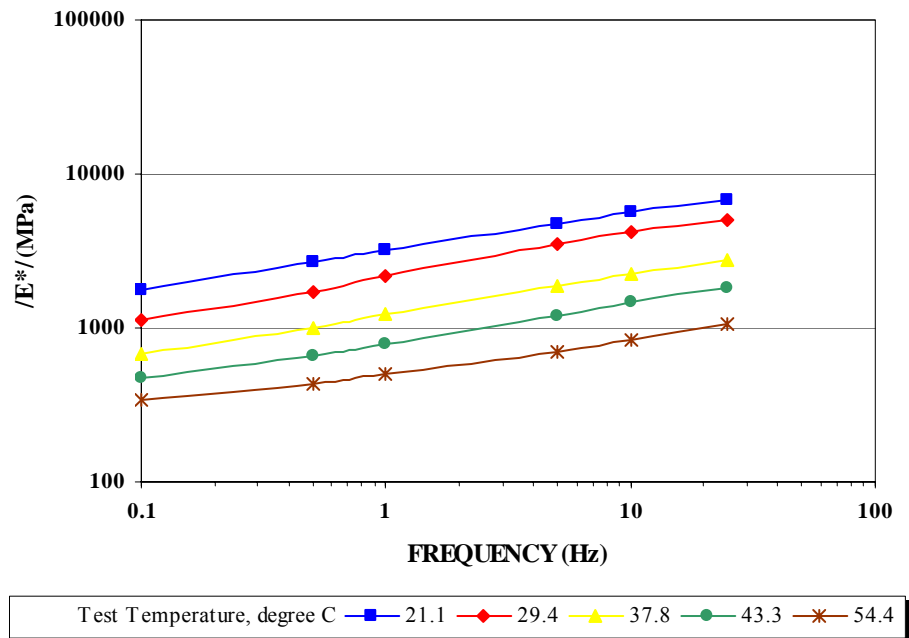
FIGURE 48   Dynamic (Complex) Modulus of the K7 40 FWD Station Case 1 and Case 3
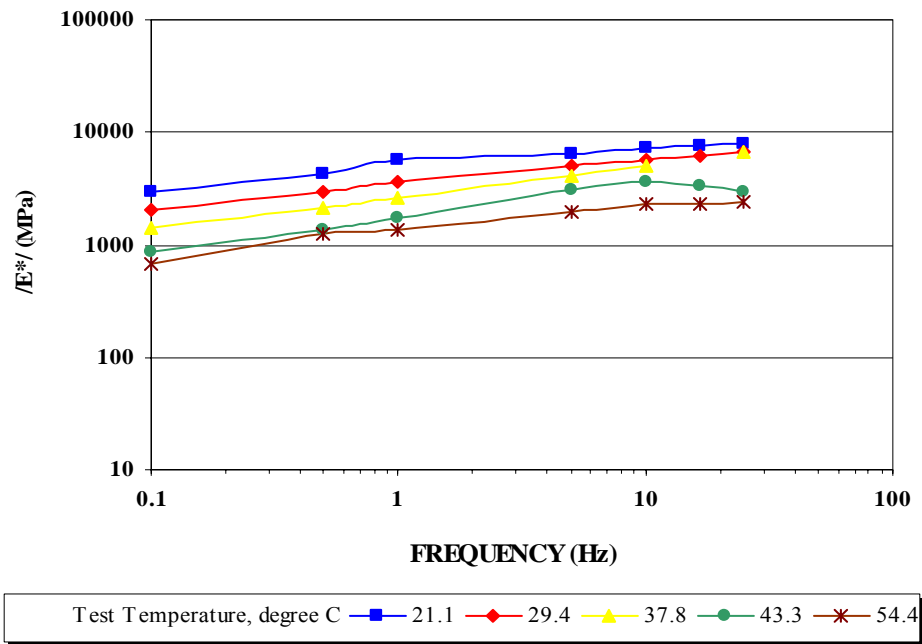
**FIGURE 49   Dynamic (Complex) Modulus of the C6 Core.
Case 1 and Case 3.**

CREEP COMPLIANCE PARAMETERS

Due to the fact that the creep compliance (D) is a complex number defined as the inverse of the complex modulus (E*) for a linear viscoeslatic material (*22*) whose values, real and imaginary, were calculated with the computer programm indicated before; then, it is possible to backcalculate the parameters of the creep compliance as defined in equations 2.1, 2.2 and 2.3. Tables 31 to 41 give the predicted creep compliance parameters, D_o, D_1 and "m" , based upon values obtained from computer analysis of laboratory data. These tables also mention the Sum of Square Error (SSE) of each data set calculated. Even though all core stations were performed by computer programs to obtained the creep compliance parameters, some stations such as K6-29, K6-35, K7-3 and K7-9 could not get valid "m" values. The criteria to select valid "m" values was that the "m" values should increase as the temperature increases.

However, most "m" values of core stations fall at the higher temperature 54.4 ^{o}C (130 ^{o}F) for both the K6 and the K7 lane.

Lane K6

TABLE 31   Creep Compliance Parameters of the K6-1 FWD Station.

N°	Temperature		Case	Do	D1	m	SSE
	º C	ºF					
1	21.1	70	C1	1.48E-05	1.76E-04	3.89E-01	2.18E-01
2	29.4	85	C2	2.69E-11	5.40E-04	4.06E-01	1.68E-01
3	37.8	100	C4	1.77E-04	1.28E-03	4.29E-01	1.59E-01
4	43.3	110	C1	3.31E-04	1.39E-03	4.28E-01	5.97E-01
5	54.4	130	C4	8.68E-04	1.76E-03	5.19E-01	1.46E+00

TABLE 32   Creep Compliance Parameters of the K6-4 FWD Station.

No	Temperature		Case	Do	D1	m	SSE
	º C	º F					
1	21.1	70	C1	4.11E-05	3.47E-04	4.64E-01	2.22E-01
2	29.4	85	C2	4.89E-05	4.91E-04	4.90E-01	1.52E-01
3	37.8	100	C2	1.12E-04	1.66E-03	5.31E-01	5.61E-01
4	43.3	110	C4	3.06E-04	1.24E-03	5.62E-01	1.55E+00
5	54.4	130	C3	1.27E-04	2.72E-03	3.49E-01	7.72E-01

TABLE 33   Creep Compliance Parameters of the K6-11 FWD Station.

No	Temperature		Case	Do	D1	m	SSE
	º C	º F					
1	21.1	70	C2	2.71E-05	1.97E-04	4.50E-01	2.10E-01
2	29.4	85	C2	1.16E-04	4.81E-04	5.11E-01	4.40E-01
3	37.8	100	C1	1.76E-04	1.14E-03	5.17E-01	6.20E-01
4	43.3	110	C4	2.40E-04	1.88E-03	5.41E-01	7.98E-01
5	54.4	130	C1	2.69E-11	2.66E-03	2.89E-01	5.43E-01

TABLE 34   Creep Compliance Parameters of the K6-23 FWD Station.

No	Temperature		Case	Do	D1	m	SSE
	° C	° F					
1	21.1	70	C4	3.56E-05	4.58E-04	3.24E-01	1.41E-01
2	29.4	85	C2	9.64E-05	3.51E-04	3.78E-01	4.26E-02
3	37.8	100	C3	2.76E-04	1.18E-03	4.27E-01	1.58E-01
4	43.3	110	C4	4.45E-04	1.69E-03	4.31E-01	2.29E-01
5	54.4	130	C2	8.31E-04	1.65E-03	4.69E-01	1.12E+00

TABLE 35   Creep Compliance Parameters of the K6-48 FWD Station.

No	Temperature		Case	Do	D1	m	SSE
	° C	° F					
1	21.1	70	C1	1.53E-04	4.01E-04	3.59E-01	4.34E-02
2	29.4	85	C4	2.05E-04	6.28E-04	3.96E-01	2.47E-01
3	37.8	100	C3	2.04E-04	6.30E-04	3.99E-01	2.29E-01
4	46.6	115	C2	3.08E-04	8.23E-04	4.41E-01	7.68E-01
5	54.4	130	C3	2.69E-11	2.13E-03	3.72E-01	8.33E-01

Lane K7

TABLE 36   Creep Compliance Parameters of the K7-11 FWD Station.

No	Temperature		Case	Do	D1	m	SSE
	° C	° F					
1	21.1	70	C2	2.69E-11	1.72E-04	4.08E-01	1.74E-01
2	29.4	85	C4	9.01E-05	4.79E-04	4.81E-01	1.87E-01
3	37.8	100	C4	8.74E-05	1.00E-03	5.42E-01	5.60E-01
4	43.3	110	C4	2.97E-04	1.53E-03	5.84E-01	1.10E+00
5	54.4	130	C3	7.75E-04	2.36E-03	5.18E-01	1.22E+00

TABLE 37   Creep Compliance Parameters of the K7-15 FWD Station.

No	Temperature		Case	Do	D1	m	SSE
	º C	º F					
1	21.1	70	C2	4.31E-05	2.58E-04	3.99E-01	1.55E-01
2	29.4	85	C2	5.91E-05	5.41E-04	4.41E-01	1.51E-01
3	37.8	100	C4	6.85E-05	6.51E-04	4.86E-01	7.87E-01
4	43.3	110	C4	1.47E-04	1.73E-03	4.96E-01	3.90E-01
5	54.4	130	C1	2.69E-11	3.26E-03	3.60E-01	4.06E-01

TABLE 38   Creep Compliance Parameters of the K7-20 FWD Station.

Nº	Temperature		Case	Do	D1	m	SSE
	º C	º F					
1	21.1	70	C2	1.57E-05	1.93E-04	3.93E-01	1.85E-01
2	29.4	85	C3	3.95E-05	3.25E-04	5.28E-01	4.43E-01
3	37.8	100	C4	3.39E-05	8.89E-04	6.61E-01	5.71E-01
4	43.3	110	C3	3.92E-05	1.35E-03	5.24E-01	3.32E-01

TABLE 39   Creep Compliance Parameters of the K7-31 FWD Station.

Nº	Temperature		Case	Do	D1	m	SSE
	º C	º F					
1	21.1	70	C2	1.25E-05	2.53E-04	3.50E-01	2.86E-01
2	29.4	85	C2	7.86E-05	3.75E-04	4.39E-01	1.52E-01
3	37.8	100	C3	1.02E-04	8.12E-04	4.93E-01	1.53E-01
3	43.3	110	C3	3.72E-04	1.17E-03	7.14E-01	2.13E+00
5	54.4	130	C1	3.71E-04	8.10E-04	9.88E-01	3.64E+00

TABLE 40   Creep Compliance Parameters of the K7-37 FWD Station.

No	Temperature		Case	Do	D1	m	SSE
	º C	º F					
1	21.1	70	C2	5.90E-06	1.15E-04	4.39E-01	2.73E-01
2	29.4	85	C1	2.60E-05	2.90E-04	4.63E-01	1.26E-01
3	37.8	100	C3	1.05E-04	9.87E-04	4.79E-01	9.33E-02
4	43.3	110	C2	1.31E-04	1.09E-03	5.78E-01	1.99E+00
5	54.4	130	C3	3.25E-04	2.90E-03	4.32E-01	6.60E-01

TABLE 41   Creep Compliance Parameters of K7-40 FWD Station.

Nº	Temperature		Case	Do	D1	m	SSE
	º C	º F					
1	21.1	70	C1	1.05E-04	4.48E-04	3.65E-01	9.51E-02
2	29.4	85	C1	9.53E-05	8.22E-04	3.81E-01	2.08E-01
3	37.8	100	C4	2.69E-11	1.47E-03	4.02E-01	1.20E+00
4	43.3	110	C1	6.26E-04	1.15E-03	5.05E-01	1.40E+00
5	54.4	130	C3	9.70E-04	1.38E-03	5.63E-01	1.85E+00

CHAPTER VII

TEMPERATURE CORRECTION OF BACKCALCULATED MODULUS

PREDICTION OF PAVEMENT TEMPERATURES

Before conducting the temperature correction of the backcalculated modulus it was necessary to set up which pavement temperatures would be used in this correction. This pavement temperature is based on the temperatures taken from the FWD collected data, which could be taken by direct measurements with a temperature probe or from predictive methods based on air and surface temperatures.

In the FWD survey, the operator took the surface pavement temperature at each station and the air temperatures were directly set up in the system of the FWD data. The pavement temperature was taken at 25 mm of depth below the AC surface, and was collected at every ten stations, from the first to the last FWD stations of each lane.

In TTI Research Report 1863-1 was developed software that assists in the prediction of pavement temperatures at different depths, Modulus Temperature Correction Program (MTCP) (*17*), (*18*). MTCP was utilized in this study to predict the pavement temperatures. MTCP uses the infrared surface temperature and the previous day's average air temperature to predict the pavement temperature at given depth, d.

The depth from the surface employed in this study, to predict pavement temperatures, was at the middle of the AC thickness.The surface pavement temperature was measured with a calibrated infrared surface temperature gauge and the previous day's average air temperature was found through the Texas Office of State Climatologist of the Texas A&M University.

To get a prediction of the pavement temperature, the MTCP should select one of three equations: the BELLS2, the BELLS3 and the Texas-LTPP. According to recommendations by the TTI Research Report 1863-1, the Texas-LTPP equation was

chosen due to this model's showing the least bias among than the other equations studied in that report.

Because the backcalculated moduli was determined by each FWD station, the prediction of the pavement temperature at the middle of the AC thickness was also carried out by each FWD stations using the MTCP software. Consequently, there is a predicted pavement temperature for each set of FWD data at each of the FWD stations in both lanes K6 and K7 that were taken in the period from 2001 to 2003. Tables 42 and 43 shows the predicted temperatures by month obtained by MTCP in both K6 and K7 lanes.

TABLE 42   Predicted Pavement Temperatures (^{o}C) for the K6 Lane.

Section	FWD	2001				2002		
	Station	Feb	May	Jul	Aug	Mar	Jul	Dec
K6-A	6-1	31	37	43	48	39	39	27
K6-B	6-2	26	36	43	48	39	40	27
K6-D	6-3	26	37	43	47	38	40	27
K6-D	6-4	26	38	45	50	39	41	26
K6-D	6-5	26	37	43	48	38	40	27
K6-D	6-6	26	37	44	48	38	40	27
K6-D	6-7	27	38	44	49	38	40	26
K6-D	6-8	27	37	43	47	*	40	27
K6-D	6-9	28	39	45	50	*	*	*
K6-D	6-10	27	39	44	49	39	41	26
K6-D	6-11	28	38	46	48	38	41	26
K6-D	6-12	28	38	46	48	38	41	26
K6-E	6-13	28	38	46	48	38	41	26
K6-E	6-14	27	39	46	49	39	42	27
K6-F	6-15	27	39	46	49	39	42	27
K6-F	6-16	27	38	45	48	38	41	27
K6-F	6-17	27	38	45	48	39	41	27
K6-F	6-18	27	39	46	49	39	43	27
K6-F	6-19	27	39	46	49	39	42	27
K6-F	6-20	28	39	46	49	39	42	27
K6-F	6-21	28	39	44	49	38	42	27
K6-F	6-22	28	39	44	48	38	42	27
K6-F	6-23	28	39	45	50	38	42	27
K6-G	6-24	27	38	44	48	38	41	27
K6-G	6-25	27	38	44	48	38	41	27
K6-G	6-26	27	38	44	48	38	41	27
K6-H	6-27	28	39	44	49	38	41	27
K6-H	6-28	28	39	44	49	38	41	27

TABLE 42   Continued

Section	FWD Station	2001				2002		
		Feb	May	Jul	Aug	Mar	Jul	Dec
K6-H	6-29	29	39	45	49	38	41	27
K6-H	6-30	29	39	45	49	38	41	27
K6-H	6-31	29	40	46	51	39	43	27
K6-H	6-32	28	39	45	49	39	42	27
K6-H	6-33	29	41	47	52	39	*	27
K6-H	6-34	29	42	47	52	39	44	27
K6-H	6-35	29	40	46	50	39	42	27
K6-H	6-36	29	40	46	50	39	42	27
K6-H	6-37	28	40	45	50	39	42	27
K6-H	6-38	30	41	47	52	39	44	27
K6-I	6-39	28	39	45	49	39	43	27
K6-J	6-40	28	39	45	49	38	42	27
K6-K	6-41	30	41	46	51	38	43	27
K6-K	6-42	30	40	45	49	38	43	27
K6-L	6-43	30	42	46	52	38	44	27
K6-L	6-44	28	40	44	49	39	42	27
K6-L	6-45	30	41	45	50	45	44	27
K6-L	6-46	30	42	46	52	46	46	26
K6-L	6-47	30	42	46	52	39	46	27
K6-L	6-48	28	39	44	48	39	43	27
K6-L	6-49	27	38	43	46	39	41	28
K6-M	6-50	28	39	43	48	39	43	27
K6-O	6-51	29	42	46	51	39	46	27
K6-O	6-52	29	41	45	50	39	45	27
K6-O	6-53	28	39	44	48	39	43	27
K6-O	6-54	28	39	44	48	39	43	28
K6-O	6-55	28	39	44	49	39	43	28
K6-P	6-56	29	41	44	50	48	45	27

* No Data

TABLE 43   Predicted Pavenment Temperatures (^oC) for the K7 Lane.

Section	FWD Stations	2001			2002				2003
		Feb	May	Aug	Mar	Jul	Oct	Dec	Apr
K7-A	K7-1	28	36	42	33	45	37	25	*
K7-A	K7-2	28	36	42	33	44	37	26	34
K7-A	K7-3	28	37	42	33	46	37	26	35
K7-A	K7-4	28	36	42	33	45	40	26	35
K7-A	K7-5	29	37	42	33	48	42	26	35
K7-A	K7-6	29	37	*	33	45	41	26	35
K7-A	K7-7	29	38	42	33	47	42	26	35
K7-A	K7-8	29	37	42	*	*	*	*	*
K7-A	K7-9	29	37	42	*	*	*	*	*
K7-A	K7-10	29	38	42	33	47	42	26	36
K7-A	K7-11	28	37	42	33	45	*	26	35
K7-A	K7-12	29	38	42	33	46	*	26	36
K7-A	K7-13	32	39	42	34	47	43	26	36
K7-A	K7-14	32	37	42	33	45	42	26	35
K7-A	K7-15	31	37	42	33	44	42	26	35
K7-A	K7-16	32	38	42	33	46	43	26	35
K7-A	K7-17	32	39	42	32	47	43	26	36
K7-A	K7-18	32	39	43	33	47	44	26	36
K7-A	K7-19	32	37	42	33	45	42	26	35
K7-A	K7-20	32	42	34	46	45	26	35	*
K7-A	K7-21	32	38	42	33	45	42	26	35
K7-A	K7-22	32	38	43	33	45	26	36	*
K7-A	K7-23	32	38	42	33	45	42	26	36
K7-A	K7-24	32	37	42	33	44	41	26	35
K7-A	K7-25	32	39	43	34	46	42	26	36
K7-A	K7-26	32	38	42	34	45	41	26	36
K7-A	K7-27	32	38	42	34	45	42	26	36
K7-A	K7-28	32	38	42	34	46	42	26	36
K7-A	K7-29	32	38	42	35	42	26	36	*
K7-A	K7-30	32	38	43	35	46	42	26	37
K7-A	K7-31	32	39	43	37	48	42	26	38
K7-A	K7-32	32	39	43	35	47	42	26	37
K7-A	K7-33	32	40	43	36	47	43	26	38
K7-A	K7-34	33	39	43	34	46	41	26	36
K7-A	K7-35	33	39	42	36	46	43	26	38
K7-A	K7-36	33	39	42	35	47	43	26	37
K7-B	K7-37	33	39	43	34	46	41	26	36
K7-C	K7-38	33	40	43	35	47	42	26	37
K7-D	K7-39	33	38	43	34	45	40	26	36
K7-E	K7-40	33	37	42	34	45	41	26	35
K7-E	K7-41	33	38	42	33	45	41	26	36
K7-E	K7-42	33	39	42	33	44	41	26	36
K7-E	K7-43	33	39	42	34	45	41	26	*
K7-E	K7-44	33	40	42	34	45	41	26	37

TABLE 43 Continued

Section	FWD Stations	2001			2002				2003
		Feb	May	Aug	Mar	Jul	Oct	Dec	Apr
K7-E	K7-45	33	40	42	34	46	42	26	37
K7-E	K7-46	33	42	44	35	48	44	26	39
K7-F	K7-47	33	42	43	35	46	42	26	38
K7-F	K7-48	33	42	43	35	46	42	26	38
K7-F	K7-49	34	42	44	35	48	43	26	39
K7-F	K7-50	34	42	44	35	48	42	26	38

VARIATION OF THE BACKCALCULATED AC MODULUS WITH TEMPERATURE

Even though there is a large number of stations analyzed (106 stations), only the core stations are plotted in these section. Figures 50 through 64 show the backcalculated AC moduli variation due to the predicted pavement temperature in each the core stations. In these figures are presented the results from the static analysis and the dynamic (complex) modulus obtained through laboratory tessting.

Lane K6
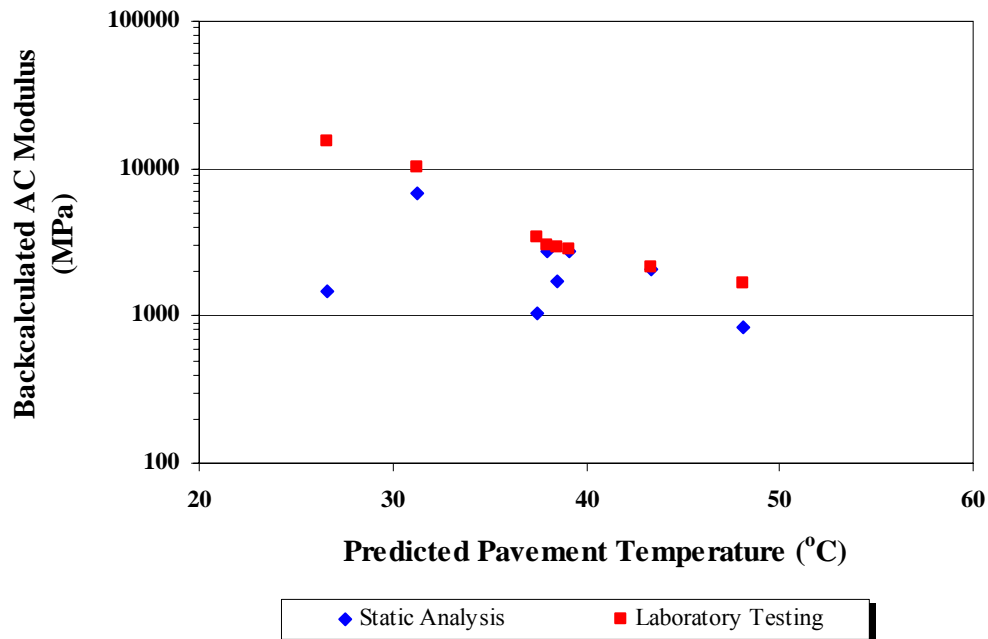
FIGURE 50 Variation of Backcalculated AC Modulus. K6-1 FWD Station.
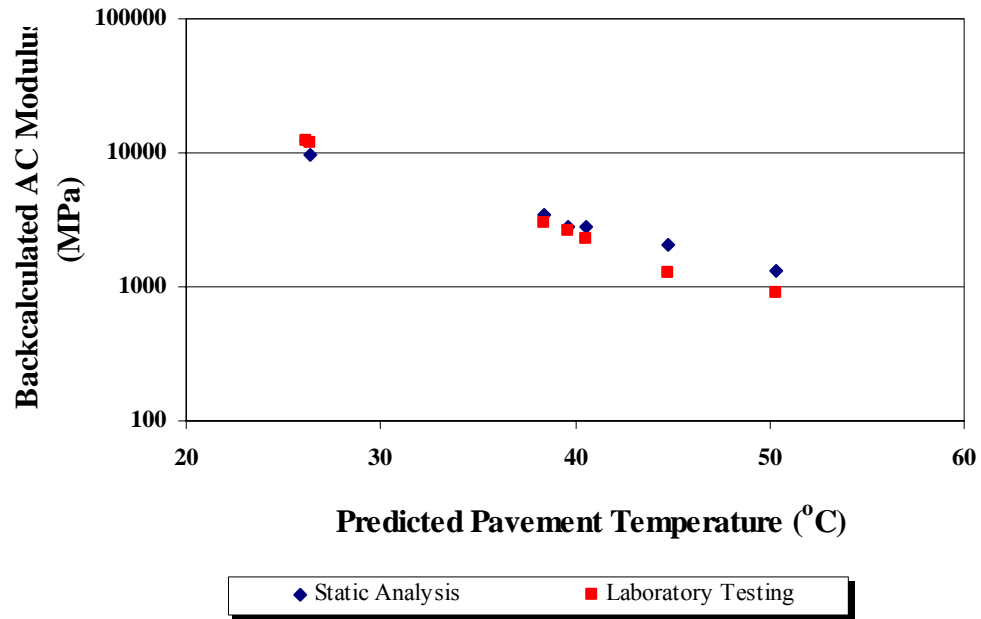
FIGURE 51   Variation of Backcalculated AC Modulus. K6-4 FWD Station.
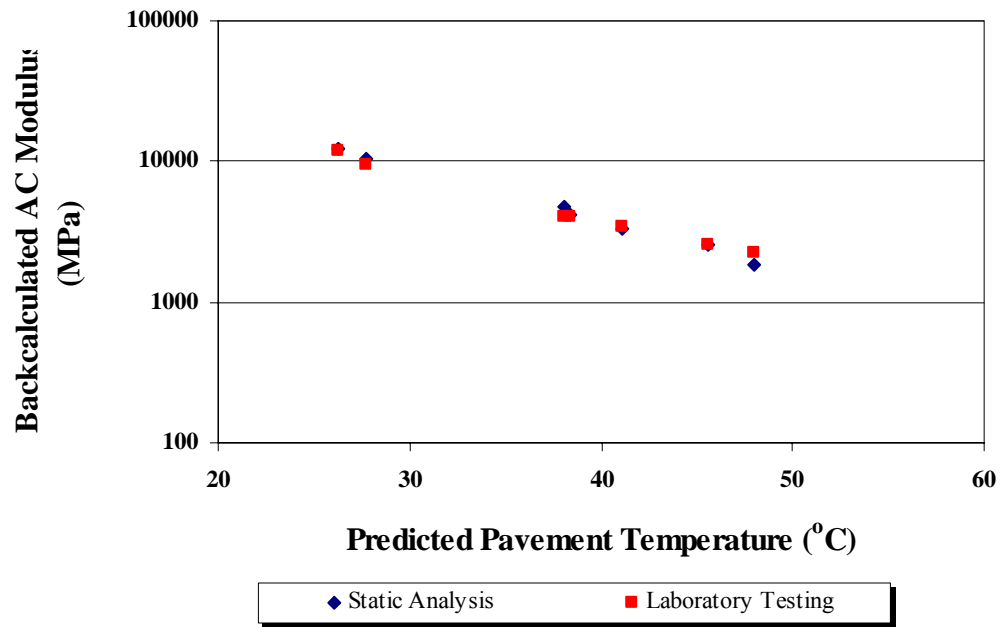
FIGURE 52   Variation of Backcalculated AC Modulus. K6-11 FWD Station.
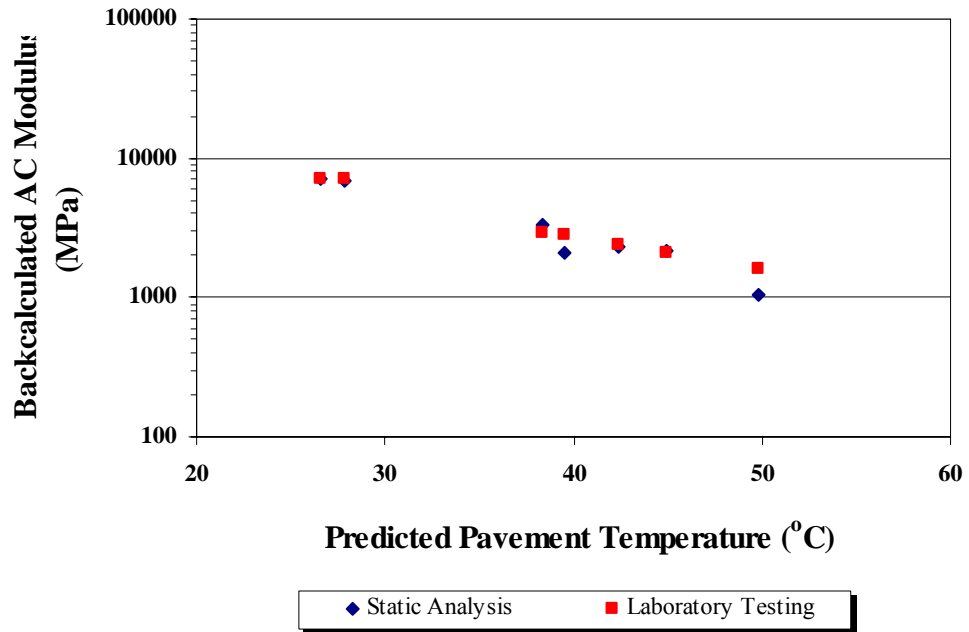
FIGURE 53   Variation of Backcalculated AC Modulus. K6-23 FWD Station.
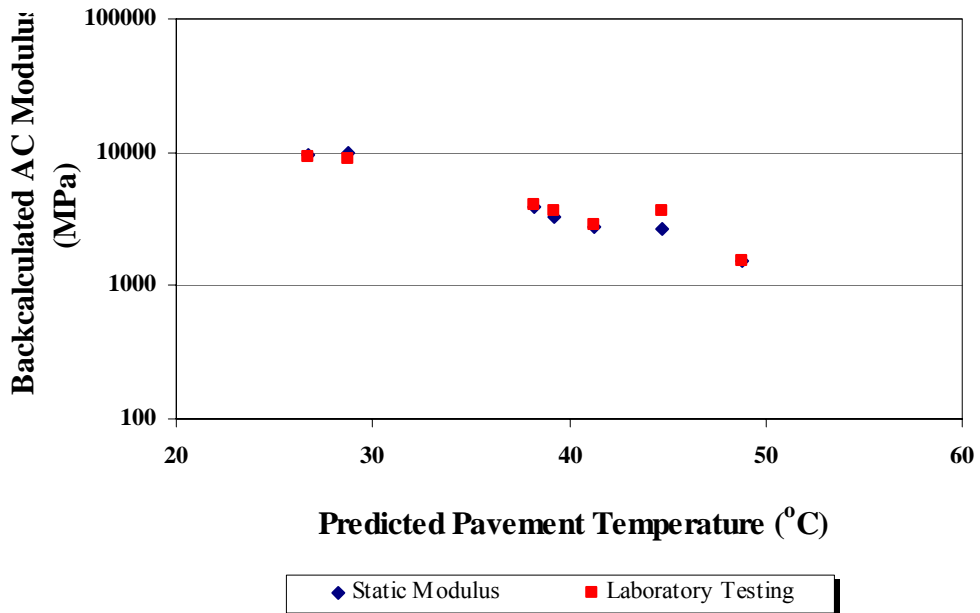
FIGURE 54   Variation of Backcalculated AC Modulus. K6-29 FWD Station.
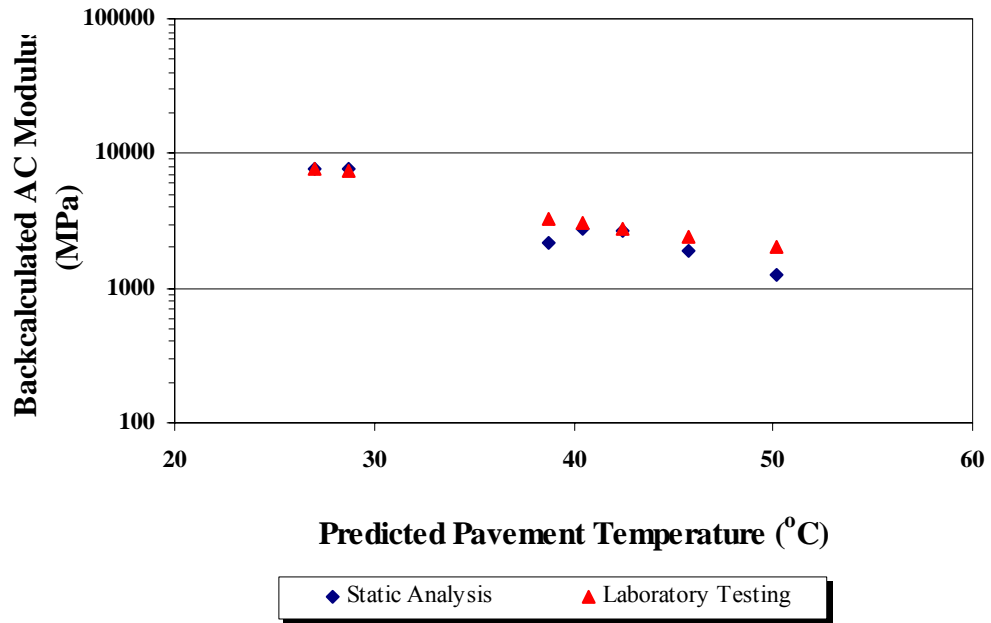
FIGURE 55   Variation of Backcalculated AC Modulus. K6-35 FWD Station.
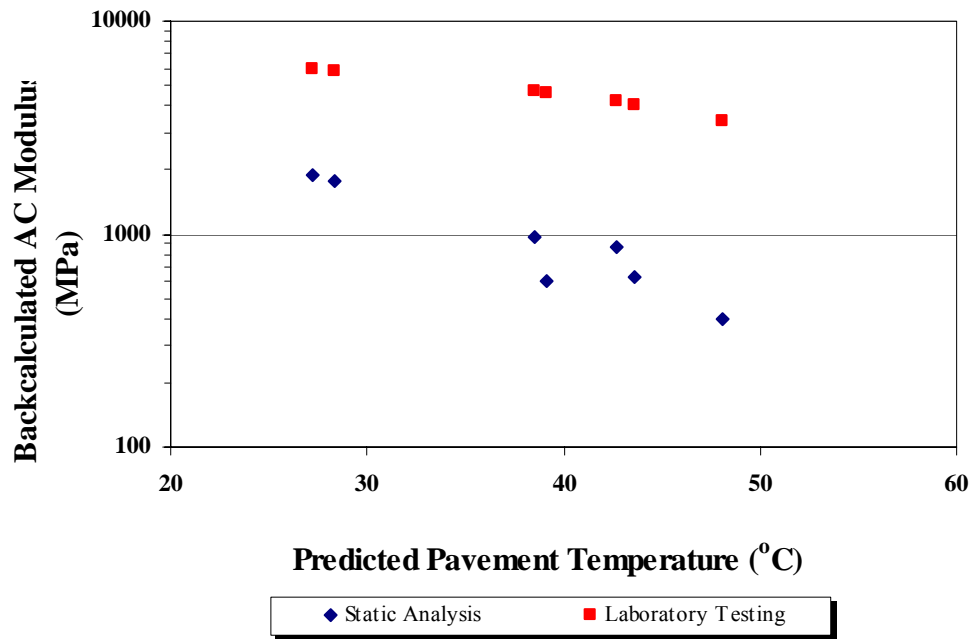
FIGURE 56   Variation of Backcalculated AC Modulus. K6-48 FWD Station.

Lane K7
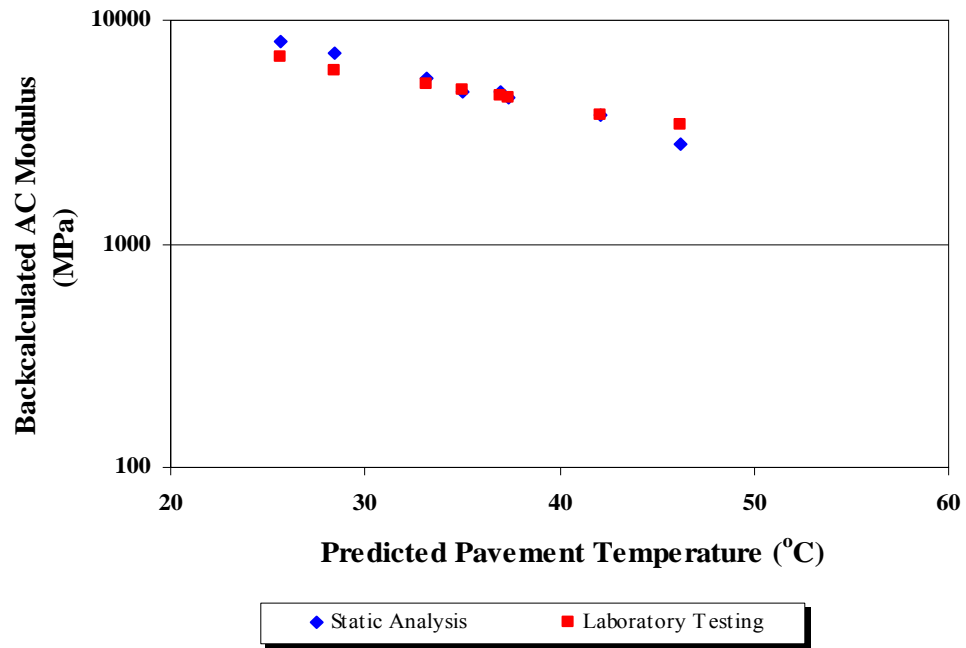
FIGURE 57   Variation of Backcalculated AC Modulus. K7-3 FWD Station.
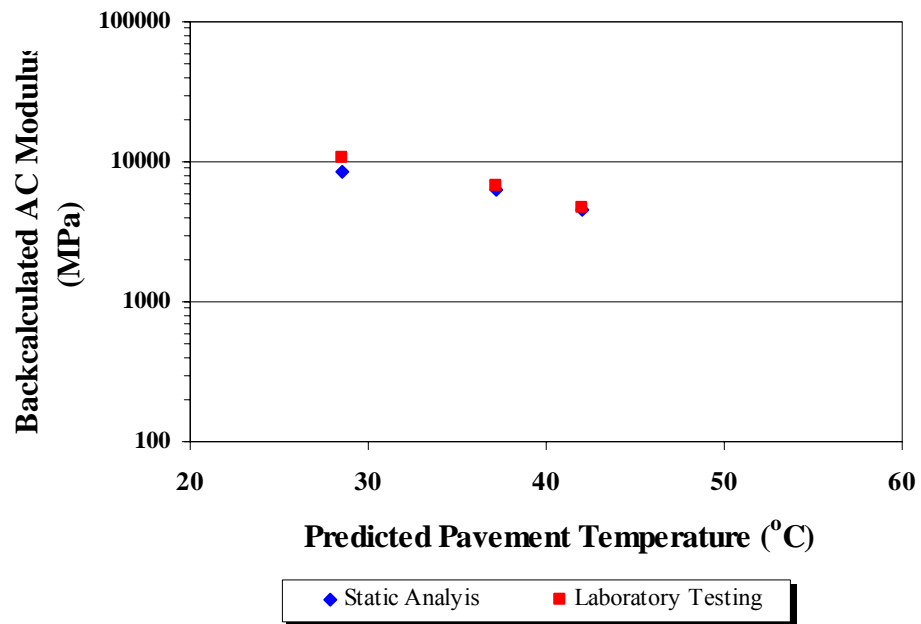
FIGURE 58   Variation of Backcalculated AC Modulus. K7-9 FWD Station.
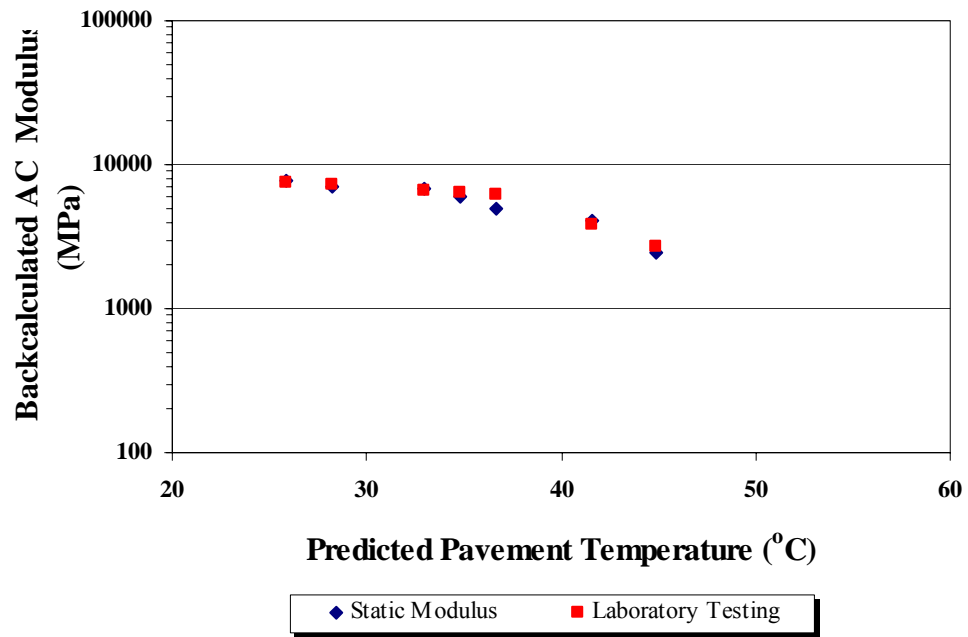
FIGURE 59   Variation of Backcalculated AC Modulus. K7-11 FWD Station.
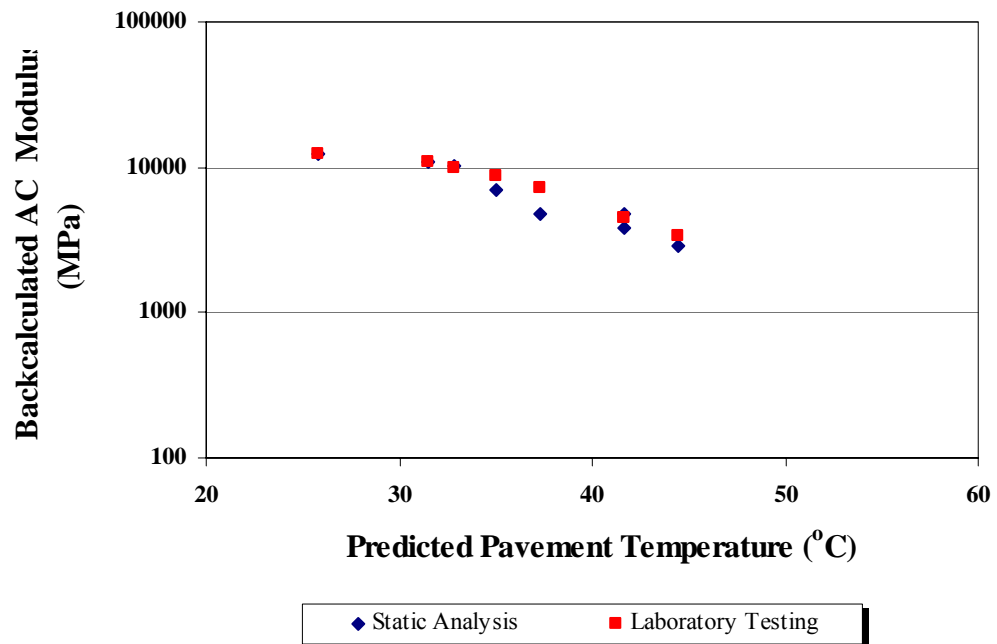
FIGURE 60   Variation of Backcalculated AC Modulus. K7-15 FWD Station.
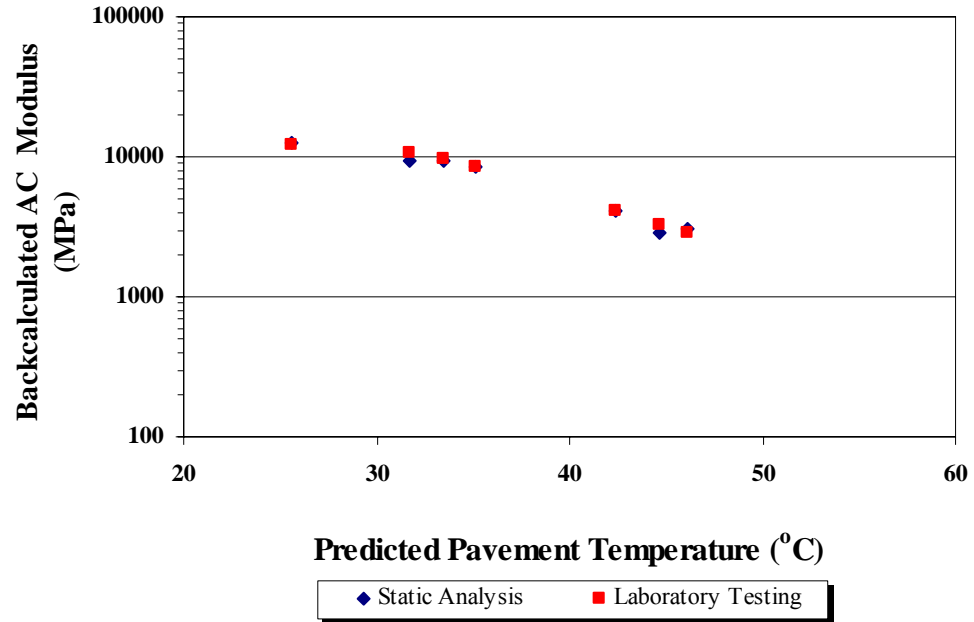
FIGURE 61   Variation of Backcalculated AC Modulus. K7-20 FWD Station.
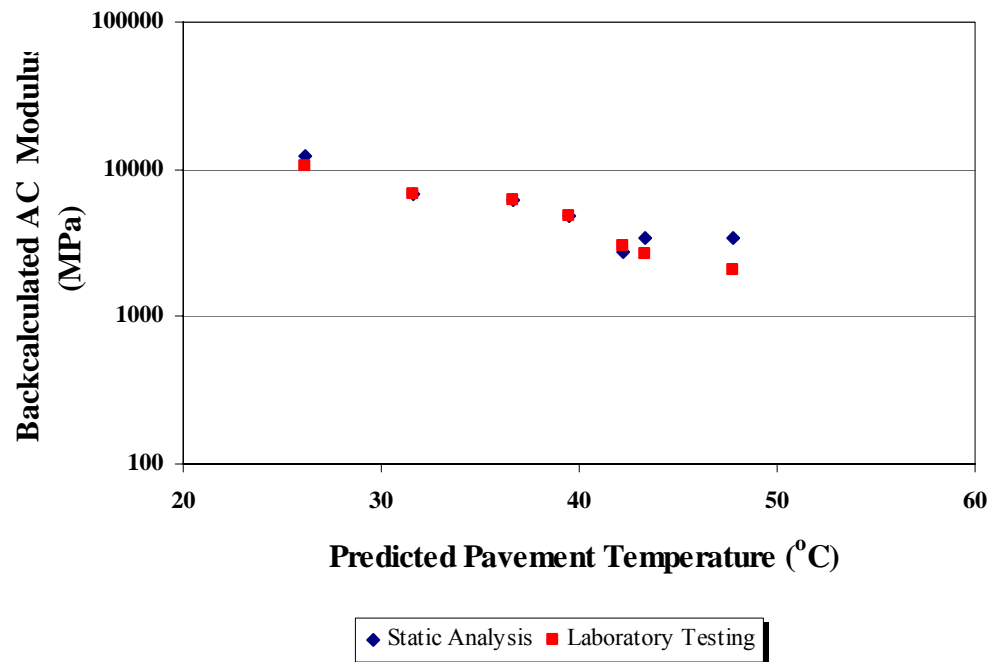
FIGURE 62   Variation of Backcalculated AC Modulus. K7-31 FWD Station.
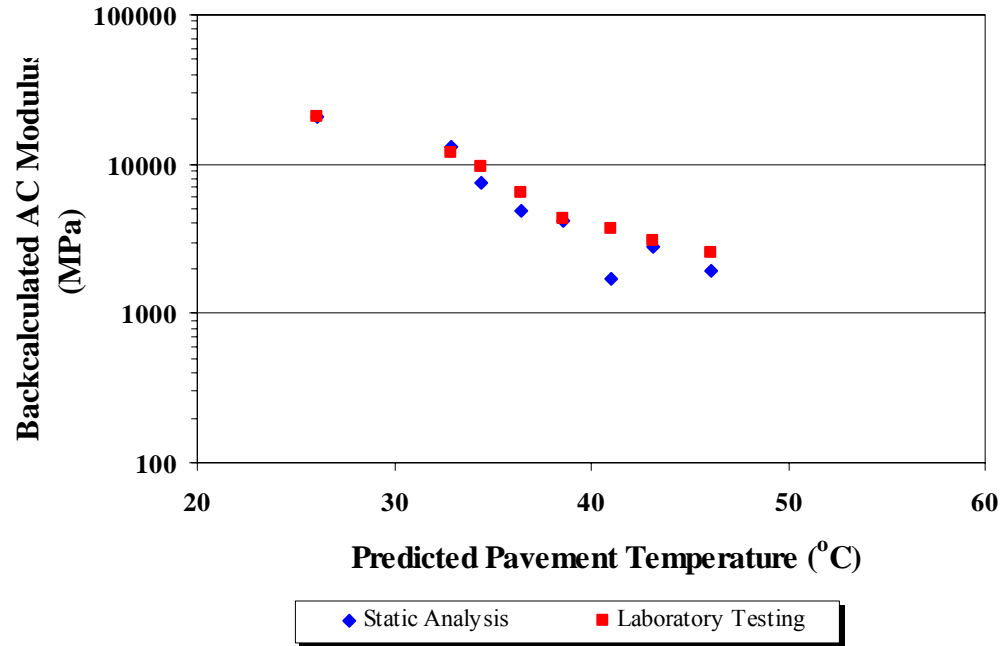
FIGURE 63   Variation of Backcalculated AC Modulus. K7-37 FWD Station.
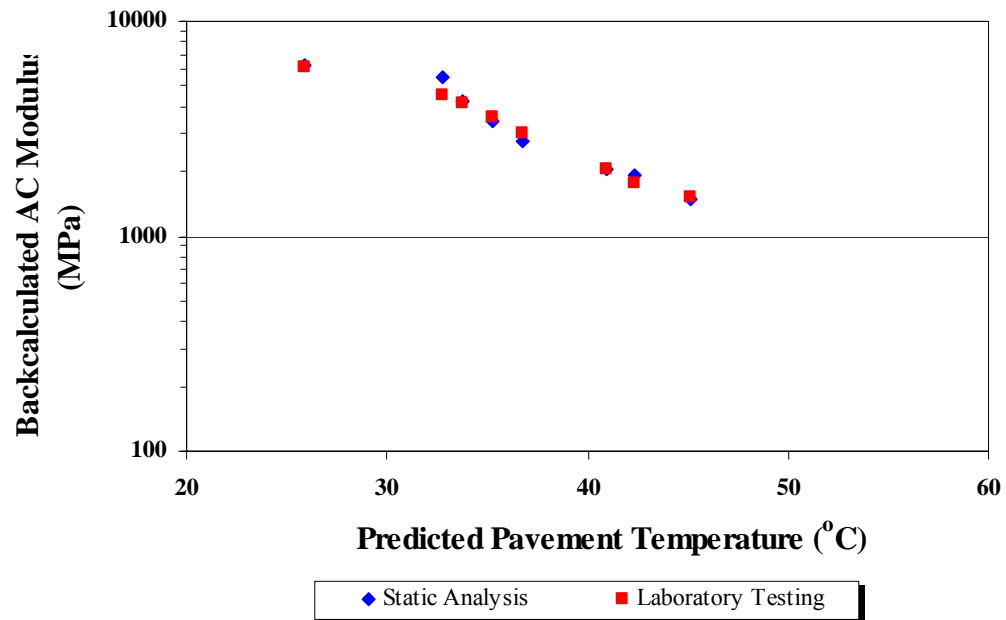
FIGURE 64   Variation of Backcalculated AC Modulus. K7-40 FWD Station.

SELECTION OF THE PAVEMENT GROUPS.

To facilitate the better interpretation of the results of backcalculated AC modulus, it was necessary to group the FWD stations of both lanes K6 and K7. The criteria to select these pavement groups was based on two major aspects:

- the physical proximity of the FWD stations, and
- the points from the plot of the backcalculated modulus versus the predicted pavement temperature of the group should have the same trend.

Once these criteria were applied to the results, the route was divided into seven pavement groups. They are:

Pavement Group 1: From FM 511 to Coffee Port Rd.

        Lane K6: FWD Stations from K6-1 to K6-15

        Lane K7: FWD Stations from K7-1 to K7-15

Pavement Group 2: From Coffee Port Rd. to Dunlap St.

        Lane K6: FWD Stations from K6-6 to K6-18

        Lane K7: FWD Stations from K7-16 to K7-17

Pavement Group 3: From Dunlap St. to Central Ave.

        Lane K6: FWD Stations from K6-19 to K6-23

        Lane K7: FWD Stations from K7-18 to K7-21

Pavement Group 4: From Central Ave. to Austin Rd.

        Lane K6: FWD Stations from K6-24 to K6-26

        Lane K7: FWD Stations from K7-22 to K7-23

Pavement Group 5: From Austin Rd. to Fruitdale Rd.

        Lane K6: FWD Stations from K6-27 to K6-36

        Lane K7: FWD Stations from K7-24 to K7-33

Pavement Group 6: Fruitdale Rd. to Boca Chica Blvd.

        Lane K6: FWD Stations from K6-37 to K6-41

        Lane K7: FWD Stations from K7-34 to K7-37

Pavement Group 7: From Boca Chica Blvd. to Cleveland St.

Lane K6: FWD Stations from K6-42 to K6-56

Lane K7: FWD Stations from K7-38 to K7-50

SELECTION OF THE TEMPERATURE CORRECTIONS METHODS

The temperature corrections methods used in the current study are as follows:

- The Chen equation uses FWD and pavement temperature data collected from TxDOT's Mobile Load Simulator (MLS) investigations.

$$E_{Tr} = E_T \left(T/T_r \right)^{2.4462} \qquad (7.1)$$

where

E_{Tr} : the modulus corrected to a reference temperature of T_r (^{o}F)

E_T : the modulus determined from testing at a temperature of T (^{o}F)

- The existing TX DOT equation used in the Flexible Pavement System (FPS) and load zoning analysis programs

$$E_{75} = E_T \left(T^{2.81} \right) / 185000 \qquad (7.2)$$

where

E_{75} : the modulus corrected to a temperature of 75 ^{o}F

E_T : the modulus determined from testing at a temperature of T (^{o}F)

- The Witczak and Fonseca equation (1996), which is proposed as a method for predicting the dynamic modulus in the AASHTO 2002 pavement design guide.

$$\log_{10} E = -0.261 + 0.008225 p_{200} - 0.0000010 (p_{200})^2 + 0.00196 p_4$$
$$- 0.03157 V_a - 0.415 \frac{V_{beff}}{(V_{beff} + V_a)}$$
$$+ \frac{\left[1.87 + 0.002808 p_4 + 0.0000404 p_{3/8} - 0.0001786 (p_{3/8})^2 + 0.0164 p_{3/4} \right]}{1 + e^{\left(-0.716 \log_{10} f - 0.7425 \log_{10} \eta \right)}} \qquad (7.3)$$

where

E : asphalt mix dynamic modulus, 10^5 psi;

η : bitumen viscosity at a given temperature and degree of aging, 10^6 poises;

f : loading frequency in Hz;

Va   : percent of air voids by volume;

V_{beff} : percent of effective binder content by volume;

$p_{3/4}$: percent retained on a ¾-inch sieve by the total aggregate weight;

$p_{3/8}$: percent retained on a 3/8-inch sieve by the total aggregate weight;

p_4 : percent retained on a No 4 sieve by the total aggregate weight;

p_{200} : percent retained on a No 200 sieve by the total aggregate weight;

From the Witczak and Fonseca equation the following equation is derived for temperature correction (*17*):

$$\log_{10} E_R = \log_{10} E_T + \alpha \left[\frac{1}{1 + e^{-(B_R + 0.7425 \log_{10} \eta_R)}} - \frac{1}{1 + e^{-(B_T + 0.7425 \log_{10} \eta_T)}} \right] \qquad (7.4)$$

where

α : $1.87 + 0.003\, p_4 + 0.00004\, p_{3/8} - 0.00018\, (p_{3/8})^2 + 0.0164\, p_{3/4}$

B_R : $0.716 \log 10\, f_R$

B_T : $0.716 \log 10\, f_T$

E_R : the AC modulus corrected for the selected reference temperature and loading frequency.

E_T : the measured backcalculated asphalt concrete modulus;

η_R : the binder viscosity corresponding to the reference temperature in 10^6 poises,

η_T : binder viscosity corresponding to the test temperature in 10^6 poises,

p_4 : the cumulative percent retained in a No. 4 sieve by the total aggregate weight;

$p_{3/8}$: the cumulative percent retained in a No. 3/8-inch sieve by the total aggregate weight;

$p_{3/4}$: the cumulative percent retained in a 3/4-inch sieve by the total aggregate weight;

f_R : the reference loading frequency in Hz; and

f_T : the test loading frequency in Hz.

In these three equations, the basic AC mixtures properties are included. The binder viscosities corresponding to test and reference temperatures are employed, to correct the measured or backcalculated moduli to specific reference temperatures.

To get the viscosity-temperature relationship for the binder used in the AC mix the equation from American Society for Testing and Material, standard ASTM-D2493 is used.

$$\log_{10} \log_{10} \eta = A + VTS \log_{10} T\,^{\circ}_R \qquad (7.5)$$

where

η : the binder viscosity in centipoises;

$T\,^{\circ}_R$: the temperature in degrees Rankine;

A and VTS: the model coefficients determined from testing.

EVALUATION OF THE BINDER-VISCOSITY RELATIONSHIP

As it was said previously it was necessary to find the parameters A, VTS, and the binder viscosity to get a corrected modulus. In this study the DSR test was not done, however the values of the parameters can be obtained by regression analysis using this formula:

$$y = \delta + \frac{\alpha}{1 + e^{(\beta - \gamma x)}} \qquad (7.6)$$

where

y : $\log_{10} E$;

δ, α : the coefficients (functions of the volumetric mixture   properties);

β : -0.716 $\log_{10} f$;

f : $1/2\pi t$;

γ : 0.7425; and

x : $\log_{10} \eta$.

Equation 7.6 was developed as a function of the test temperature using equation 7.5. Employing SAS sofware, Eq 7.6 was solved by nonlinear regression to find the coefficients A, VTS, δ and α. Since there were no data from volumetric mixture

properties from the laboratory testing conducted for this project, a range of δ and α were obtained from the LTPP database and the results from the TTI Research Report 1863-1. These ranges were used as boundaries values in the nonlinear regression analysis to obtain the coefficients.

Tables 44 and 45 show the coefficients obtained by the nonlinear regression of each group for lanes K6 and K7. Tables 46 and 47 show the results of analysis of the variance (ANOVA) in these regression analyses. Being the p value < 0.001, these regression equations may be aceptable. Figures 65 to 79 show a comparison between the predicted AC modulus using the Witczak and Fonseca equation (Eq. 7.6) and backcalculated AC modulus**.**

TABLE 44   Coefficients of the Binder-Viscosity Relationship for the K6 Lane.

Pavement Group	Range of Fwd Stations	A	VTS	α	δ
1	K6 1 to K6 15	11.122	-3.747	2.587	-0.500
2	K6 16 to K6 18	8.987	-3.000	3.000	-0.510
3	K6 19 to K6 23	9.011	-3.000	3.000	-0.202
4	K6 24 to K6 26	9.000	-2.989	2.474	-0.511
5	K6 27 to K6 36	10.000	-3.343	2.662	-0.500
6	K6 37 to K6 41	12.171	-4.247	6.790	0.141
7	K6 42 to K6 56	10.000	-3.380	2.521	-0.500

TABLE 45   Coefficients of the Binder-Viscosity Relationship of the K7 Lane.

Pavement Group	Range of FWD Stations	A	VTS	α	δ
1	K7 1 to K7 15	10.367	-3.464	2.450	-0.50
2	K7 16 to K7 17	10.000	-3.335	2.856	-0.51
3	K7 18 to K7 21	10.000	-3.331	2.605	-0.50
4	K7 22 to K7 23	10.000	-3.324	2.450	-0.50
5	K7 24 to K7 33	10.335	-3.449	2.450	-0.50
6	K7 34 to K7 37	10.000	-3.338	2.771	-0.50
7	K7 38 to K7 50	12.011	-4.080	2.451	-0.50
C6	K6 -4 Station	8.918	-3	-3	-0.26

TABLE 46   Analysis of Variance of Non-linear Regression for the K6 Lane.

Pavement Group	Source	DF	Sum of Squares	Mean Squares	F Value	Approx Pr > F
1	Regression	3	68.07	22.69	1015.13	<.0001
	Residual	99	2.21	0.02		
	Uncorrected Total	102	70.29			
	Corrected Total	101	11.14			
2	Regression	3	3.48	1.16	15.54	0.0001
	Residual	18	0.58	0.03		
	Uncorrected Total	21	4.06			
	Corrected Total	20	1.58			
3	Regression	3	23.58	7.86	109.15	<.0001
	Residual	32	0.37	0.01		
	Uncorrected Total	35	23.95			
	Corrected Total	34	2.90			
4	Regression	3	5.85	1.95	9.69	0.0014
	Residual	18	2.27	0.13		
	Uncorrected Total	21	8.13			
	Corrected Total	20	4.72			
5	Regression	3	36.27	12.09	828.40	<.0001
	Residual	66	0.96	0.01		
	Uncorrected Total	69	37.23			
	Corrected Total	68	6.02			
6	Regression	4	11.37	2.84	9.24	0.0002
	Residual	31	1.09	0.04		
	Uncorrected Total	35	12.46			
	Corrected Total	34	2.06			
7	Regression	3	5.05	1.68	42.43	<.0001
	Residual	102	4.05	0.04		
	Uncorrected Total	105	9.10			
	Corrected Total	104	8.92			

TABLE 47   Analysis of Variance of Non-linear Regression for the K7 Lane.

Pavement Group	Source	DF	Sum of Squares	Mean Squares	F Value	Approx Pr > F
1	Regression	4	90.28	22.57	122.2	<.0001
	Residual	102	0.87	0.01		
	Uncorrected Total	106	91.16			
	Corrected Total	105	4.01			
2	Regression	3	16.06	5.35	81.9	<.0001
	Residual	13	0.09	0.01		
	Uncorrected Total	16	16.14			
	Corrected Total	15	1.16			
3	Regression	3	29.44	9.81	1602.8	<.0001
	Residual	28	0.17	0.01		
	Uncorrected Total	31	29.61			
	Corrected Total	30	1.98			
4	Regression	2	15.88	7.94	1743.0	<.0001
	Residual	13	0.06	0.00		
	Uncorrected Total	15	15.93			
	Corrected Total	14	0.69			
5	Regression	3	69.88	23.29	2782.2	<.0001
	Residual	76	0.64	0.01		
	Uncorrected Total	79	70.52			
	Corrected Total	78	4.44			
6	Regression	3	25.48	8.49	46.1	<.0001
	Residual	29	0.88	0.03		
	Uncorrected Total	32	26.35			
	Corrected Total	31	3.66			
7	Regression	4	32.84	8.21	268.3	<.0001
	Residual	99	3.03	0.03		
	Uncorrected Total	103	35.87			
	Corrected Total	102	8.65			
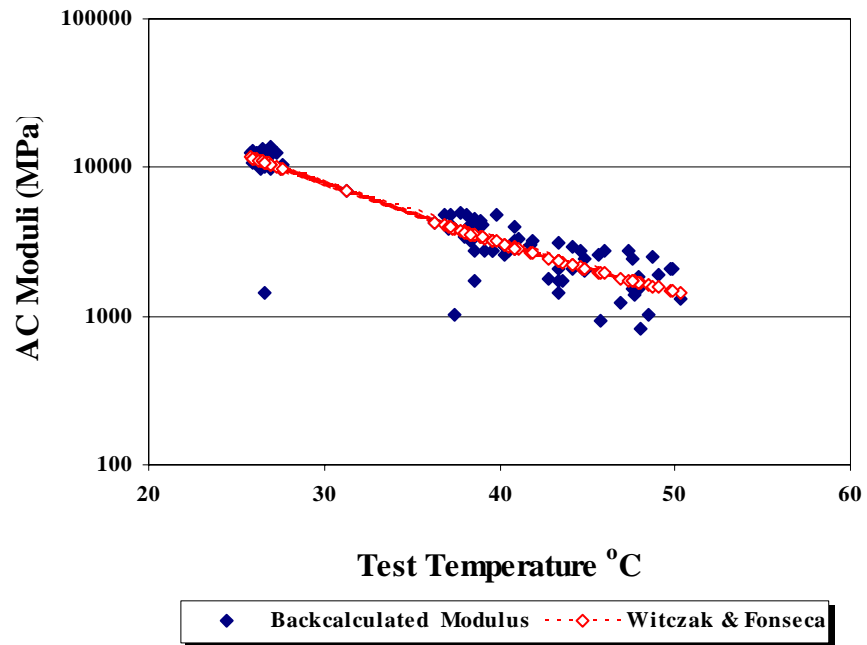
FIGURE 65   **Comparison of the Backcalculated AC Modulus with Eq 7.6. Pavement Group 1 of the K6 Lane.**
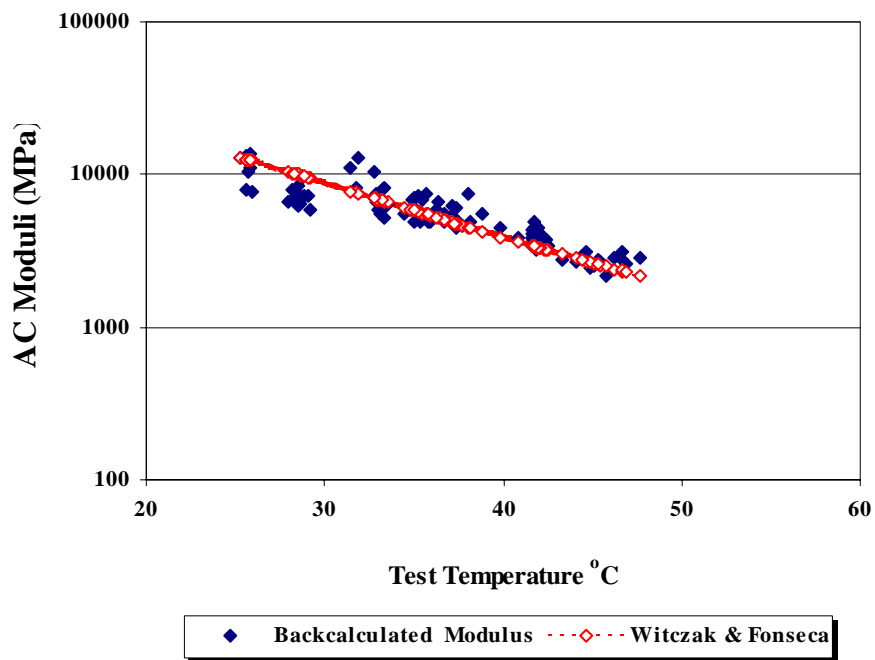
FIGURE 66   **Comparison of the Backcalculated AC Modulus with Eq 7.6. Pavement Group 1 of the K7 Lane.**
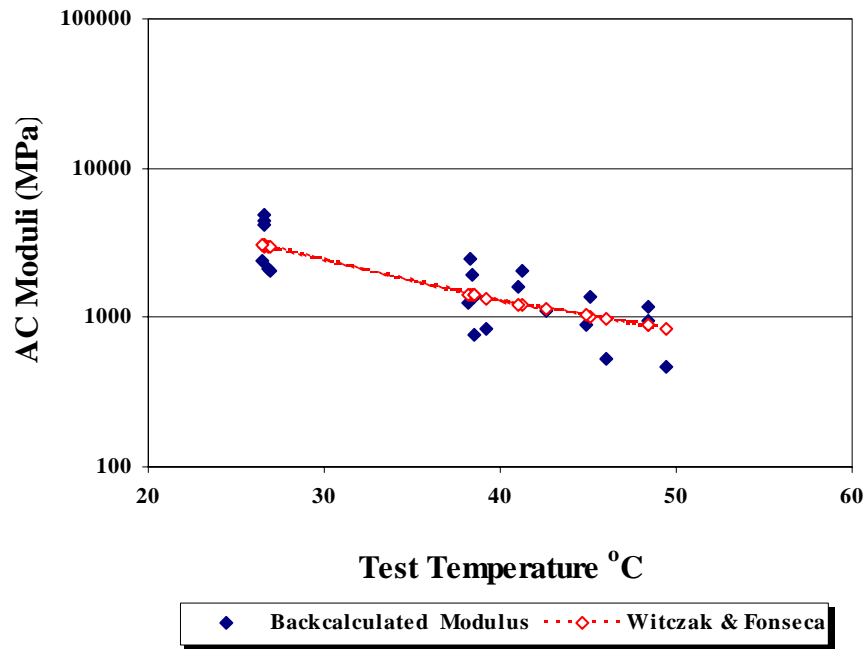
FIGURE 67   Comparison of the Backcalculated AC Modulus with Eq 7.6. Pavement Group 2 of the K6 Lane.
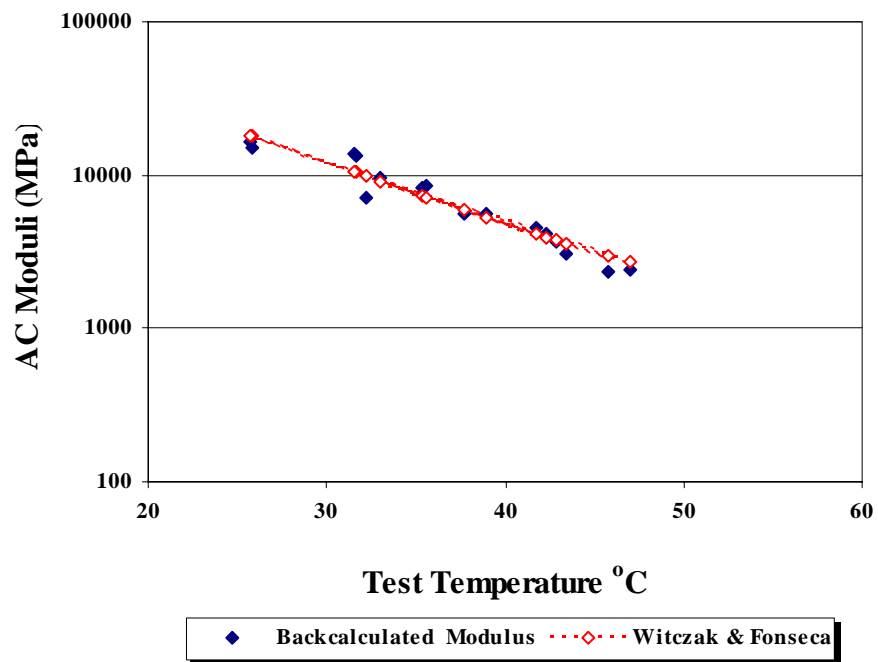
FIGURE 68   Comparison of the Backcalculated AC Modulus with Eq 7.6. Pavement Group 2 of the K7 Lane.
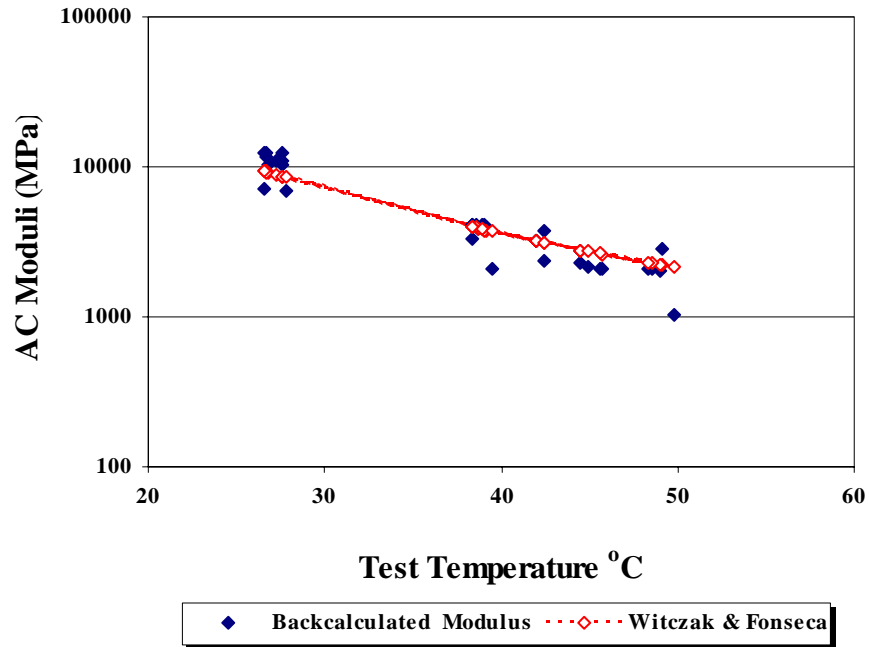
FIGURE 69   Comparison of the Backcalculated AC Modulus with Eq 7.6. Pavement Group 3 of the K6 Lane.
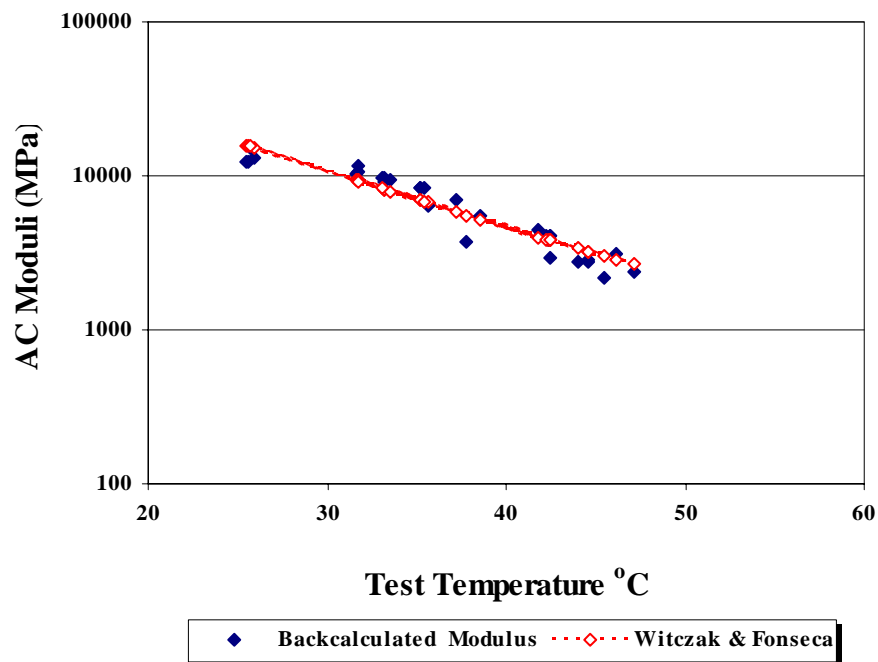
FIGURE 70   Comparison of the Backcalculated AC Modulus with Eq 7.6. Pavement Group 3 of the K7 Lane.
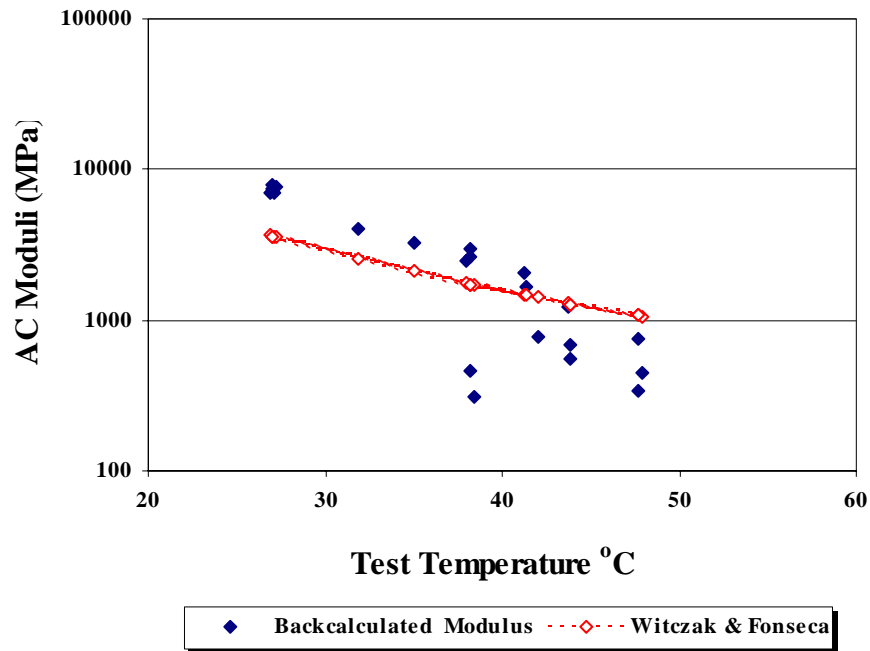
FIGURE 71 **Comparison of the Backcalculated AC Modulus with Eq 7.6. Pavement Group 4 of the K6 Lane.**
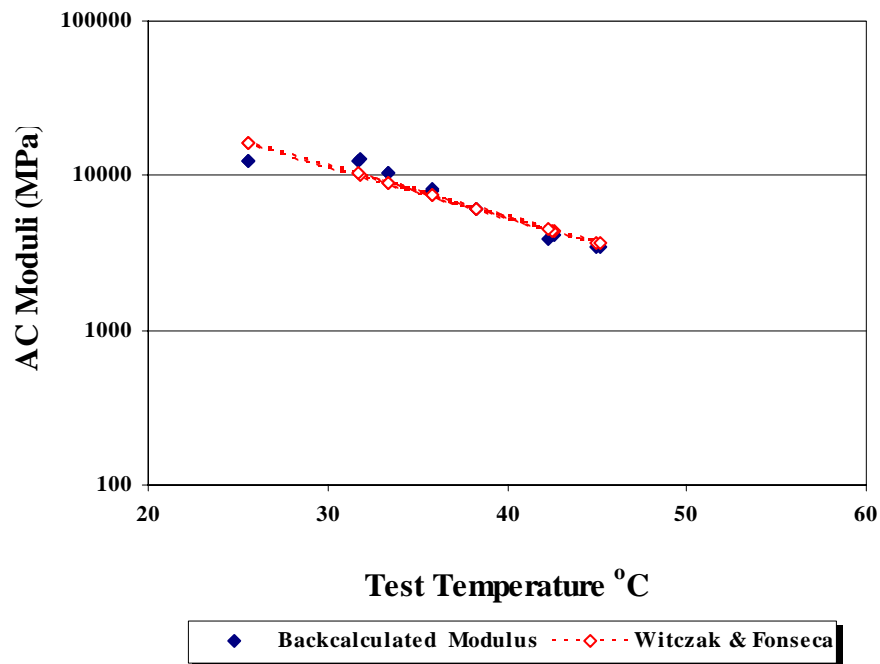
FIGURE 72 **Comparison of the Backcalculated AC Modulus with Eq 7.6. Pavement Group 4 of the K7 Lane.**
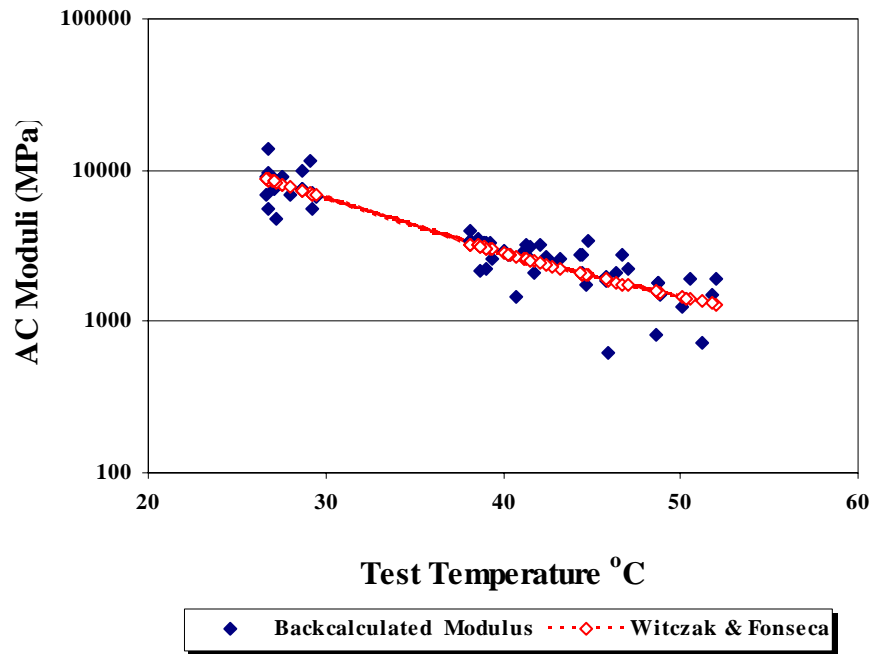
FIGURE 73   **Comparison of the Backcalculated AC Modulus with Eq 7.6. Pavement Group 5 of the K6 Lane.**
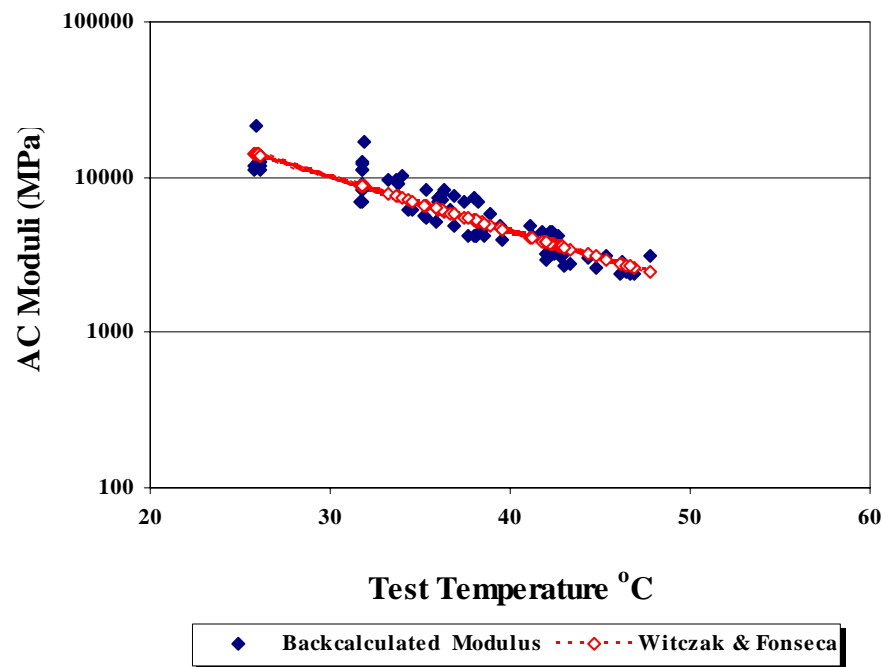
FIGURE 74   **Comparison of the Backcalculated AC Modulus with Eq 7.6. Pavement Group 5 of the K7 Lane.**
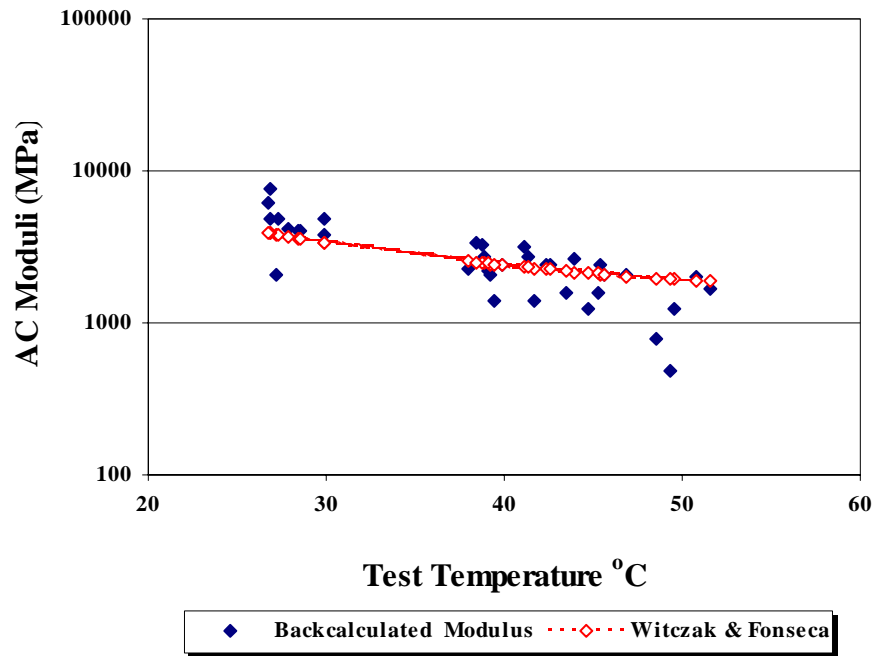
FIGURE 75   Comparison of the Backcalculated AC Modulus with Eq 7.6. Pavement Group 6 of the K6 Lane.
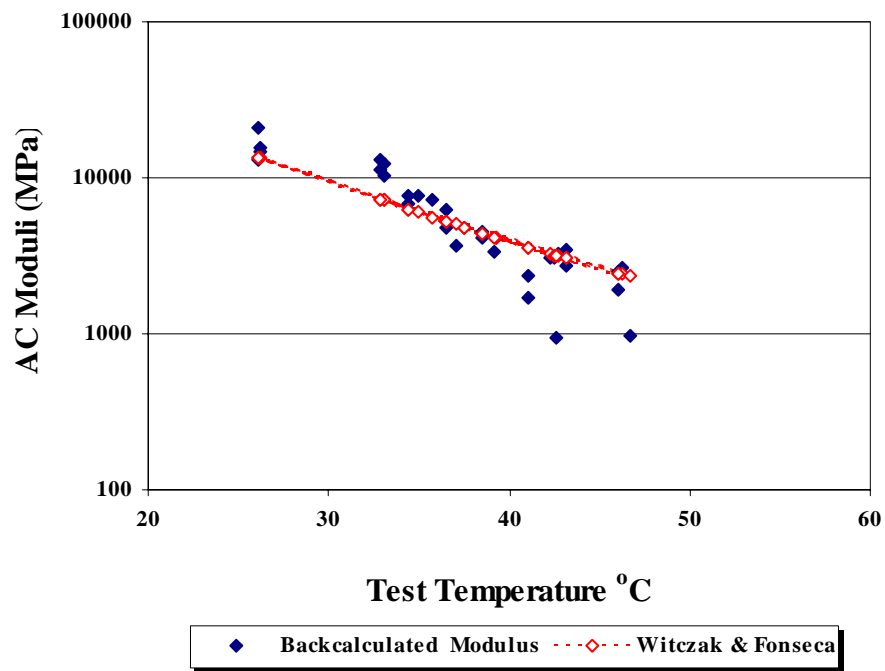
FIGURE 76   Comparison of the Backcalculated AC Modulus with Eq 7.6. Pavement Group 6 of the K7 Lane.
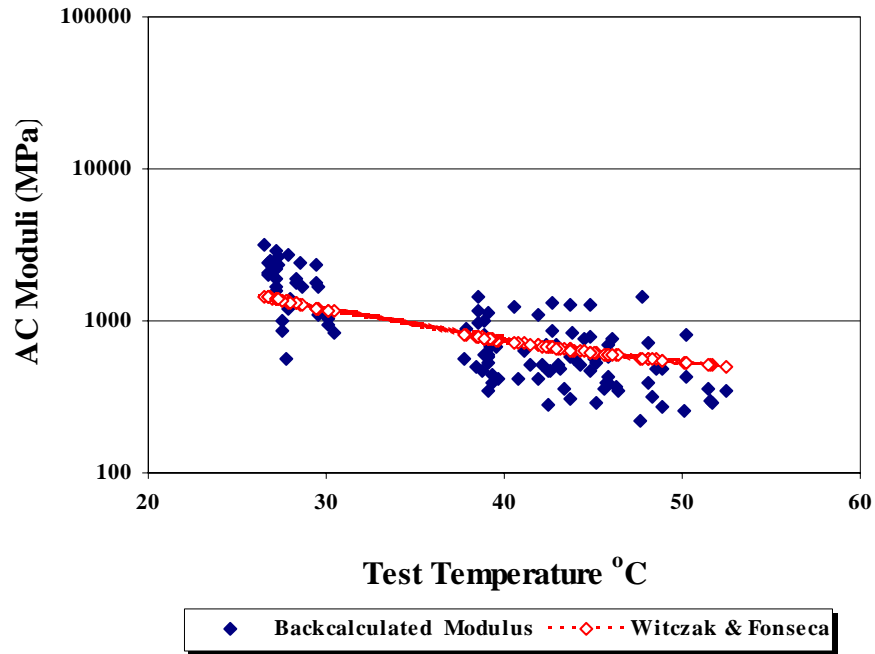
FIGURE 77 **Comparison of the Backcalculated AC Modulus with Eq 7.6. Pavement Group 7 of the K6 Lane.**
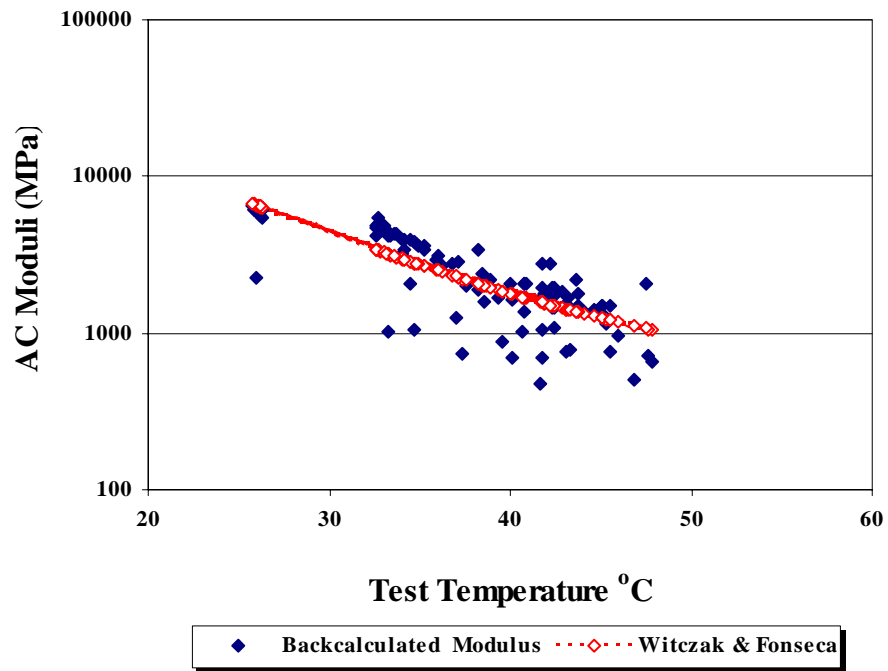
FIGURE 78 **Comparison of the Backcalculated AC Modulus with Eq 7.6. Pavement Group 7 of the K7 Lane.**
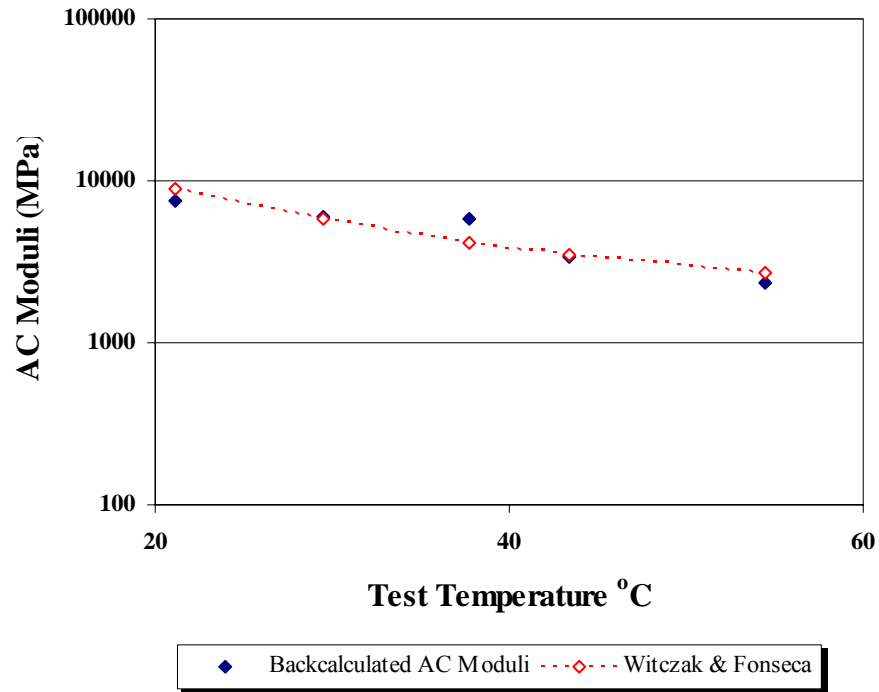
FIGURE 79 **Comparison of the Backcalculated AC Modulus with Eq 7.6.**
C6 Core.

Since the figures of the modulus comparison between the backcalculated and the predicted by Witczak and Fonseca have been set by pavement groups and lanes, the comparison between both lanes can be seen by observing two consecutive figures.

It is important to note that the AC moduli from the K6 lane has a lesser value than the K7 lane in the same group, indicating possible damage on the K6 lane. This is supported by the field data, since the K6 lane (outside) is more frequently used by overweight trucks than K7 lane (inside).

Figure 79 belongs to the C6 core taken in the center left turn lane in the vicinity of the K6-4 FWD station. This data will be very useful later when it will be focused on the corrected modulus by temperature.

CALCULATIONS OF THE CORRECTED BACKCALCULATED AC MODULUS

Three equations of making temperature corrections were selected for this research: the Chen, the Tx DOT and the Witczak and Fonseca. The reference temperature for these corrections was determined to be 23.8 ^{o}C (75 ^{o}F). The corrected modulus by each group and by each lane were calculated using equations 7.1, 7.2, 7.4 and 7.5. The last two equations used the coefficients taken from Tables 44 and 45.

The corrected moduli were plotted by each method, with the best results coming from the Witczak and Fonseca equation. In spite of the fact that FWD data was taken in the K6 lane until December of 2002, this month was not included due to the fact that the K6 lane was being milled in that month. Thus, the FWD data analyzed for the K6 lane is only until July of 2002.

However, when the Witczak and Fonseca equations are plotted, the corrected AC modulus values from the K6 lane were rather flat or with a small decreasing slope, which show an insignificantly decreasing trend with time indicating a negligible increase in damage on this lane. This could be explained if it is considered that FWD data incorporates two effects: load and environmental conditions, since the data were taken in the wheel paths. To verify this, two additional corrections were made. First, the corrected backcalculated AC moduli from the K6 lane were corrected using the modulus temperature relationship from frequency sweep tests done in the laboratory on the core sample taken at the center left turn lane, C6. The second was using the modulus temperature relationship from K7 lane on K6 lane. The mixtures of both lanes should be the same and in the K7 lane which would have smaller load effects because it is the passing lane.

From these two additional corrections, evidence of damage was found on the K6 lane when the correction was carried out with the modulus temperature relationship from the C6 core. Figures 80 through 86 present plots of all groups of the K6 lane with the modulus temperature relationship from the C6 core. Appendix E shows the results of the temperature corrected modulus aalysed in all groups stations using the Chen and TxDOT temperature corrections methods.
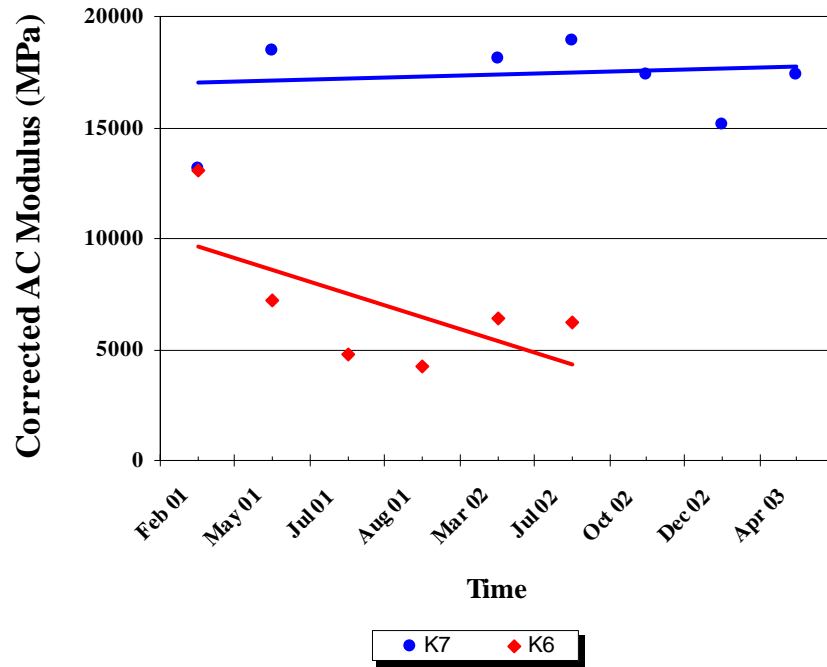
FIGURE 80   Evidence of Damage in the Pavement Group 1 of SH 4/48.
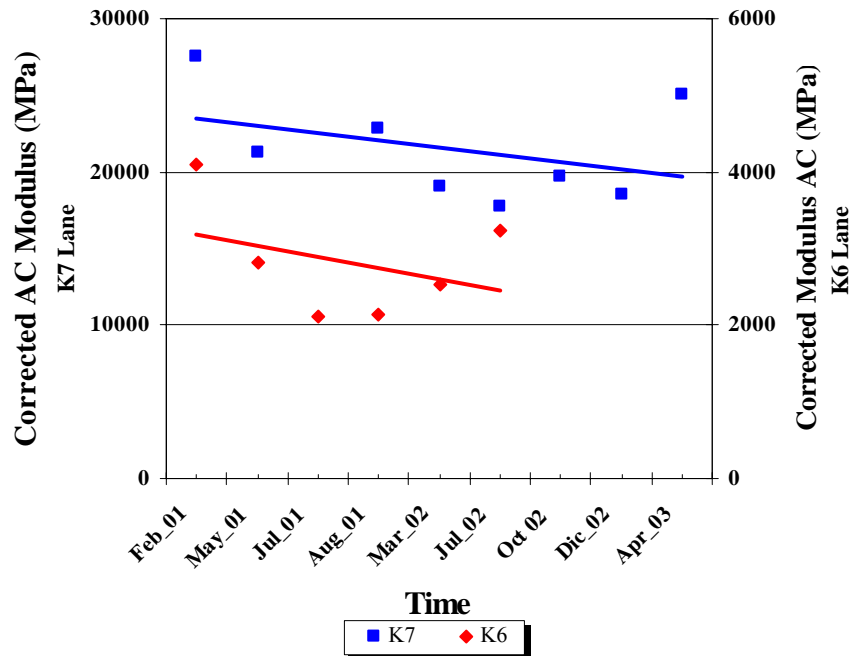
FIGURE 81   Evidence of Damage in the Pavement Group 2 of SH4/48.
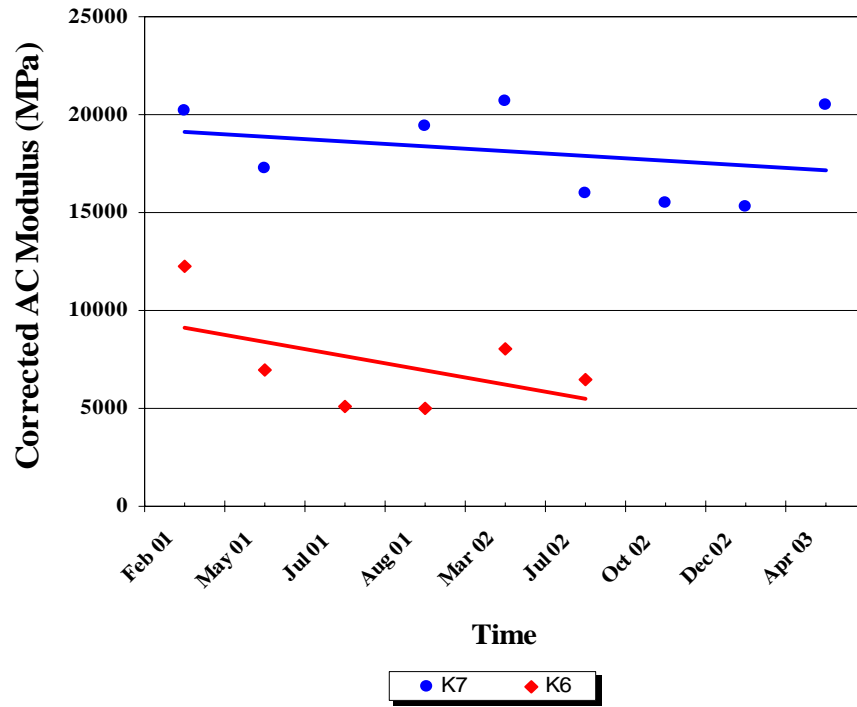
FIGURE 82   Evidence of Damage in the Pavement Group 3 of SH4/48.
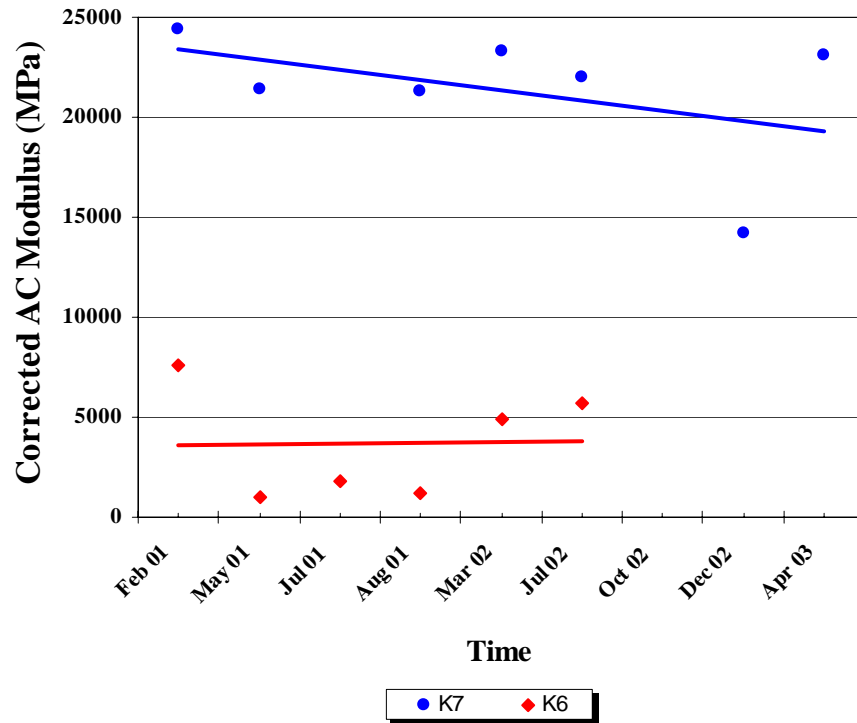
FIGURE 83   Evidence of Damage in the Pavement Group 4 of SH4/48.
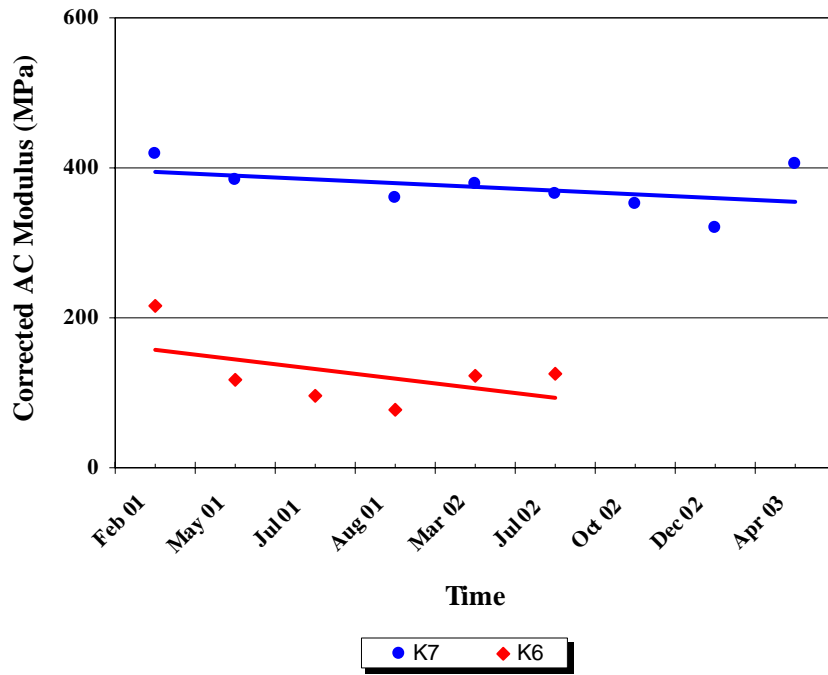
FIGURE 84   Evidence of Damage in the Pavement Group 5 of SH4/48.
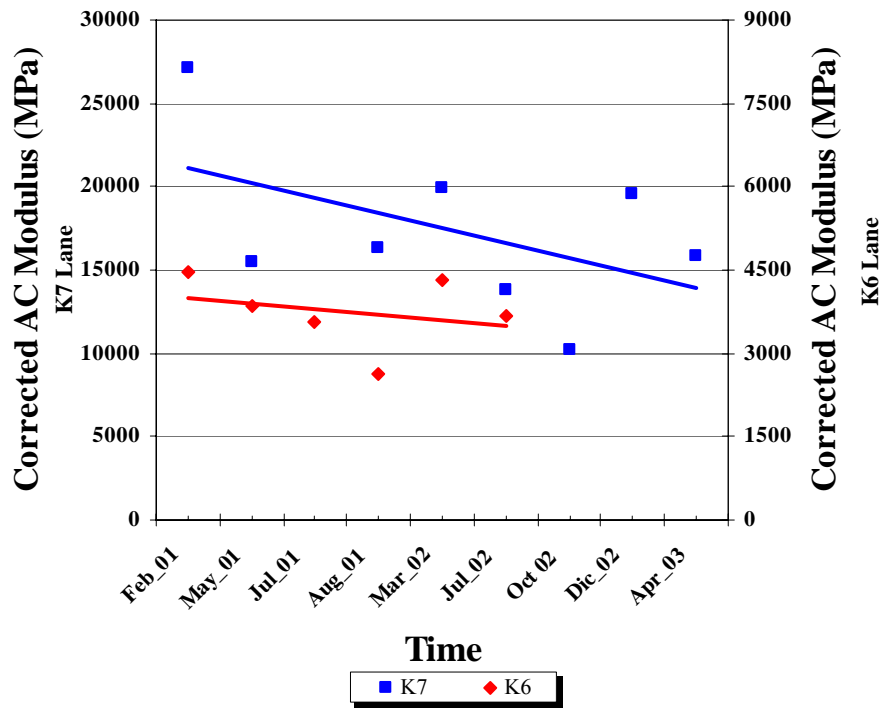
FIGURE 85   Evidence of Damage in the Pavement Group 6 of SH4/48.
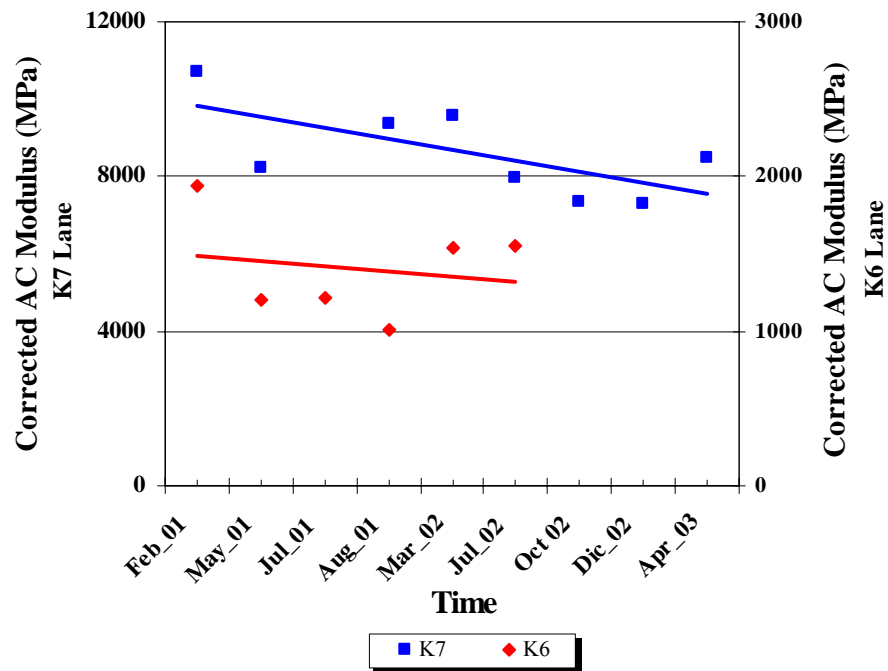
FIGURE 86   Evidence of Damage in the Pavement Group 7 of SH4/48.

As it was said earlier, Figures 80 to 86 show the corrections done to the backcalculated AC modulus using the modulus temperature relationship from the C6 core. The corrected backcalculated AC moduli from the K6 lane show in these plots a decreasing line over time, evidence of damage to this lane. Group stations 1, 3, 5, 6 and 7 show more damage. The number of the FWD stations included in these three groups on the K6 lane are more than 50 % of segment route SH4/48.

CHAPTER VIII

DISCUSSION OF THE RESULTS

BACKCALCULATED MODULUS ERROR

Tables 12 and 13 on pages 46 through 48 reflect the accuracy of the backcalculated modulus values. Since the maximum error should be 5 %, the values obtained from these tables are less than 5 % with three exceptionsat the K6-42, K6-43 and K7-38 FWD stations.

The possible reasons for these anomalie could be they are located at the beginning of the downtown area where the truck traffic is not only due to overweight loads but also due to normal traffic. It means the number of repetitions of load would be increasing more in this intersection of Boca Chica Boulevard and SH 48 with dense traffic.

BACKCALCULATED AC MODULI RELATIONSHIP BETWEEN THE STATIC ANALYSIS AND THE DYNAMIC (COMPLEX) MODULUS /E*/.

The backcalculated AC results at core locations from static analysis (MODULUS) are compared with the dynamic (complex) modulus /E*/ obtained from the laboratory testing. Figures 87, and 88 show theses plots and theirs linear correlations correspondient to a los values got from K6 and K7 lane, respectively. The Figure 89 present the combination of both K6 and K7 lane values. The linear regression found was comparable with the form:

$$/E*/ = (1+a) \ E_{static} \qquad\qquad (8.1)$$

where

$/E*/$: dynamic (complex) modulus get from Labotatory testing,

E_{static} : backcalculated AC Modulus gets from Static Analyis,

$(1+a)$: slope;

- Regression Linear for K6 Lane values.

$$/E*/ = 1.087\ E_{static}$$

TABLE 48   Testing of Significance for the Linear Regression between Backcalculated AC Modulus from Static Analysis and Dynamic (Complex) Modulus /E*/ for the K6 Lane.

Source of Variation	Sum of Squares	Degree of Freedom	Mean Square	f_o	$f_{0.01,1,34}$	P value
Regression	238376337	1	238376337.2	37.22	7.46	< 0.0005
Error	6405116	34	6405116.4			
Total	244781454	35				
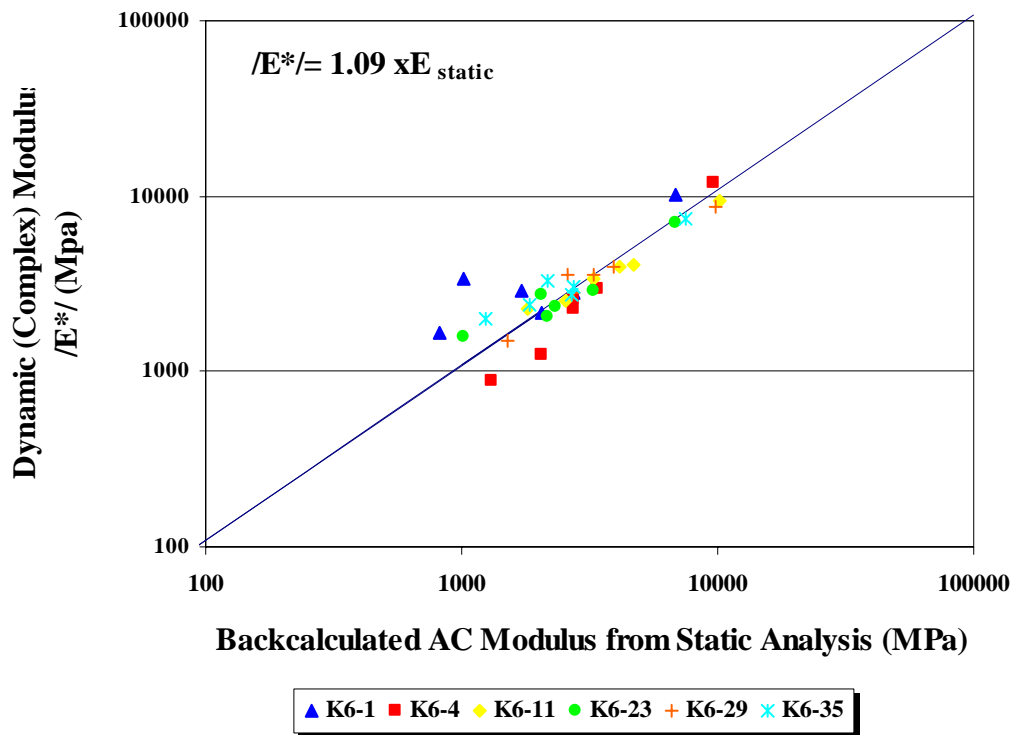
FIGURE 87   Backcalculated AC Moduli Relationship between the Static Analysis and the Dynamic (Complex) Modulus for the K6 Lane.

- Regression Linear for K7 Lane values.

$$/E*/ = 1.042\ E_{static}$$

TABLE 49 Testing of Significance for the Linear Regression between Backcalculated AC Modulus from Static Analysis and Dynamic (Complex) Modulus /E*/ for the K7 Lane.

Source of Variation	Sum of Squares	Degree of Freedom	Mean Square	f_o	$f_{0.01,1,54}$	P value
Regression	431907550	1	431907550	7096.9113	7.1605	< 0.0005
Error	3225502	53	60859			
Total	435133052	54				
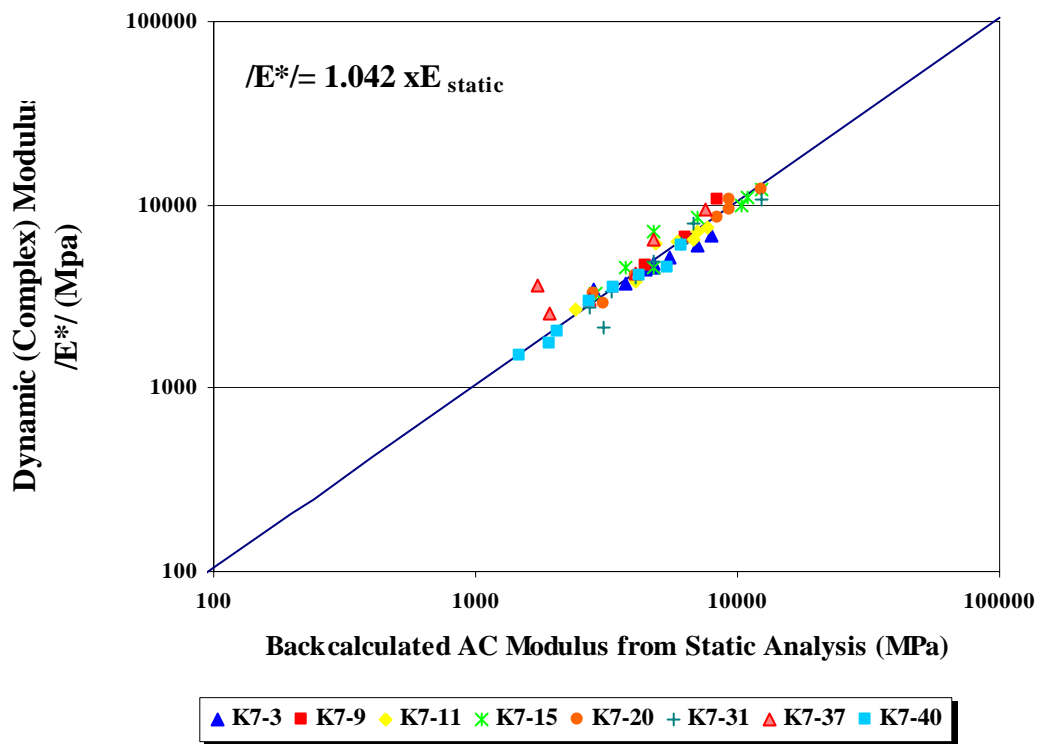
FIGURE 88 Backcalculated AC Moduli Relationship between the Static Analysis and the Dynamic (Complex) Modulus for the K7 Lane.

- Regression Linear for the combination of K6 and K7 lane values.

$$/E*/ = 1.055 \; E_{static}$$

TABLE 50   Testing of Significance for the Linear Regression between Backcalculated AC Modulus from Static Analysis and Dynamic (Complex) Modulus /E*/ for Both K6 and K7 Lanes.

Source of Variation	Sum of Squares	Degree of Freedom	Mean Square	f_o	$f_{0.01,1,89}$	P value
Regession	892634944	1	892634944	22438	6.968	<< 0.0005
Error	3540696	89	39783			
Total	896175640	90				
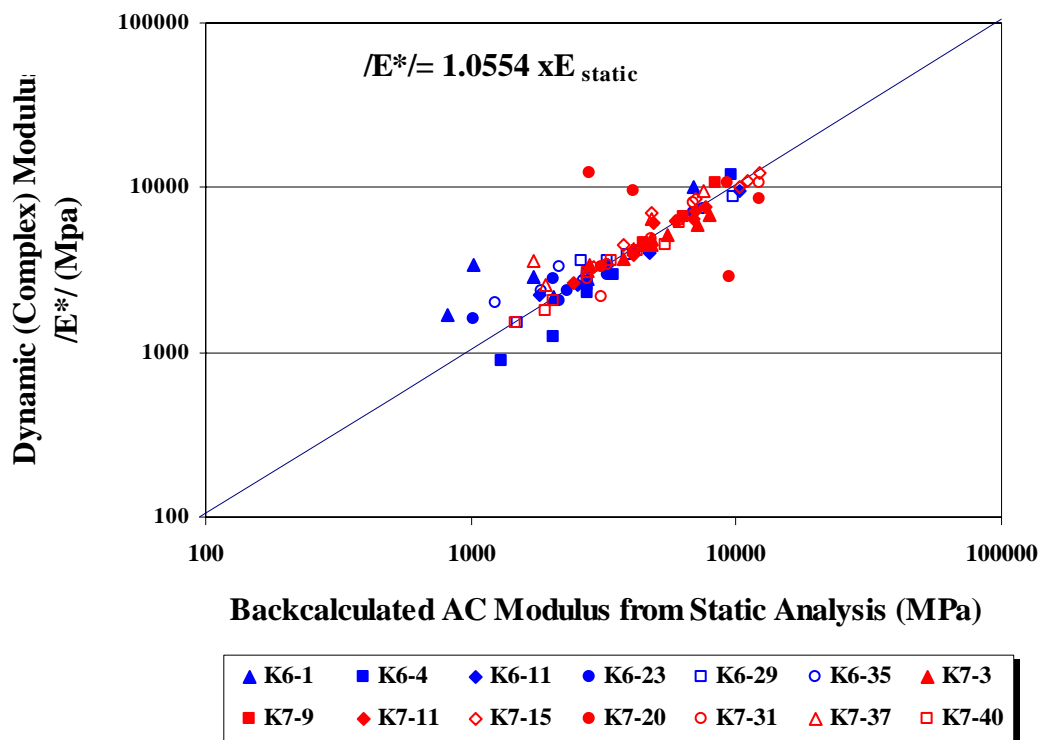
FIGURE 89   Backcalculated AC Moduli Relationship between the Static Analysis and the Dynamic (Complex) Modulus for Both Lanes.

In these comparisons the values of K6-48 core station were separated because the values did not show the same tendency as the other cores. This deviation is explained because of K6 48 is located in the downtown area where most of the extracted core samples from the K6 lane lacked a homogeneous AC mixture as it shown in Figures 87, pictures a, b, c and d.

In the K7 lane, contrary to the K6 lane, the results from the FWD stations, K7-37 and K7 40 downtown area, fit well with the results of laboratory testing. The interpretation of this is reflected on pictures e) and f) of Figure 90 where the quality of the cores is stronger and more uniform than those in the K6 lane.

Figure 91 presents the comparison of the backcalculated AC modulus from the MODULUS program versus Dynamic (Complex) Modulus from the laboratory testing corresponding to group stations 1, 3, 4, 5 and 6 from the K6 lane. Groups 2 and 7 did not have good correlations with the closer FWD core station results. Because Group 7 is located in the downtown area, it is expected that the results from laboratory testing will not be exact.

According to Figure 92 shows that in all group stations from the K7 lane, the correlation between laboratory testing and static analysis is accurate, even in the group station 7. Once again is shown how the overweight truck traffic is impacting more on the K6 lane than K7 lane.

a) K6 42 FWD Station.   b) K6 46 FWD Station.

c) K6 50 FWD Station.   d) K6 53 FWD Station.

e) K7 40 FWD Station.   f) K7 37 FWD Station.

FIGURE 90   The Core Samples from Downtown Area.
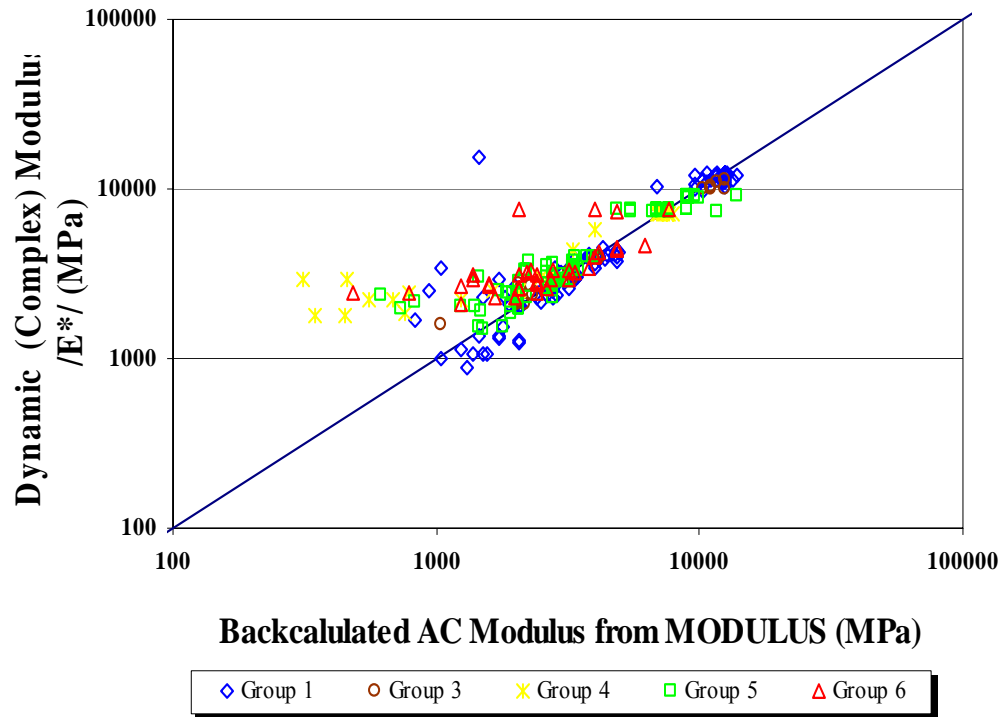
FIGURE 91   Backcalculated AC Moduli from Static Analysis versus Dynamic (Complex) Modulus by K6 Lane Pavement Groups.
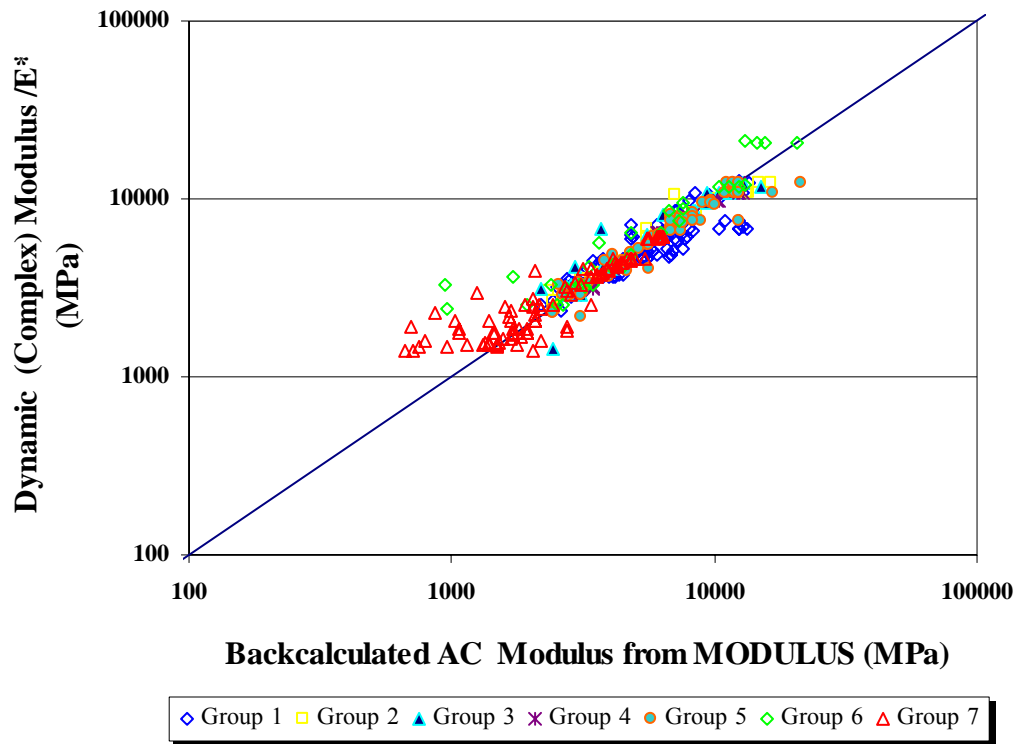
FIGURE 92   Backcalculated AC Moduli from Static Analysis versus Dynamic (Complex) Modulus by K7 Lane Pavement Groups.

BACKCALCULATED AC MODULI RELATIONSHIP BETWEEN THE STATIC ANALYSIS AND THE DYNAMIC ANALYSIS.

Figures 93 and 94 plot the backcalculated AC modulus obtained from DBISD (dynamic analysis) versus those obtained from the MODULUS program (static analysis) and show theirs linear regression for both K6 and K7 lane. The Tables 50 and 51 present the significance of their linear regression done. Figure 95 joins both K6 and K7 lane values and present its linear regression. Table 52 show the significance of its linear regression. The linear regression found was comparable with the form:

$$\mathbf{E_{static} = (1+b)\, E_{DBSID}} \qquad\qquad (8.2)$$

where

E_{DBSID} : backcalculated AC modulus gets from dynamic analyis

E_{static} : backcalculated AC modulus gets from static analyis,

$(1+b)$: slope;

It is significant to point out that the pavement structure thicknesses selected in the static analysis (Figure 30) fit well with the dynamic analysis in both lanes K6 and K7. However, it is observed that in some stations values obtained from the MODULUS are slightly greater than the DBISD especially in the K7 lane.

- Regression Linear for K6 Lane values.

$$E_{static} = 1.047\ E_{DBSID}$$

TABLE 51   Testing of Significance for the Linear Regression between Backcalculated AC Modulus from Static and Dynamic Analysis for the K6 Lane.

Source of Variation	Sum of Squares	Degree of Freedom	Mean Square	f_o	$f_{0.01,1,34}$	P value
Regression	271068416	1	271068416	4930	7.46	< 0.0005
Error	1869347	34	54981			
Total	272937763	35				
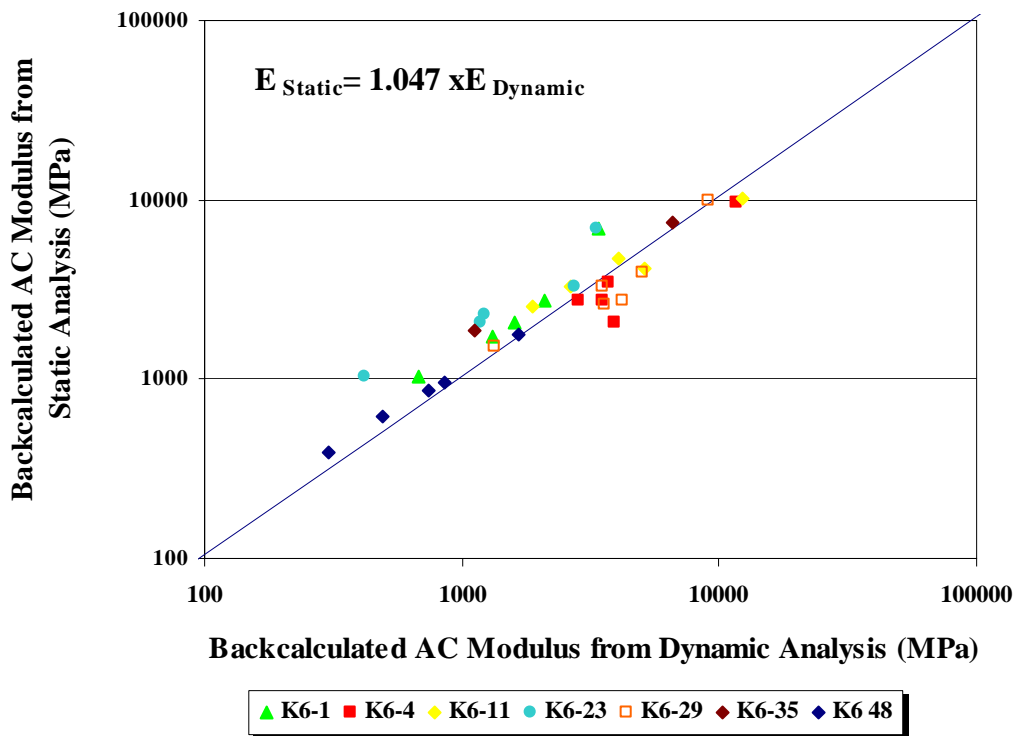
FIGURE 93   Backcalculated AC Moduli Relationship between the Static Analysis and the Dynamic Analyis for the K6 Lane.

- Regression Linear for K7 Lane values.

$$E_{static} = 1.0308\ E_{DBSID}$$

TABLE 52   Testing of Significance for the Linear Regression between Backcalculated AC Modulus from Static and Dynamic Analysis for the K7 Lane.

Source of Variation	Sum of Squares	Degree of Freedom	Mean Square	f_o	$f_{0.01,1,35}$	P value
Regression	202716160	1	202716160	87.936736	7.435	< 0.0005
Error	80683750	35	2305250			
Total	283399910	36				
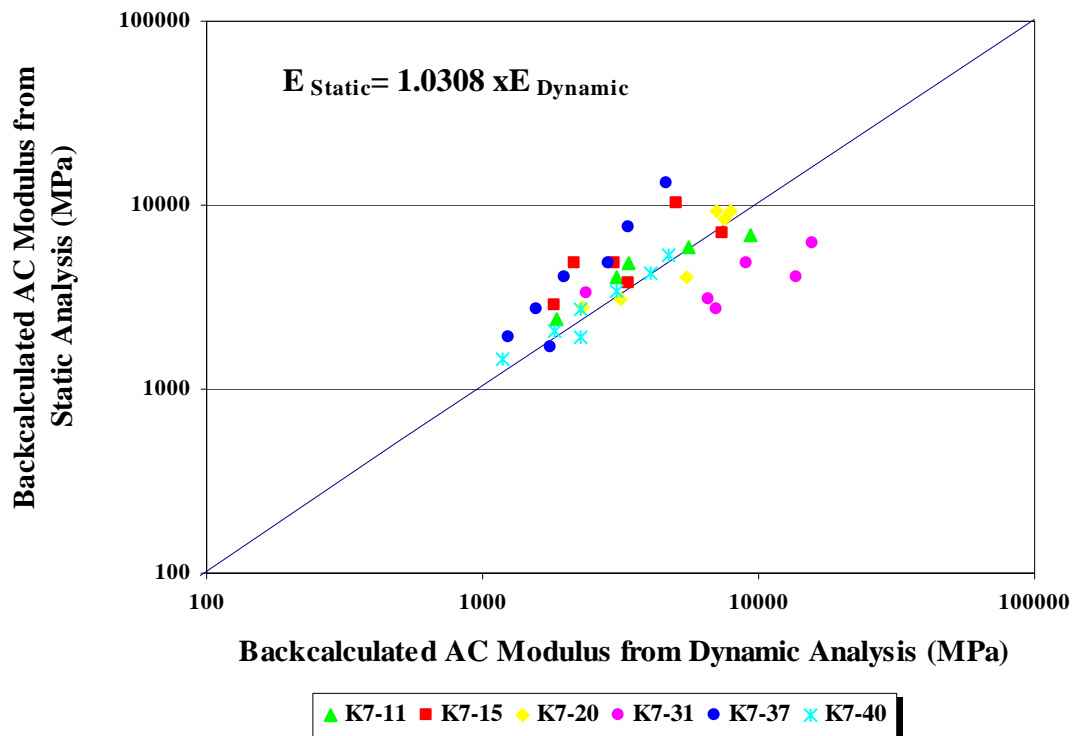
FIGURE 94   Backcalculated AC Moduli Relationship between the Static Analysis and the Dynamic Analyis for the K7 Lane.

- Regression Linear for combination both K6 and K7 Lane values.

$$E_{static} = 1.065\ E_{DBSID}$$

TABLE 53   Testing of Significance for the Linear Regression between Backcalculated AC Modulus from Static and Dynamic Analysis for Both K6 and K7 Lanes.

Source of Variation	Sum of Squares	Degree of Freedom	Mean Square	f_o	$f_{0.01,1,71}$	P value
Regression	448017558	1	448017558	357.7	7.0378	<< 0.0005
Error	88923870	71	1252449			
Total	536941428	72				
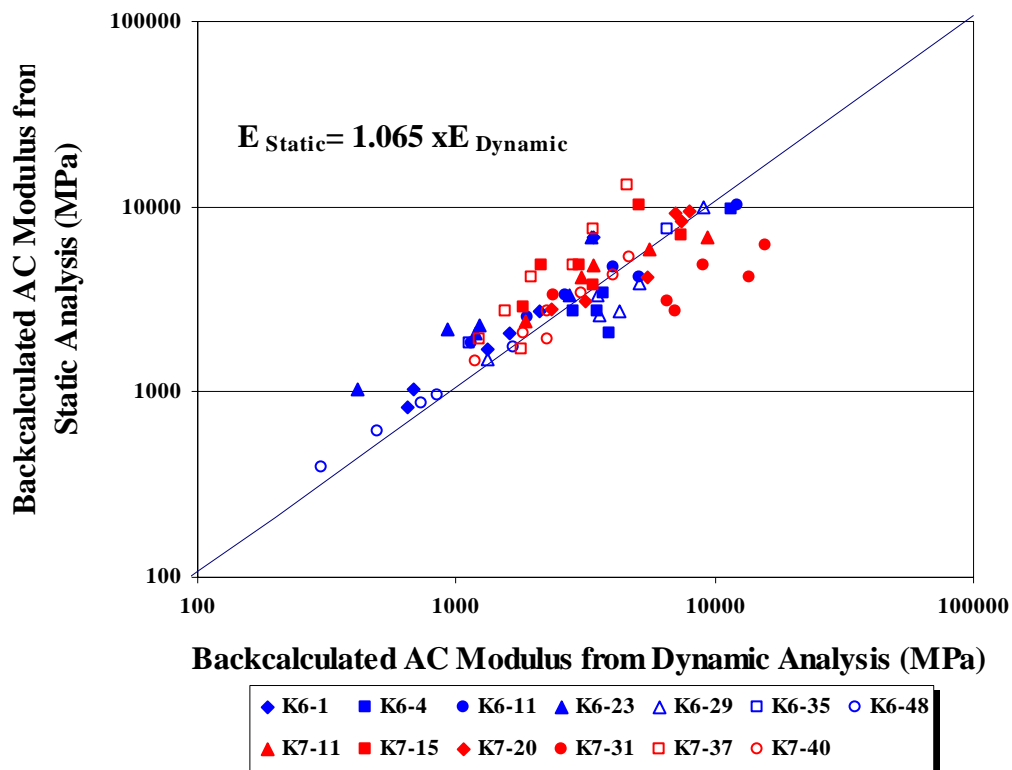
FIGURE 95   Backcalculated AC Moduli Relationship between the Static Analysis and the Dynamic Analyis for Both Lanes.

As it known backcalculated AC modulus from dynamic analysis (DBSID) is an isotropic modulus which follow this laws:

$$E_{DBSID} = \sqrt{E_{VERTICAL} * E_{HORIZONTAL}} \qquad (8.3)$$

$$E_{HORIZONTAL} = \frac{E_{VERTICAL}}{c} \qquad (8.4)$$

and $E_{vertical}$ is the AC modulus gets in the laboratory testing (/E*/) , then it may obtained "c" value combining the Eq. 8.3 and 8.4 with 8.1 and 8.2 given this expression:

$$c = (1 + a)^2 * (1 + b)^2 \qquad (8.5)$$

In this study was calculated "c" value for each lane. They are 1.3 and 1.15 for the K6 and K7 lanes, respectively. However a better result of "c" was obtained when both K6 and K7 data are analyzed together. This value is 1.26.

COMPARISON OF THE CREEP COMPLIANCE PARAMETERS OBTAINED FROM THE DYNAMIC ANALYSIS AND FROM THE LABORATORY TESTING

As it was explained in Chapter VI only the cores stations K6-1, K6-4, K6-11, K6-23 and K6-48 offered valid creep compliance parameters in the K6 lane. In the same way, the following core stations: K7-11, K7-15, K7-20, K7-31, K7-37 and K7-40, offered valid creep compliance paameters.

To process and compare "m" values between those obtained from dynamic analysis and laboratory data, it was necessary to set up a reference temperature. For convenience 23.8 ^{o}C (75 ^{o}F) was chosen. This is the same reference temperature used in the temperature corrected modulus. The "m" value from the laboratory was corrected to this reference temperature which is possible with the trendline of "m" from the laboratory temperature data as see in Figure 96 a).

The ratio m_{ref}/m_{temp} for each "m" value is used to get the correction factor line. See Figure 96 b). As the correction factor line is a function of temperature, the correction factor is calculated for each 'm" value The corrected value of "m" is called "m_c" is obtained multiplying the correction factor by the "m" values from DBSID.

a) **Temperature and "m" Reference.**   b) **Correction Factor Line.**
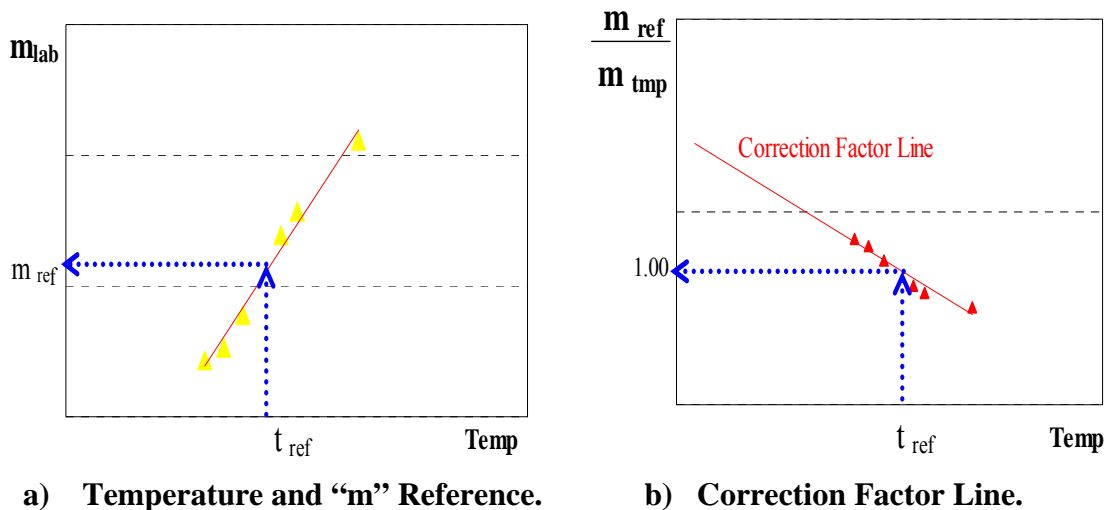
FIGURE 96   Procedure to Obtain "m_c" .

Figures 97 and 98 show the variation of "m_c" with time for both the K6 and K7 lanes, respectively. The increasing values of "m_c" over time in the K6 lane reflects deterioration. The "m" value is related to two major problems with the asphalt pavement, fatigue cracking and permanent deformation. The increasing "m" values obtained in this analysis confirms the deterioration of the K6 lane with time. Contrary to the trends in the K6 lane, in the K7 lane "m_c" values show a flat line, or a very small positive slope indicating that in the K7 lane, the initial conditions of the road have undergone little change.
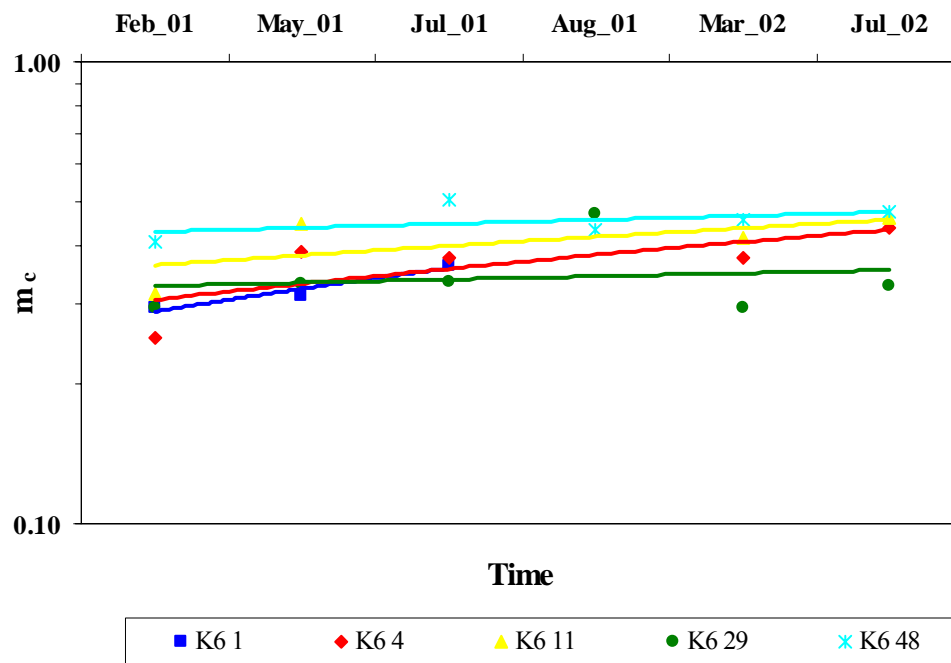
FIGURE 97   Variation of the "m$_c$" Values for the K6 Lane.
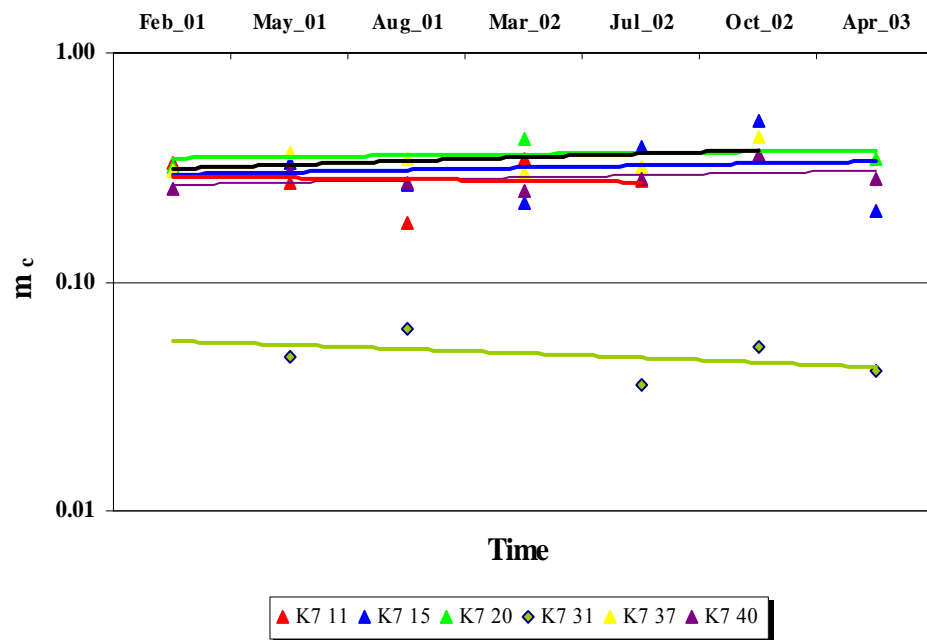
FIGURE 98   Variation of "m$_c$" Values for the K7 Lane.

CORRECTED BACKCALCULATED AC MODULUS WITH ENVIRONMENTAL CONDITIONS

Figures 80 trough 86 present the corrected backcalculated AC moudlus with environmental conditions. The fact that corrected bakcalculated AC modulus from the K6 lane show a greater decresing line overtime and lower AC moduli than the K7 lane indicate that there is evidency of damage in K6 lane.

RELATIONSHIP BETWEEN CORRECTED BACKCALCULATED AC MODULUS AND CUMULATIVE 18-kip ESALs.

A reduction in asphalt moduli with increasing amounts of 18-kip Equivalent Single Axle (ESAL) provides evidence that pavements are damaged by increasing numbers of load repetititons.

The fact that a greater amount of truck traffic travels in the K6 lane than in the K7 lane provides an opportunity to evaluate the amount of damage that is done by this traffic by plotting the observed reduction in modulus against the accumulate 18-kip Equivalent Single Axle Loads in both lanes.

To analyse the number of the ESALs in each lane it was necessary to request the current traffic data and the historical Average Daily Traffic (ADT) from Tx DOT traffic record.

TxDOT sent data corresponding to the Fiscal Year 2003, from September 2002 to August 2003, which was collected and recorded by the weigh-in-motion (WIM) stations along the SH 4/48 roadway. Table 54 shows the number of 18-kip ESALs separated into axle configuration: single, tandem, triple or quad, by monthly mean and per year (2003). In addition, the historical average daily traffic (ADT) from SH 4/48 provided by the Pharr District office was useful to calculate the traffic growth rate "g and to project backward in time to obtain the 18-kip ESALs for the past years.

Because SH 4/48 was divided on seven Pavement Groups in Chapter VII, it was necessary to select the ADT values in the same Pavement Groups to get the 18-kip ESAL in each of them. Table 55 presents the greater ADT selected values by Pavement Group.

It notes that the ADT values are the same in the Pavement Group 2, 3, 4, and 5, but different in the Pavement Group 1, 6 and 7. Equation 8.6 was used to determine the values of the Growth Rate "g" which are shown in Table 55 too.

$$g = \left(\frac{ADT_n}{ADT_o}\right)^{\frac{1}{n}} - 1 \qquad (8.6)$$

where;

g   :   Growth rate;

ADT o :   Average daily traffic at the start of the design period;

ADT n :   Average daily traffic at the end of the design period;

n   :   Number of the years of the design period.

TABLE 54   Results of 18-kip ESALs in the Fiscal Year 2003 by Axle Configuration.

Axle configuration	By Month	By Year
Single axle	6878	82535
Tandem axle	17990	215880
Triple axle	1496	17957
Quad axle	1	13
TOTAL ESALs	**26365**	**316385**

TABLE 55   Growth Rate "g" by Pavement Group.

Pavement Group	ADT$_o$ 1993	ADT$_n$ 2003	Growth Factor "g"
1	14079	18974	0.0303
2,3,4,5	23511	28344	0.0189
6	28022	34356	0.0206
7	27148	29253	0.0075

Equation (8.7) was used to compute the total number of 18-kip ESAL's for each year before 2003.

$$\text{Cumulative } 18 - \text{kip ESAL}_n = (\text{Total } 18 - \text{kip ESAL}_O) * \left(\frac{(1+g)^n - 1}{g} \right)$$
(8.7)

where;

Cumulative 18-kip ESAL_n : It is the total number of the 18-kip ESAL at the year "n";

Total 18-kip ESAL_o : It is the total number of the 18-kip ESAL at the year "o" ;

g   : growth rate;

n   : the number of the years between the year_n and the year_o.

The Table 56 presents the total number of 18-kip ESAL by year, from 1993 up to 2003. The year 1993 was chosen because it was during that year the SH 4/48 sections in this study were repaved.

TABLE 56   Number of the Total 18-kip ESAL by Year and Pavement Groups.

Year	Pavement Groups			
	1-1A	2 to 5	6	7
1993	2.3E+05	2.6E+05	2.6E+05	2.9E+05
1994	2.3E+05	2.6E+05	2.6E+05	2.9E+05
1995	4.8E+05	5.3E+05	5.2E+05	5.9E+05
1996	7.3E+05	8.0E+05	7.9E+05	8.9E+05
1997	9.8E+05	1.1E+06	1.1E+06	1.2E+06
1998	1.2E+06	1.4E+06	1.3E+06	1.5E+06
1999	1.5E+06	1.7E+06	1.6E+06	1.8E+06
2000	1.8E+06	1.9E+06	1.9E+06	2.1E+06
2001	2.1E+06	2.2E+06	2.2E+06	2.4E+06
2002	2.4E+06	2.5E+06	2.5E+06	2.7E+06
2003	2.7E+06	2.9E+06	2.8E+06	3.0E+06

Table 57 presents the percentage of incidence of each vehicle class in the westbound direction, from Port of Brownsville to Mexico. Table 58 shows the percentages that were used to compute the FHWA vehicle class distribution in both the K6 and K7 lanes. The lane distribution of traffic along of SH4/48 were provided by TxDOT.

TABLE 57   FHWA Class Distribution in the Westbound Direction.

FHWA Class	Description (Texas 6 Vehicle Classifications)	Monthly Mean	Percentage of Incidence
4	2D-Six Tre Single Unit	1854	12%
5	3 Axles Single Unit	2821	18%
6	4, or more, Axles Single Unit	1307	8%
7	3 Axles Single Trailer	237	1%
8	4 Axles Single Trailer	486	3%
9	5 Axles Single Trailer	7755	49%
10	6, or more, Axles Single Trailer	1304	8%
11	5, or Less, Axles Multi-Trailers	153	1%
12	6 Axles, Multi-Trailers	16	0.10%
13	7, or More, Axles Multi-Trailers	3	0.02%
	Total number of vehicles	15936	1

TABLE 58   Traffic   Distribution by Lanes.

FHWA Class	Description (Texas 6 Vehicle Classifications	Percentage of Incidence	Traffic Distribution	
			K6 Lane	K7 Lane
4	2D-Six Tre Single Unit	12%	0.70	0.30
5	3 Axles Single Unit	18%	0.70	0.30
6	4, or more, Axles Single Unit	8%	0.60	0.40
7	3 Axles Single Trailer	1%	0.80	0.20
8	4 Axles Single Trailer	3%	0.80	0.20
9	5 Axles Single Trailer	49%	0.78	0.22
10	6, or more, Axles Single Trailer	8%	0.70	0.30
11	5, or Less, Axles Multi-Trailers	1%	0.40	0.60
12	6 Axles, Multi-Trailers	0.10%	0.40	0.60
13	7, or More, Axles Multi-Trailers	0.02%	0.40	0.60

Table 59 shows the cumulative 18-kip ESALs by Pavemenet Group which is generated with the data in Table 56 using the percentages from the Tables 57 and 58 for each lane and each vehicle class.

TABLE 59 Cumulative 18-kip ESALs by Lanes and by Pavement Group.

Lane	Date	Cumulative 18-kip ESALs				
		1A	1	2 to 5	6	7
K7	Feb 01	5.0E+05	5.0E+05	5.4E+05	5.3E+05	5.8E+05
	May 01	5.2E+05	5.2E+05	5.6E+05	5.5E+05	6.0E+05
	Aug 01	5.4E+05	5.4E+05	5.8E+05	5.7E+05	6.2E+05
	Mar 02	5.8E+05	5.8E+05	6.3E+05	6.2E+05	6.7E+05
	Jul 02	6.1E+05	6.1E+05	6.5E+05	6.5E+05	7.0E+05
	Oct 02	6.3E+05	6.3E+05	6.7E+05	6.7E+05	7.2E+05
	Dec 02	6.4E+05	6.4E+05	6.9E+05	6.8E+05	7.4E+05
	Apr 03	6.7E+05	6.7E+05	7.2E+05	7.1E+05	7.6E+05
	Sep 03	7.1E+05	7.1E+05	7.5E+05	7.4E+05	8.0E+05
K6	Feb 01	1.3E+06	1.3E+06	1.5E+06	1.4E+06	1.6E+06
	May 01	1.4E+06	1.4E+06	1.5E+06	1.5E+06	1.6E+06
	Jul 01	1.4E+06	1.4E+06	1.5E+06	1.5E+06	1.7E+06
	Aug 01	1.5E+06	1.5E+06	1.6E+06	1.5E+06	1.7E+06
	Mar 02	1.6E+06	1.6E+06	1.7E+06	1.7E+06	1.8E+06
	Jul 02	1.7E+06	1.7E+06	1.8E+06	1.7E+06	1.9E+06
	Sep 03	1.9E+06	1.9E+06	2.0E+06	2.0E+06	2.2E+06

TABLE 60   Corrected Backcalculated E_{AC} by Pavement Groups.

Lane	Date	Corrected Backcalculated E_{AC} by Groups (MPa)							
		1A	1	2	3	4	5	6	7
K6	Feb-01	12684	13109	4106	12214	7587	10238	4454	1937
	May-01	6625	7232	2824	6935	1014	5568	3867	1207
	Jul-01	4332	4776	2108	5123	1801	4560	3575	1219
	Aug-01	3520	4224	2148	4959	1243	3636	2635	1002
	Mar-02	5627	6433	2521	7303	4931	5860	4306	1535
	Jul-02	5957	6372	3247	6479	4475	5386	3685	1547
K7	Feb-01	9997	12516	27496	20156	22364	19148	27120	10699
	May-01	14919	16201	21203	17260	18087	16961	15492	8209
	Aug-01	17078	17290	22886	19356	17137	16093	16358	9342
	Mar-02	13054	14594	22886	19356	17137	16093	16358	9342
	Jul-02	16338	15731	19027	20683	20854	17095	19967	9582
	Oct 02	16070	14519	17771	15945	17302	16123	13762	7955
	Dec 02	13325	13365	19698	15459		15128	10192	7364
	Apr 03	14684	15597	18503	15277	13965	15045	19618	7286

Figures 99 through 106 presents the plots of the cumulative 18-kip ESAL versus corrected backcalculated AC modulus belong to westbound direction, K6 and K7 lanes to each Pavement Group. The Figure 106 belongs to Pavement Group 1A corresponds to the first eight FWD stations to both lanes and it starts in FM 511 and ends in FM 802. These plots utilize the data from Tables 59 and 60.

In addition, a fitted curve has beed added to each of the plots. Equation 8.8 was used to obtain these fitted curve. The coefficients ρ, β, E_{Asym}, and E_o from the Equation 8.8 were obtained by nonlinear regression. Table 61 show the results of analysis of variance (ANOVA) for each Pavement Groups.

$$E = E_{ASYM} + E_0 * (1 - e^{-\left(\frac{\rho}{N}\right)^{\beta}}) \qquad (8.8)$$

where : E_{ASYM} , E_o, ρ, β : Coefficeints;

  E : Corrected Backcalculated AC Modulus;

  N : Cumulative 18-kip ESAL.
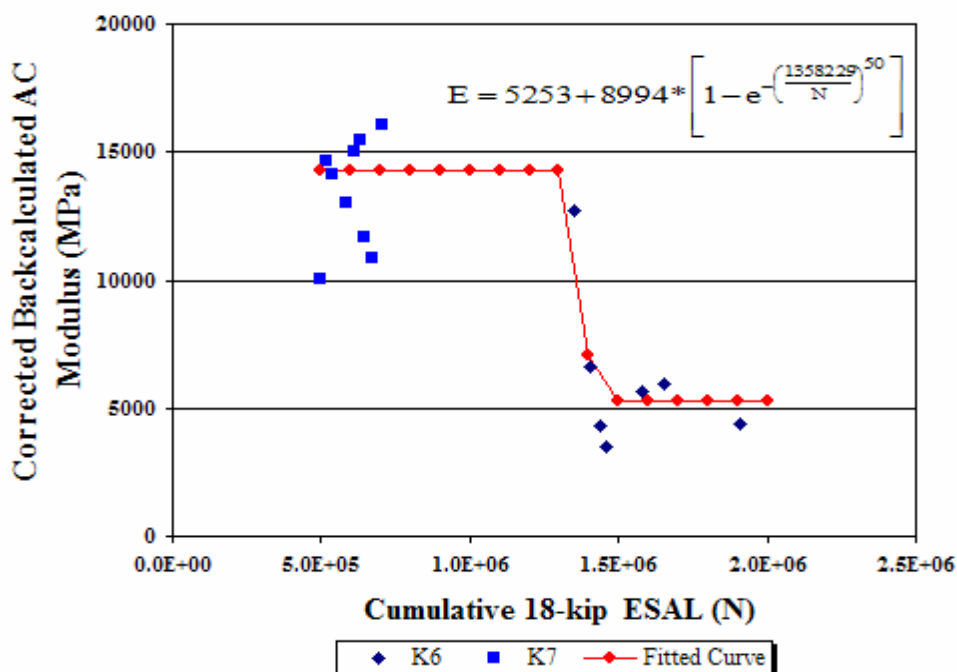
FIGURE 99 **Plot of Cumulative 18-kip ESAL versus Corrected Backcalculated AC Modulus in the Pavement Group 1A.**

$$E = 5503 + 9509 * \left[1 - e^{-\left(\frac{1359759}{N}\right)^{67}} \right]$$
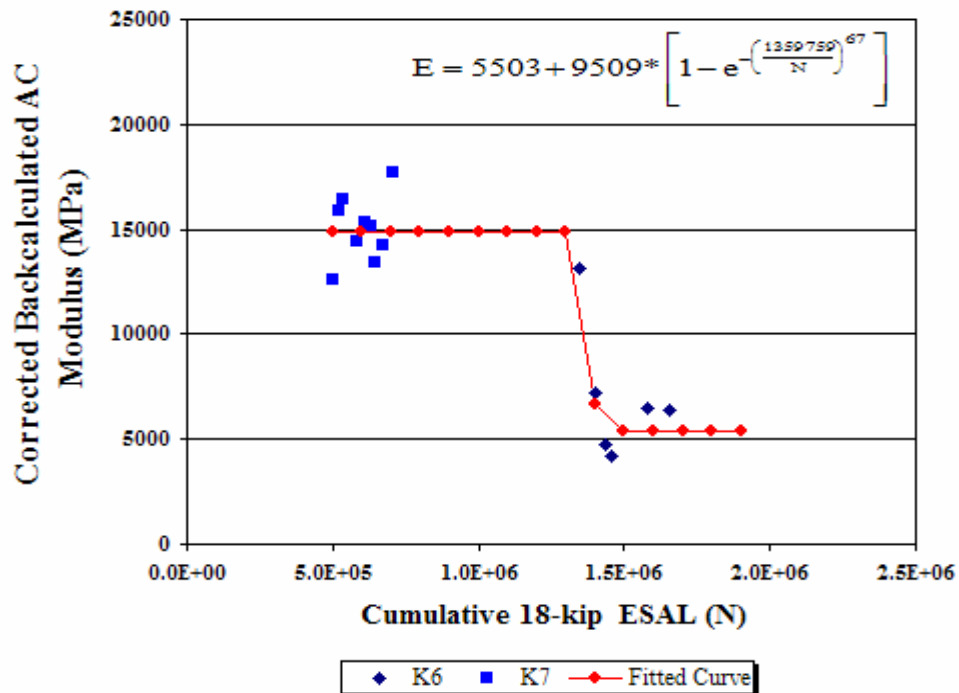
FIGURE 100   Plot of Cumulative 18-kip ESALs versus Corrected Backcalculated AC Modulus in the Pavement Group 1.

$$E = 2647 + 19989 * \left[1 - e^{-\left(\frac{1403440}{N}\right)^{70}} \right]$$
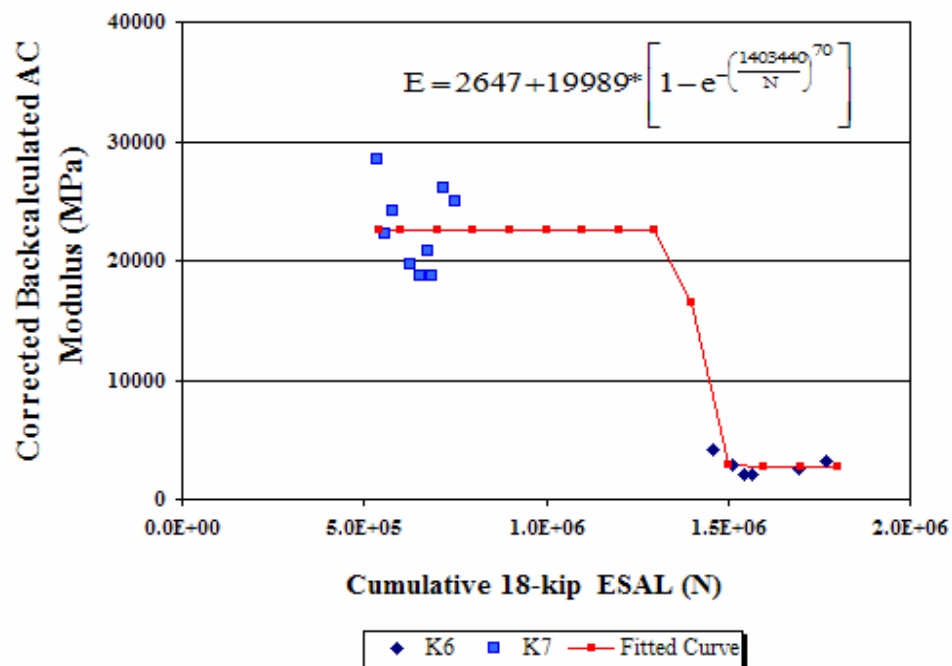
FIGURE 101   Plot of Cumulative 18-kip ESALs versus Corrected Backcalculated AC Modulus in the Pavement Group 2.

$$E = 7431 + 10883 * \left[1 - e^{-\left(\frac{1456682}{N} \right)^{70}} \right]$$
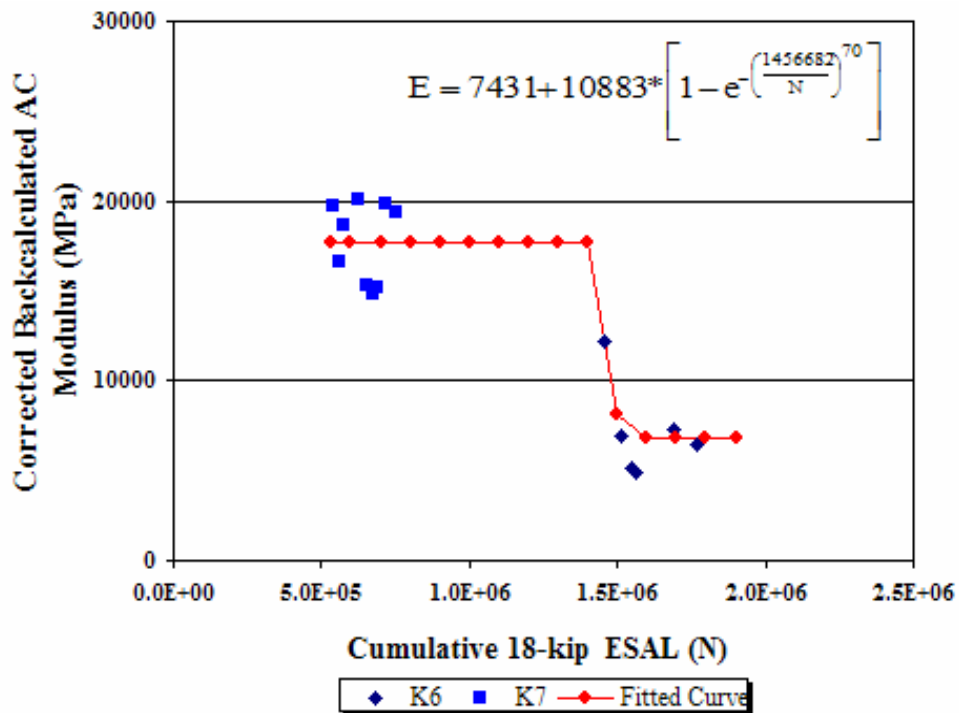
FIGURE 102   Plot of Cumulative 18-kip ESALs versus Corrected Backcalculated AC Modulus in the Pavement Group 3.

$$E = 5113 + 13645 * \left[1 - e^{-\left(\frac{1011486}{N} \right)^{30}} \right]$$
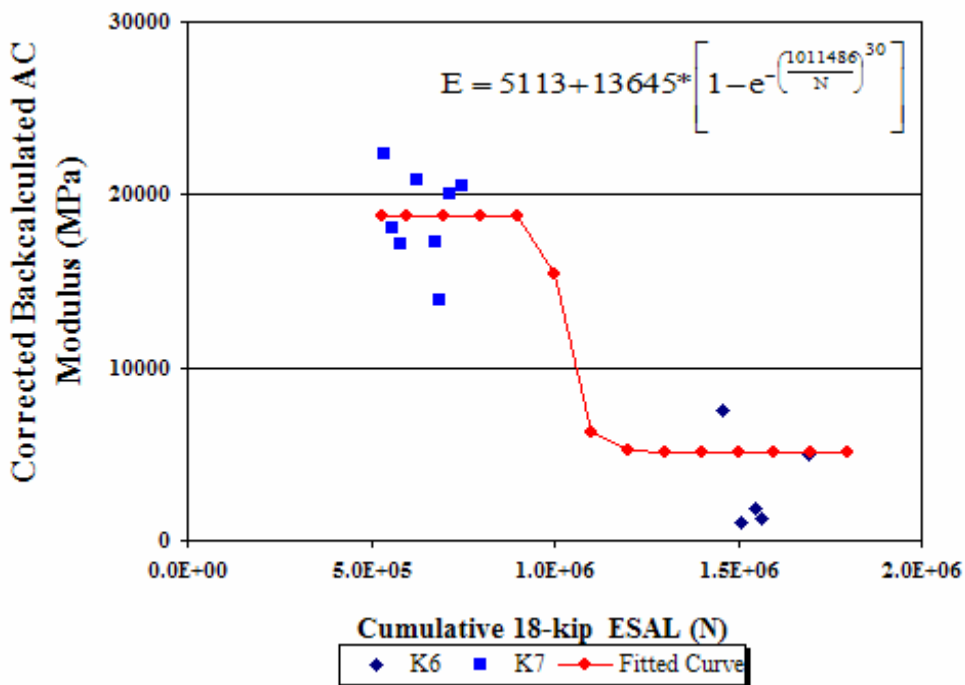
FIGURE 103   Plot of Cumulative 18-kip ESALs versus Corrected Backcalculated AC Modulus in the Pavement Group 4.

$$E = 4866 + 11877 * \left[1 - e^{-\left(\frac{1442190}{N}\right)^{70}} \right]$$
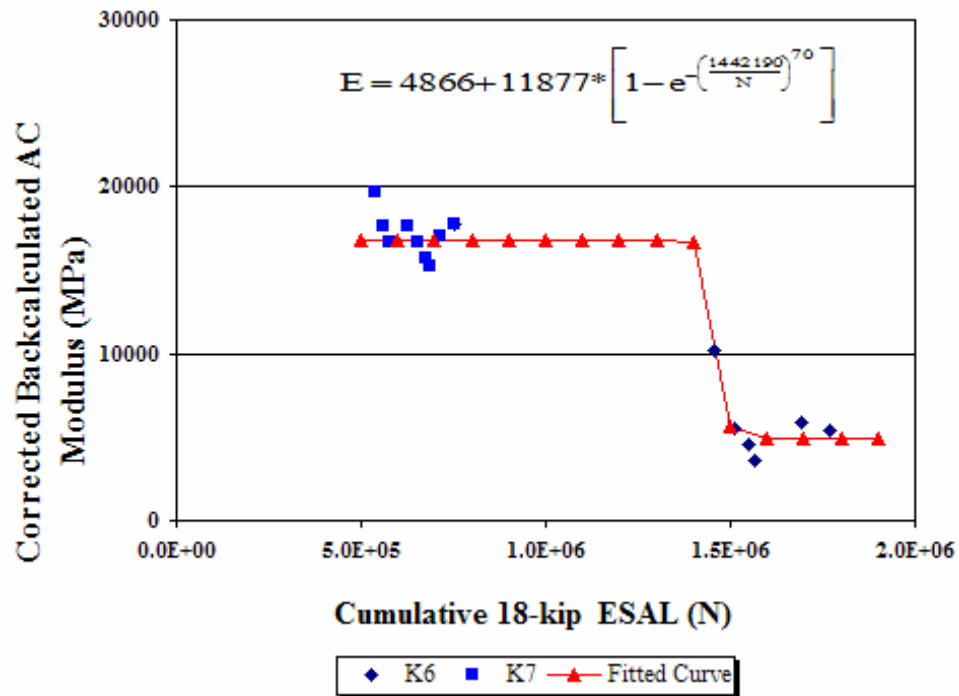
FIGURE 104   Plot of Cumulative 18-kip ESALs versus Corrected Backcalculated AC Modulus in the Pavement Group 5.

$$E = 3590 + 17753 * \left[1 - e^{-\left(\frac{1374560}{N}\right)^{65}} \right]$$
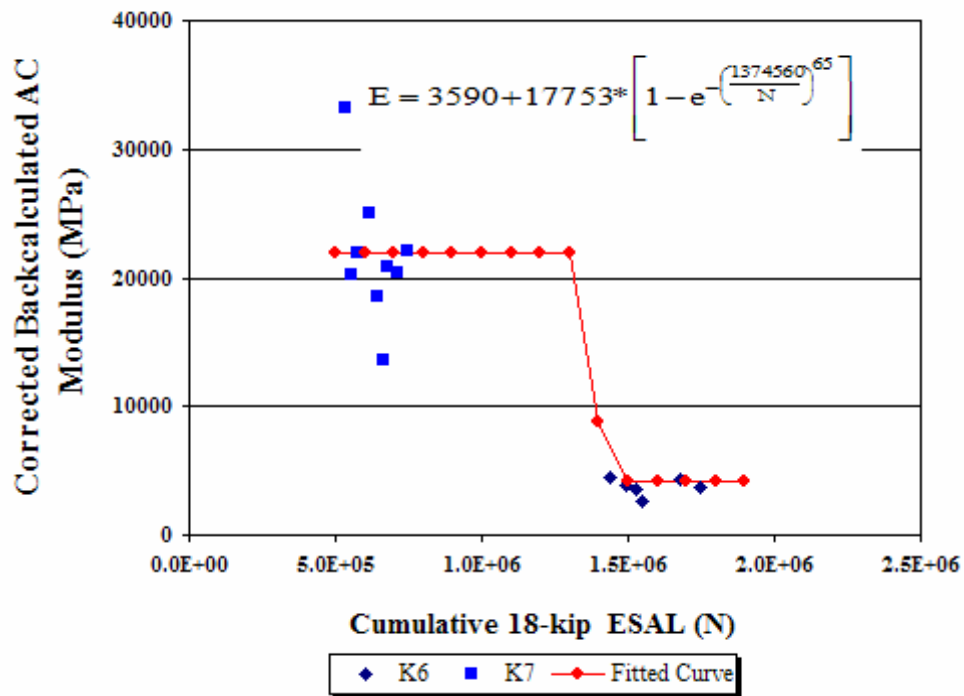
FIGURE 105   Plot of Cumulative 18-kip ESALs versus Corrected Backcalculated AC Modulus in the Pavement Group 6.
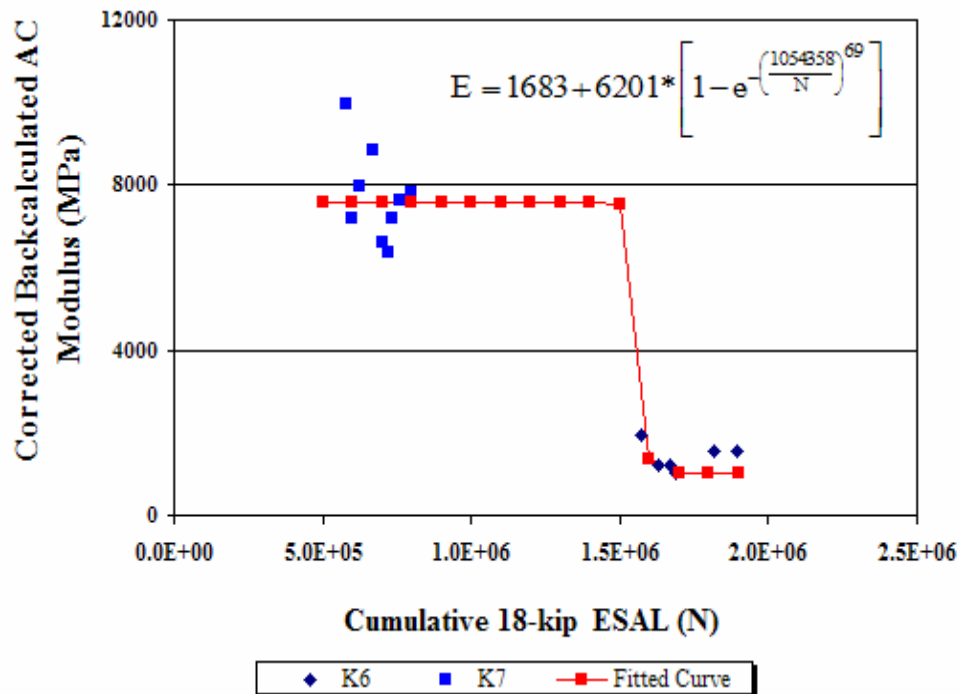
FIGURE 106   Plot of Cumulative 18-kip ESALs versus Corrected Backcalculated AC Modulus in the Pavement Group 7.

These eight figures, Figures 99 through 106, point out how the traffic affects each lane. In each of figure the cumulative 18-kip ESAL is greater in the K6 lane than in the K7 lane, confirming the fact that the K6 lane is more heavily used by all vehicle classes. These plots clearly demonstrate that this greater cumulative 18-kip ESAL is associated with lower corrected backcalculated AC moduli in the K6 lane. It is important to note that the K7 lane carries lower cumulative 18-kip ESAL and higher corrected backcalculated AC modulus than in the K6 lane. These data confirm that more damage is produced by the greater amount of 18-kip ESALs in the K6 lane.

TABLE 61   Analysis of Variance of Non-Linear Regression of the Eq. 8.8.

Pavement Group No	Source	DF	Sum of Squares	Mean of Square	F Value	Approx. Pr > F
1A	Regression	3	45040517	15013506	165.62	<.0001
	Residual	13	1178459	90650.7		
	Uncorrected Total	16	46218976			
	Corrected Total	15	7605180			
1	Regression	3	49832570	16610857	394.95	<.0001
	Residual	12	504693	42057.7		
	Uncorrected Total	15	50337263			
	Corrected Total	14	6290649			
2	Regression	3	98195065	32731688	192.82	<.0001
	Residual	12	2037067	169756		
	Uncorrected Total	15	100230000			
	Corrected Total	14	31839626			
3	Regression	3	66578186	22192729	249.99	<.0001
	Residual	12	1065291	88774.3		
	Uncorrected Total	15	67643477			
	Corrected Total	14	10023397			
4	Regression	3	60469580	20156527	105.92	<.0001
	Residual	11	2093336	190303		
	Uncorrected Total	14	62562915			
	Corrected Total	13	18543367			
5	Regression	3	60133474	20044491	444.06	<.0001
	Residual	12	541666	45138.8		
	Uncorrected Total	15	60675140			
	Corrected Total	14	10405033			
6	Regression	3	91572515	30524172	76.57	<.0001
	Residual	12	4783480	398623		
	Uncorrected Total	15	96355995			
	Corrected Total	14	29367555			
7	Regression	3	11568756	3856252	194.67	<.0001
	Residual	12	237711	19809.3		
	Uncorrected Total	15	11806468			
	Corrected Total	14	3255912			

CHAPTER IX

CONCLUSIONS AND RECOMMENDATIONS

The impact of overweight truck traffic (OTT) on the segment route SH4/48 has been analyzed in this research by carrying out a monitoring process of FWD testing for three years on the road and breaking down their data by static and dynamic analysis. In addition, a frequency sweep test was conducted to get the Dynamic (Complex) Modulus and creep compliance parameters neccesary to compare with those static and dynamic analysis and to find their correlations.

With the purpose of finding out if these OTTs produce damage to the pavement on the route SH4/48 the backcalculated AC moduli were corrected to a common temperature using the Witczak and Fonseca Equation.

These are the conclusions reached in this research:

1. There is evidence of damage on the route SH4/48 due to overweight truck traffic.

2. Combining the thickness of the flexible base layer with the salvage base layer and the treated limestone layer (Figure 32) produce the smallest errors in the backcalculated moduli in both lanes. Only the K6 42, K6 43 and K7 38 FWD stations gave errors in the order of 10% in some months.

3. A linear regression between backcalculated AC modulus from static analysis and dynamic (complex) modulus /E*/ from the frequency sweep lab test gave the best equation /E*/ =1.0554 E $_{static}$ when the core stations from both lanes are analyzed together. The results are shown in Figure 89 and Table 50.

4. The correlation between the backcalculated AC modulus from the static analysis and the Dynamic (Complex) Modulus obtained through frequency sweep test in the laboratory are very acceptable in all FWD stations of the K7 lane (Figure 92). In the K6 lane there is a good correlations except for those values from Pavement Group 2 and the downtown area (Figure 91).

5. The AC mixture in the K6 lane in the downtown area gave the lowest backcalculated AC moduli and the dispersion of the dynamic (complex) modulus /E*/ (Figures B42 up to B56 and Figure 90 pictures a), b), and c) of all pavements sections in this study. This is also supported by the laboratory testing results in which from ten core samples taken in the downtown area in the K6 lane, four were disintegrated in the handling process, six were tested in the laboratory and only one core sample had acceptable values.

6. The linear regression between backcalculated AC moduli from dynamic analysis and static analysis gave the equation $E_{static} = 1.065 \ E_{DBSID}$, when the core stations from both lanes were analyzed together. The results are shown in the Figure 95 and Table 52.

7. The best "c" value that correlates $E_{horinzontal}$ with $E_{vertical}$ was 1.26. This is when all data from both K6 and K7 lane are combinated.

8. The greater "c" value obtained in the K6 lane, 1.3, than 1.15 in the K7 lane, indicates that as damage increases, the anysotropy of the asphalt layer increase.

9. Since the corrected backcalculated AC moduli by temperature show a decreasing line on the K6 lane in mostly all Pavement Groups, this lane must have more damage than the K7 lane (Figures 98 to 104). This conclusion is supported by the m_c values from the K6 lane whose values increase with time, indicating te presence of large fatigue cracking or permanent deformation over time. Unlike the m_c values from the K7 lane which show a flat trend (Figures 97 and 98), indicating little damage.

10. The total number of the 18-kip ESAL by year (Tables 56 and 59) provides evidence of a greater use in the K6 lane than the K7 lane for all vehicle classes.

11. The greater cumulative 18-kip ESALs with lower corrected backcalculated AC modulus shown in the Figures 106 up to 113 confirm again the damage which occurred in the K6 lane due to current traffic (overweight truck).

12. The percentage by incidence of the FHWA classes 9 and 10 (overweight truck class) gave 4.21% and 0.73% porcentages, respectively, (Table 57 and 58) the porcentage of the ESALs for tandem axle produced by these classes is 35 % of the total 18-kip ESALs obtained from the axle distribution (Table 56).

13. Damage to asphalt flexible pavement can be detected by non-destructive FWD testing.

14. This research has proved that FWD data must be corrected for the effects of load level and environmental conditions and the resulting backcalculated modulus values are consistent with laboratory data.

RECOMMENDATIONS

Because the SH 4/48 is a segmened route which carries overweight truck traffic, it is necessary to have a homogenous hardening AC layer in all downtown areas, especially in the K6 lane FWD stations from K6 42 up to K6 56 (From Boca Chica Blvd. to Cleveland St.).

REFERENCES

1. Nguyen, C., C. Lau, and T. Scullion. *Design Concepts for a Miniature Pavement GPR Antenna.* Texas Transportation Institute. Research Report 1341-3F, College Station, TX., November 1995.

2. Scullion, T., S. Servos, J. Ragsdale, and T. Saarenketo. *Applications of Ground-Coupled GPR to Pavement Evaluation.* Texas Transportation Institute. Research Report 2947-S, College Station, TX. November 1997.

3. Scullion, T., C. Lau, and Y. Chen. *Implementation of the Texas Ground Penetrating Radar System.* Texas Transportation Institute. Research Report 1233-1, College Station, TX. November 1994.

4. Scullion, T., Y. Chen, and C. Lau. *COLORMAP-User's Manual with Case Studies.* Texas Transportation Institute. Research Report 1341-1, College Station, TX. November 1995.

5. Magnuson, A. *Calculation of the Pavement Layer Properties Using Dynamic Analysis of Falling-Weight Deflectometer Data.* Final Report SHRP/IDEA Project Number SHRP-88-ID025. Texas Transportation Institute. Division II, Materials, Pavements, and Construction. Texas A&M University. College Station TX, September 1993.

6. Lytton, R., F. Germann, Y. Chou, and S. Stofels. Determining Asphaltic Concrete Pavement Structural Properties by Nondestructive Testing. *National Cooperative Highway Research Report 327.* Transportation Research Board. National Research Council. Washington, DC. June 1990.

7. Lytton, R. Backcalculation of Pavement Layers Properties. *Nondestructive Testing of Pavements and Backcalculations of Moduli. ASTM STP 1026.* A.J. Bush III and G. Y. Baladi Eds. American Society for Testing and Materials. Philadelphia, 1989 pp. 7-38.

8. Michalak, C., and T. Scullion. *MODULUS 5.0: User's Manual*. Texas Transportation Institute. The Texas A&M University System. Research Report 1987-1. College Station, TX. November 1995.

9. Kausel, E., and R. Peek. Dynamic Loads I the Interior of a Layered Stratum: An Explicit Solution. *Bulletin of the Seismological Society of America* 72(5): 1459-1481. 1982.

10. Roesset, J. *Computer Program UTFWIBM*. The University of Texas. Austin TX. 1987.

11. Magnuson, A., and R. Lytton. *Development of Dynamic Analysis Techniques for Falling Weight Deflectometer Data.* Texas Transportation Institute. The Texas A&M University System. Research Report 1175-2, College Station, TX. July 1997.

12. Foinquinos, R., J. Roesset, and K. Stokoe. *FWD-DYN: A Computer Program for Forward Analysis and Inversion of Falling Weight Deflection Data*. Research Report 1970-1F, Center for Transportation Research, The University of Texas, Austin, TX. 1993.

13. Fernando, E., and W. Liu. *Dynamic Analysis of FWD Data for Pavement Evaluation.* Proceedings 6th International Conference of the Bearing Capacity of Roads and Airfield, Lisboa, Portugal, Vol 1, 2002, pp 159-167.

14. Lukanen, E., N. Stubstad, and R. Briggs. *Temperature Predictions and Adjustment Factors for Asphalt Pavements*. Research Report FHWA-RD-98-085, Federal Highway Administration, McLean. VA., 1998

15. Stubstad, N., E. Lukanen, C. Ritcher, and S. Baltzer. Calculation of AC Layer Temperatures from FWD Field Data. *Proceedings 5th Conference on the Bearing Capacity of Roads and Airfields.* Trondheim, Norway, 1998, pp 919-928.

16. Fernando, E., W. Liu, and D. Ryu. *Development of a Procedure for Temperature Corrections of Backcalculated AC Modulus.* Texas Transportation Institute. The Texas A&M University System. Research Report 1863-1, College Station, TX. September 2001.

17. Fernando, E., and W. Liu. *User's Guide for the Modulus Temperature Corrections Program (MTCP).* Texas Transportation Institute. The Texas A&M University System. Research Report 1863-2, College Station, TX. January 2001.

18. Fernando, E., and W. Liu. *User's Manual for Pavement Dynamic Back-Calculation Procedure with Systems Identification Method (DBSID).* Texas Transportation Institute. The Texas A&M University System. RF Project 7265, College Station, TX. 2001

19. *AASHTO Guide for Design Pavement Structures.* AASHTO, Washington DC, 1993.

20. *NCHRP 1-37A Draft Test Method DM-1, Standard Test Method for Dynamic Modulus of Asphalt Concrete Mixtures.* NCHRP. RF Project 9-29, Washington DC, May 2002.

21. *Standard Test Method for Dynamic Modulus of Asphalt Mixtures D-3497-79 (Reapproved 1995).* American Society of Material Testing. ASTM. West Conshohocken, PA. Vol 04: pp 334-336.

22. Yoder, E., and M. Witczak. *Principles of Pavement Design.* Second Edition. John Willey & Sons, New York, Inc. 1975, Chapter VIII, pp. 271-272.

Supplemented Source Consulted

- Lee, J., C. Nguyen, and T. Scullion. *Development of a Prototype High Frequency Ground Penetrating Radar System.* Texas Transportation Institute. Research Report 1702-S, College Station, TX. January 2002.

- Scullion, T., and Y. Chen . *Using Ground Penetrating Radar for Real-Time Quality Control Measurements on New HMA Surfaces.* Texas Transportation Institute. Research Report 1702-5, College Station, TX. November 2002.

- Scullion, T., and E. Rmeili. *Detecting Stripping in Asphalt Concrete Layers Using Ground-Penetrating Radar.* Texas Transportation Institute. Research Report 2964-S, College Station, TX. November 1997.

- Maser, K., and T. Scullion. *Influence of Asphalt Layering and Surface Treatments on Asphalt and Base Layer Thickness Computations Using Radar.* Texas Transportation Institute. Research Report 1923-1 College Station, TX. 1992.

APPENDIX A

K6 AND K7 SECTIONS
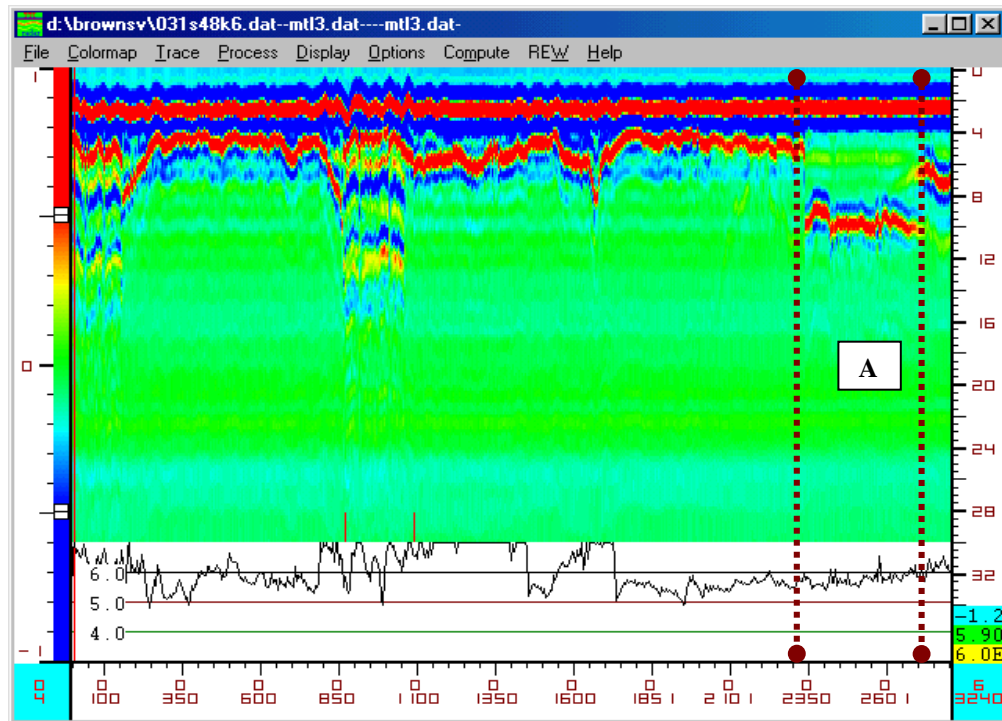
FIGURE A1   K6-A and K6-B Section
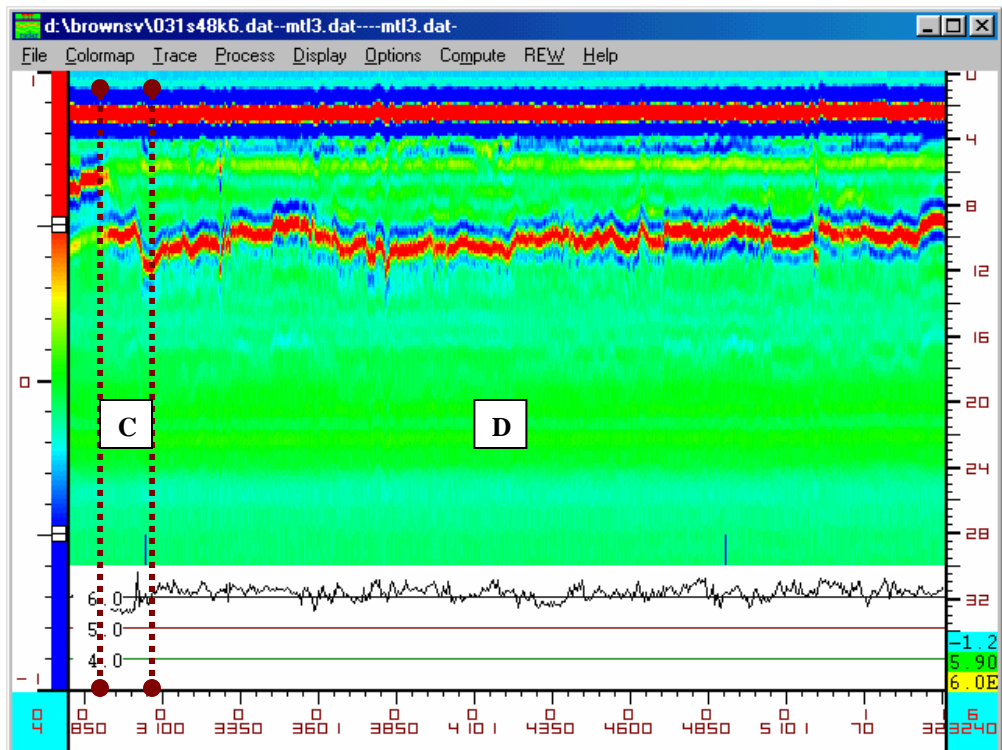
FIGURE A2   K6-B, K6-C, and K6-D Section
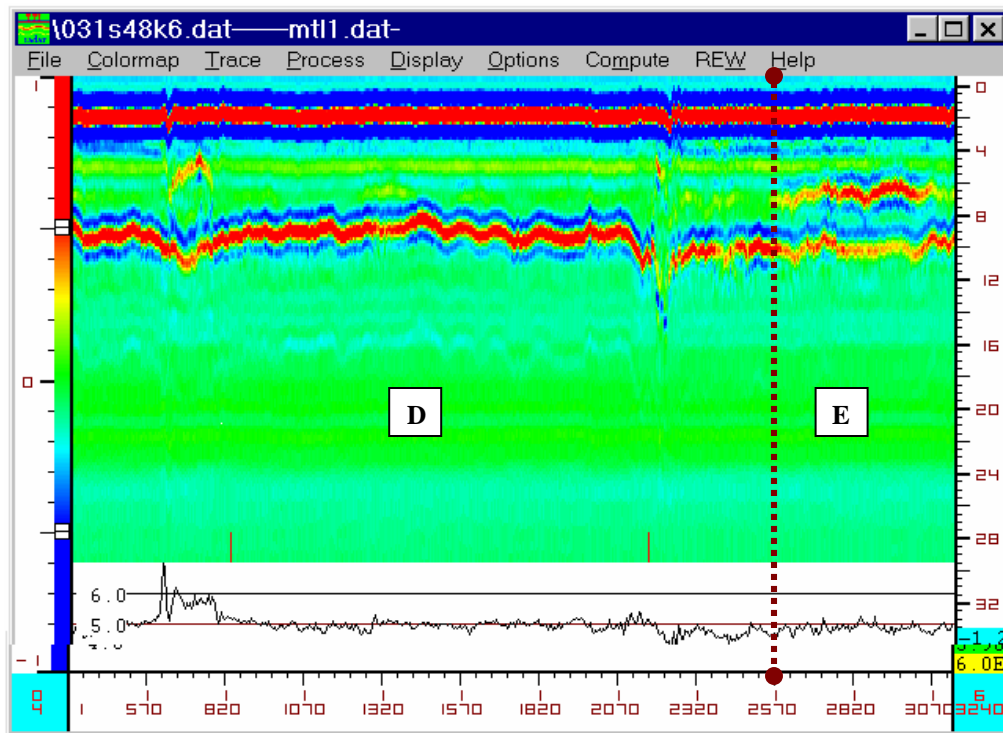
FIGURE A3   K6-D and K6-E Sections
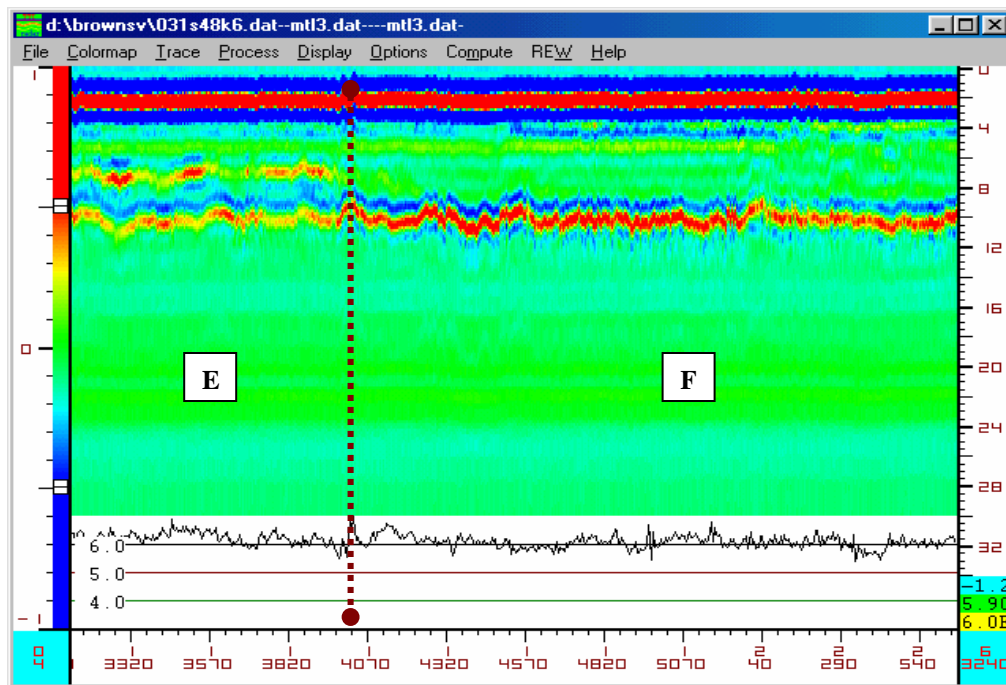
FIGURE A4   K6-E and K6-F Sections
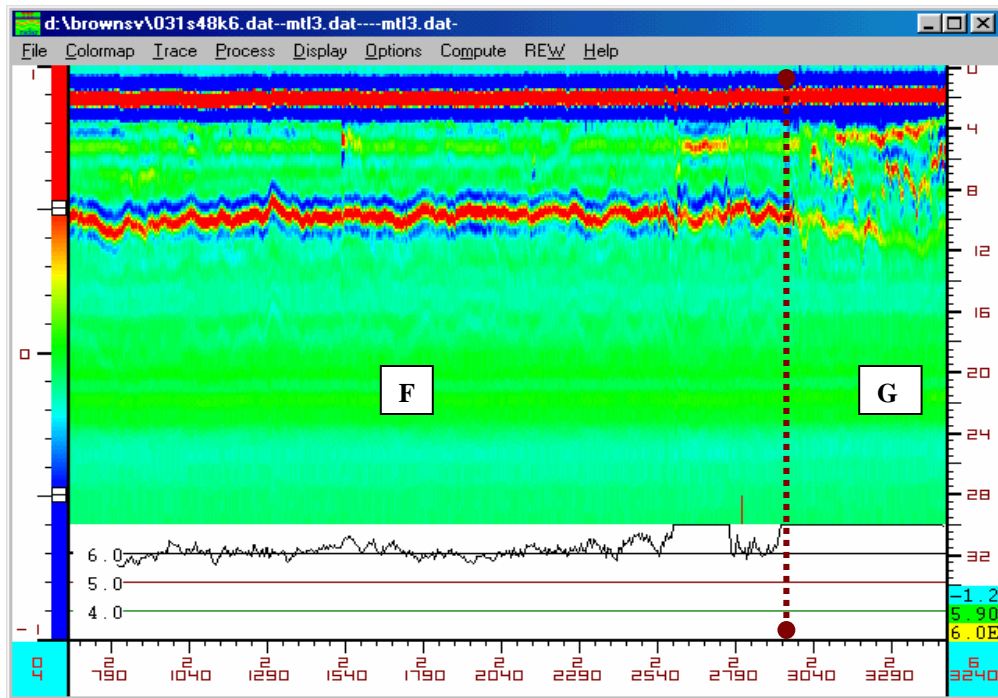
FIGURE A5   K6-F and K6-G Sections
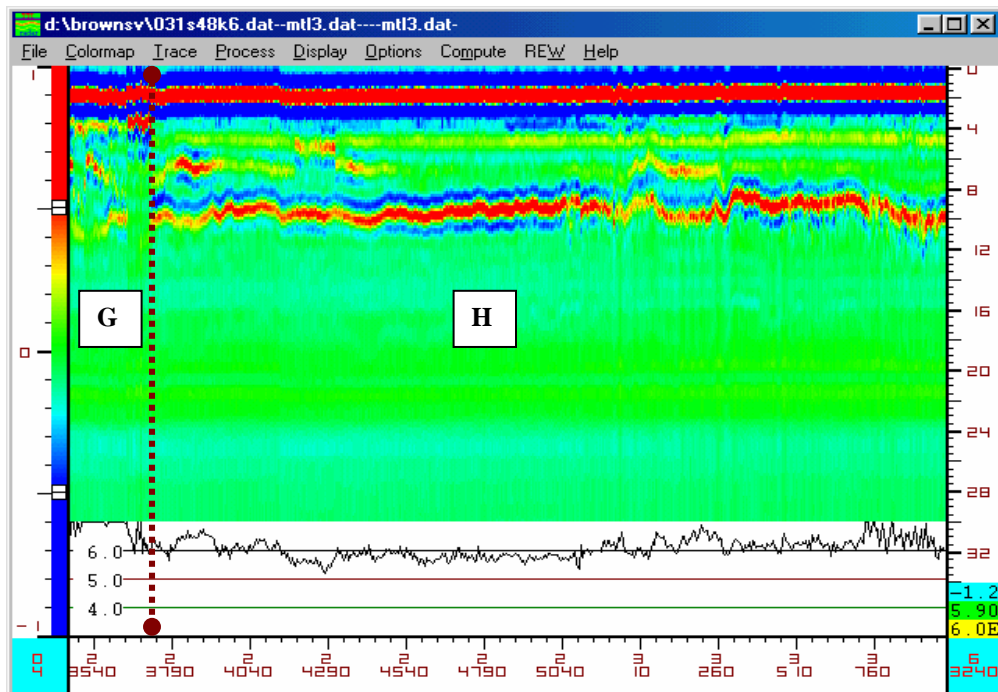
FIGURE A6   K6-G and K6-H Sections
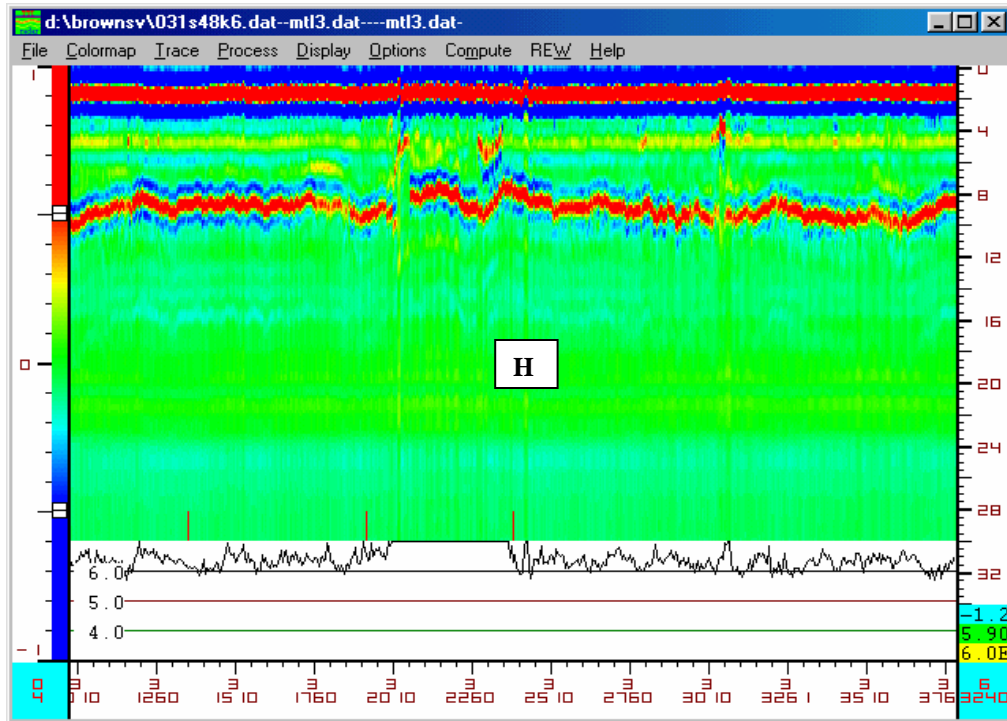
FIGURE A7   K6-H Section
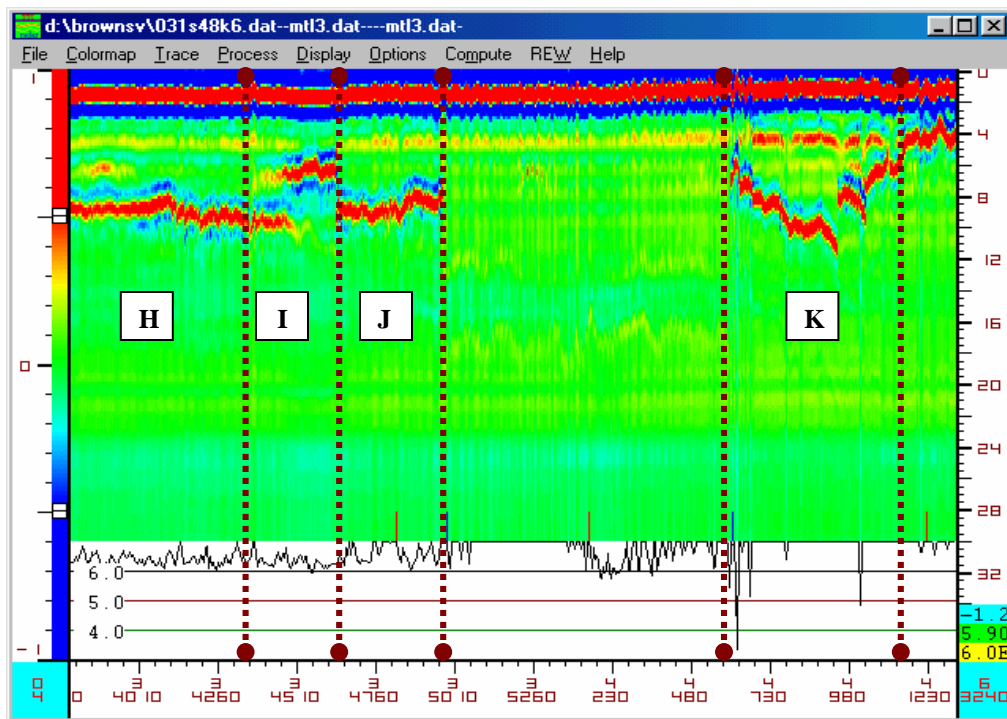
FIGURE A8   K6-H, K6-I, K6-J, and K6-K Sections

FIGURE A9   K6-L Section

FIGURE A10   K6-L, K6-M, K6-N, and K6-O Sections
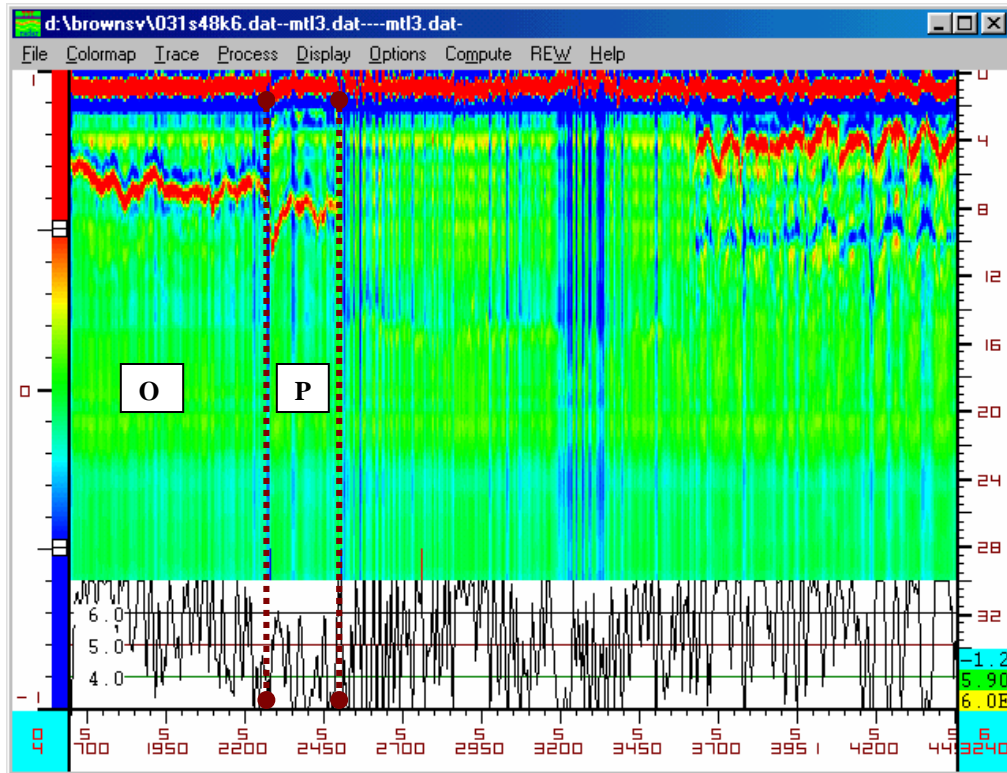
FIGURE A11   K6-O and K6-P Sections
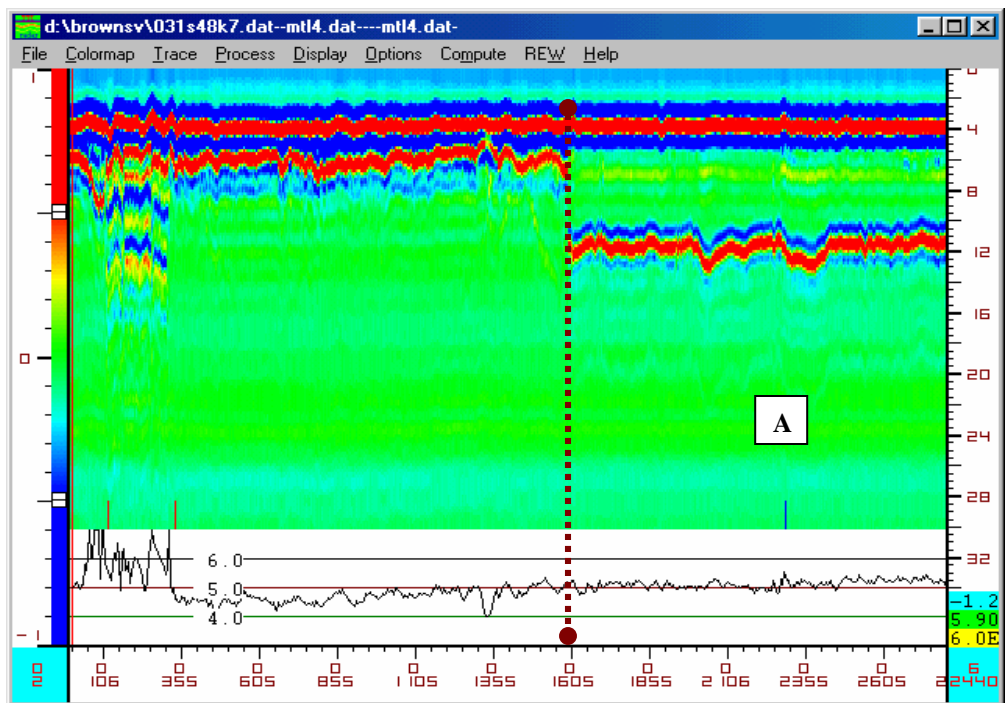
FIGURE A12   K7-A Section
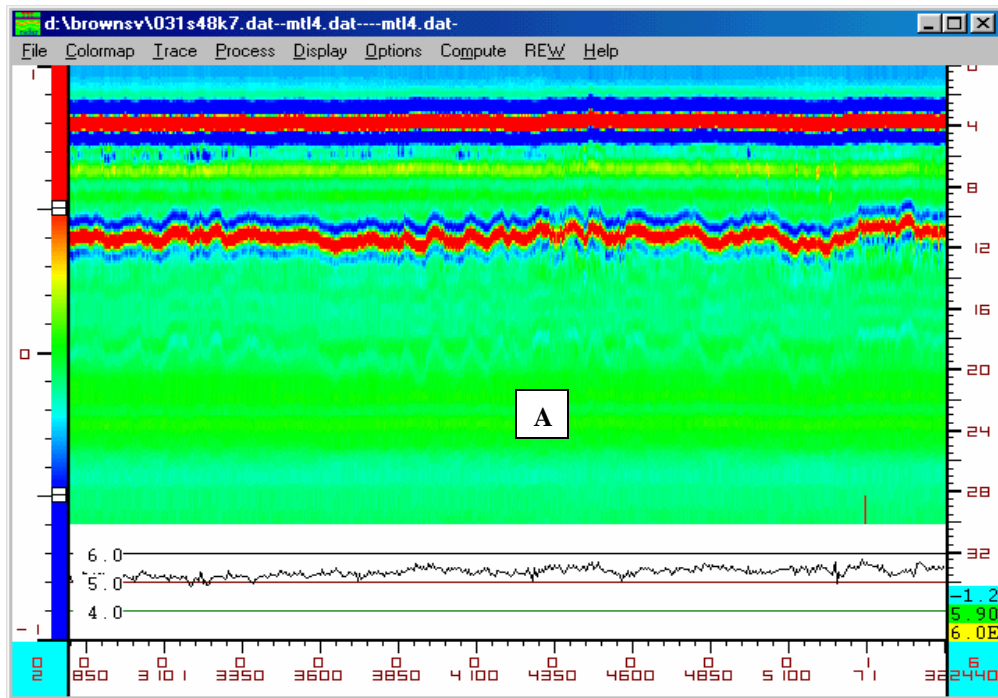
FIGURE A13   K7-A Section
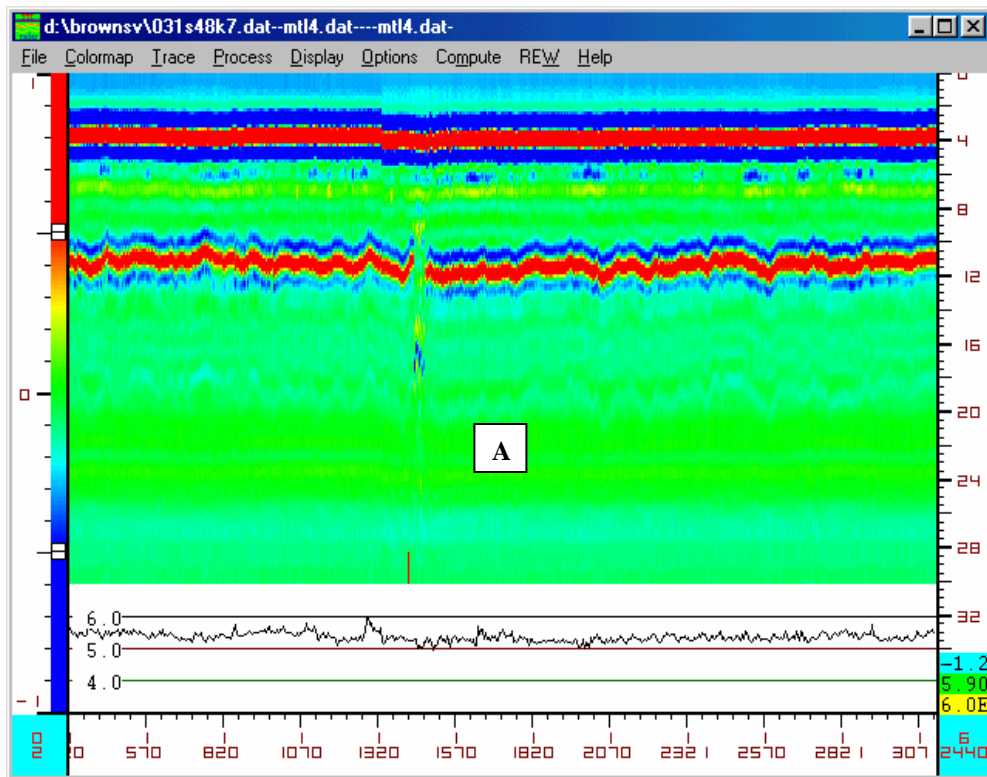
FIGURE A14   K7-A Section
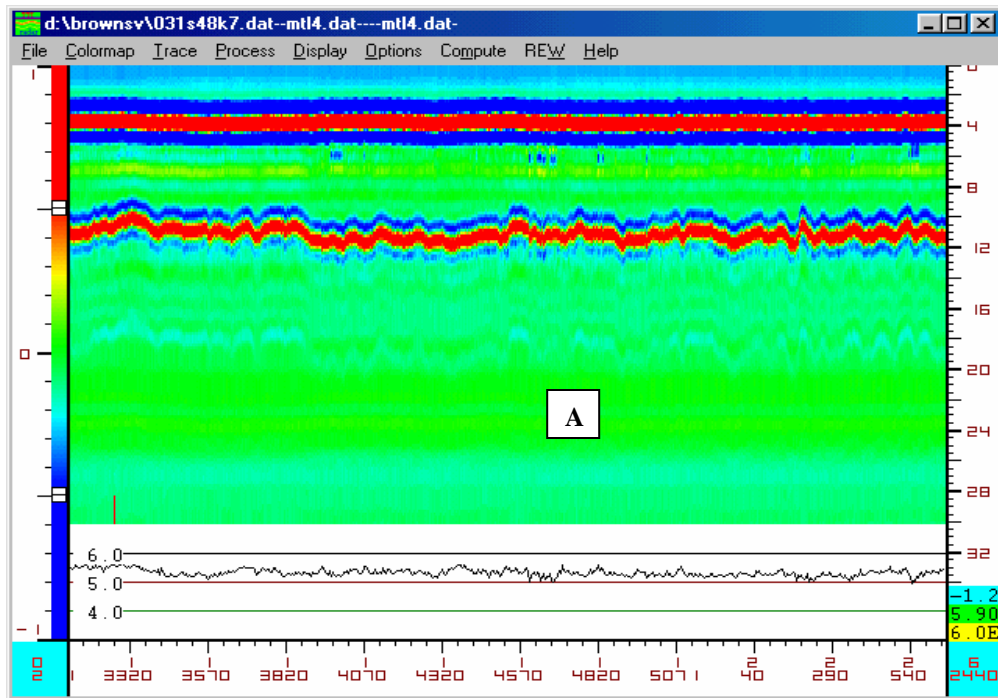
FIGURE A15   K7-A Section
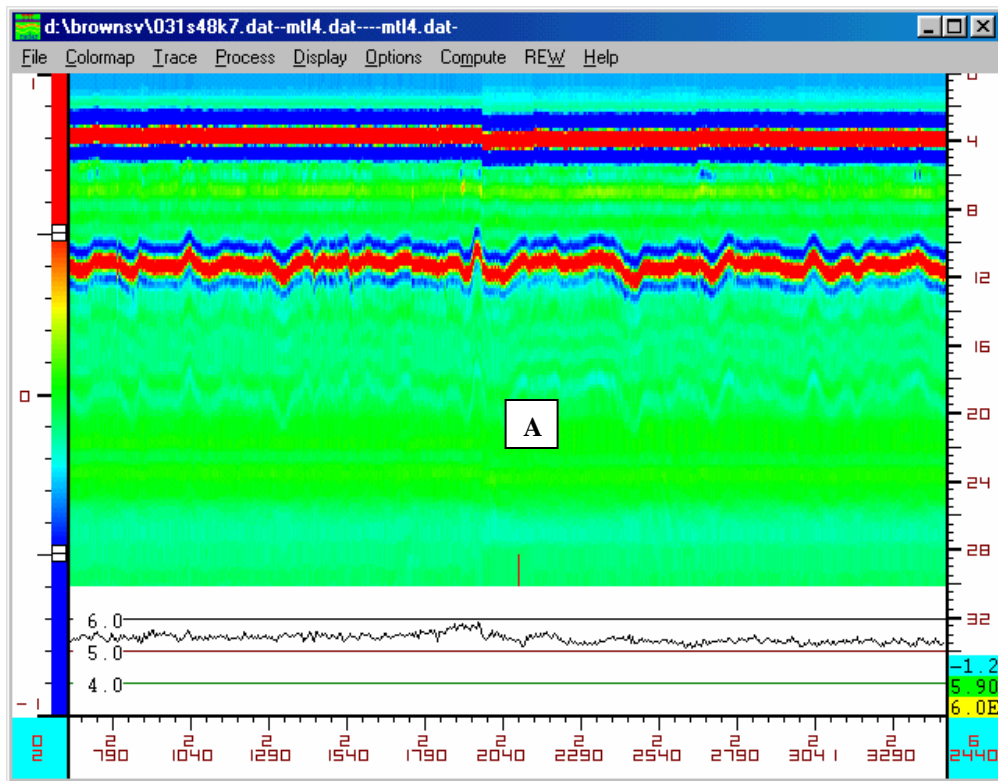
FIGURE A16   K7-A Section
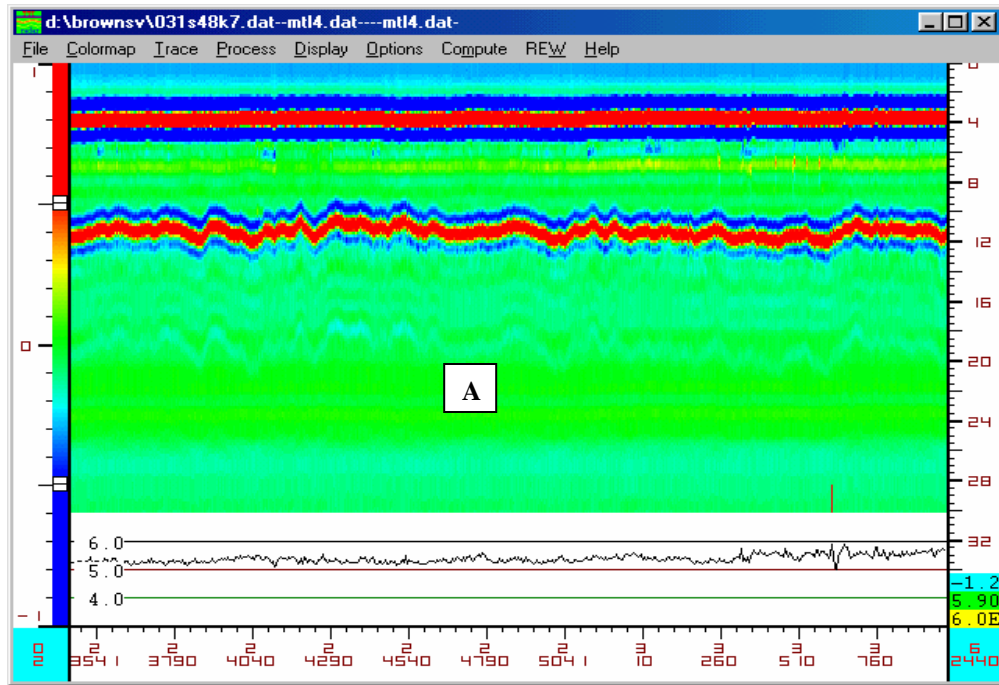
FIGURE A17   K7-A Section
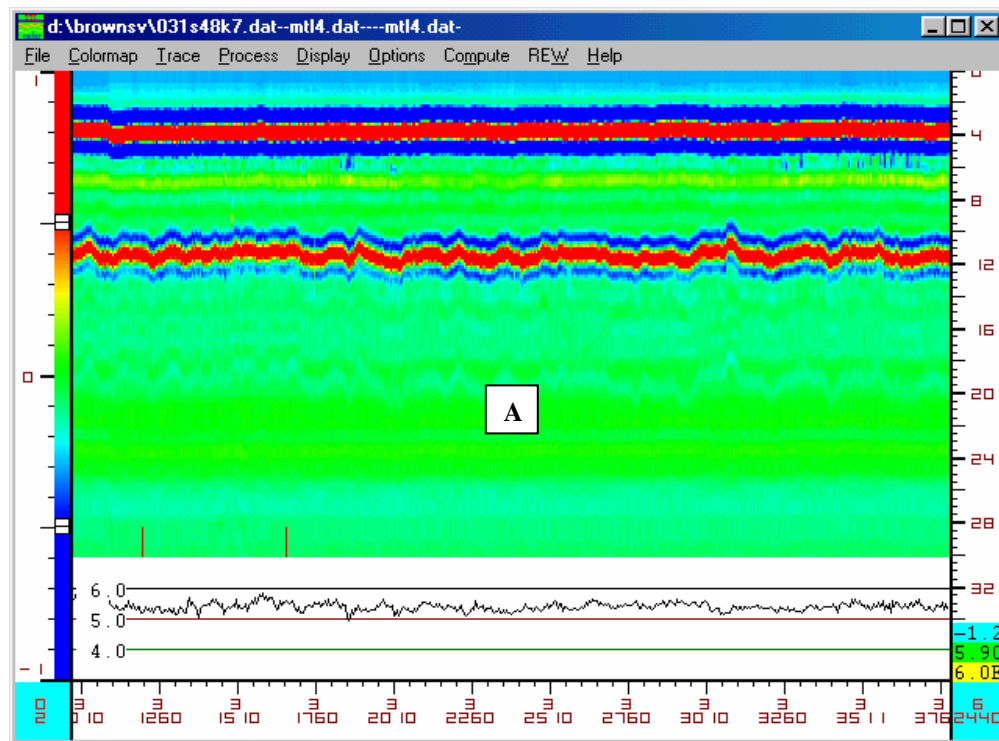
FIGURE A18   K7-A Section
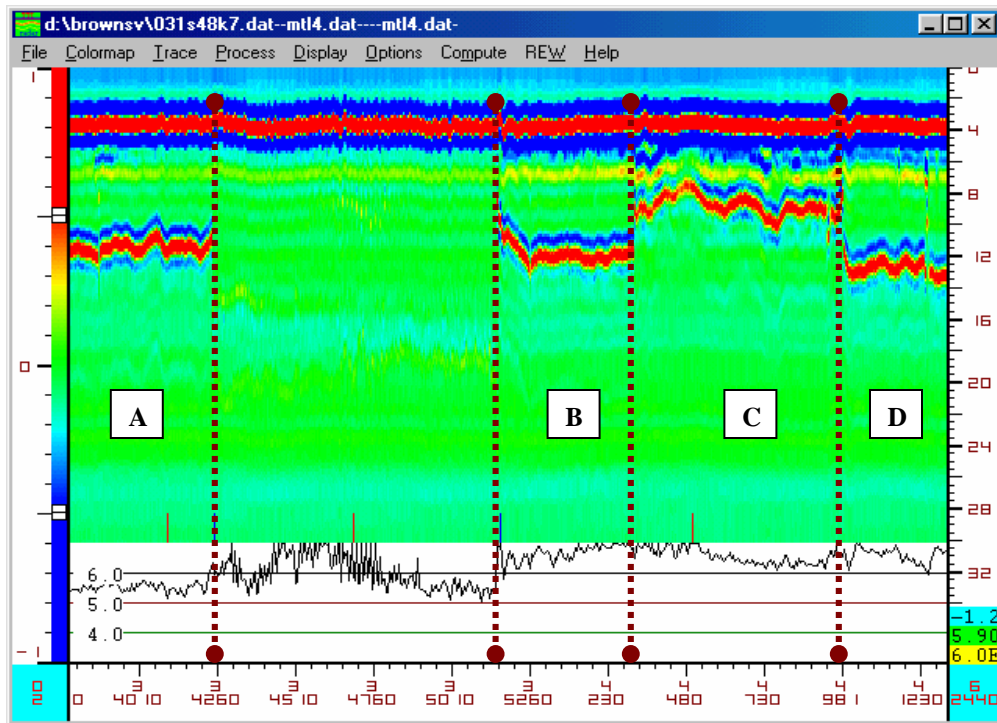
FIGURE A19   K7- A, K7-B, K7-C, and K7-D Sections
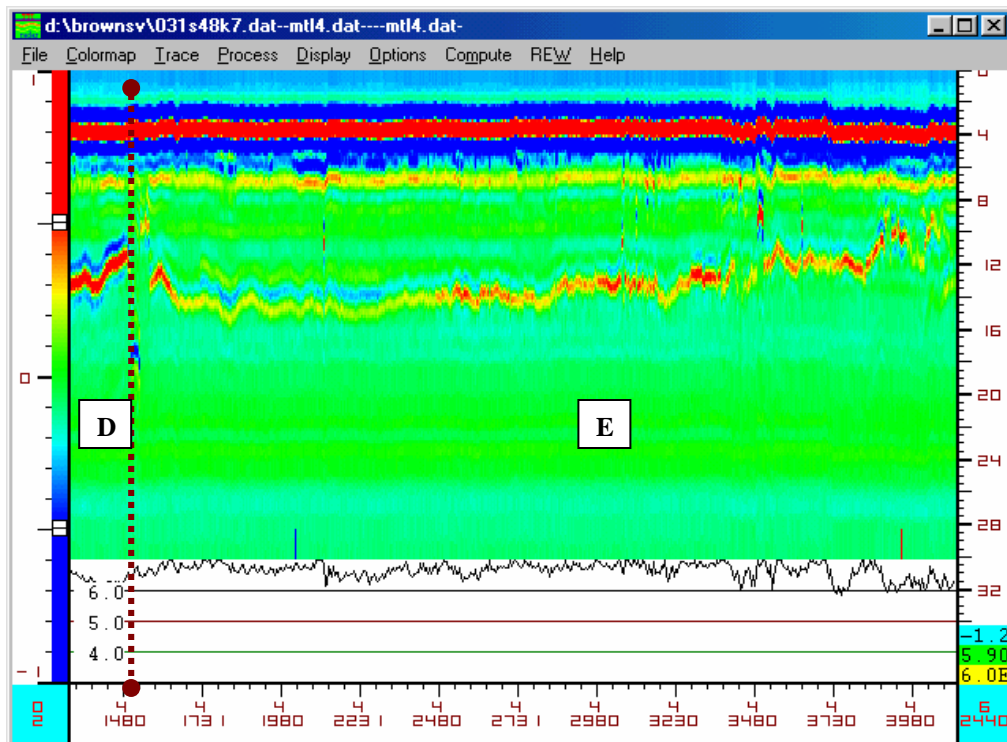
FIGURE A20   K7-D and K7- E Sections
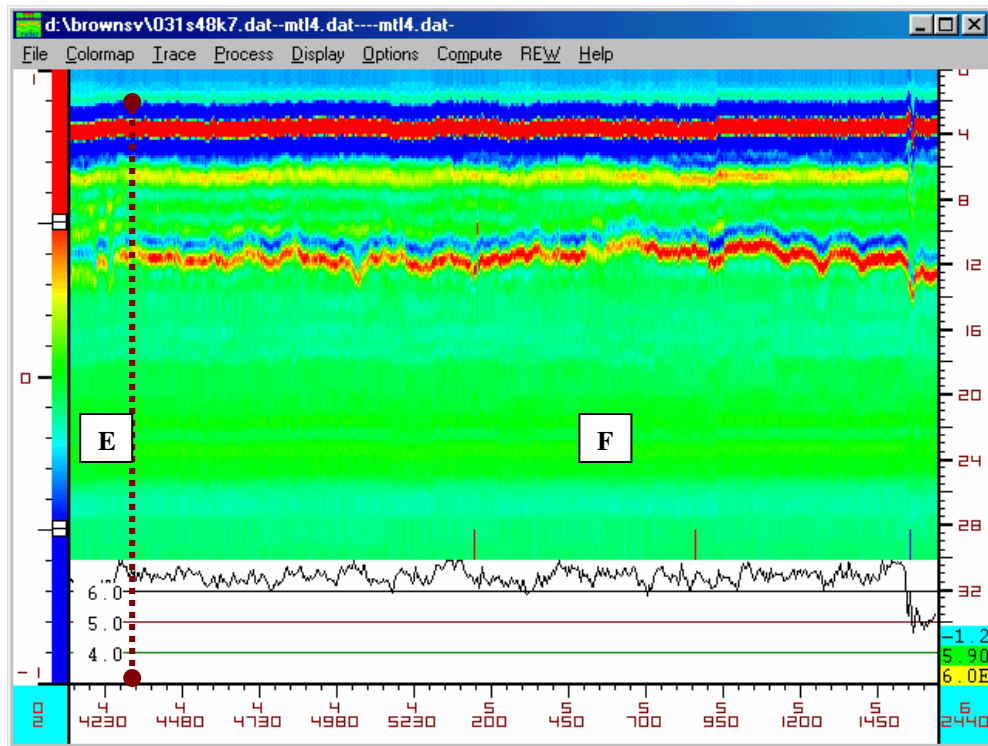
FIGURE A21   K7- E and K7- F Sections
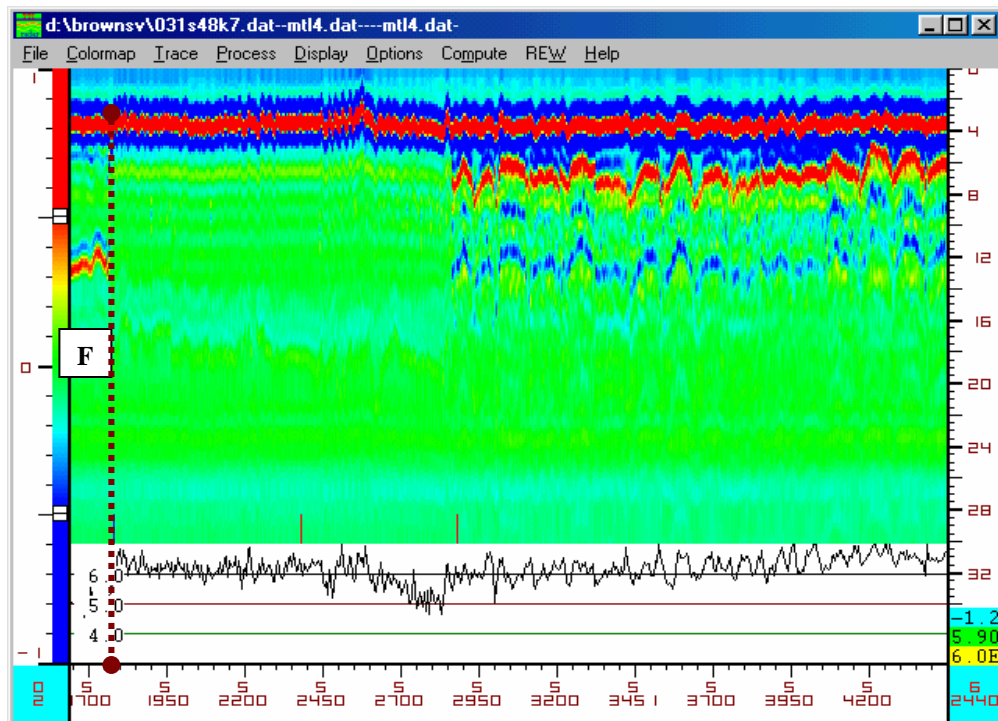
FIGURE A22   K7- F Section

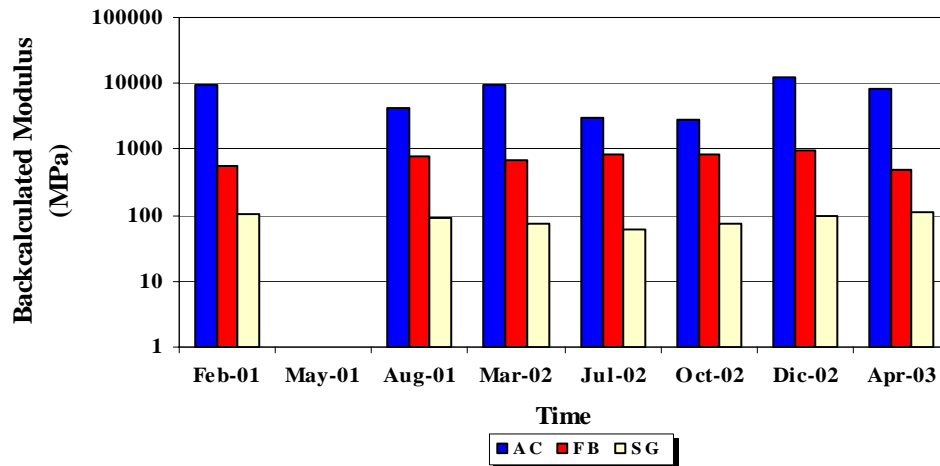**APPENDIX B**

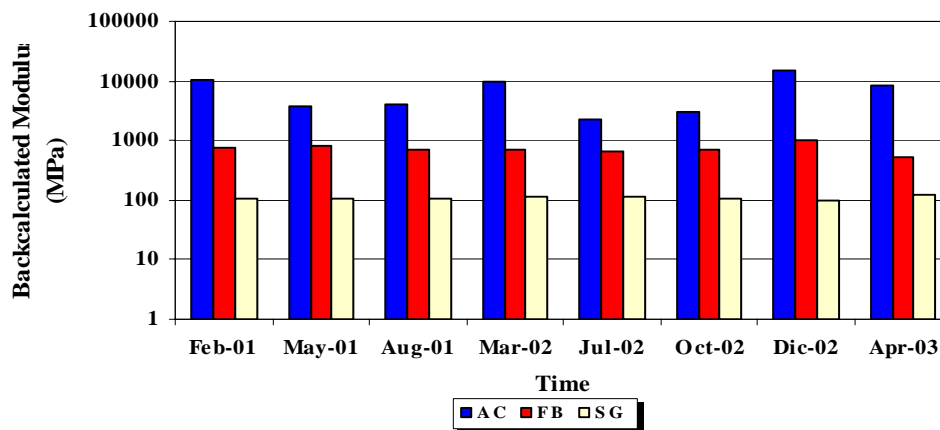**PLOTS OF BACKCALCULATED MODULI**
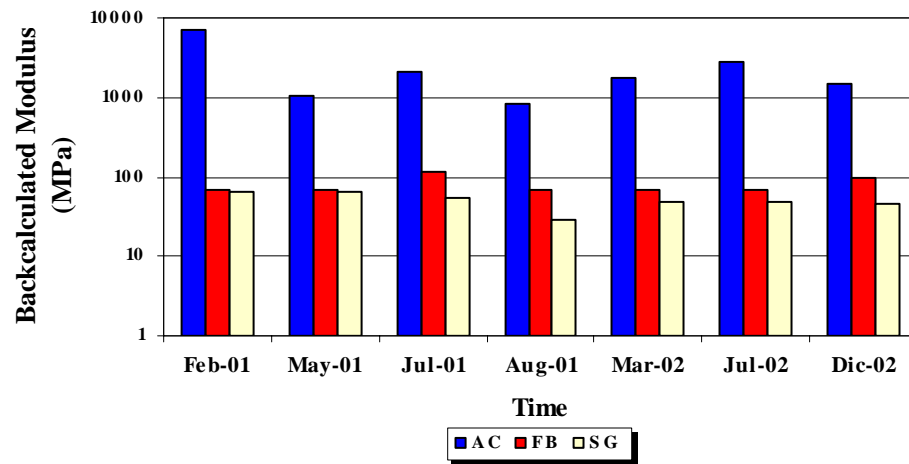
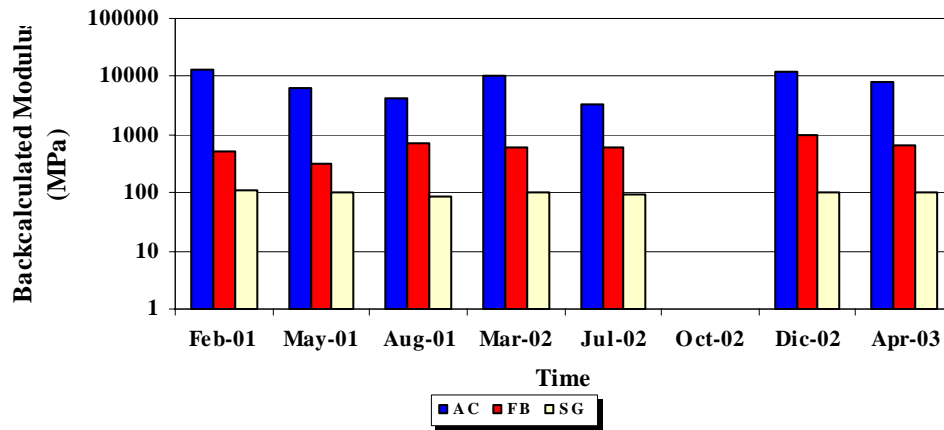**FIGURE B1 Backcalculated Modulus of K6 1 FWD Station**
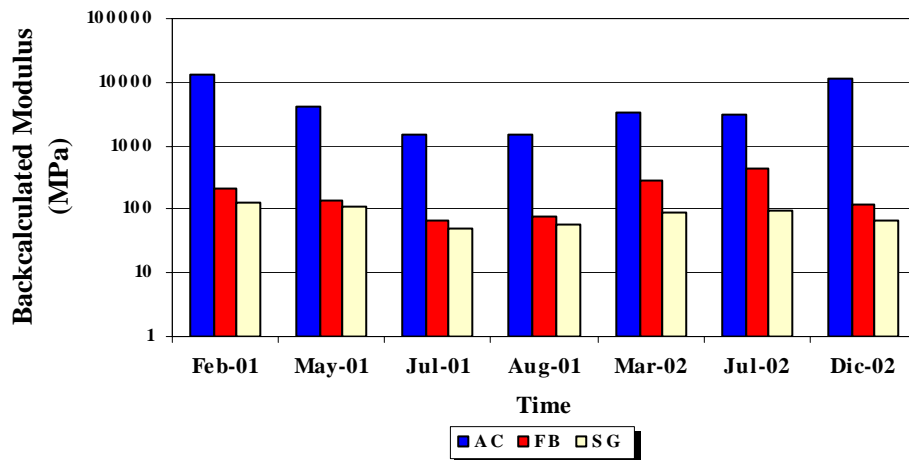
FIGURE B2 Backcalculated Modulus of K6 2 FWD Station
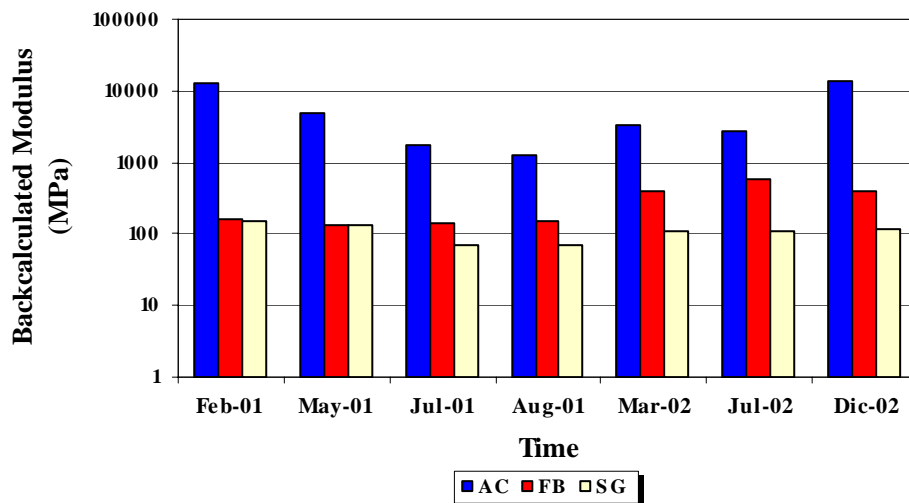
FIGURE B3 Backcalculated Modulus of K6 3 FWD Station
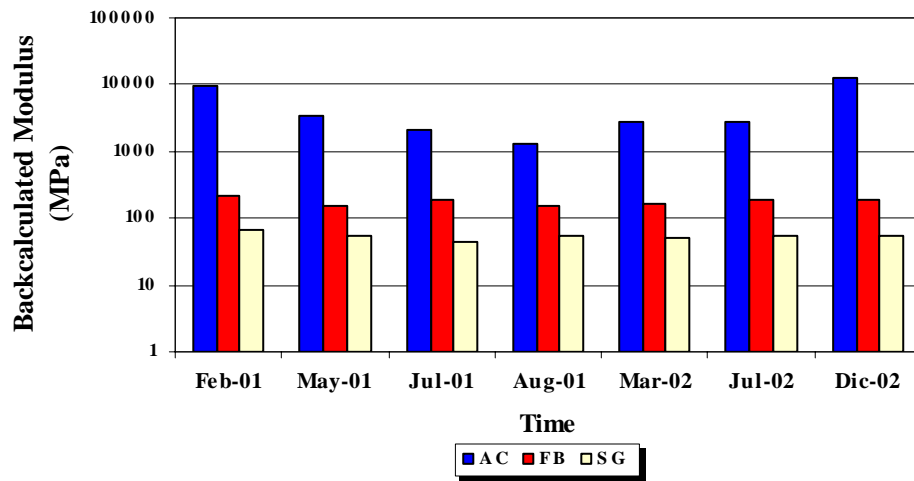
FIGURE B4 Backcalculated Modulus of K6 4 FWD Station
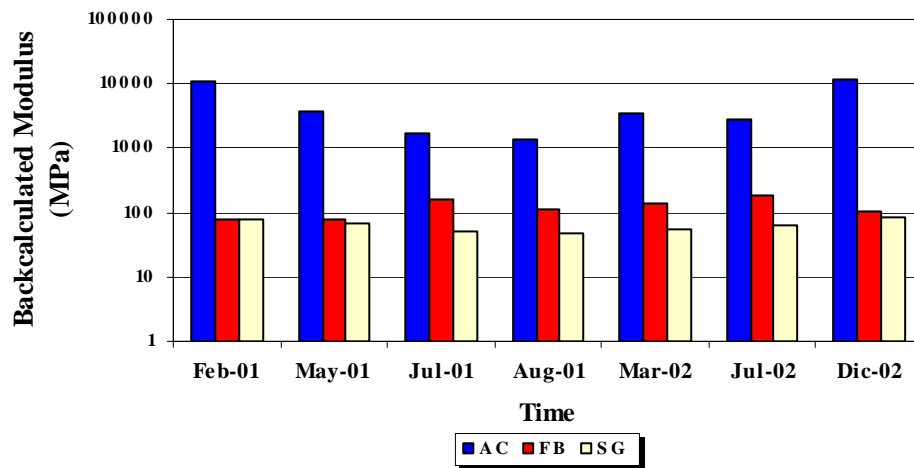
FIGURE B5 Backcalculated Modulus of K6 5 FWD Station
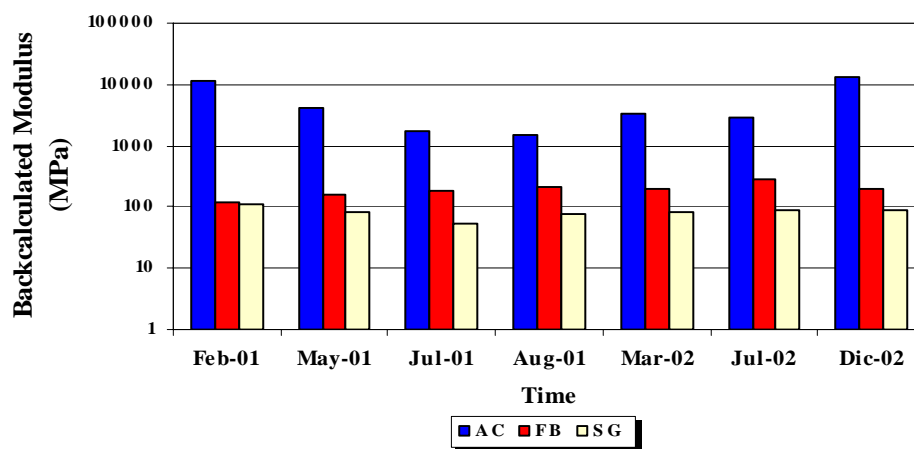
FIGURE B6 Backcalculated Modulus of K6 6 FWD Station
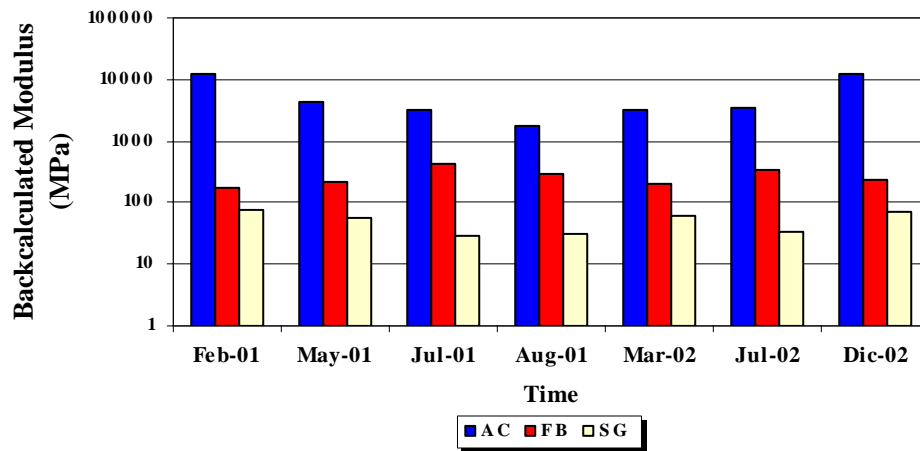
FIGURE B7 Backcalculated Modulus of K6 7 FWD Station
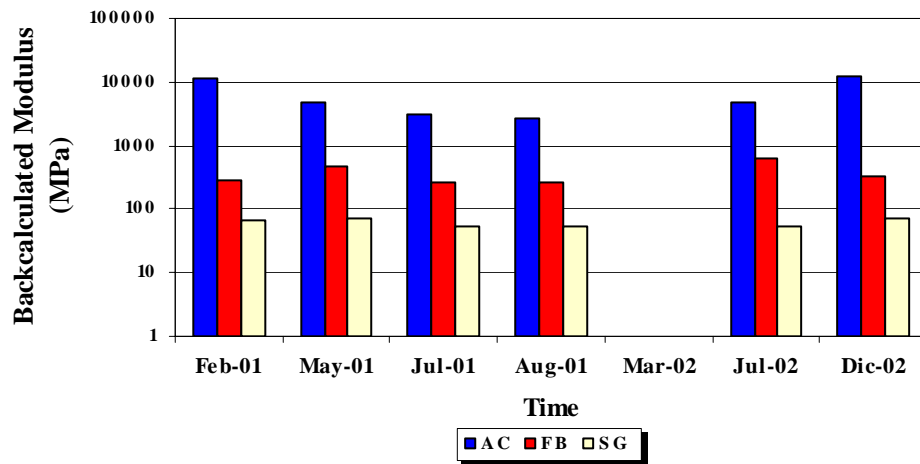
FIGURE B8 Backcalculated Modulus of K6 8 FWD Station
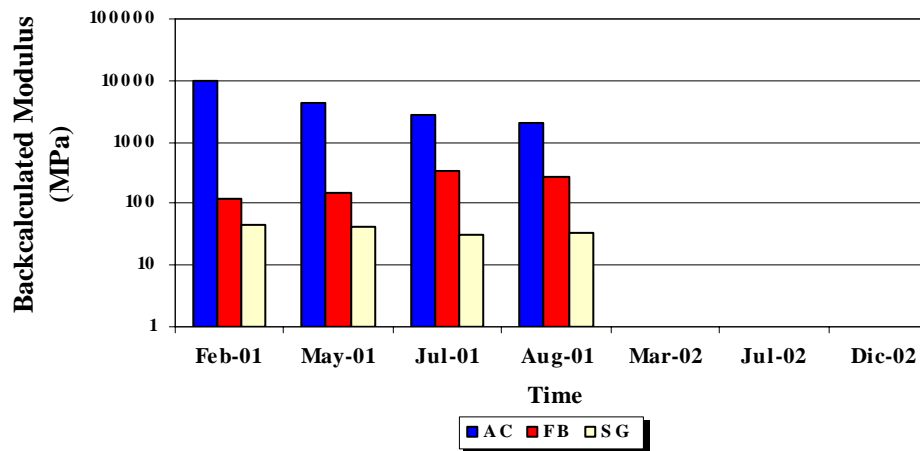
FIGURE B9 Backcalculated Modulus of K6-9 FWD Station
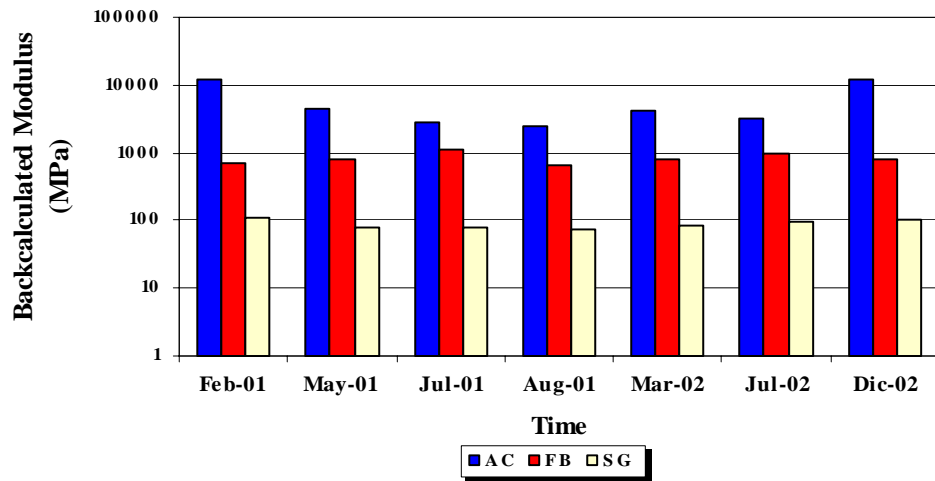
FIGURE B10   Backcalculated Modulus of K6-10 FWD Station
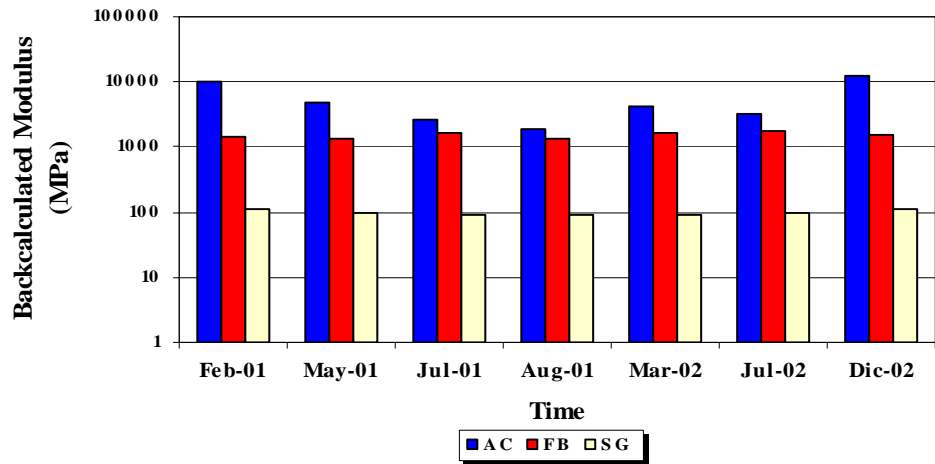
FIGURE B11   Backcalculated Modulus of K6-11 FWD Station
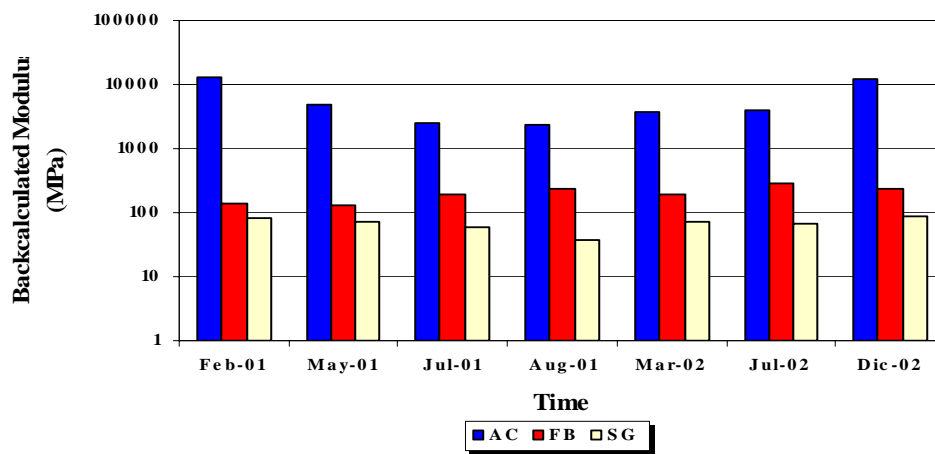
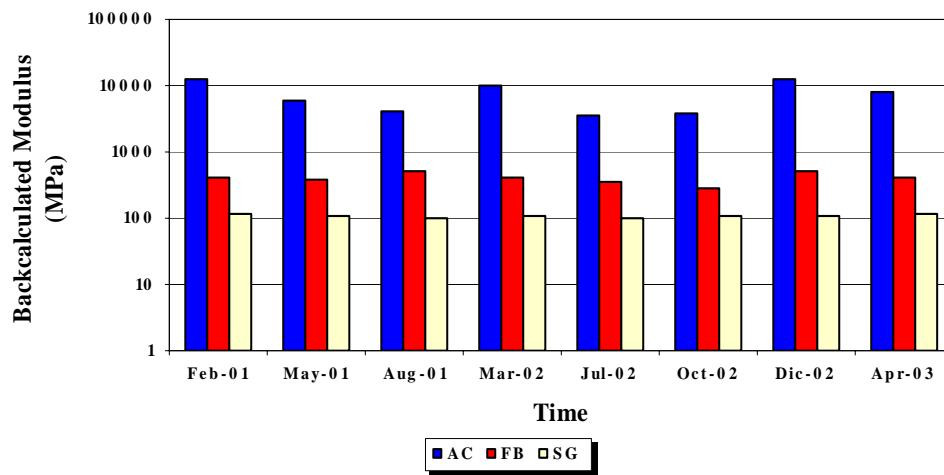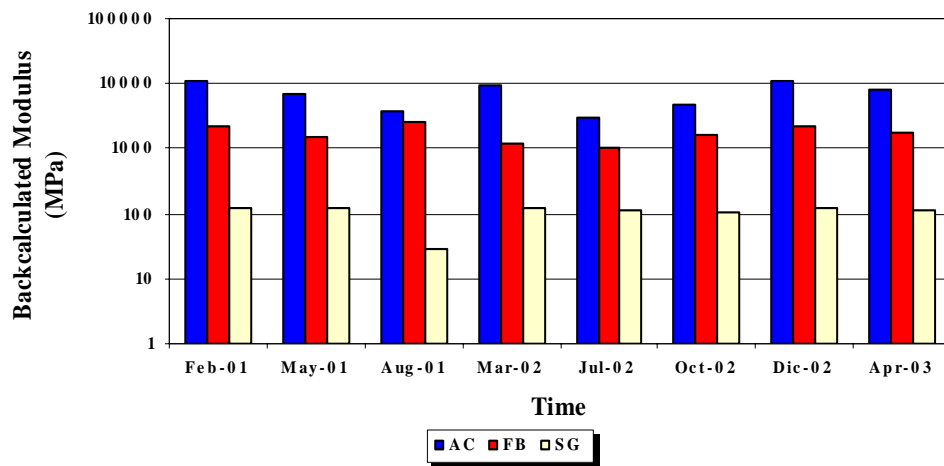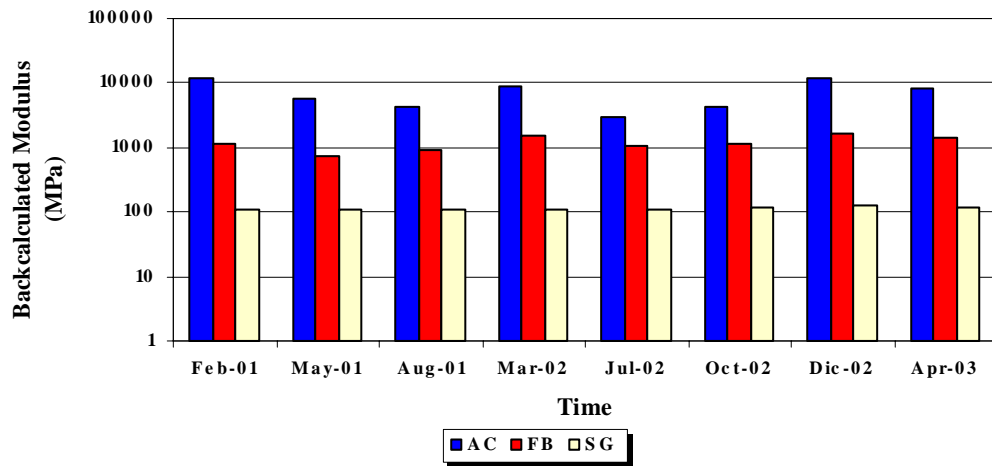FIGURE B12   Backcalculated Modulus of K6-12 FWD Station
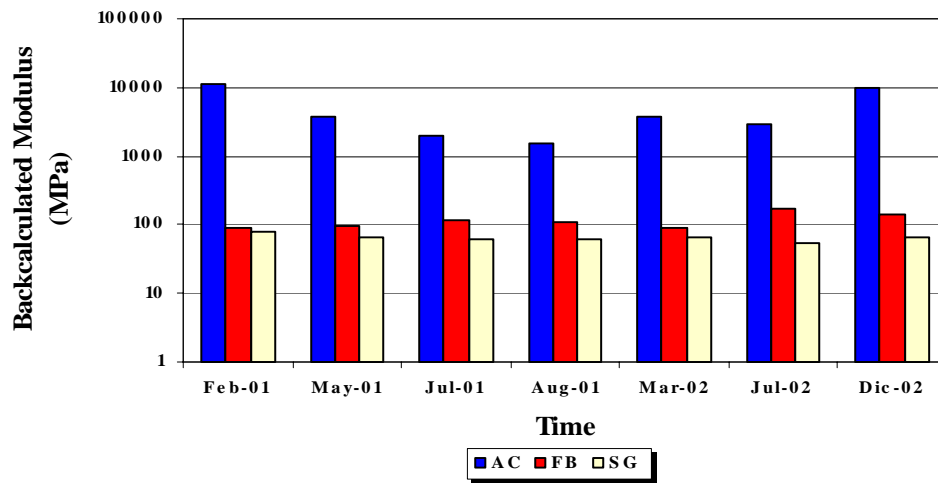
FIGURE B13   Backcalculated Modulus of K6-13 FWD Station
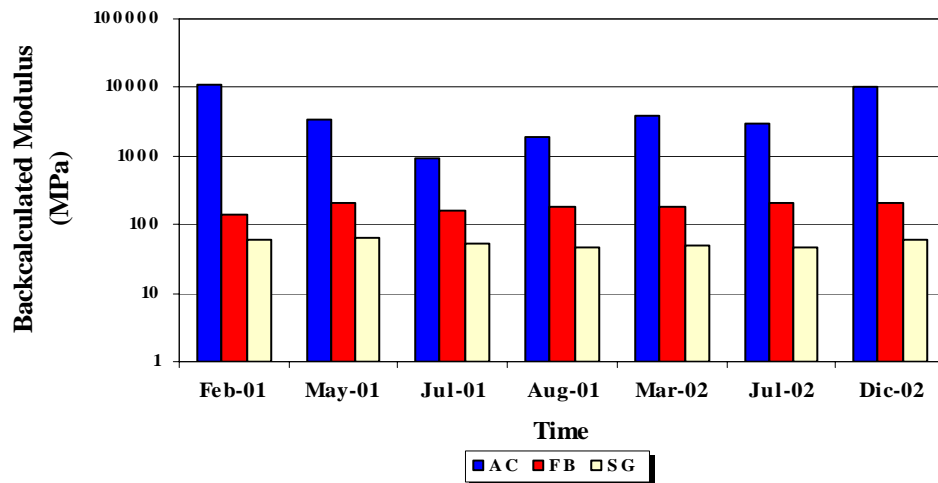
FIGURE B14   Backcalculated Modulus of K6-14 FWD Station
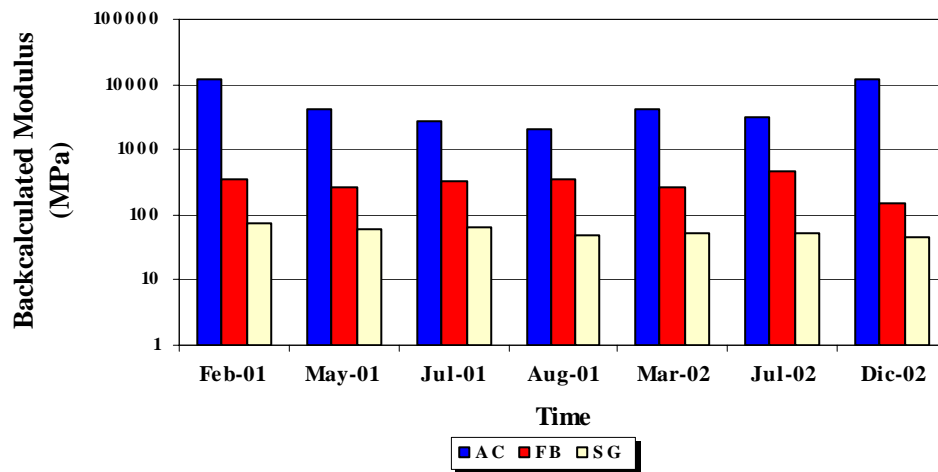
FIGURE B15   Backcalculated Modulus of K6-15 FWD Station
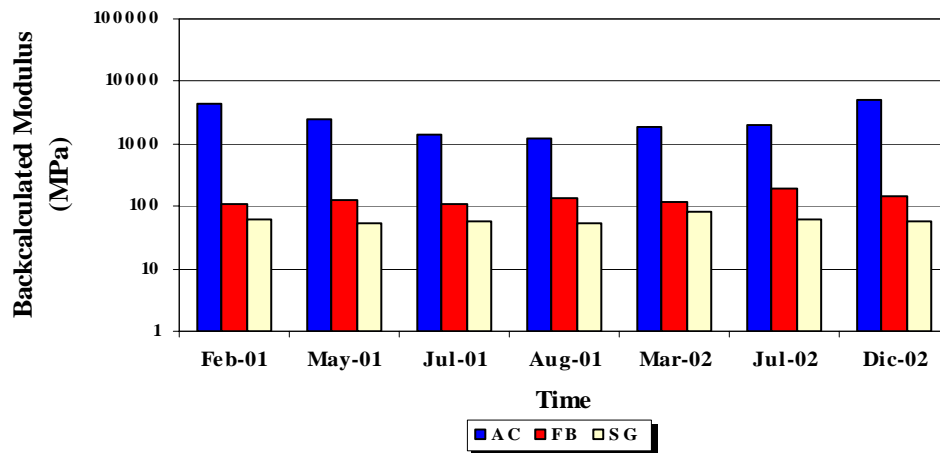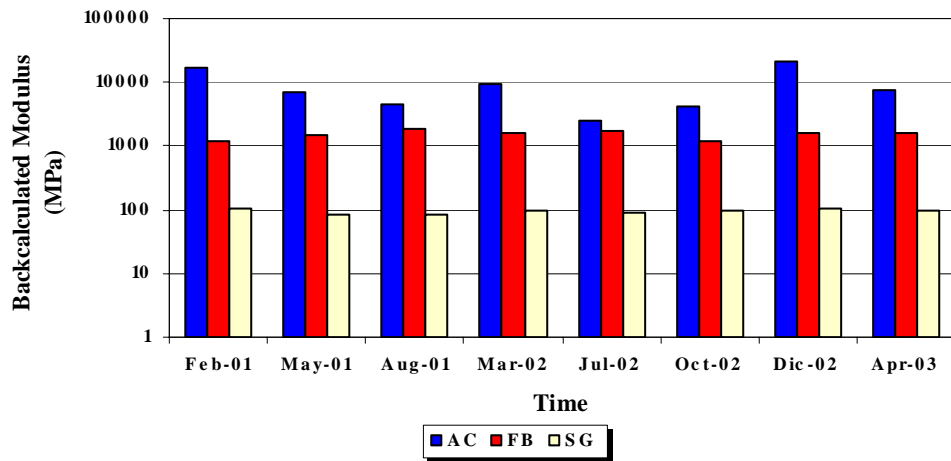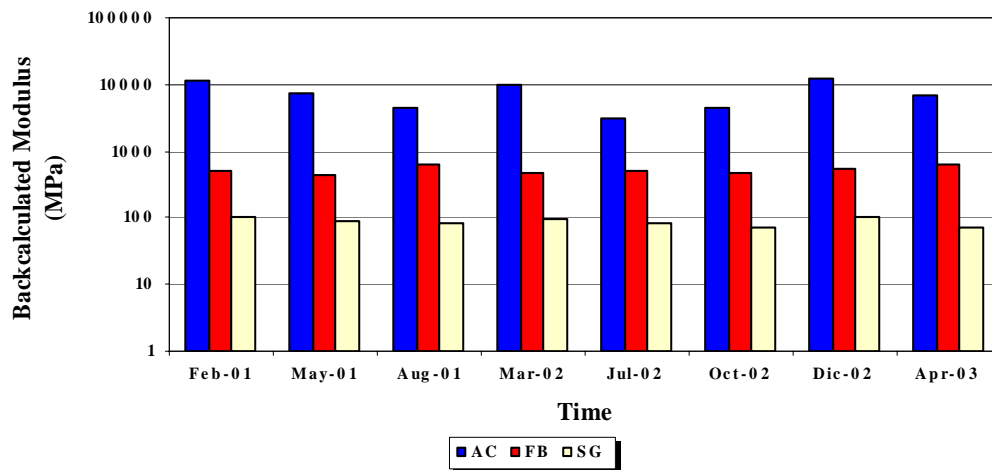
FIGURE B16   Backcalculated Modulus of K6-16 FWD Station
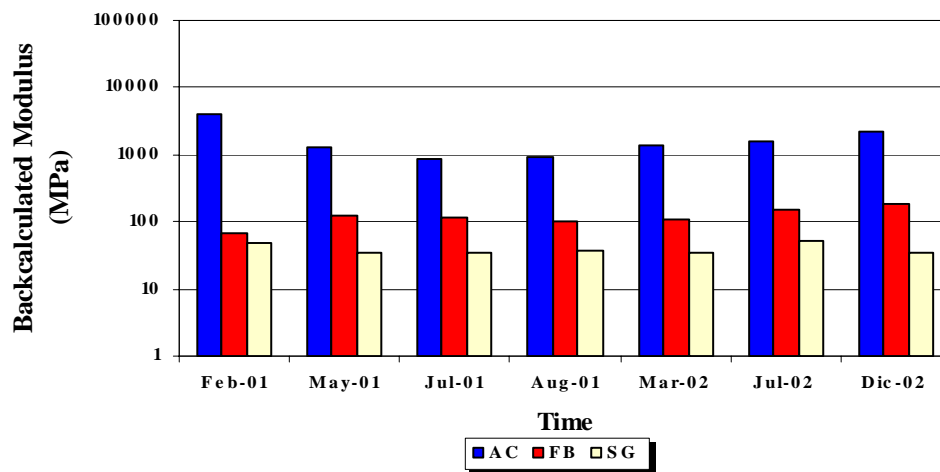
FIGURE B17   Backcalculated Modulus of K6-17 FWD Station
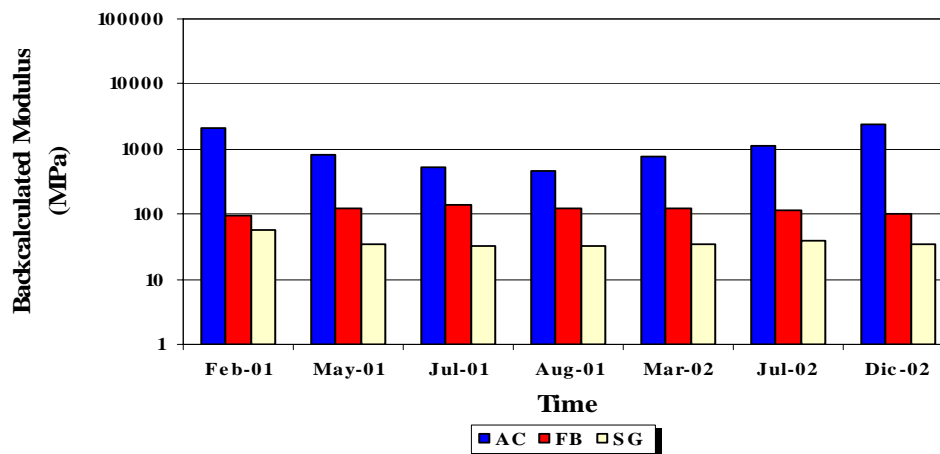
FIGURE B18   Backcalculated Modulus of K6-18 FWD Station
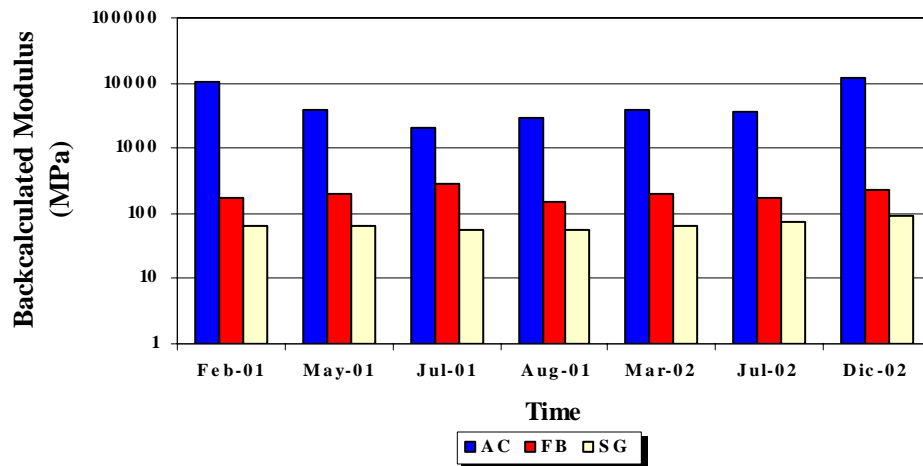
FIGURE B19   Backcalculated Modulus of FWD Station K6-19
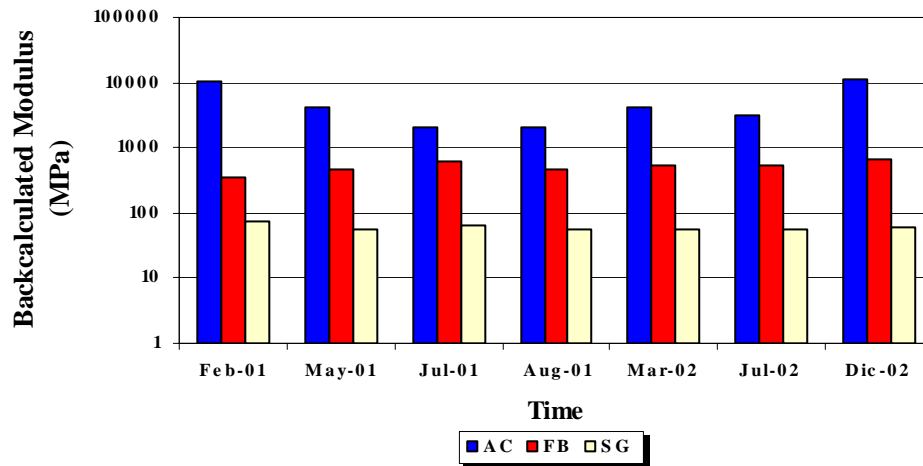
FIGURE B20   Backcalculated Modulus of FWD Station K6-20
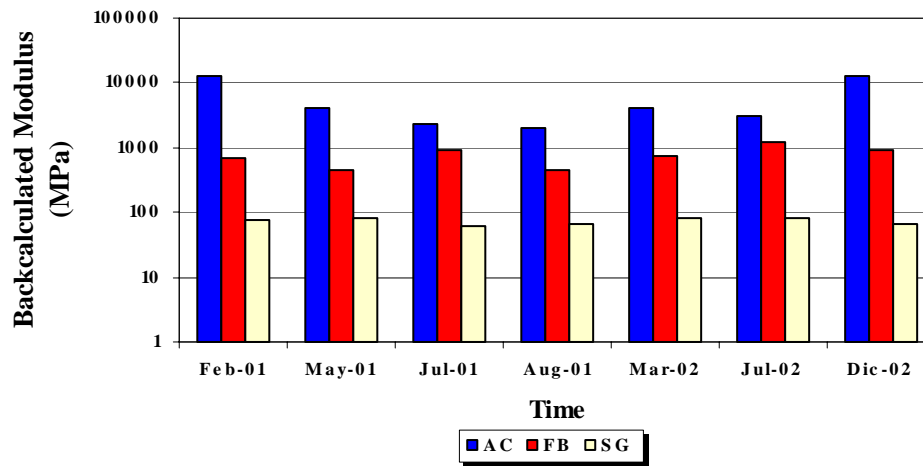
FIGURE B21   Backcalculated Modulus of FWD Station K6-21
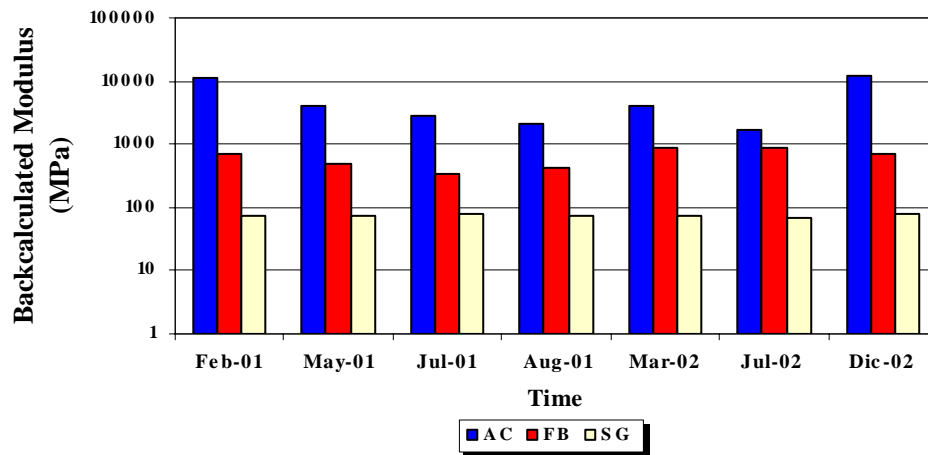
FIGURE B22   Backcalculated Modulus of K6-22 FWD Station
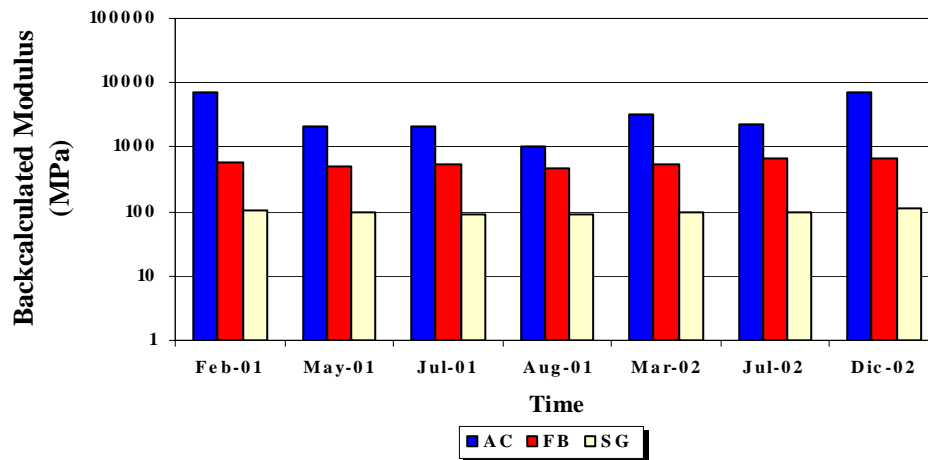
FIGURE B23   Backcalculated Modulus of K6-23 FWD Station
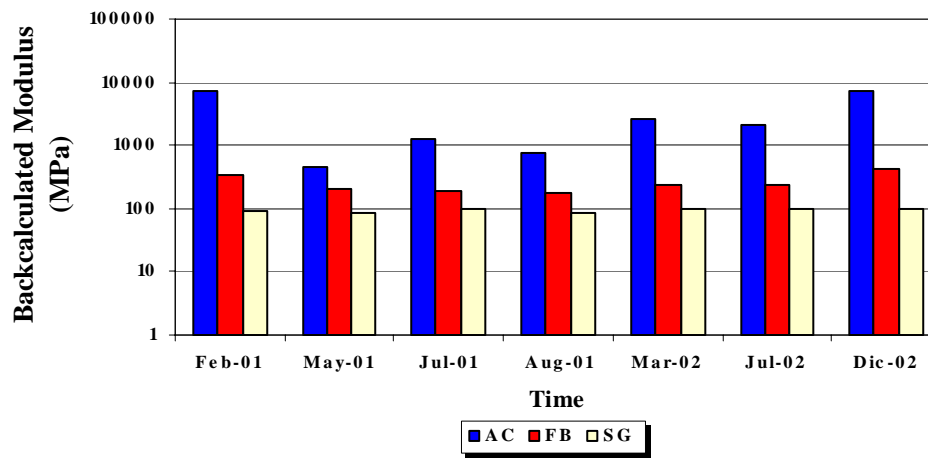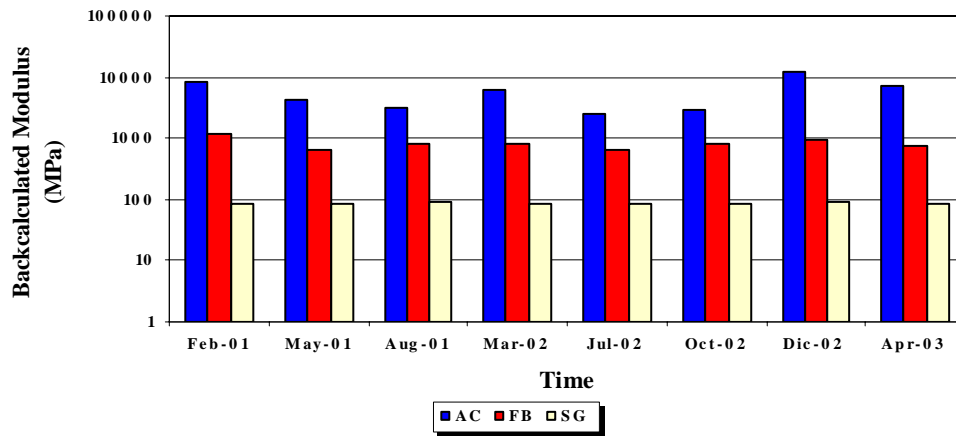

FIGURE B24   Backcalculated Modulus of K6-24 FWD Station
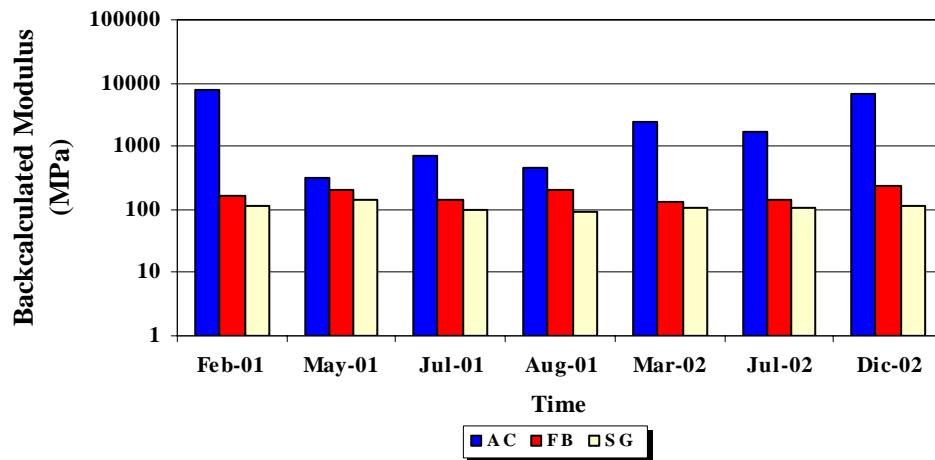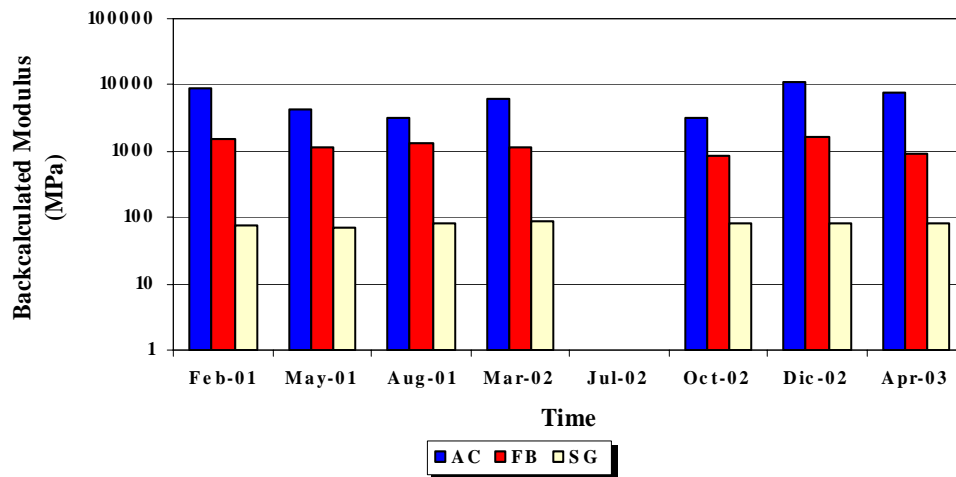
FIGURE B25   Backcalculated Modulus of K6-25 FWD Station
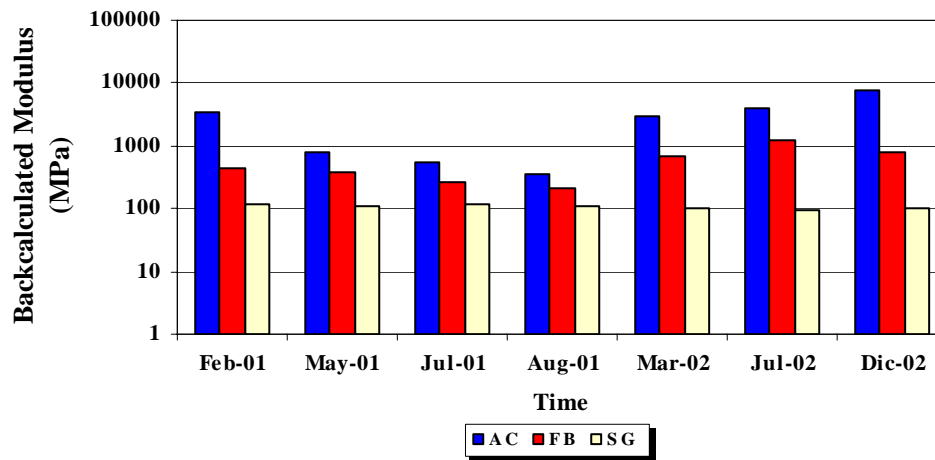
FIGURE B26   Backcalculated Modulus of K6-26 FWD Station
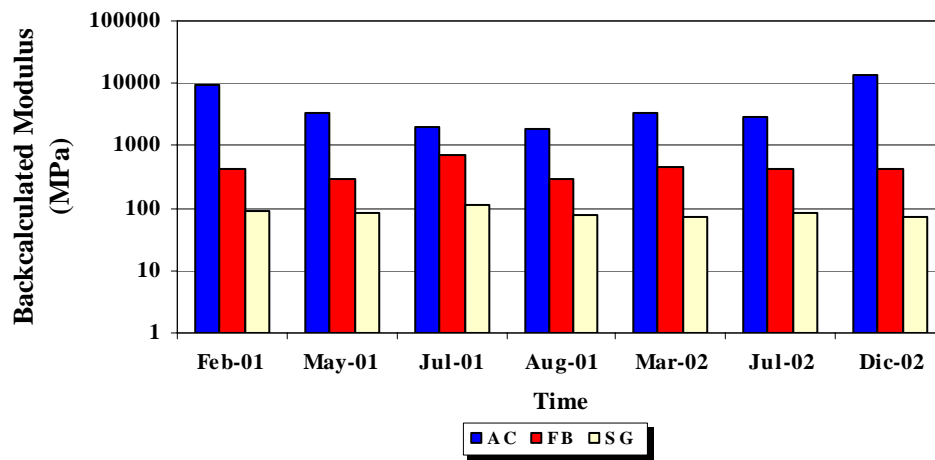
FIGURE B27   Backcalculated Modulus of K6-27 FWD Station
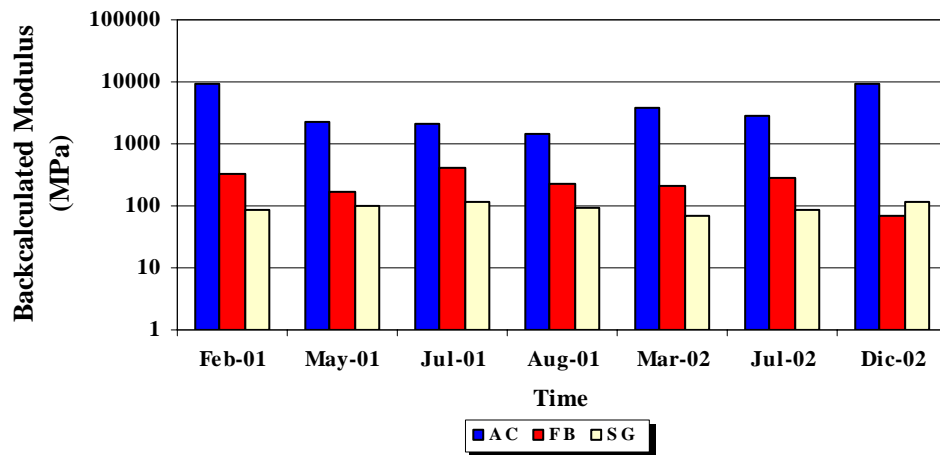
FIGURE B28   Backcalculated Modulus of K6-28 FWD Station
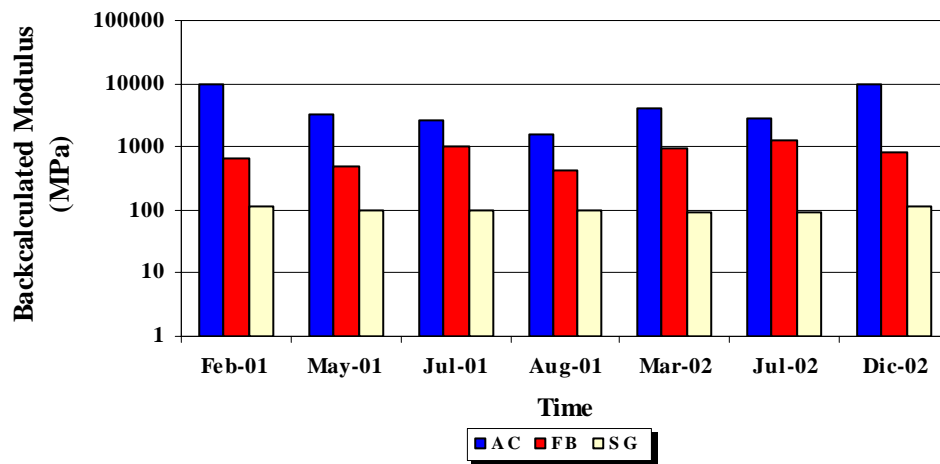
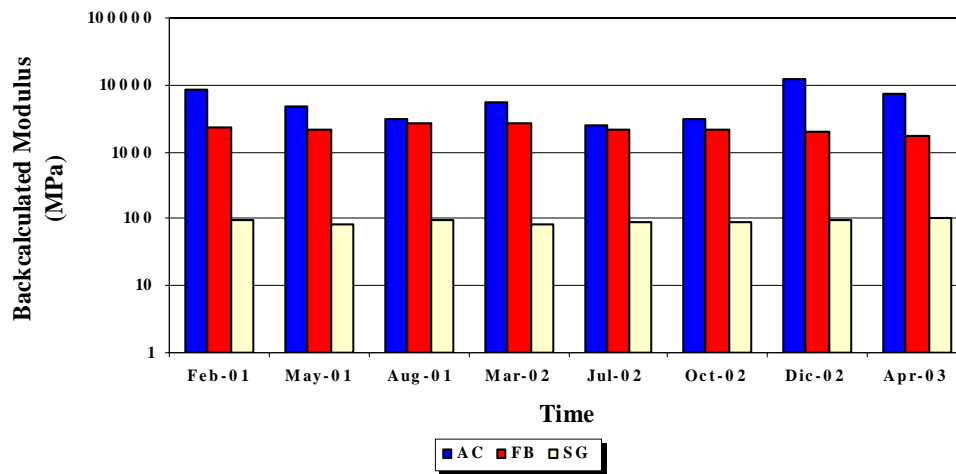**FIGURE B29   Backcalculated Modulus of K6-29 FWD Station**
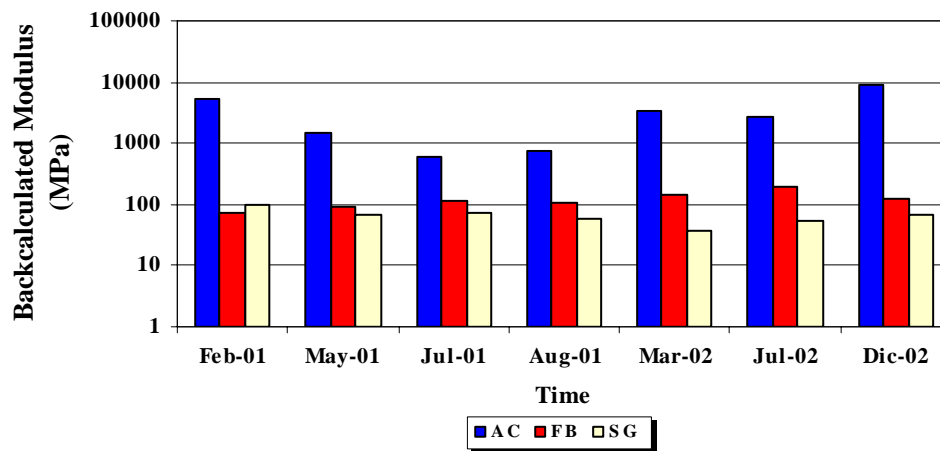
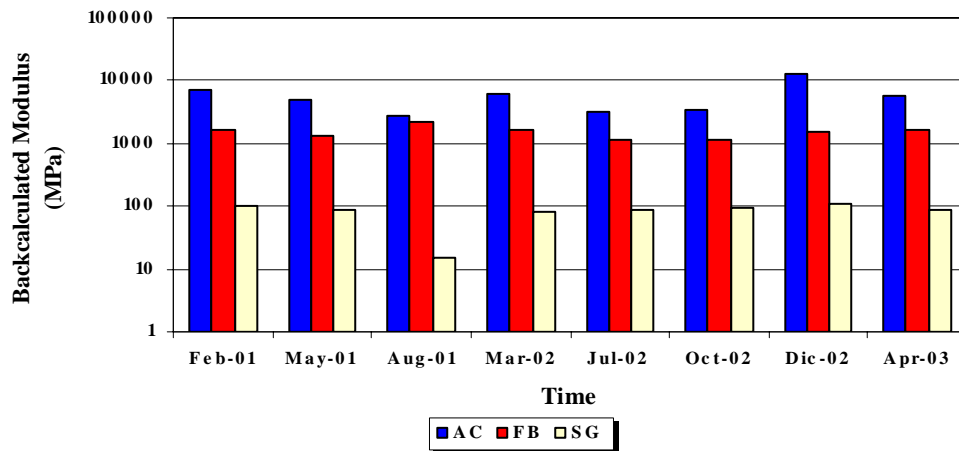**FIGURE B30   Backcalculated Modulus of K6-30 FWD Station**
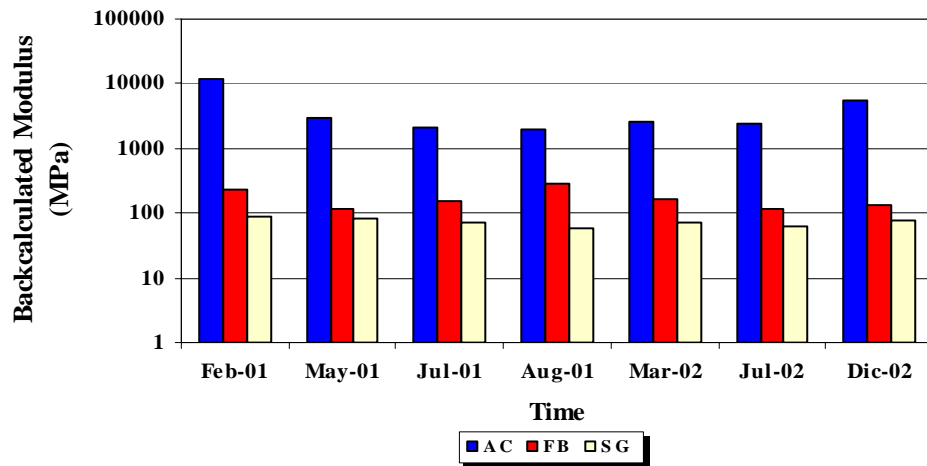
FIGURE B31   Backcalculated Modulus of K6-31 FWD Station
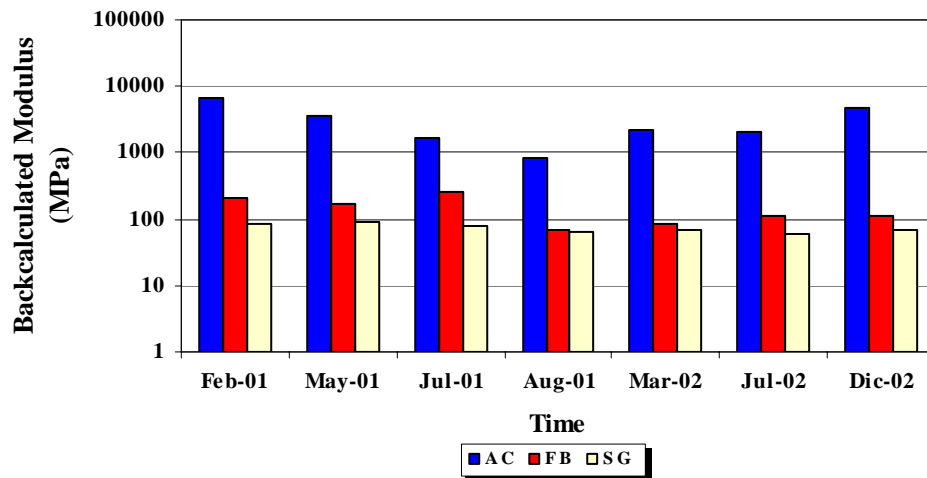
FIGURE B32   Backcalculated Modulus of K6-32 FWD Station
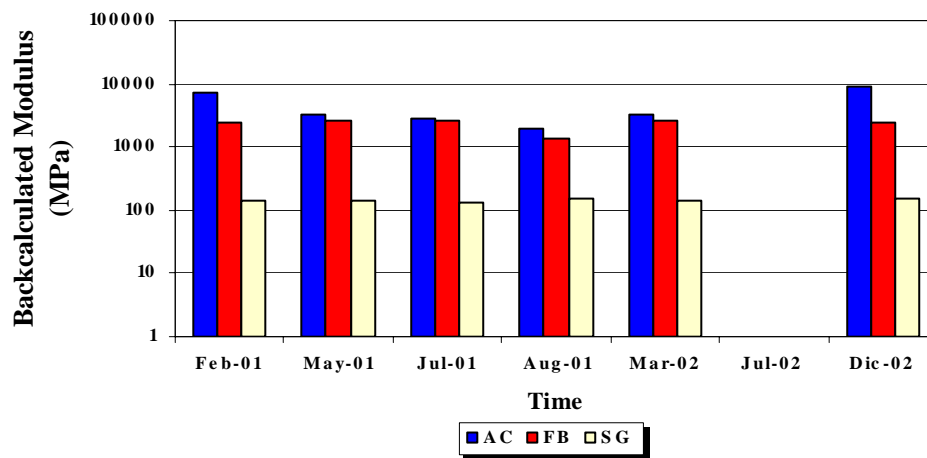
FIGURE B33   Backcalculated Modulus of K6-33 FWD Station
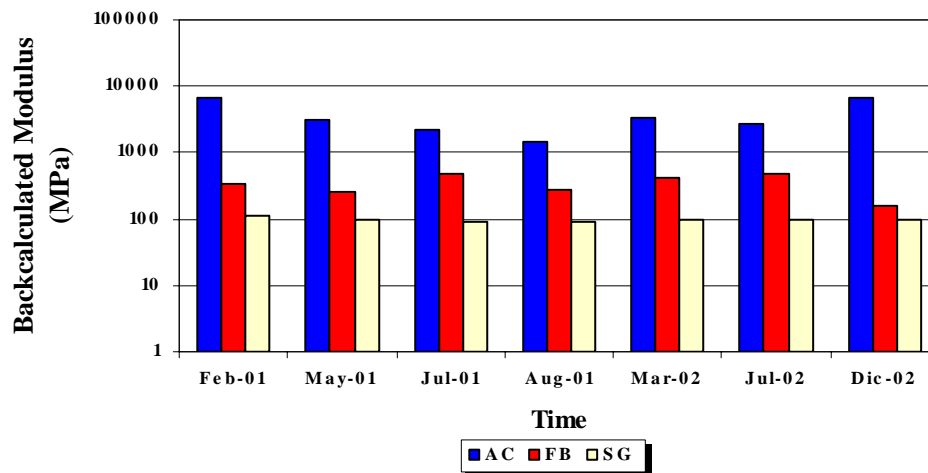
FIGURE B34   Backcalculated Modulus of K6-34 FWD Station
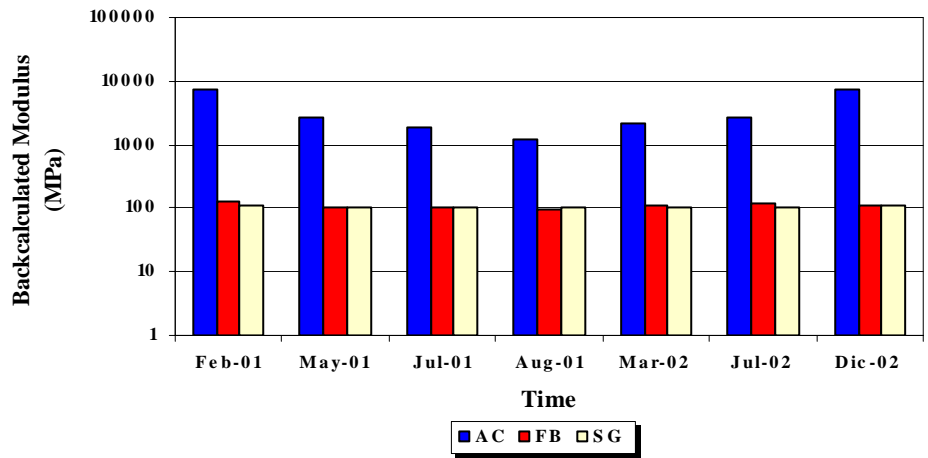
FIGURE B35   Backcalculated Modulus of K6-35 FWD Station
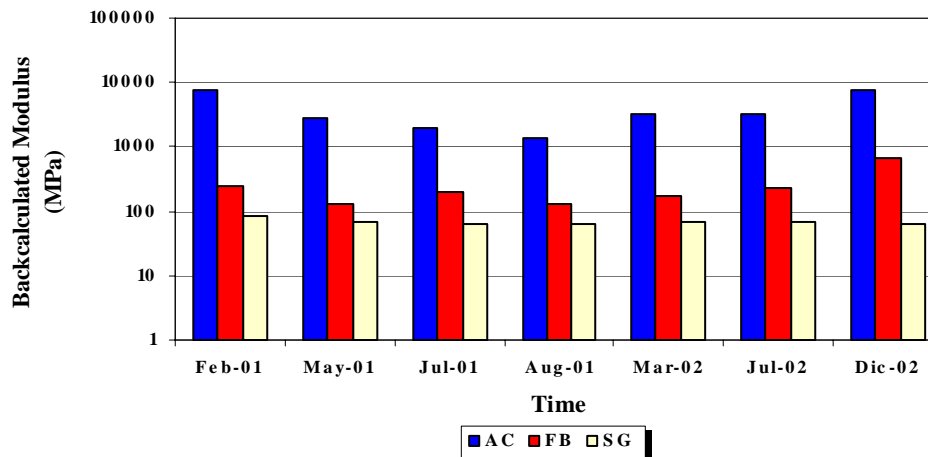
FIGURE B36   Backcalculated Modulus of K6-36 FWD Station
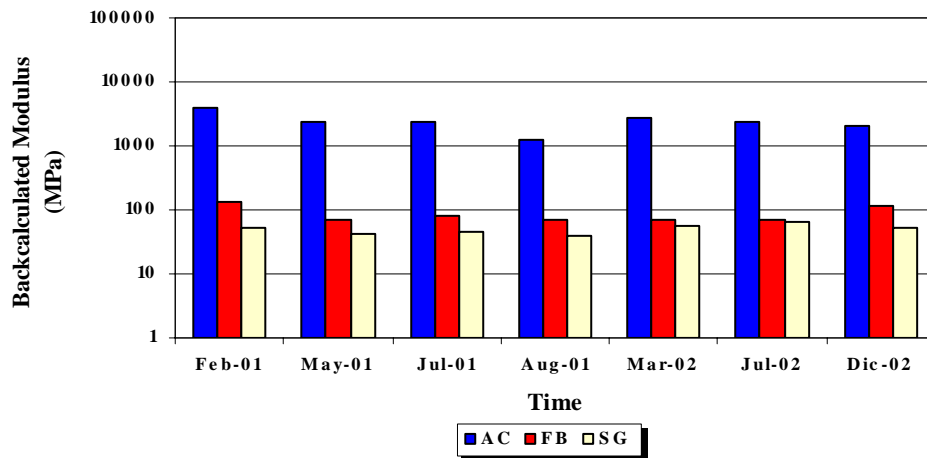
FIGURE B37   Backcalculated Modulus of K6-37 FWD Station
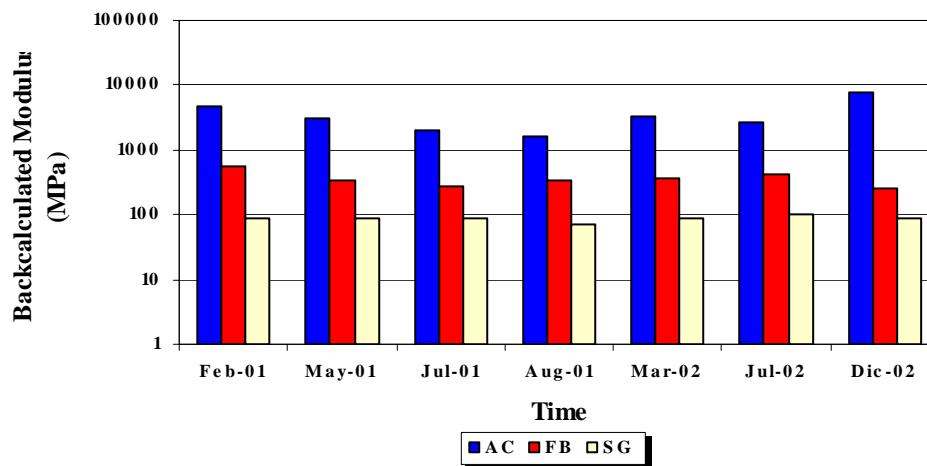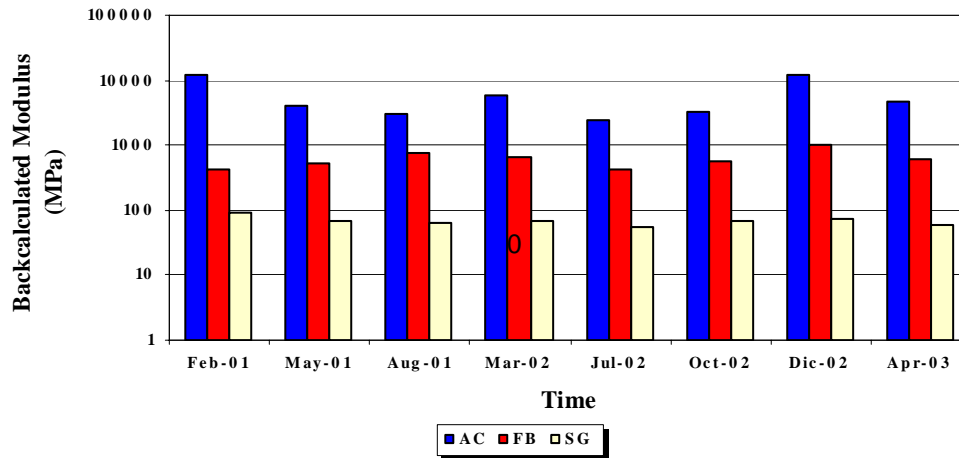

FIGURE B38   Backcalculated Modulus of K6-38 FWD Station
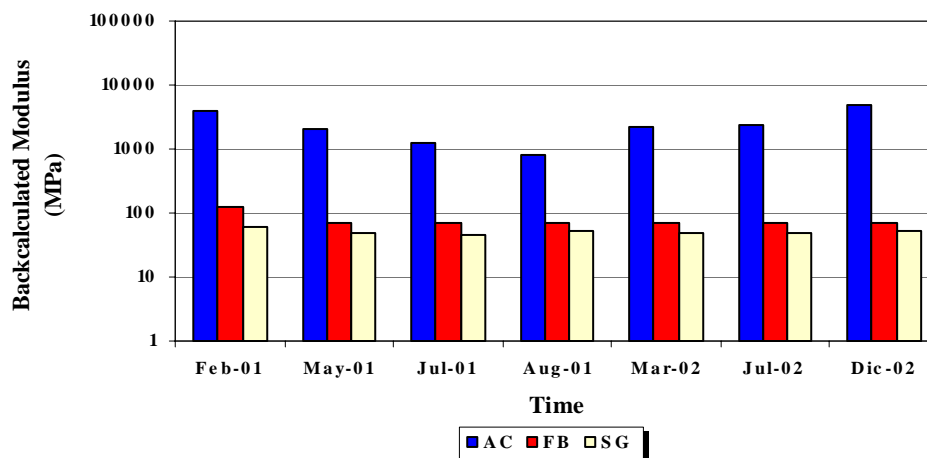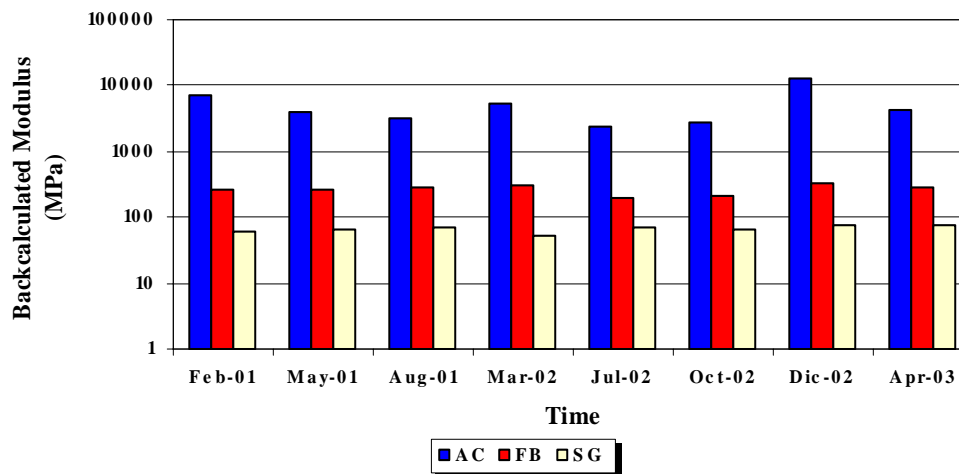

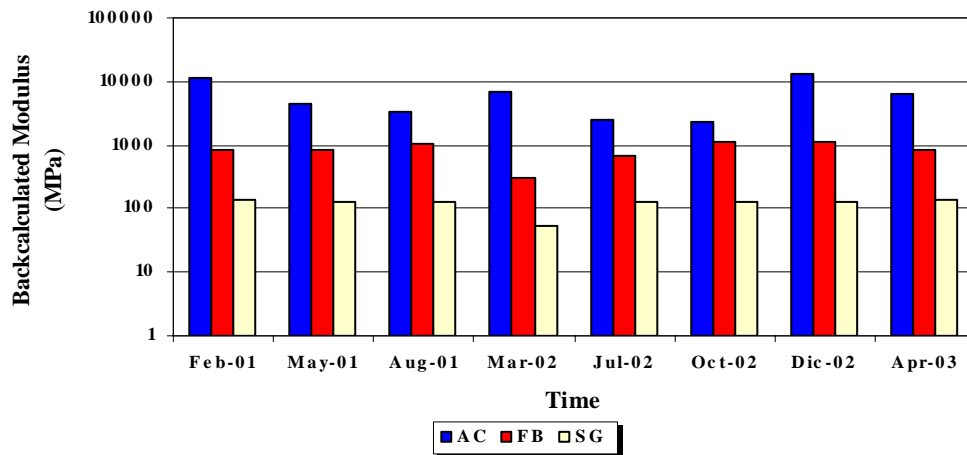FIGURE B39   Backcalculated Modulus of K6-39 FWD Station
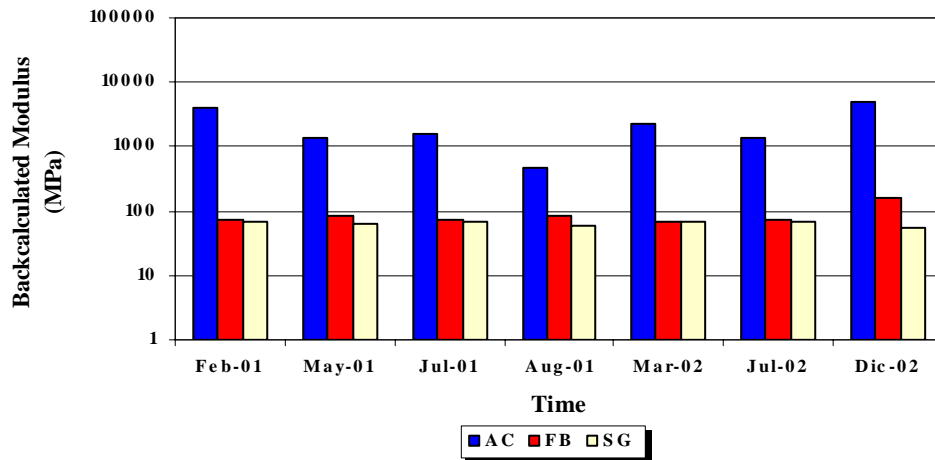
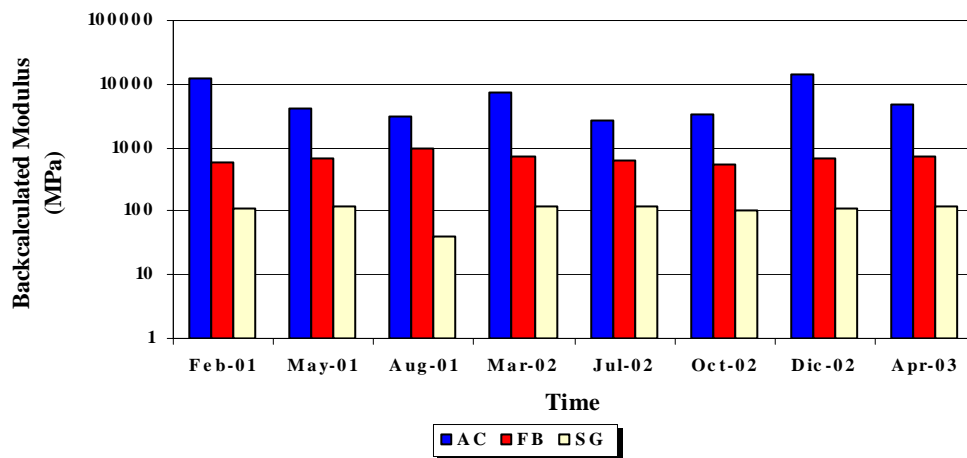FIGURE B40   Backcalculated Modulus of K6-40 FWD Station
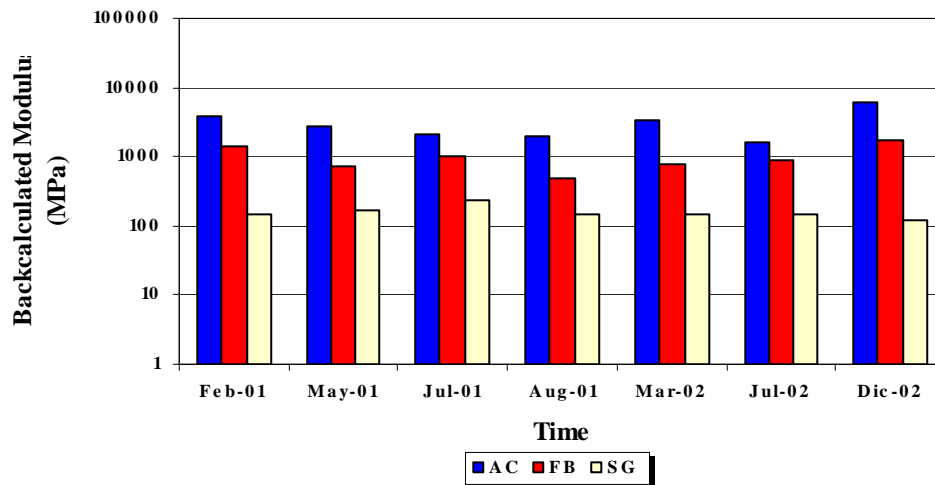
FIGURE B41   Backcalculated Modulus of K6-41 FWD Station
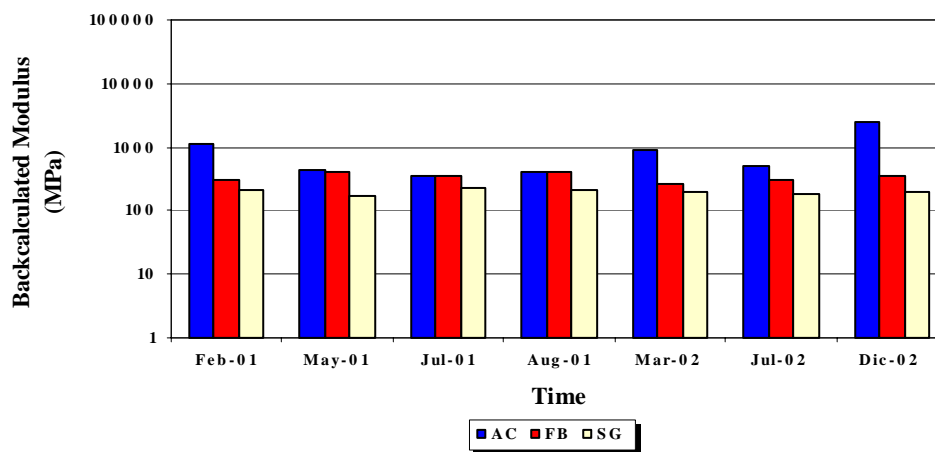
FIGURE B42   Backcalculated Modulus of K6-42 FWD Station
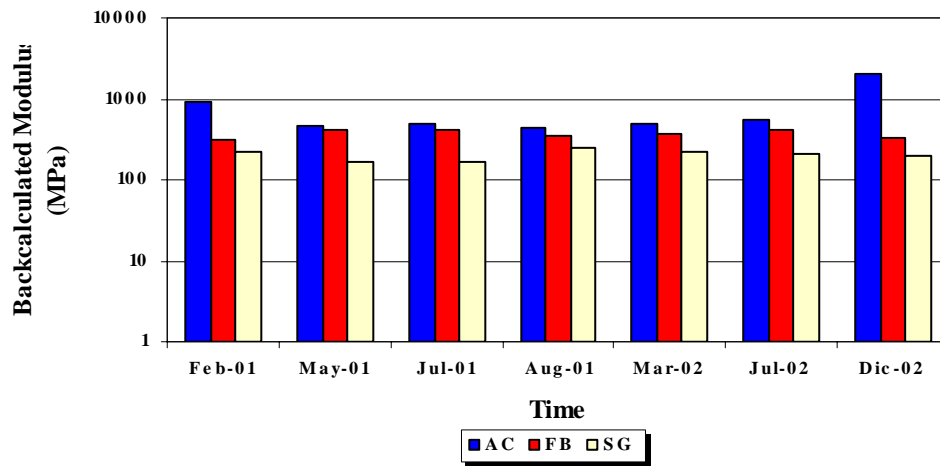
FIGURE B43   Backcalculated Modulus of K6-43 FWD Station
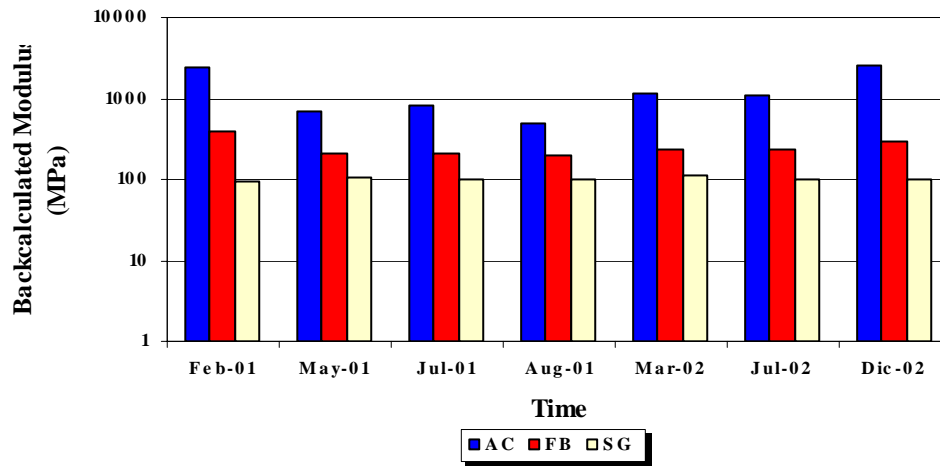
FIGURE B44   Backcalculated Modulus of K6-44 FWD Station
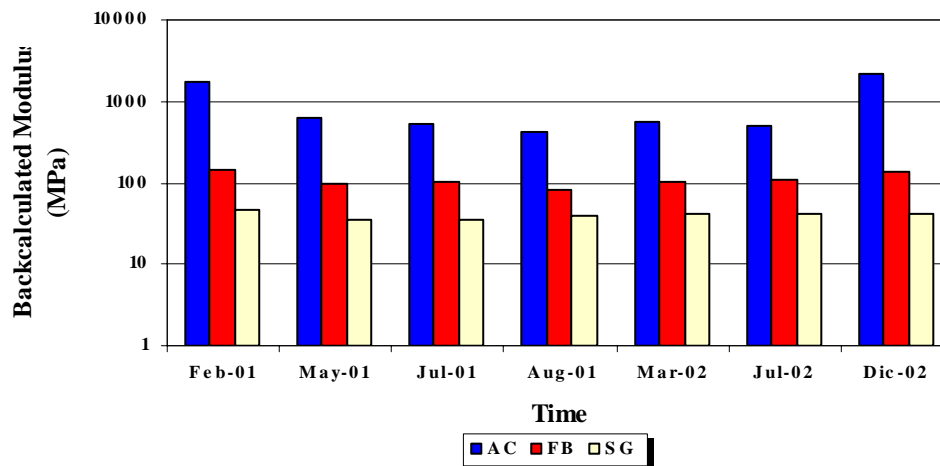
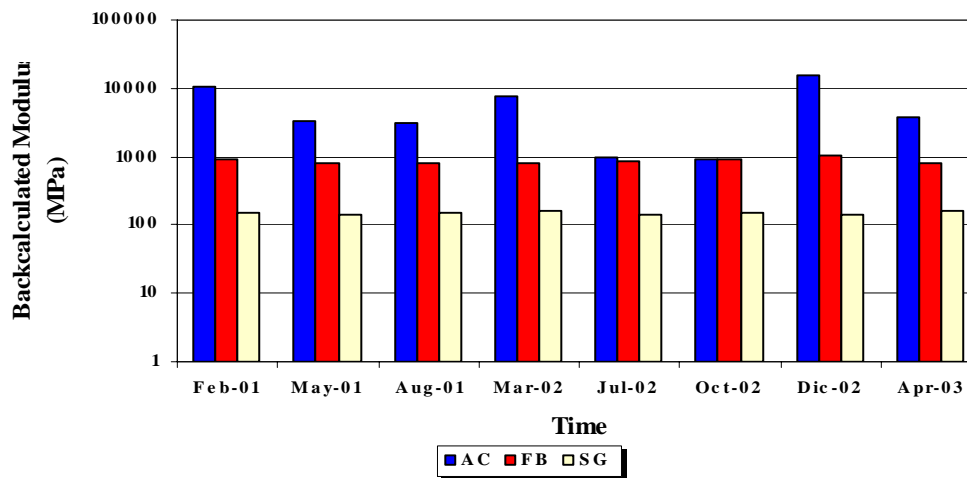FIGURE B45   Backcalculated Modulus of K6-45 FWD Station
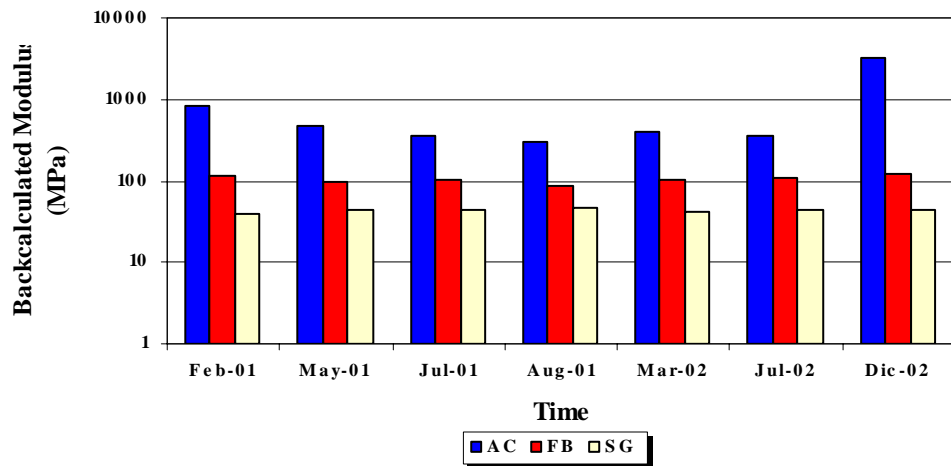
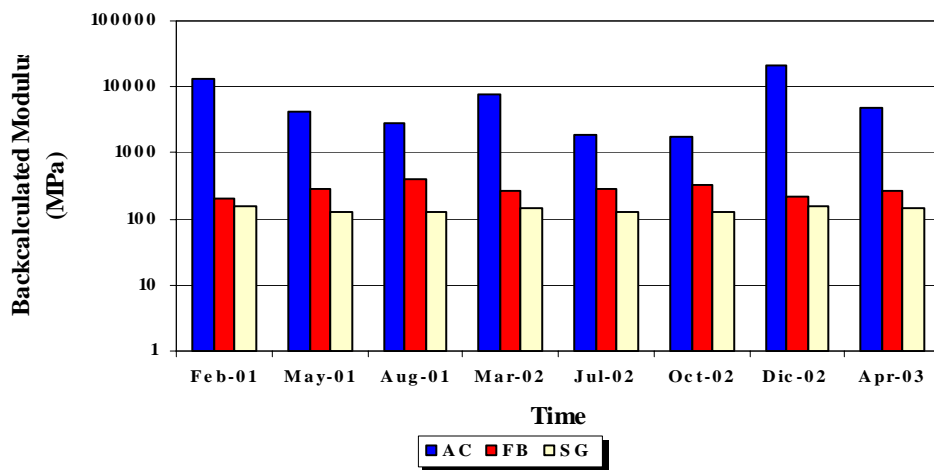FIGURE B46   Backcalculated Modulus of K6-46 FWD Station
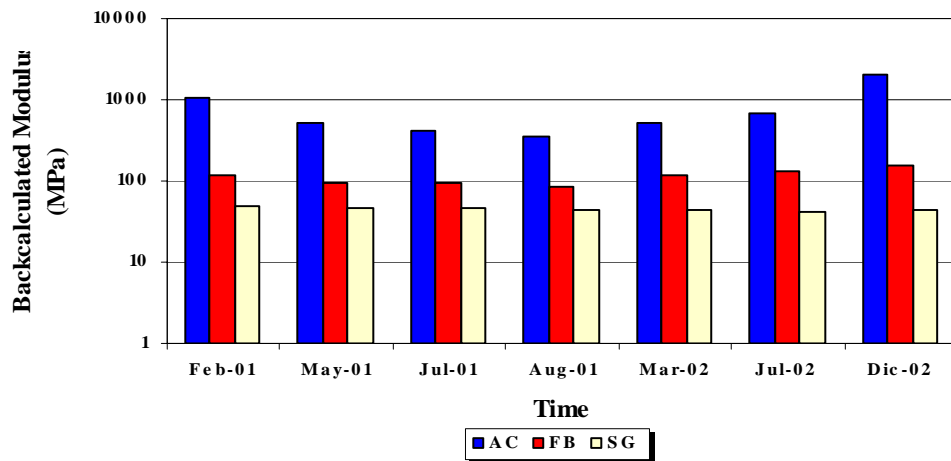
FIGURE B47   Backcalculated Modulus of K6-47 FWD Station
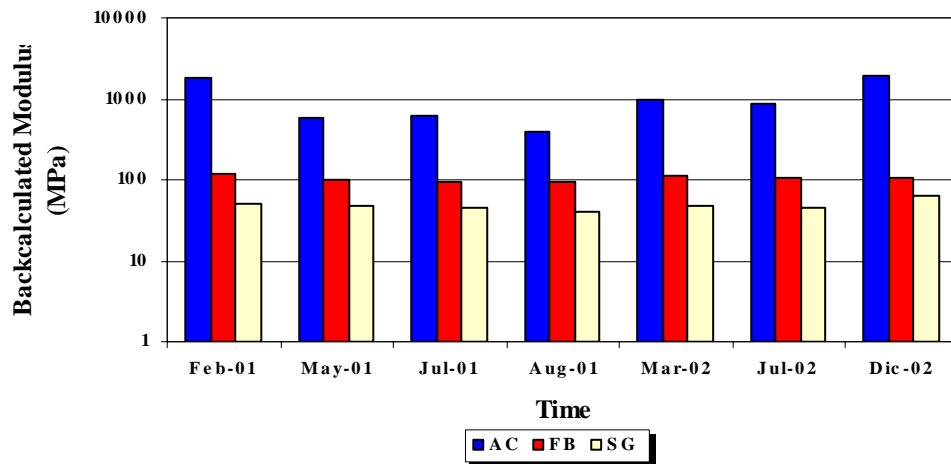
FIGURE B48   Backcalculated Modulus of K6-48 FWD Station
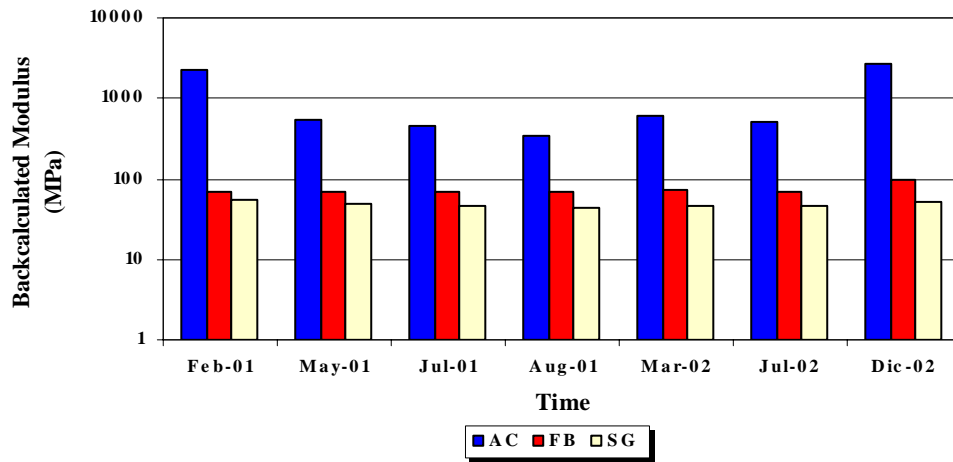
FIGURE B49   Backcalculated Modulus of K6-49 FWD Station
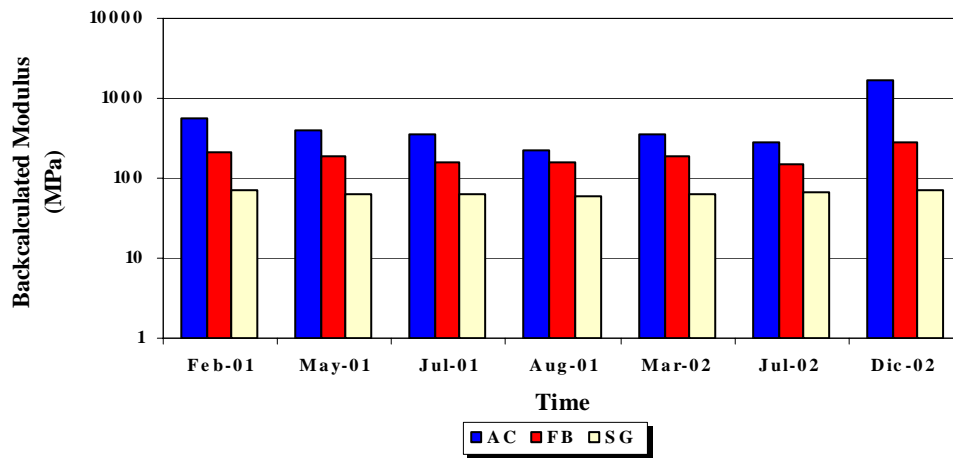
FIGURE B50   Backcalculated Modulus of K6-50 FWD Station
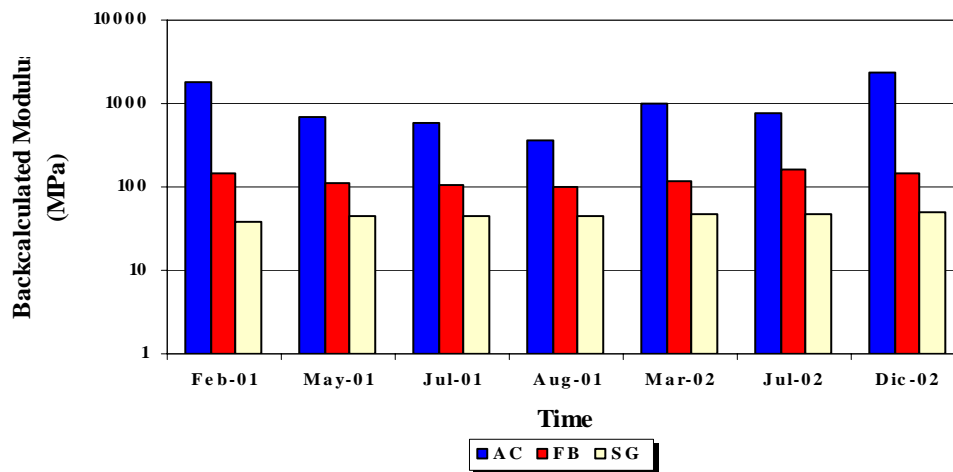
FIGURE B51   Backcalculated Modulus of K6-51 FWD Station
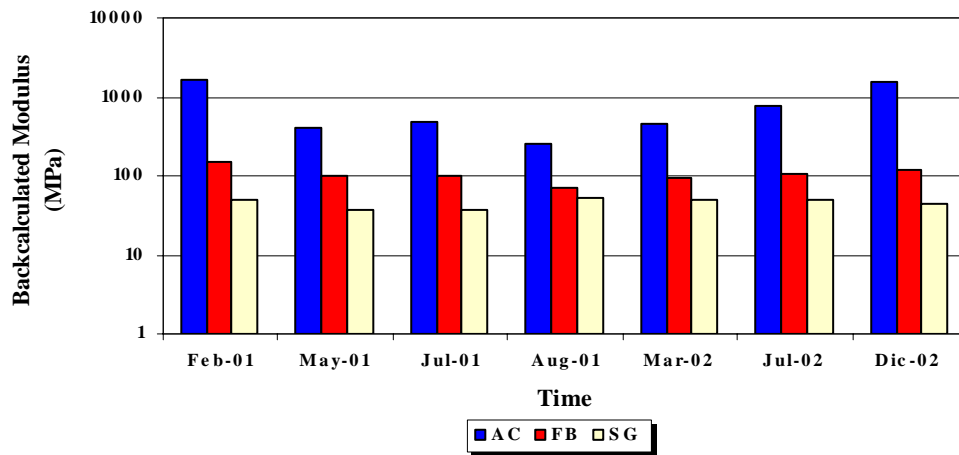
FIGURE B52   Backcalculated Modulus of K6-52 FWD Station
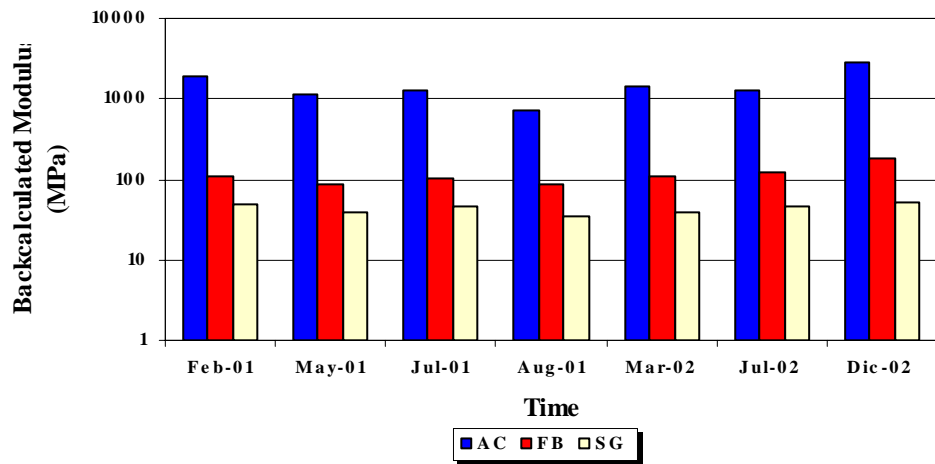
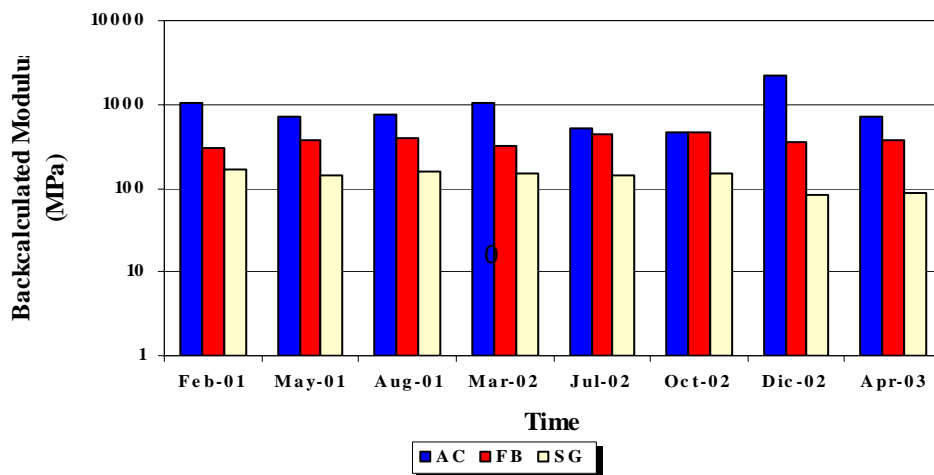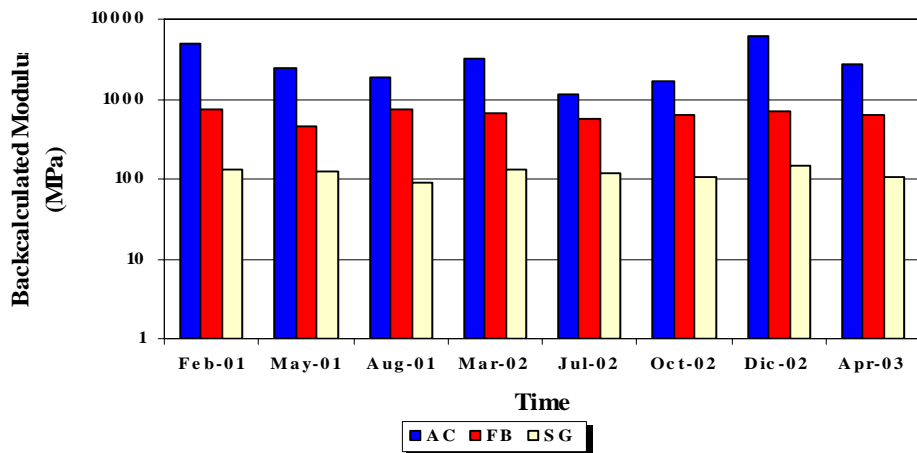FIGURE B53   Backcalculated Modulus of K6-53 FWD Station
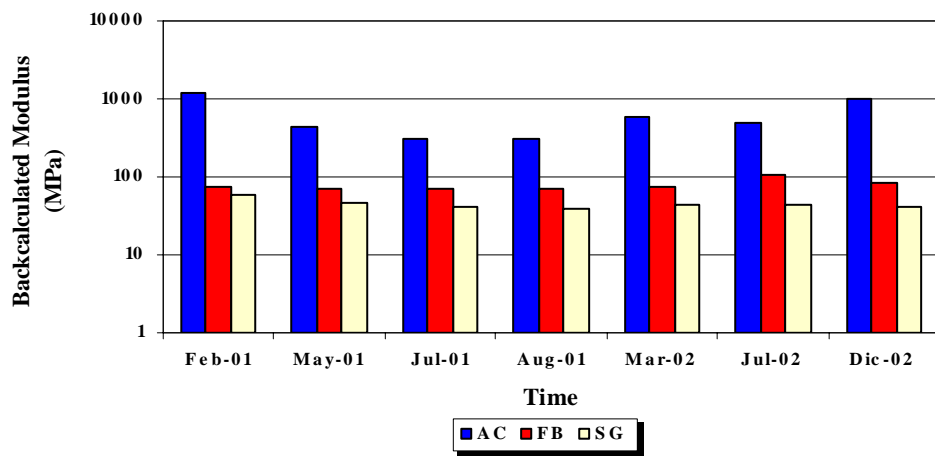
FIGURE B54   Backcalculated Modulus of K6-54 FWD Station
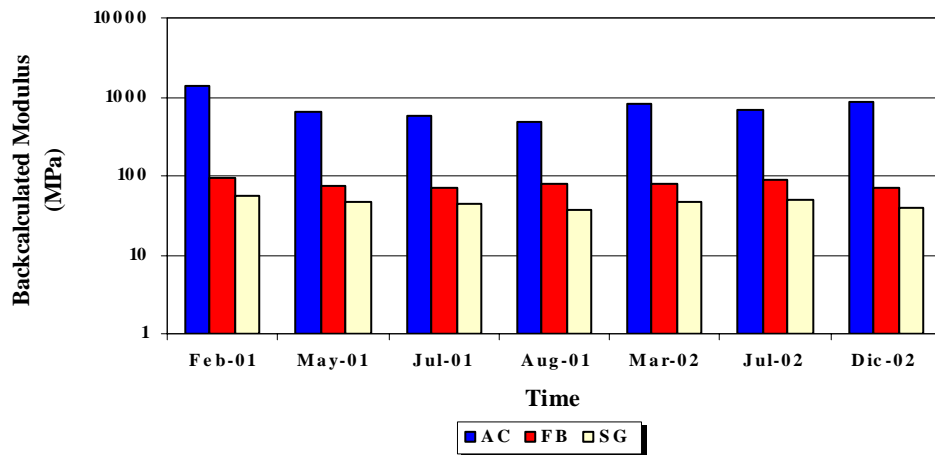
FIGURE B55   Backcalculated Modulus of K6-55 FWD Station
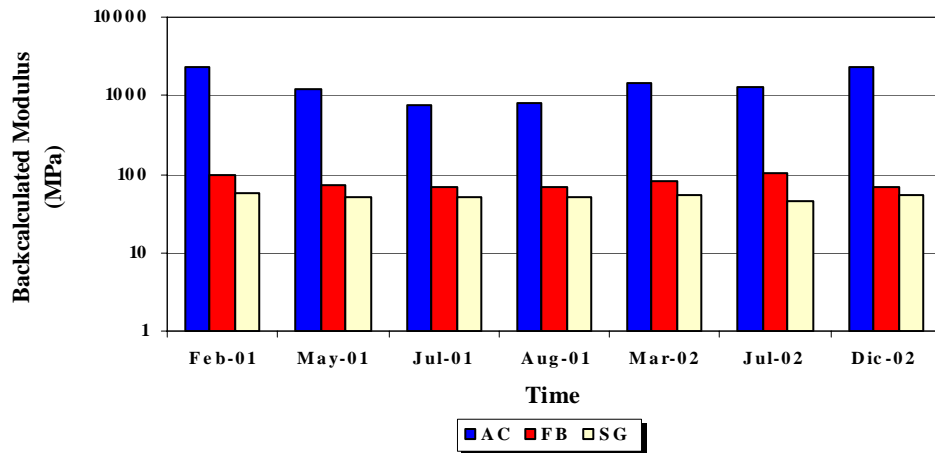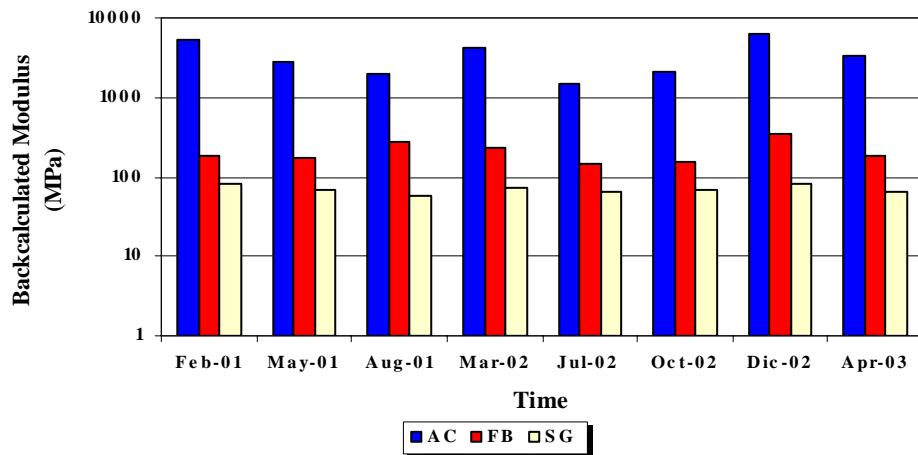

FIGURE B56   Backcalculated Modulus of K6-56 FWD Station
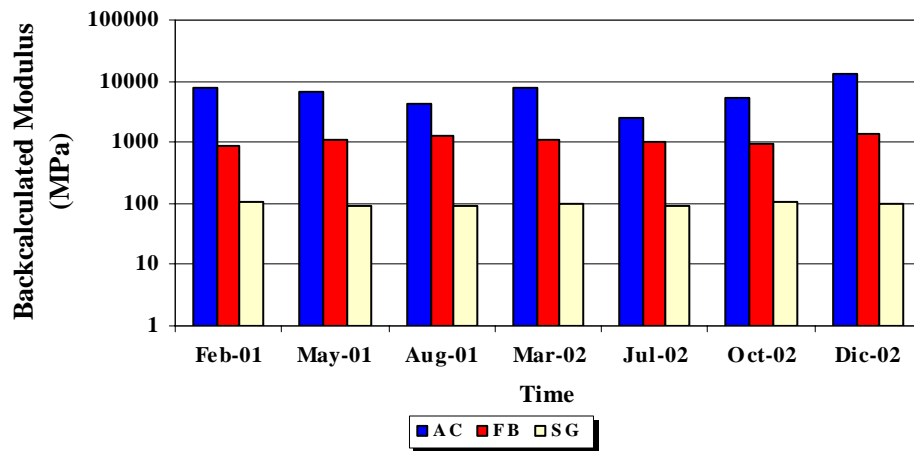
FIGURE B57   Backcalculated Modulus of K7-1 FWD Station
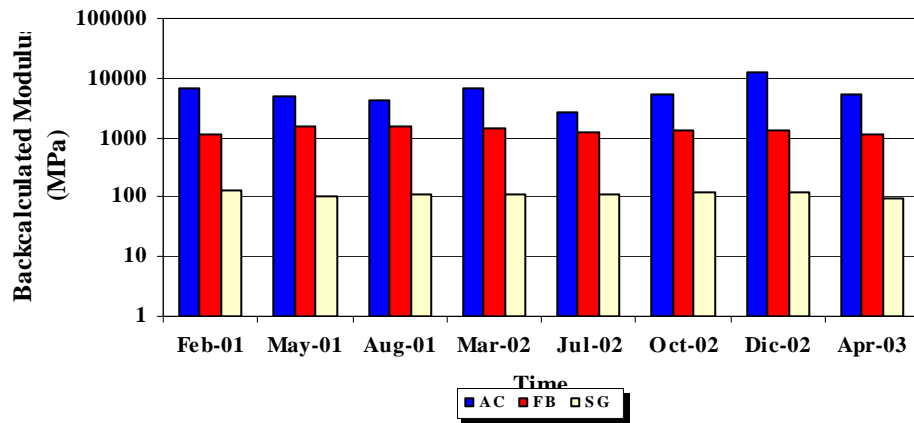
FIGURE B58   Backcalculated Modulus of K7-2 FWD Station
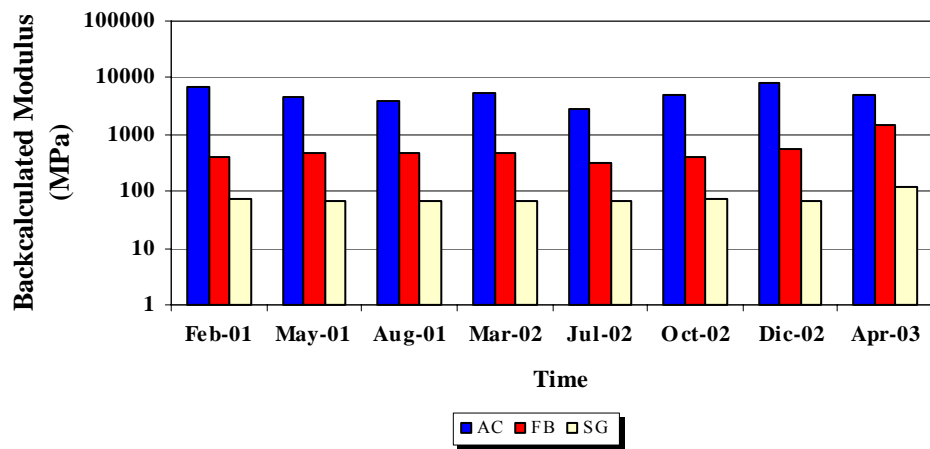
FIGURE B59   Backcalculated Modulus of K7-3 FWD Station
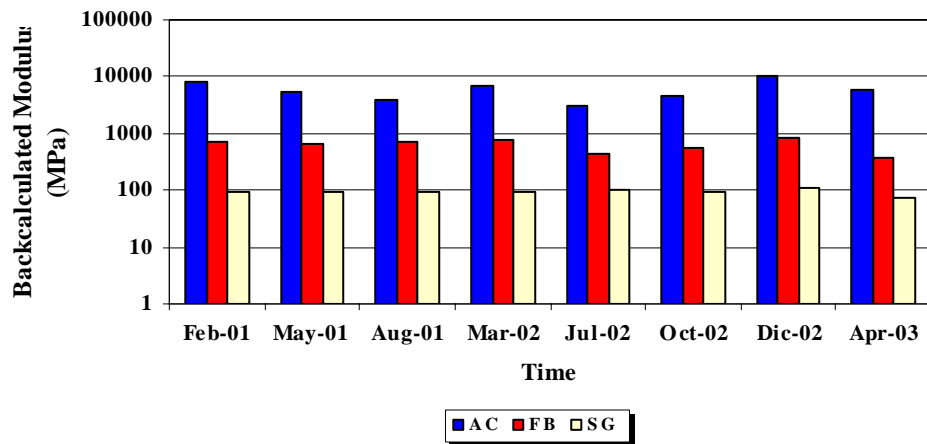
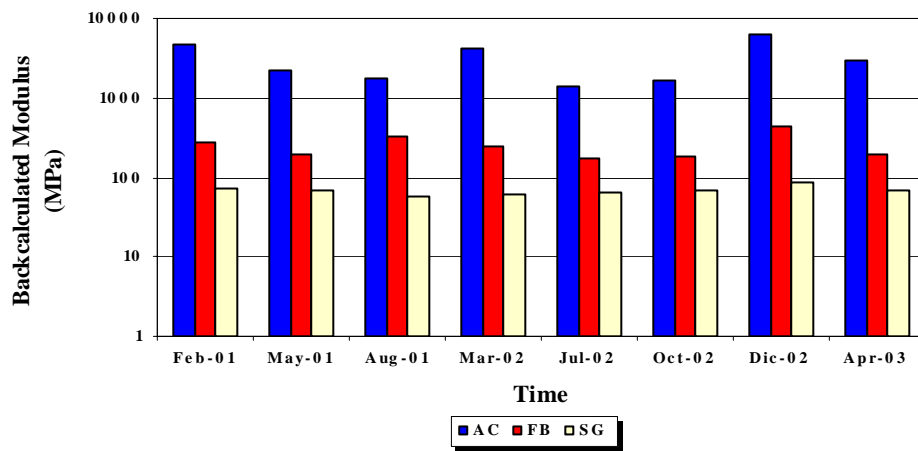**FIGURE B60   Backcalculated Modulus of K7-4 FWD Station**
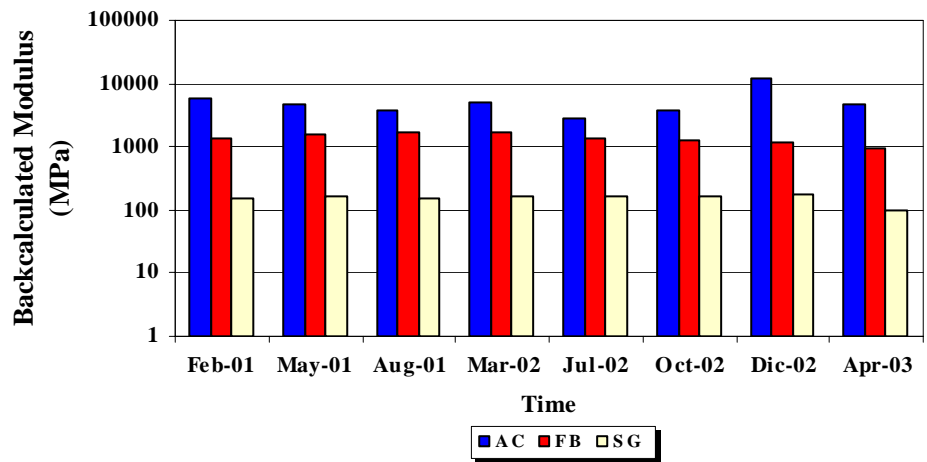
FIGURE B61   Backcalculated Modulus of K7-5 FWD Station
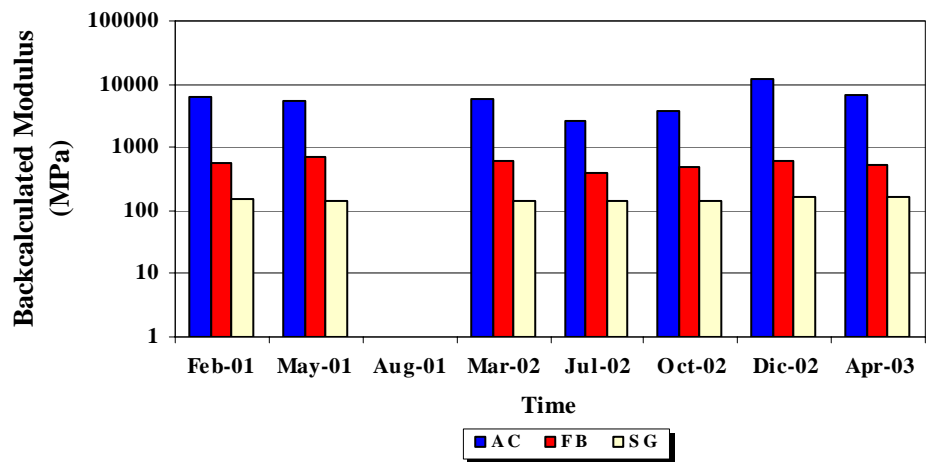
FIGURE B62   Backcalculated Modulus of K7-6 FWD Station
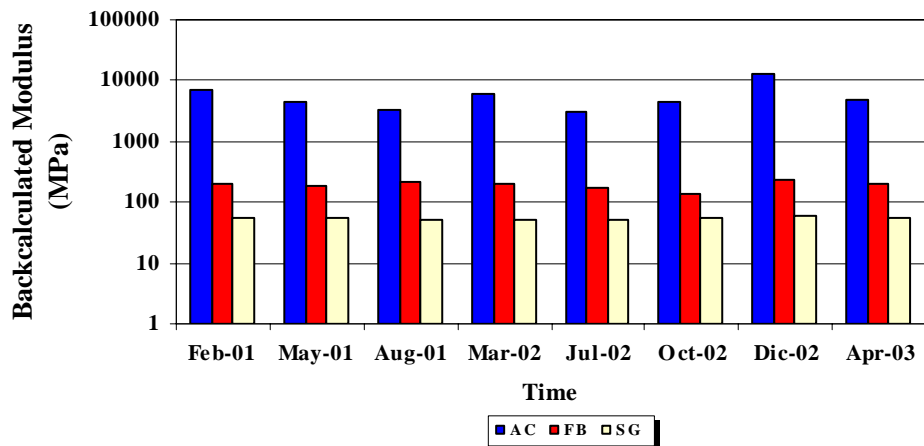
FIGURE B63   Backcalculated Modulus of K7-7 FWD Station
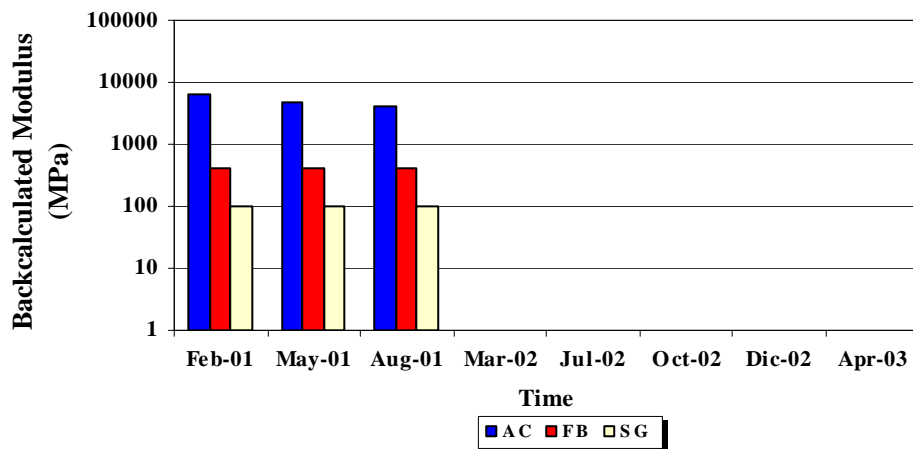
FIGURE B64   Backcalculated Modulus of K7-8 FWD Station
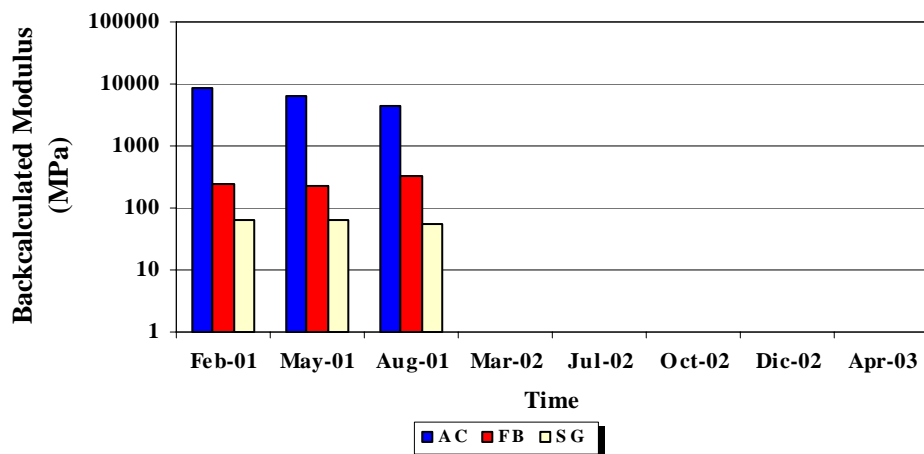
FIGURE B65   Backcalculated Modulus of K7-9 FWD Station
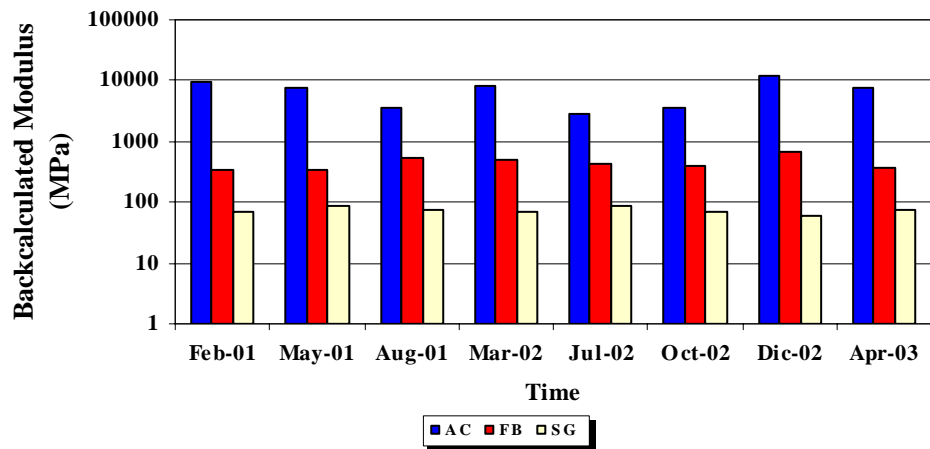
FIGURE B66   Backcalculated Modulus of K7-10 FWD Station
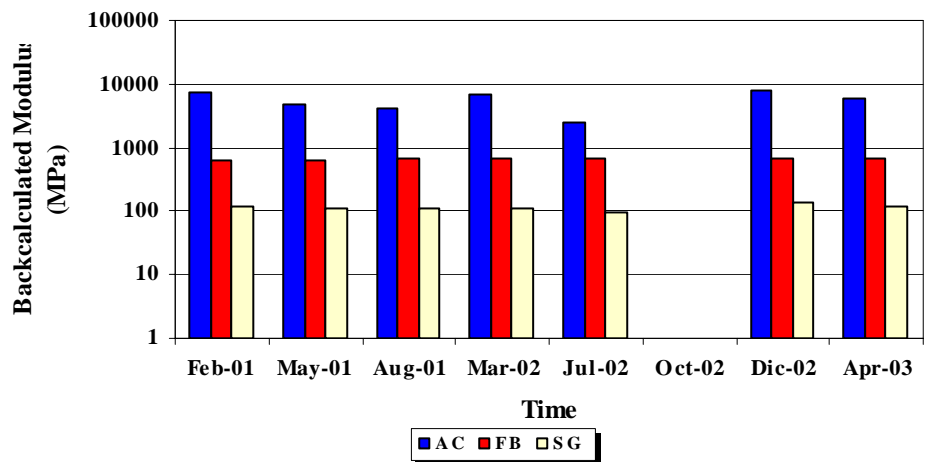
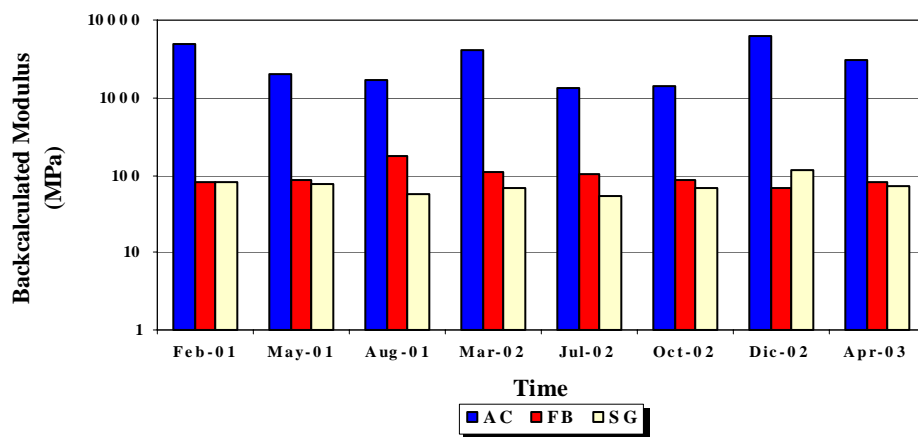**FIGURE B67   Backcalculated Modulus of K7-11 FWD Station**
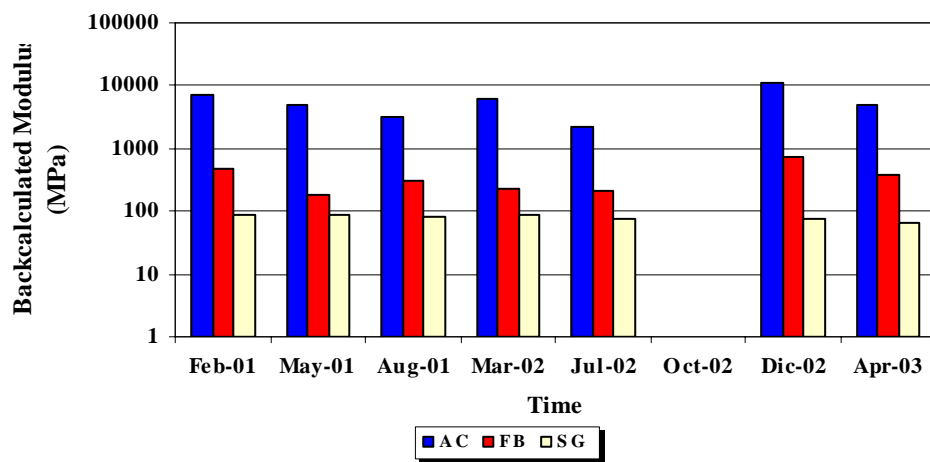
FIGURE B68   Backcalculated Modulus of K7-12 FWD Station
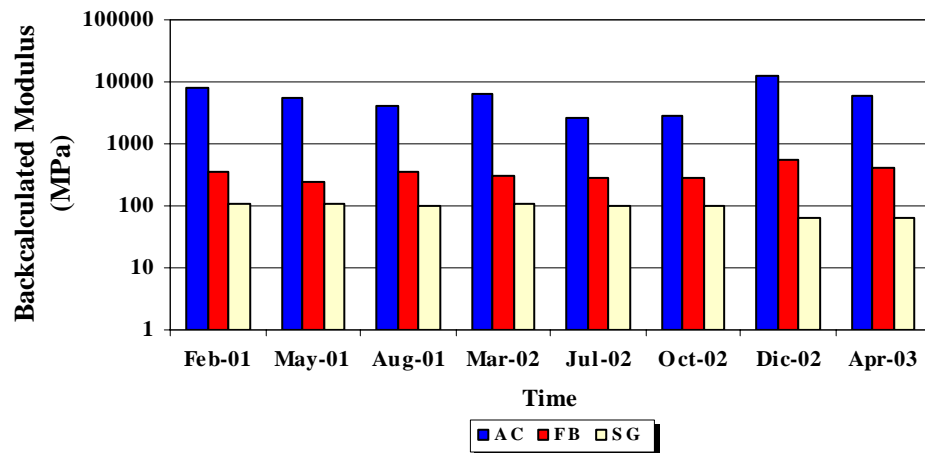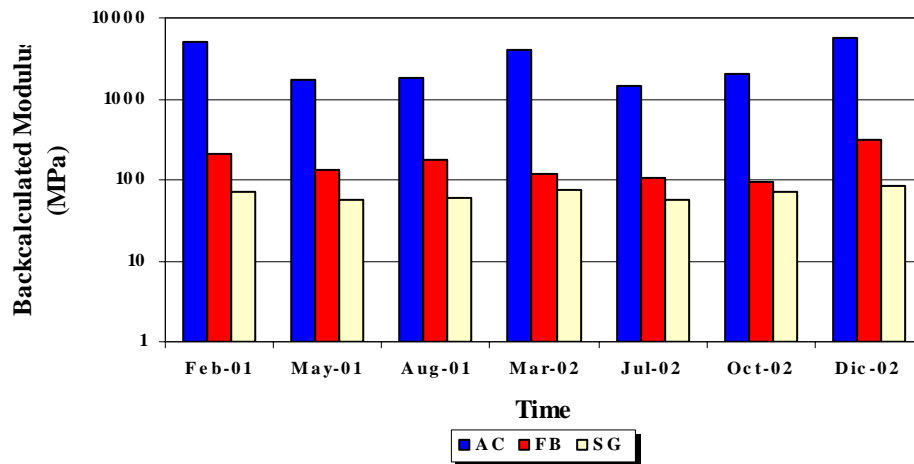
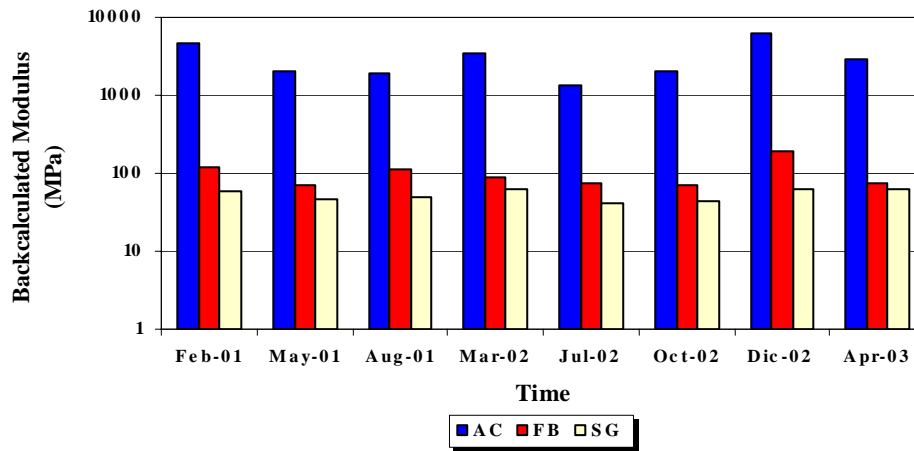**FIGURE B69   Backcalculated Modulus of K7-13 FWD Station**
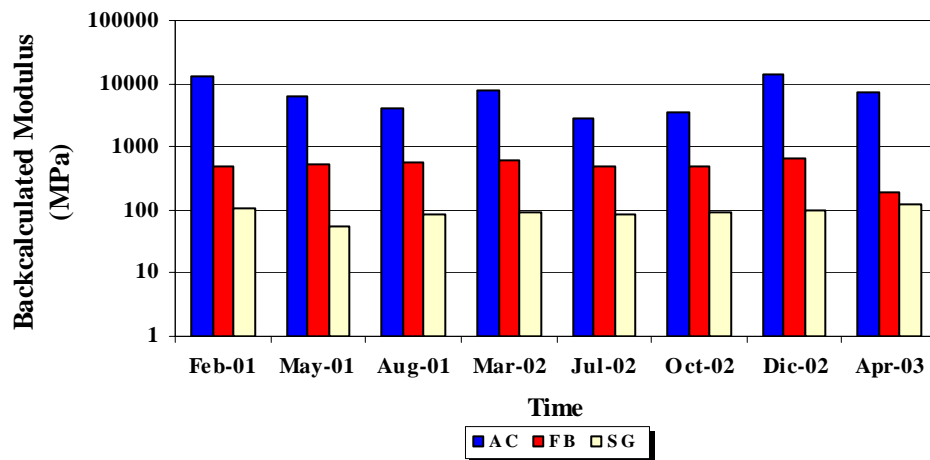
FIGURE B70   Backcalculated Modulus of K7-14 FWD Station
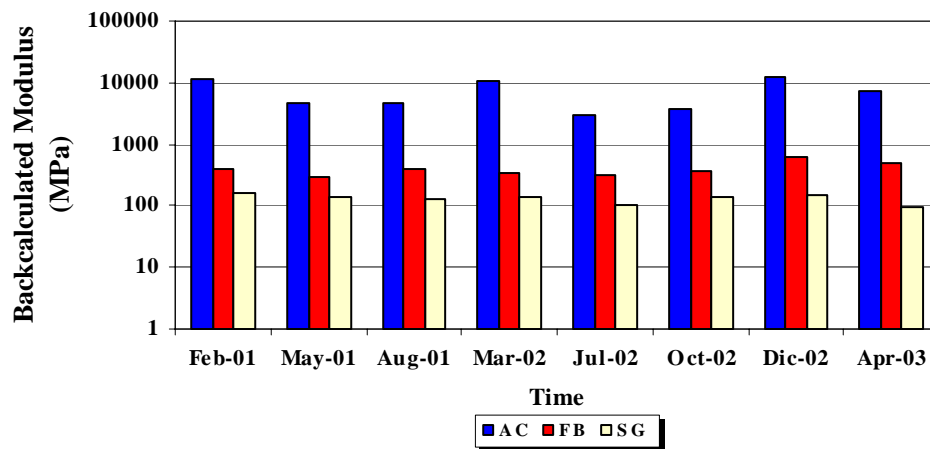
FIGURE B71   Backcalculated Modulus of K7-15 FWD Station
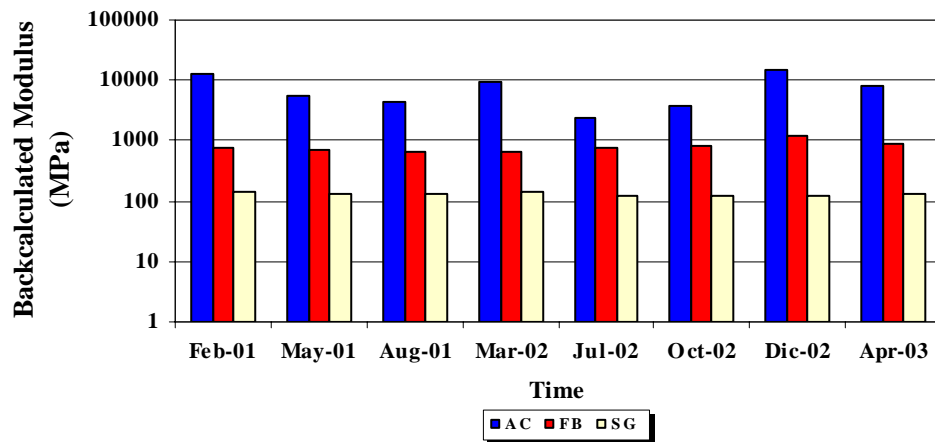
FIGURE B72   Backcalculated Modulus of K7-16 FWD Station
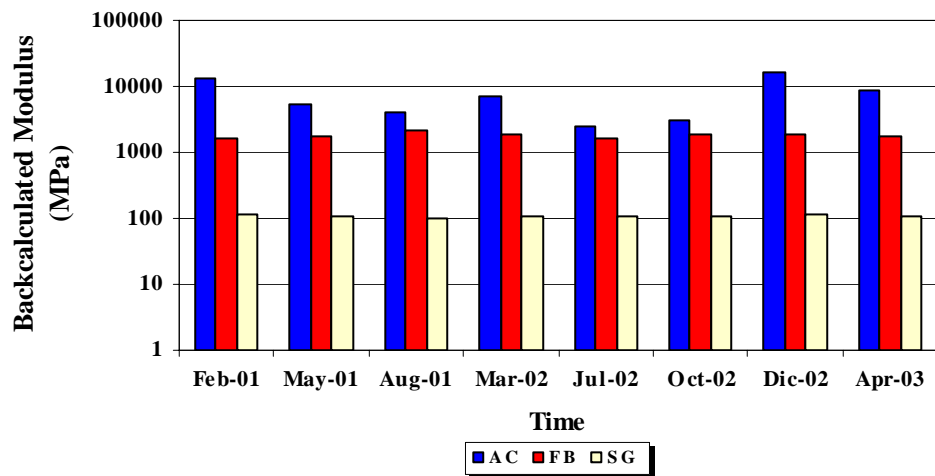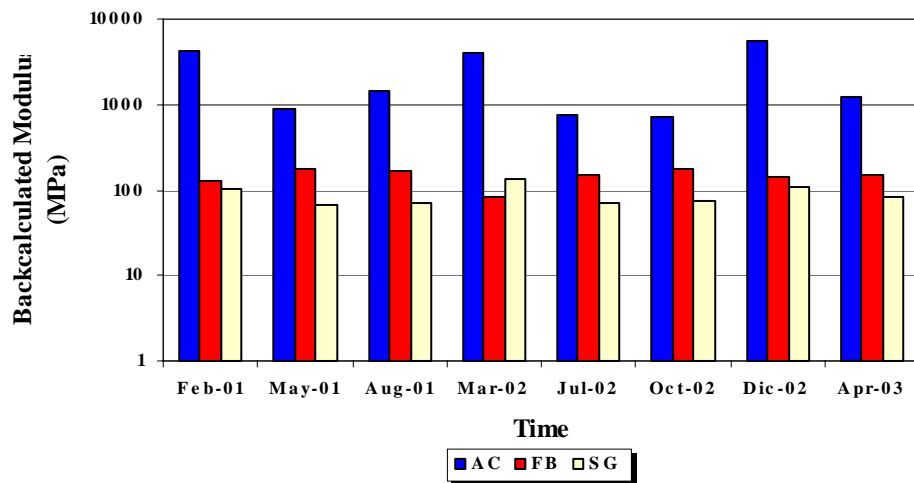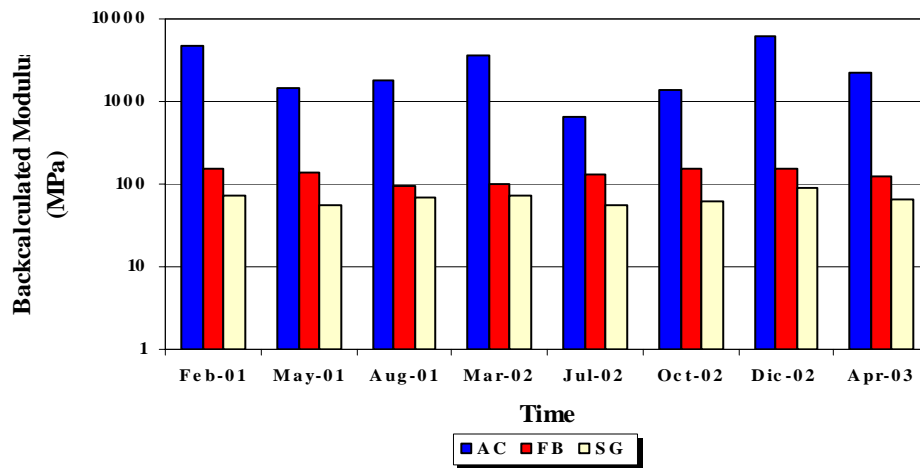

FIGURE B73   Backcalculated Modulus of K7-17 FWD Station
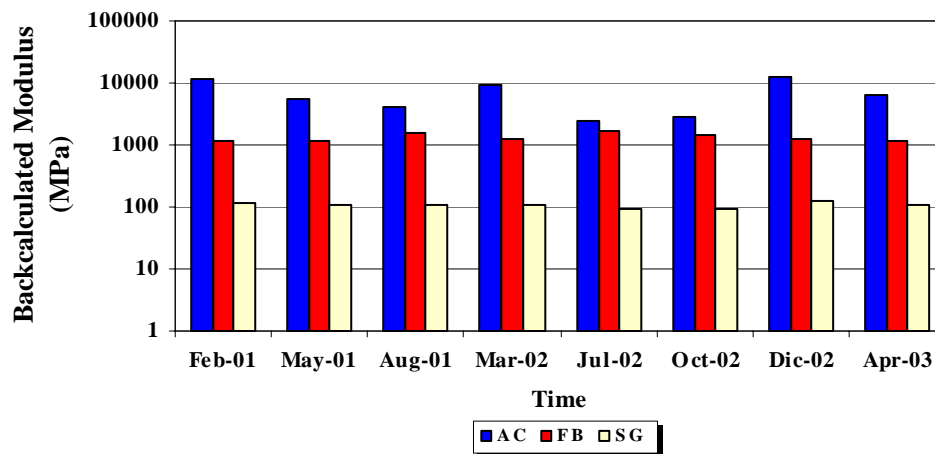
FIGURE B74   Backcalculated Modulus of K7-18 FWD Station
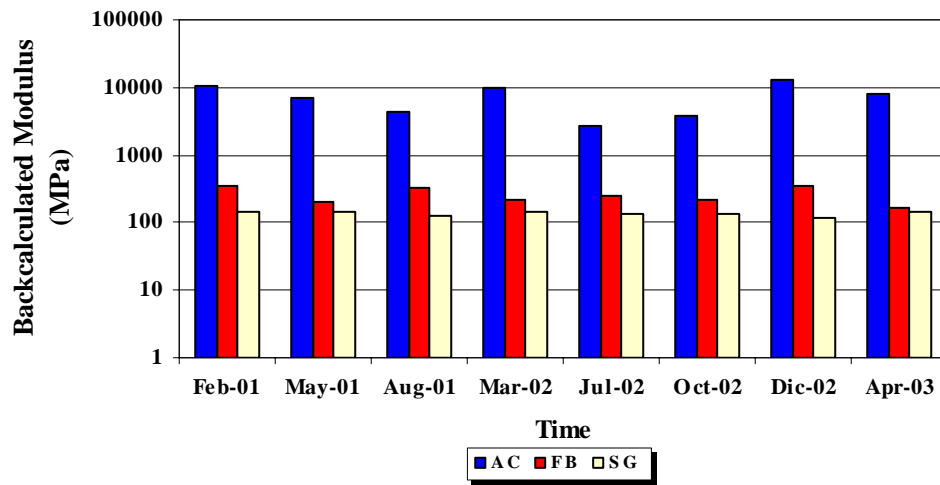
FIGURE B75   Backcalculated Modulus of K7-19 FWD Station

FIGURE B76   Backcalculated Modulus of K7-20 FWD Station

FIGURE B77   Backcalculated Modulus of K7-21 FWD Station

FIGURE B78   Backcalculated Modulus of K7-22 FWD Station

FIGURE B79   Backcalculated Modulus of K7-23 FWD Station

FIGURE B80   Backcalculated Modulus of K7-24 FWD Station

FIGURE B81   Backcalculated Modulus of K7-25 FWD Station

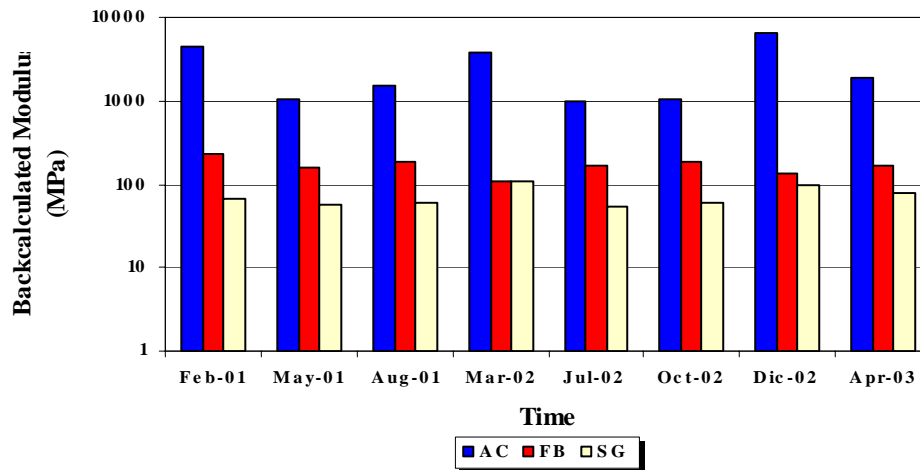**FIGURE B82   Backcalculated Modulus of K7-26 FWD Station**

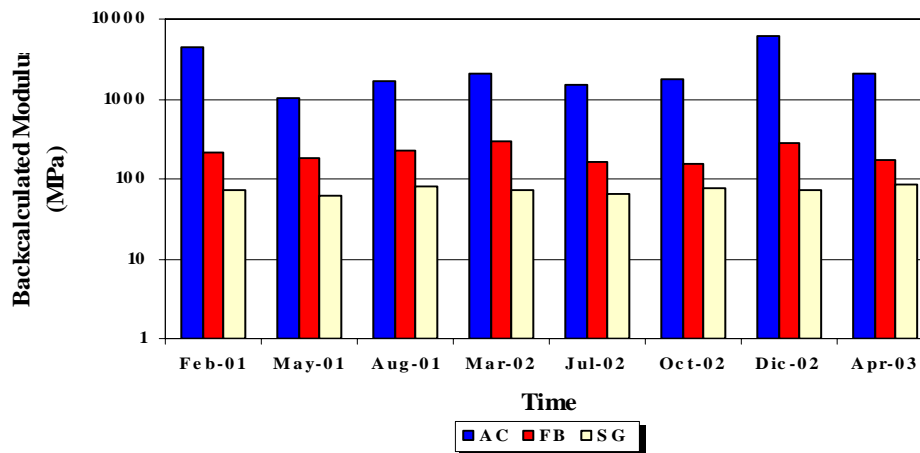**FIGURE B83   Backcalculated Modulus of K7-27 FWD Station**

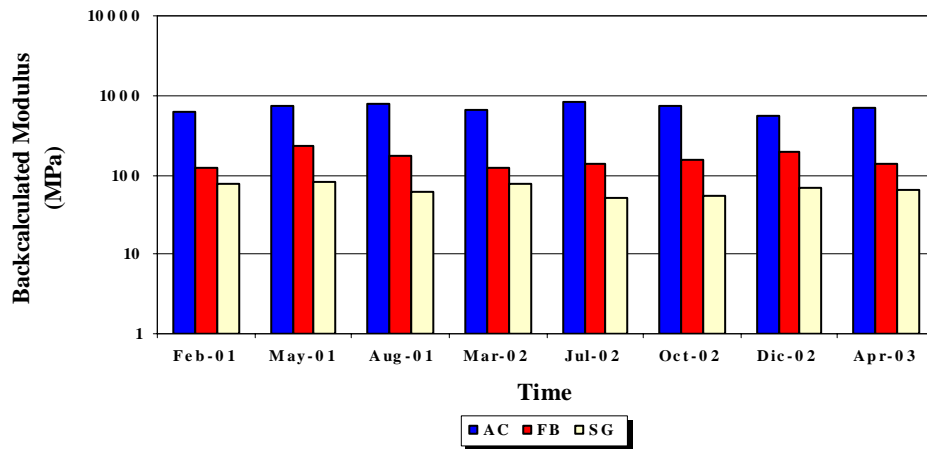**FIGURE B84   Backcalculated Modulus of K7-28 FWD Station**

FIGURE B85   Backcalculated Modulus of K7-29 FWD Station

FIGURE B86   Backcalculated Modulus of K7-30 FWD Station

FIGURE B87   Backcalculated Modulus of K7-31 FWD Station

FIGURE B88   Backcalculated Modulus of K7-32 FWD Station

FIGURE B89   Backcalculated Modulus of K7-33 FWD Station

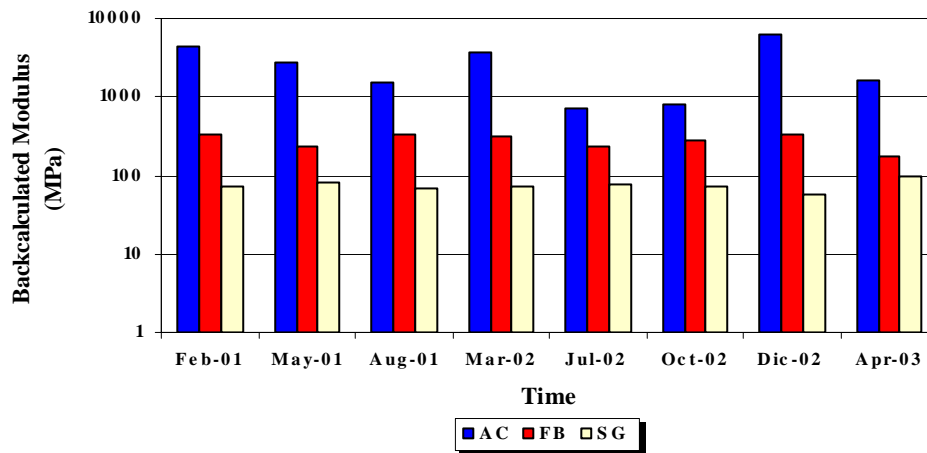**FIGURE B90   Backcalculated Modulus of K7-34 FWD Station**

FIGURE B91   Backcalculated Modulus of K7-35 FWD Station

FIGURE B92   Backcalculated Modulus of K7-36 FWD Station

FIGURE B93   Backcalculated Modulus of K7-37 FWD Station

FIGURE B94   Backcalculated Modulus of K7-38 FWD Station

FIGURE B95   Backcalculated Modulus of K7-39 FWD Station

FIGURE B96   Backcalculated Modulus of K7-40 FWD Station

FIGURE B97   Backcalculated Modulus of K7-41 FWD Station

FIGURE B98   Backcalculated Modulus of K7-42 FWD Station

FIGURE B99   Backcalculated Modulus of K7-43 FWD Station

FIGURE B100   Backcalculated Modulus of K7-44 FWD Station

FIGURE B101   Backcalculated Modulus of K7-45 FWD Station

FIGURE B102 Backcalculated Modulus of K7-46 FWD Station

FIGURE B103 Backcalculated Modulus of K7-47 FWD Station

FIGURE B104 Backcalculated Modulus of K7-48 FWD Station

FIGURE B105   Backcalculated Modulus of K7-49 FWD Station

FIGURE B106   Backcalculated Modulus of K7-50 FWD Station

APPENDIX C

**PLOTS OF MEASURED AND PREDICTED DISPLACEMENT
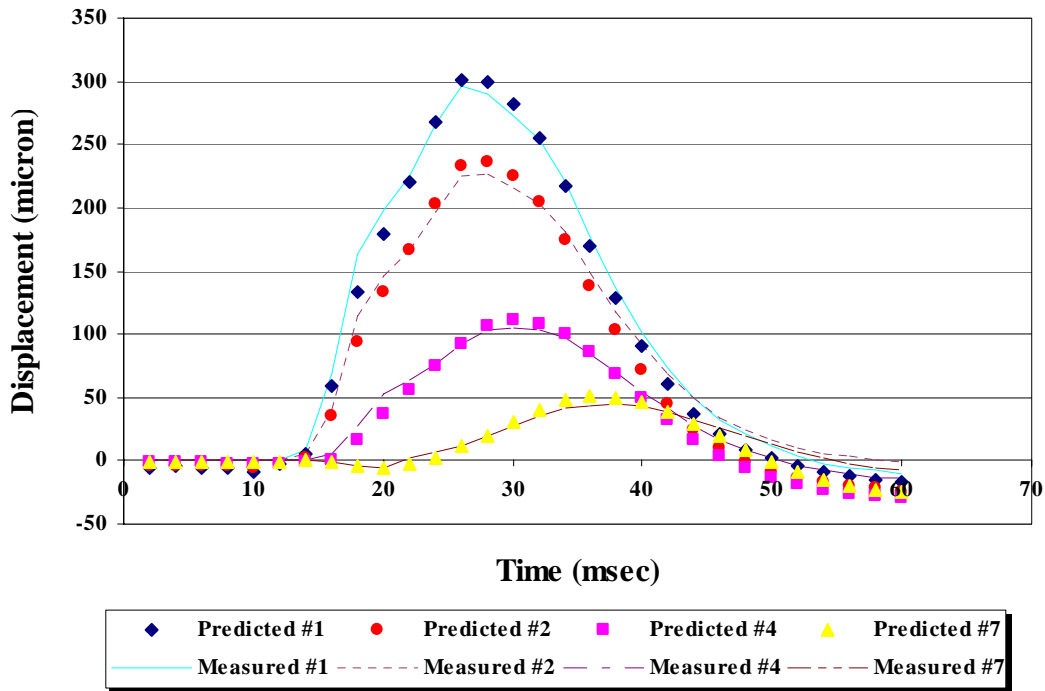HISTORIES**
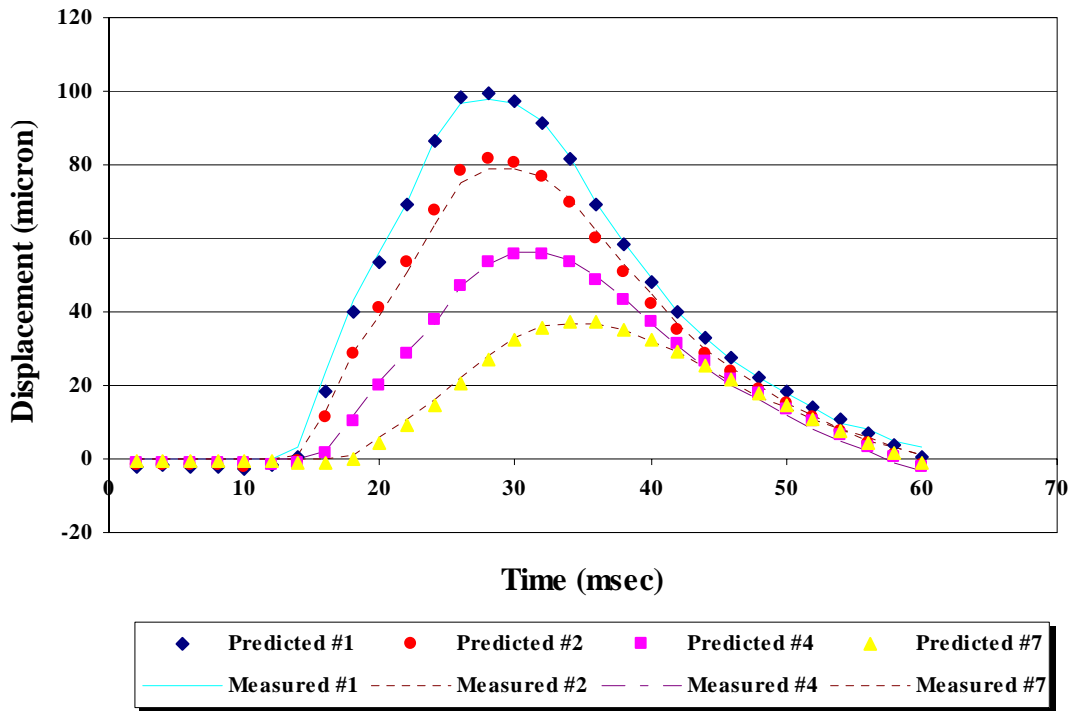
FIGURE C1   Comparison of Measured and Predicted Displacement Histories on K6 11 FWD Station in February 01
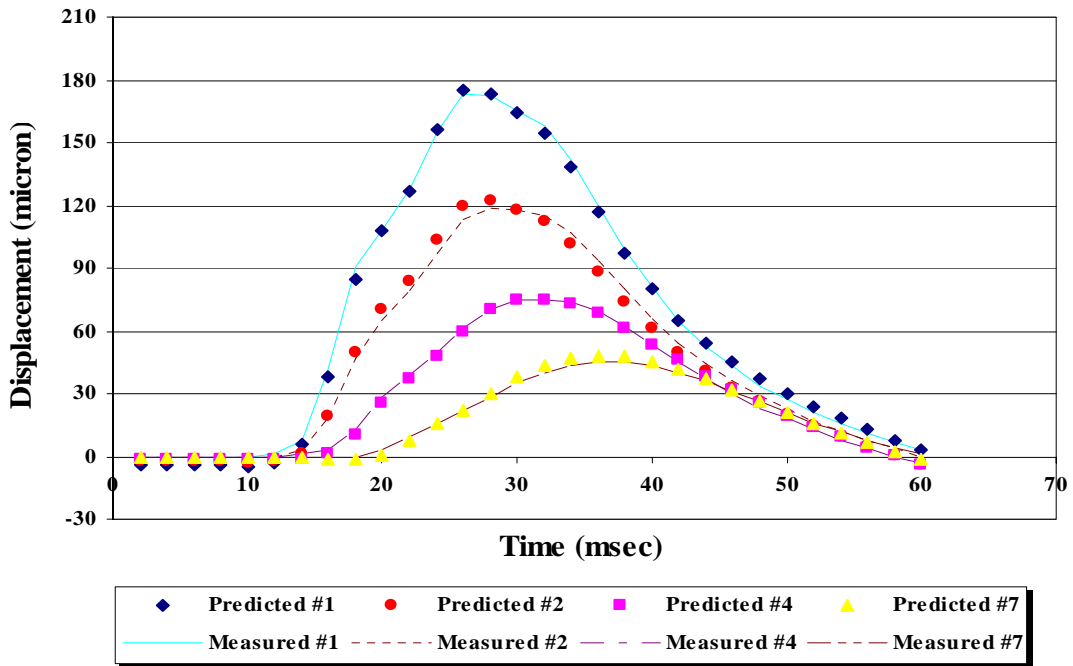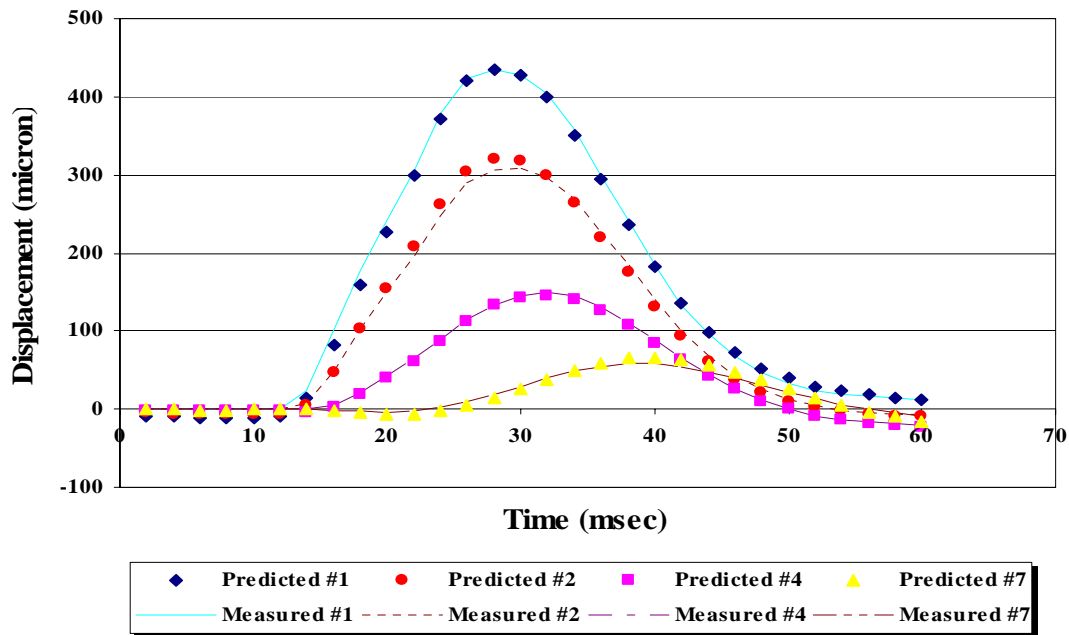

FIGURE C2   Comparison of Measured and Predicted Displacement Histories on K6 23 FWD Station in February 01
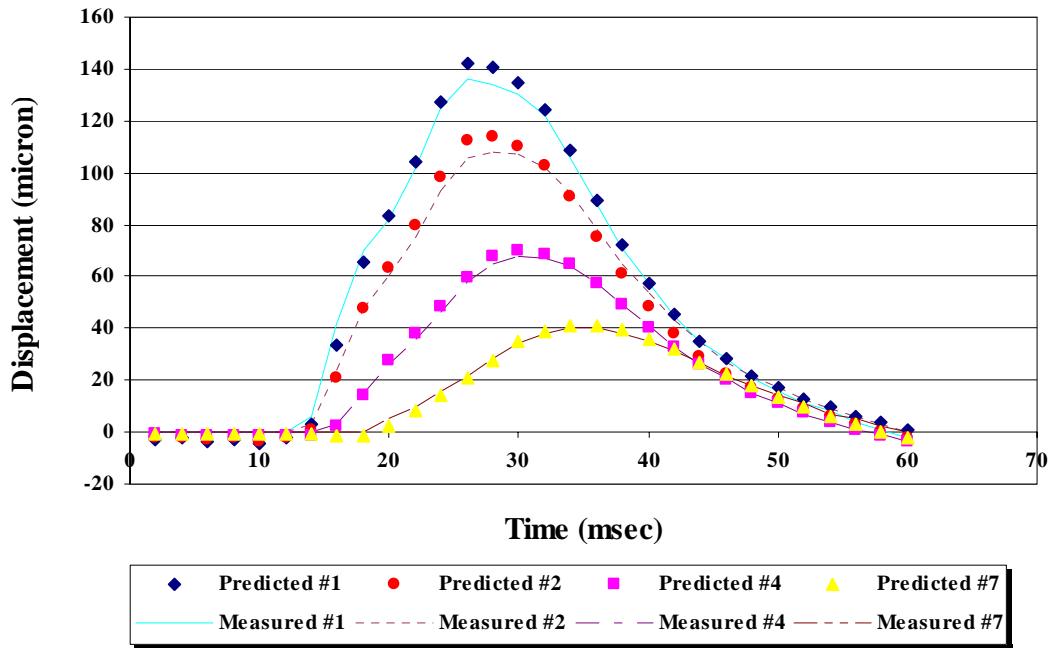
FIGURE C3   Comparison of Measured and Predicted Displacement Histories on K6 29 FWD Station in February 01

FIGURE C4   Comparison of Measured and Predicted Displacement Histories on K6 35 FWD Station in February 01

FIGURE C5   Comparison of Measured and Predicted Displacement Histories on K6 48 FWD Station in February 01
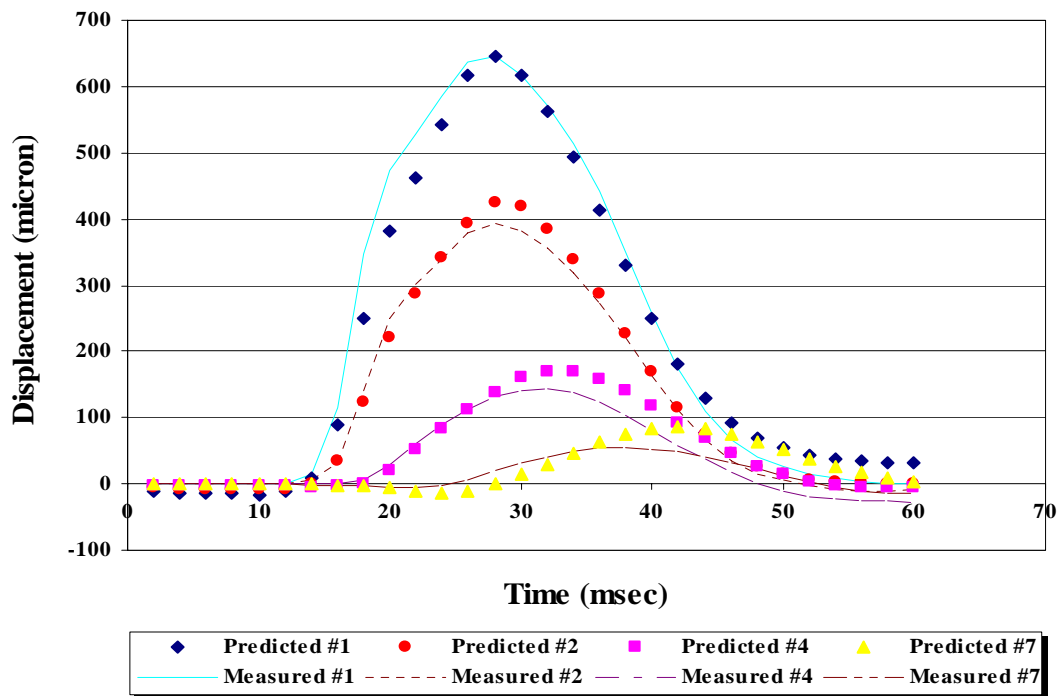

FIGURE C6   Comparison of Measured and Predicted Displacement Histories on K6 1 FWD Station in May 01
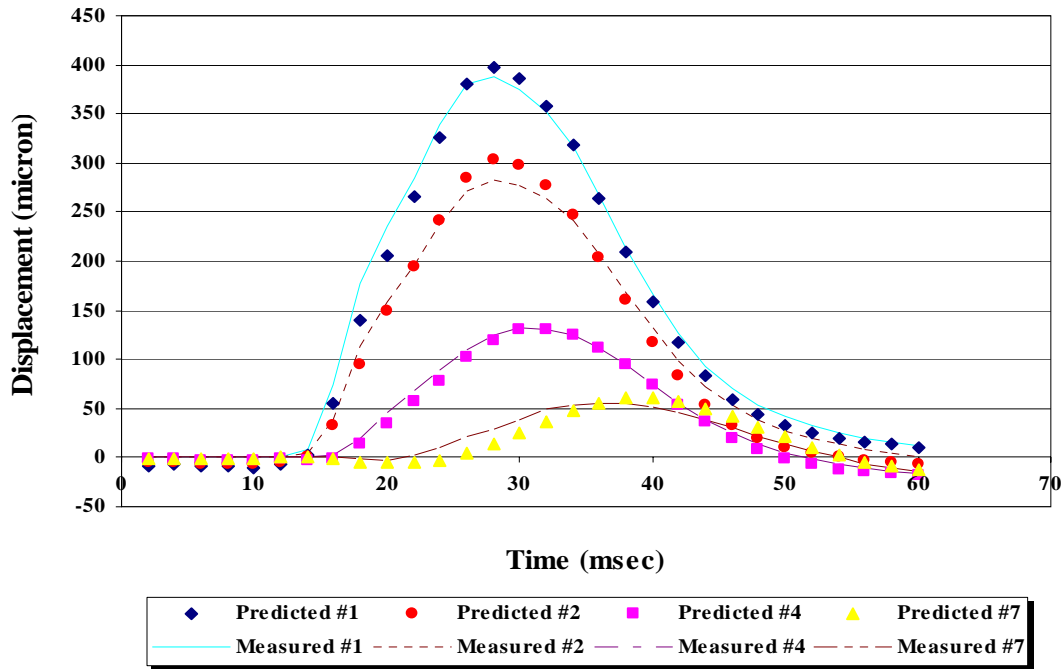
FIGURE C7   **Comparison of Measured and Predicted Displacement Histories on K6 4 FWD Station in May 01**
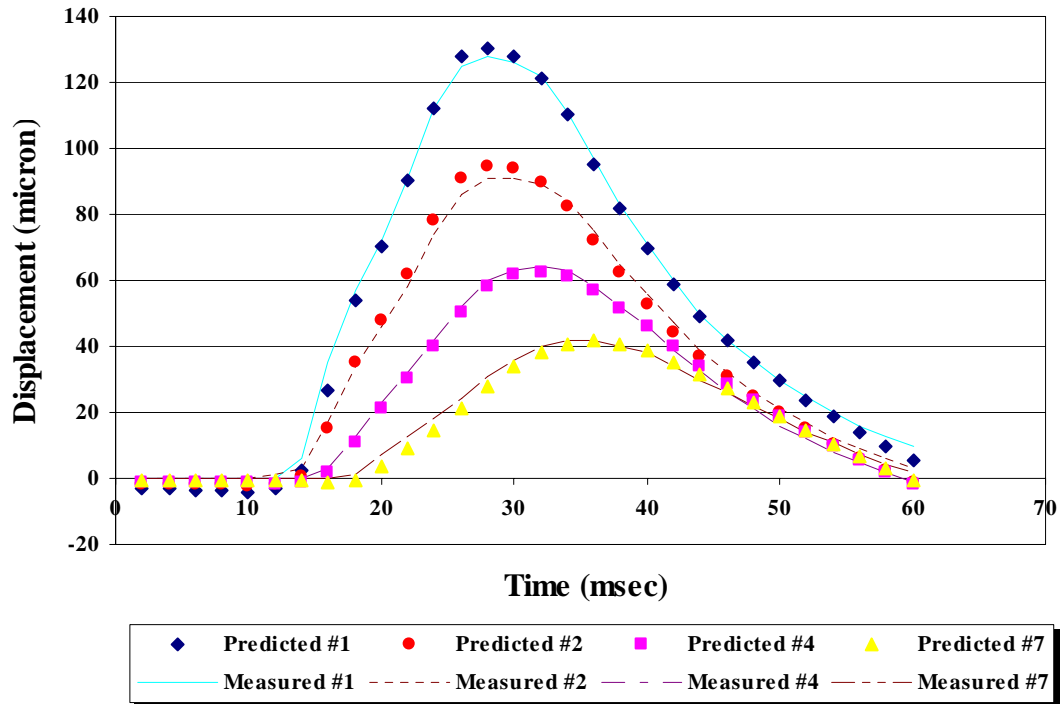

FIGURE C8   **Comparison of Measured and Predicted Displacement Histories on K6 11 FWD Station in May 01**
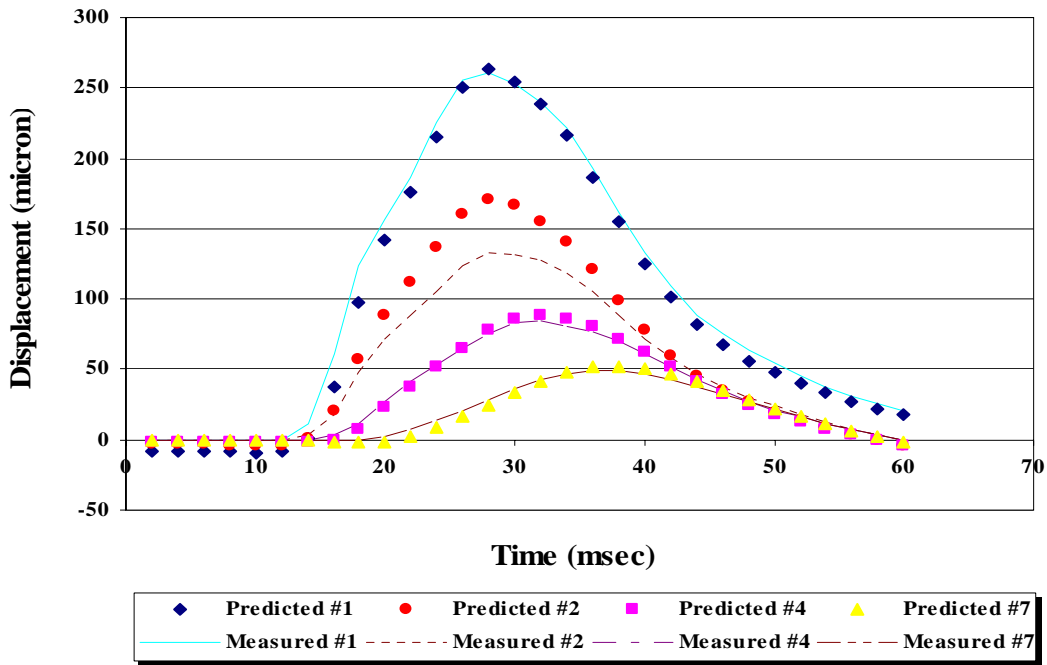
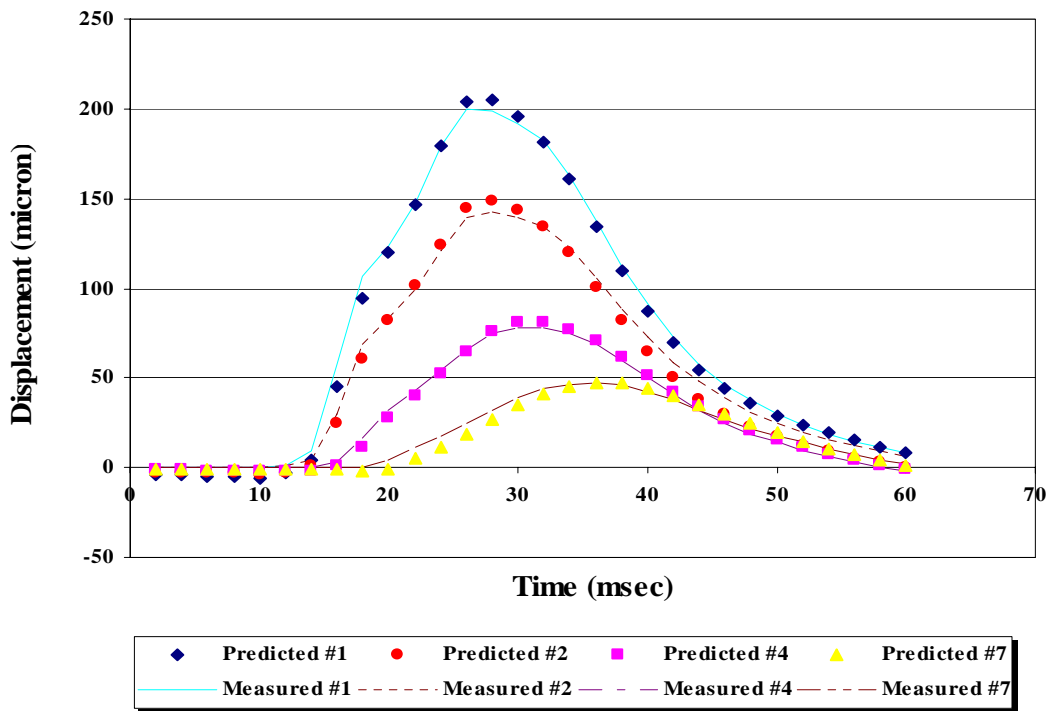**FIGURE C9   Comparison of Measured and Predicted Displacement Histories on K6 23 FWD station in May 01**

FI GURE C10   Comparison of Measured and Predicted Displacement Histories on K6 29 FWD station in May 01

FIGURE C11   Comparison of Measured and Predicted Displacement Histories   on K6 1 FWD station in July 01

FIGURE C12   Comparison of Measured and Predicted Displacement Histories on K6 4 FWD station in July 01
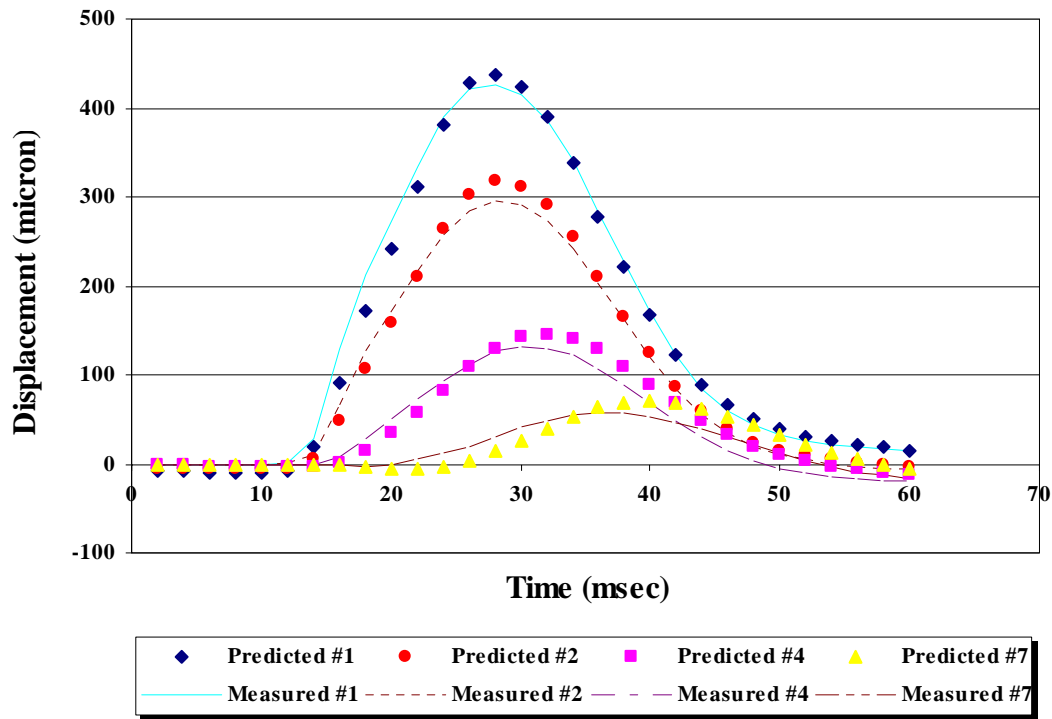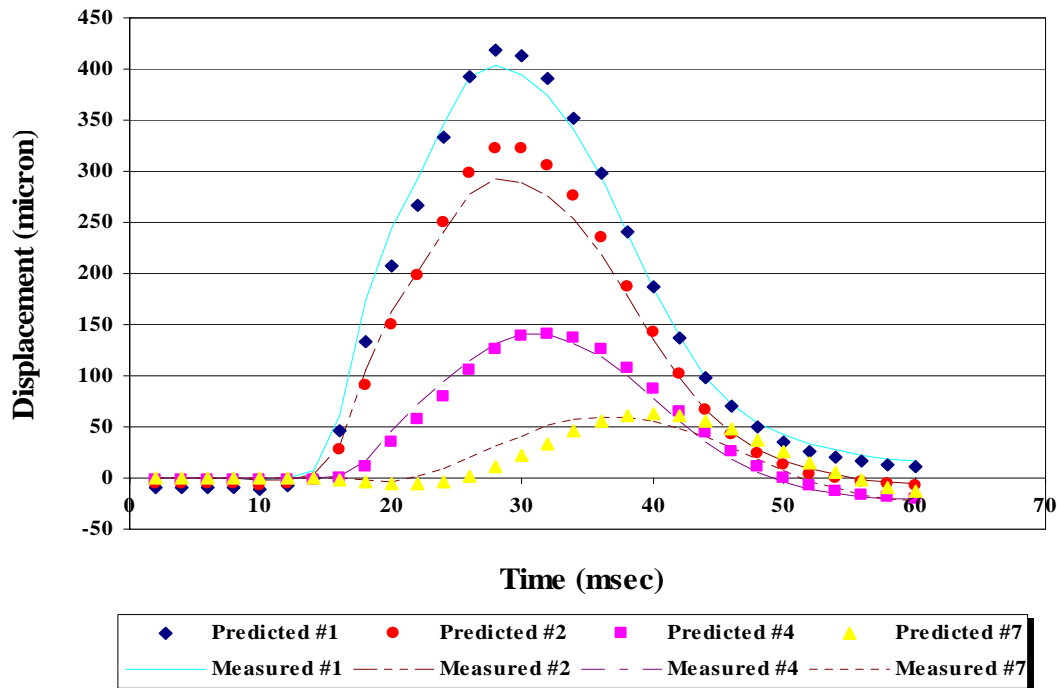
FIGURE C13   Comparison of Measured and Predicted Displacement Histories on K6 11 FWD station in July 01

FIGURE C14   Comparison of Measured and Predicted Displacement Histories on K6 23 FWD station in July 01

FIGURE C15 Comparison of Measured and Predicted Displacement Histories on K6 29 FWD station in July 01

FIGURE C16 Comparison of Measured and Predicted Displacement Histories on K6 35 FWD station in July 01
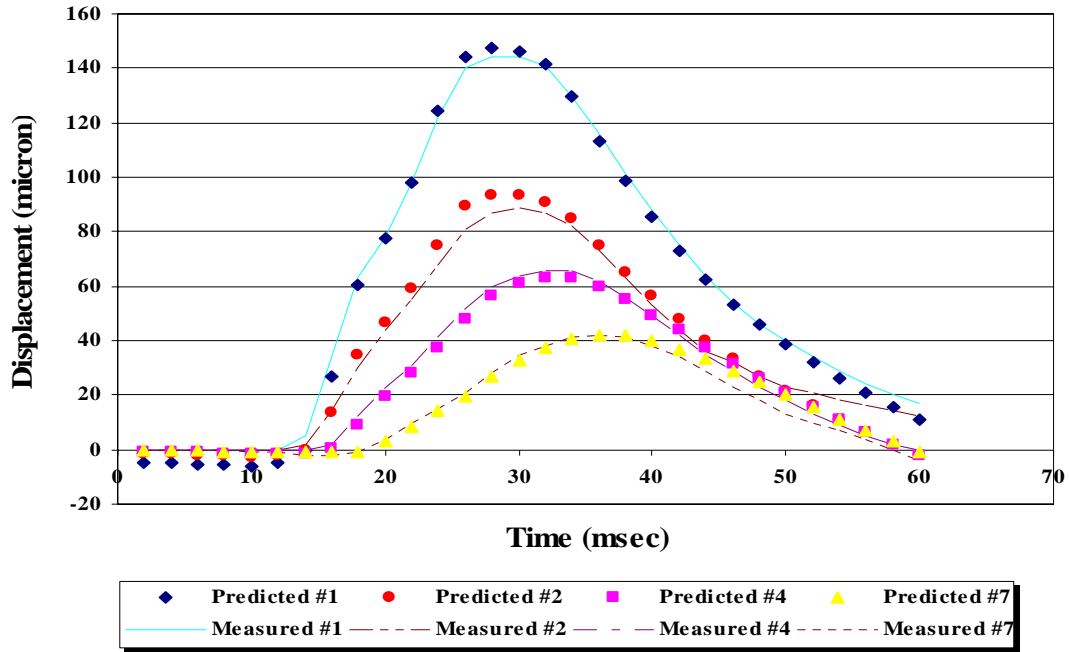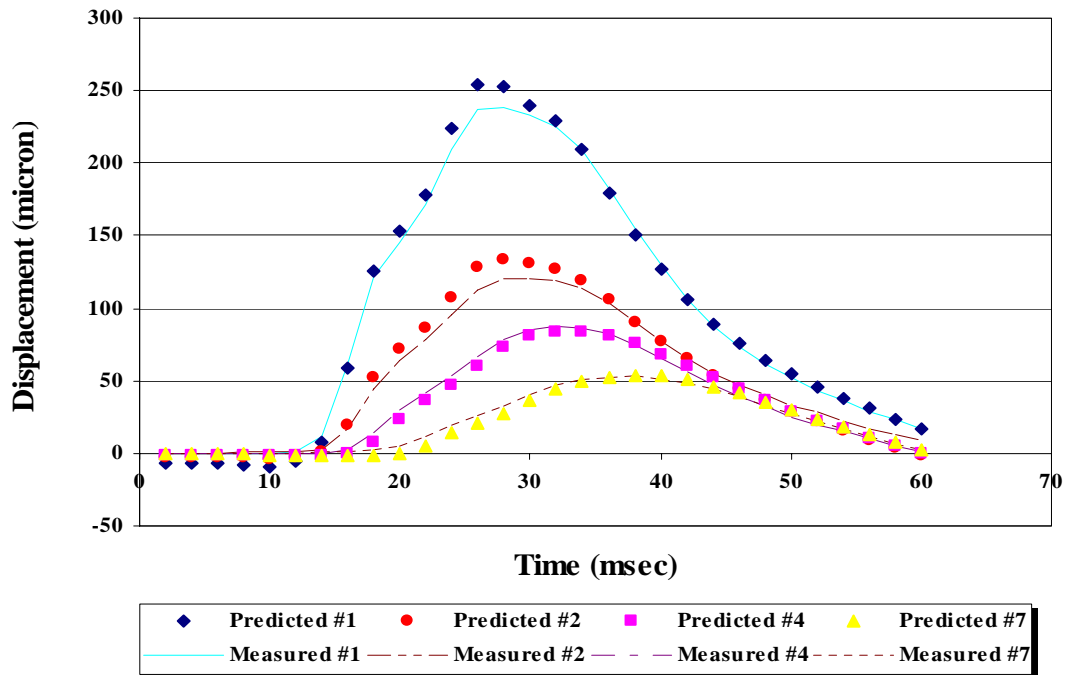
FIGURE C17   Comparison of Measured and Predicted Displacement Histories on K6 48 FWD Station in July 01

FIGURE C18   Comparison of Measured and Predicted Displacement Histories on K6 1 FWD Station in August 01

FIGURE C19 Comparison of Measured and Predicted Displacement Histories on K6 11 FWD Station in August 01

FIGURE C20 Comparison of Measured and Predicted Displacement Histories on K6 23 FWD Station in August 01
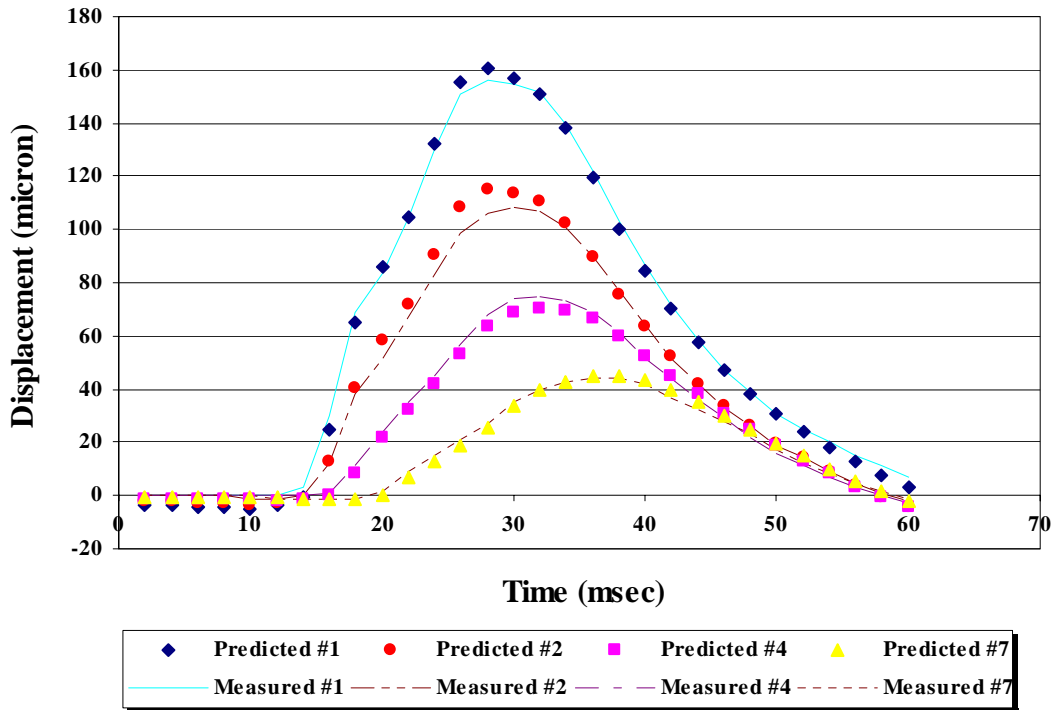
FIGURE C21   Comparison of Measured and Predicted Displacement Histories on K6 29 FWD Station in August 01
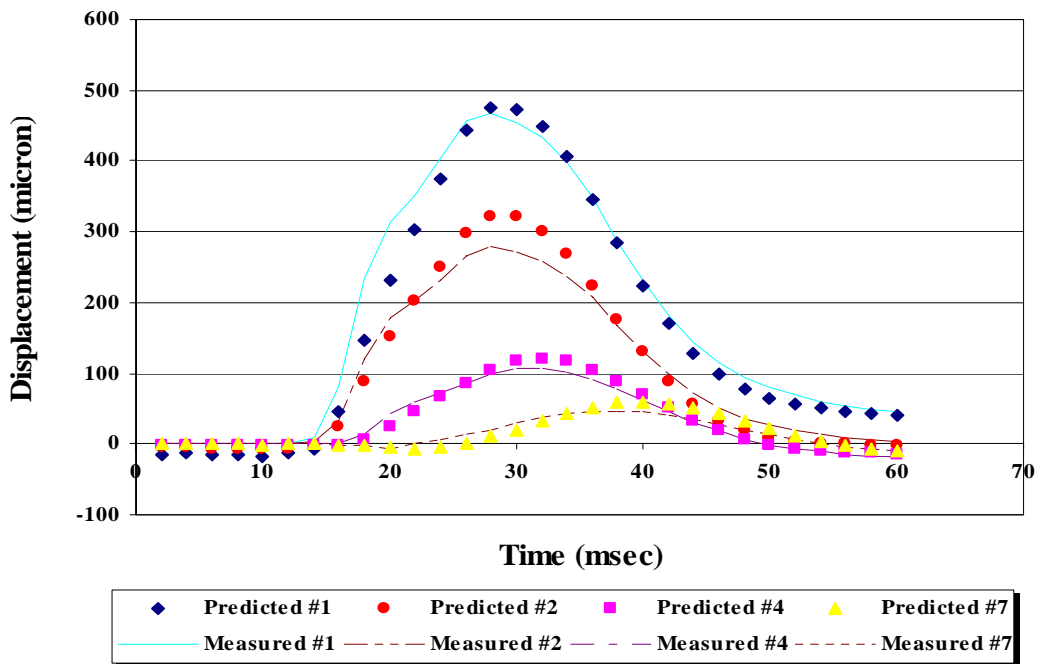

FIGURE C22   Comparison of Measured and Predicted Displacement Histories on K6 48 FWD Station in August 01

FIGURE C23   Comparison of Measured and Predicted Displacement Histories on K6 1 FWD Station in March 02
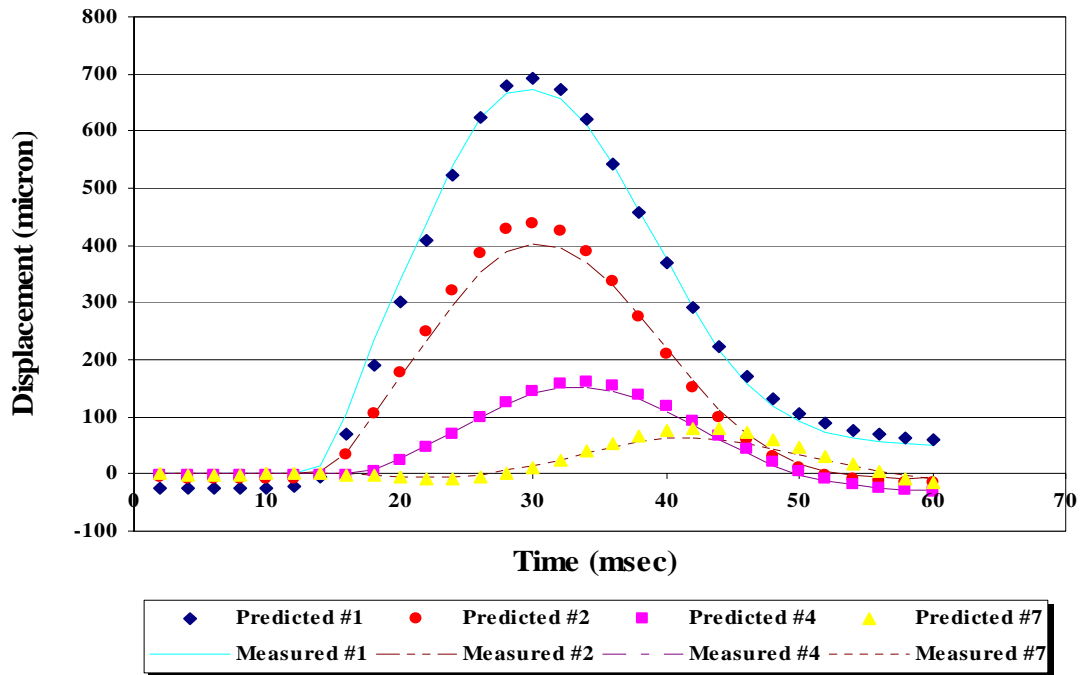

FIGURE C24   Comparison of Measured and Predicted Displacement Histories on K6 4 FWD Station in March 02

FIGURE C25 Comparison of Measured and Predicted Displacement Histories on K6 11 FWD Station in March 02

FIGURE C26 Comparison of Measured and Predicted Displacement Histories on K6 23 FWD Station in March 02

FIGURE C27 Comparison of Measured and Predicted Displacement Histories on K6 29 FWD Station in March 02

FIGURE C28 Comparison of Measured and Predicted Displacement Histories on K6 48 FWD Station in March 02

FIGURE C29   Comparison of Measured and Predicted Displacement Histories on K6 4 FWD Station in July 02

FIGURE C29   Comparison of Measured and Predicted Displacement Histories on K6 11 FWD Station in July 02
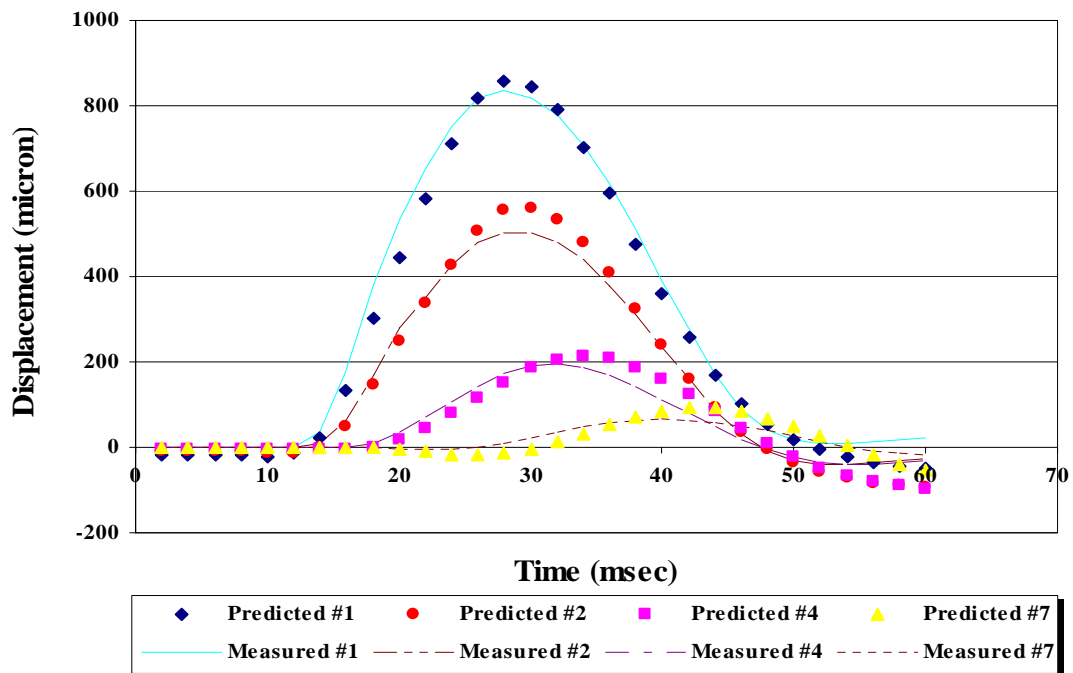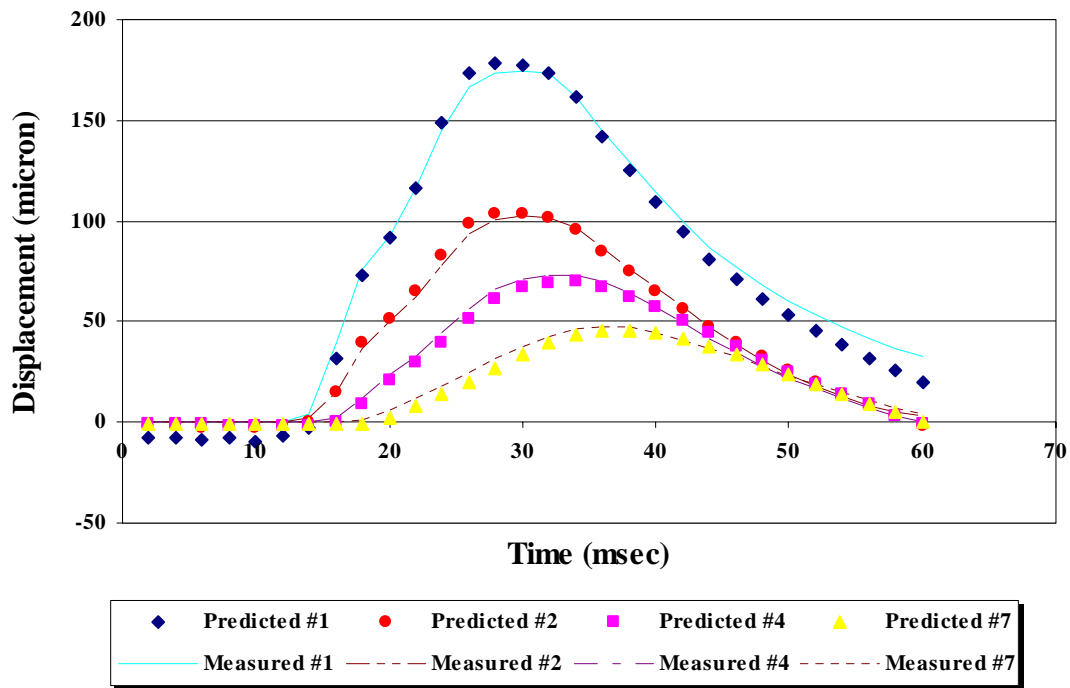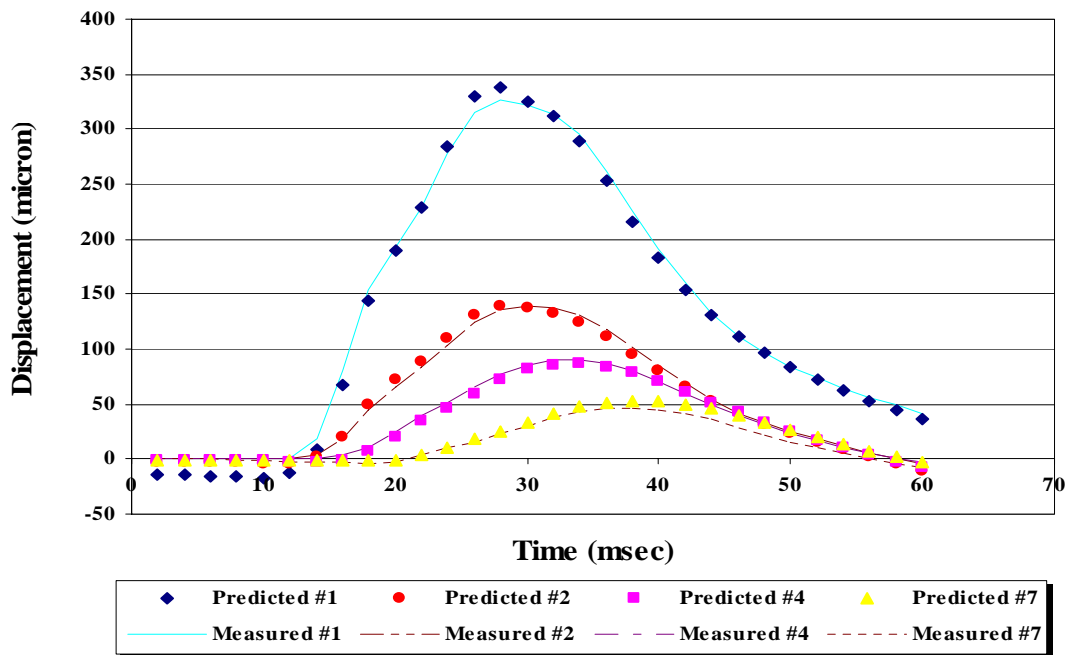
FIGURE C30   Comparison of Measured and Predicted Displacement Histories on K6 23 FWD Station in July 02
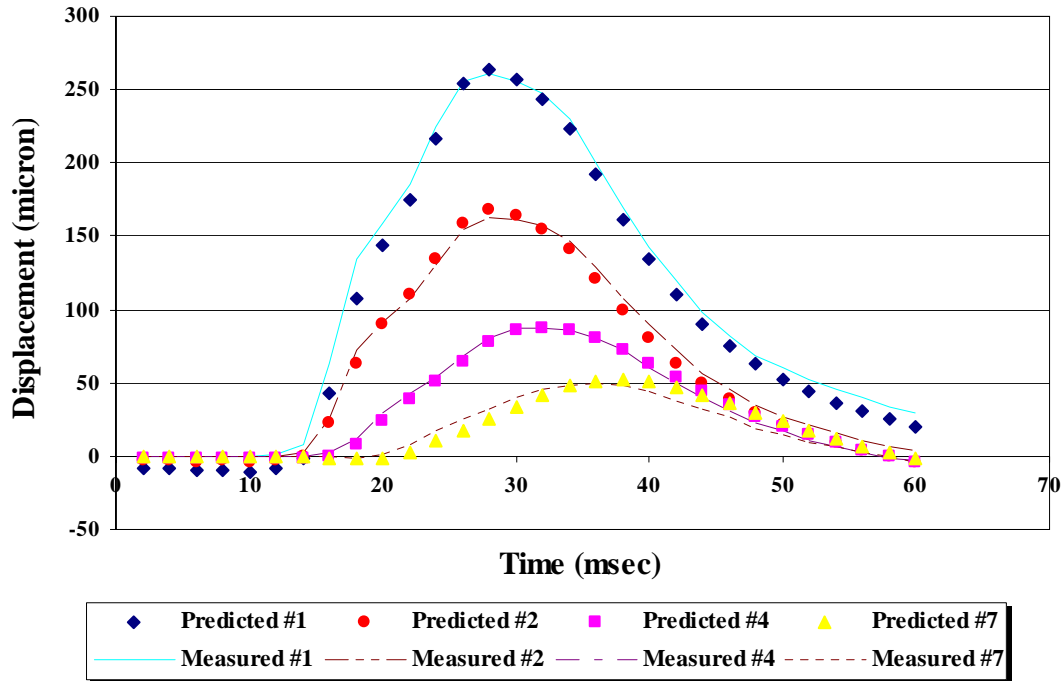

FIGURE C31   Comparison of Measured and Predicted Displacement Histories on K6 29 FWD Station in July 02
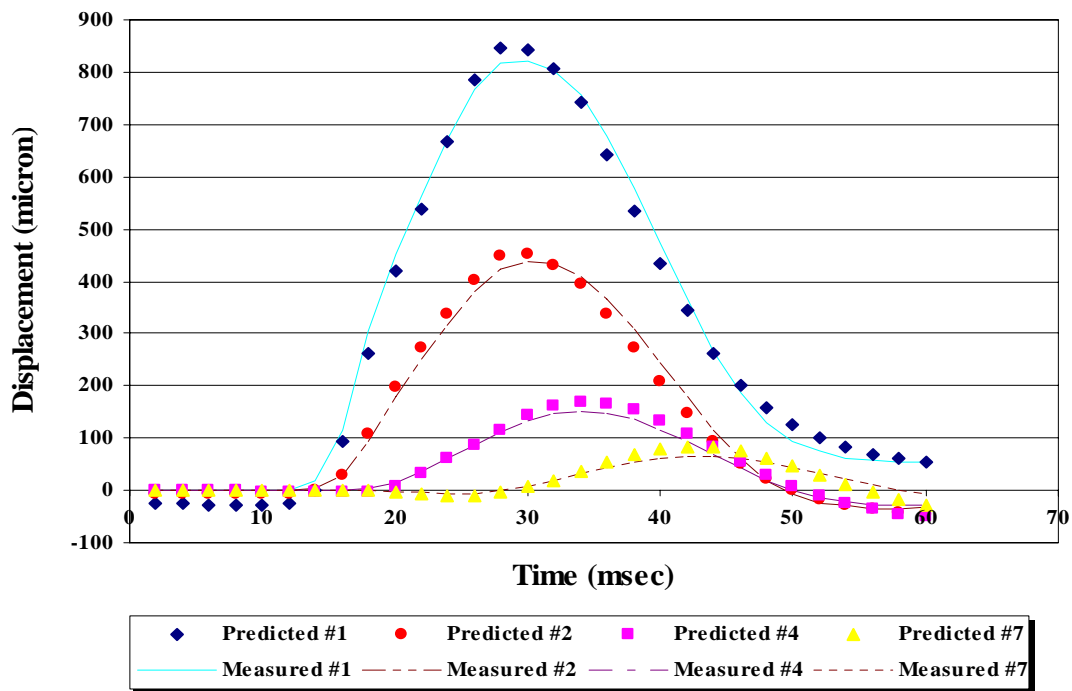
FIGURE C32   Comparison of Measured and Predicted Displacement Histories on K6 48 FWD Station in July 02

FIGURE C33   Comparison of Measured and Predicted Displacement Histories on K7 20 FWD Station in February 01

FIGURE C34   Comparison of Measured and Predicted Displacement Histories on K7 37 FWD Station in February 01

FIGURE C35   Comparison of Measured and Predicted Displacement Histories on K7 40 FWD Station in February 01
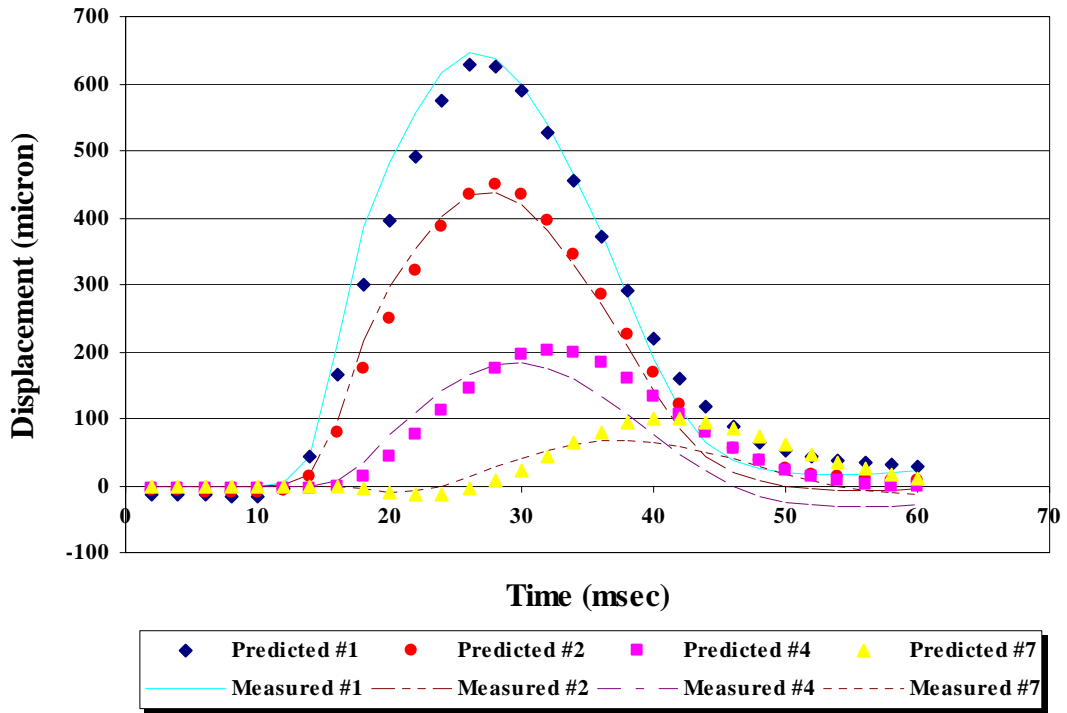
FIGURE C36   Comparison of Measured and Predicted Displacement Histories on K7 11 FWD Station in May 01

FIGURE C37   Comparison of Measured and Predicted Displacement Histories on K7 15 FWD Station in May 01
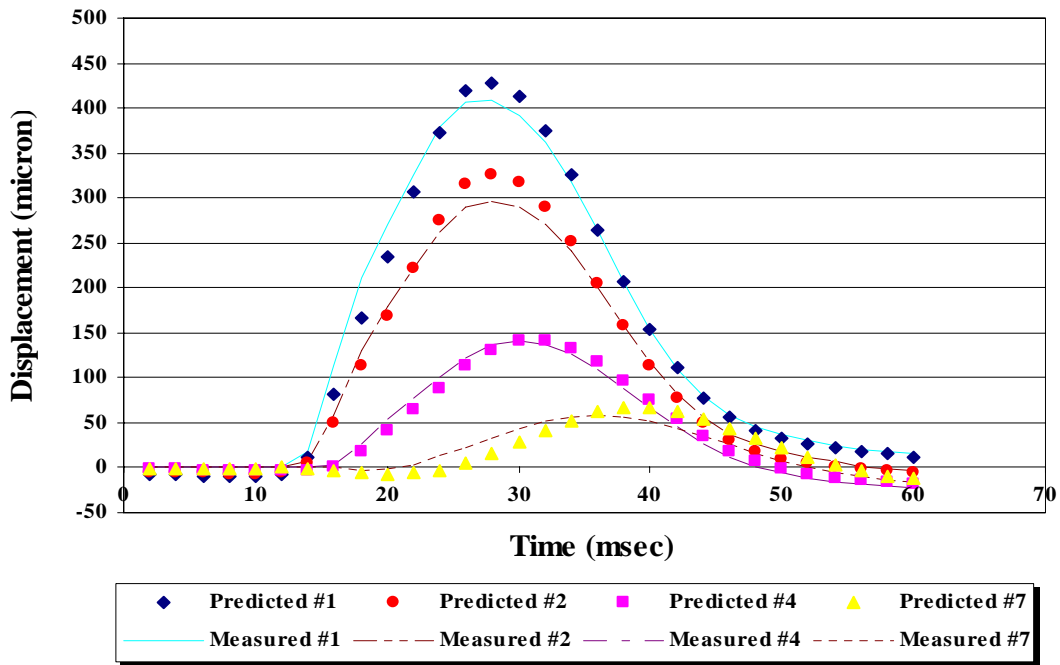
FIGURE C38   Comparison of Measured and Predicted Displacement Histories on K7 31 FWD Station in May 01
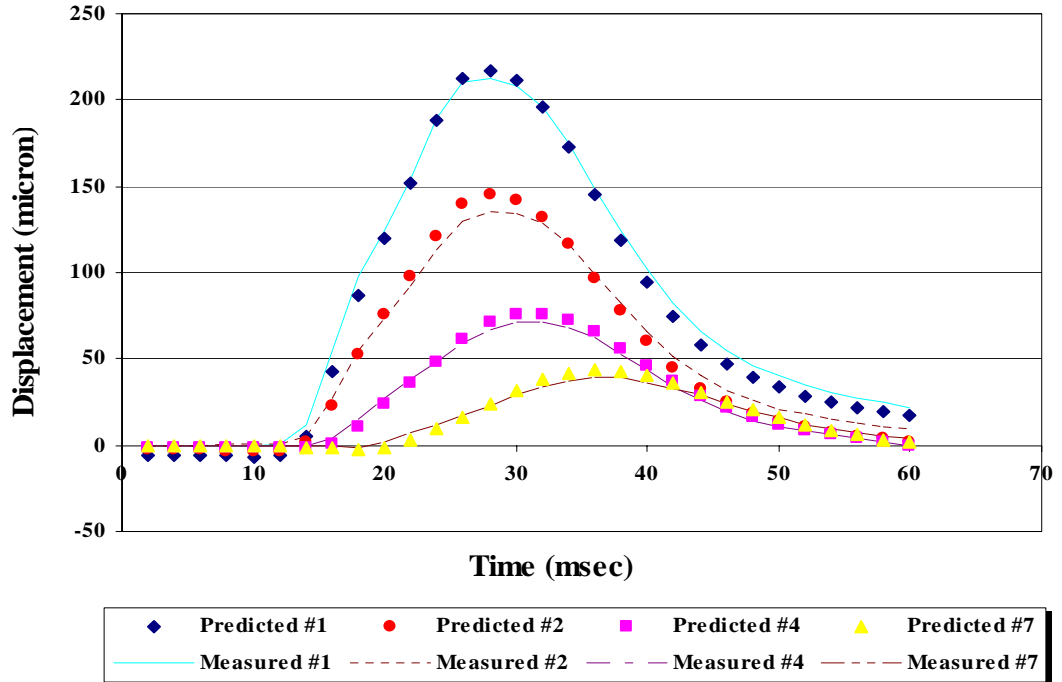
FIGURE C38   Comparison of Measured and Predicted Displacement Histories on K7 37 FWD Station in May 01
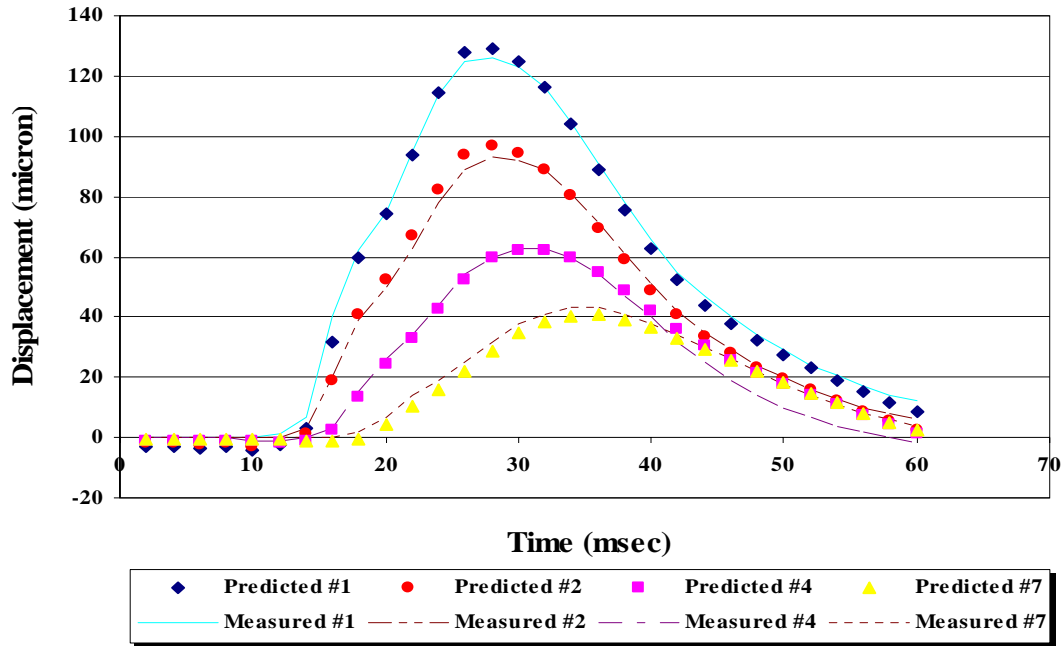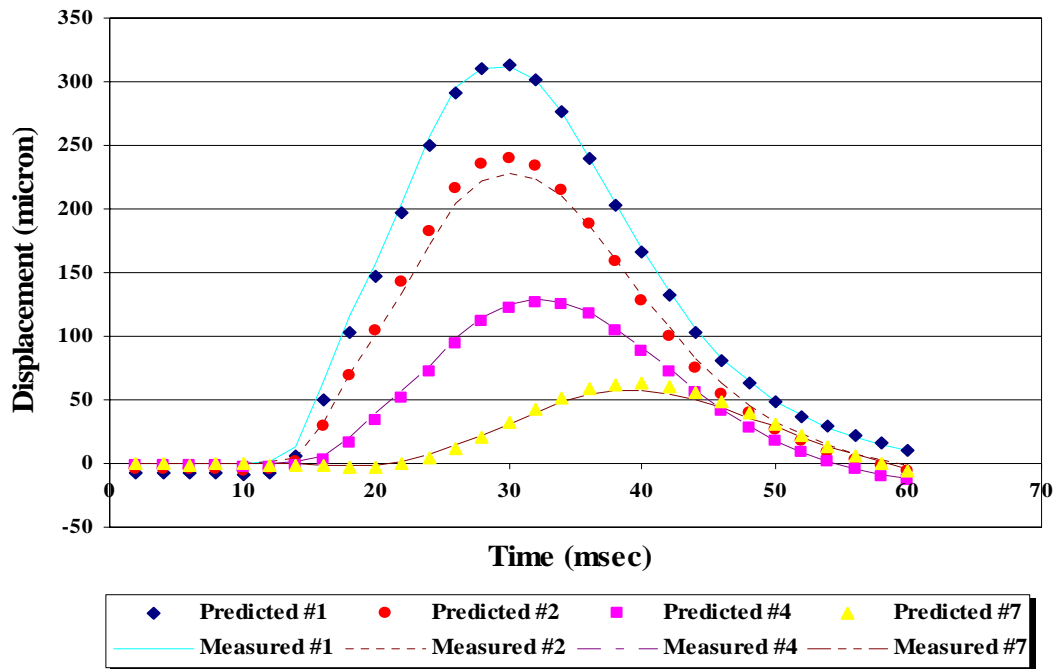
FIGURE C39 Comparison of Measured and Predicted Displacement Histories on K7 40 FWD Station in May 01
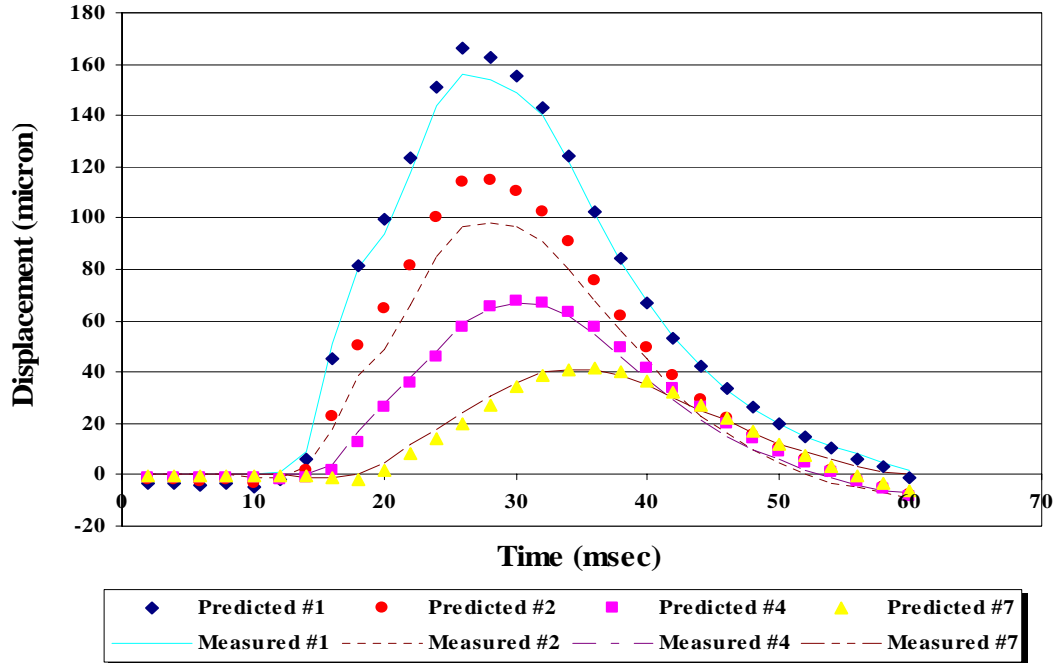
FIGURE C40 Comparison of Measured and Predicted Displacement Histories on K7 11 FWD Station in August 01
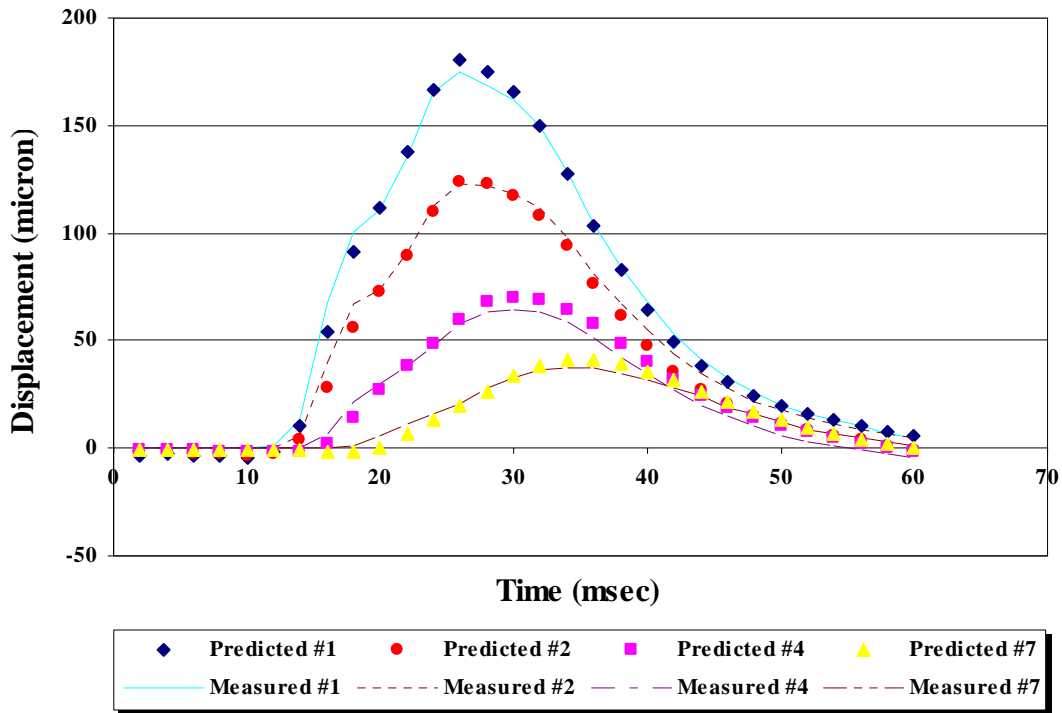
FIGURE C40   Comparison of Measured and Predicted Displacement Histories on K7 15 FWD Station in August 01
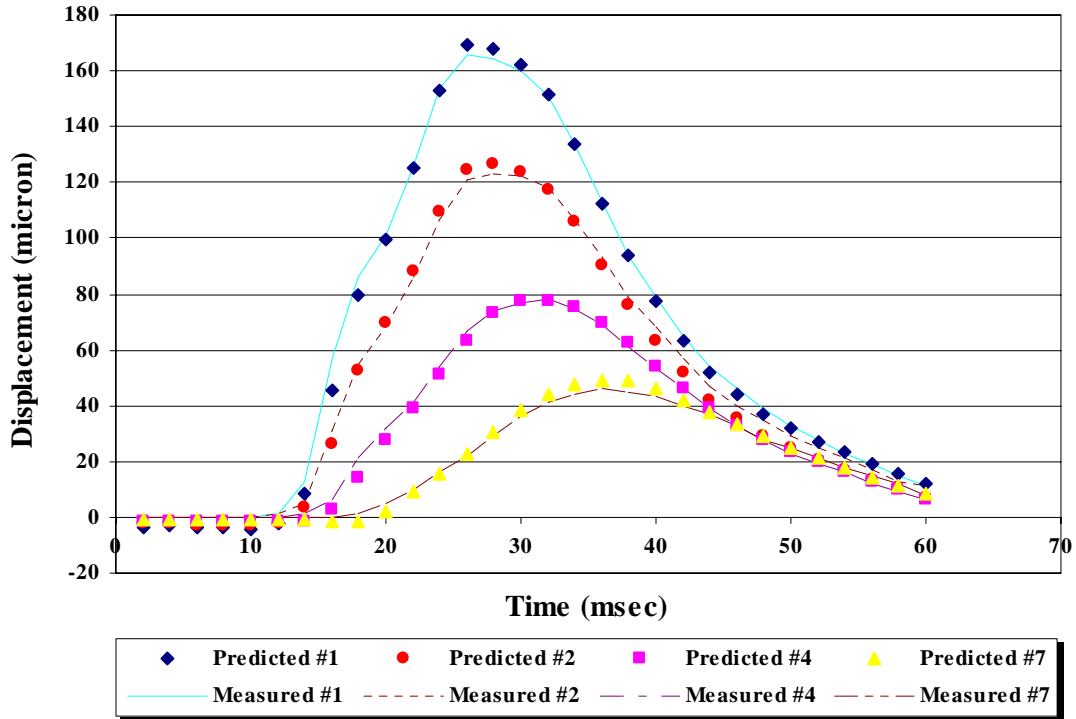
FIGURE C41   Comparison of Measured and Predicted Displacement Histories on K7 20 FWD Station in August 01
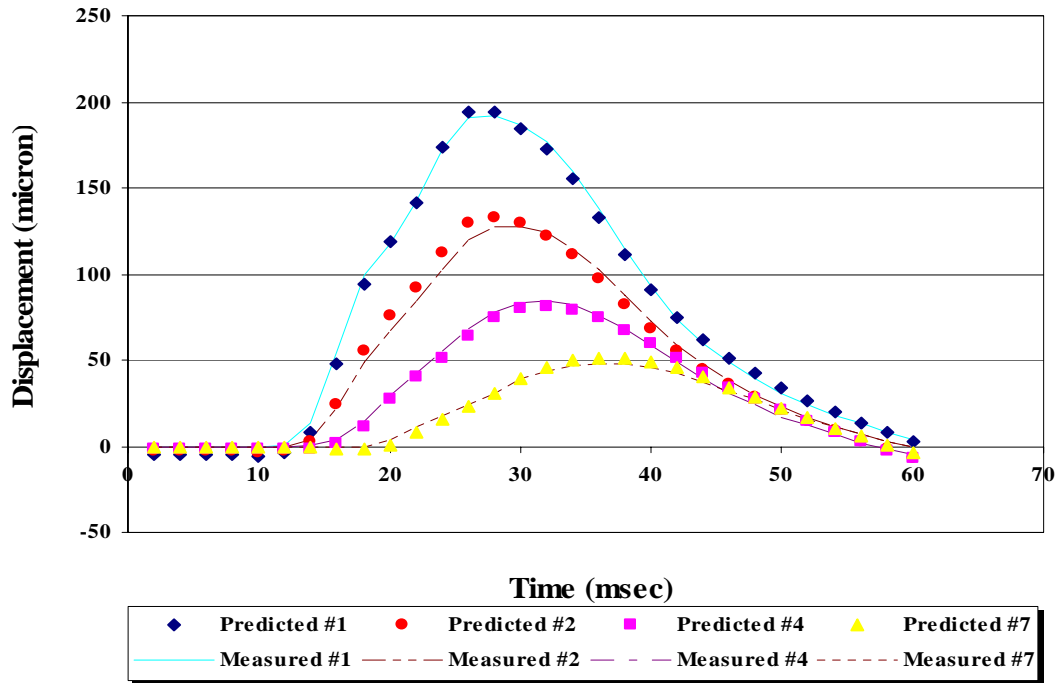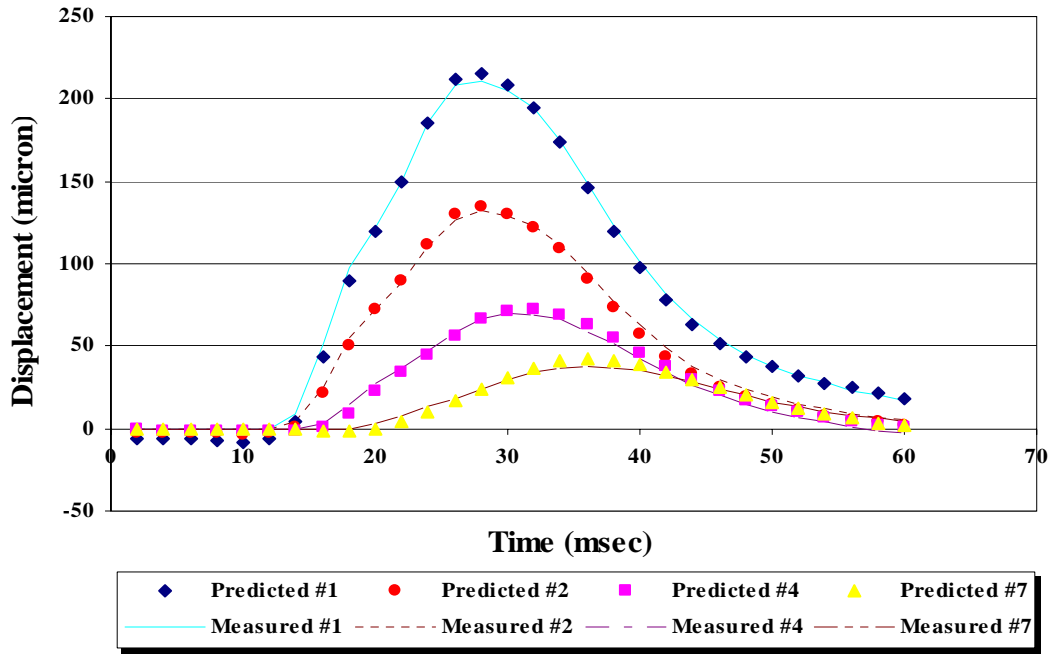
FIGURE C42   Comparison of Measured and Predicted Displacement Histories on
K7 37 FWD Station in August 01
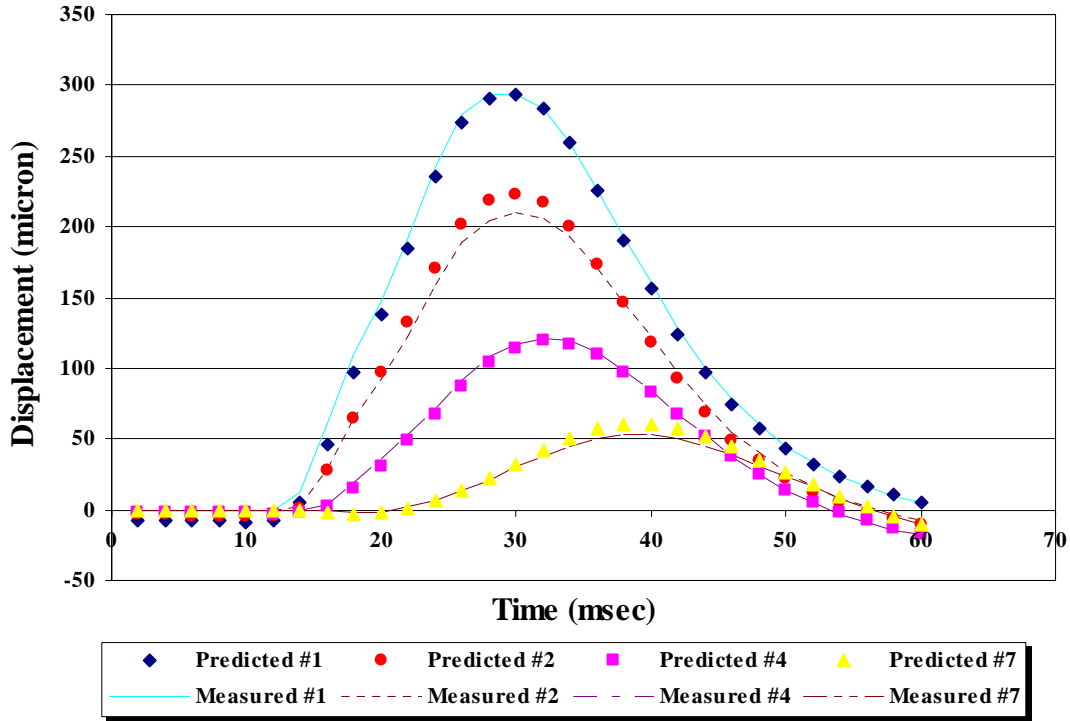
FIGURE C43   Comparison of Measured and Predicted Displacement Histories on
K7 40 FWD Station in August 01
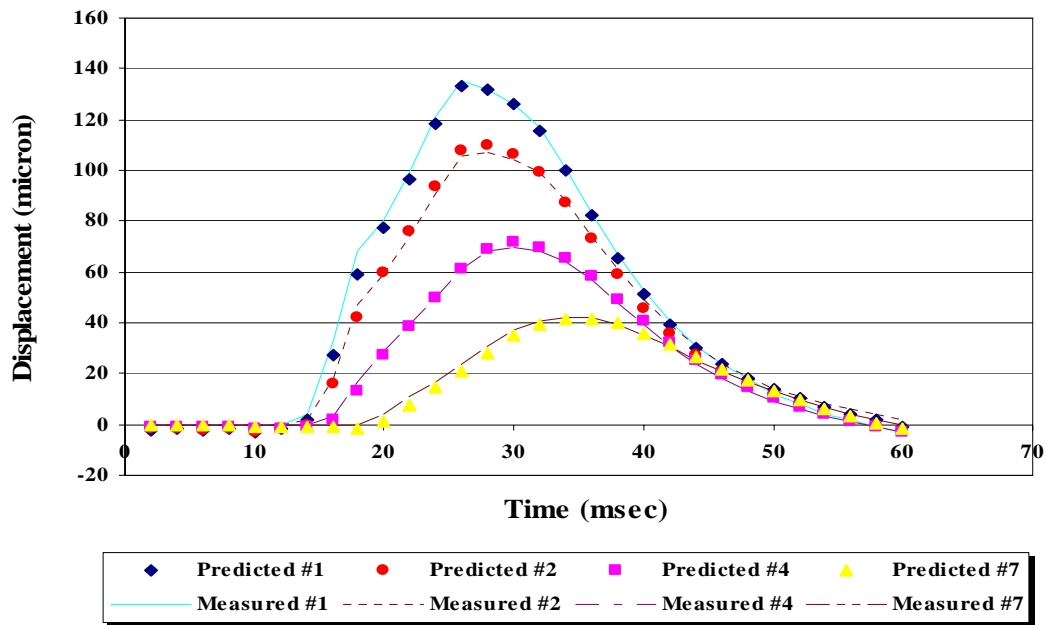
FIGURE C44   Comparison of Measured and Predicted Displacement Histories on K7 11 FWD Station in March 02
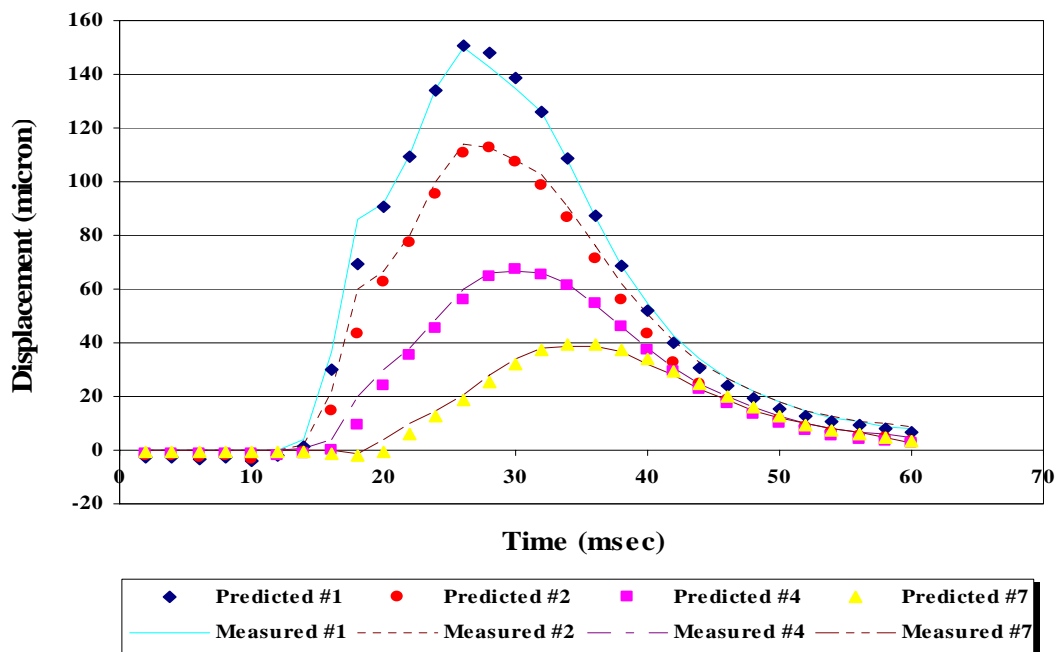
FIGURE C45   Comparison of Measured and Predicted Displacement Histories on K7 15 FWD Station in March 02
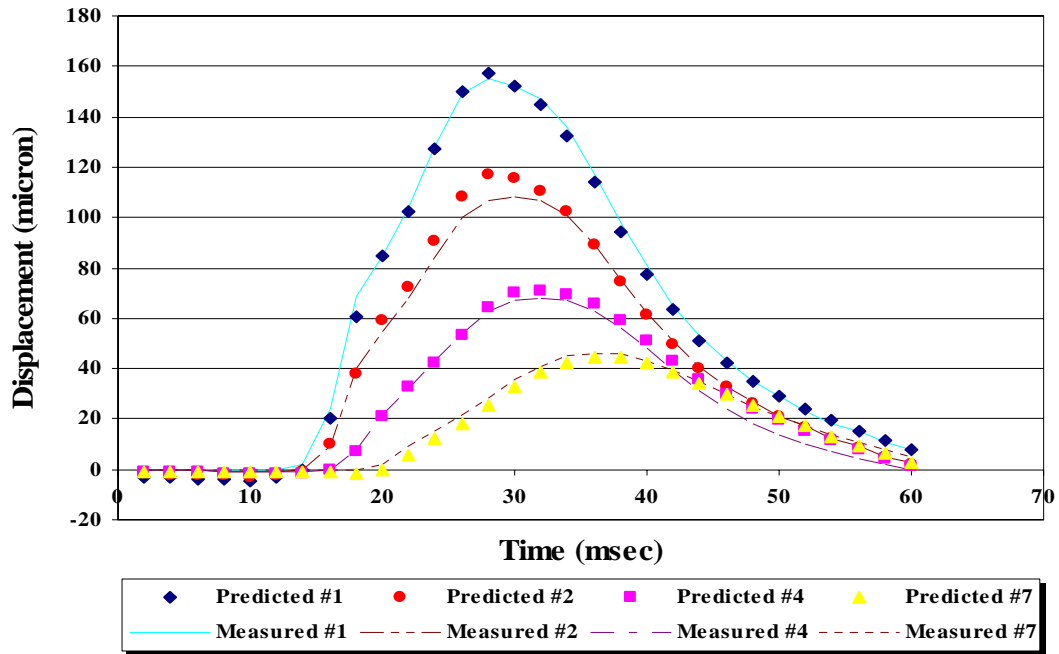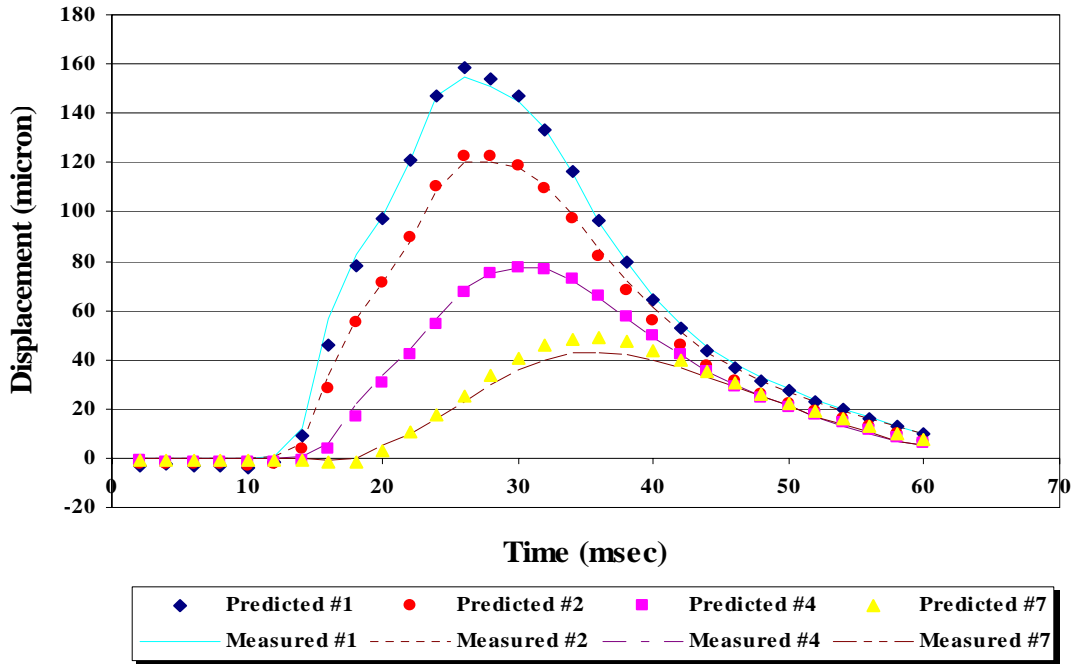
FIGURE C46   Comparison of Measured and Predicted Displacement Histories on K7 20 FWD Station in March 02
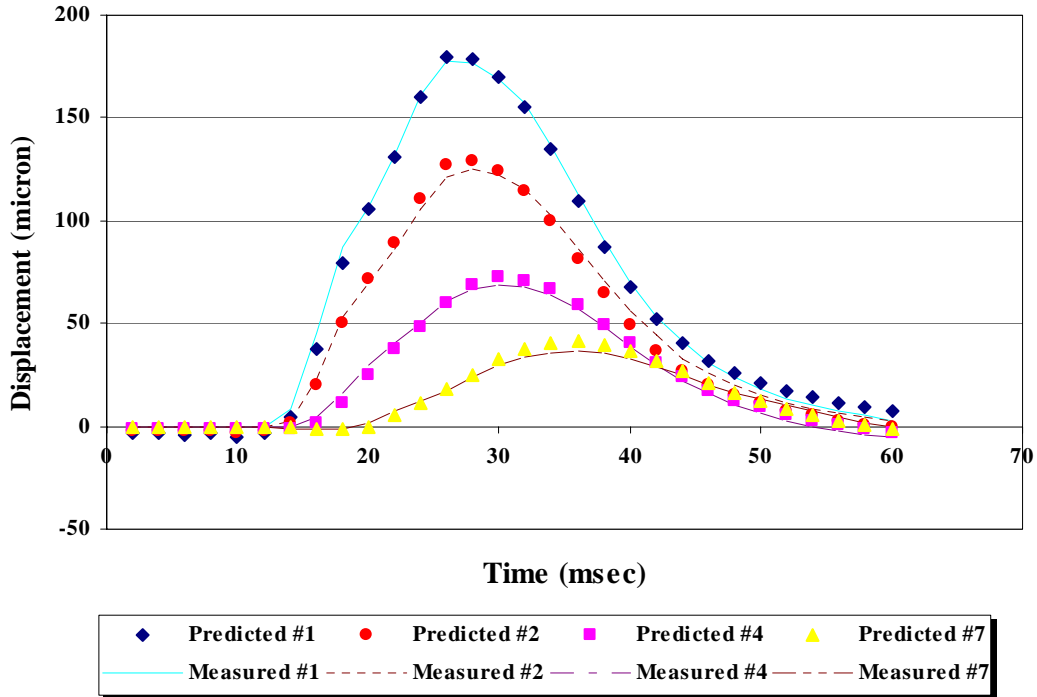
FIGURE C47   Comparison of Measured and Predicted Displacement Histories on K7 37 FWD Station in March 02
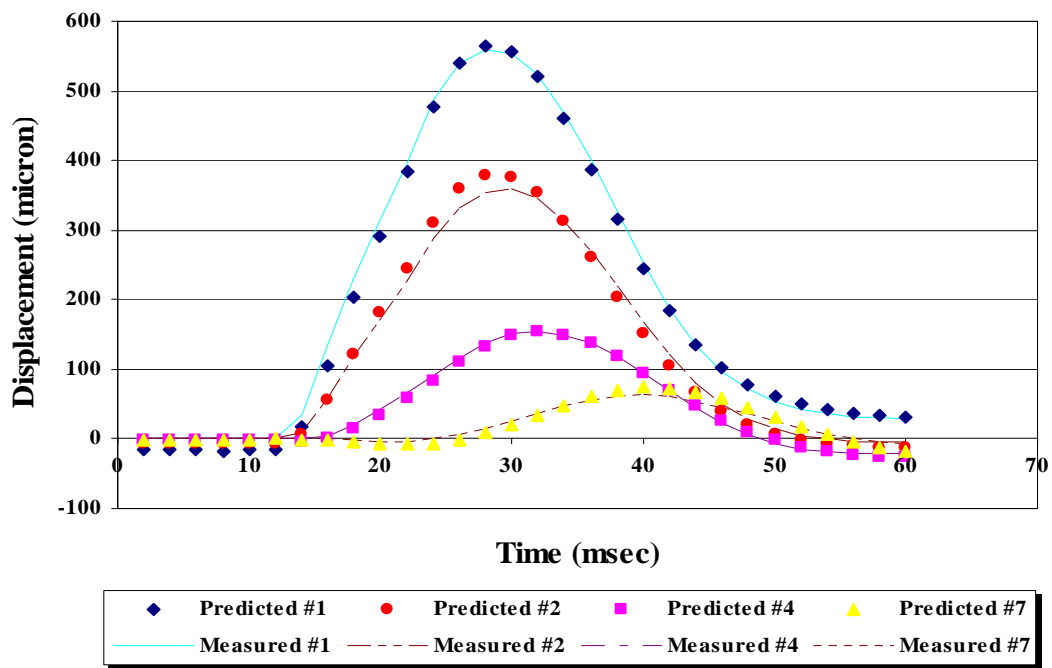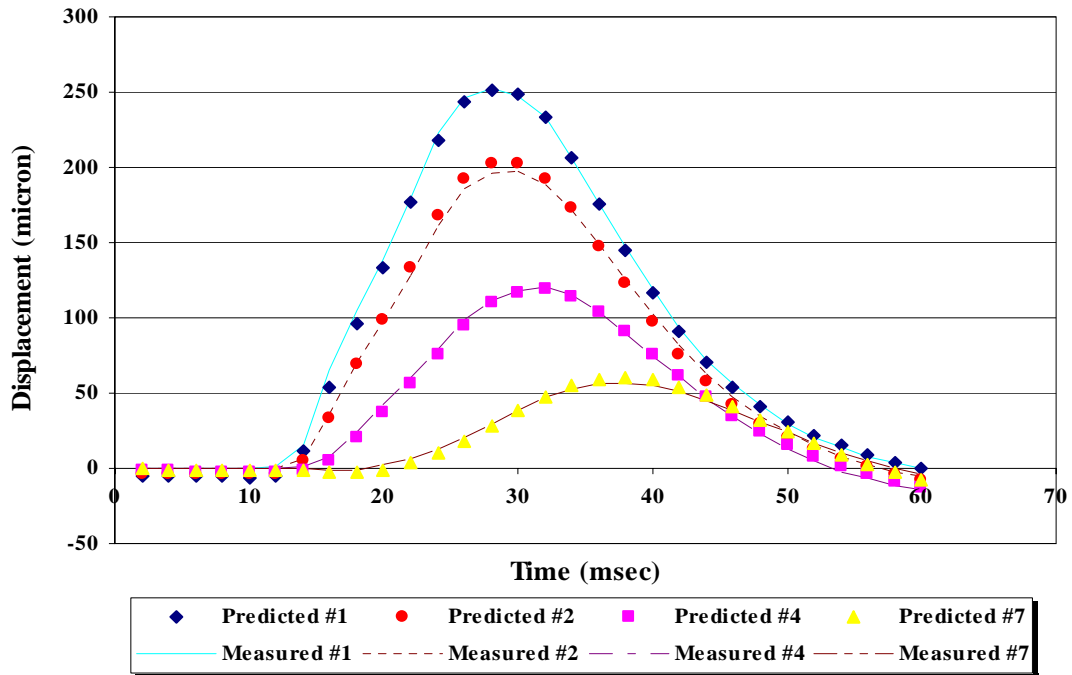
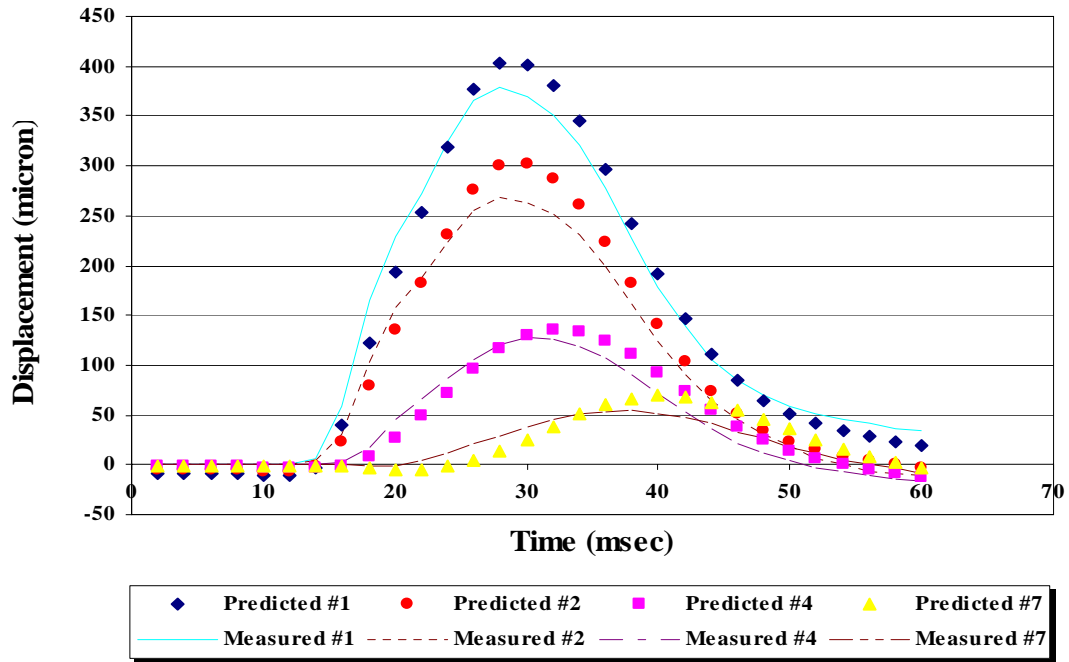**FIGURE C48   Comparison of Measured and Predicted Displacement Histories on K7 40 FWD Station in March 02**
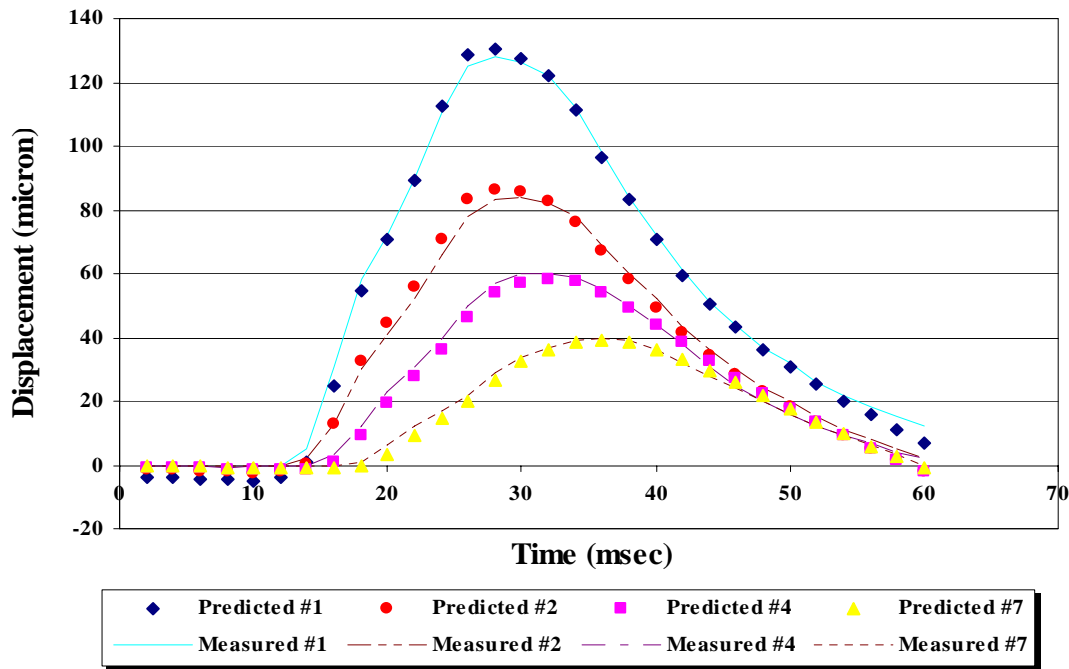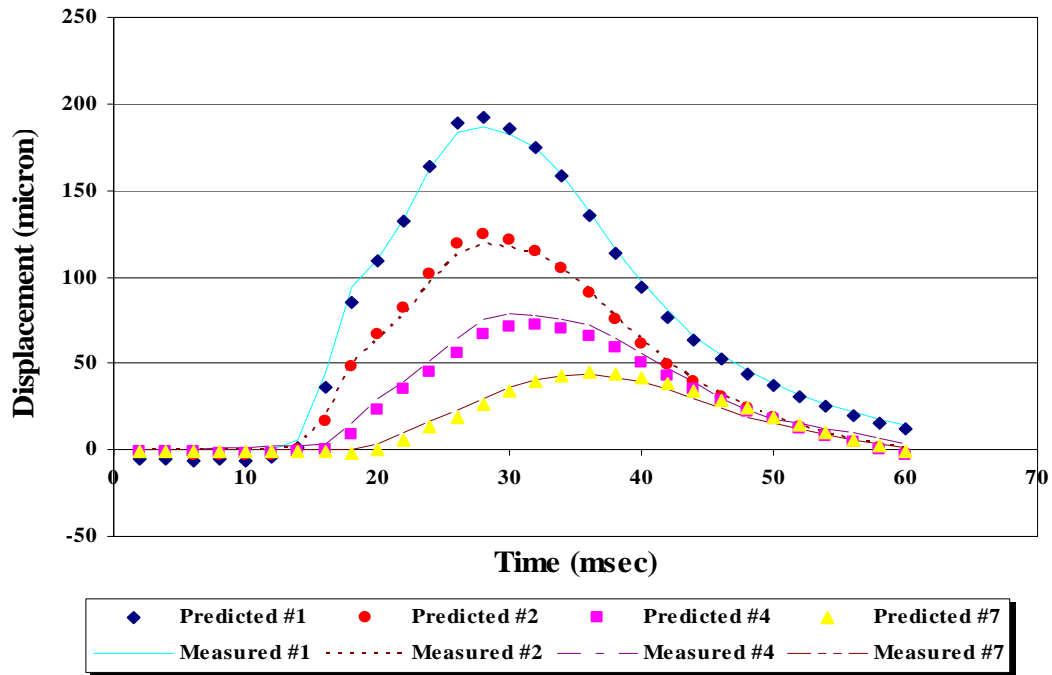

FIGURE C49   Comparison of Measured and Predicted Displacement Histories on K7 11 FWD Station in July 02
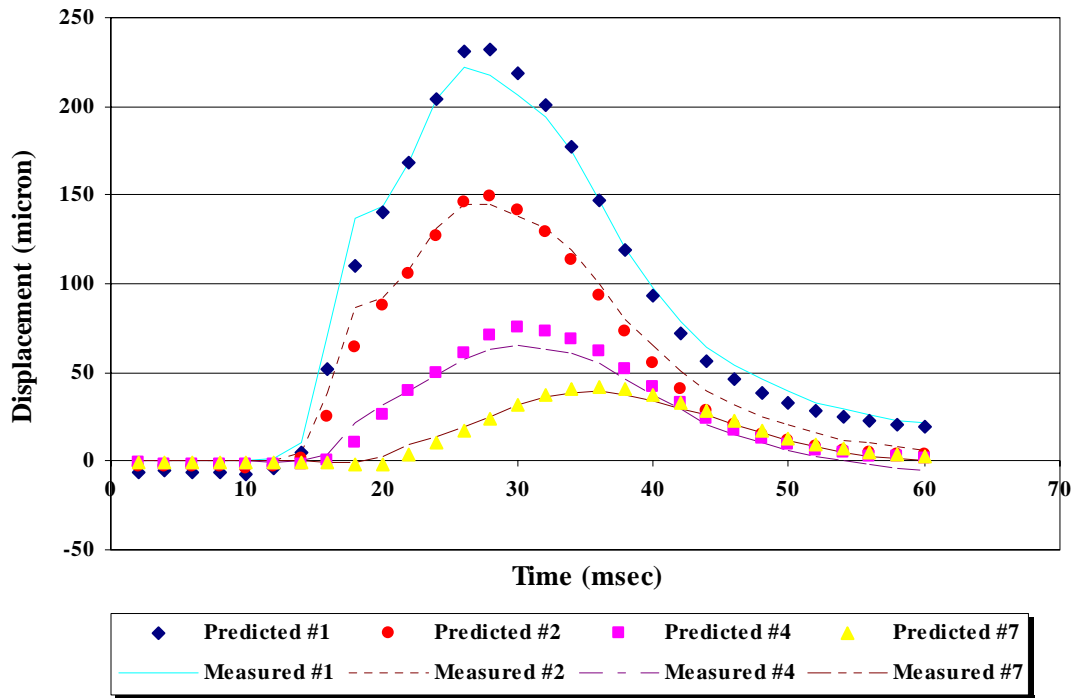
FIGURE C49   Comparison of Measured and Predicted Displacement Histories on K7 15 FWD Station in July 02
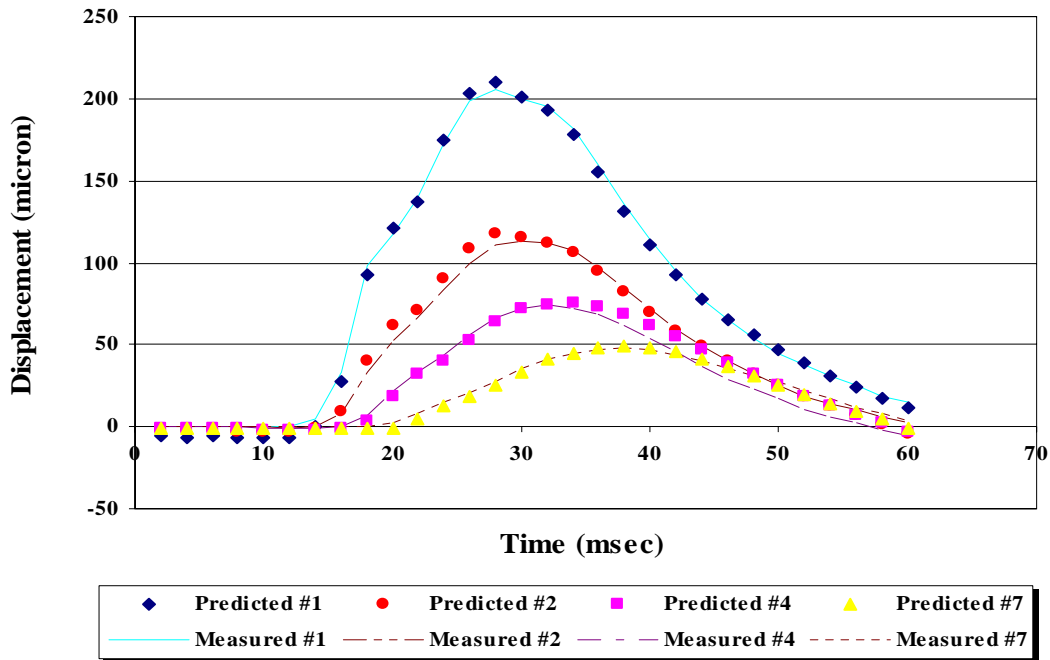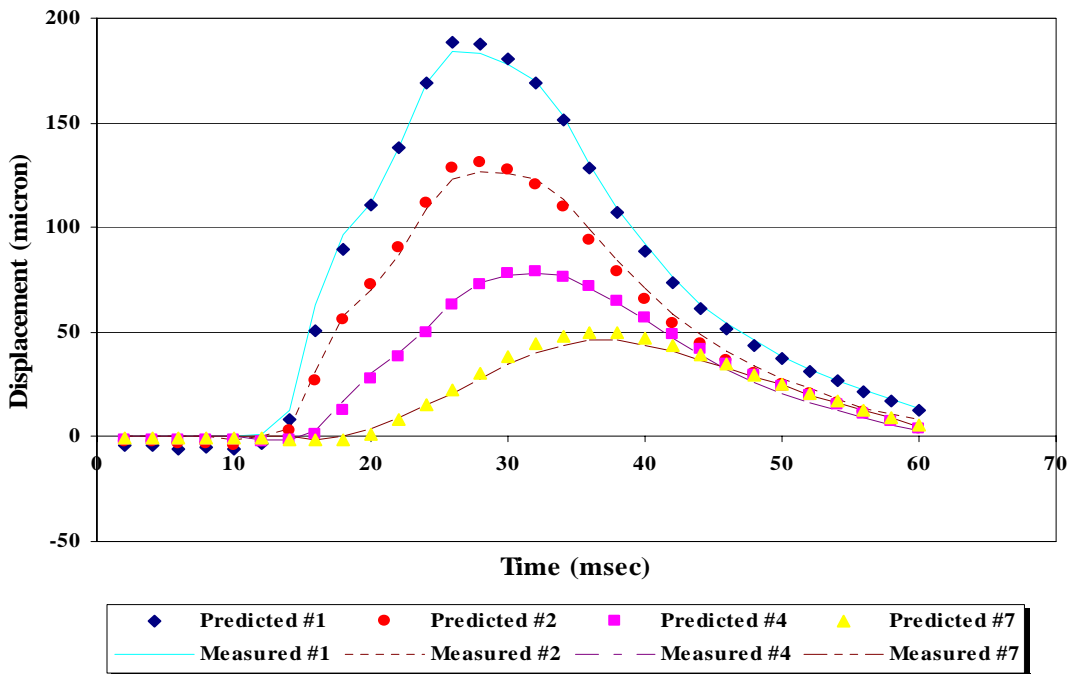

FIGURE C50   Comparison of Measured and Predicted Displacement Histories on K7 20 FWD Station in July 02
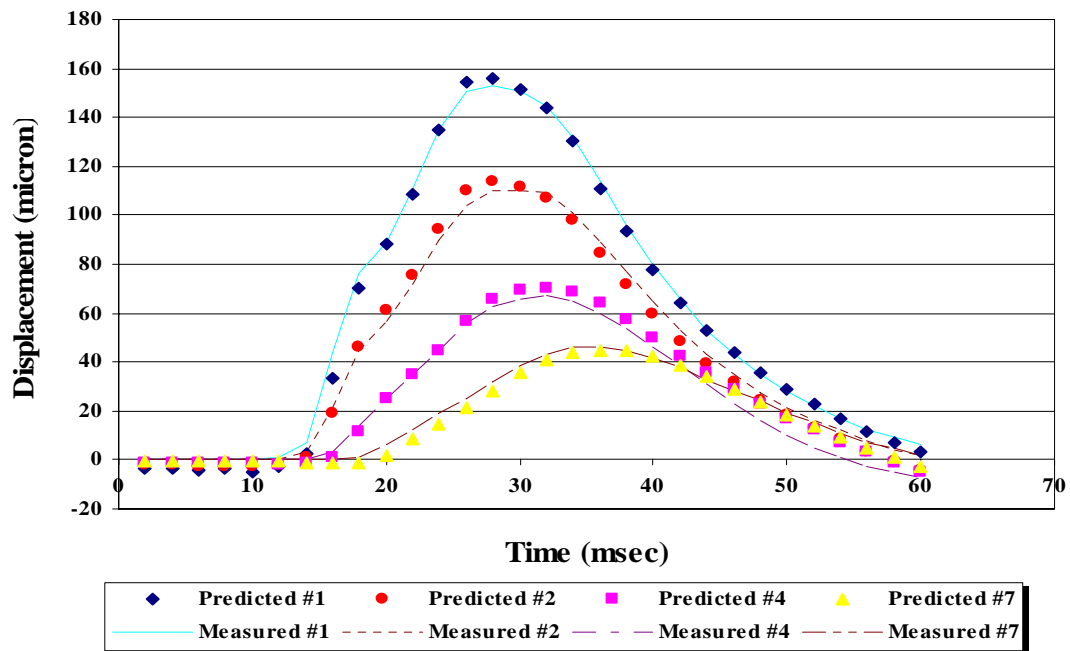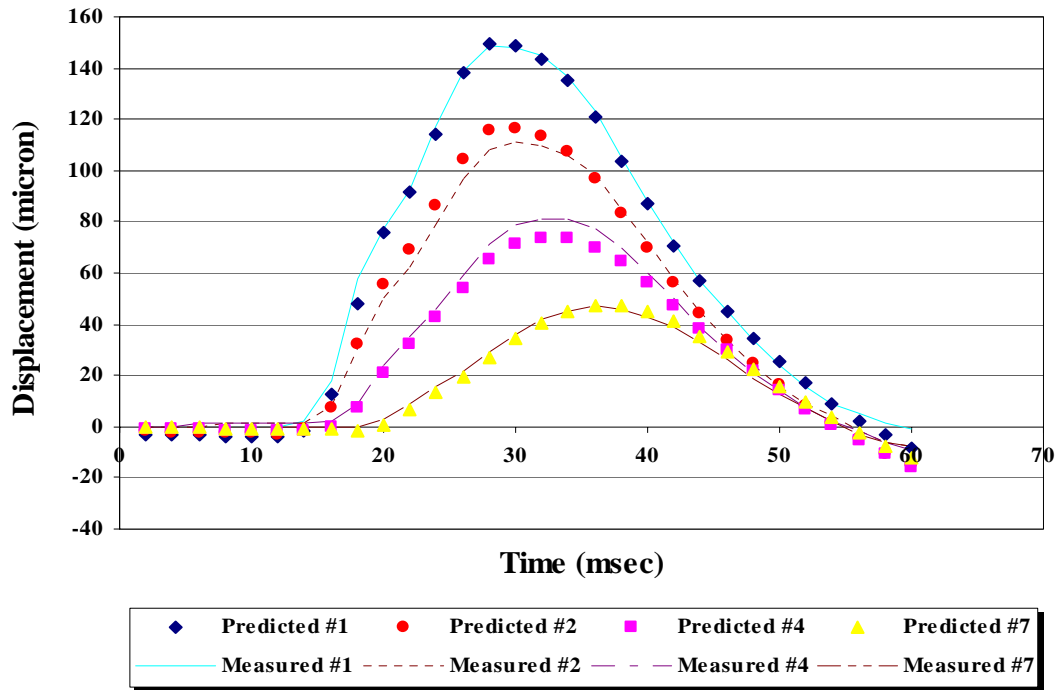
FIGURE C51   Comparison of Measured and Predicted Displacement Histories on K7 31 FWD Station in July 02
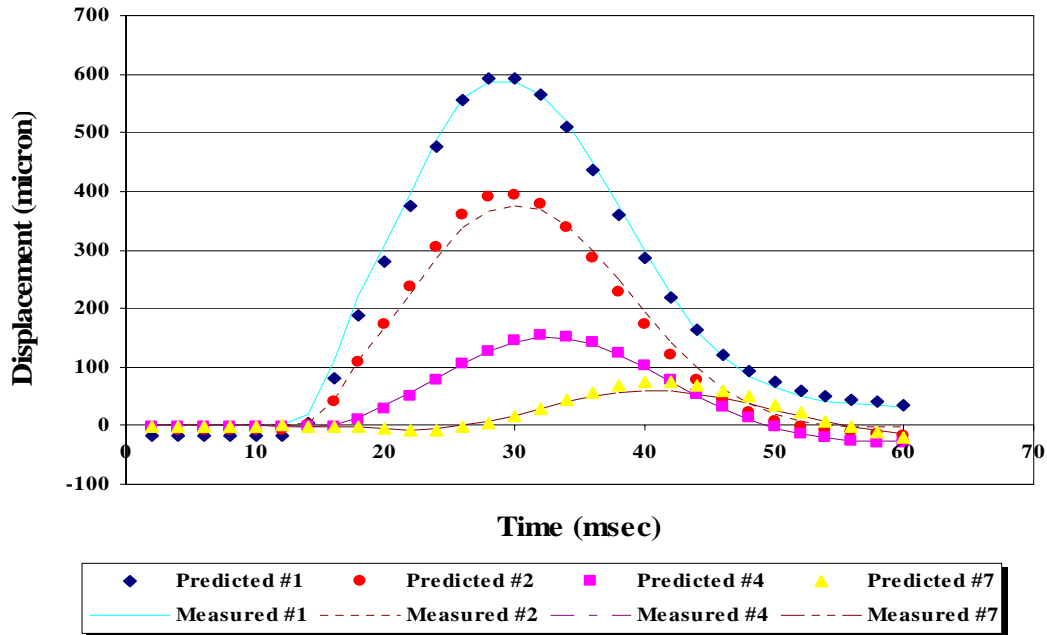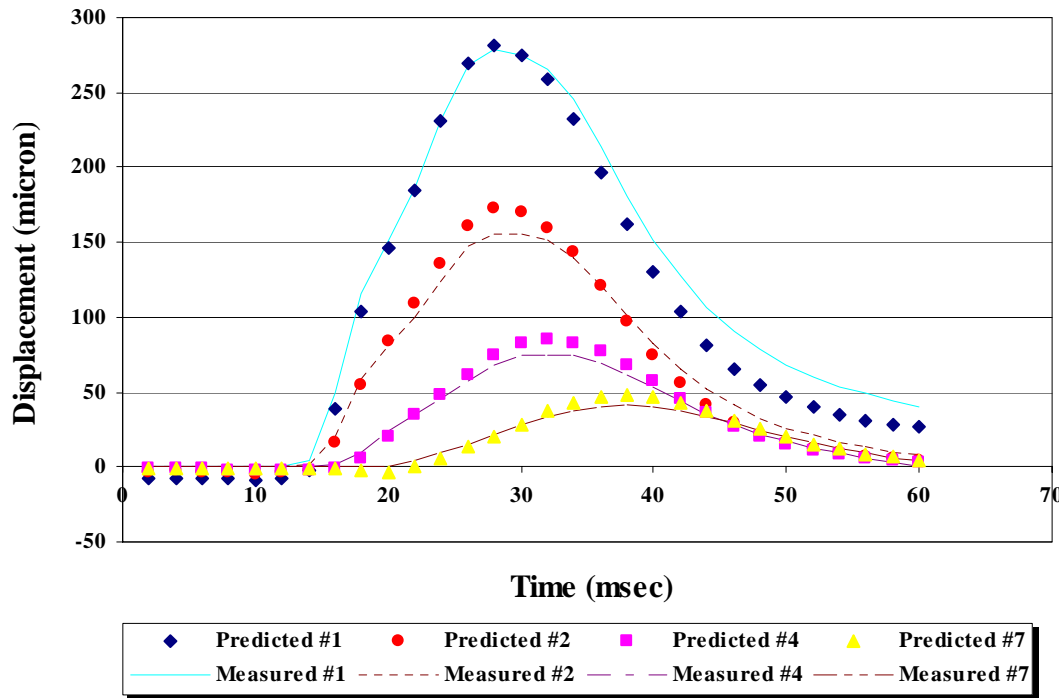

FIGURE C52   Comparison of Measured and Predicted Displacement Histories on K7 37 FWD Station in July 02
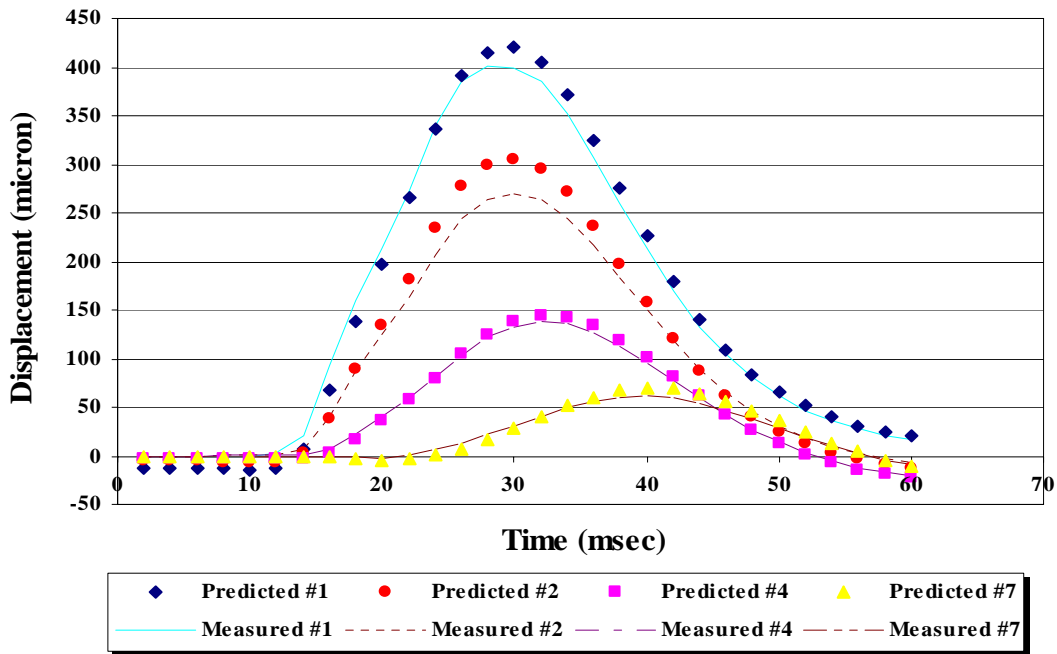
FIGURE C53   Comparison of Measured and Predicted Displacement Histories on K7 40 FWD Station in July 02
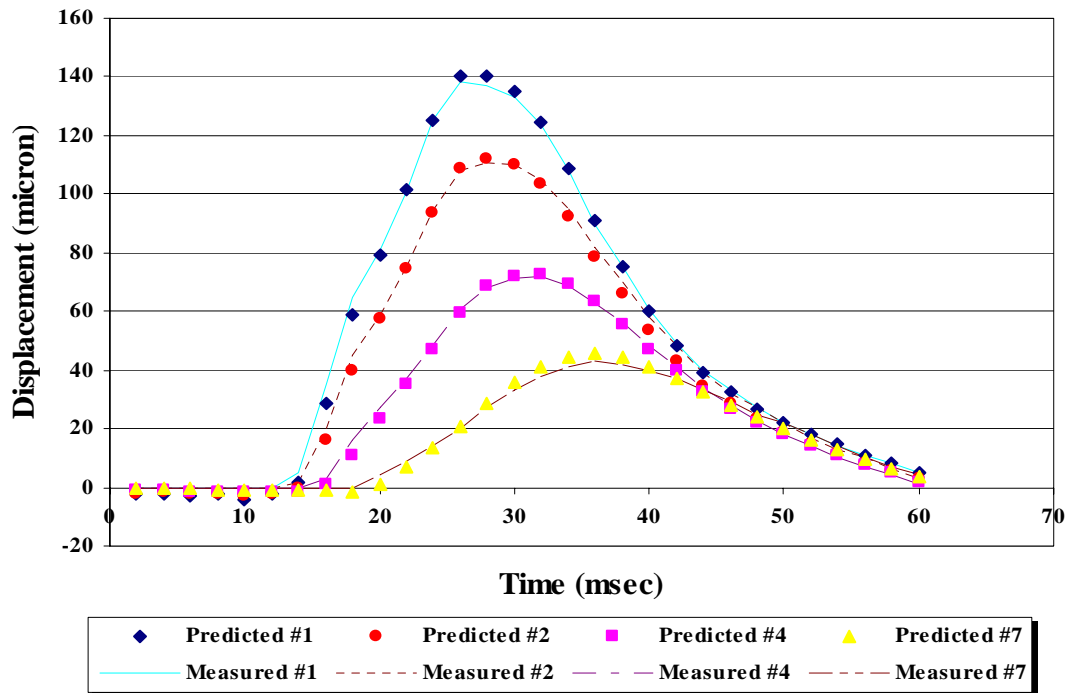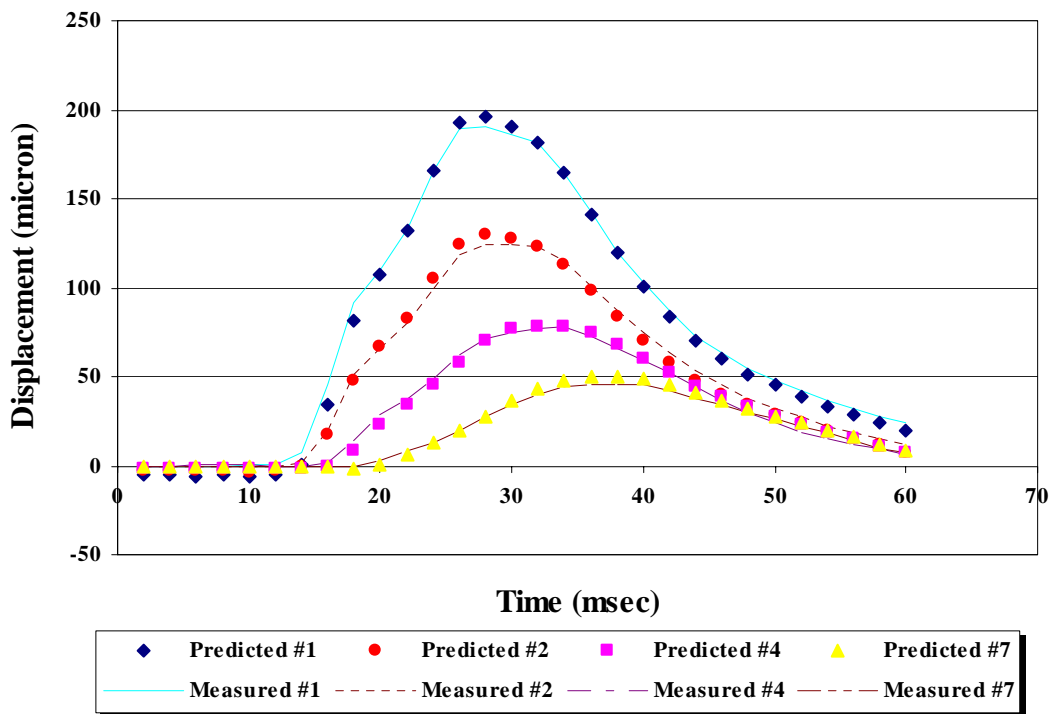

FIGURE C54   Comparison of Measured and Predicted Displacement Histories on K7 20 FWD Station in October 02
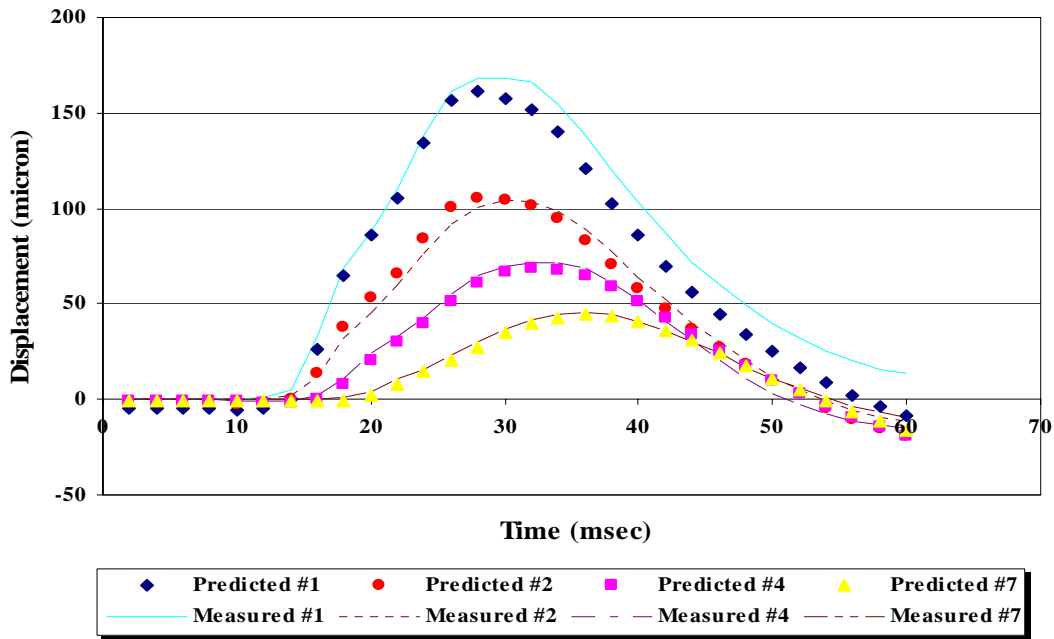
FIGURE C55   Comparison of Measured and Predicted Displacement Histories on K7 31 FWD Station in October 02
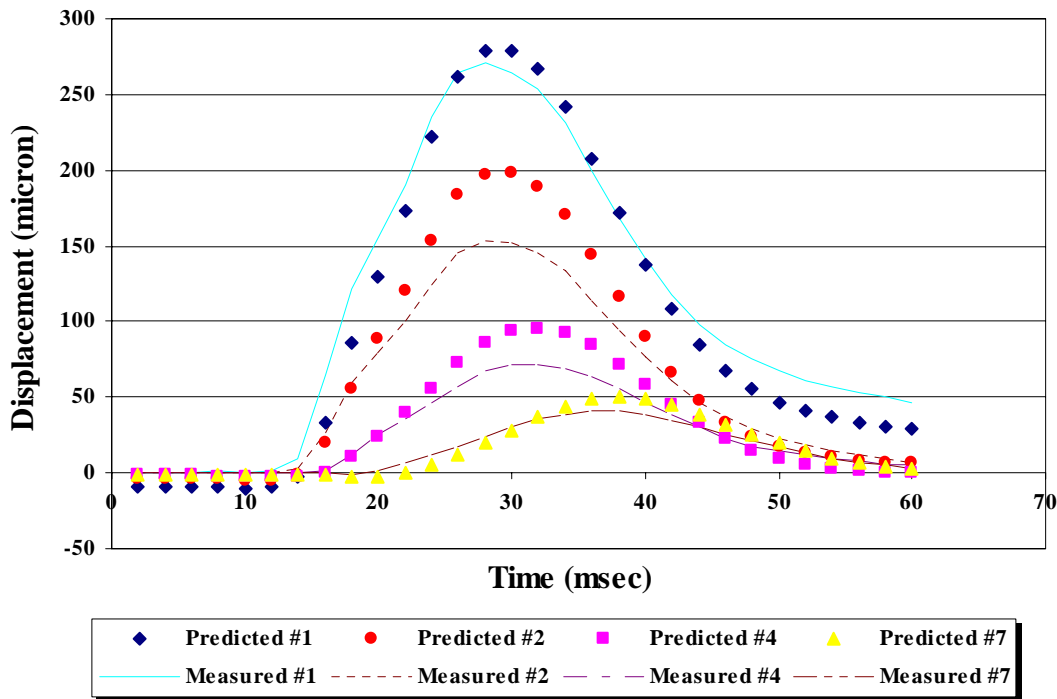
FIGURE C56   Comparison of Measured and Predicted Displacement Histories on K7 37 FWD Station in October 02
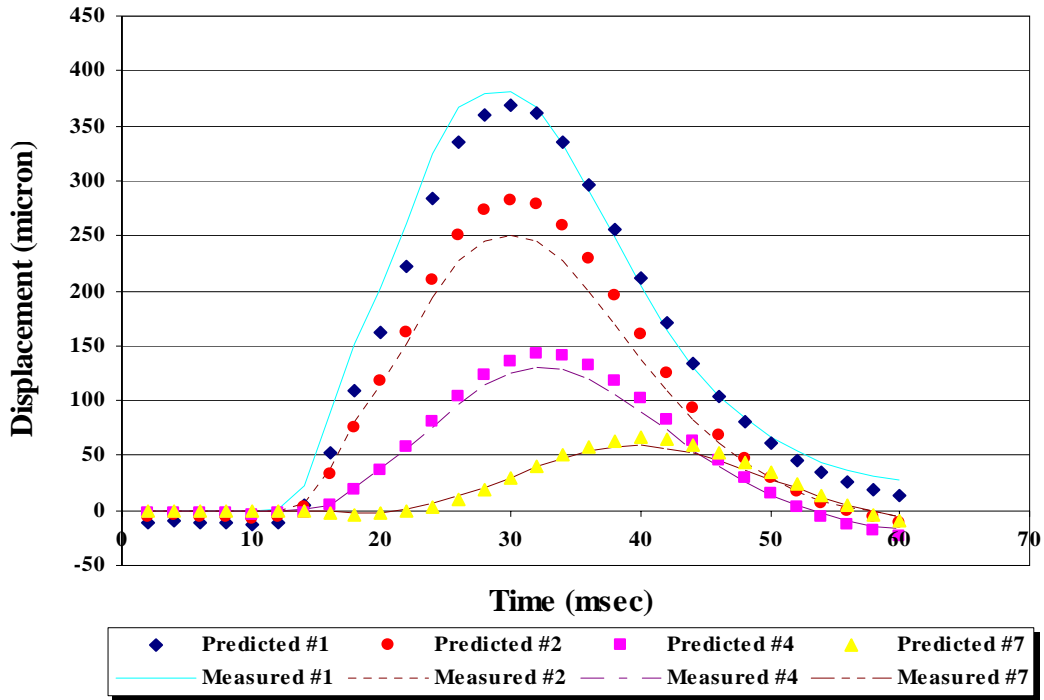
**FIGURE C57   Comparison of Measured and Predicted Displacement Histories on
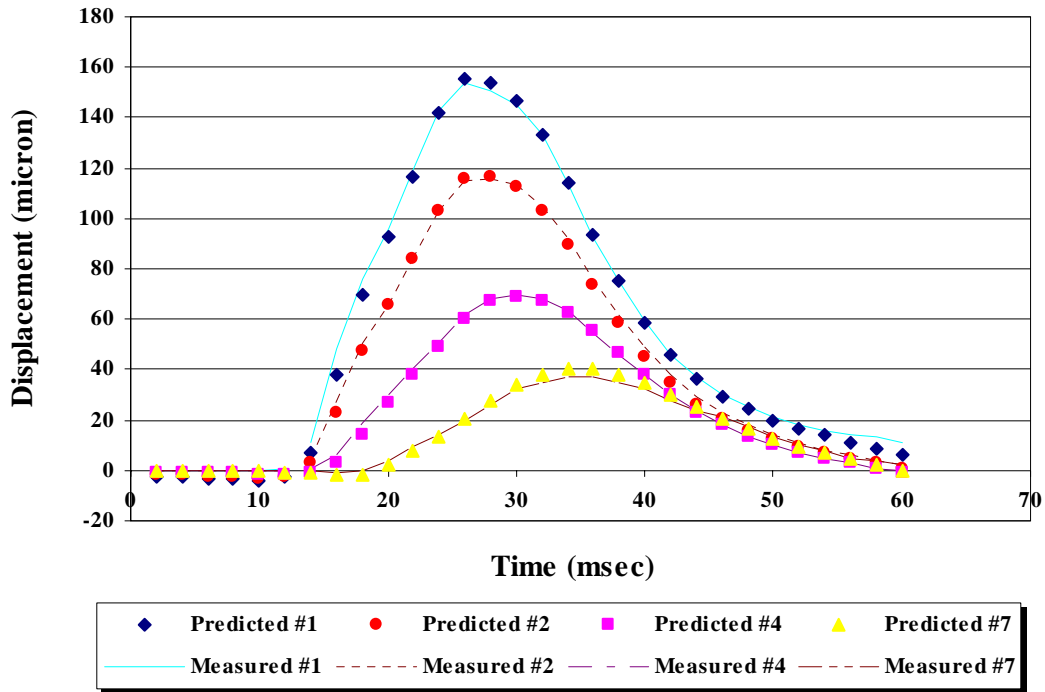K7 40 FWD Station in October 02**
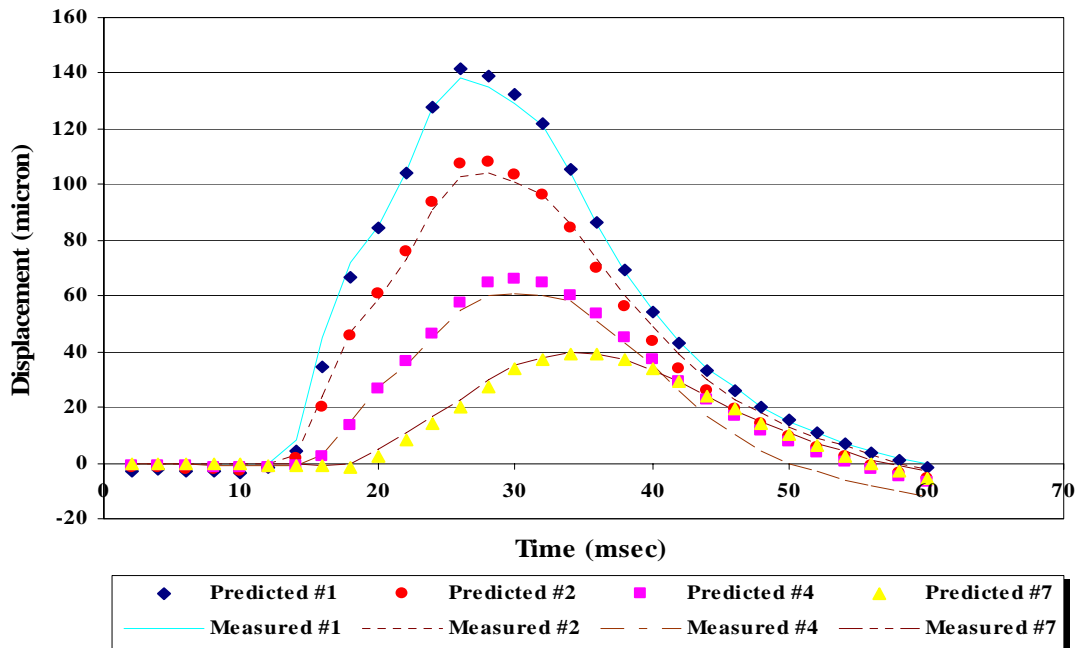
**FIGURE C58   Comparison of Measured and Predicted Displacement Histories on
K7 11 FWD Station in April 03**
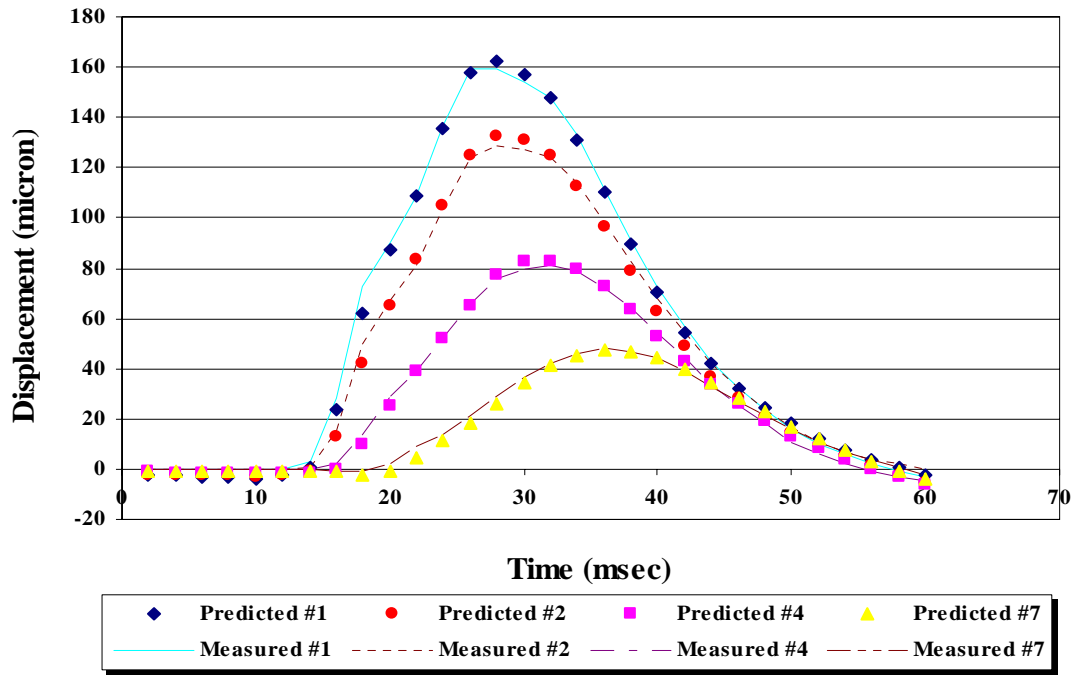
FIGURE C59   Comparison of Measured and Predicted Displacement Histories s on K7 15 FWD Station in April 03
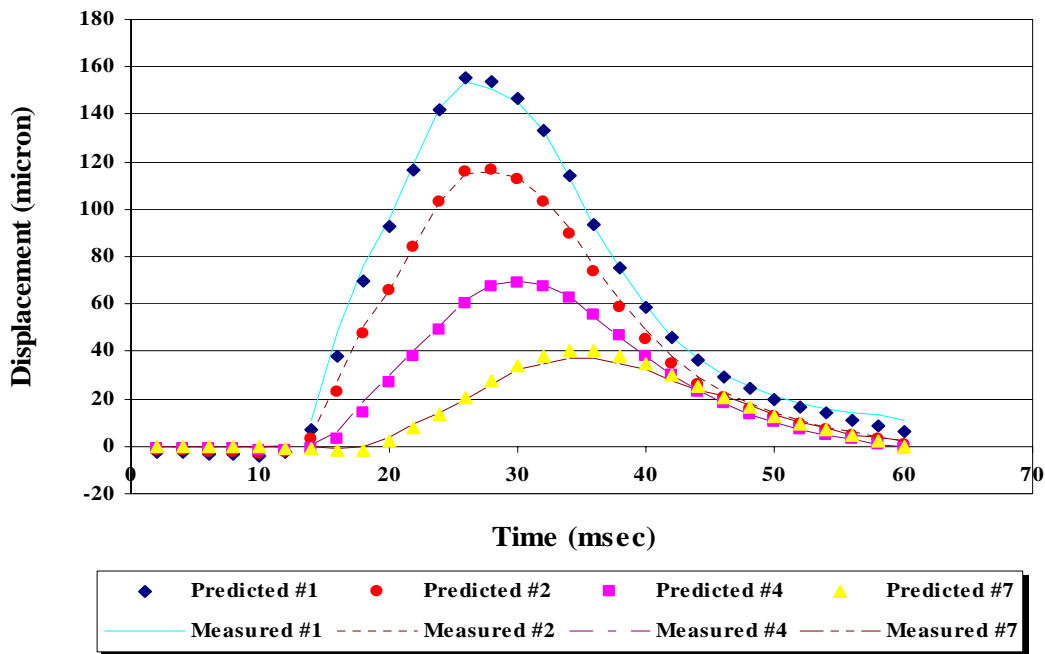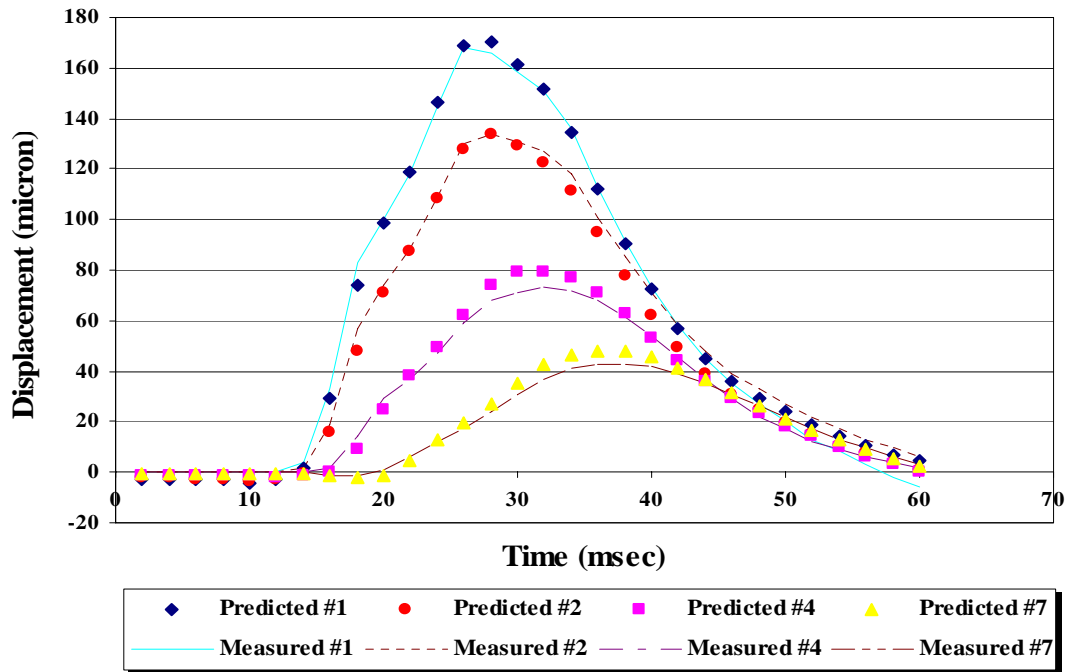

FIGURE C60   Comparison of Measured and Predicted Displacement Histories on K7 20 FWD Station in April 03
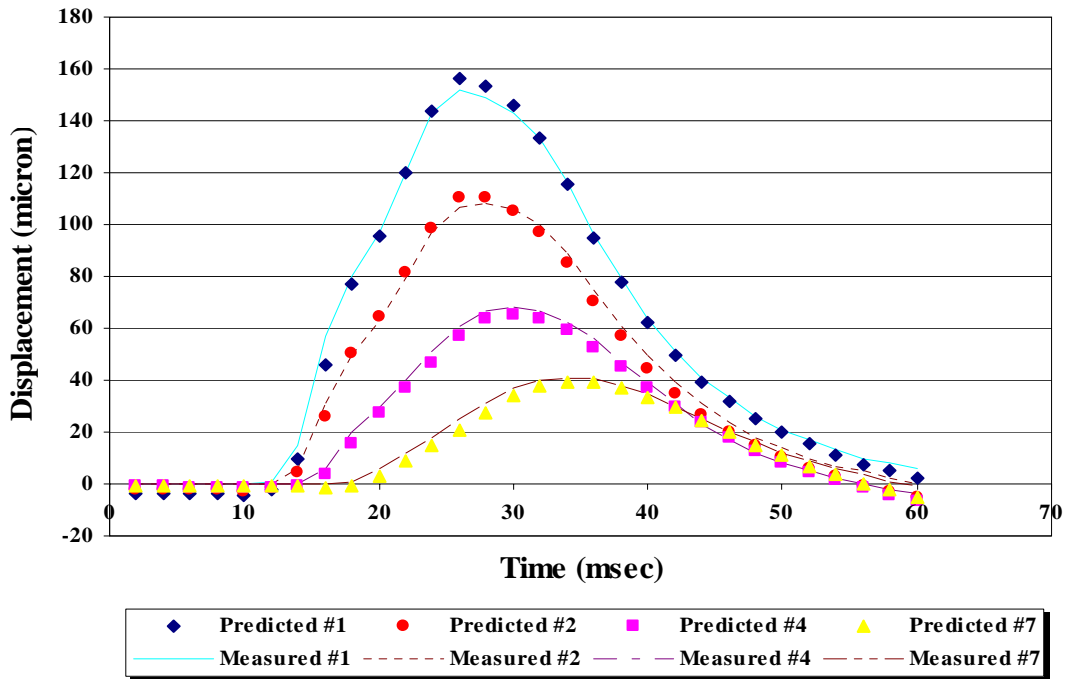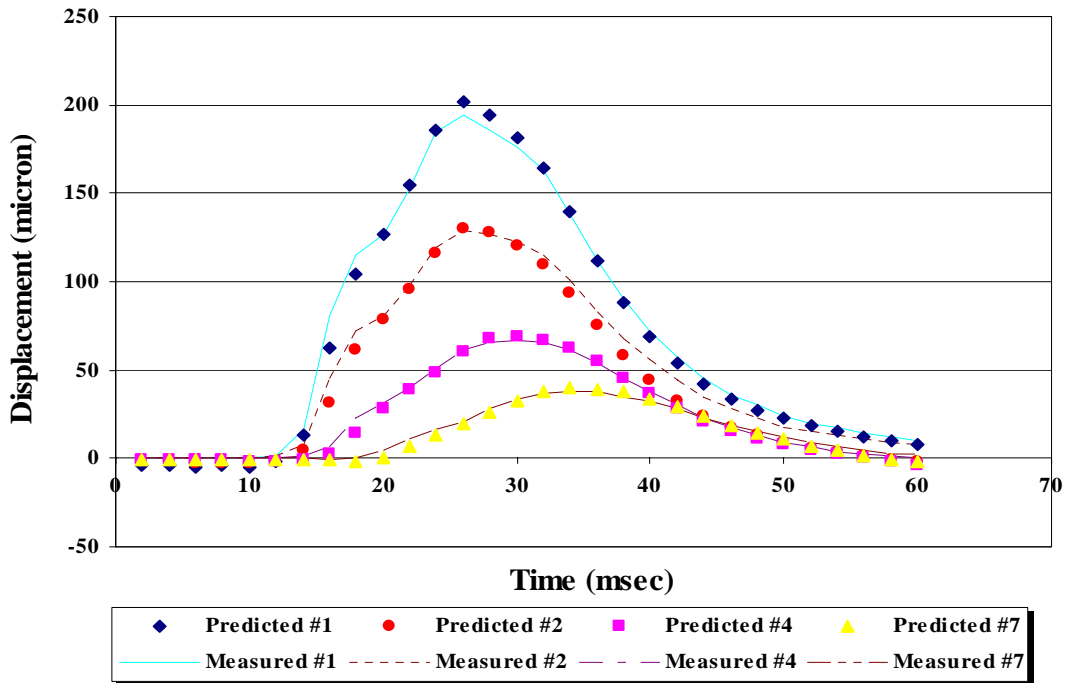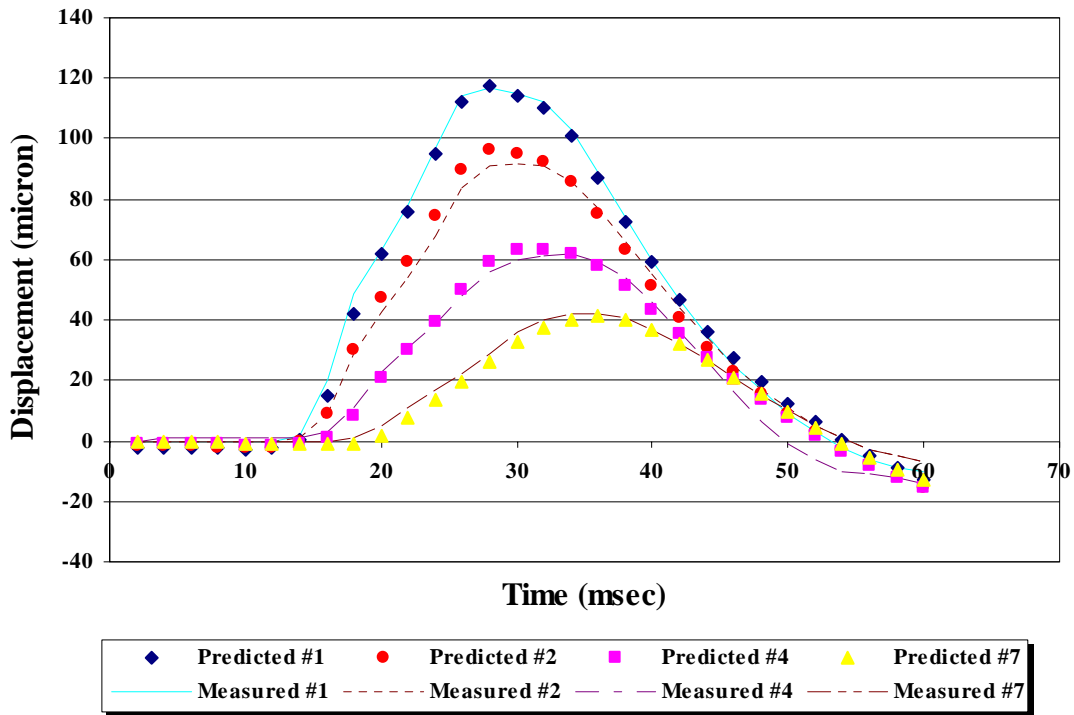
FIGURE C61   Comparison of Measured and Predicted Displacement Histories on K7 31 FWD Station in April 03
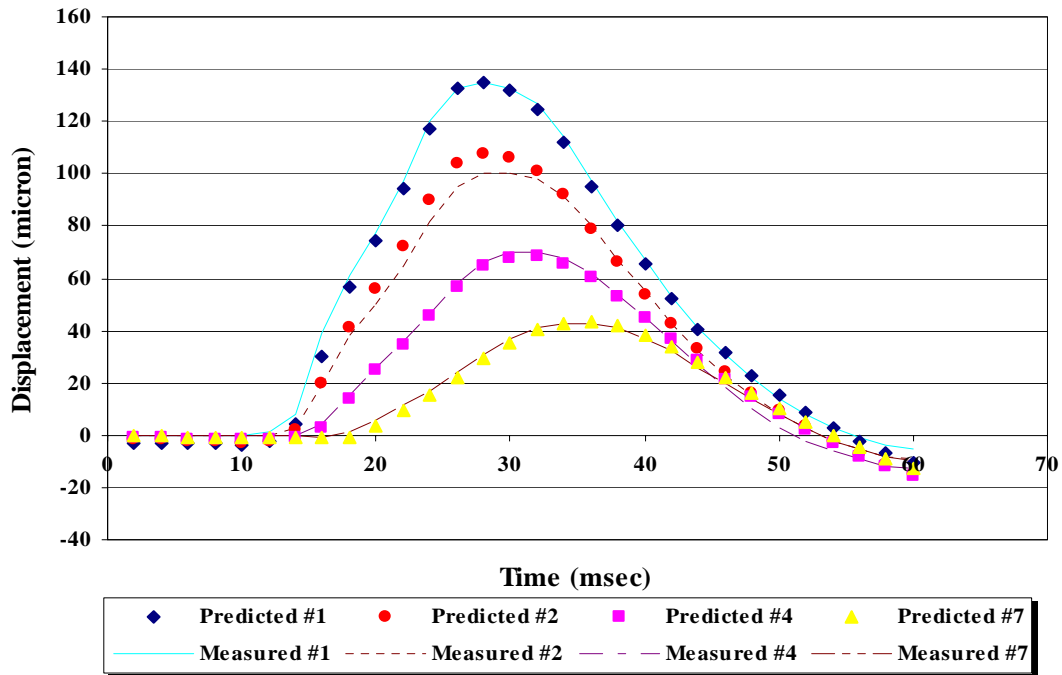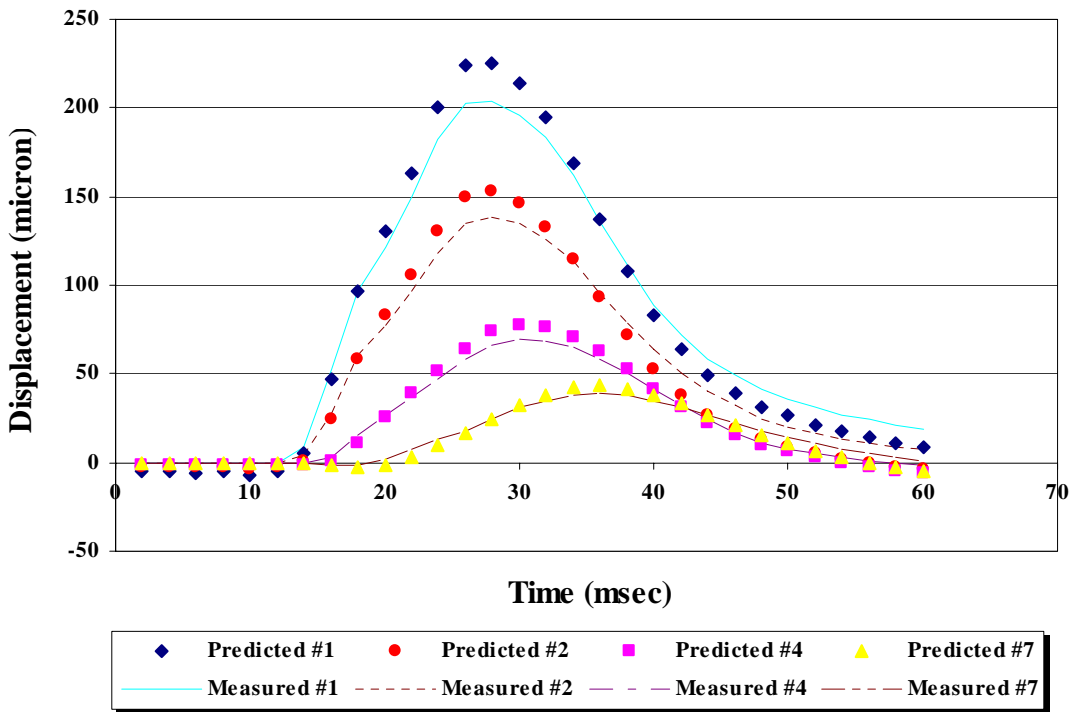

FIGURE C62   Comparison of Measured and Predicted Displacement Histories on K7 37 FWD Station in April 03
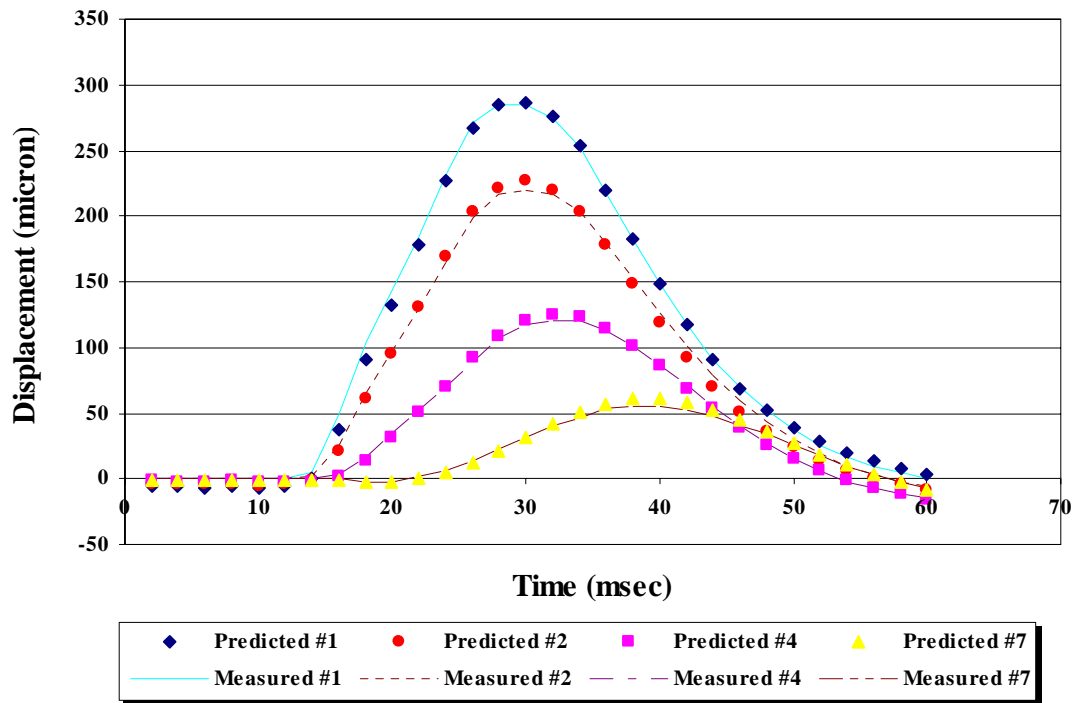
FIGURE C63   Comparison of Measured and Predicted Displacement Histories on K7 40 FWD Station in April 03

APPENDIX D

PLOTS OF DYNAMIC (COMPLEX) MODULUS VERSUS FREQUENCIES AT DIFFERENT TEST TEMPERATURES
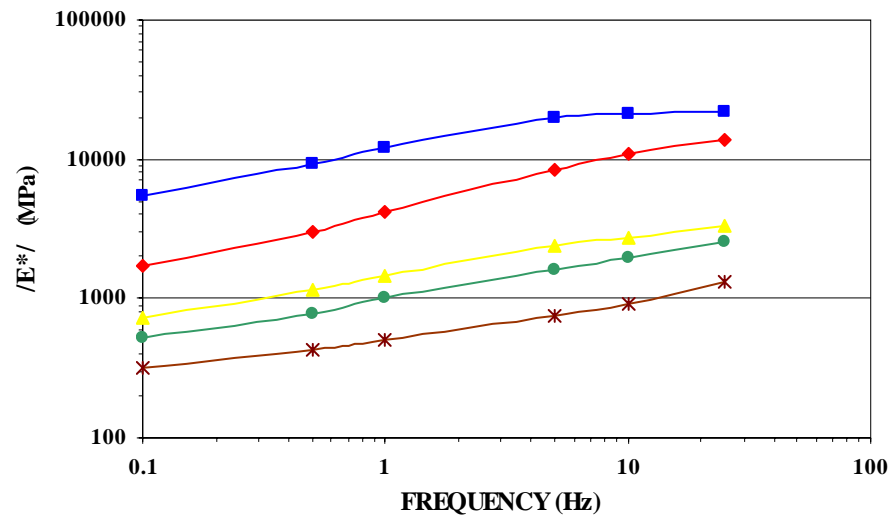
FIGURE D1   Dynamic (Complex) Modulus of K6-1 FWD Station.
Case 1 and Case 3 (LVDT 1).
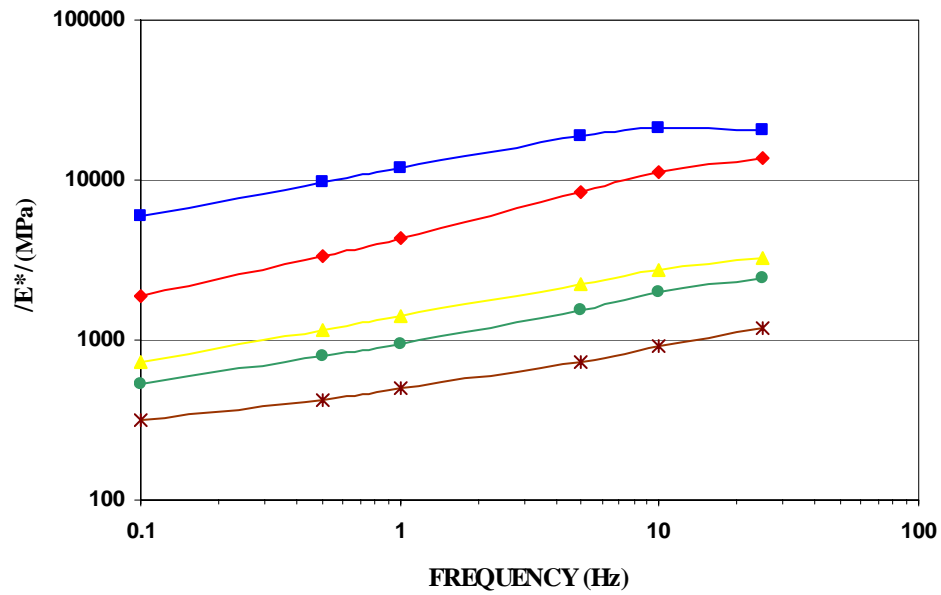
FIGURE D2   Dynamic (Complex) Modulus of K6-1 FWD Station.
CASE 2 AND CASE 4 (LVDT 1)
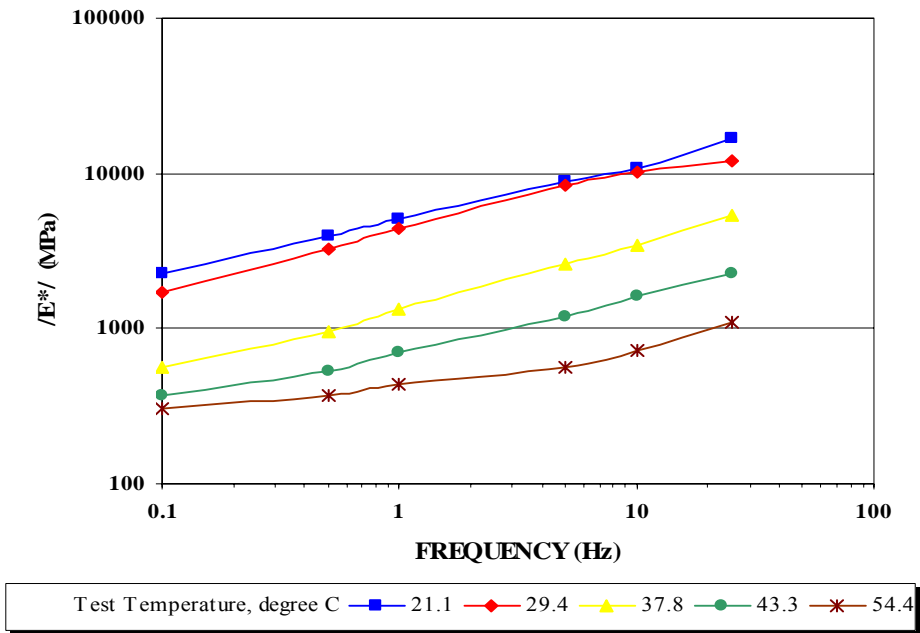
FIGURE D3   Dynamic (Complex) Modulus of K6-4 FWD Station.
Case 1 and Case 3 (Average)
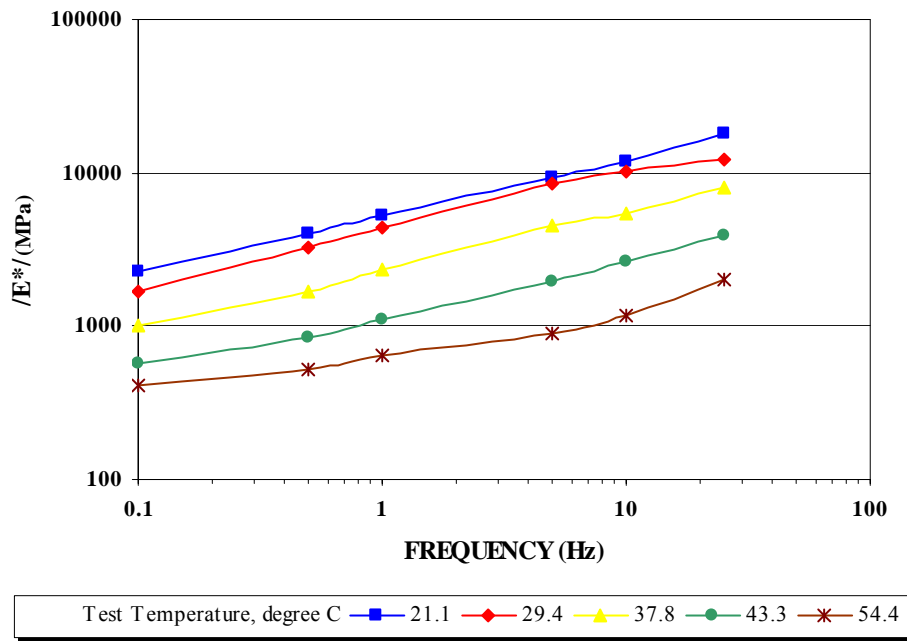
FIGURE D4   Dynamic (Complex) Modulus of K6-4 FWD Station.
Case 1 and Case 3 (LVDTs)
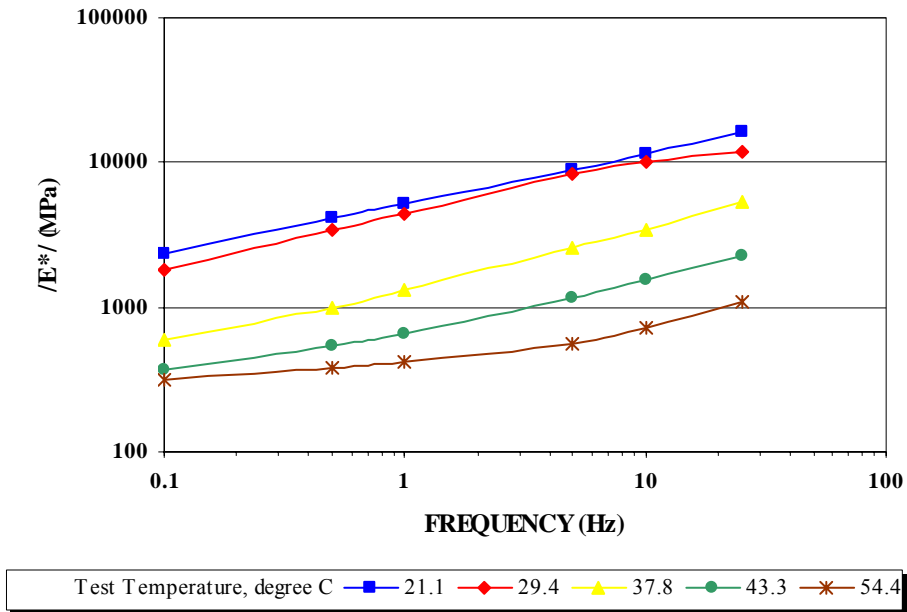
FIGURE D5   Dynamic (Complex) Modulus of K6-4 FWD Station.
Case 2 and Case 4 (Average)
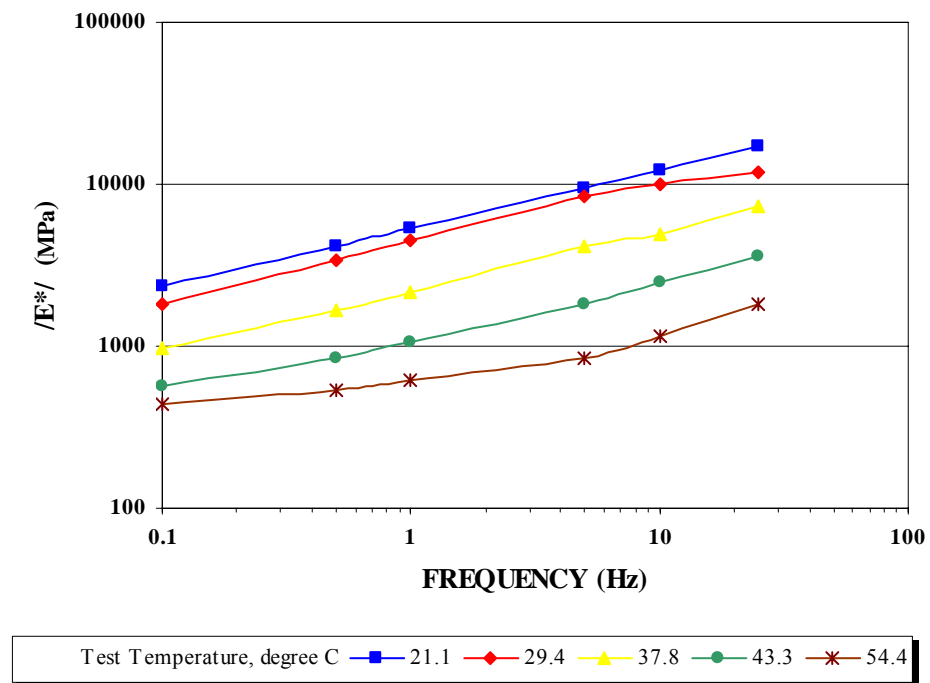
FIGURE D6   Dynamic (Complex) Modulus of K6-4 FWD Station.
Case 2 and Case 4 (LVDTs)
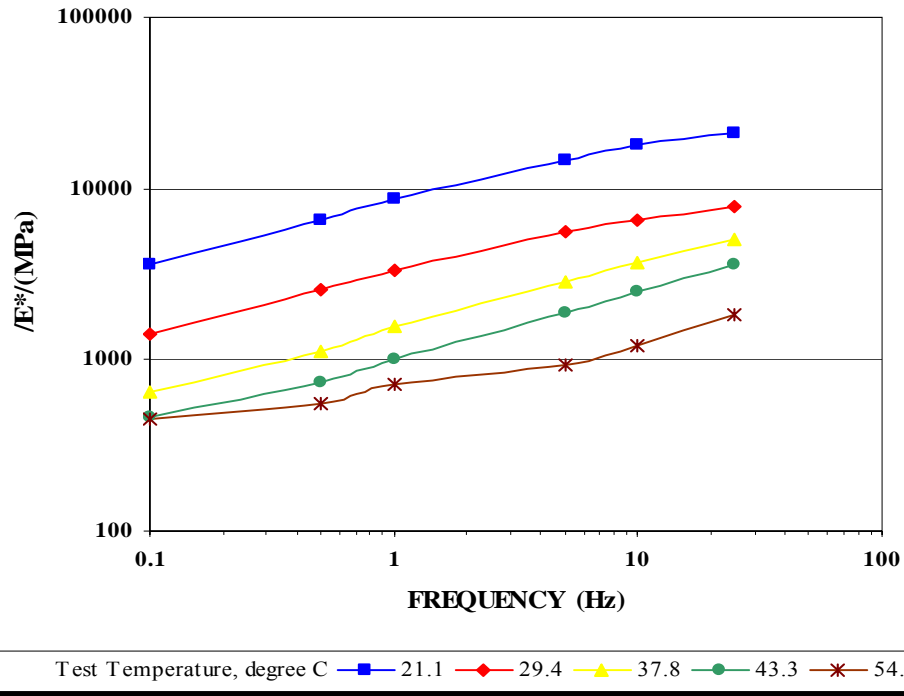
FIGURE D7 Dynamic (Complex) Modulus of K6-11 FWD Station.
Case 1 and Case 3 (Average)
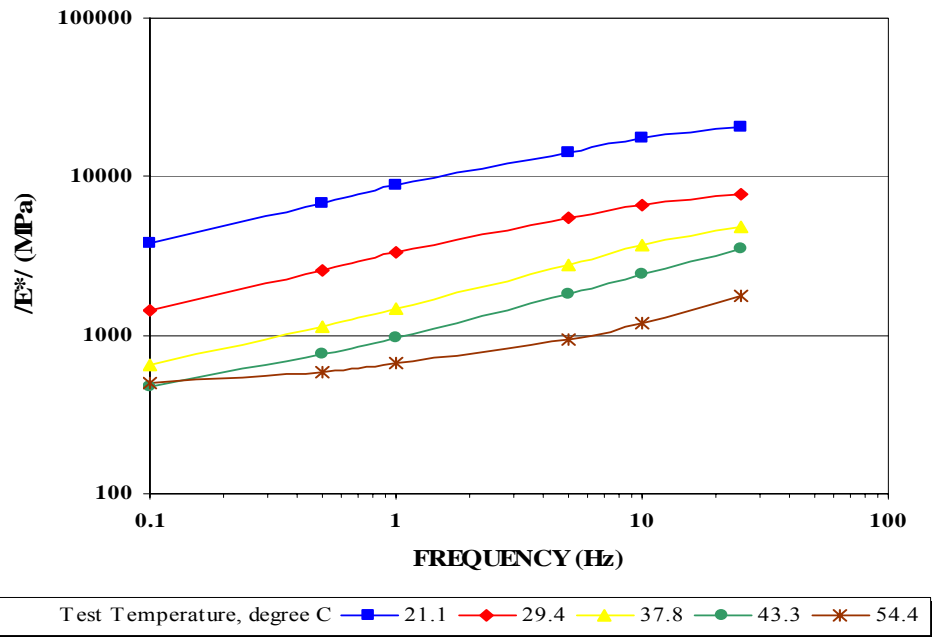
FIGURE D8   Dynamic (Complex) Modulus of K6-11 FWD Station.
Case 2 and Case 4 (Average)
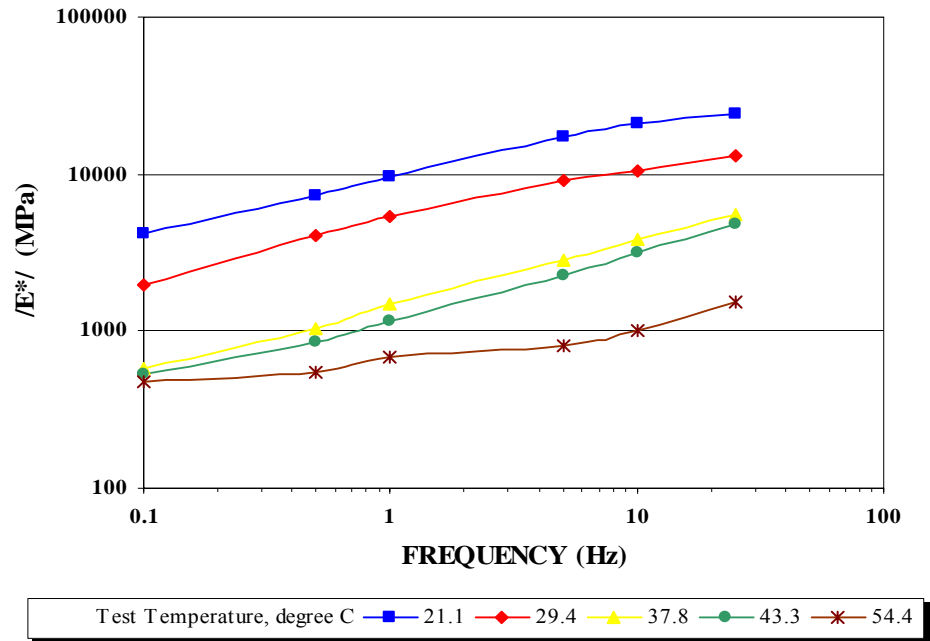
FIGURE D9   Dynamic (Complex) Modulus of K6-11 FWD Station   Case
              1 and Case 3 (LVDT 1)
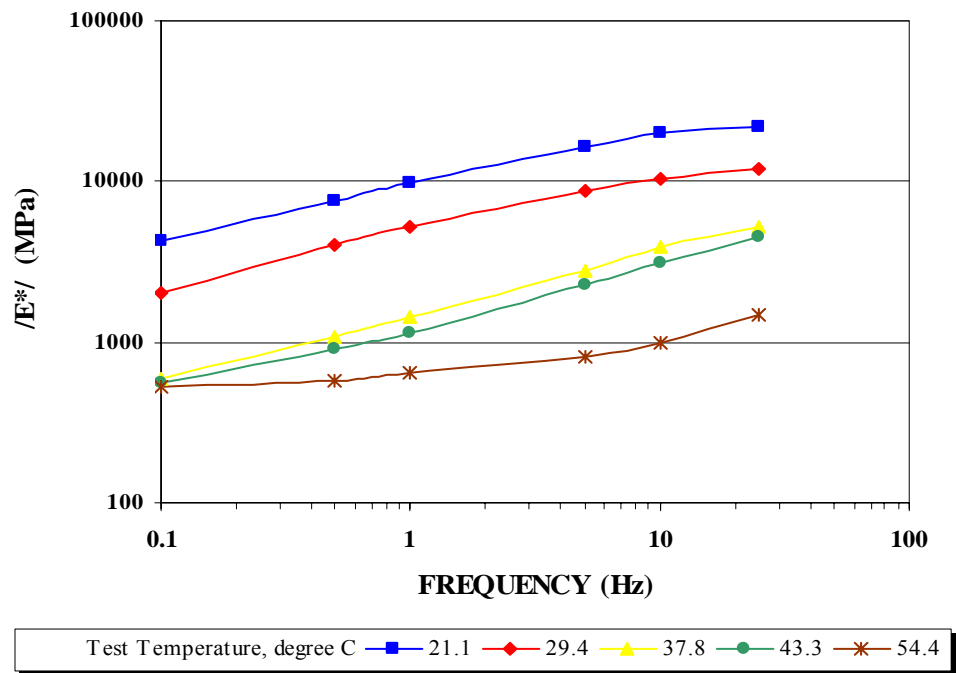
FIGURE D12   Dynamic (Complex) Modulus of K6-11 FWD Station.
               Case 2 and Case 4 (LVDT 1)
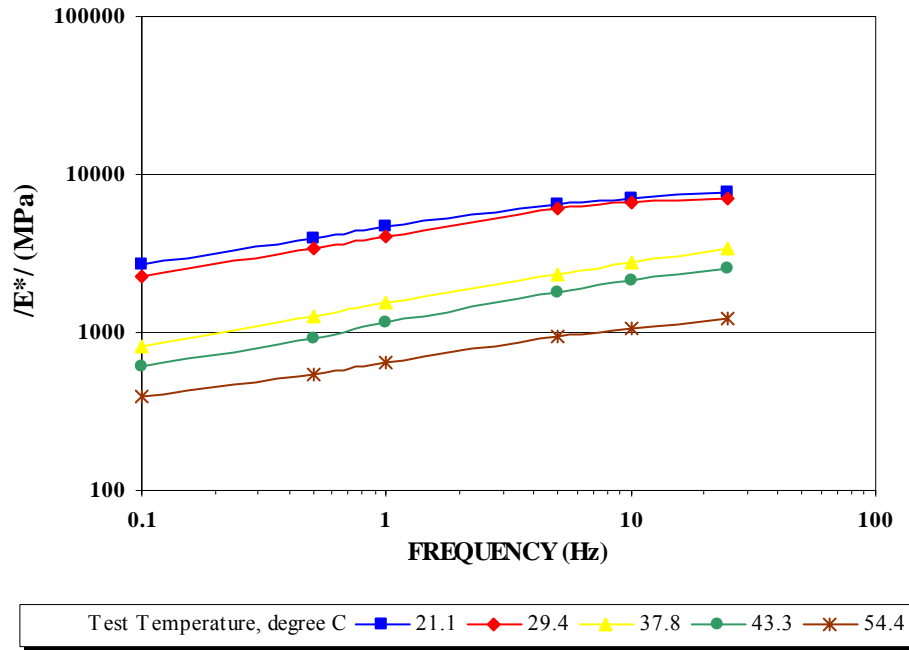
FIGURE D13   Dynamic (Complex) Modulus of K6-23 FWD Station.
Case 1 and Case 3 (Average)
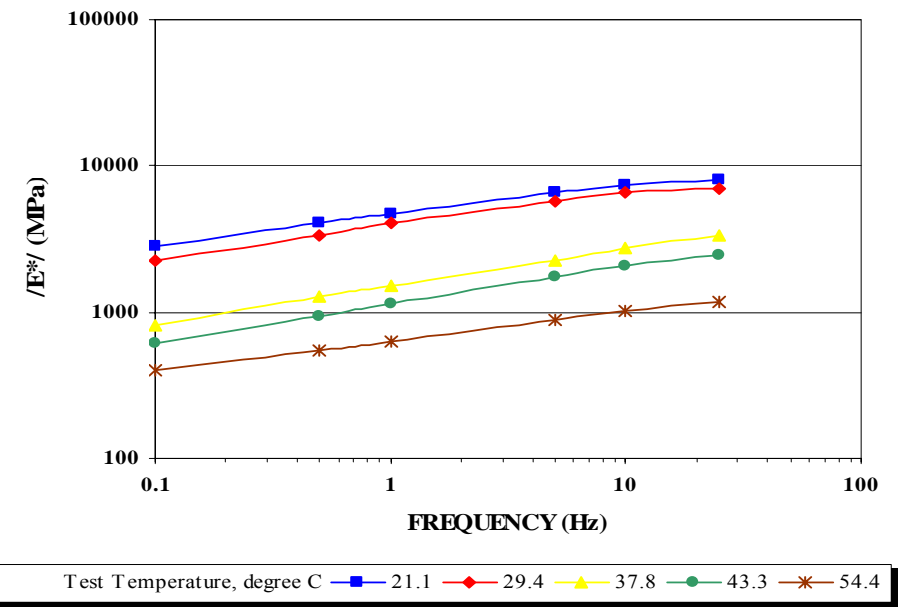
FIGURE D14   Dynamic (Complex) Modulus of K6-23 FWD Station.
Case 2 and Case 4 (Average)
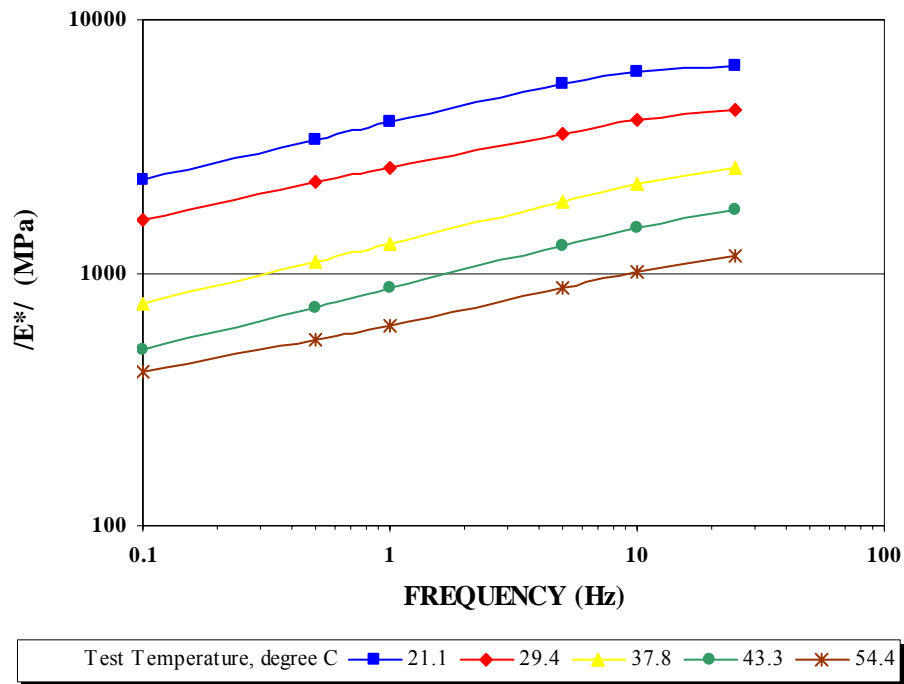
FIGURE D15   Dynamic (Complex) Modulus of K6-23 FWD Station.
             Case 1 and Case 3 (LVDTs)
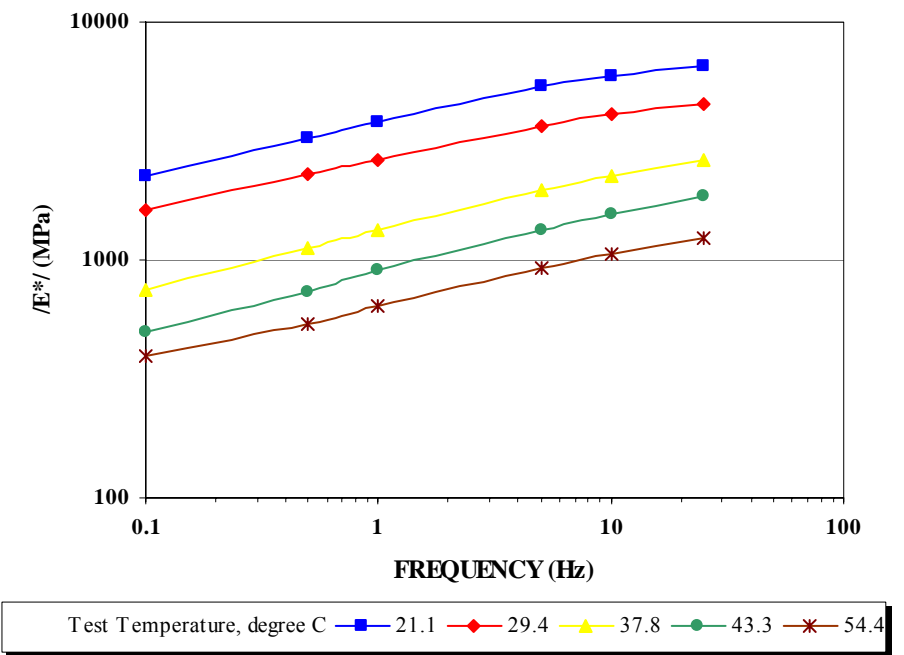
FIGURE D16   Dynamic (Complex) Modulus of K6-23 FWD Station.
             Case 2 and Case 4 (LVDTs)
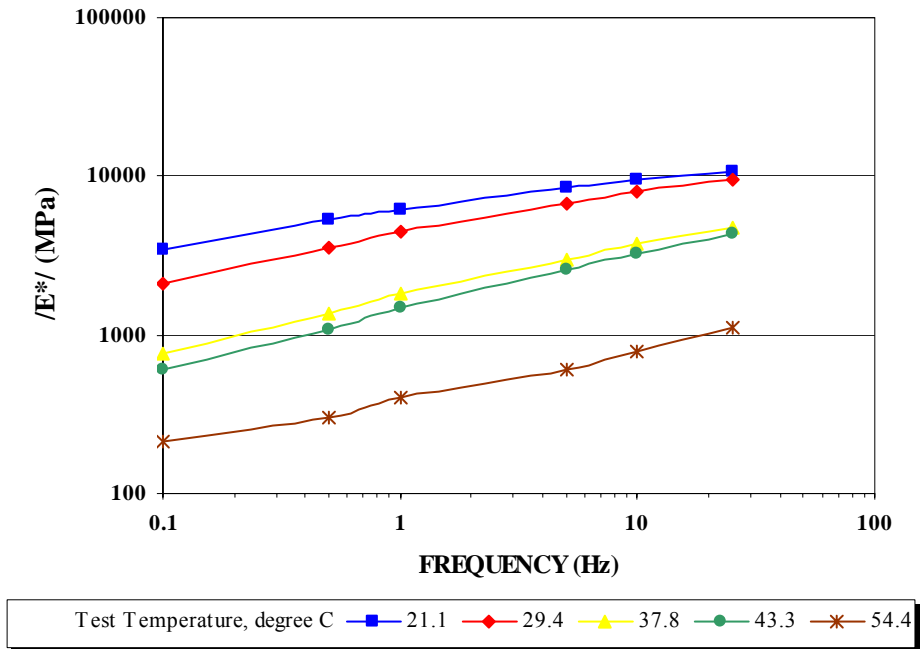
FIGURE D17   Dynamic (Complex) Modulus of K6-29 FWD Station.
Case 1 and Case 3 (LVDT 2)
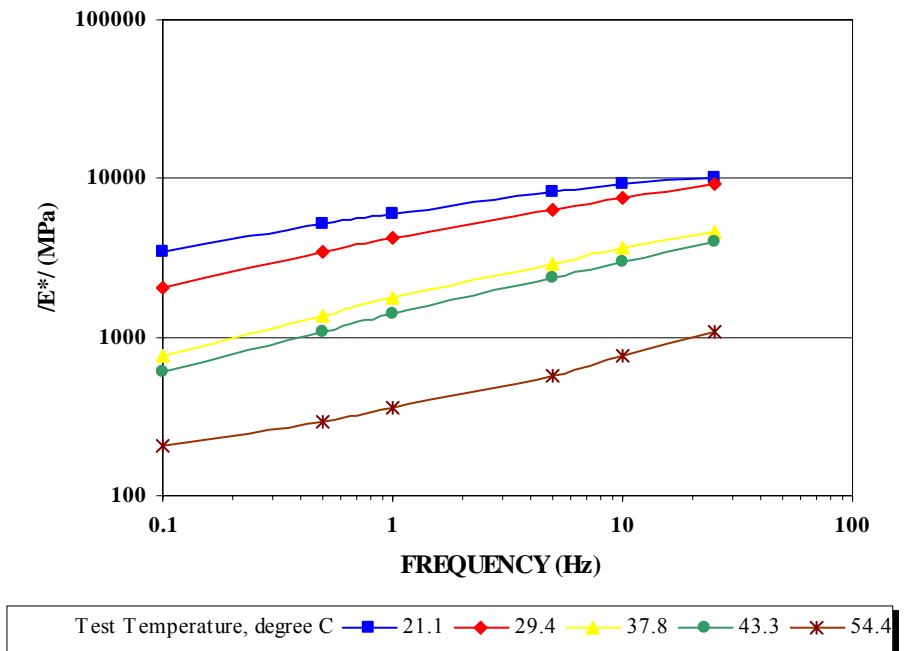
FIGURE D18   Dynamic (Complex) Modulus of K6-29 FWD Station.
Case 2 and Case 4 (LVDT-2)
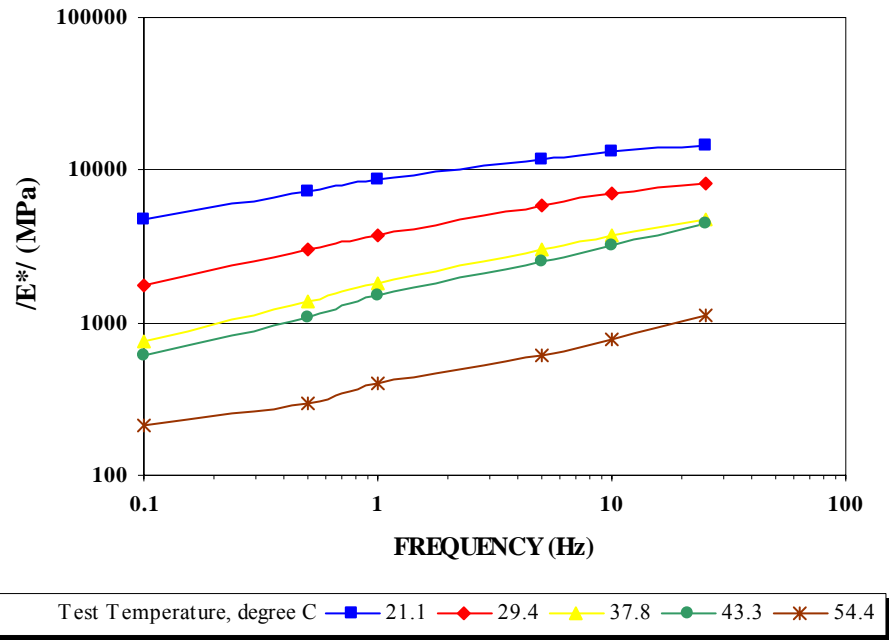
FIGURE D19   Dynamic (Complex) Modulus of K6-29 FWD Station.
Case 1 and Case 3 (LVDTs)
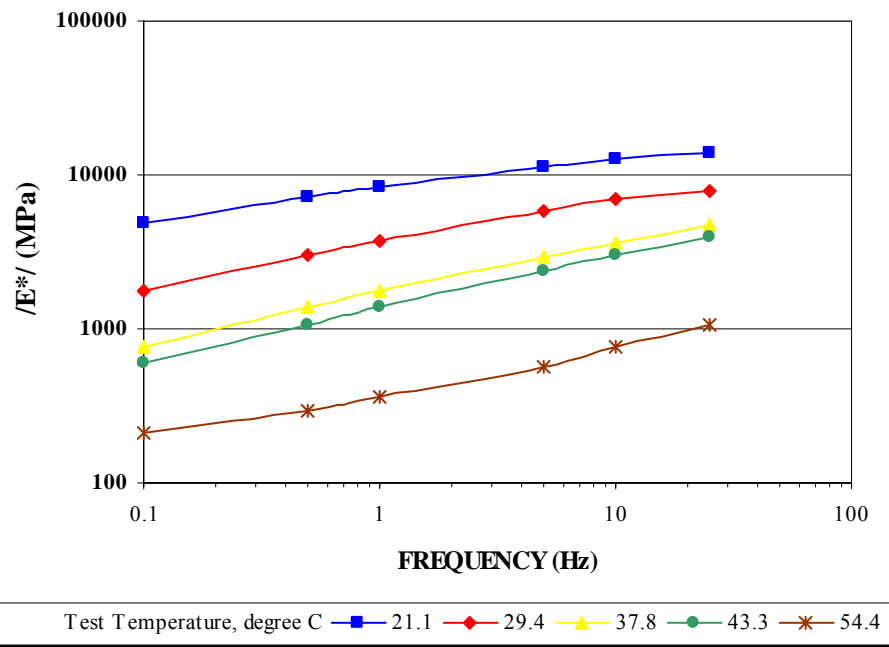
FIGURE D20   Dynamic (Complex) Modulus of K6-29 Fwd Station.
Case 2 and Case 4 (LVDTs)
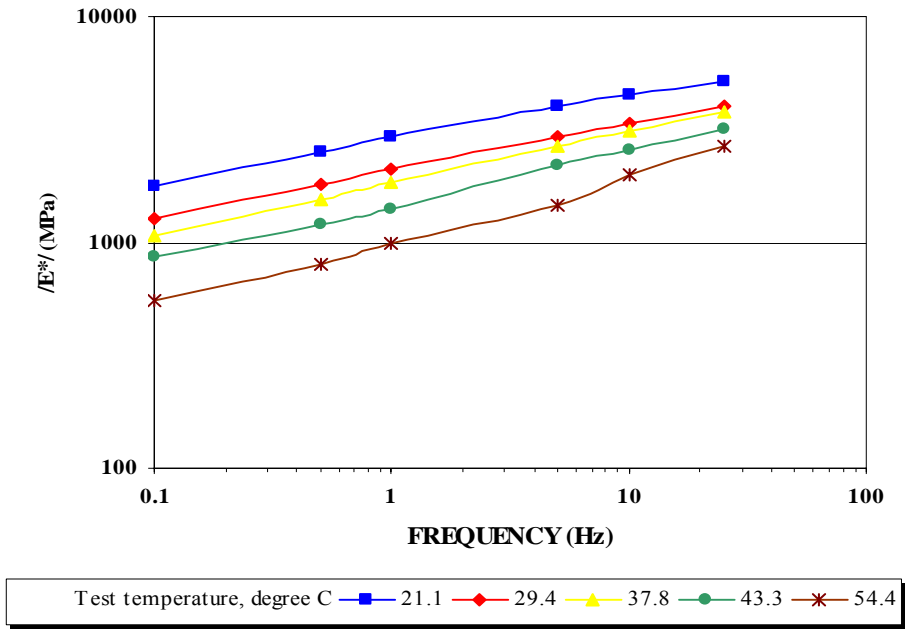
FIGURE D21   Dynamic (Complex) Modulus of K6-48 FWD Station.
Case 1 and 3 (LVDT-2)
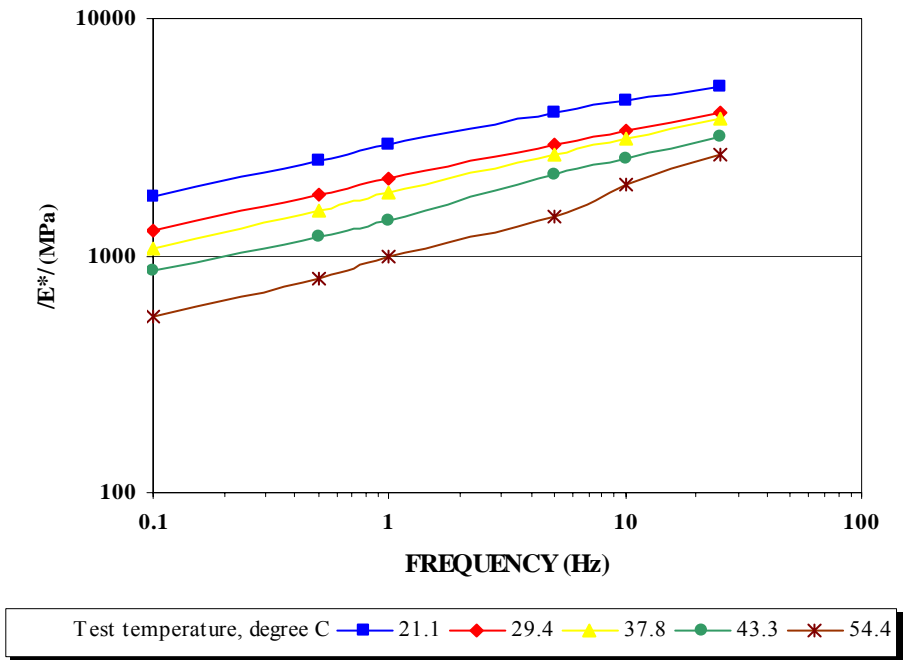
FIGURE D22   Dynamic (Complex) Modulus of K6-48 FWD Station.
Case 2 and 4 (LVDT 2)
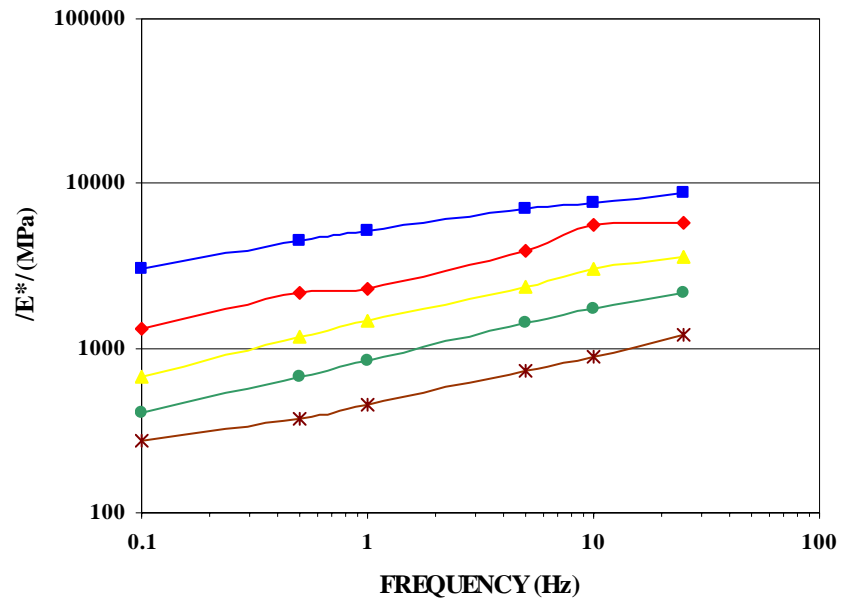
FIGURE D23   Dynamic (Complex) Modulus of Fwd Station K7-3
Case 2 And Case 4 (LVDTs)
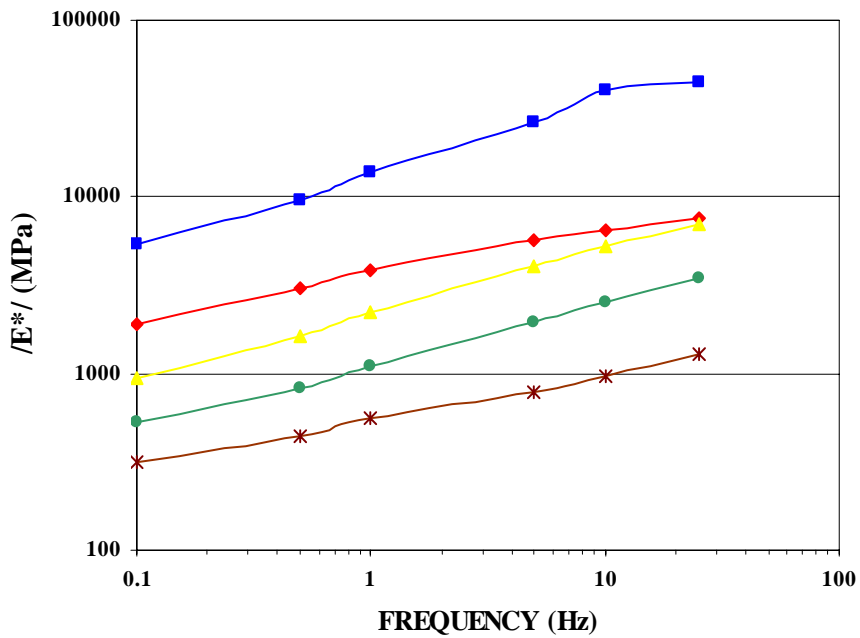
FIGURE C24   Dynamic (Complex) Modulus of K7-11 FWD Station.
Case 1 and Case 3 (LVDTs)
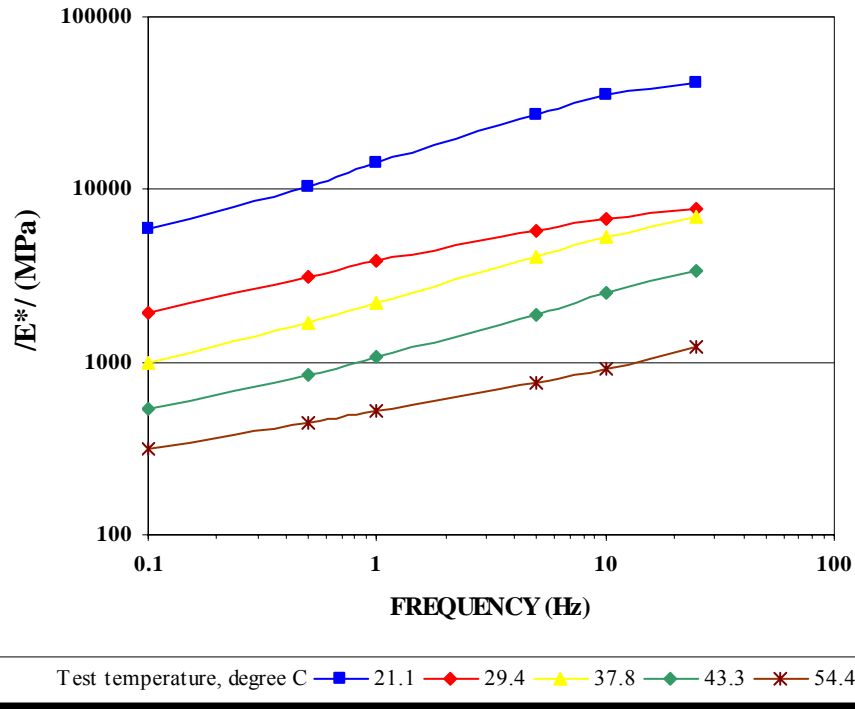
FIGURE C25   Dynamic (Complex) Modulus of K7-11 FWD Station.
Case 2 and Case 4 (LVDTs)
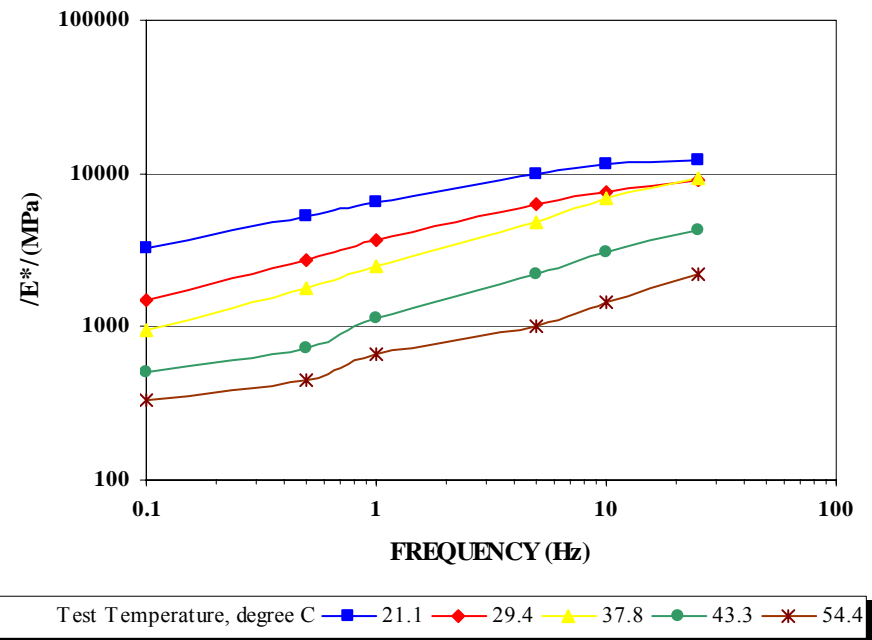
FIGURE C26   Dynamic (Complex) Modulus of K7-15 FWD Station
Case 1 and Case 3 (LVDTs)
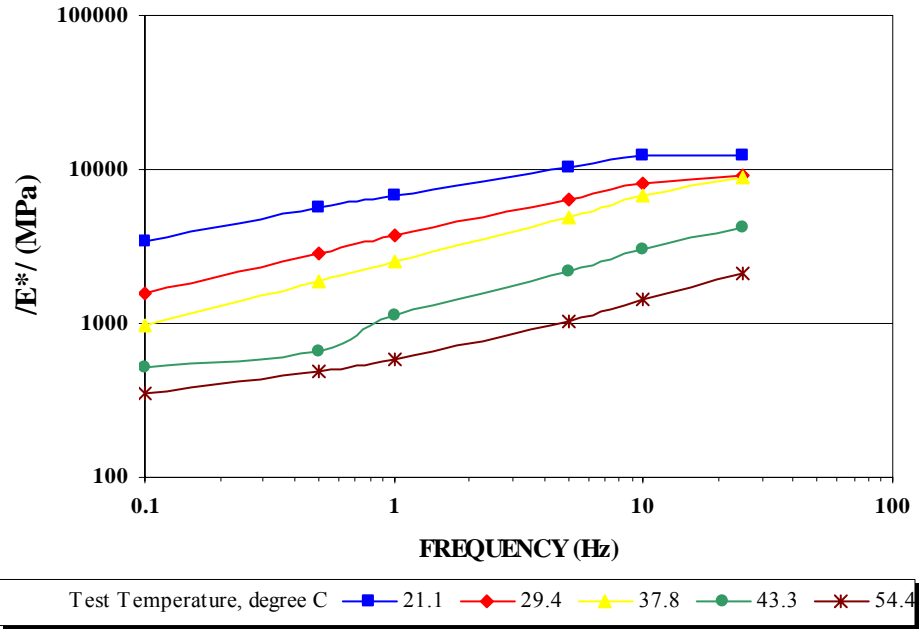
FIGURE C27   Dynamic (Complex) Modulus of K7-15 FWD Station
                   Case 2 and Case 4 (LVDTS)
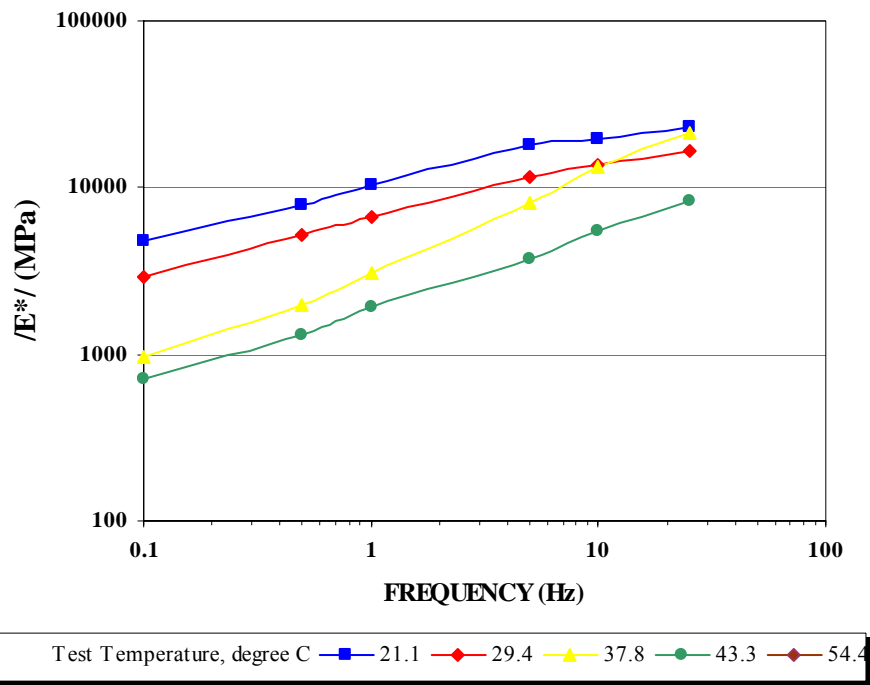
FIGURE C28   Dynamic (Complex) Modulus of K7-20 FWD Station
                   Case 1 and Case 3 (LVDTs)
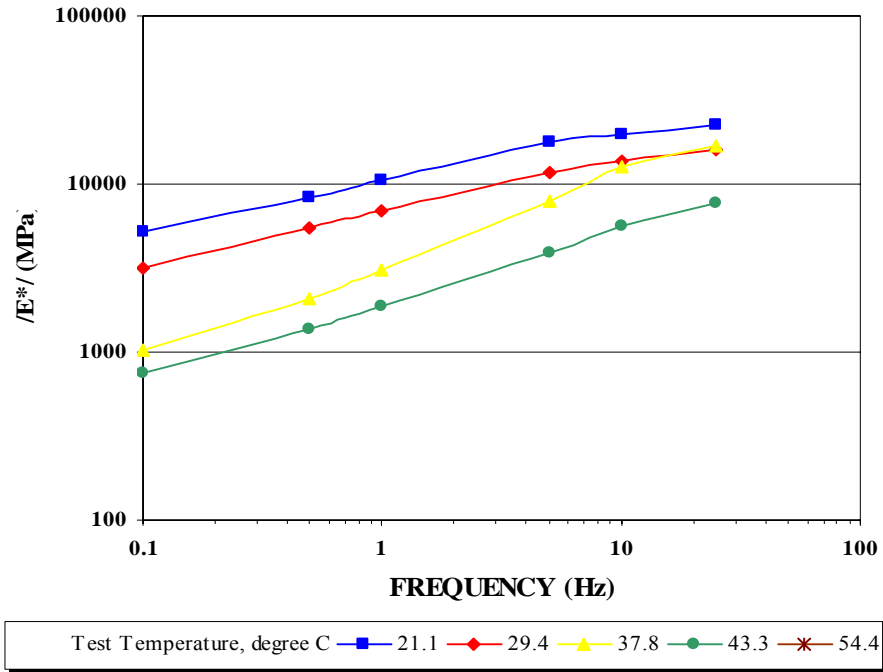
FIGURE C29   Dynamic (Complex) Modulus of K7-20 FWD Station
Case 2 And Case 4 (LVDTs)
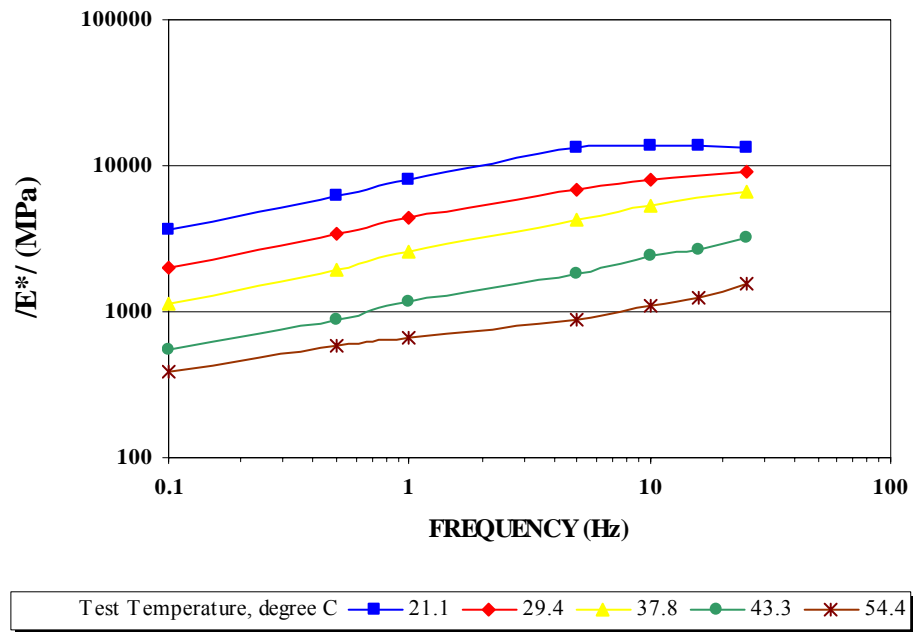
FIGURE C30   Dynamic (Complex) Modulus of K7-31 FWD Station
Case 1 and Case 3 (LVDTs)
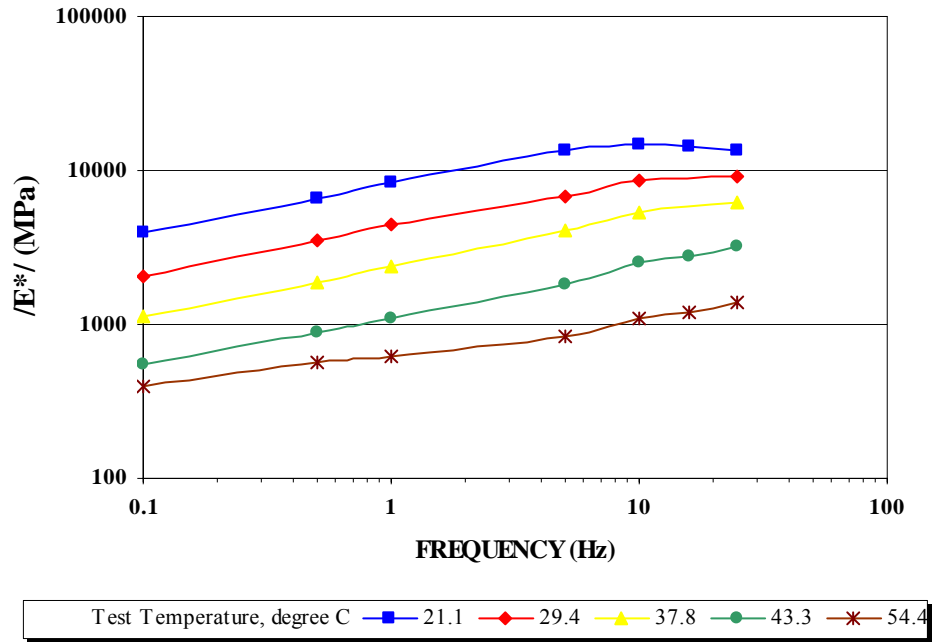
FIGURE C31   Dynamic (Complex) Modulus of K7-31 FWD Station
                      Case 2 and Case 4 (LVDTs)
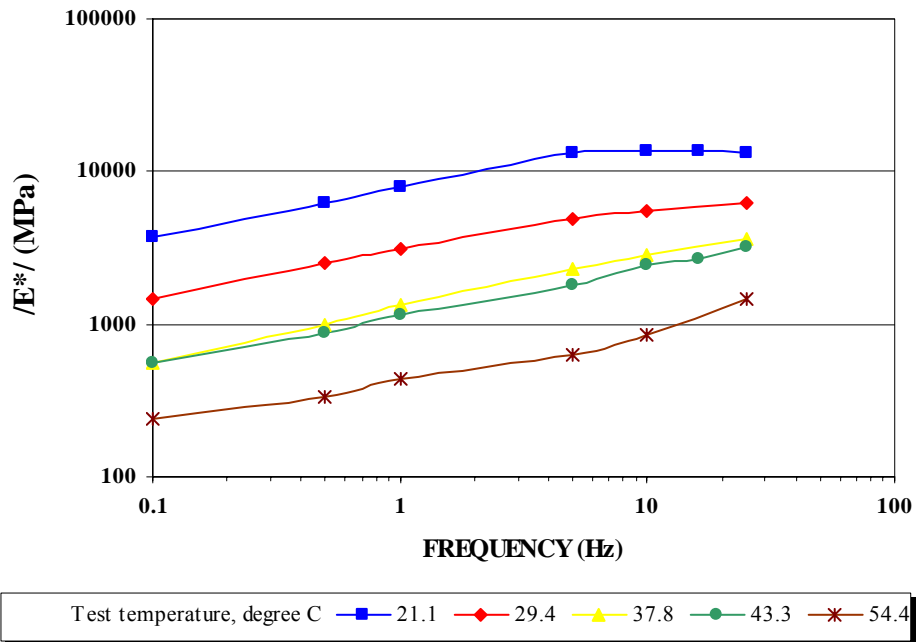
FIGURE C32   Dynamic (Complex) Modulus of K7-31 FWD Station
                      Case 1 and Case 3 (LVDT 2)
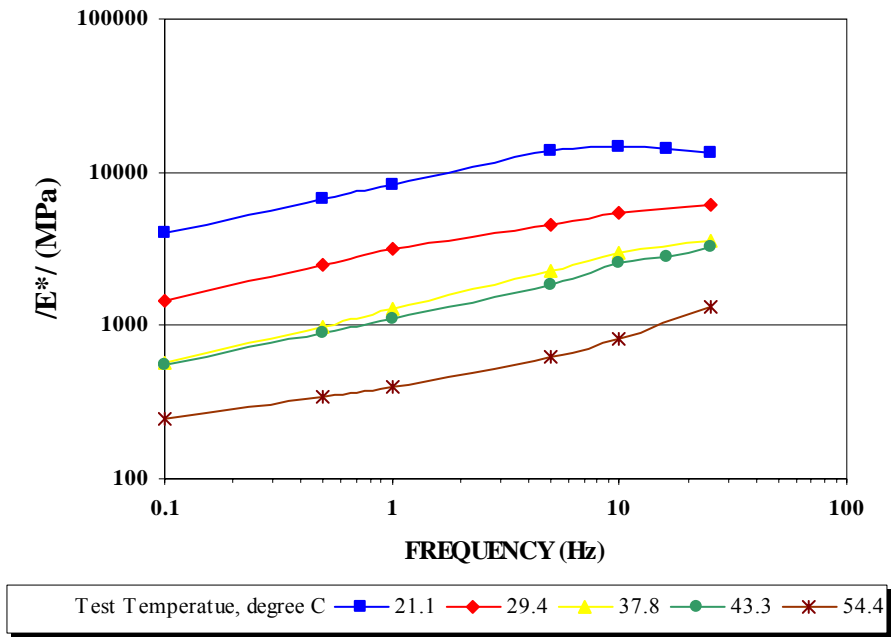
FIGURE C33   Dynamic (Complex) Modulus of K7-31 FWD Station
CASE 2 AND CASE 4 (LVDT 2)
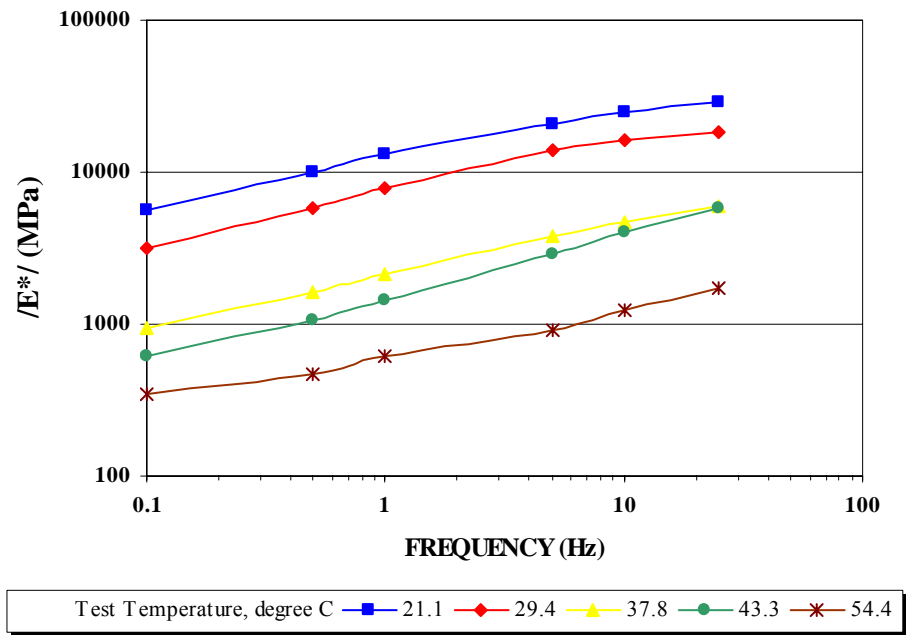
FIGURE C34   Dynamic (Complex) Modulus of K7-37 FWD Station
Case 1 and Case 3 (Average)
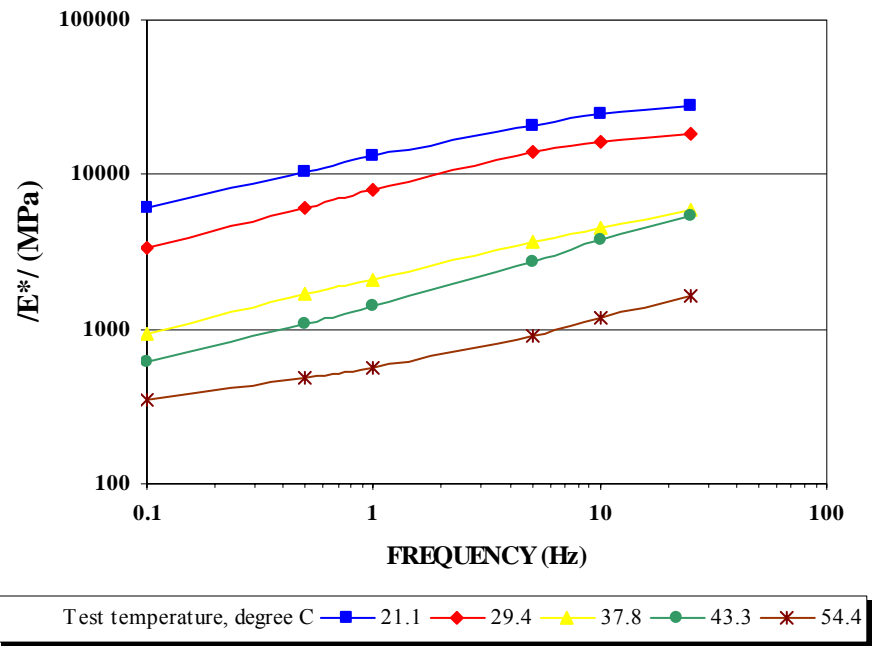
FIGURE C35   Dynamic (Complex) Modulus of K7-37 FWD Station
Case 2 and Case 4 (Average)
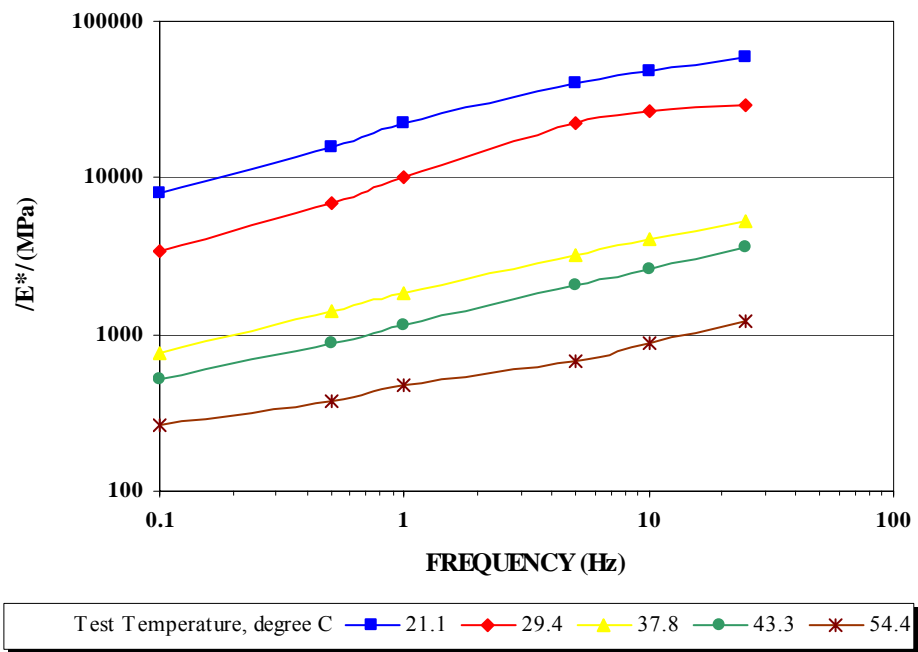
FIGURE C36   Dynamic (Complex) Modulus of K7-37 FWD Station
Case 1 and Case 3 (LVDT 2)
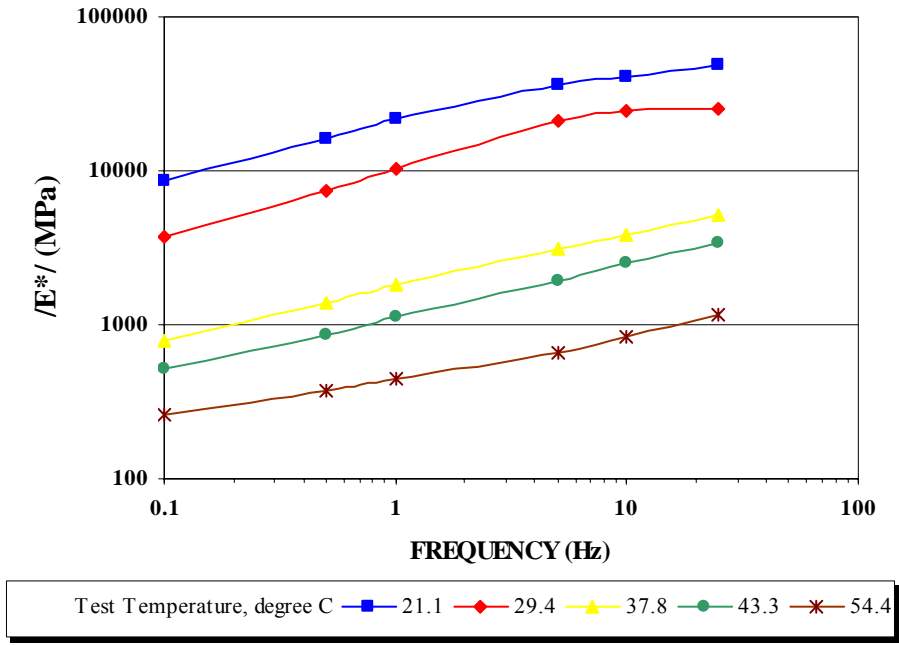
FIGURE C37   Dynamic (Complex) Modulus of K7-37 FWD Station
Case 2 and Case 4 (LVDT 2)
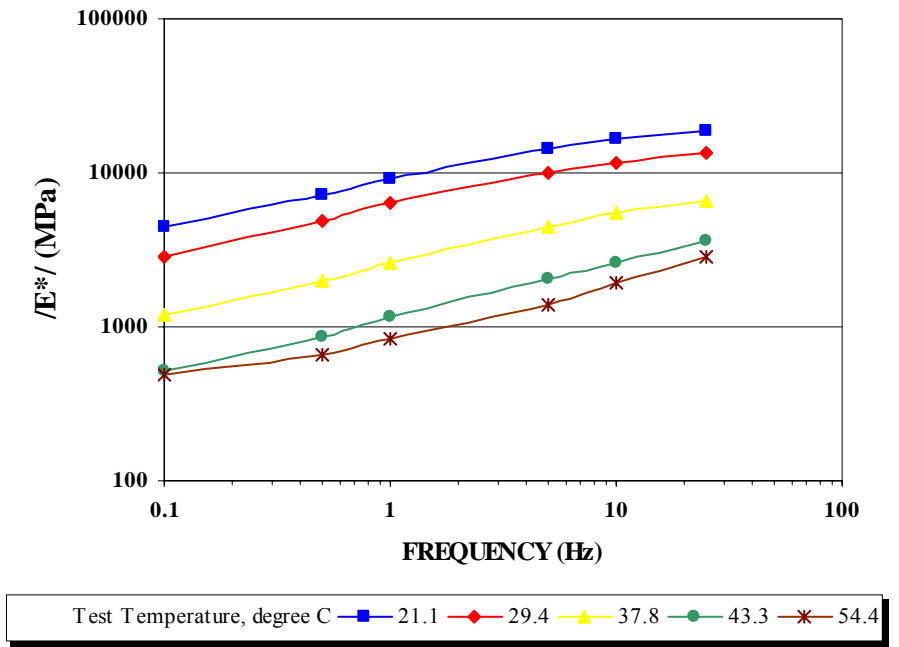
FIGURE C38   Dynamic (Complex) Modulus of K7-37 FWD Station
Case 1 and Case 3 (LVDTs)
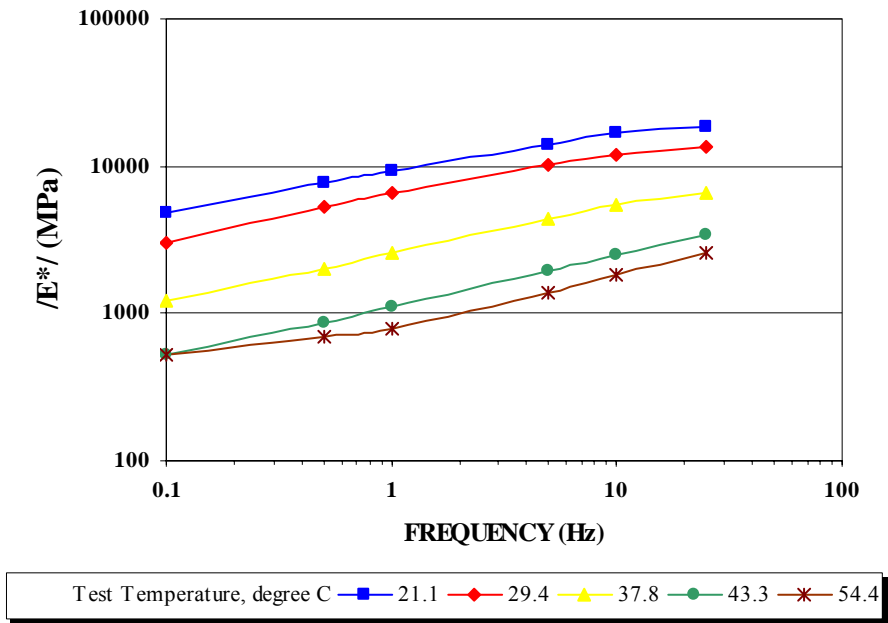
FIGURE C39   Dynamic (Complex) Modulus of K7-37 FWD Station
Case 2 and Case 4 (LVDTs)
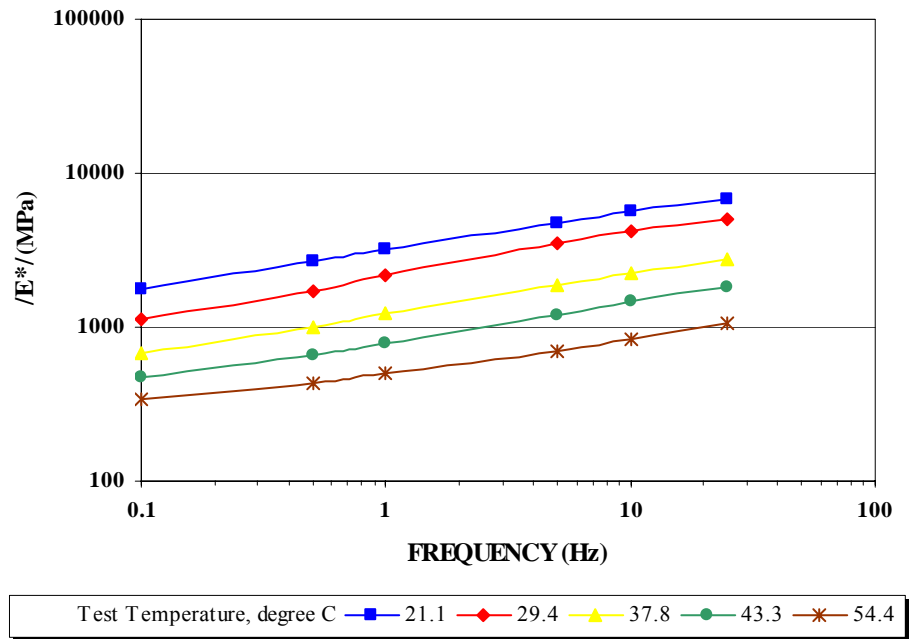
FIGURE C40   Dynamic (Complex) Modulus of K7-40 FWD Station
Case 1 and Case 3 (Average)
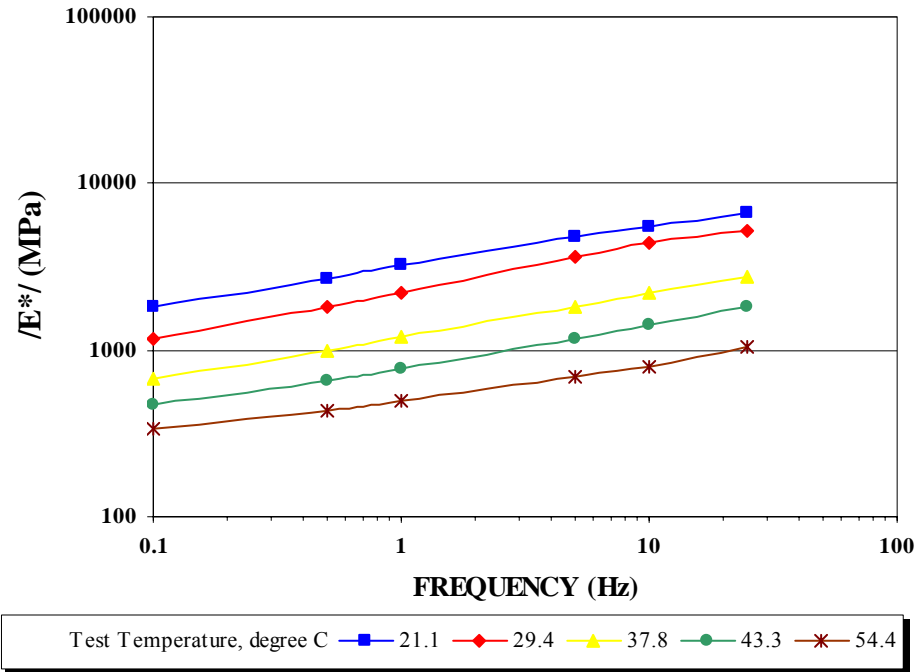
FIGURE C41   Dynamic (Complex) Modulus of K7-40 FWD Station
Case 2 and Case 4 (Average)
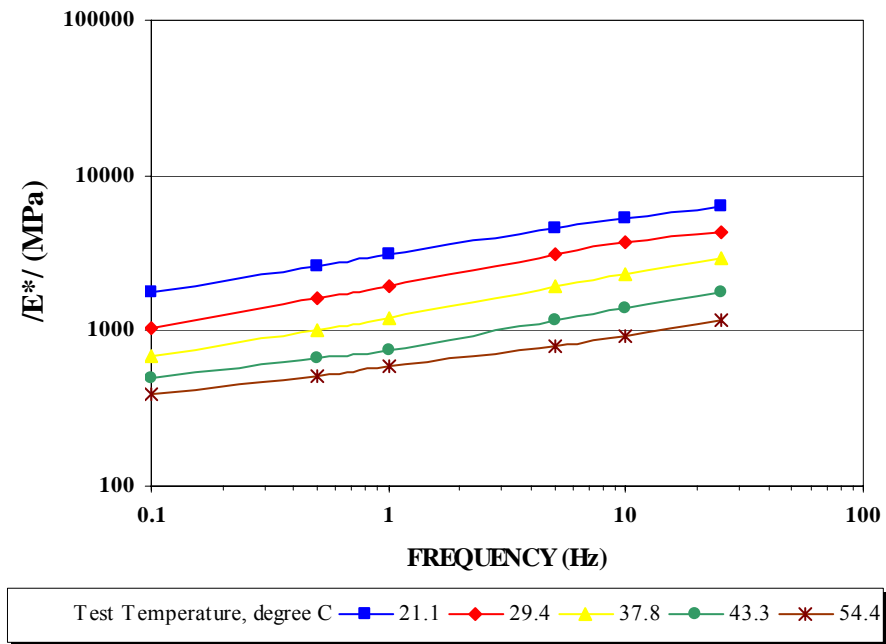
FIGURE C 42   Dynamic (Complex) Modulus of K7-40 FWD Station
Case 2 and Case 4 (LVDTs)
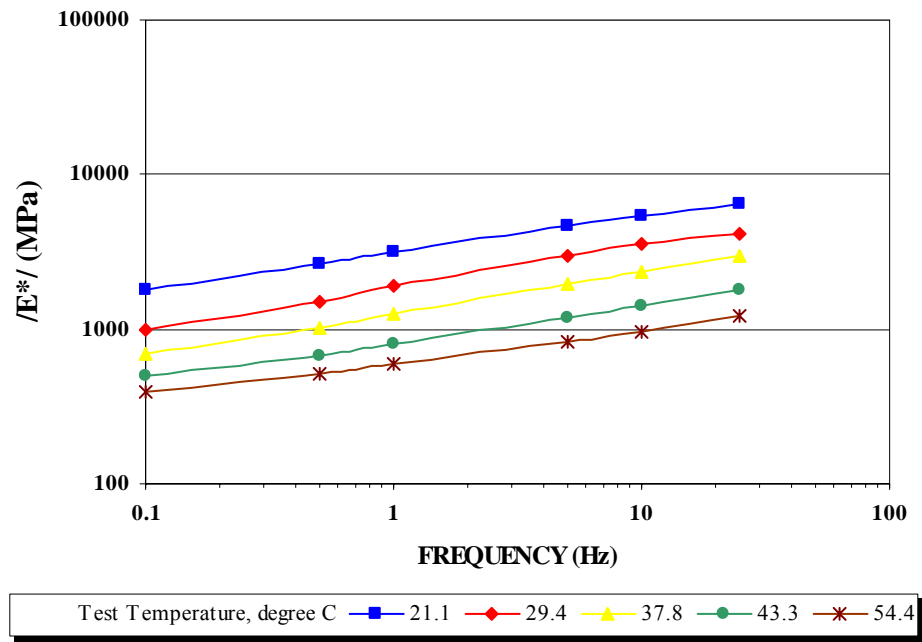
FIGURE D43   Dynamic (Complex) Modulus of K7-40 FWD Station
Case 1 and Case 3 (LVDTs)

D2 BACKCALCULATION OF THE CREEP COMPLIANCE COEFFICIENTS

The program FREQSWP is used to backcalculate the creep compliance coefficients, which uses data from frequency sweep tests. The input data to this program are the storage and loss compliances at various frequencies which have been determined by the frequency sweep test data. The J_1 and J_2 are the real and imaginary part of the Creep Compliance obtained on the laboratory testing.

TABLE D1   Measured and Predicted values of Creep Compliance of K6-1 FWD Station at 21.1 $^{\circ}$C (70 $^{\circ}$F)

No	Frequency (Hz.)	J1 (1/MPa)		J2 (1/MPa)	
		Measured	Predicted	Measured	Predicted
1	25	4.47E-05	3.27E-05	1.22E-05	1.25E-05
2	10	4.22E-05	4.04E-05	2.09E-05	1.79E-05
3	5	4.15E-05	4.83E-05	2.97E-05	2.34E-05
4	1	7.27E-05	7.74E-05	4.22E-05	4.39E-05
5	0.5	8.70E-05	9.67E-05	6.46E-05	5.74E-05
6	0.1	1.47E-04	1.68E-04	1.06E-04	1.07E-04

Backcalculated Creep Compliance Coefficients of K6-1 FWD Station at 21.1 $^{\circ}$C

Do	D1	m	SSE
1.48E-05	1.76E-04	3.89E-01	2.18E-01

FIGURE D44   Comparison between the Measured and Predicted Values of Creep Compliance of K6-1 FWD Station at 21.1 $^{\circ}$C

TABLE D2   Measured and Predicted Values of Creep Compliance of K6-1 FWD Station at 29.4 °C (85 °F)

No	Frequency (Hz.)	J1 (1/MPa)		J2 (1/MPa)	
		Measured	Predicted	Measured	Predicted
1	25	5.93E-05	4.96E-05	4.31E-05	3.67E-05
2	10	6.56E-05	7.19E-05	5.87E-05	5.32E-05
3	5	8.15E-05	9.52E-05	8.52E-05	7.04E-05
4	1	1.93E-04	1.83E-04	1.24E-04	1.35E-04
5	0.5	2.26E-04	2.42E-04	2.00E-04	1.79E-04
6	0.1	4.14E-04	4.65E-04	3.37E-04	3.44E-04

Backcalculated Creep Compliance Coefficients of K6-1 FWD Station at 29.4 °C

Do	D1	m	SSE
2.69E-11	5.40E-04	4.06E-01	1.68E-01

FIGURE D45   Comparison between the Measured and Predicted Values of Creep Compliance of K6-1 FWD Station at 29.4 °C

TABLE D3   Measured and Predicted values of Creep Compliance of K6-1 FWD Station at 37.8 $^{\circ}$C (100 $^{\circ}$F)

No	Frequency	J1 (1/MPa)		J2 (1/MPa)	
	(Hz.)	Measured	Predicted	Measured	Predicted
1	10	3.48E-04	3.27E-04	1.12E-04	1.20E-04
2	5	4.09E-04	3.79E-04	1.72E-04	1.62E-04
3	1	5.18E-04	5.80E-04	4.61E-04	3.23E-04
4	0.5	7.20E-04	7.20E-04	4.80E-04	4.34E-04
5	0.1	1.11E-03	1.26E-03	7.88E-04	8.67E-04

Backcalculated Creep Compliance Coefficients of K6-1 FWD Station at 37.8 $^{\circ}$C

Do	D1	m	SSE
1.77E-04	1.28E-03	4.29E-01	1.59E-01

FIGURE D46   Comparison between the Measured and Predicted Values of Creep Compliance of K6-1 FWD Station at 37.8 $^{\circ}$C

TABLE D4 Measured and Predicted values of Creep Compliance of K6-1 FWD Station at 43.3 °C (110 °F)

No	Frequency	J1 (1/MPa)		J2 (1/MPa)	
	(Hz.)	Measured	Predicted	Measured	Predicted
1	25	3.90E-04	4.42E-04	6.27E-05	8.79E-05
2	10	4.73E-04	4.95E-04	1.87E-04	1.30E-04
3	5	5.58E-04	5.51E-04	2.70E-04	1.75E-04
4	1	9.13E-04	7.69E-04	3.99E-04	3.49E-04
5	0.5	1.14E-03	9.20E-04	5.68E-04	4.69E-04
6	0.1	1.74E-03	1.50E-03	7.34E-04	9.34E-04

Backcalculated Creep Compliance Coefficients of K6-1 FWD Station at 43.3 °C

Do	D1	m	SSE
3.31E-04	1.39E-03	4.28E-01	5.97E-01
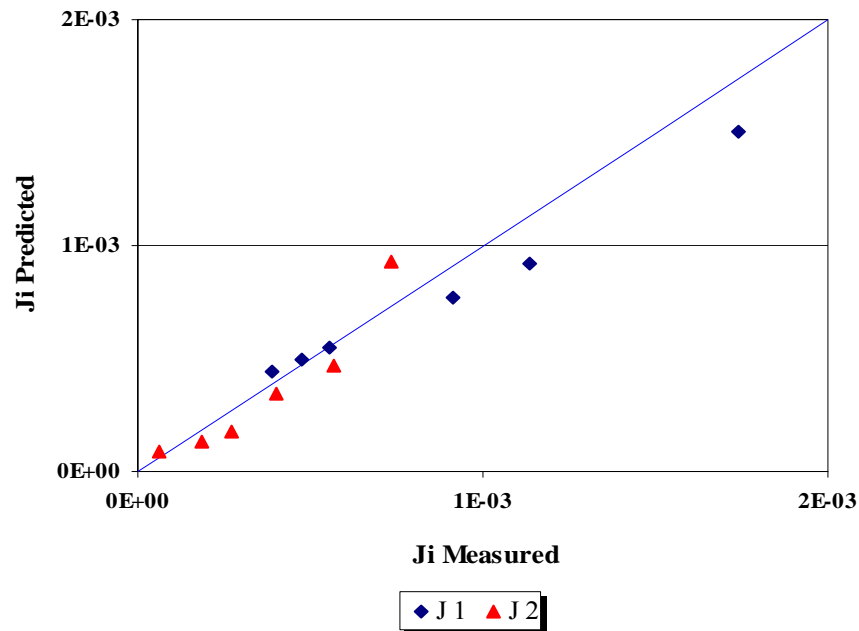
FIGURE D47 Comparison between the Measured and Predicted Values of Creep Compliance of K6-1 FWD Station at 43.3 °C

TABLE D5 Measured and Predicted values of Creep Compliance of K6-1 FWD
Station at 54.4 ^{o}C (130 ^{o}F)

No	Frequency	J1 (1/MPa)		J2 (1/MPa)	
	(Hz.)	Measured	Predicted	Measured	Predicted
1	25	8.32E-04	9.46E-04	6.59E-05	8.25E-05
2	10	1.02E-03	9.93E-04	4.16E-04	1.33E-04
3	5	1.22E-03	1.05E-03	6.20E-04	1.90E-04
4	1	1.06E-03	1.28E-03	3.43E-04	4.39E-04
5	0.5	2.12E-03	1.46E-03	1.01E-03	6.29E-04
6	0.1	2.83E-03	2.23E-03	1.32E-03	1.45E-03

Backcalculated Creep Compliance Coefficients of K6-1 FWD Station at 54.4 ^{o}C

Do	D1	m	SSE
8.68E-04	1.76E-03	5.19E-01	1.46E+00

FIGURE D48   Comparison between the Measured and Predicted Values of Creep
Compliance of K6-1 FWD Station at 54.4 ^{o}C

TABLE D6   Measured and Predicted values of Creep Compliance of K6-4
FWD Station at 21.1 ^{o}C (70 ^{o}F)

No	Frequency	J1 (1/MPa)		J2 (1/MPa)	
	(Hz.)	Measured	Predicted	Measured	Predicted
1	25	5.51E-05	6.30E-05	1.54E-05	1.96E-05
2	10	7.46E-05	7.47E-05	3.26E-05	3.00E-05
3	5	9.33E-05	8.74E-05	5.17E-05	4.13E-05
4	1	1.69E-04	1.39E-04	8.37E-05	8.72E-05
5	0.5	2.01E-04	1.76E-04	1.29E-04	1.20E-04
6	0.1	3.58E-04	3.26E-04	2.25E-04	2.54E-04

Backcalculated Creep Compliance Coefficients of K6-4 FWD Station at 21.1 ^{o}C

Do	D1	m	SSE
4.11E-05	3.47E-04	4.64E-01	2.22E-01

FIGURE D49   Comparison between the Measured and Predicted values of Creep
Compliance of K6-4 FWD Station at 21.1 ^{o}C

TABLE D7   Measured and Predicted values of Creep Compliance of K6-4 FWD Station at 29.4 ^{o}C (85 ^{o}F)

No	Frequency (Hz.)	J1 (1/MPa)		J2 (1/MPa)	
		Measured	Predicted	Measured	Predicted
1	25	8.23E-05	7.51E-05	2.15E-05	2.54E-05
2	10	8.80E-05	8.99E-05	4.83E-05	3.98E-05
3	5	9.64E-05	1.07E-04	7.16E-05	5.59E-05
4	1	1.90E-04	1.76E-04	1.16E-04	1.23E-04
5	0.5	2.24E-04	2.27E-04	1.87E-04	1.73E-04
6	0.1	4.31E-04	4.41E-04	3.53E-04	3.80E-04

Backcalculated Creep Compliance Coefficients of K6-4 FWD Station at 29.4 ^{o}C

Do	D1	m	SSE
4.89E-05	4.91E-04	4.90E-01	1.52E-01

FIGURE D50   Comparison between the Measured and Predicted values of Creep Compliance of K6-4 FWD Station at 29.4 ^{o}C

TABLE D8   Measured and Predicted values of Creep Compliance of K6-4 FWD Station at 37.8 °C (100 °F)

No	Frequency (Hz.)	J1 (1/MPa) Measured	J1 (1/MPa) Predicted	J2 (1/MPa) Measured	J2 (1/MPa) Predicted
1	25	1.79E-04	1.79E-04	5.65E-05	7.43E-05
2	10	2.32E-04	2.21E-04	1.73E-04	1.21E-04
3	5	2.82E-04	2.70E-04	2.60E-04	1.75E-04
4	1	3.98E-04	4.84E-04	5.82E-04	4.10E-04
5	0.5	7.67E-04	6.50E-04	7.29E-04	5.93E-04
6	0.1	1.37E-03	1.38E-03	1.11E-03	1.39E-03

Backcalculated Creep Compliance Coefficients of K6-4 FWD Station at 37.8 °C

Do	D1	m	SSE
1.12E-04	1.66E-03	5.31E-01	5.61E-01

FIGURE D51   Comparison between the Measured and Predicted values of Creep Compliance of K6-4 FWD Station at 37.8 °C

TABLE D9   Measured and Predicted values of Creep Compliance of K6-4 FWD Station at 43.3 ᵒC (110 ᵒF)

No	Frequency	J1 (1/MPa)		J2 (1/MPa)	
	(Hz.)	Measured	Predicted	Measured	Predicted
1	25	2.78E-04	3.47E-04	3.31E-05	4.96E-05
2	10	3.69E-04	3.74E-04	1.70E-04	8.29E-05
3	5	4.74E-04	4.07E-04	2.68E-04	1.22E-04
4	1	6.10E-04	5.55E-04	6.53E-04	3.03E-04
5	0.5	1.03E-03	6.73E-04	6.08E-04	4.47E-04
6	0.1	1.58E-03	1.21E-03	8.14E-04	1.10E-03

Backcalculated Creep Compliance Coefficients of K6-4 FWD Station at 43.3 ᵒC

Do	D1	m	SSE
3.06E-04	1.24E-03	5.62E-01	1.55E+00

FIGURE D52   Comparison between the Measured and Predicted values of Creep Compliance of K6-4 FWD Station at 43.3 ᵒC

TABLE D10   Measured and Predicted values of Creep Compliance of K6-4 FWD Station at 54.4 ^{o}C (130 ^{o}F)

No	Frequency	J_1 (1/MPa)		J_2 (1/MPa)	
	(Hz.)	Measured	Predicted	Measured	Predicted
1	25	4.70E-04	4.81E-04	1.70E-04	2.16E-04
2	10	7.00E-04	6.14E-04	4.70E-04	2.98E-04
3	5	9.10E-04	7.48E-04	6.70E-04	3.79E-04
4	1	1.00E-03	1.22E-03	1.10E-03	6.65E-04
5	0.5	1.60E-03	1.51E-03	1.00E-03	8.47E-04
6	0.1	2.00E-03	2.56E-03	1.30E-03	1.49E-03

Backcalculated Creep Compliance Coefficients of K6-4 FWD Station at 54.4 ^{o}C

Do	D1	m	SSE
1.27E-04	2.72E-03	3.49E-01	7.72E-01

FIGURE D53   Comparison between the Measured and Predicted values of Creep Compliance of K6-4 FWD Station at 54.4 ^{o}C

TABLE D11   Measured and Predicted values of Creep Compliance of K6-11
FWD Station at 21.1 ^{o}C (70 ^{o}F)

No	Frequency	J1 (1/MPa)		J2 (1/MPa)	
	(Hz.)	Measured	Predicted	Measured	Predicted
1	25	4.46E-05	4.07E-05	9.62E-06	1.16E-05
2	10	4.51E-05	4.76E-05	2.14E-05	1.76E-05
3	5	5.07E-05	5.52E-05	3.30E-05	2.40E-05
4	1	9.15E-05	8.50E-05	4.46E-05	4.95E-05
5	0.5	1.09E-04	1.06E-04	7.66E-05	6.76E-05
6	0.1	1.92E-04	1.90E-04	1.27E-04	1.39E-04

Backcalculated Creep Compliance Coefficients of K6-11 FWD Station at 21.1 ^{o}C

Do	D1	m	SSE
2.71E-05	**1.97E-04**	**4.50E-01**	**2.10E-01**

FIGURE D54   Comparison between the Measured and Predicted values of Creep
Compliance of K6-11 FWD Station at 21.1 ^{o}C

TABLE D12   Measured and Predicted values of Creep Compliance of K6-11 FWD Station at 29.4 ^{o}C (85 ^{o}F)

No	Frequency	J1 (1/MPa)		J2 (1/MPa)	
	(Hz.)	Measured	Predicted	Measured	Predicted
1	25	1.26E-04	1.39E-04	1.76E-05	2.32E-05
2	10	1.41E-04	1.52E-04	5.05E-05	3.70E-05
3	5	1.64E-04	1.67E-04	7.86E-05	5.27E-05
4	1	2.83E-04	2.32E-04	1.05E-04	1.20E-04
5	0.5	3.38E-04	2.82E-04	1.87E-04	1.71E-04
6	0.1	6.12E-04	4.92E-04	3.46E-04	3.89E-04

Backcalculated Creep Compliance Coefficients of K6-11 FWD Station at 29.4 ^{o}C

Do	D1	m	SSE
1.16E-04	4.81E-04	5.11E-01	4.40E-01

FIGURE D55   Comparison between the Measured and Predicted values of Creep Compliance of K6-11 FWD Station at 29.4 ^{o}C

**TABLE D13   Measured and Predicted values of Creep Compliance of K6-11
FWD Station at 37.8 ^{o}C (100 ^{o}F)**

No	Frequency	J1 (1/MPa)		J2 (1/MPa)	
	(Hz.)	Measured	Predicted	Measured	Predicted
1	25	1.97E-04	2.26E-04	3.77E-05	5.36E-05
2	10	2.46E-04	2.57E-04	1.08E-04	8.61E-05
3	5	3.05E-04	2.92E-04	1.82E-04	1.23E-04
4	1	5.34E-04	4.44E-04	3.39E-04	2.83E-04
5	0.5	7.55E-04	5.60E-04	4.66E-04	4.05E-04
6	0.1	1.38E-03	1.06E-03	7.27E-04	9.31E-04

Backcalculated Creep Compliance Coefficients of K6-11 FWD Station at 37.8 ^{o}C

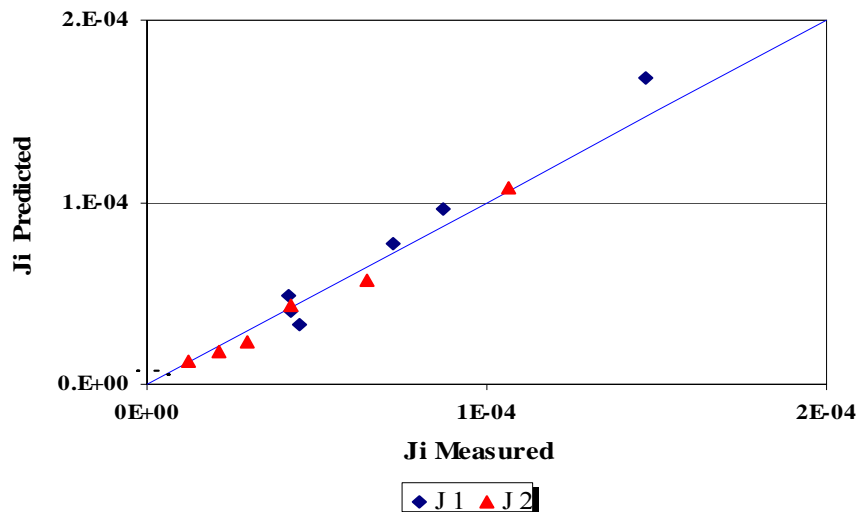| Do	D1	m	SSE
1.76E-04	1.14E-03	5.17E-01	6.20E-01

**FIGURE D56   Comparison between the Measured and Predicted values of Creep
Compliance of K6-11 FWD Station at 37.8 ^{o}C**

TABLE D14   Measured and Predicted values of Creep Compliance of K6-11
FWD Station at 43.3 °C (110 °F)

No	Frequency	J1 (1/MPa)		J2 (1/MPa)	
	(Hz.)	Measured	Predicted	Measured	Predicted
1	25	2.82E-04	3.12E-04	5.71E-05	8.15E-05
2	10	3.59E-04	3.58E-04	2.12E-04	1.34E-04
3	5	4.40E-04	4.11E-04	3.27E-04	1.95E-04
4	1	6.54E-04	6.49E-04	7.54E-04	4.65E-04
5	0.5	1.04E-03	8.35E-04	8.17E-04	6.77E-04
6	0.1	1.70E-03	1.66E-03	1.25E-03	1.62E-03

Backcalculated Creep Compliance Coefficients of K6-11 FWD Station at 43.3 °C

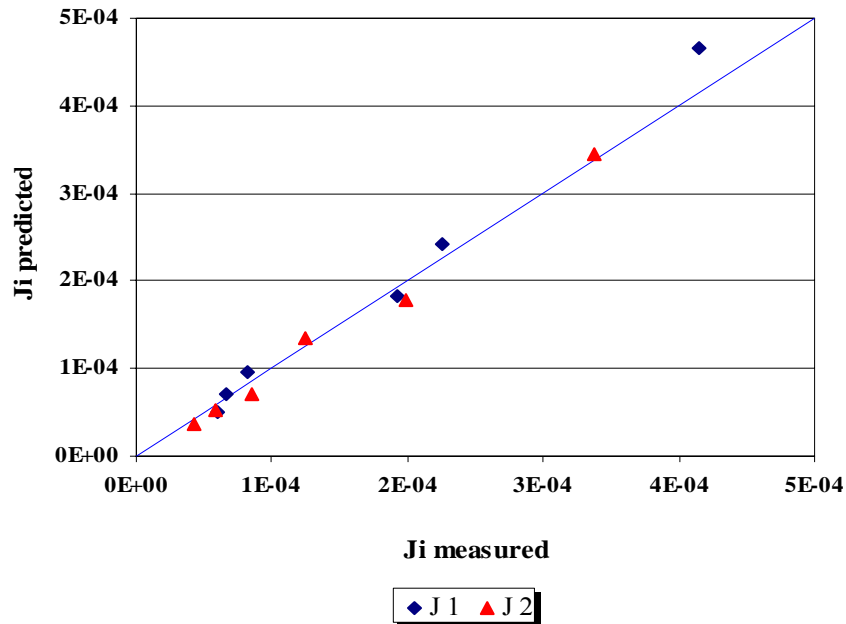| Do	D1	m	SSE
2.40E-04	1.88E-03	5.41E-01	7.98E-01

FIGURE D57   Comparison between the Measured and Predicted values of Creep
Compliance of K6-11 FWD Station at 43.3 °C

TABLE D15   Measured and Predicted values of Creep Compliance of K6-11 FWD Station at 54.4 ^{o}C (130 ^{o}F)

No	Frequency	J1 (1/MPa)		J2 (1/MPa)	
	(Hz.)	Measured	Predicted	Measured	Predicted
1	25	4.55E-04	5.00E-04	2.88E-04	2.44E-04
2	10	6.33E-04	6.51E-04	5.16E-04	3.17E-04
3	5	7.79E-04	7.95E-04	7.20E-04	3.88E-04
4	1	1.28E-03	1.27E-03	5.60E-04	6.17E-04
5	0.5	1.55E-03	1.55E-03	9.35E-04	7.54E-04
6	0.1	1.92E-03	2.46E-03	1.05E-03	1.20E-03

Backcalculated Creep Compliance Coefficients of K6-11 FWD Station at 54.4 ^{o}C

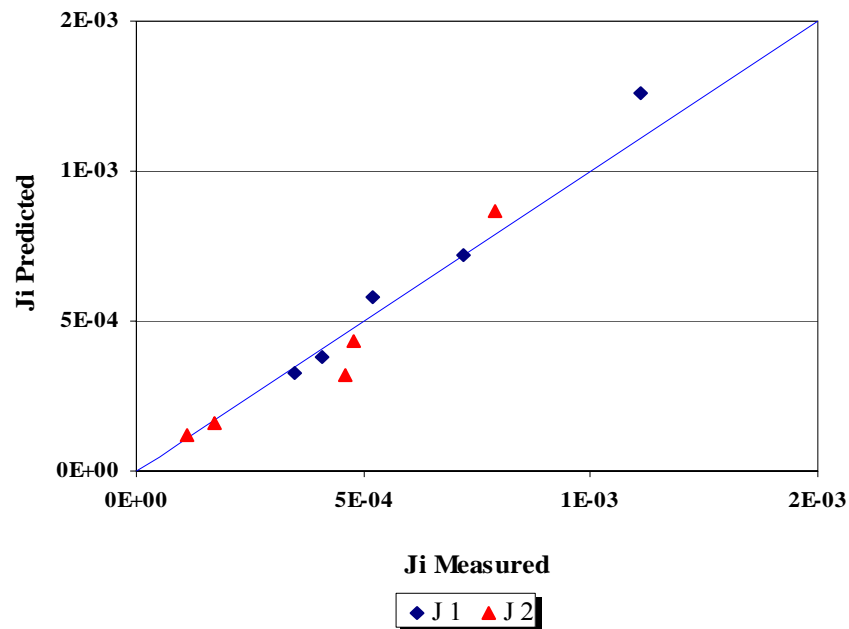| Do	D1	m	SSE
2.69E-11	2.66E-03	2.89E-01	5.43E-01

FIGURE D58   Comparison between the Measured and Predicted values of Creep Compliance of K6-11 FWD Station at 54.4 ^{o}C

**TABLE D16   Measured and Predicted values of Creep Compliance of K6-23
FWD Station at 21.1 ^{o}C (70 ^{o}F)**

No	Frequency	J1 (1/MPa)		J2 (1/MPa)	
	(Hz.)	Measured	Predicted	Measured	Predicted
1	10	1.50E-04	1.29E-04	5.22E-05	5.22E-05
2	5	1.65E-04	1.53E-04	7.35E-05	6.54E-05
3	1	2.18E-04	2.33E-04	1.30E-04	1.10E-04
4	0.5	2.56E-04	2.83E-04	1.48E-04	1.38E-04
5	0.1	3.64E-04	4.52E-04	2.32E-04	2.32E-04

Backcalculated Creep Compliance Coefficients of K6-23 FWD Station at 21.1 ^{o}C

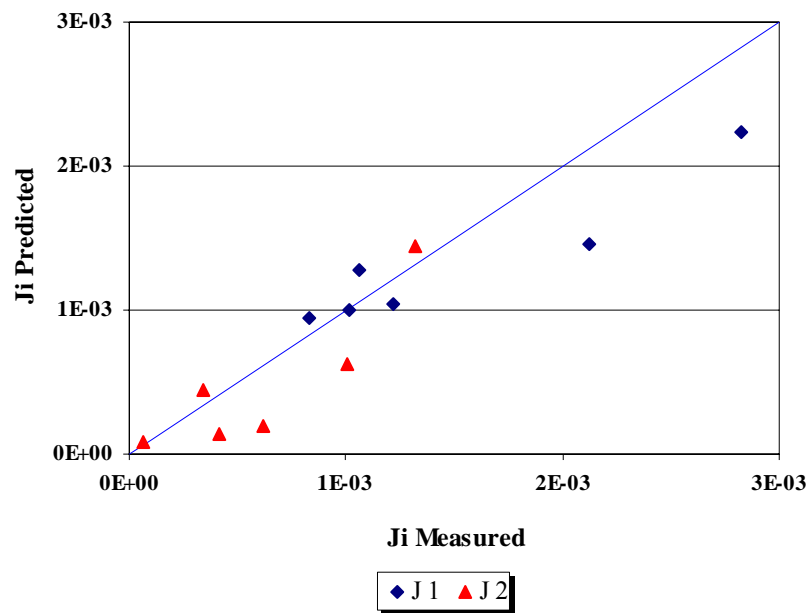| Do	D1	m	SSE
3.56E-05	4.58E-04	3.24E-01	1.41E-01

**FIGURE D59   Comparison between the Measured and Predicted values of Creep
Compliance of K6-23 FWD Station at 21.1 ^{o}C**

**TABLE D17   Measured and Predicted values of Creep Compliance of K6-23
FWD Station at 29.4 ^{o}C (85 ^{o}F)**

No	Frequency	J1 (1/MPa)		J2 (1/MPa)	
	(Hz.)	Measured	Predicted	Measured	Predicted
1	10	1.50E-04	1.50E-04	3.35E-05	3.65E-05
2	5	1.64E-04	1.67E-04	5.47E-05	4.74E-05
3	1	2.34E-04	2.25E-04	8.21E-05	8.70E-05
4	0.5	2.67E-04	2.64E-04	1.25E-04	1.13E-04
5	0.1	3.92E-04	4.04E-04	2.01E-04	2.08E-04

Backcalculated Creep Compliance Coefficients of K6-23 FWD Station at 21.1 ^{o}C

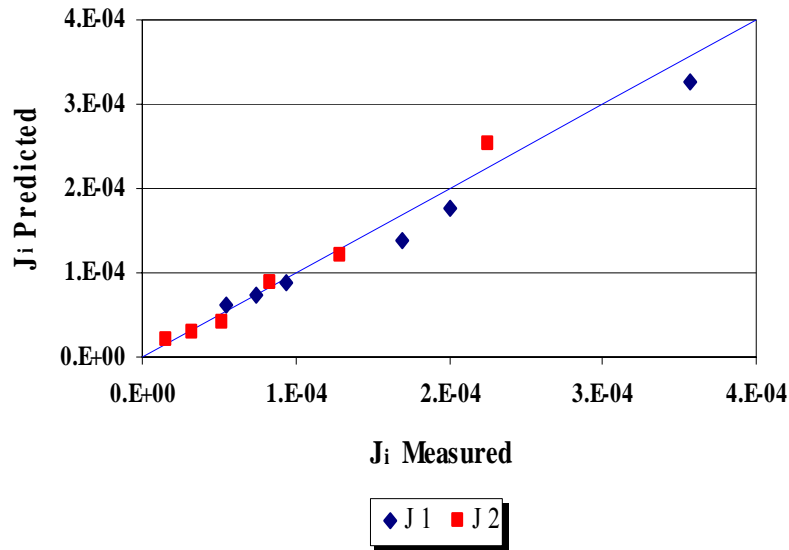| Do	D1	m	SSE
9.64E-05	3.51E-04	3.78E-01	4.26E-02

**FIGURE D60   Comparison between the Measured and Predicted values of Creep
Compliance of K6-23 FWD Station at 29.4 ^{o}C**

TABLE D18   Measured and Predicted values of Creep Compliance of K6-23 FWD Station at 37.8 °C (100 °F)

No	Frequency (Hz.)	J1 (1/MPa)		J2 (1/MPa)	
		Measured	Predicted	Measured	Predicted
1	10	4.35E-04	4.15E-04	9.74E-05	1.11E-04
2	5	4.82E-04	4.63E-04	1.69E-04	1.49E-04
3	1	6.18E-04	6.48E-04	4.16E-04	2.96E-04
4	0.5	7.85E-04	7.76E-04	4.33E-04	3.98E-04
5	0.1	1.12E-03	1.27E-03	7.15E-04	7.91E-04

Backcalculated Creep Compliance Coefficients of K6-23 FWD Station at 37.8 °C

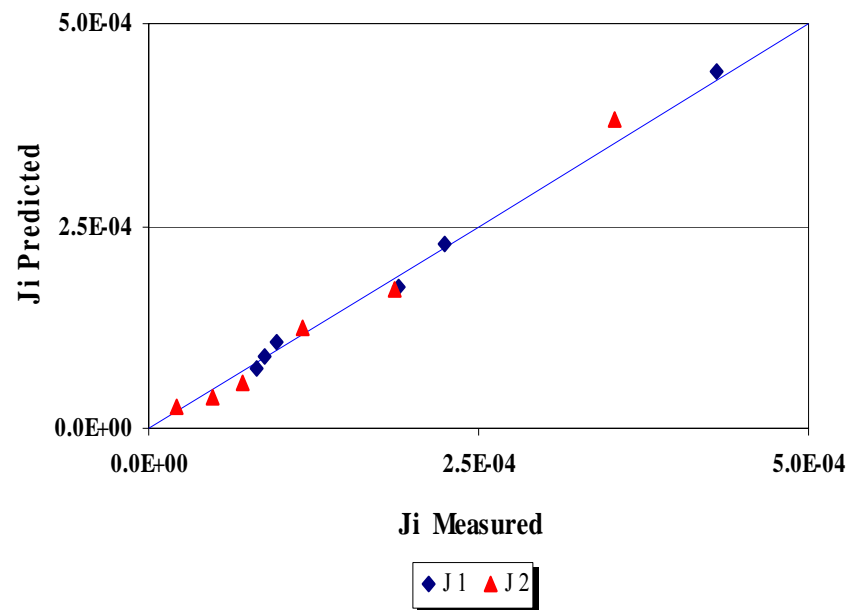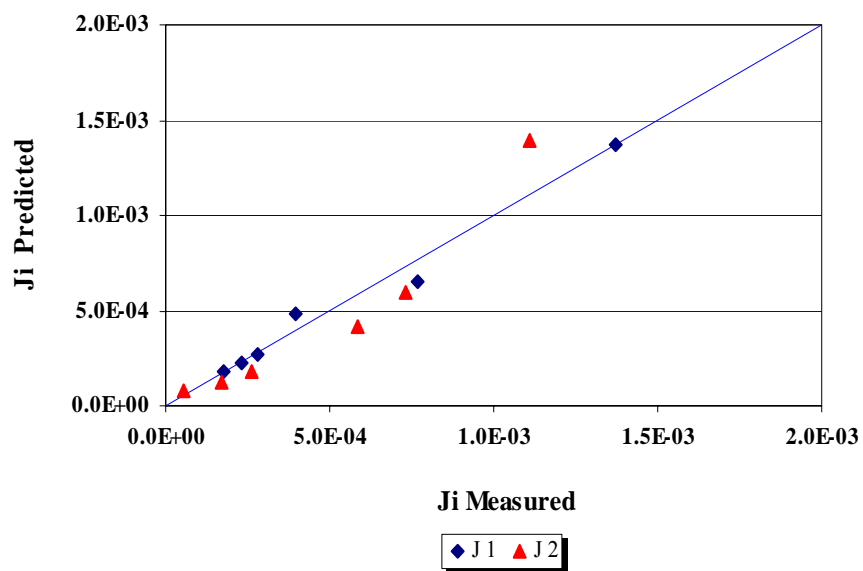| Do	D1	M	SSE
2.76E-04	1.18E-03	4.27E-01	1.58E-01

FIGURE D61   Comparison between the Measured and Predicted values of Creep Compliance of K6-23 FWD Station at 37.8 °C

TABLE D19   Measured and Predicted values of Creep Compliance of K6-23 FWD Station at 43.3 ^{o}C (110 ^{o}F)

No	Frequency (Hz.)	J1 (1/MPa)		J2 (1/MPa)	
		Measured	Predicted	Measured	Predicted
1	10	6.56E-04	6.42E-04	1.36E-04	1.58E-04
2	5	7.45E-04	7.11E-04	2.34E-04	2.13E-04
3	1	8.97E-04	9.76E-04	6.96E-04	4.26E-04
4	0.5	1.22E-03	1.16E-03	6.28E-04	5.74E-04
5	0.1	1.75E-03	1.87E-03	1.00E-03	1.15E-03

Backcalculated Creep Compliance Coefficients of K6-23 FWD Station at 43.3 ^{o}C

Do	D1	m	SSE
4.45E-04	1.69E-03	4.31E-01	2.29E-01

FIGURE D62   Comparison between the Measured and Predicted Values of Creep Compliance of K6-23 FWD Station at 43.3 ^{o}C

TABLE D20   Measured and Predicted values of Creep Compliance of K6-23 FWD Station at 54.4 ^{o}C (130 ^{o}F)

No	Frequency	J1 (1/MPa)		J2 (1/MPa)	
	(Hz.)	Measured	Predicted	Measured	Predicted
1	25	8.51E-04	9.32E-04	6.53E-05	9.19E-05
2	10	9.24E-04	9.87E-04	3.39E-04	1.41E-04
3	5	1.04E-03	1.05E-03	4.69E-04	1.96E-04
4	1	1.49E-03	1.29E-03	5.95E-04	4.16E-04
5	0.5	1.71E-03	1.47E-03	7.22E-04	5.75E-04
6	0.1	2.29E-03	2.18E-03	9.46E-04	1.22E-03

Backcalculated Creep Compliance Coefficients of K6-23 FWD Station at 54.4 ^{o}C

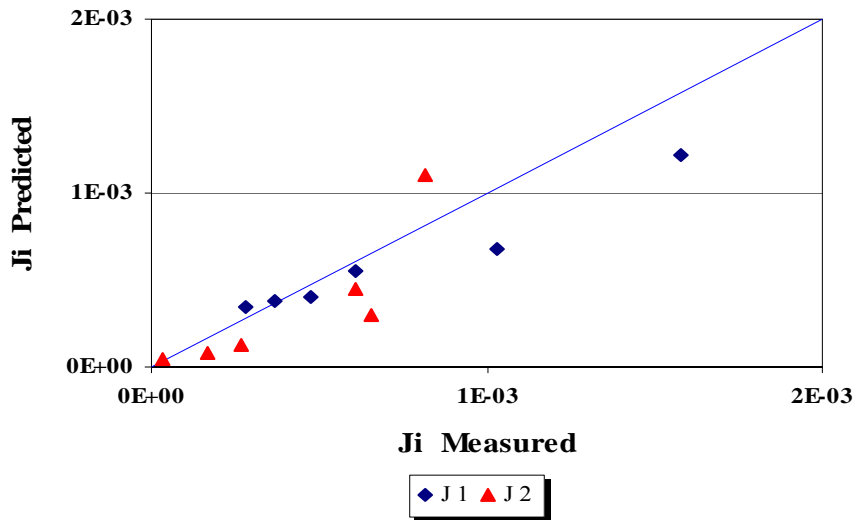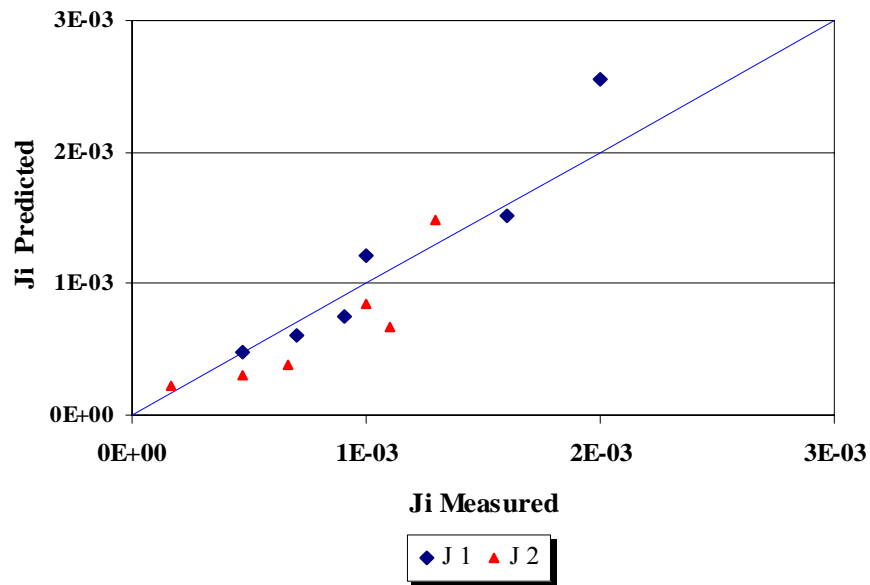| Do	D1	m	SSE
8.31E-04	1.65E-03	4.69E-01	1.12E+00

FIGURE D63   Comparison between the Measured and Predicted Values of Creep Compliance of K6-23 FWD Station at 54.4 ^{o}C

TABLE D21   **Measured and Predicted values of Creep Compliance of K6-29 FWD Station at 21.1 ^{o}C (70 ^{o}F)**

No	Frequency (Hz.)	J1 (1/MPa)		J2 (1/MPa)	
		Measured	Predicted	Measured	Predicted
1	10	7.80E-05	8.22E-05	1.00E-05	1.21E-05
2	5	8.60E-05	8.73E-05	1.90E-05	1.65E-05
3	1	1.10E-04	1.08E-04	5.00E-05	3.43E-05
4	0.5	1.30E-04	1.23E-04	4.90E-05	4.69E-05
5	0.1	1.90E-04	1.81E-04	8.50E-05	9.73E-05

Backcalculated Creep Compliance Coefficients of K6-23 FWD Station at 54.4 ^{o}C

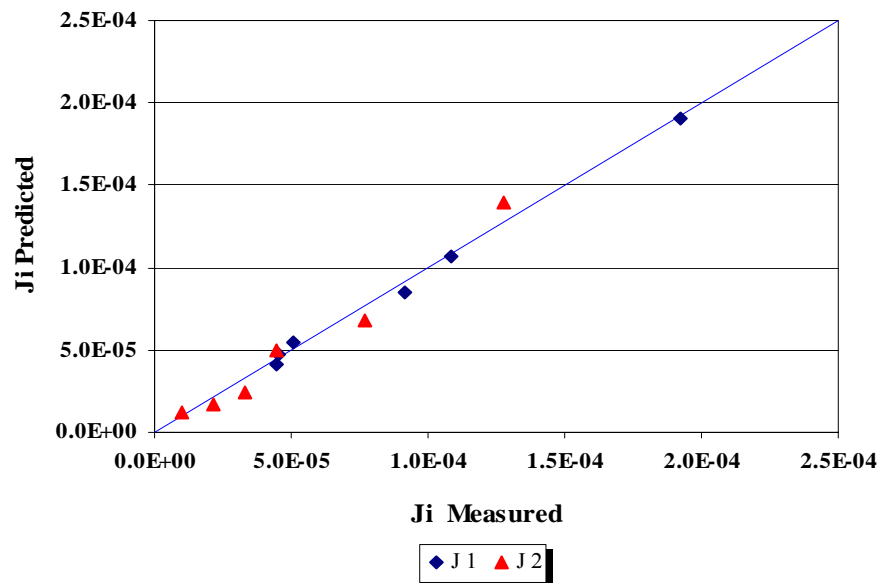| Do	D1	m	SSE
6.82E-05	1.36E-04	4.53E-01	1.91E-01
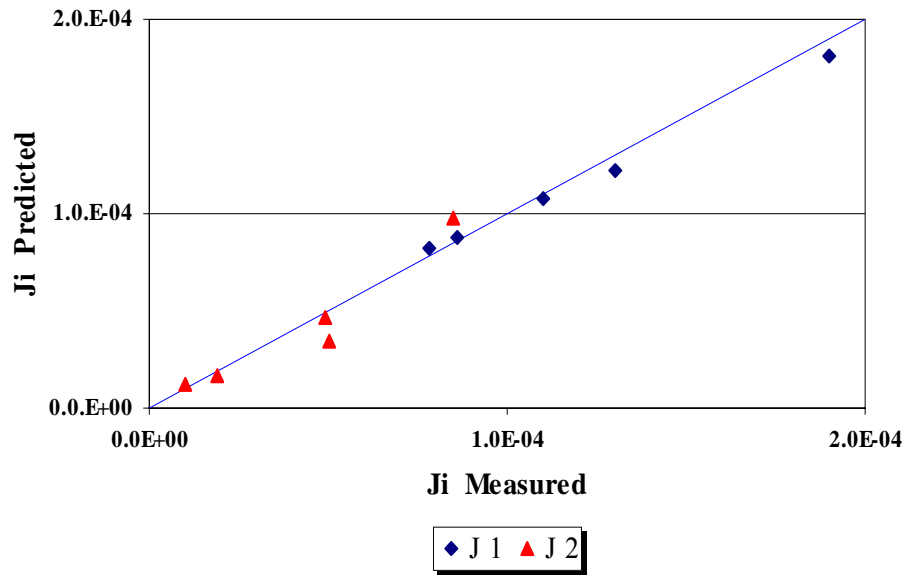
FIGURE D64   **Comparison between the Measured and Predicted Values of Creep Compliance of K6-29 FWD Station at 21.1 ^{o}C**

TABLE D22   Measured and Predicted values of Creep Compliance of K6-29 FWD Station at 29.4 $^{\circ}$C (85 $^{\circ}$F)

No	Frequency	J1 (1/MPa)		J2 (1/MPa)	
	(Hz.)	Measured	Predicted	Measured	Predicted
1	10	1.23E-04	1.26E-04	2.74E-05	3.02E-05
2	5	1.41E-04	1.39E-04	4.67E-05	4.31E-05
3	1	1.98E-04	1.92E-04	1.07E-04	9.82E-05
4	0.5	2.42E-04	2.32E-04	1.50E-04	1.40E-04
5	0.1	3.76E-04	4.05E-04	3.00E-04	3.19E-04

Backcalculated Creep Compliance Coefficients of K6-29 FWD Station at 29.4 $^{\circ}$C

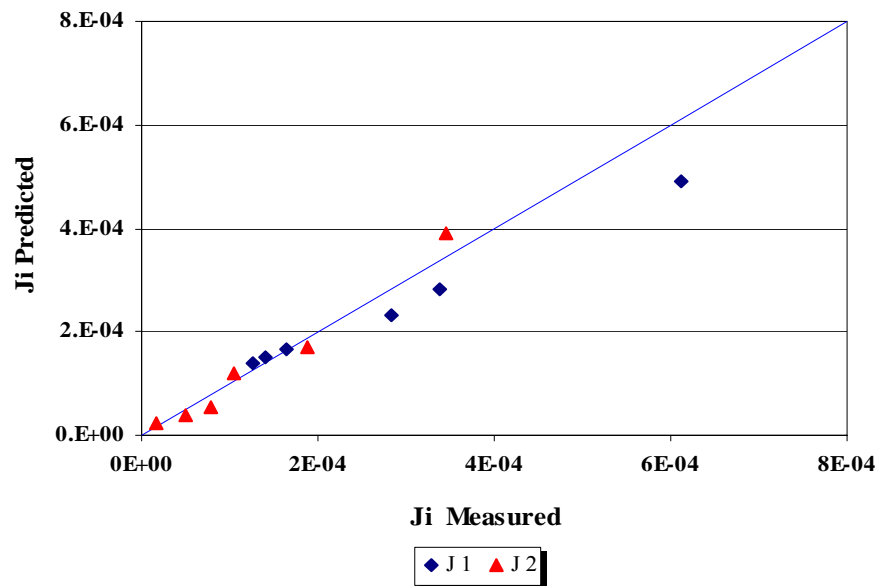| Do	D1	m	SSE
9.71E-05	3.94E-04	5.12E-01	4.21E-02
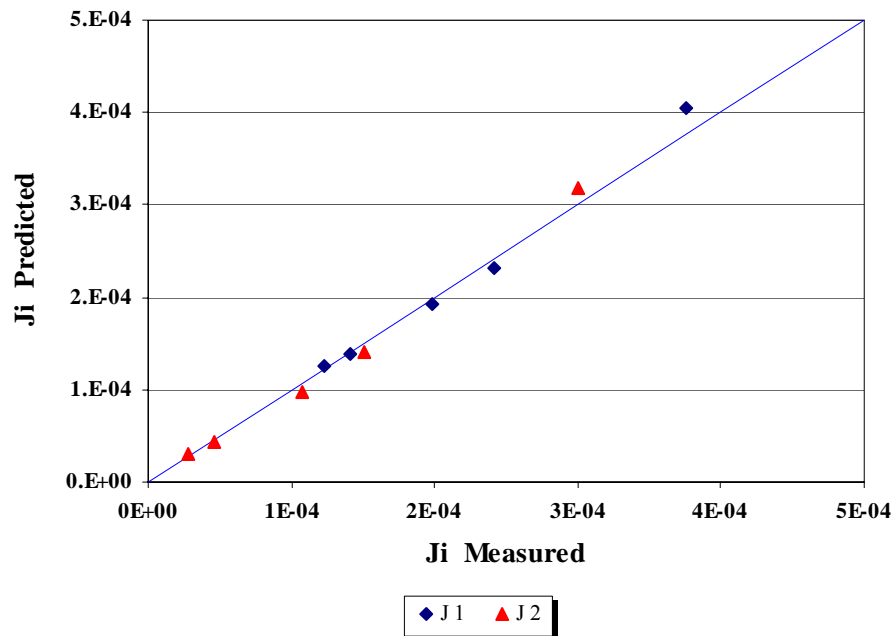
FIGURE D65   Comparison between the Measured and Predicted Values of Creep Compliance of K6-29 FWD Station at 29.4 $^{\circ}$C

TABLE D23   Measured and Predicted values of Creep Compliance of K6-29 FWD Station at 37.8 ^{o}C (100 ^{o}F)

No	Frequency (Hz.)	J1 (1/MPa)		J2 (1/MPa)	
		Measured	Predicted	Measured	Predicted
1	25	2.14E-04	2.70E-04	1.40E-05	2.07E-05
2	10	2.55E-04	2.80E-04	9.70E-05	3.78E-05
3	5	3.09E-04	2.93E-04	1.49E-04	5.96E-05
4	1	5.23E-04	3.60E-04	2.29E-04	1.72E-04
5	0.5	6.44E-04	4.19E-04	3.44E-04	2.71E-04
6	0.1	1.16E-03	7.23E-04	5.98E-04	7.82E-04

Backcalculated Creep Compliance Coefficients of K6-29 FWD Station at 37.8 ^{o}C

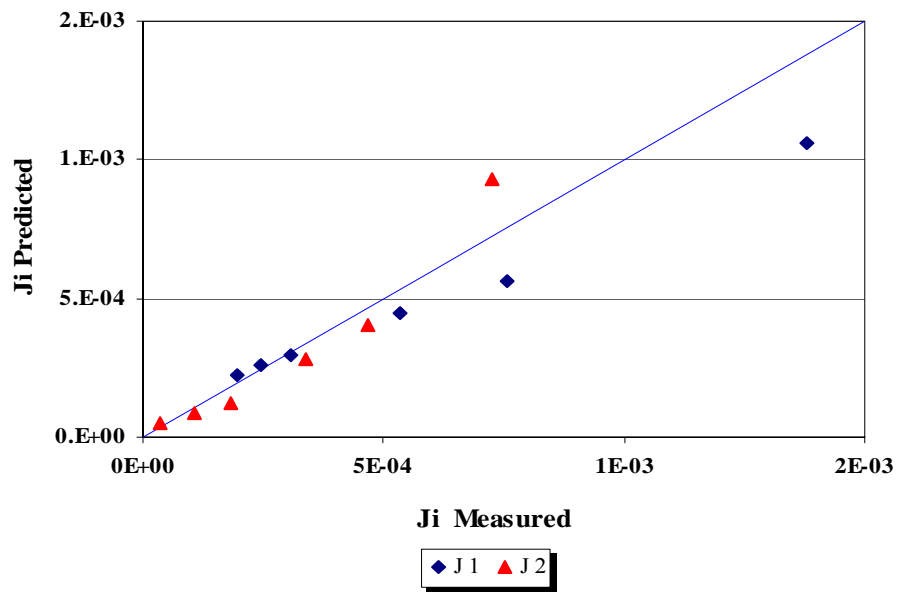| Do	D1	m	SSE
2.58E-04	7.44E-04	6.58E-01	1.61E+00

FIGURE D66   Comparison between the Measured and Predicted Values of Creep Compliance of K6-29 FWD Station at 37.8 ^{o}C

TABLE D24   Measured and Predicted values of Creep Compliance of K6-29 FWD Station at 43.3 ^{o}C (110 ^{o}F)

No	Frequency (Hz.)	J1 (1/MPa)		J2 (1/MPa)	
		Measured	Predicted	Measured	Predicted
1	25	2.26E-04	2.96E-04	1.71E-05	2.53E-05
2	10	2.91E-04	3.09E-04	1.07E-04	4.55E-05
3	5	3.52E-04	3.25E-04	1.73E-04	7.08E-05
4	1	6.31E-04	4.06E-04	2.23E-04	1.98E-04
5	0.5	8.22E-04	4.76E-04	4.18E-04	3.09E-04
6	0.1	1.51E-03	8.29E-04	6.66E-04	8.64E-04

Backcalculated Creep Compliance Coefficients of K6-29 FWD Station at 43.3 ^{o}C

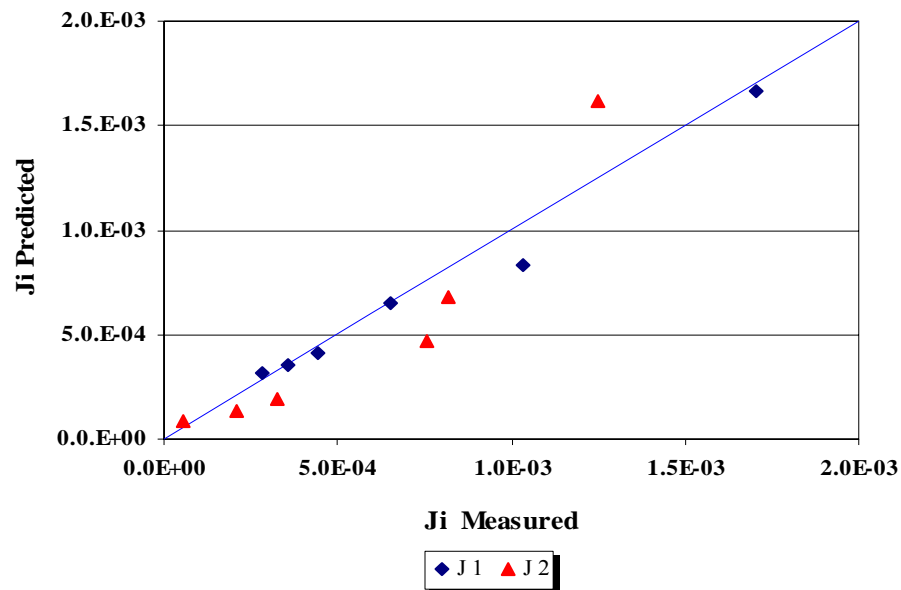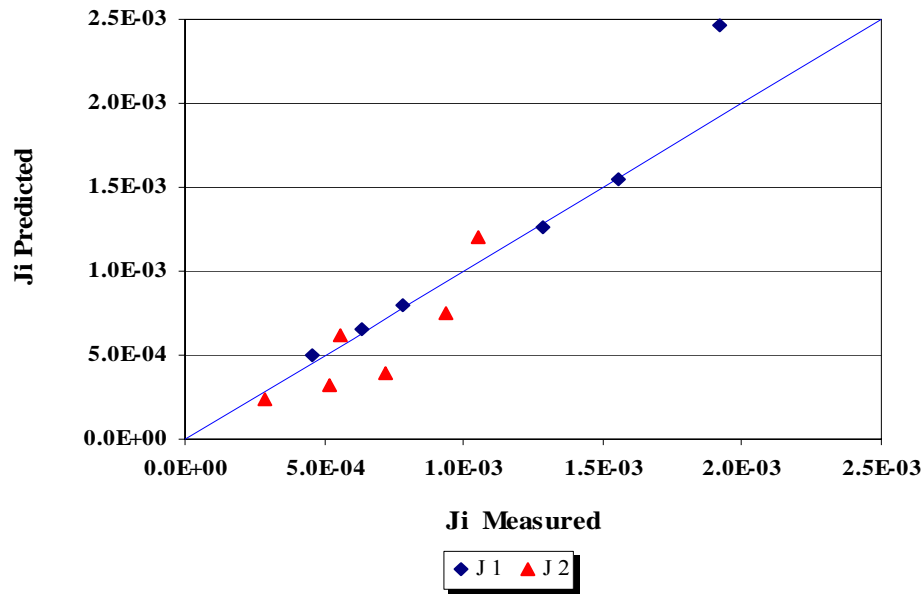| Do	D1	m	SSE
2.80E-04	8.46E-04	6.39E-01	1.69E+00

FIGURE D67   Comparison between the Measured and Predicted Values of Creep Compliance of K6-29 FWD Station at 43.3 ^{o}C

TABLE D25   **Measured and Predicted values of Creep Compliance of K6-29 FWD Station at 54.4 ^{o}C (130 ^{o}F)**

No	Frequency	J1 (1/MPa)		J2 (1/MPa)	
	(Hz.)	Measured	Predicted	Measured	Predicted
1	25	8.77E-04	9.27E-04	1.41E-04	1.90E-04
2	10	1.15E-03	1.04E-03	5.49E-04	3.04E-04
3	5	1.41E-03	1.16E-03	8.60E-04	4.34E-04
4	1	1.28E-03	1.69E-03	1.20E-03	9.92E-04
5	0.5	2.84E-03	2.10E-03	1.73E-03	1.42E-03
6	0.1	3.99E-03	3.85E-03	2.59E-03	3.24E-03

Backcalculated Creep Compliance Coefficients of K6-29 FWD Station at 54.4 ^{o}C

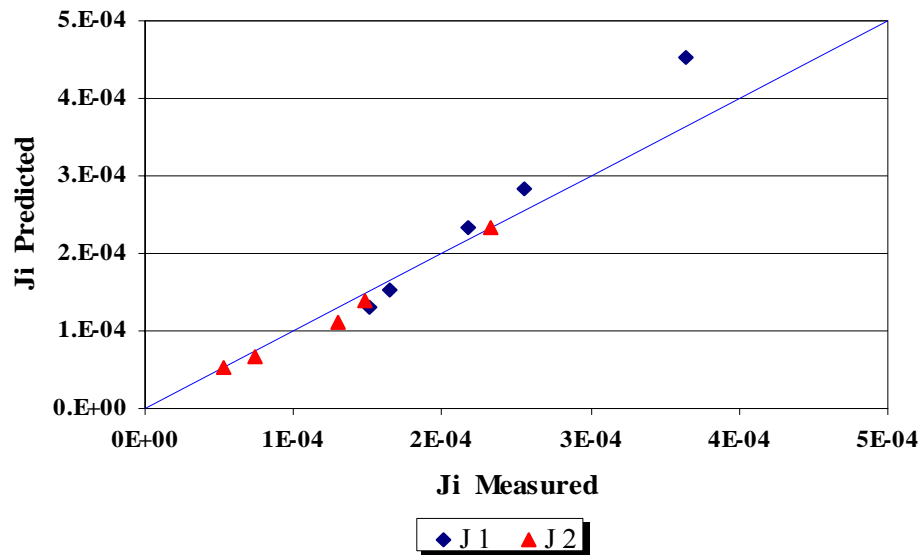| Do	D1	m	SSE
7.46E-04	3.98E-03	5.14E-01	9.09E-01

FIGURE D68   **Comparison between the Measured and Predicted Values of Creep Compliance of K6-29 FWD Station at 54.4 ^{o}C**

TABLE D26   Measured and Predicted values of Creep Compliance of K6-48 FWD Station at 21.1 ^{o}C (70 ^{o}F)

No	Frequency	J1 (1/MPa)		J2 (1/MPa)	
	(Hz.)	Measured	Predicted	Measured	Predicted
1	10	2.18E-04	2.22E-04	3.95E-05	4.31E-05
2	5	2.41E-04	2.41E-04	5.96E-05	5.53E-05
3	1	3.00E-04	3.09E-04	9.67E-05	9.86E-05
4	0.5	3.71E-04	3.53E-04	1.46E-04	1.26E-04
5	0.1	5.23E-04	5.10E-04	2.09E-04	2.25E-04

Backcalculated Creep Compliance Coefficients of K6-48 FWD Station at 21.1 ^{o}C

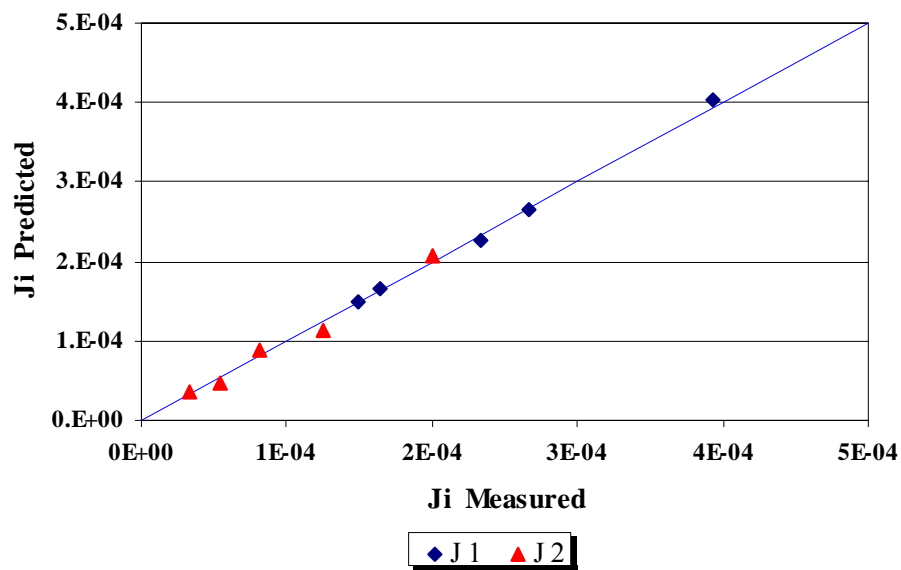| Do	D1	m	SSE
1.53E-04	4.01E-04	3.59E-01	4.34E-02

FIGURE D69   Comparison between the Measured and Predicted Values of Creep Compliance of K6-48 FWD Station at 21.1 ^{o}C

TABLE D27   Measured and Predicted values of Creep Compliance of K6-48 FWD Station at 29.4 ^{o}C (85 ^{o}F)

No	Frequency	J1 (1/MPa)		J2 (1/MPa)	
	(Hz.)	Measured	Predicted	Measured	Predicted
1	10	2.94E-04	2.93E-04	5.18E-05	6.31E-05
2	5	3.29E-04	3.21E-04	1.03E-04	8.30E-05
3	1	4.20E-04	4.24E-04	2.36E-04	1.57E-04
4	0.5	5.05E-04	4.94E-04	2.36E-04	2.06E-04
5	0.1	7.02E-04	7.50E-04	3.36E-04	3.90E-04

Backcalculated Creep Compliance Coefficients of K6-48 FWD Station at 29.4 ^{o}C

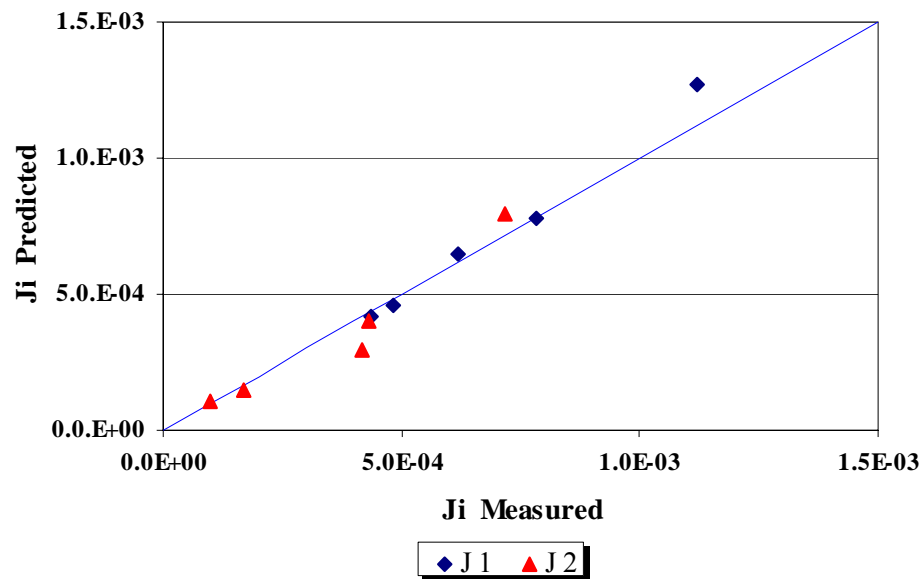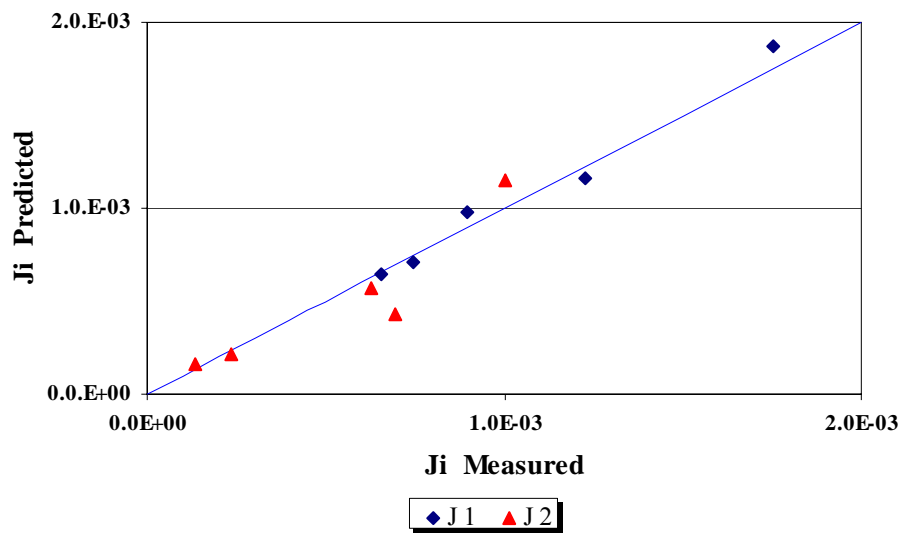| Do	D1	m	SSE
2.05E-04	6.28E-04	3.96E-01	2.47E-01

FIGURE D70   Comparison between the Measured and Predicted Values of Creep Compliance of K6-48 FWD Station at 29.4 ^{o}C

TABLE D28   Measured and Predicted values of Creep Compliance of K6-48 FWD Station at 37.8 ^{o}C (100 ^{o}F)

No	Frequency (Hz.)	J1 (1/MPa)		J2 (1/MPa)	
		Measured	Predicted	Measured	Predicted
1	10	2.95E-04	2.91E-04	5.19E-05	6.29E-05
2	5	3.22E-04	3.19E-04	1.01E-04	8.29E-05
3	1	4.16E-04	4.22E-04	2.35E-04	1.58E-04
4	0.5	5.05E-04	4.92E-04	2.36E-04	2.08E-04
5	0.1	7.10E-04	7.50E-04	3.40E-04	3.94E-04

Backcalculated Creep Compliance Coefficients of K6-48 FWD Station at 37.8 ^{o}C

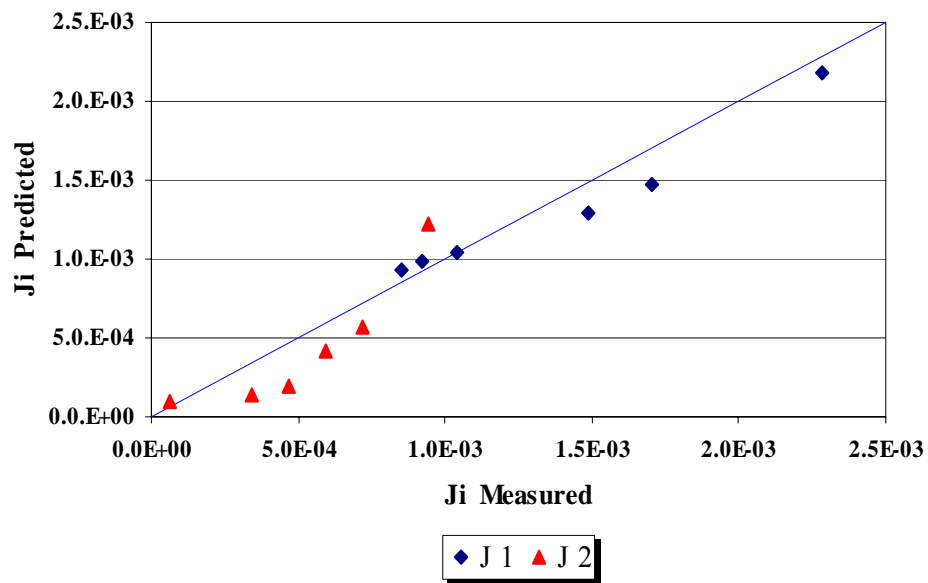| Do	D1	m	SSE
2.04E-04	6.30E-04	3.99E-01	2.29E-01

FIGURE D71   Comparison between the Measured and Predicted Values of Creep Compliance of K6-48 FWD Station at 37.8 ^{o}C

TABLE D29   Measured and Predicted values of Creep Compliance of K6-48 FWD Station at 46.6 ^{o}C (115 ^{o}F)

No	Frequency	J1 (1/MPa)		J2 (1/MPa)	
	(Hz.)	Measured	Predicted	Measured	Predicted
1	25	3.28E-04	3.69E-04	3.53E-05	5.00E-05
2	10	3.72E-04	3.99E-04	1.31E-04	7.49E-05
3	5	4.37E-04	4.31E-04	1.73E-04	1.02E-04
4	1	6.75E-04	5.58E-04	2.70E-04	2.07E-04
5	0.5	7.76E-04	6.47E-04	3.32E-04	2.81E-04
6	0.1	1.08E-03	9.97E-04	4.47E-04	5.72E-04

Backcalculated Creep Compliance Coefficients of K6-48 FWD Station at 37.8 ^{o}C

| Do	D1	m	SSE
3.08E-04	8.23E-04	4.41E-01	7.68E-01

FIGURE D72   Comparison between the Measured and Predicted Values of Creep Compliance of K6-48 FWD Station at 46.6 ^{o}C

272

TABLE D30   Measured and Predicted values of Creep Compliance of K6-48 FWD Station at 54.4 °C (130 °F)

No	Frequency (Hz.)	J1 (1/MPa)		J2 (1/MPa)	
		Measured	Predicted	Measured	Predicted
1	25	1.81E-04	2.40E-04	3.32E-04	1.59E-04
2	10	3.46E-04	3.38E-04	3.56E-04	2.23E-04
3	5	4.99E-04	4.37E-04	4.70E-04	2.89E-04
4	1	8.18E-04	7.95E-04	5.89E-04	5.26E-04
5	0.5	9.97E-04	1.03E-03	7.74E-04	6.81E-04
6	0.1	1.55E-03	1.87E-03	9.69E-04	1.24E-03

Backcalculated Creep Compliance Coefficients of K6-48 FWD Station at 54.4 °C

| Do	D1	m	SSE
2.69E-11	2.13E-03	3.72E-01	8.33E-01

FIGURE D73   Comparison between the Measured and Predicted Values of Creep Compliance of K6-48 FWD Station at 54.4 °C

Lane K7

TABLE D31 Measured and Predicted values of Creep Compliance of K7-3 FWD Station at 21.1 ^{o}C (70 ^{o}F)

No	Frequency	J1 (1/MPa)		J2 (1/MPa)	
	(Hz.)	Measured	Predicted	Measured	Predicted
1	10	1.29E-04	1.30E-04	2.01E-05	2.31E-05
2	5	1.39E-04	1.40E-04	3.40E-05	3.04E-05
3	1	1.77E-04	1.78E-04	7.17E-05	5.77E-05
4	0.5	2.07E-04	2.03E-04	7.78E-05	7.60E-05
5	0.1	2.99E-04	2.97E-04	1.31E-04	1.44E-04

Backcalculated Creep Compliance Coefficients of K7-3 FWD Station at 21.1 ^{o}C

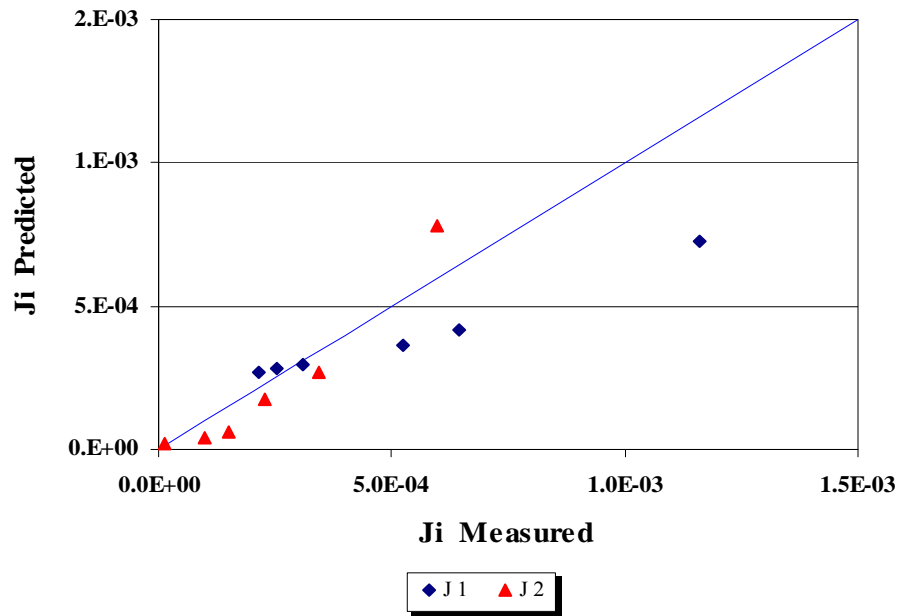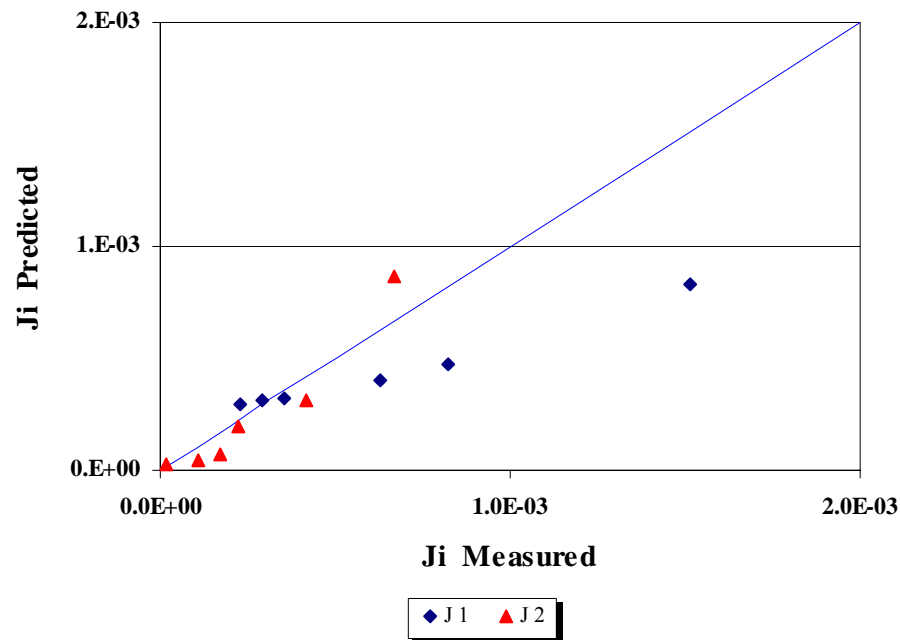| Do	D1	m	SSE
9.76E-05	2.31E-04	3.98E-01	8.31E-02

FIGURE D74   Comparison between the Measured and Predicted Values of Creep Compliance of K7-3 FWD Station at 21.1 ^{o}C

TABLE D31 Measured and Predicted values of Creep Compliance of K7-3 FWD Station at 29.4 °C (85 °F)

No	Frequency (Hz.)	J1 (1/MPa)		J2 (1/MPa)	
		Measured	Predicted	Measured	Predicted
1	25	1.70E-04	1.30E-04	3.63E-05	4.21E-05
2	10	1.31E-04	1.53E-04	1.19E-04	7.05E-05
3	5	2.08E-04	1.81E-04	1.54E-04	1.04E-04
4	1	3.27E-04	3.06E-04	2.91E-04	2.57E-04
5	0.5	3.17E-04	4.07E-04	3.31E-04	3.79E-04

Backcalculated Creep Compliance Coefficients of K7-3 FWD Station at 29.4 °C

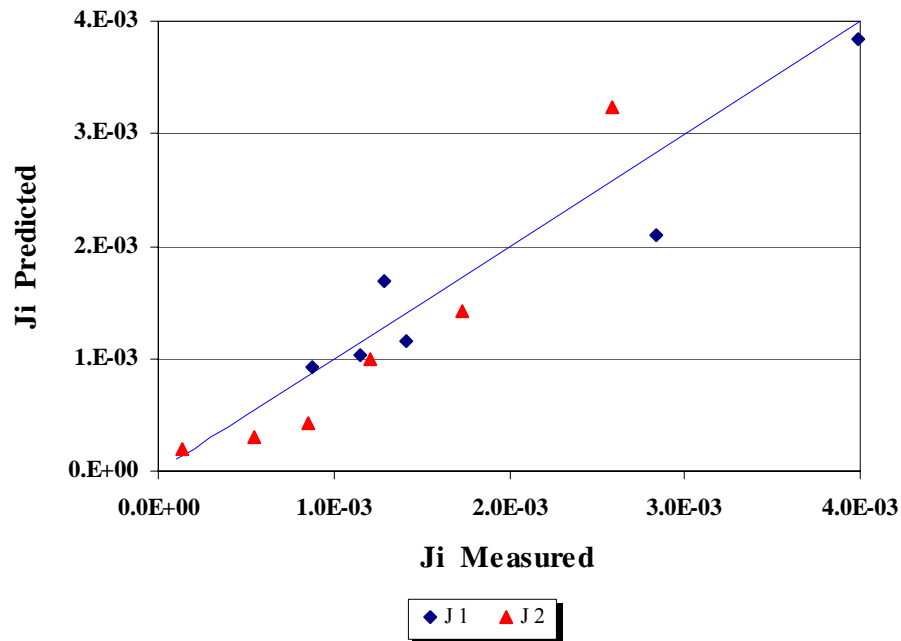| Do	D1	m	SSE
9.50E-05	1.05E-03	5.61E-01	5.23E-01

FIGURE D75 Comparison between the Measured and Predicted Values of Creep Compliance of K7-3 FWD Station at 29.4 °C

TABLE D31   Measured and Predicted values of Creep Compliance of K7-3 FWD Station at 37.8 °C (100 °F)

No	Frequency	J1 (1/MPa)		J2 (1/MPa)	
	(Hz.)	Measured	Predicted	Measured	Predicted
1	25	2.81E-04	2.99E-04	4.09E-05	5.60E-05
2	10	3.11E-04	3.31E-04	1.22E-04	8.91E-05
3	5	3.63E-04	3.68E-04	1.91E-04	1.27E-04
4	1	5.91E-04	5.24E-04	3.22E-04	2.87E-04
5	0.5	7.39E-04	6.42E-04	4.60E-04	4.07E-04
6	0.1	1.32E-03	1.14E-03	7.46E-04	9.21E-04

Backcalculated Creep Compliance Coefficients of K7-3 FWD Station at 37.84 °C

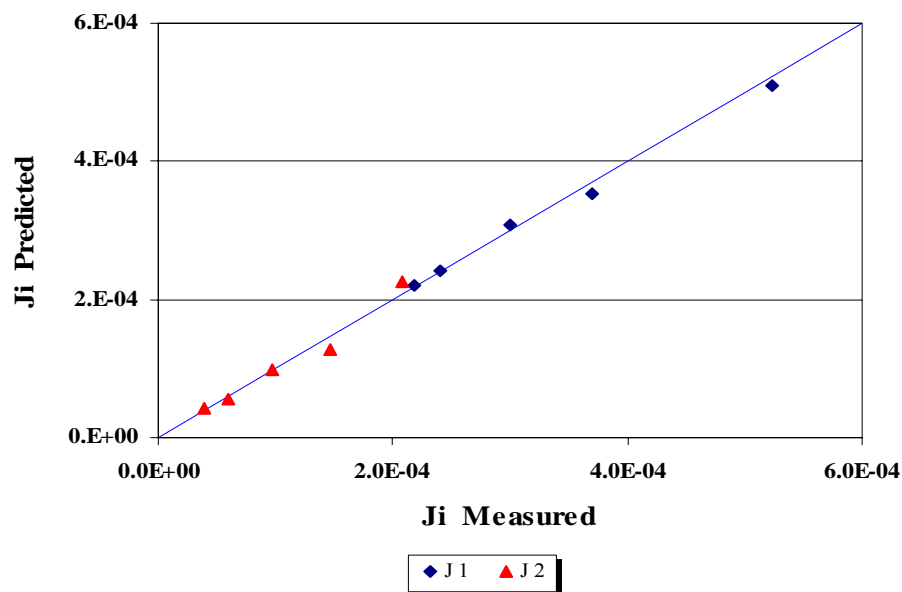| Do	D1	m	SSE
2.44E-04	1.15E-03	5.07E-01	4.59E-01

FIGURE D76   Comparison between the Measured and Predicted Values of Creep Compliance of K7-3 FWD Station at 37.8 °C

TABLE D32   Measured and Predicted values of Creep Compliance of K7-3 FWD Station at 43.3 °C (110 °F)

No	Frequency	J1 (1/MPa)		J2 (1/MPa)	
	(Hz.)	Measured	Predicted	Measured	Predicted
1	10	5.20E-04	5.11E-04	1.61E-04	1.87E-04
2	5	6.10E-04	5.90E-04	2.88E-04	2.58E-04
3	1	8.15E-04	9.11E-04	7.49E-04	5.44E-04
4	0.5	1.24E-03	1.14E-03	8.30E-04	7.50E-04
5	0.1	2.04E-03	2.07E-03	1.38E-03	1.58E-03

Backcalculated Creep Compliance Coefficients of K7-3 FWD Station at 43.3 °C

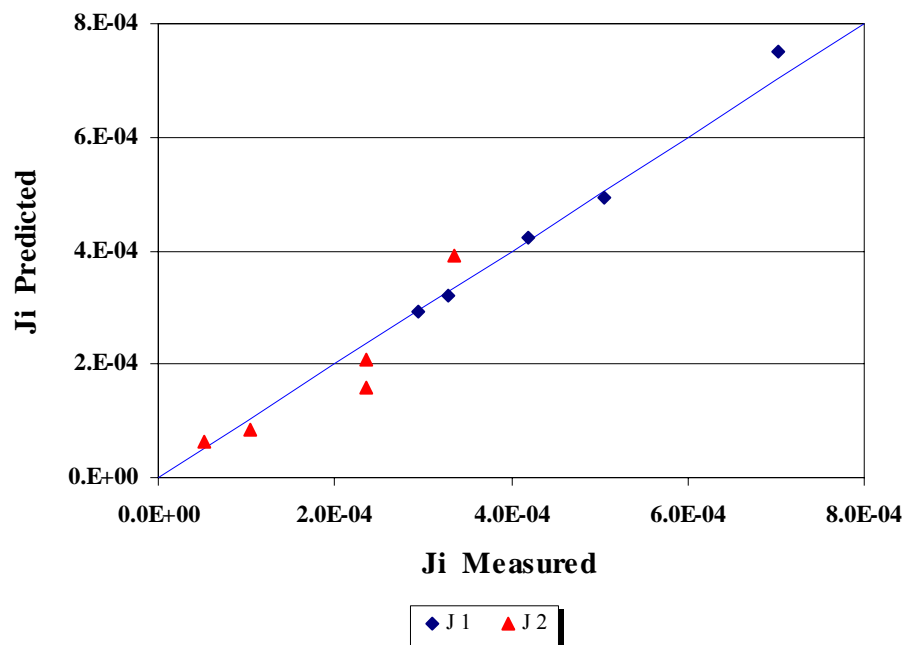| Do	D1	m	SSE
3.01E-04	2.16E-03	4.64E-01	1.64E-01

FIGURE D77   Comparison between the Measured and Predicted Values of Creep Compliance of K7-3 FWD Station at 43.3 °C

TABLE D33   Measured and Predicted values of Creep Compliance of K7-3 FWD Station at 54.4 ^{o}C (130 ^{o}F)

No	Frequency	J1 (1/MPa)		J2 (1/MPa)	
	(Hz.)	Measured	Predicted	Measured	Predicted
1	25	7.74E-04	8.85E-04	1.41E-04	2.00E-04
2	10	9.58E-04	1.01E-03	4.94E-04	2.79E-04
3	5	1.16E-03	1.13E-03	6.39E-04	3.59E-04
4	1	1.85E-03	1.58E-03	6.61E-04	6.43E-04
5	0.5	2.43E-03	1.86E-03	1.06E-03	8.28E-04
6	0.1	3.43E-03	2.89E-03	1.17E-03	1.48E-03

Backcalculated Creep Compliance Coefficients of K7-3 FWD Station at 54.4 ^{o}C

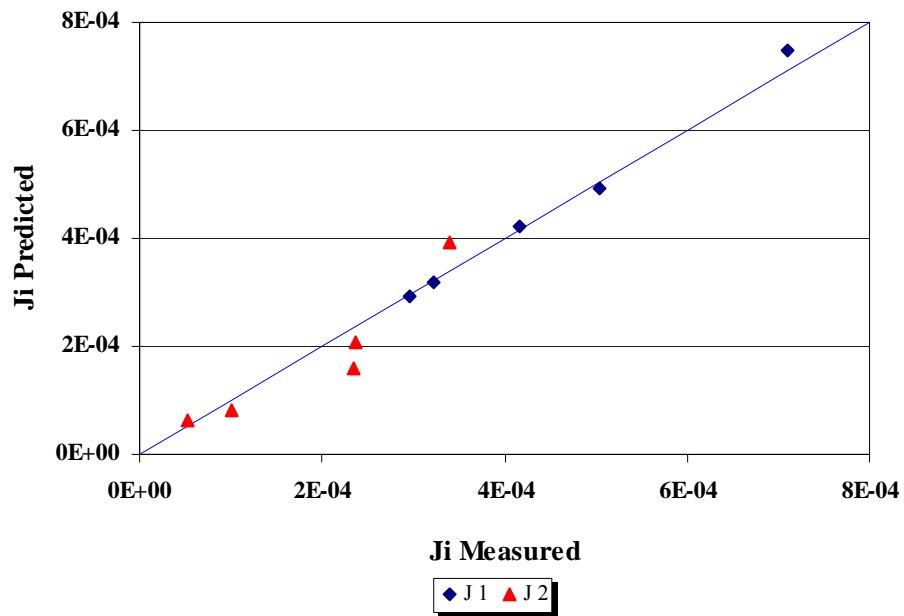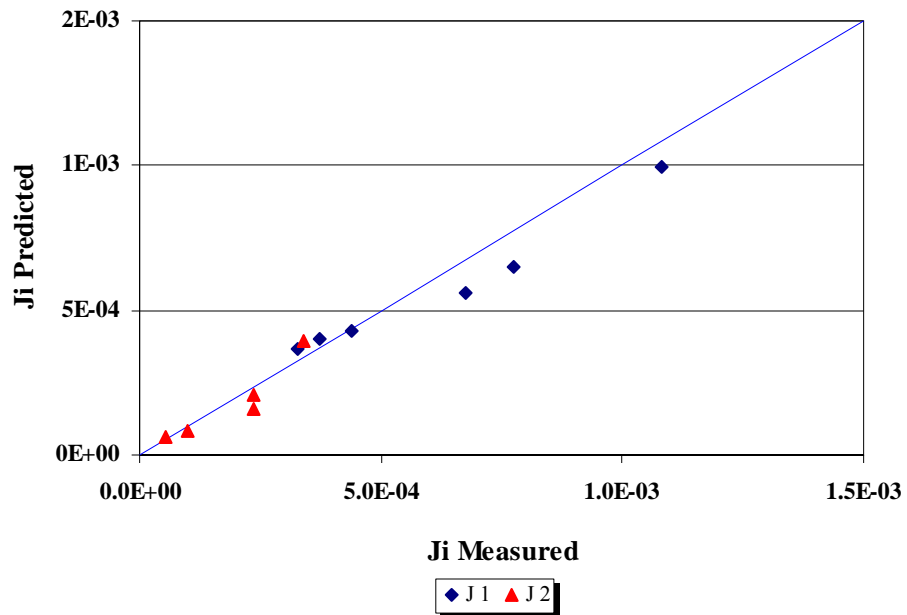| Do	D1	m	SSE
5.73E-04	2.61E-03	3.63E-01	8.02E-01

FIGURE D78   Comparison between the Measured and Predicted Values of Creep Compliance of K7-3 FWD Station at 54.4 ^{o}C

TABLE D34   Measured and Predicted values of Creep Compliance of K7-11 FWD Station at 21.1 °C (70 °F)

No	Frequency	J1 (1/MPa)		J2 (1/MPa)	
	(Hz.)	Measured	Predicted	Measured	Predicted
1	25	2.02E-05	1.55E-05	1.25E-05	1.16E-05
2	10	2.16E-05	2.25E-05	1.85E-05	1.68E-05
3	5	2.58E-05	2.99E-05	2.70E-05	2.23E-05
4	1	5.43E-05	5.77E-05	4.29E-05	4.30E-05
5	0.5	6.98E-05	7.65E-05	6.56E-05	5.70E-05
6	0.1	1.30E-04	1.47E-04	1.07E-04	1.10E-04

Backcalculated Creep Compliance Coefficients of K7-11 FWD Station at 21.1 °C

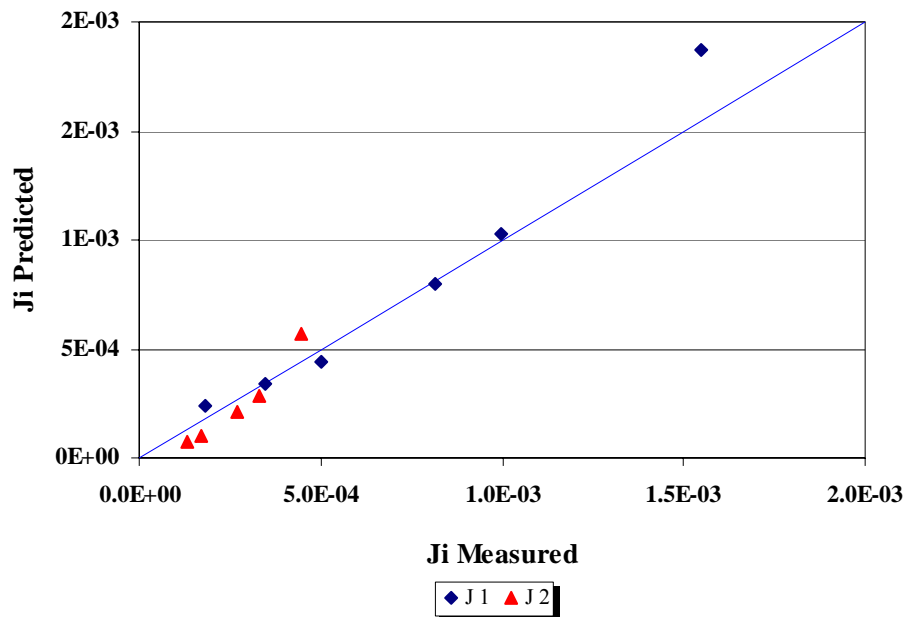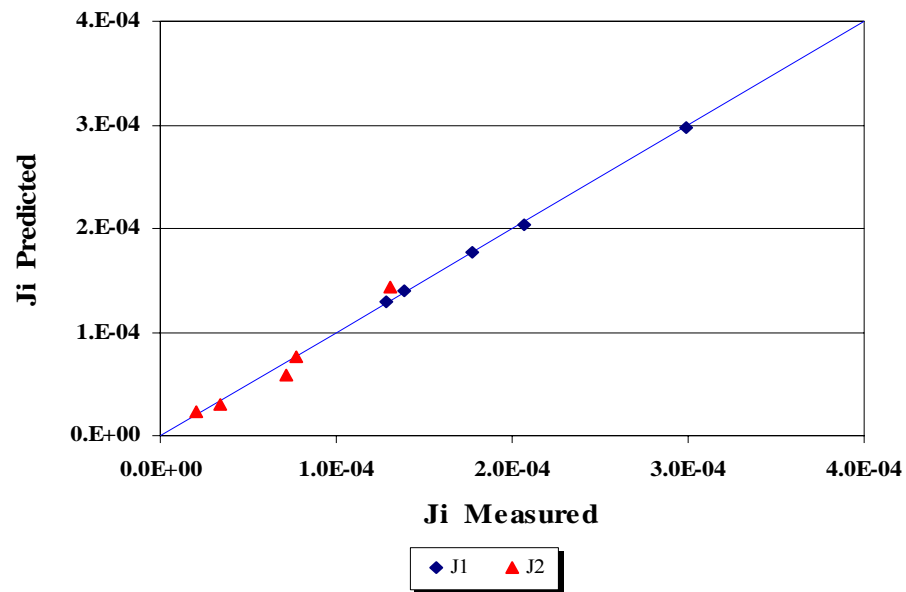| Do	D1	m	SSE
2.69E-11	1.72E-04	4.08E-01	1.74E-01

FIGURE D79   Comparison between the Measured and Predicted Values of Creep Compliance of K7-11 FWD Station at 21.1 °C

TABLE D35   Measured and Predicted values of Creep Compliance of K7-11 FWD Station at 29.4 ^{o}C (85 ^{o}F)

No	Frequency (Hz.)	J1 (1/MPa)		J2 (1/MPa)	
		Measured	Predicted	Measured	Predicted
1	10	1.44E-04	1.32E-04	3.70E-05	3.97E-05
2	5	1.63E-04	1.49E-04	6.52E-05	5.54E-05
3	1	2.03E-04	2.18E-04	1.63E-04	1.20E-04
4	0.5	2.61E-04	2.68E-04	1.82E-04	1.68E-04
5	0.1	3.82E-04	4.76E-04	3.44E-04	3.64E-04

Backcalculated Creep Compliance Coefficients of K7-11 FWD Station at 29.4 ^{o}C

Do	D1	m	SSE
9.01E-05	4.79E-04	4.81E-01	1.87E-01

FIGURE D80   Comparison between the Measured and Predicted Values of Creep Compliance of K7-11 FWD Station at 29.4 ^{o}C

**TABLE D36   Measured and Predicted values of Creep Compliance of K7-11
FWD Station at 37.8 ^{o}C (100 ^{o}F)**

No	Frequency	J1 (1/MPa)		J2 (1/MPa)	
	(Hz.)	Measured	Predicted	Measured	Predicted
1	25	1.40E-04	1.25E-04	3.70E-05	4.33E-05
2	10	1.53E-04	1.50E-04	1.08E-04	7.11E-05
3	5	1.92E-04	1.78E-04	1.58E-04	1.04E-04
4	1	2.56E-04	3.04E-04	3.63E-04	2.48E-04
5	0.5	3.96E-04	4.03E-04	4.35E-04	3.60E-04
6	0.1	6.44E-04	8.43E-04	7.65E-04	8.62E-04

Backcalculated Creep Compliance Coefficients of K7-11 FWD Station at 37.8 ^{o}C

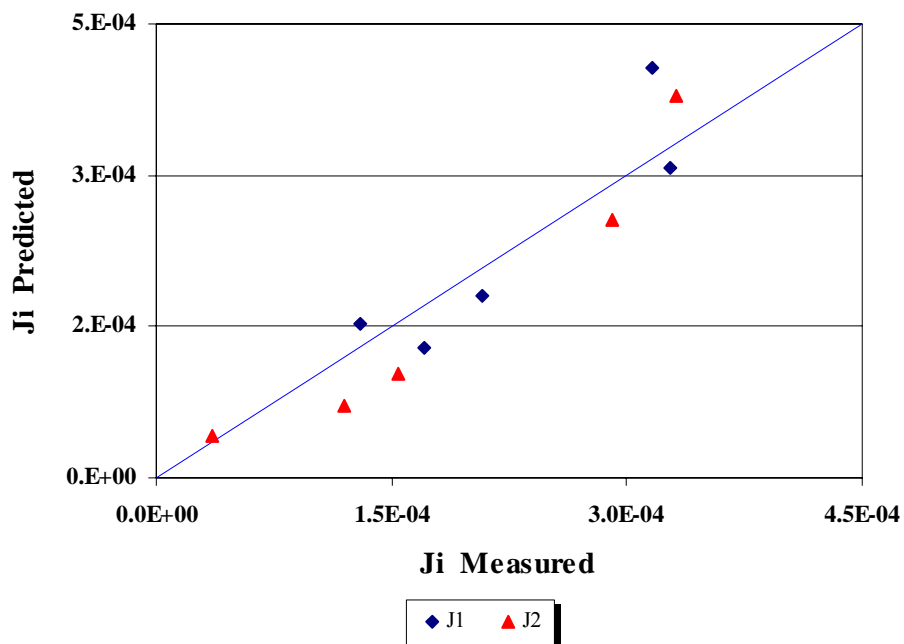| Do	D1	m	SSE
8.74E-05	1.00E-03	5.42E-01	5.60E-01

**FIGURE D81   Comparison between the Measured and Predicted Values of Creep
Compliance of K7-11 FWD Station at 37.8 ^{o}C**

TABLE D37   Measured and Predicted values of Creep Compliance of K7-11 FWD Station at 43.3 °C (110 °F)

No	Frequency	J1 (1/MPa)		J2 (1/MPa)	
	(Hz.)	Measured	Predicted	Measured	Predicted
1	25	2.94E-04	3.40E-04	3.85E-05	5.63E-05
2	10	3.59E-04	3.71E-04	1.77E-04	9.62E-05
3	5	4.59E-04	4.08E-04	2.72E-04	1.44E-04
4	1	6.03E-04	5.80E-04	6.60E-04	3.69E-04
5	0.5	9.60E-04	7.21E-04	6.98E-04	5.54E-04
6	0.1	1.54E-03	1.38E-03	1.07E-03	1.42E-03

Backcalculated Creep Compliance Coefficients of K7-11 FWD Station at 43.3 °C

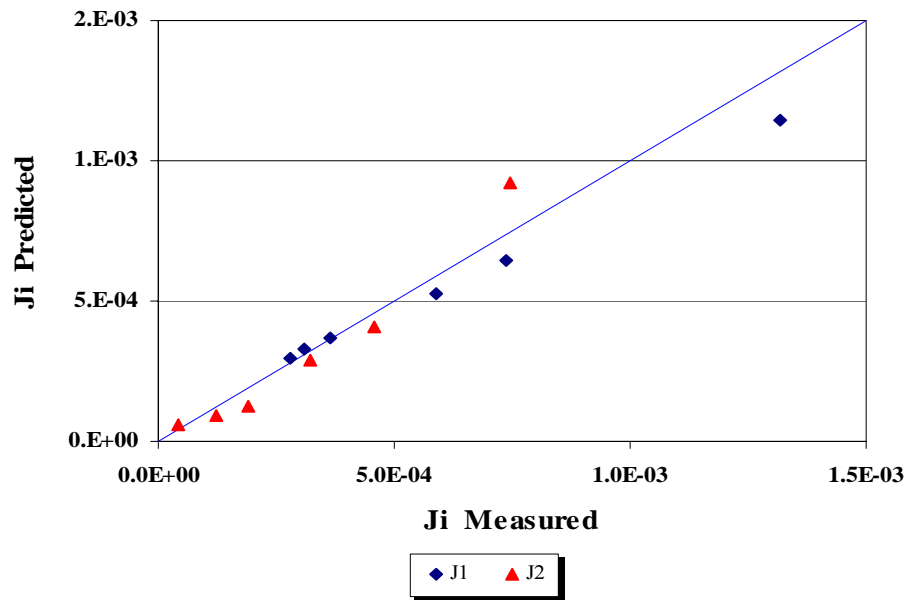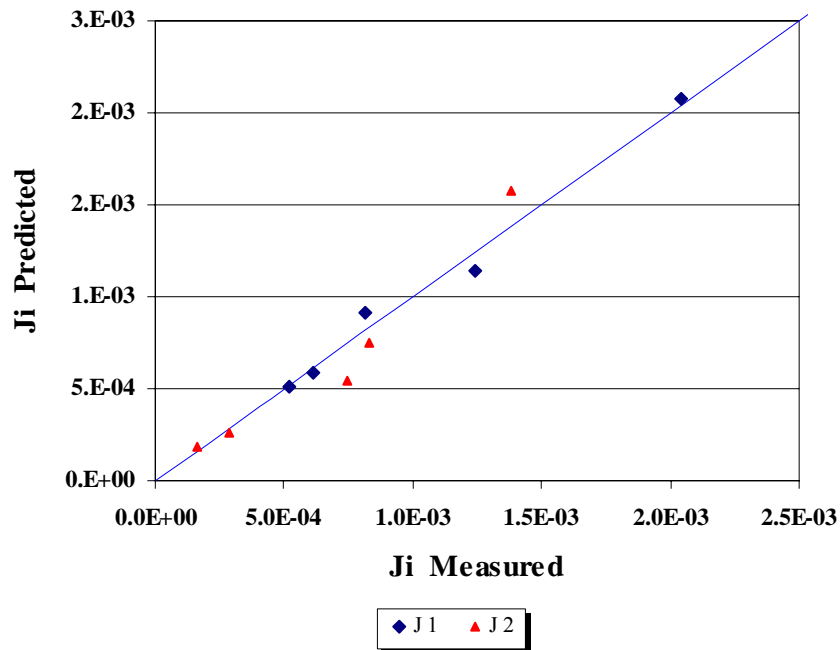| Do	D1	m	SSE
2.97E-04	1.53E-03	5.84E-01	1.10E+00

FIGURE D82   Comparison between the Measured and Predicted Values of Creep Compliance of K7-11 FWD Station at 43.3 °C

**TABLE D38   Measured and Predicted values of Creep Compliance of K7-11
FWD Station at 54.4 ^{o}C (130 ^{o}F)**

No	Frequency	J1 (1/MPa)		J2 (1/MPa)	
	(Hz.)	Measured	Predicted	Measured	Predicted
1	25	7.68E-04	8.80E-04	7.79E-05	1.11E-04
2	10	9.50E-04	9.43E-04	3.97E-04	1.78E-04
3	5	1.13E-03	1.02E-03	5.66E-04	2.55E-04
4	1	1.27E-03	1.33E-03	1.15E-03	5.87E-04
5	0.5	2.00E-03	1.57E-03	1.01E-03	8.41E-04
6	0.1	2.77E-03	2.60E-03	1.49E-03	1.94E-03

Backcalculated Creep Compliance Coefficients of K7-11 FWD Station at 54.4 ^{o}C

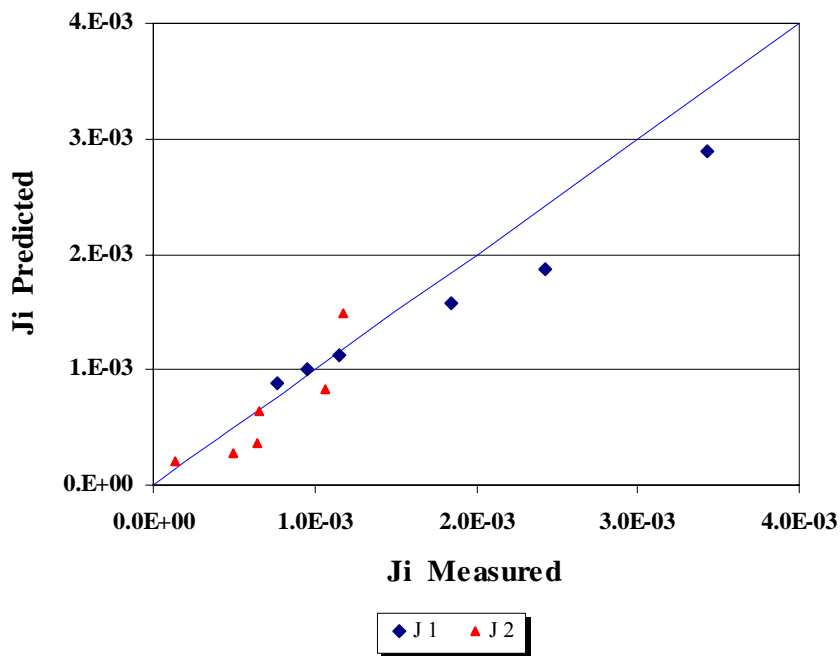| Do	D1	m	SSE
7.75E-04	2.36E-03	5.18E-01	1.22E+00

**FIGURE D83   Comparison between the Measured and Predicted Values of Creep
Compliance of K7-11 FWD Station at 54.4 ^{o}C**

TABLE D39 Measured and Predicted values of Creep Compliance of K7-15 FWD Station at 21.1 ^{o}C (70 ^{o}F)

No	Frequency	J1 (1/MPa)		J2 (1/MPa)	
	(Hz.)	Measured	Predicted	Measured	Predicted
1	25	7.94E-05	6.78E-05	1.52E-05	1.79E-05
2	10	7.51E-05	7.87E-05	3.06E-05	2.58E-05
3	5	8.51E-05	9.01E-05	4.45E-05	3.40E-05
4	1	1.30E-04	1.32E-04	6.83E-05	6.46E-05
5	0.5	1.56E-04	1.61E-04	8.76E-05	8.52E-05
6	0.1	2.54E-04	2.67E-04	1.49E-04	1.62E-04

Backcalculated Creep Compliance Coefficients of K7-15 FWD Station at 21.1 ^{o}C

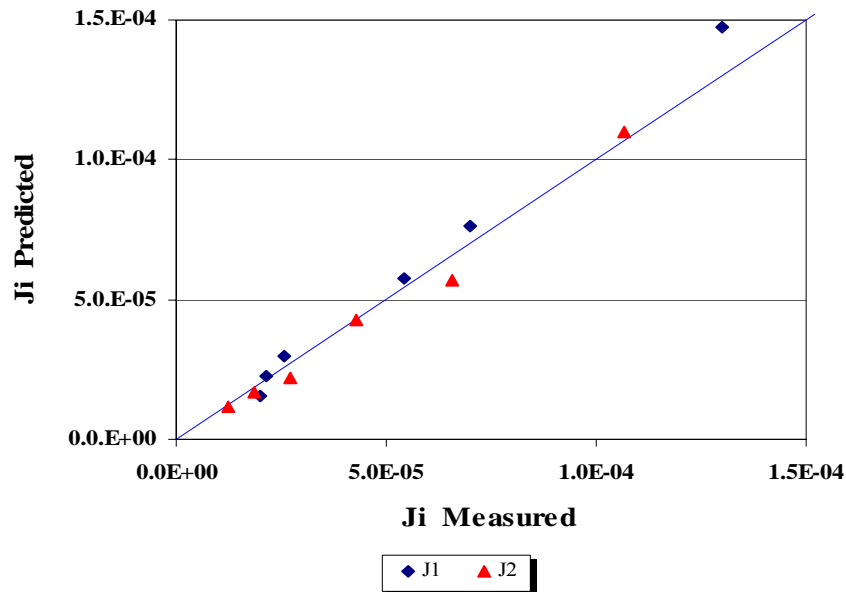| Do	D1	m	SSE
4.31E-05	2.58E-04	3.99E-01	1.55E-01

FIGURE D84   Comparison between the Measured and Predicted Values of   Creep Compliance of K7-15 FWD Station at 21.1 ^{o}C

TABLE D40   Measured and Predicted values of Creep Compliance of K7-15 FWD Station at 29.4 (85 °F)

No	Frequency	J1 (1/MPa)		J2 (1/MPa)	
	(Hz.)	Measured	Predicted	Measured	Predicted
1	25	1.07E-04	9.88E-05	2.75E-05	3.29E-05
2	10	1.09E-04	1.18E-04	6.04E-05	4.93E-05
3	5	1.31E-04	1.40E-04	8.31E-05	6.69E-05
4	1	2.38E-04	2.23E-04	1.25E-04	1.36E-04
5	0.5	2.95E-04	2.82E-04	1.90E-04	1.85E-04
6	0.1	5.42E-04	5.12E-04	3.52E-04	3.75E-04

Backcalculated Creep Compliance Coefficients of K7-15 FWD Station at 29.4 °C

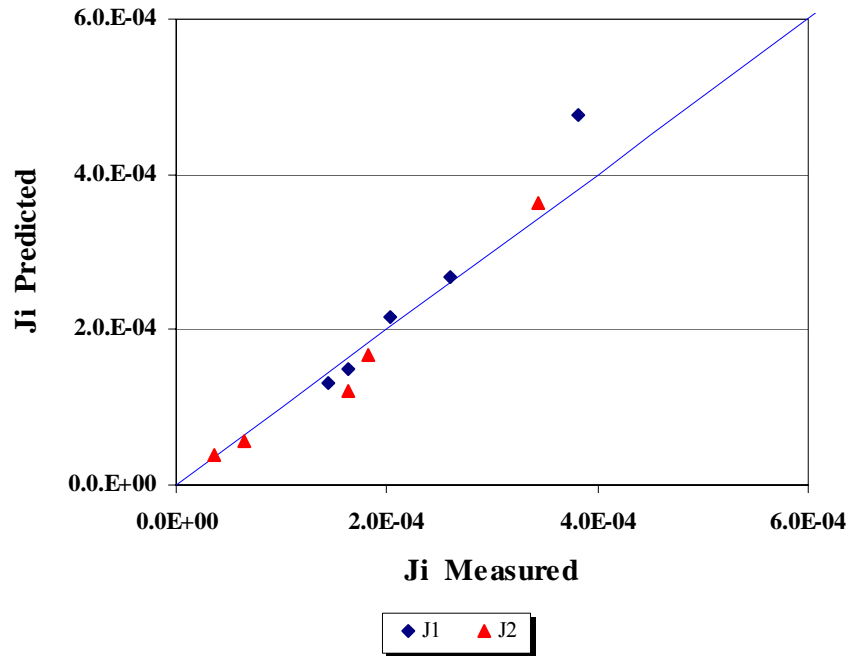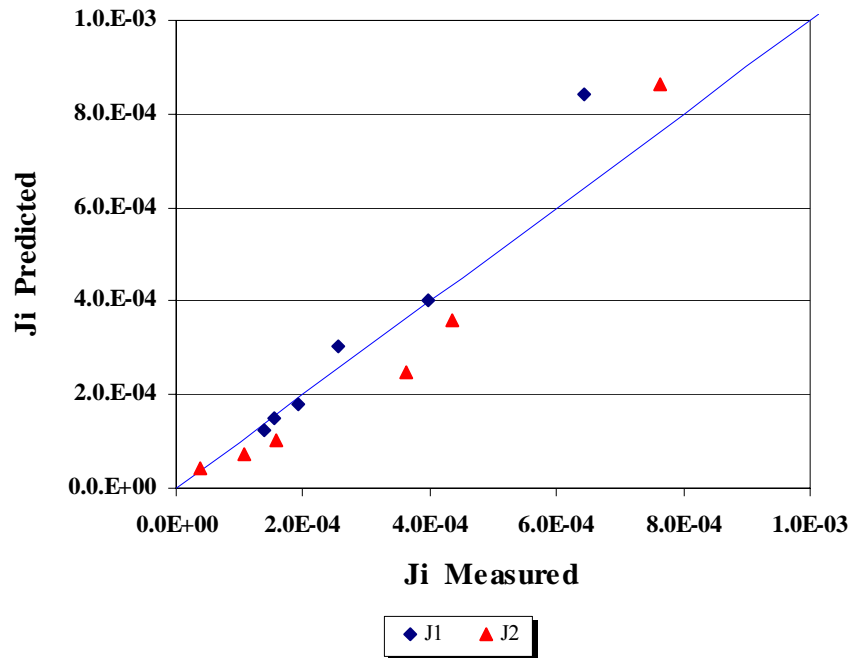| Do	D1	m	SSE
5.91E-05	5.41E-04	4.41E-01	1.51E-01

FIGURE D85   Comparison between the Measured and Predicted Values of Creep Compliance of K7-15 FWD Station at 29.4 °C

TABLE D41   Measured and Predicted values of Creep Compliance of K7-15
FWD Station at 37.8 °C (100 °F)

No	Frequency	J1 (1/MPa)		J2 (1/MPa)	
	(Hz.)	Measured	Predicted	Measured	Predicted
1	25	1.05E-04	1.04E-04	2.75E-05	3.41E-05
2	10	1.10E-04	1.24E-04	9.56E-05	5.33E-05
3	5	1.47E-04	1.46E-04	1.39E-04	7.46E-05
4	1	2.55E-04	2.39E-04	1.25E-04	1.63E-04
5	0.5	3.87E-04	3.07E-04	1.90E-04	2.29E-04
6	0.1	7.75E-04	5.91E-04	6.64E-04	5.00E-04

Backcalculated Creep Compliance Coefficients of K7-15 FWD Station at 37.8 °C

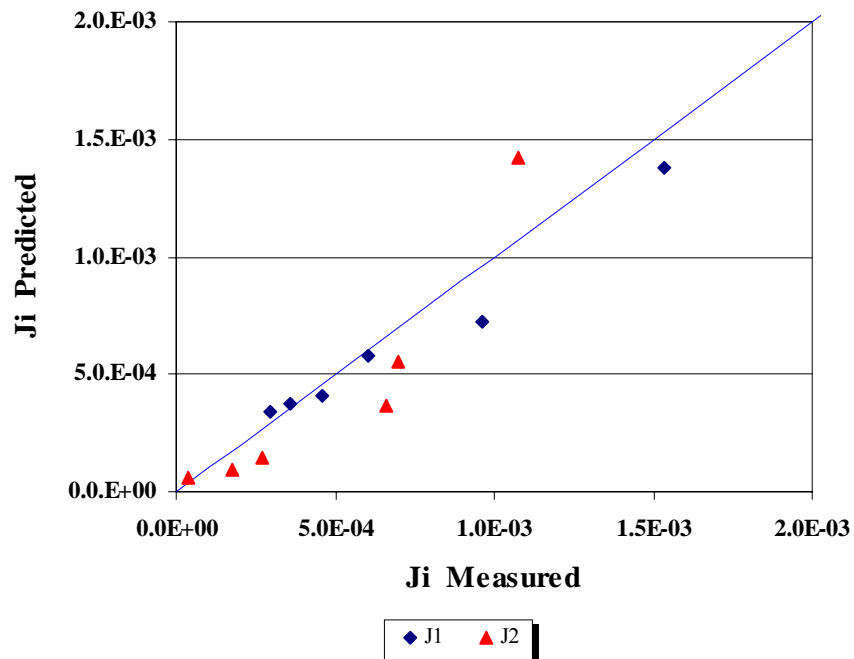| Do	D1	m	SSE
6.85E-05	6.51E-04	4.86E-01	7.87E-01

FIGURE D86   Comparison between the Measured and Predicted Values of Creep
Compliance of K7-15 FWD Station at 37.8 °C

TABLE D42   Measured and Predicted values of Creep Compliance of K7-15 FWD Station at 43.3 ^{o}C (110 ^{o}F)

No	Frequency	J1 (1/MPa)		J2 (1/MPa)	
	(Hz.)	Measured	Predicted	Measured	Predicted
1	25	2.30E-04	2.37E-04	6.65E-05	8.79E-05
2	10	2.79E-04	2.88E-04	1.78E-04	1.38E-04
3	5	3.61E-04	3.45E-04	2.85E-04	1.95E-04
4	1	6.24E-04	5.87E-04	6.27E-04	4.34E-04
5	0.1	1.54E-03	1.52E-03	1.14E-03	1.36E-03

Backcalculated Creep Compliance Coefficients of K7-15 FWD Station at 43.3 ^{o}C

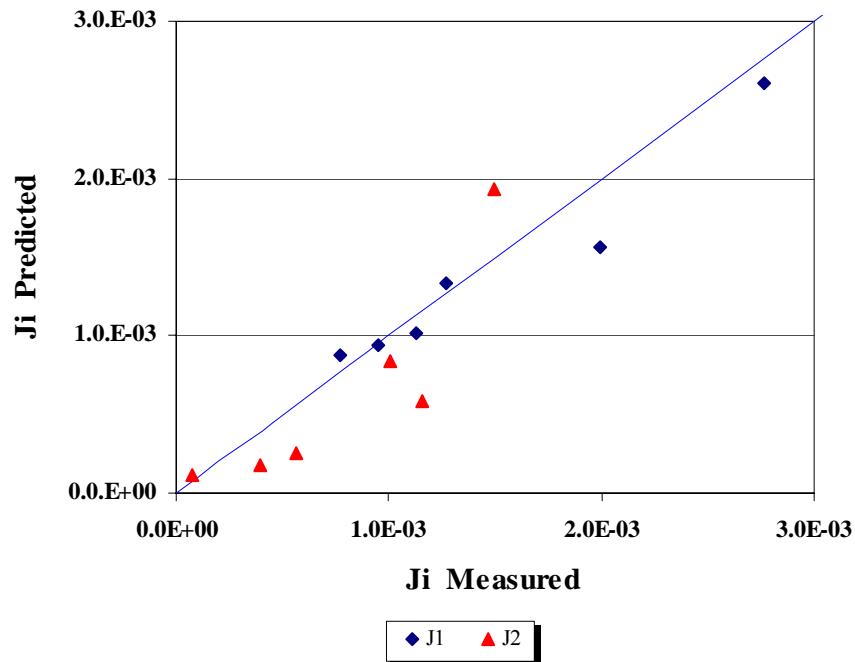| Do	D1	m	SSE
1.47E-04	**1.73E-03**	**4.96E-01**	**3.90E-01**

FIGURE D87   Comparison between the Measured and Predicted Values of Creep Compliance of K7-15 FWD Station at 43.3 ^{o}C

TABLE D43 Measured and Predicted values of Creep Compliance of K7-15 FWD Station at 54.4 °C (130 °F)

No	Frequency	J1 (1/MPa)		J2 (1/MPa)	
	(Hz.)	Measured	Predicted	Measured	Predicted
1	25	3.42E-04	3.96E-04	2.88E-04	2.52E-04
2	10	4.88E-04	5.51E-04	4.92E-04	3.50E-04
3	5	6.91E-04	7.07E-04	7.03E-04	4.49E-04
4	1	1.27E-03	1.26E-03	8.39E-04	8.02E-04
5	0.5	1.82E-03	1.62E-03	1.23E-03	1.03E-03
6	0.1	2.69E-03	2.90E-03	1.42E-03	1.84E-03

Backcalculated Creep Compliance Coefficients of K7-15 FWD Station at 54.4 °C

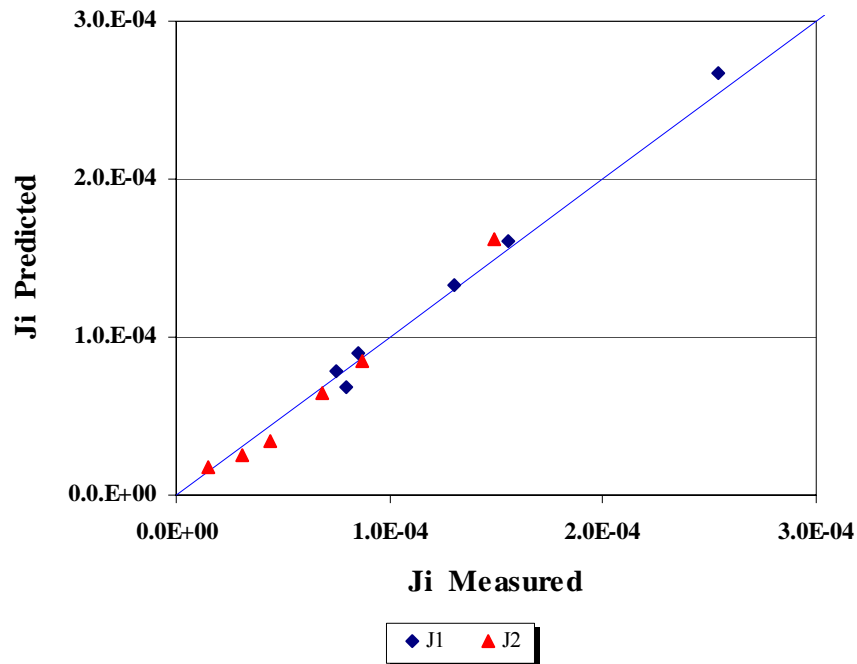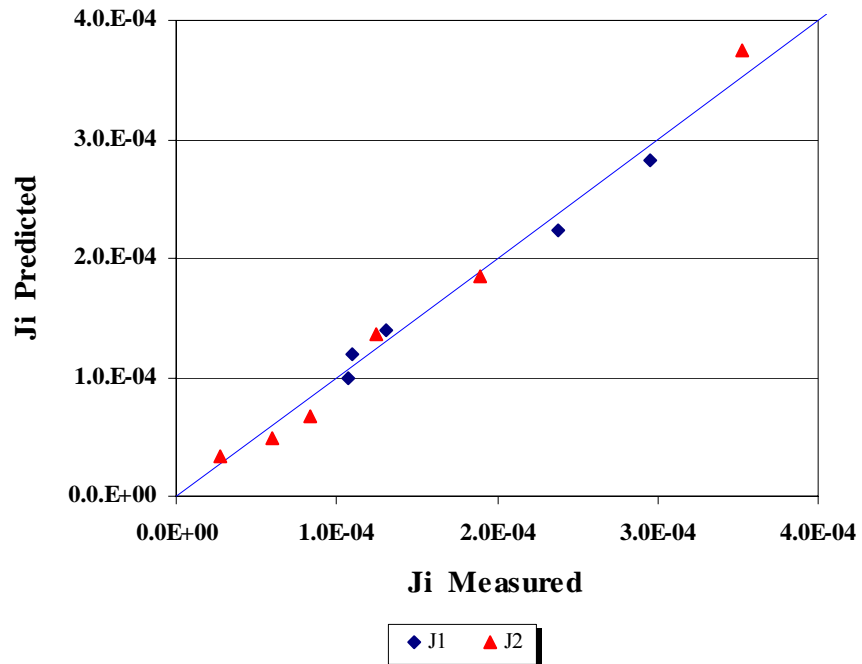| Do	D1	m	SSE
2.69E-11	3.26E-03	3.60E-01	4.06E-01

FIGURE D88 Comparison between the Measured and Predicted Values of Creep Compliance of K7-15 FWD Station at 54.4 °C

TABLE D44   Measured and Predicted values of Creep Compliance of K7-20 FWD Station at 21.1 ^{o}C (70 ^{o}F)

No	Frequency	J1 (1/MPa)		J2 (1/MPa)	
	(Hz.)	Measured	Predicted	Measured	Predicted
1	25	4.28E-05	3.49E-05	1.26E-05	1.36E-05
2	10	4.55E-05	4.32E-05	2.27E-05	1.95E-05
3	5	4.68E-05	5.18E-05	3.22E-05	2.56E-05
4	1	7.68E-05	8.36E-05	5.40E-05	4.82E-05
5	0.5	9.64E-05	1.05E-04	6.92E-05	6.32E-05
6	0.1	1.56E-04	1.83E-04	1.12E-04	1.19E-04

Backcalculated Creep Compliance Coefficients of K7-20 FWD Station at 21.1 ^{o}C

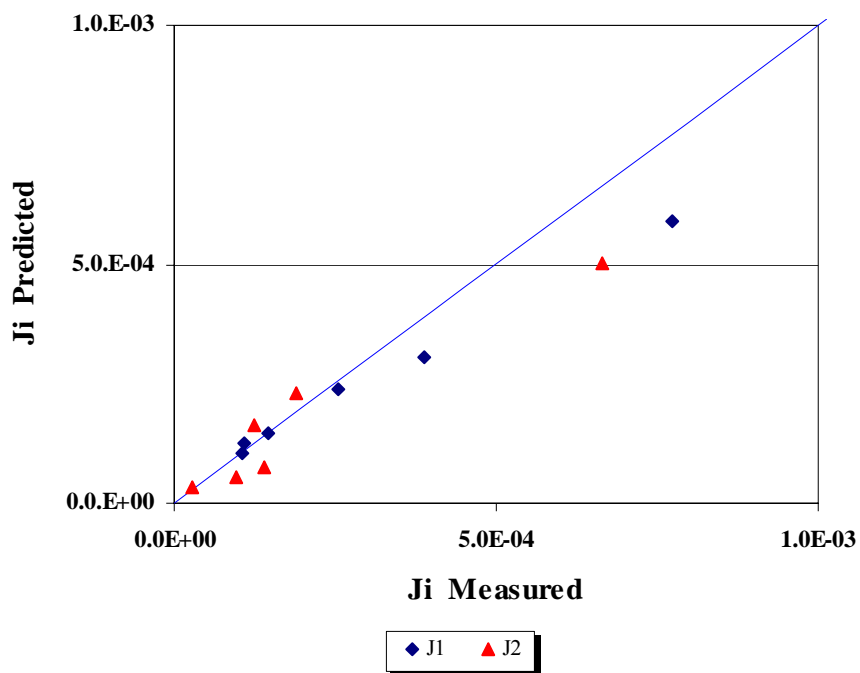| Do	D1	m	SSE
1.57E-05	1.93E-04	3.93E-01	1.85E-01

FIGURE D89   Comparison between the Measured and Predicted Values of Creep Compliance of K7-20 FWD Station at 21.1 ^{o}C

TABLE D45   Measured and Predicted values of Creep Compliance of K7-20 FWD Station at 29.4 °C (85 °F)

No	Frequency	J1 (1/MPa)		J2 (1/MPa)	
	(Hz.)	Measured	Predicted	Measured	Predicted
1	25	5.87E-05	5.30E-05	1.18E-05	1.47E-05
2	10	6.31E-05	6.13E-05	3.63E-05	2.39E-05
3	5	7.02E-05	7.10E-05	5.12E-05	3.44E-05
4	1	1.00E-04	1.13E-04	1.09E-04	8.05E-05
5	0.5	1.44E-04	1.46E-04	1.29E-04	1.16E-04
6	0.1	2.50E-04	2.88E-04	2.33E-04	2.72E-04

Backcalculated Creep Compliance Coefficients of K7-20 FWD Station at 29.4 °C

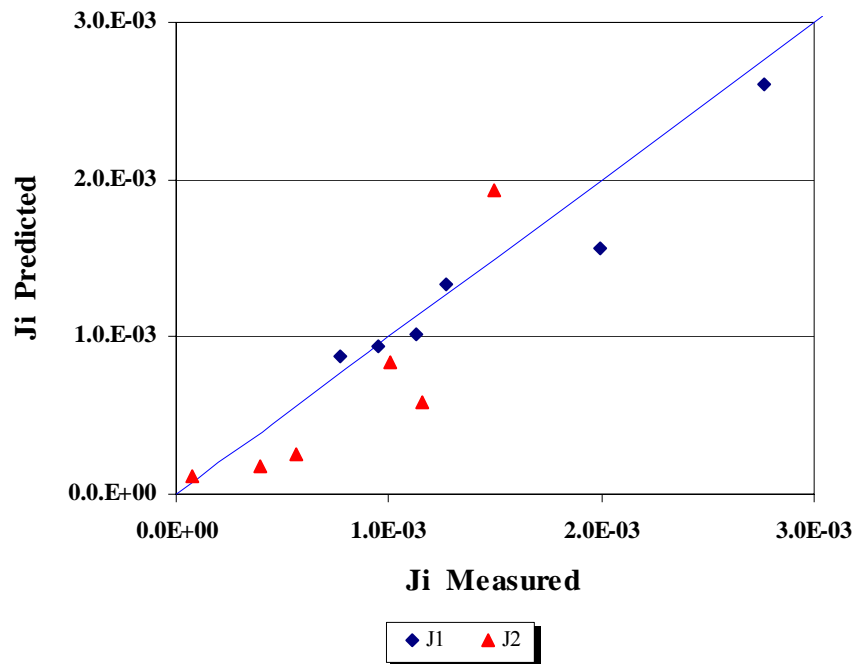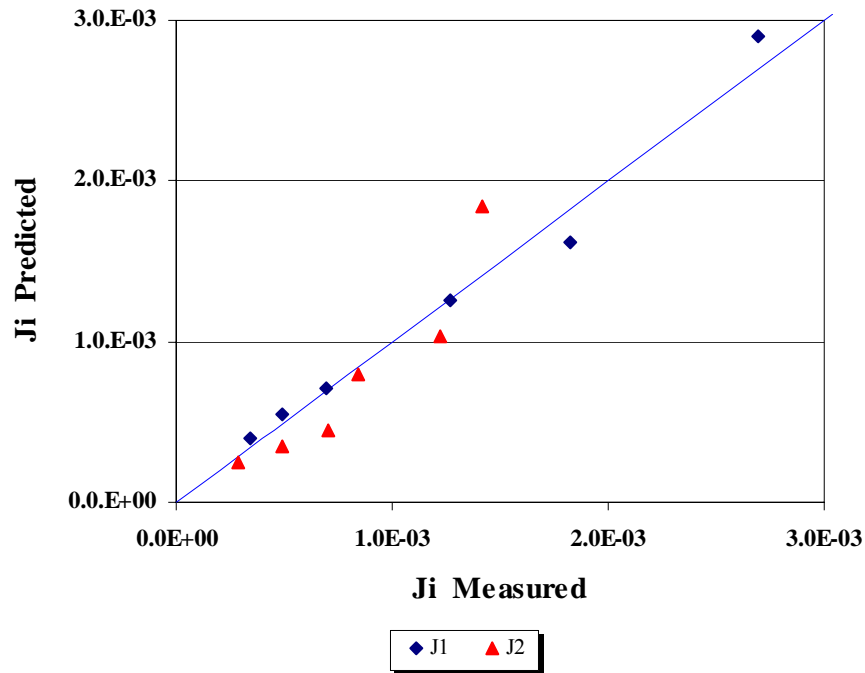| Do	D1	m	SSE
3.95E-05	3.25E-04	5.28E-01	4.43E-01

FIGURE D90   Comparison between the Measured and Predicted Values of Creep Compliance of K7-20 FWD Station at 29.4 °C

TABLE D46   Measured and Predicted values of Creep Compliance of K7-20 FWD Station at 37.8 $^{\circ}$C (100 $^{\circ}$F)

No	Frequency	J1 (1/MPa)		J2 (1/MPa)	
	(Hz.)	Measured	Predicted	Measured	Predicted
1	25	5.70E-05	4.83E-05	1.80E-05	2.44E-05
2	10	5.24E-05	6.03E-05	5.99E-05	4.47E-05
3	5	7.49E-05	7.56E-05	1.04E-04	7.07E-05
4	1	1.45E-04	1.55E-04	2.89E-04	2.05E-04
5	0.5	2.71E-04	2.25E-04	3.90E-04	3.24E-04
6	0.1	6.38E-04	5.87E-04	7.32E-04	9.39E-04

Backcalculated Creep Compliance Coefficients of K7-20 FWD Station at 37.8 $^{\circ}$C

Do	D1	m	SSE
3.39E-05	8.89E-04	6.61E-01	5.71E-01

FIGURE D91   Comparison between the Measured and Predicted Values of Creep Compliance of K7-20 FWD Station at 37.8 $^{\circ}$C

TABLE D47   Measured and Predicted values of Creep Compliance of K7-20 FWD Station at 43.3 °C (110 °F)

No	Frequency	J1 (1/MPa)		J2 (1/MPa)	
	(Hz.)	Measured	Predicted	Measured	Predicted
1	25	1.06E-04	9.68E-05	5.55E-05	6.20E-05
2	10	1.33E-04	1.32E-04	1.21E-04	1.00E-04
3	5	1.80E-04	1.73E-04	1.94E-04	1.44E-04
4	1	2.62E-04	3.50E-04	4.22E-04	3.35E-04
5	0.5	5.52E-04	4.86E-04	5.42E-04	4.81E-04
6	0.1	1.01E-03	1.08E-03	9.61E-04	1.12E-03

Backcalculated Creep Compliance Coefficients of K7-20 FWD Station at 43.3 °C

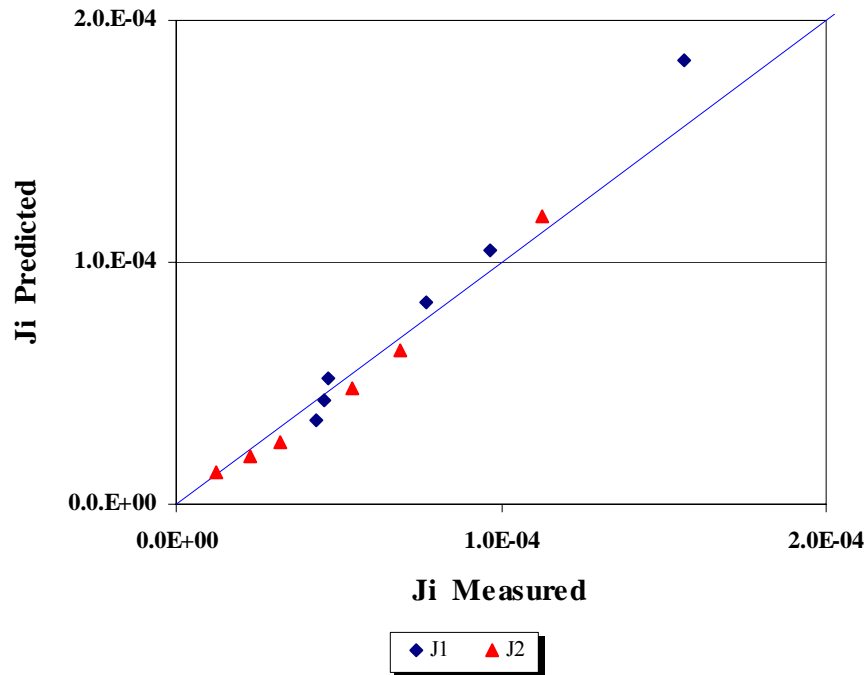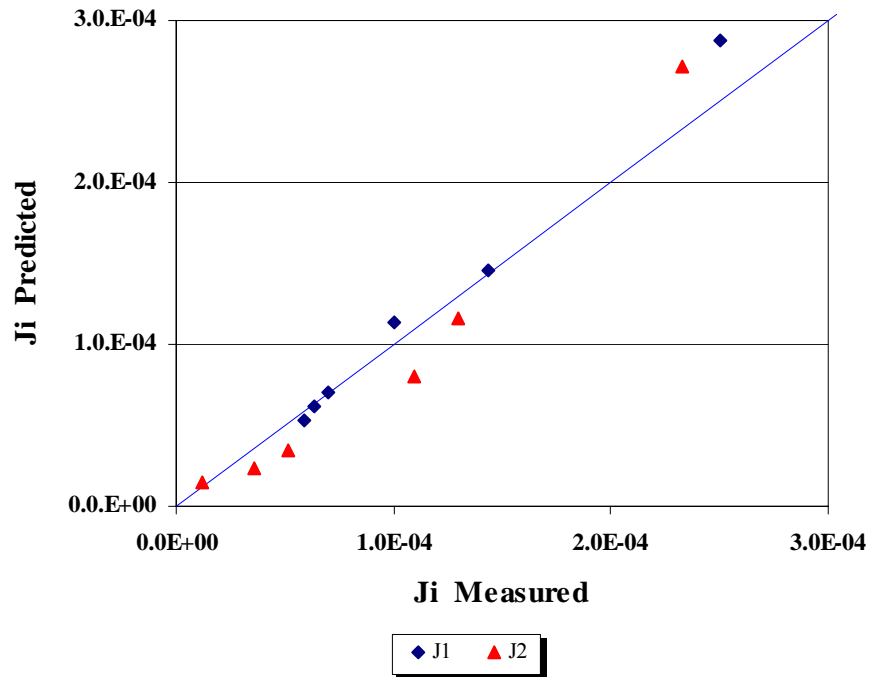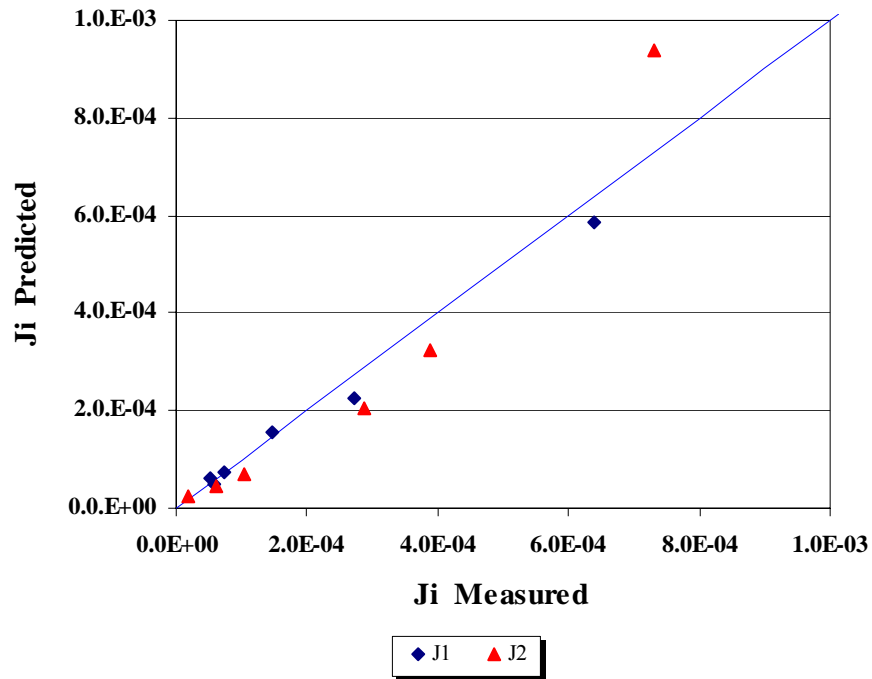| Do	D1	m	SSE
3.92E-05	1.35E-03	5.24E-01	3.32E-01

FIGURE D92   Comparison between the Measured and Predicted Values of Creep Compliance of K7-20 FWD Station at 43.3 °C

TABLE D48   Measured and Predicted values of Creep Compliance of K7-31 FWD Station at 21.1 ^{o}C (70 ^{o}F)

No	Frequency	J1 (1/MPa)		J2 (1/MPa)	
	(Hz.)	Measured	Predicted	Measured	Predicted
1	25	7.11E-05	4.52E-05	2.10E-05	2.01E-05
2	10	5.98E-05	5.76E-05	3.17E-05	2.76E-05
3	5	5.92E-05	7.00E-05	4.35E-05	3.52E-05
4	1	1.05E-04	1.13E-04	5.91E-05	6.19E-05
5	0.5	1.23E-04	1.41E-04	8.78E-05	7.89E-05
6	0.1	2.07E-04	2.39E-04	1.43E-04	1.39E-04

Backcalculated Creep Compliance Coefficients of K7-31 FWD Station at 21.1 ^{o}C

Do	D1	m	SSE
1.25E-05	2.53E-04	3.50E-01	2.86E-01

FIGURE D93   Comparison between the Measured and Predicted Values of Creep Compliance of K7-31 FWD Station at 21.1 ^{o}C

**TABLE D49   Measured and Predicted values of Creep Compliance of K7-31
FWD Station at 29.4 ^{o}C (85 ^{o}F)**

No	Frequency	J1 (1/MPa)		J2 (1/MPa)	
	(Hz.)	Measured	Predicted	Measured	Predicted
1	25	1.08E-04	1.06E-04	1.95E-05	2.29E-05
2	10	1.11E-04	1.20E-04	3.57E-05	3.43E-05
3	5	1.32E-04	1.35E-04	6.23E-05	4.65E-05
4	1	2.10E-04	1.93E-04	8.59E-05	9.43E-05
5	0.5	2.47E-04	2.34E-04	1.43E-04	1.28E-04
6	0.1	4.31E-04	3.93E-04	2.36E-04	2.59E-04

Backcalculated Creep Compliance Coefficients of K7-31 FWD Station at 29.4 ^{o}C

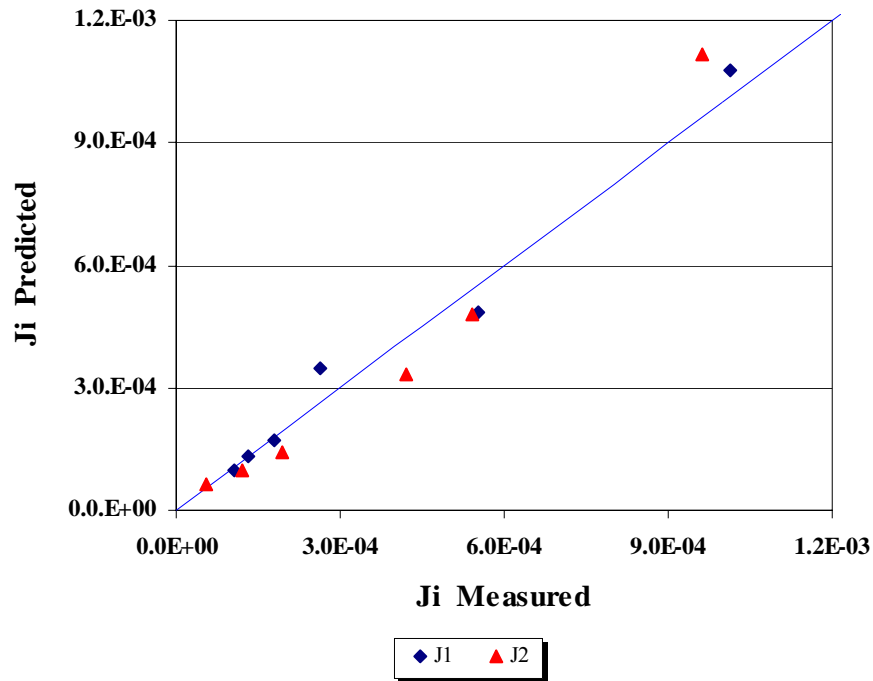| Do	D1	m	SSE
7.86E-05	3.75E-04	4.39E-01	1.52E-01

**FIGURE D94   Comparison between the Measured and Predicted Values of Creep
Compliance of K7-31 FWD Station at 29.4 ^{o}C**

TABLE D50   Measured and Predicted values of Creep Compliance of K7-31 FWD Station at 37.8 ^{o}C (100 ^{o}F)

No	Frequency	J1 (1/MPa)		J2 (1/MPa)	
	(Hz.)	Measured	Predicted	Measured	Predicted
1	10	1.79E-04	1.68E-04	5.98E-05	6.53E-05
2	5	2.10E-04	1.95E-04	1.01E-04	9.19E-05
3	1	2.66E-04	3.09E-04	2.75E-04	2.03E-04
4	0.5	4.05E-04	3.94E-04	3.20E-04	2.86E-04
5	0.1	6.89E-04	7.48E-04	5.65E-04	6.33E-04

Backcalculated Creep Compliance Coefficients of K7-31 FWD Station at 37.8 ^{o}C

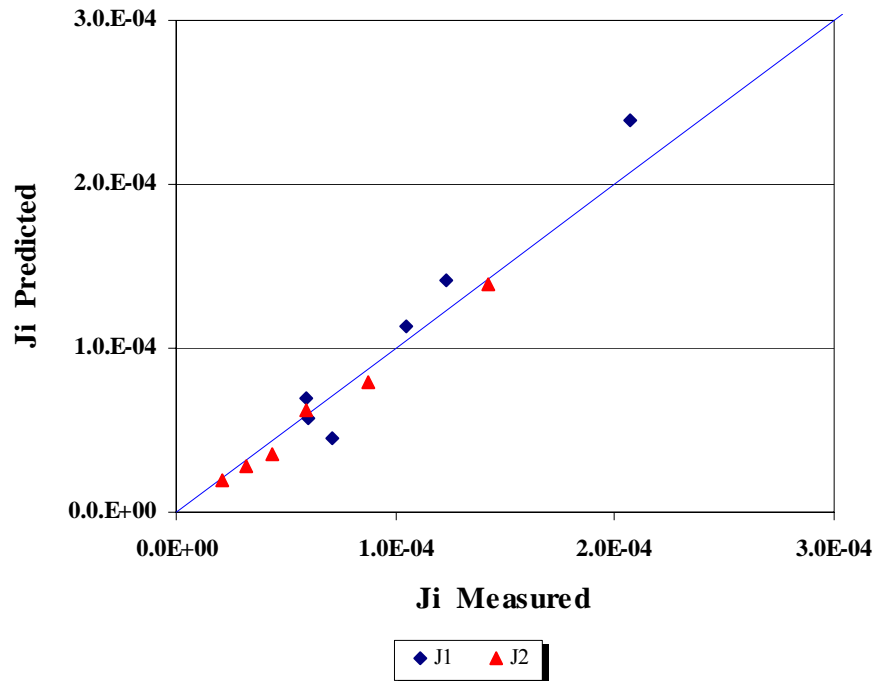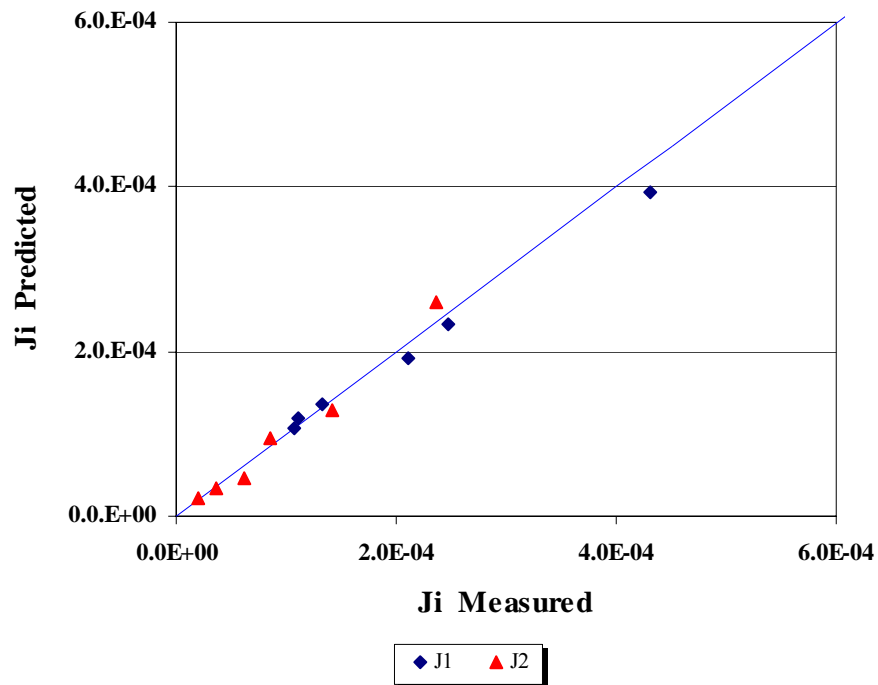| Do	D1	m	SSE
1.02E-04	8.12E-04	4.93E-01	1.53E-01

FIGURE D95   Comparison between the Measured and Predicted Values of Creep Compliance of K7-31 FWD Station at 37.8 ^{o}C

TABLE D51   Measured and Predicted values of Creep Compliance of K7-31 FWD Station at 43.3 °C (110 °F)

No	Frequency	J1 (1/MPa)		J2 (1/MPa)	
	(Hz.)	Measured	Predicted	Measured	Predicted
1	25	3.07E-04	3.85E-04	1.77E-05	2.59E-05
2	10	3.79E-04	3.96E-04	1.66E-04	4.99E-05
3	5	4.59E-04	4.12E-04	2.93E-04	8.18E-05
4	1	5.20E-04	4.97E-04	6.32E-04	2.58E-04
5	0.5	9.23E-04	5.76E-04	6.49E-04	4.23E-04
6	0.1	1.51E-03	1.02E-03	1.01E-03	1.34E-03

Backcalculated Creep Compliance Coefficients of K7-31 FWD Station at 43.3 °C

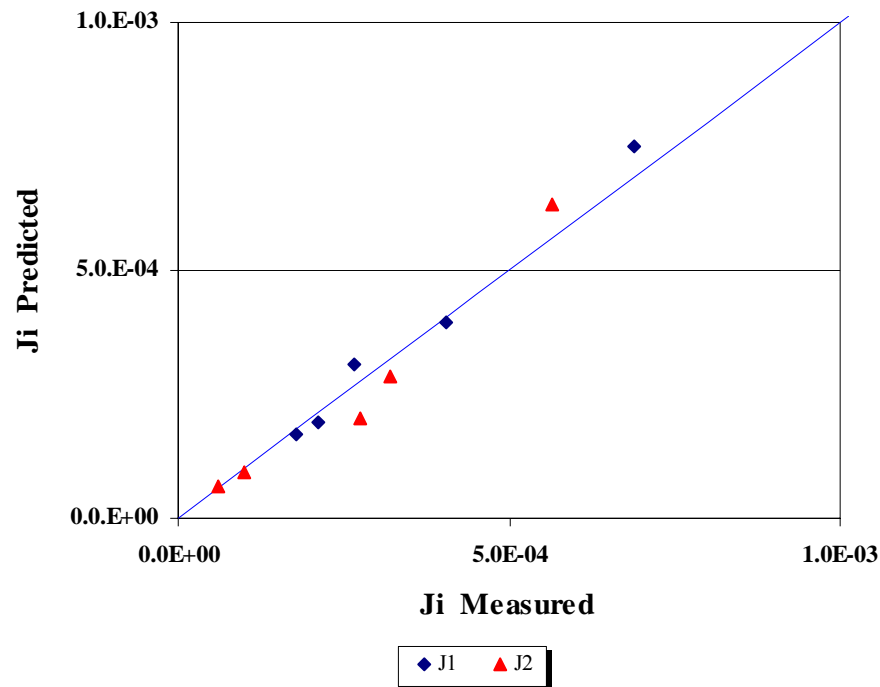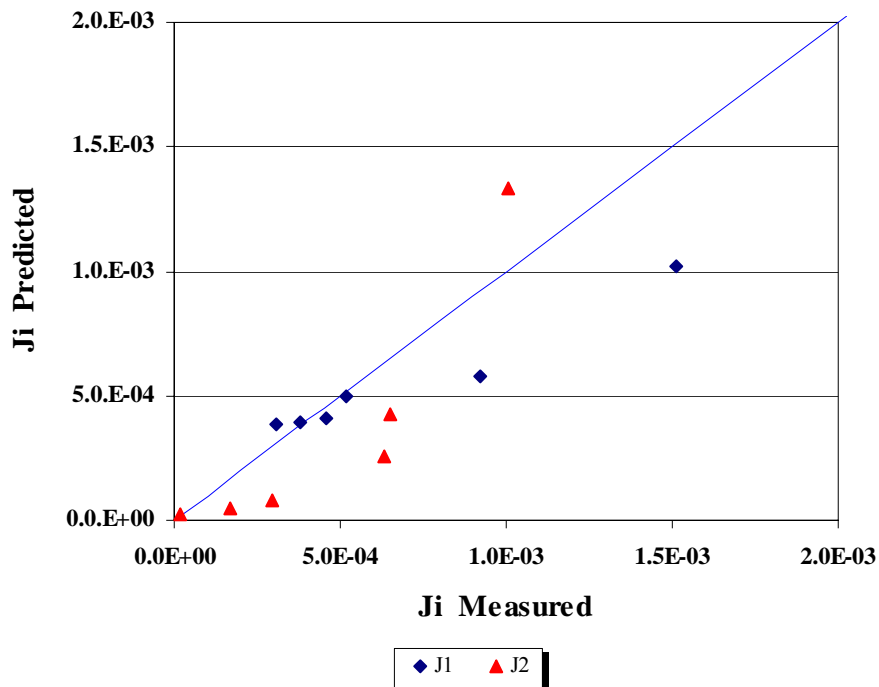| Do	D1	m	SSE
3.72E-04	1.17E-03	7.14E-01	2.13E+00

FIGURE D96   Comparison between the Measured and Predicted Values of Creep Compliance of K7-31 FWD Station at 43.3 °C

TABLE D52   Measured and Predicted values of Creep Compliance of K7-31 FWD Station at 54.4 ^{o}C (130°F)

No	Frequency	J1 (1/MPa)		J2 (1/MPa)	
	(Hz.)	Measured	Predicted	Measured	Predicted
1	25	2.77E-04	3.71E-04	3.89E-06	5.45E-06
2	10	3.16E-04	3.71E-04	1.20E-04	1.35E-05
3	5	3.89E-04	3.72E-04	2.12E-04	2.67E-05
4	1	4.86E-04	3.74E-04	5.87E-04	1.31E-04
5	0.5	7.63E-04	3.76E-04	6.62E-04	2.60E-04
6	0.1	1.32E-03	3.95E-04	1.19E-03	1.28E-03

Backcalculated Creep Compliance Coefficients of K7-31 FWD Station at 54.4 ^{o}C

Do	D1	m	SSE
3.71E-04	8.10E-04	9.88E-01	3.64E+00

FIGURE D97   Comparison between the Measured and Predicted Values of Creep Compliance of K7-31 FWD Station at 54.4 ^{o}C

**TABLE D53   Measured and Predicted values of Creep Compliance of K7-37
FWD Station at 21.1 ^{o}C (70°F)**

No	Frequency	J1 (1/MPa)		J2 (1/MPa)	
	(Hz.)	Measured	Predicted	Measured	Predicted
1	25	1.91E-05	1.44E-05	7.55E-06	7.02E-06
2	10	2.07E-05	1.86E-05	1.27E-05	1.05E-05
3	5	2.07E-05	2.32E-05	1.77E-05	1.42E-05
4	1	3.39E-05	4.09E-05	3.09E-05	2.88E-05
5	0.5	4.52E-05	5.33E-05	4.28E-05	3.91E-05
6	0.1	8.74E-05	1.02E-04	7.90E-05	7.91E-05

Backcalculated Creep Compliance Coefficients of K7-37 FWD Station at 21.1^{o}C

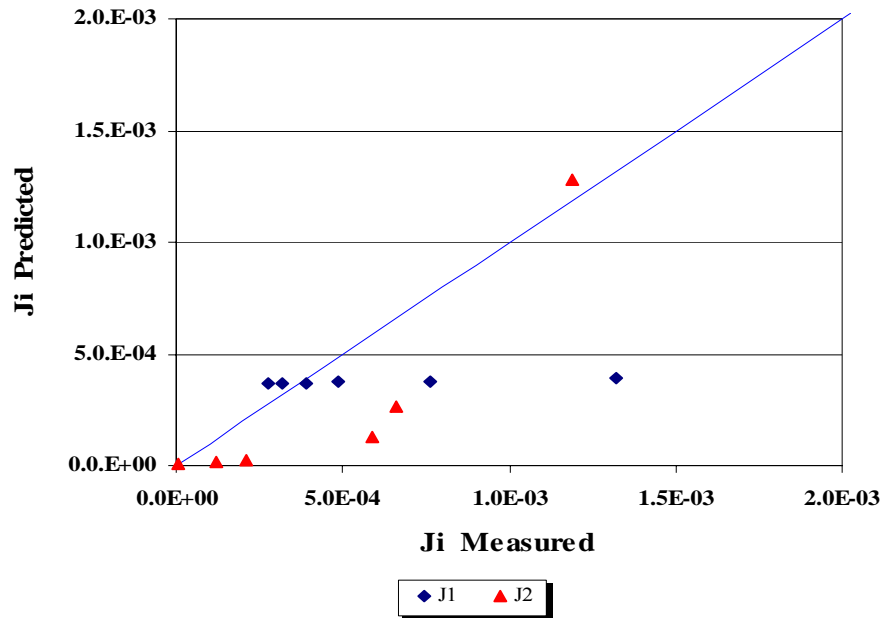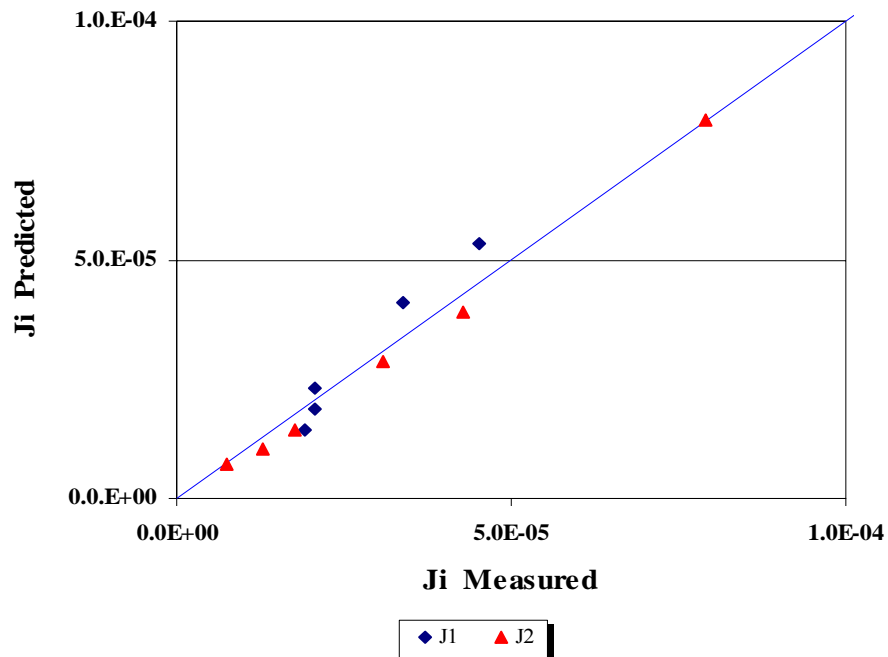| Do	D1	m	SSE
5.90E-06	1.15E-04	4.39E-01	2.73E-01

**FIGURE D98   Comparison between the Measured and Predicted Values of Creep
Compliance of K7-37 FWD Station at 21.1 ^{o}C**

**TABLE D54   Measured and Predicted values of Creep Compliance of K7-37
FWD Station at 29.4 ^{o}C (85°F)**

No	Frequency	J1 (1/MPa)		J2 (1/MPa)	
	(Hz.)	Measured	Predicted	Measured	Predicted
1	25	5.22E-05	4.45E-05	1.50E-05	1.64E-05
2	10	5.42E-05	5.43E-05	2.94E-05	2.51E-05
3	5	5.79E-05	6.50E-05	4.18E-05	3.46E-05
4	1	1.09E-04	1.08E-04	6.86E-05	7.29E-05
5	0.5	1.29E-04	1.39E-04	1.14E-04	1.00E-04
6	0.1	2.50E-04	2.64E-04	2.01E-04	2.12E-04

Backcalculated Creep Compliance Coefficients of K7-37 FWD Station at 29.4 ^{o}C

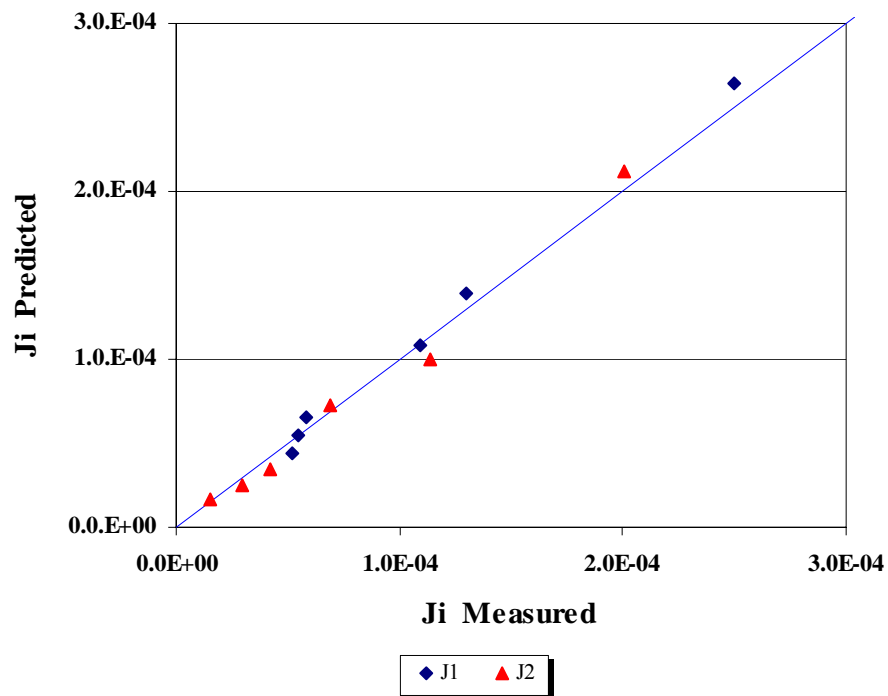| Do	D1	m	SSE
2.60E-05	2.90E-04	4.63E-01	1.26E-01

**FIGURE D99   Comparison between the Measured and Predicted Values of Creep
Compliance of K7-37 FWD Station at 29.4 ^{o}C**

TABLE D55 Measured and Predicted values of Creep Compliance of K7-37 FWD Station at 37.8 ^{o}C (100°F)

No	Frequency	J1 (1/MPa)		J2 (1/MPa)	
	(Hz.)	Measured	Predicted	Measured	Predicted
1	10	2.01E-04	1.93E-04	7.64E-05	8.23E-05
2	5	2.38E-04	2.28E-04	1.22E-04	1.15E-04
3	1	3.39E-04	3.70E-04	3.13E-04	2.48E-04
4	0.5	4.70E-04	4.74E-04	3.84E-04	3.45E-04
5	0.1	8.36E-04	9.03E-04	6.75E-04	7.46E-04

Backcalculated Creep Compliance Coefficients of K7-37 FWD Station at 37.8 ^{o}C

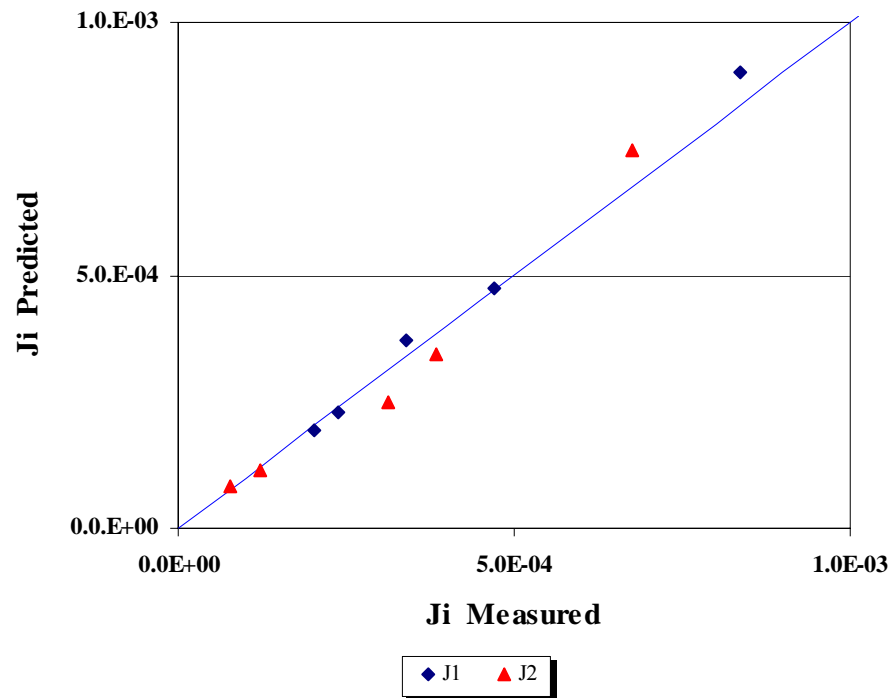| Do	D1	m	SSE
1.05E-04	9.87E-04	4.79E-01	9.33E-02

FIGURE D100   Comparison between the Measured and Predicted Values of   Creep Compliance of K7-37 FWD Station at 37.8 ^{o}C

**TABLE D56   Measured and Predicted values of Creep Compliance of K7-37
FWD Station at 43.3 ^{o}C (110 ^{o}F)**

No	Frequency	J1 (1/MPa)		J2 (1/MPa)	
	(Hz.)	Measured	Predicted	Measured	Predicted
1	25	1.83E-04	1.64E-04	2.71E-05	4.12E-05
2	10	1.32E-04	1.86E-04	2.29E-04	7.00E-05
3	5	2.98E-04	2.13E-04	2.06E-04	1.05E-04
4	1	6.07E-04	3.38E-04	3.53E-04	2.65E-04
5	0.5	7.78E-04	4.40E-04	5.00E-04	3.96E-04
6	0.1	1.43E-03	9.15E-04	7.44E-04	1.00E-03

Backcalculated Creep Compliance Coefficients of K7-37 FWD Station at 43.3 ^{o}C

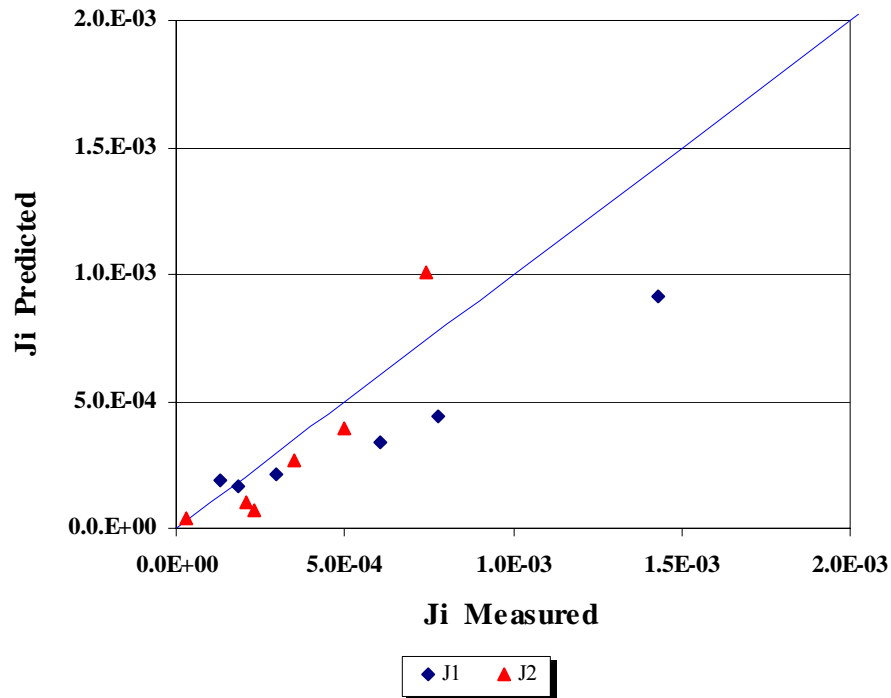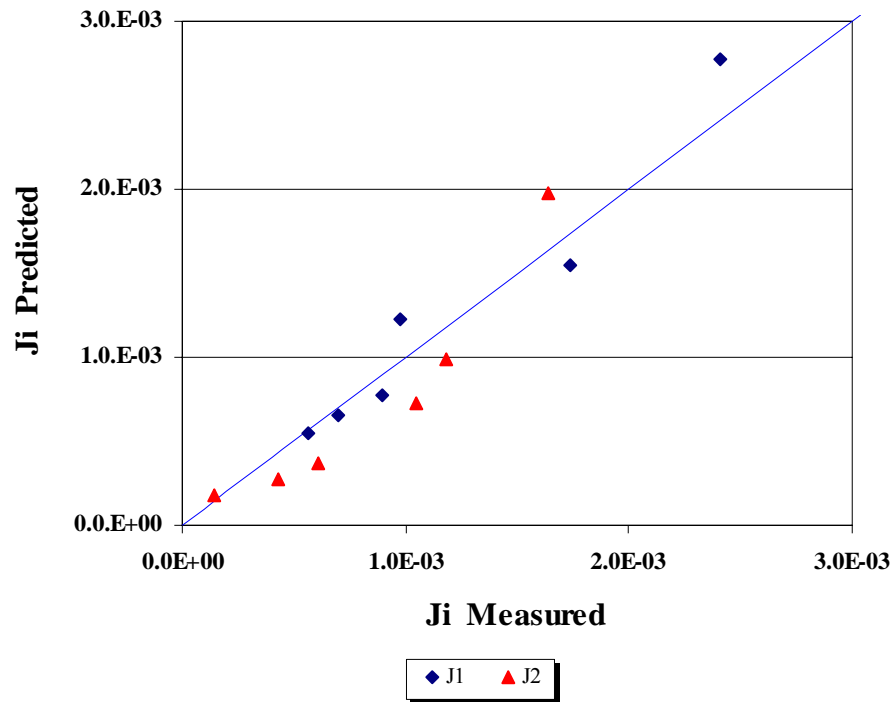| Do	D1	m	SSE
1.31E-04	1.09E-03	5.78E-01	1.99E+00

**FIGURE D101   Comparison between the Measured and Predicted Values of
Creep Compliance of K7-37 FWD Station at 43.3 ^{o}C**

**TABLE D57   Measured and Predicted values of Creep Compliance of K7-37
FWD Station at 54.4 ^{o}C (130°F)**

No	Frequency	J1 (1/MPa)		J2 (1/MPa)	
	(Hz.)	Measured	Predicted	Measured	Predicted
1	25	5.63E-04	5.51E-04	1.41E-04	1.82E-04
2	10	6.99E-04	6.60E-04	4.25E-04	2.70E-04
3	5	8.97E-04	7.77E-04	6.07E-04	3.64E-04
4	1	9.77E-04	1.23E-03	1.05E-03	7.30E-04
5	0.5	1.74E-03	1.55E-03	1.18E-03	9.84E-04
6	0.1	2.40E-03	2.77E-03	1.64E-03	1.97E-03

Backcalculated Creep Compliance Coefficients of K7-37 FWD Station at 54.4 ^{o}C

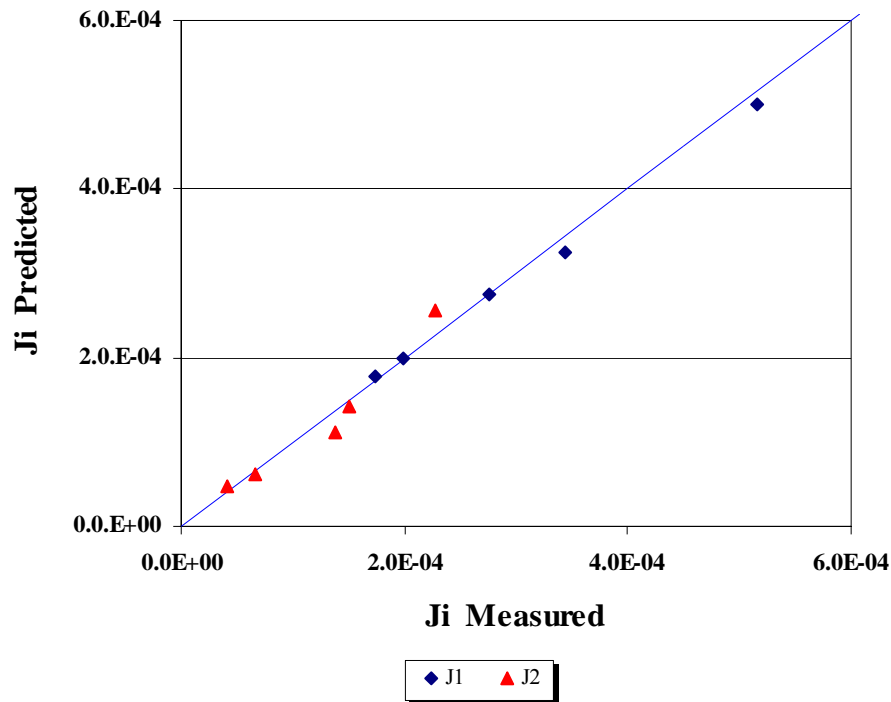| Do	D1	m	SSE
3.25E-04	2.90E-03	4.32E-01	6.60E-01

**FIGURE D102   Comparison between the Measured and Predicted Values of
Creep Compliance of K7-37 FWD Station at 54.4 ^{o}C**

TABLE D58 **Measured and Predicted values of Creep Compliance of K7-40 FWD Station at 21.1 ^{o}C (70°F)**

No	Frequency	J1 (1/MPa)		J2 (1/MPa)	
	(Hz.)	Measured	Predicted	Measured	Predicted
1	10	1.73E-04	1.78E-04	4.12E-05	4.77E-05
2	5	1.99E-04	2.00E-04	6.63E-05	6.14E-05
3	1	2.75E-04	2.76E-04	1.39E-04	1.10E-04
4	0.5	3.44E-04	3.25E-04	1.50E-04	1.42E-04
5	0.1	5.15E-04	5.01E-04	2.28E-04	2.56E-04

Backcalculated Creep Compliance Coefficients of K7-40 FWD Station at 21.1^{o}C

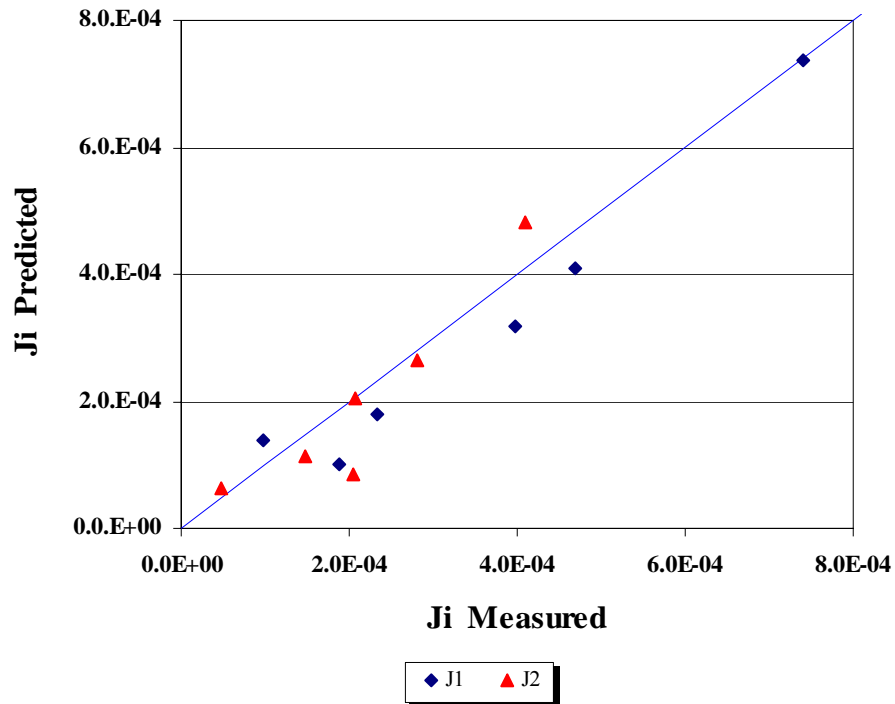| Do	D1	m	SSE
1.05E-04	4.48E-04	3.65E-01	9.51E-02

FIGURE D103 **Comparison between the Measured and Predicted Values of Creep Compliance of K7-40 FWD Station at 21.1 ^{o}C**

TABLE D59   Measured and Predicted values of Creep Compliance of K7-40 FWD Station at 29.4 ^{o}C (85 ^{o}F)

No	Frequency	J1 (1/MPa)		J2 (1/MPa)	
	(Hz.)	Measured	Predicted	Measured	Predicted
1	25	1.88E-04	1.02E-04	4.69E-05	6.15E-05
2	10	9.84E-05	1.40E-04	2.05E-04	8.66E-05
3	5	2.34E-04	1.78E-04	1.47E-04	1.12E-04
4	1	3.97E-04	3.17E-04	2.08E-04	2.04E-04
5	0.5	4.69E-04	4.08E-04	2.82E-04	2.65E-04
6	0.1	7.40E-04	7.36E-04	4.10E-04	4.82E-04

Backcalculated Creep Compliance Coefficients of K7-40 FWD Station at 29.4 ^{o}C

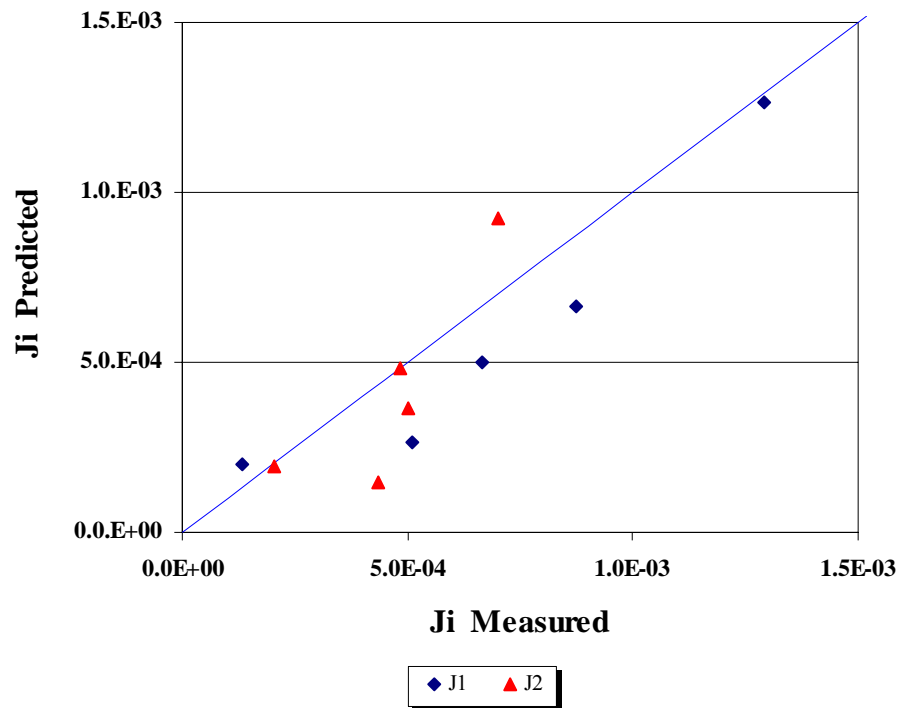| Do	D1	m	SSE
9.09E-06	8.25E-04	3.73E-01	1.02E+00

FIGURE D104   Comparison between the Measured and Predicted Values of Creep Compliance of K7-40 FWD Station at 29.4 ^{o}C

TABLE D60   Measured and Predicted values of Creep Compliance of K7-40 FWD Station at 37.8 °C (100 °F)

No	Frequency	J1 (1/MPa)		J2 (1/MPa)	
	(Hz.)	Measured	Predicted	Measured	Predicted
1	10	1.35E-04	1.99E-04	4.34E-04	1.45E-04
2	5	5.10E-04	2.62E-04	2.03E-04	1.92E-04
3	1	6.65E-04	5.01E-04	5.01E-04	3.67E-04
4	0.5	8.74E-04	6.62E-04	4.85E-04	4.85E-04
5	0.1	1.29E-03	1.26E-03	7.03E-04	9.26E-04

Backcalculated Creep Compliance Coefficients of K7-40 FWD Station at 37.8 °C

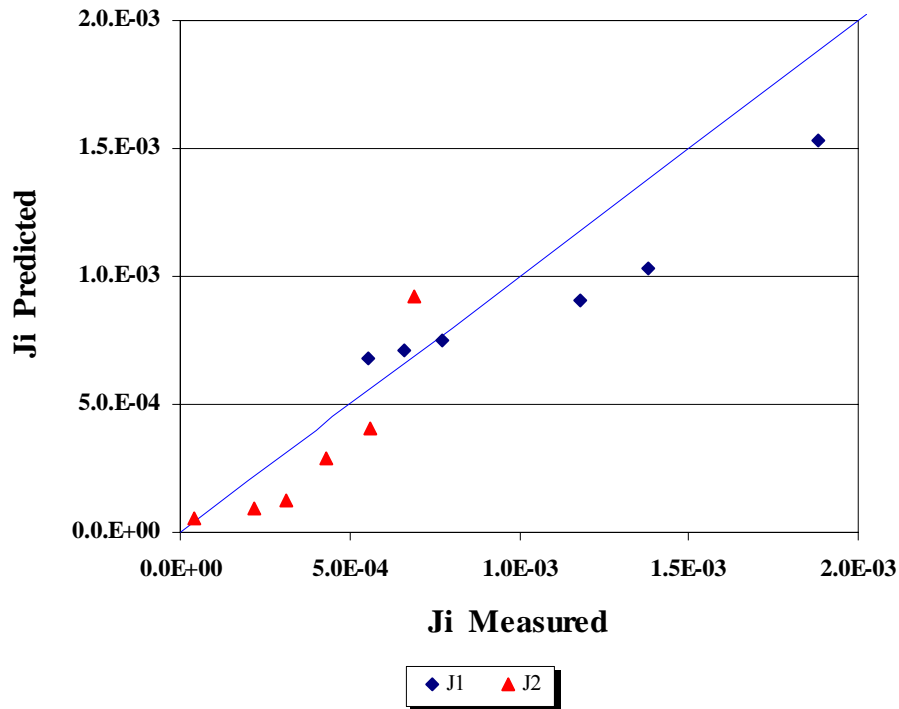| Do	D1	m	SSE
2.69E-11	1.47E-03	4.02E-01	1.20E+00

FIGURE D105   Comparison between the Measured and Predicted Values of Creep Compliance of K7-40 FWD Station at 37.8 °C

TABLE D61   Measured and Predicted values of Creep Compliance of K7-40
FWD Station at 43.3 ^{o}C (110 ^{o}F)

No	Frequency	J1 (1/MPa)		J2 (1/MPa)	
	(Hz.)	Measured	Predicted	Measured	Predicted
1	25	5.57E-04	6.82E-04	3.91E-05	5.66E-05
2	10	6.63E-04	7.15E-04	2.21E-04	8.99E-05
3	5	7.76E-04	7.52E-04	3.12E-04	1.28E-04
4	1	1.18E-03	9.09E-04	4.28E-04	2.88E-04
5	0.5	1.38E-03	1.03E-03	5.61E-04	4.08E-04
6	0.1	1.88E-03	1.53E-03	6.91E-04	9.21E-04

Backcalculated Creep Compliance Coefficients of K7-40 FWD Station at 43.3 ^{o}C

Do	D1	m	SSE
6.26E-04	1.15E-03	5.05E-01	1.40E+00

FIGURE D105   Comparison between the Measured and Predicted Values of
Creep Compliance of K7-40 FWD Station at 43.3 ^{o}C

TABLE D62 Measured and Predicted values of Creep Compliance of K7-40 FWD Station at 54.4 ^{o}C (130 ^{o}F)

No	Frequency	J1 (1/MPa)		J2 (1/MPa)	
	(Hz.)	Measured	Predicted	Measured	Predicted
1	25	8.23E-04	1.01E-03	3.94E-05	5.53E-05
2	10	9.99E-04	1.05E-03	3.35E-04	9.26E-05
3	5	1.13E-03	1.08E-03	4.59E-04	1.37E-04
4	1	1.44E-03	1.25E-03	7.80E-04	3.39E-04
5	0.5	1.82E-03	1.38E-03	7.09E-04	5.00E-04
6	0.1	2.34E-03	1.98E-03	9.36E-04	1.24E-03

Backcalculated Creep Compliance Coefficients of K7-40 FWD Station at 54.4 ^{o}C

Do	D1	m	SSE
9.70E-04	1.38E-03	5.63E-01	1.85E+00
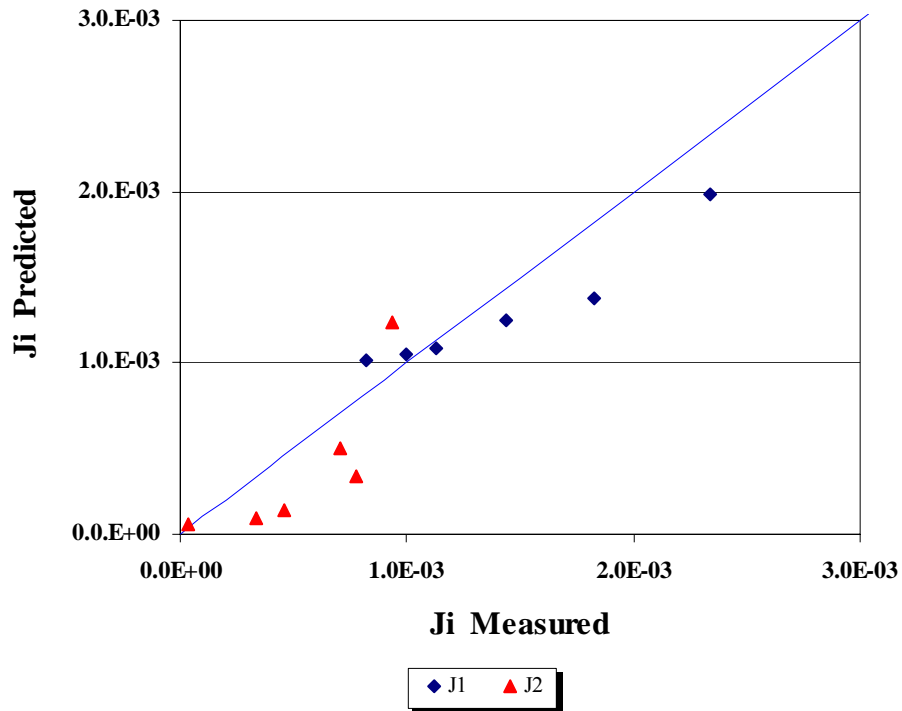
FIGURE D106   Comparison between the Measured and Predicted Values of Creep Compliance of K7-40 FWD Station at 54.4 ^{o}C

APPENDIX E

PLOTS OF DYNAMIC (COMPLEX) MODULUS VERSUS FREQUENCIES AT DIFFERENT TEST TEMPERATURES

USING CHEN EQUATION
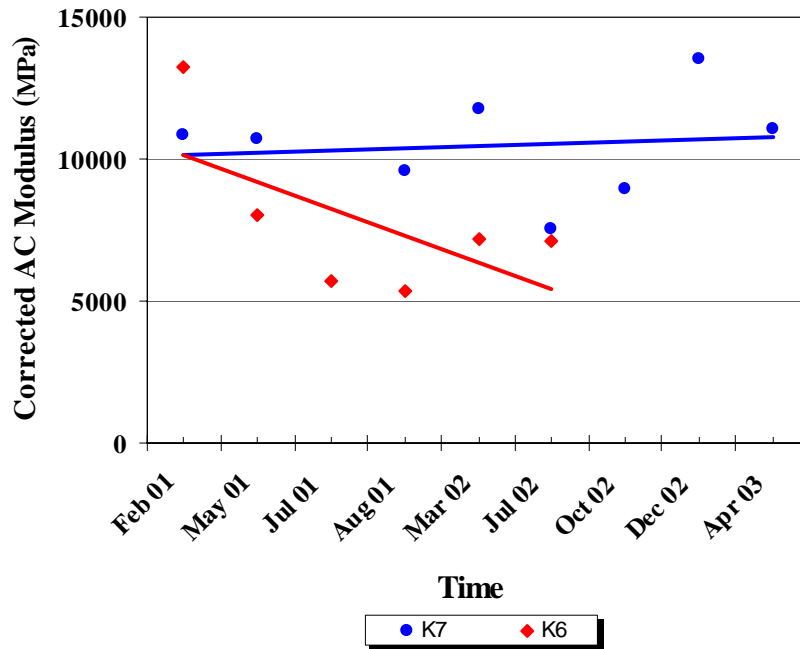
FIGURE D1   Corrected AC Moduli using Eq. 7.1 in the Pavement Group 1.
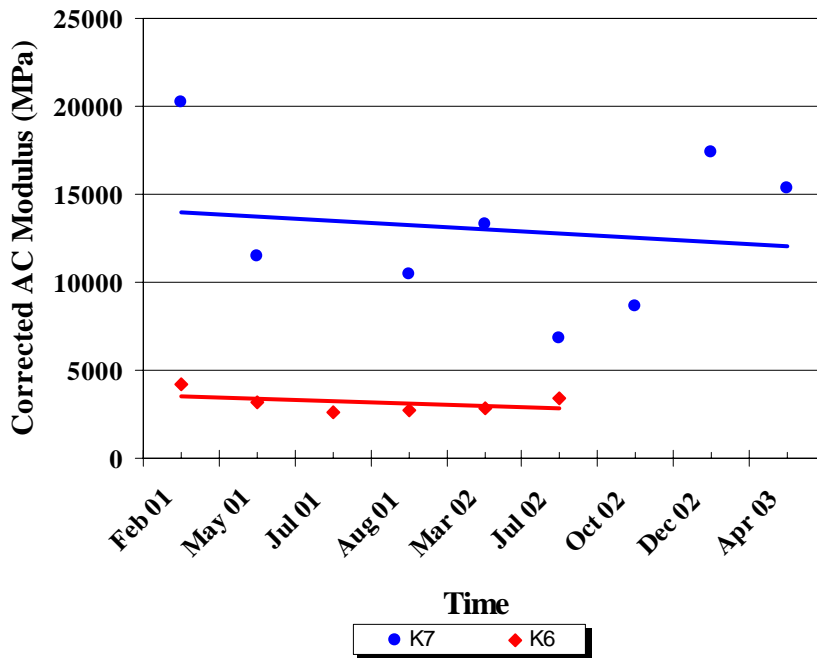
FIGURE D2   Corrected AC Moduli Using Eq. 7.1 in the Pavement Group 2
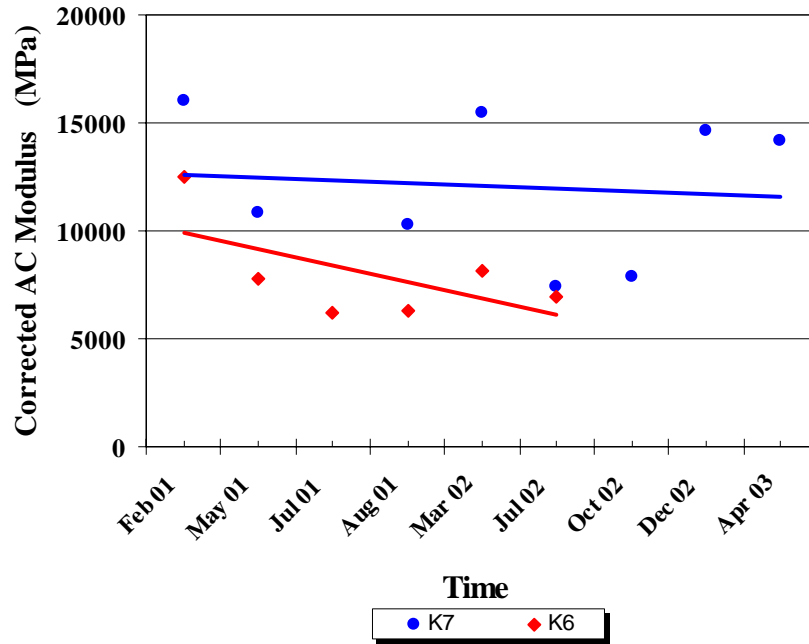
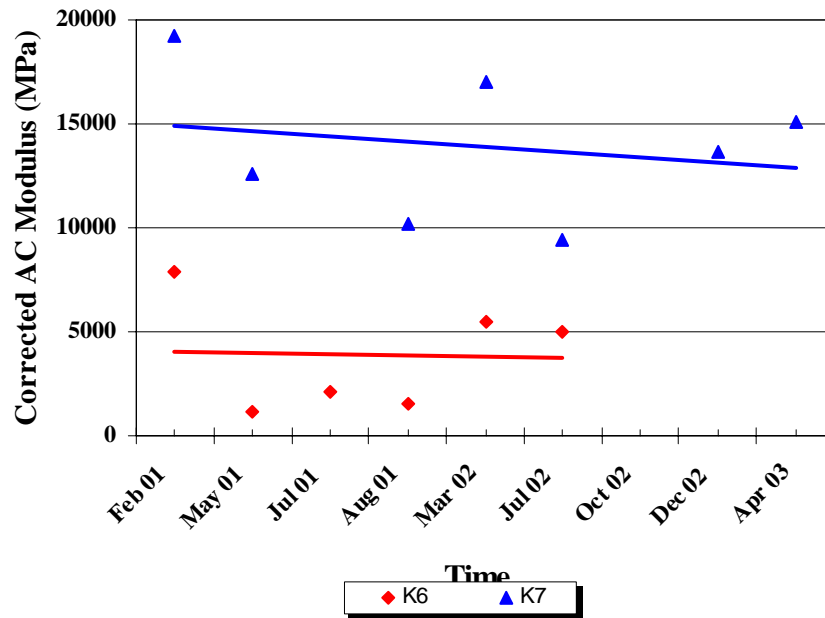**FIGURE D3   Corrected AC Moduli Using Eq. 7.1 in the Pavement Group 3.**

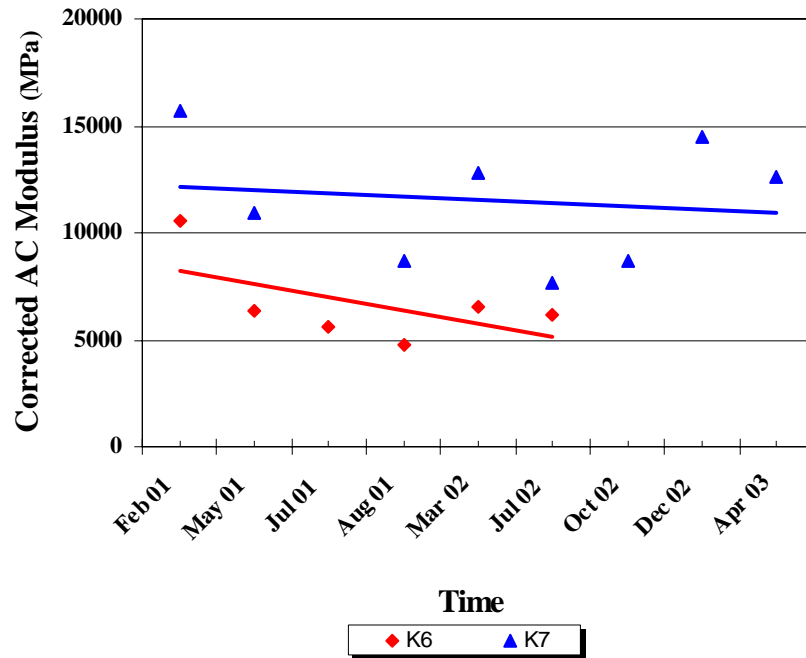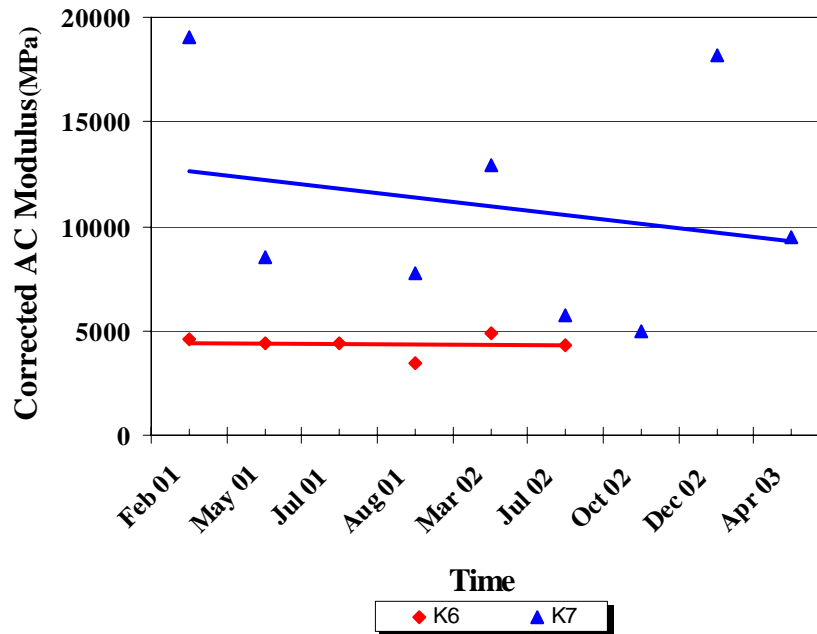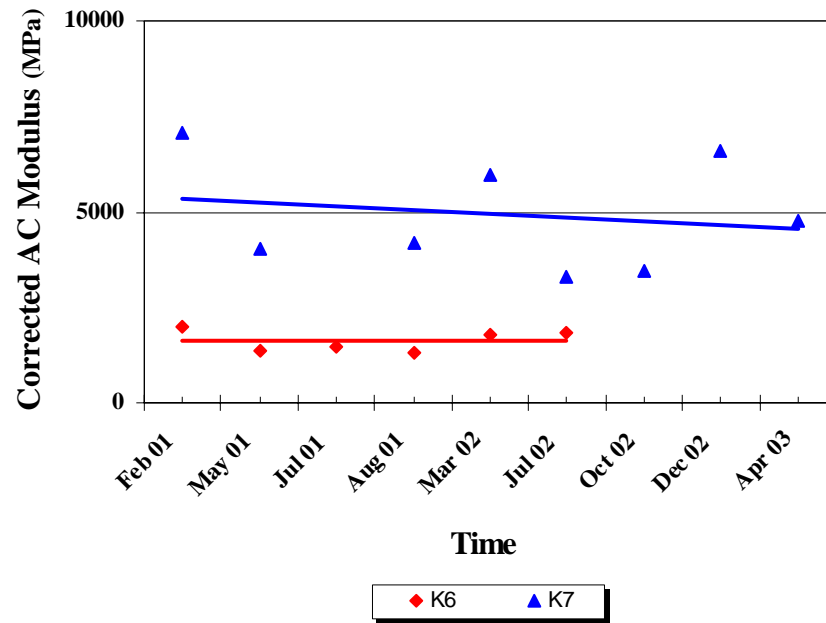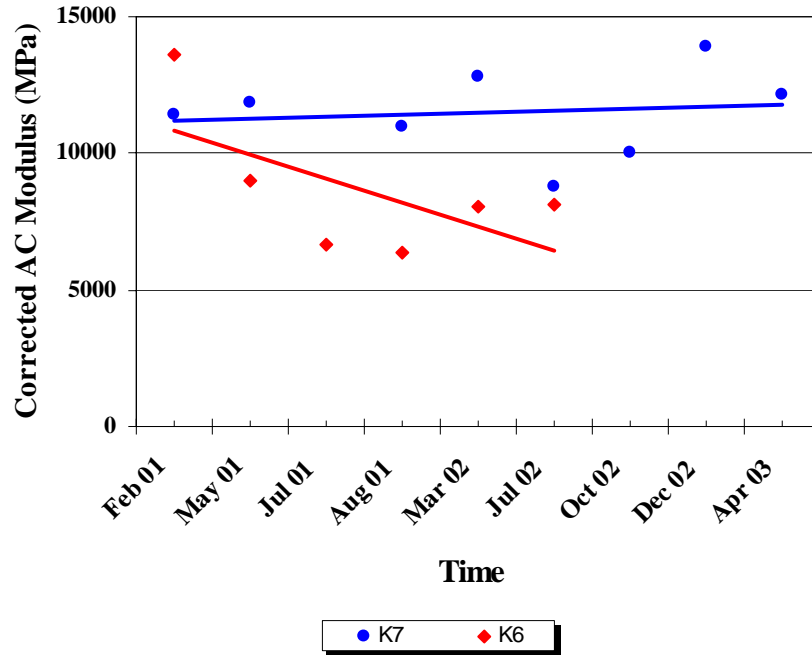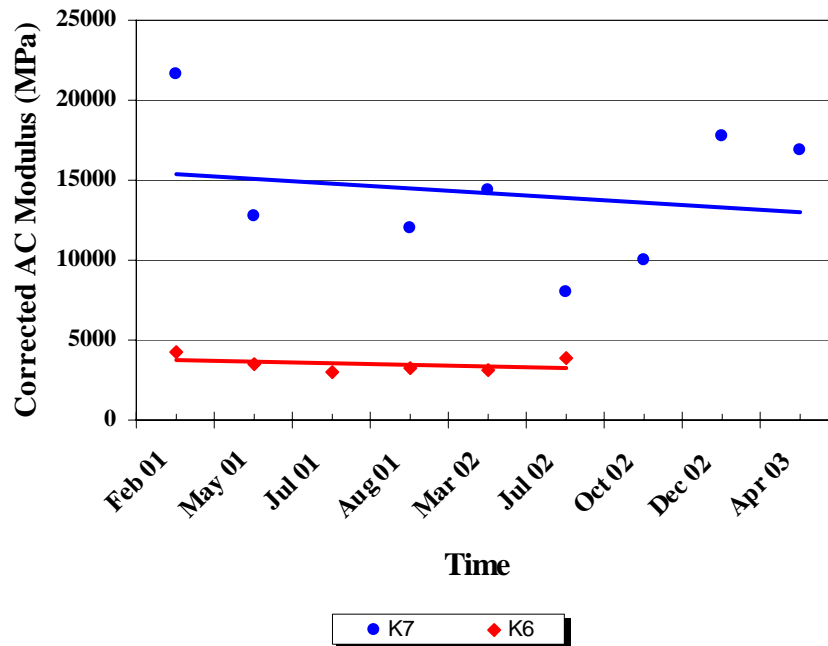**FIGURE D4   Corrected AC Moduli Using Eq. 7.1 in the Pavement Group 4.**

FIGURE D5   Corrected AC Moduli Using Eq. 7.1 in the Pavement Group 5.

FIGURE D6   Corrected AC Moduli Using Eq. 7.1 in the Pavement Group 6.

FIGURE D7   Corrected AC Moduli Using Eq. 7.1 in the Pavement Group 7.

USING TX DOT EQUATION

FIGURE D8   Corrected AC Moduli Using Eq. 7.2 in the Pavement Group 1.

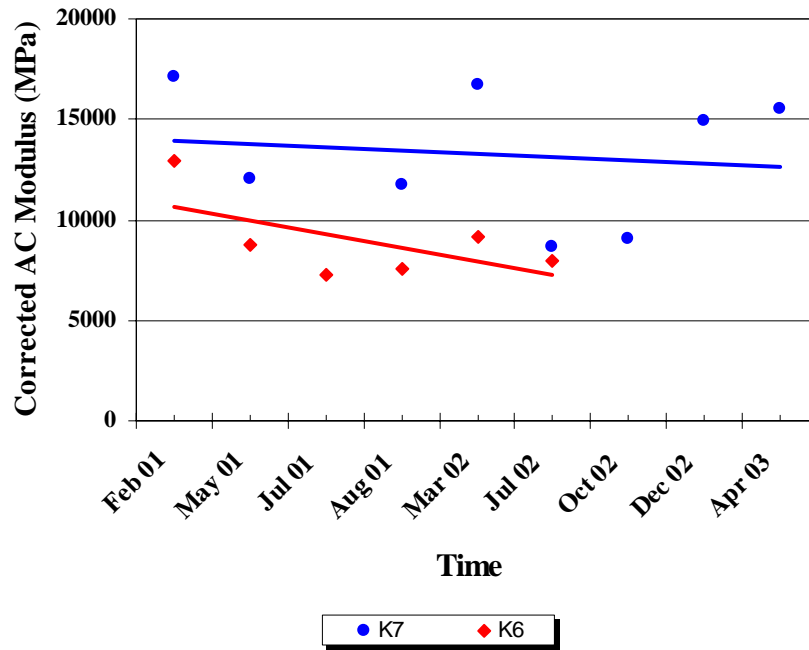**FIGURE D9   Corrected AC Moduli Using Eq. 7.2 in the Pavement Group 2.**

FIGURE D10   Corrected AC Moduli Using Eq. 7.2 in the Pavement Group 3.
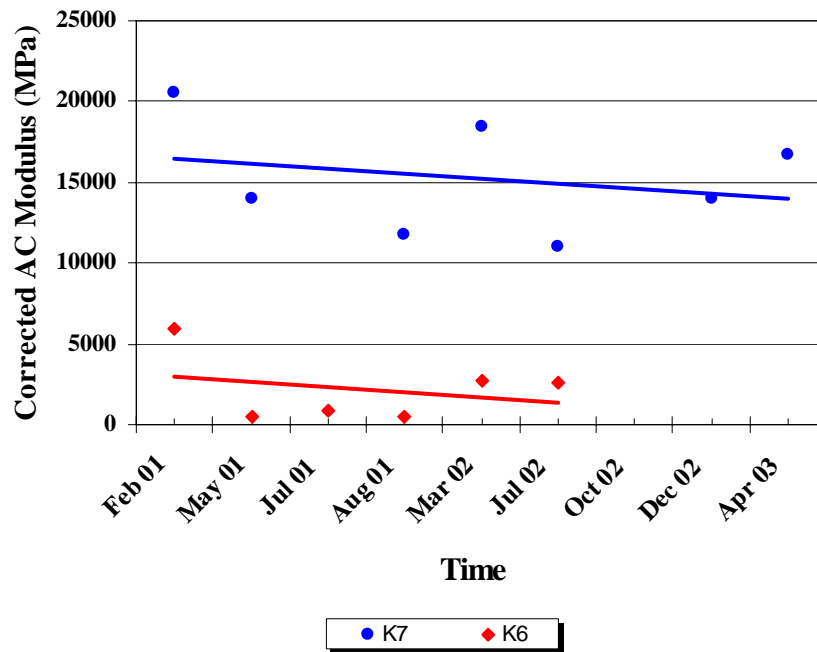

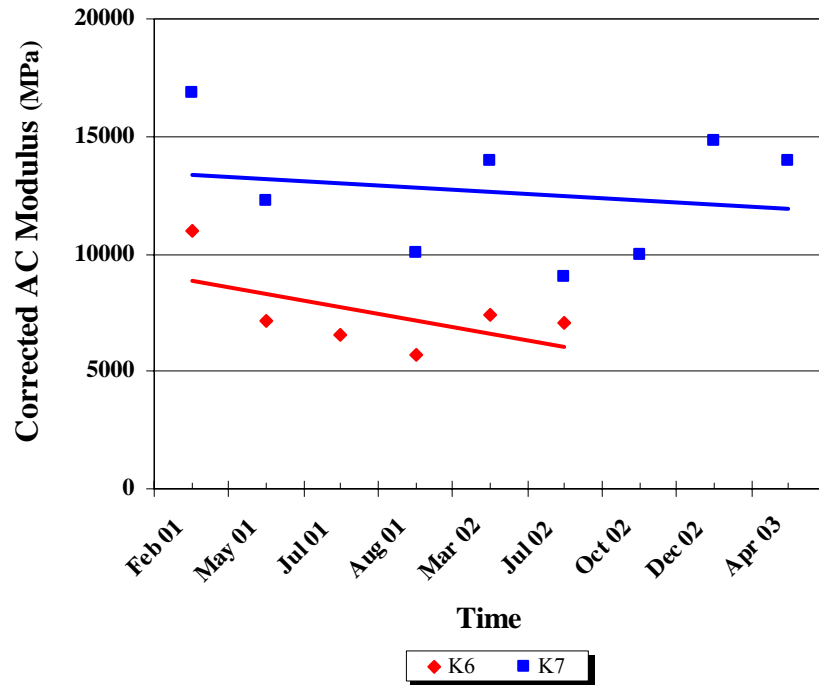**FIGURE D11   Corrected AC Moduli Using Eq. 7.2 in the Pavement Group 4.**

FIGURE D12   Corrected AC Moduli Using Eq. 7.2 in the Pavement Group 5.
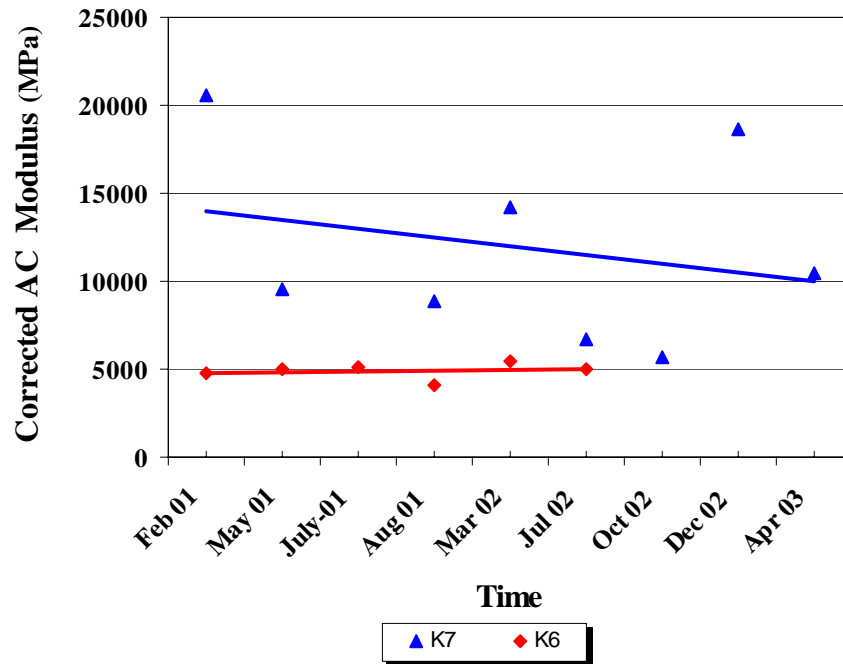

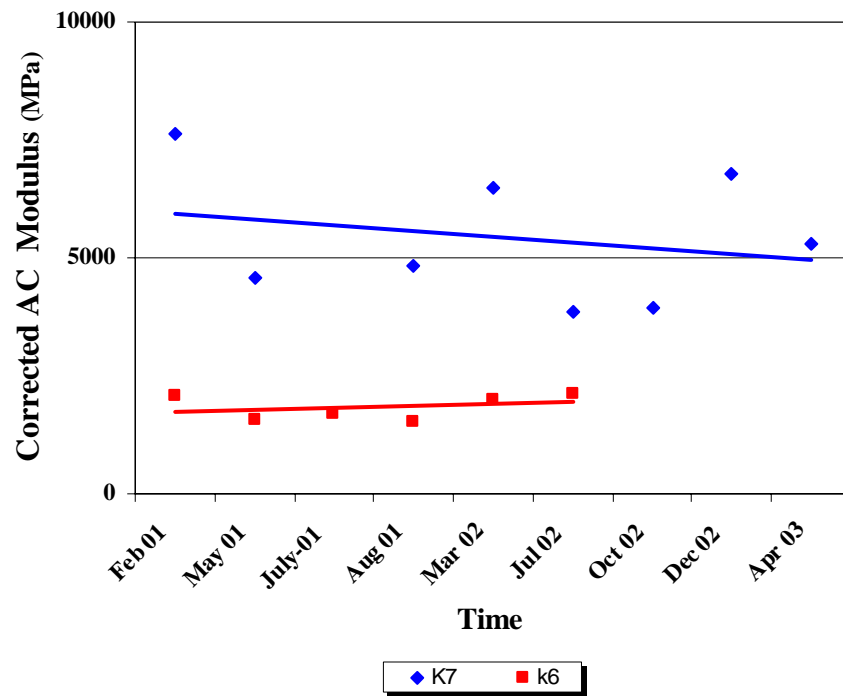FIGURE D13   Corrected AC Moduli Using Eq. 7.2 in the Pavement Group 6.

FIGURE D14   Corrected AC Moduli Using Eq. 7.2 in the Pavement Group 7.

VITA

SONIA INES RAMOS APARICIO

PERMANENT ADDRESS

Av Morro Solar 2204 Urb Monterrico Sur Lima 33 Peru
(511) 2749512)

EDUCATION

- Texas A&M University
  Master of Science in Civil Engineering, May 2003

- Universidad Nacional de Ingenieria
  Bachelor of Science in Civil Engineering, December 1988

EXPERIENCE

- Texas Transportation Institute, Texas A&M System. College Station, Texas.
  Research Assistant, Project: " Characterize the Effects of Permitted Overweight
  Loads on SH 4/48 in the Port of Brownsville." Aug 2000- Aug 2003.

- Ministry of the Presidency. Peru Government.
  Inspector and Coordinator Engineer of civil work related to highways. Jan 1998-
  April 1999.

- Peru Government and Inter-American Development Bank.
  Inspector and Coordinator Engineer of civil works from Ministry of Education
  especially the elementary and high schools built in the coast and mountain of
  Peru. Jan 1997- Dec 1997.

- Fletcher Challenge Group, Firth Industries Peru, Premix Concrete
  Aggregate Plant Supervisor Engineer with training in New Zealand in aggregate
  plants operations and quality control of aggregate production. 1996.

- Universidad Nacional de Ingenieria.
  Assistant Professor, Department of Civil Engineering. Jan 1991- Dec 1995.